Western Indian Ocean
JOURNAL OF
Marine Science

Special Issue 2/ 2021 | e-ISSN 2683-6416

Studies on the Mascarene Plateau

Guest Editor | Ranjeet Bhagooli

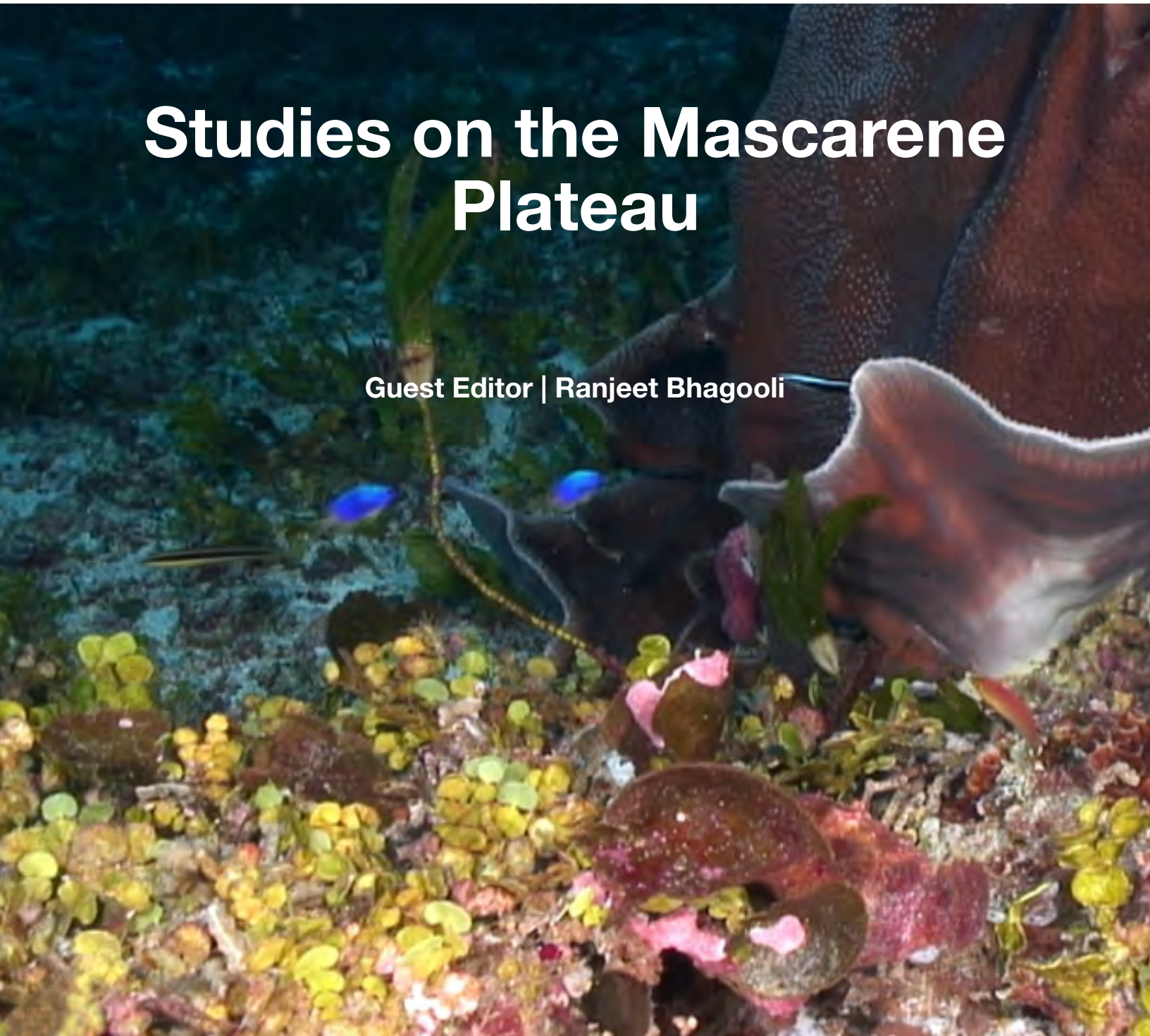

Western Indian Ocean
JOURNAL OF
Marine Science

Published biannually

Aims and scope: The *Western Indian Ocean Journal of Marine Science* provides an avenue for the wide dissemination of high quality research generated in the Western Indian Ocean (WIO) region, in particular on the sustainable use of coastal and marine resources. This is central to the goal of supporting and promoting sustainable coastal development in the region, as well as contributing to the global base of marine science. The journal publishes original research articles dealing with all aspects of marine science and coastal management. Topics include, but are not limited to: theoretical studies, oceanography, marine biology and ecology, fisheries, recovery and restoration processes, legal and institutional frameworks, and interactions/relationships between humans and the coastal and marine environment. In addition, *Western Indian Ocean Journal of Marine Science* features state-of-the-art review articles and short communications. The journal will, from time to time, consist of special issues on major events or important thematic issues. Submitted articles are subjected to standard peer-review prior to publication.

Manuscript submissions should be preferably made via the African Journals Online (AJOL) submission platform (http://www.ajol.info/index.php/wiojms/about/submissions). Any queries and further editorial correspondence should be sent by e-mail to the Chief Editor, wiojms@fc.ul.pt. Details concerning the preparation and submission of articles can be found in each issue and at http://www.wiomsa.org/wio-journal-of-marine-science/ and AJOL site.

Disclaimer: Statements in the Journal reflect the views of the authors, and not necessarily those of WIOMSA, the editors or publisher.

e-ISSN 2683-6416

Cover image: Benthos at location 37 surveyed at Saya de Malha Bank, Western Indian Ocean © FAO, DA and IMR/EAF Nansen Programme

Western Indian Ocean
JOURNAL OF
Marine Science

Special Issue 2/ 2021

Studies on the Mascarene Plateau

Guest Editor | Ranjeet Bhagooli

The EAF-Nansen Programme is executed by the Food and Agriculture Organization (FAO) of the United Nations with the scientific support of the Institute of Marine Research (IMR). The Marine Scientific Research Survey was carried out in 2018 within the project framework entitled "Characterising the marine ecosystem and morphology of the Saya de Malha Bank" between the FAO and the Designated Authority (DA) of the Extended Continental Shelf, Mascarene Plateau Region.

Table of Contents

Studies on the Mascarene Plateau

A survey was conducted from on board the R/V Dr Fridtjof Nansen in May/June 2018 with the aim of characterizing the marine ecosystems and morphology of the Saya de Malha Bank, part of the Mascarene Plateau. The survey formed part of the EAF-Nansen Programme, executed by the Food and Agriculture Organization of the United Nations (FAO).

The Saya de Malha Bank is part of a jointly managed area (JMA) between the Republics of Mauritius and Seychelles. The survey was organized following a request in February 2017 by the Department for Continental Shelf, Maritime Zones Administration and Exploration, Prime Minister's Office, Mauritius on behalf of the JMA, and after authorization was obtained to conduct Marine Scientific Research from the concerned Authorities. Some studies were also carried out on the Nazareth Bank.

The scientific team was led by the principal investigator and cruise leader, Dr Odd Aksel Bergstad from the Institute of Marine Research (IMR), Norway and co-led by Dr Dass Bissessur from the Department for Continental Shelf, Maritime Zones Administration & Exploration, Prime Minister's Office, Republic of Mauritius. A core team of scientists and technicians from IMR, appointed scientists from various institutions from the Republic of Mauritius and Seychelles, as well as guest scientists from overseas constituted the scientific team. Additionally, an engineer from the engineering firm Argus Remote Systems ASA, and a trainee from the University of Bergen participated.

Some of the major research findings from this FAO / EAF-Nansen 2018 research cruise are presented in this special issue of the Western Indian Ocean Journal of Marine Science entitled "Studies on the Mascarene Plateau". The papers include both original articles and field notes. The physical and chemical oceanography aspects include reports from Coopen *et al.* on observations of circulation over the Saya de Malha Bank and Audit-Manna *et al.* documenting the inorganic nutrient distribution at Saya de Malha and the eastern slope of the Nazareth Banks. Soondur *et al.* then present two papers on phytoplankton; firstly documenting the spatial distribution of surface chlorophyll *a* and micro-phytoplankton in the Mascarene region, and secondly on the variations in density, diversity, photo-physiology and estimated productivity of micro-phytoplankton with depth at the Saya de Malha Bank. Ramah *et al.* report on the distribution and diversity of the benthic habitats at 23-50 m at the Saya de Malha Bank, while Nicholas and Bhiwajee document the sediment characteristics at these Banks. Additionally, Bhagooli *et al.* present two contributions on photo-physiology of marine organisms from the Banks on the Mascarene Plateau through assessment of the variable photo-physiology of healthy and bleached corals, and seaweeds and seagrasses from the Saya de Malha and Nazareth Banks. Ramah *et al.* then present investigations on marine mollusc diversity in the surveyed area. The original article by Bergstad *et al.* provides a first characterization of the distribution and composition of benthic and demersal macro- and megafauna from 1000 m depth up the slope on the western, northern and eastern sides of the Saya de Malha Bank while Caussy *et al.* documents the pelagic and demersal fish diversity at the Saya de Malha and Nazareth Banks. The field notes include highlights on Rhodolith beds by Ramah *et al.*, seagrasses by Ramah and Bhagooli, *Halimeda* beds and coral diseases by Bhagooli *et al.*, and the endemic giant clam and sea star sightings by Ramah *et al.*

These contributions present new scientific knowledge for the Mascarene Plateau and would help inform policy and decision making in the Mascarene region. These scientific data provide a basis for comparison with findings of potential future oceanic research cruises and marine spatial planning processes on the Mascarene Plateau, Western Indian Ocean.

Associate Professor (Dr) Ranjeet Bhagooli
CMarSci (Oceanography) CSci CBiol FRSB FIMarEST FMBA (UK),
Fellow (ICRS), FMAST (MU), FSB (MU)
University of Mauritius
Guest Editor

Ocean circulation over the Saya de Malha Bank in the South West Indian Ocean

Priscilla Coopen[1]*, Yuneeda B. N. Oozeeraully[1], Marek Ostrowski[2]

[1] Department for Continental Shelf, Maritime Zones Administration and Exploration, Prime Minister's Office, Belmont House 2nd Floor, Intendance Street, Port Louis, 11328, Republic of Mauritius

[2] Institute of Marine Research (IMR), PO Box 1870 Nordnes, N-5817 Bergen, Norway

* Corresponding author: pcoopen@govmu.org

Abstract

The Saya de Malha Bank is one of the major banks of the Mascarene Plateau in the South West Indian Ocean. It is known for its unique ecosystem, remoteness (nearest island is about 300 km away) and complex oceanographic conditions. This study presents the results of a survey conducted in May 2018 on-board the R/V Dr Fridtjof Nansen, and aims to provide a descriptive overview of the interaction of the large-scale South Equatorial Current (SEC) over the shallow Saya de Malha Bank. The analysis of the current pattern revealed a two-layered structure of the current over the shallow topography of the bank compared to the vertically rigid-structure of the SEC throughflow in its deeper region. This two-layered flow consists of a surface layer and a sub-thermocline layer. The top layer flow, carrying the lower salinity mass (Tropical Surface Water) is driven by the Ekman dynamics observed in the southern hemisphere whereas the sub-thermocline current layer is most likely governed by the tidal and internal wave dynamics generated by the topographic relief of the bank.

Keywords: Saya de Malha Bank, South Equatorial Current, thermocline, Mascarene Plateau, ocean circulation

Introduction

The tropical south Indian Ocean is characterized by the large-scale circulation called the South Equatorial Current (SEC), which is a major westward current in the latitude band between 10° to 20°S and is most intense at the surface, reaching a depth of 1400 m (Schott and McCreary, 2001; New *et al*., 2007; New *et al*., 2005). When the SEC meets the Mascarene Plateau, an arch-shaped submarine ridge comprising of a series of shallow banks (Cargados Carajos Bank, Nazareth Bank, Saya de Malha Bank and Seychelles Bank) that rise sharply from the deep ocean in the South West Indian Ocean (SWIO), it has a profound effect on the basin-scale current system (Schott and McCreary, 2001).

The overall effect of the Mascarene Plateau is to split the SEC into two cores, forming the northern and southern cores of the SEC downstream of the plateau and the current is forced to follow the bathymetric contours of the banks (New *et al*., 2007) which are eventually funnelled across to the SWIO through the gaps found between the shoals of the plateau (New *et al*., 2007; Vianello *et al*., 2017). Most of the SEC flows through three gaps (channels): between Seychelles and the Saya de Malha Banks; between the Saya de Malha and Nazareth Banks; and between Cargados Carajos Bank and Mauritius island. The volume transported in these gaps varies due to the varying influence of the two monsoon seasons (northeast Monsoon and southwest Monsoon) on the SEC (Vianello *et al*., 2017). In addition, the interaction of incident currents with the abrupt topographical changes prompts local oceanographic conditions to support the formation of unique mid-ocean shallow sea ecosystems (Genin, 2004; Payet, 2005).

The SEC also acts as a barrier in the upper ocean between water masses of southern and northern origins (Schott and McCreary, 2001; New *et al.,* 2007; New *et al.,* 2005). For instance, the Subtropical Surface Water (STSW), Sub-Antarctic Mode Water (SAMW)

http://dx.doi.org/10.4314/wiojms.si2021.2.1

and Antarctic Intermediate Water (AAIW) are present on the southern side of the SEC as compared to the Arabian Sea High Salinity Water (ASHSW) and Red Sea Water (RSW) on its northern side (New *et al.,* 2007). Tropical Surface Water (TSW) is also evident as a fresh surface layer which is carried westward by the SEC in the upper 50–100 m. At deeper depths, the North Indian Deep Water (NIDW) and Antarctic Bottom Water (AABW) are found to the west of the Mascarene Plateau (New *et al*., 2007; Pous *et al*., 2014). The SEC therefore forms a sharp boundary between the subtropical water masses from further north (nutrient-rich waters) and south (nutrient-poor waters) of the bank (New *et al*., 2007; Vortsepneva, 2008). The interaction of the SEC with the Mascarene Plateau further plays a significant role in the supply of water masses to the SWIO (New *et al.*, 2005; New *et al.*, 2007; Vianello *et al.*, 2017).

The Saya de Malha Bank is one of the major banks of the Mascarene Plateau and has an area of about 40, 808 km^2 (Vortsepneva, 2008), and is comprised of the smaller Ritchie Bank and the South Bank. This paper focuses on the latter which will be hereafter referred as Saya de Malha (SDM). The SDM has been the target of various scientific research works during recent years due to the uniqueness of its ecosystems (Bergstad *et al.,* 2021; Ramah *et al.,* 2022), the complexity of its oceanographic processes (da Silva *et al.*, 2011; New *et al.*, 2013; Lindhorst *et al*., 2019) as well as its geological nature and biogeochemistry (Lindhorst *et al.,* 2019). The oceanographic conditions that develop over SDM and their impact on local biological productivity are strongly influenced by a superposition of the steady SEC flow with barotropic tides (da Silva *et al.*, 2015) upon interacting with the relief of the bank. As a result of these interactions, barotropic tidal energy is transferred to internal solitary waves (ISWs) at the southern end of the bank, which propagate towards the shallow bathymetry where they break (New *et al.*, 2013). The ISW breaking induces turbulence and intense mixing, which appears to boost nutrient supply and chlorophyll production in otherwise oligotrophic environments (New *et al.*, 2013; Ostrowski *et al.*, 2009; Zeng *et al.*, 2021).

In May 2018, the Norwegian research vessel, R/V Dr Fridtjof Nansen, in collaboration with the Mauritius and Seychelles Joint Management Authority, conducted a survey over the SDM that lasted almost three weeks. It is to be noted that the SDM is within the Joint Management Area and is jointly managed by both the Republic of Mauritius and the Republic of Seychelles under the Joint Management Treaty (Treaty Concerning the Joint Management of the Continental Shelf in the Mascarene Plateau Region - CLCS, 2011). The aim of the survey was to carry out a systematic study of the benthic ecosystems and morphology of the bank. The survey covered the entire area of the bank with an adequate spatial resolution with the vessel-mounted Acoustic Doppler Current Profiler (ADCP) operated continuously underway. In this paper, the collected ADCP data were used to provide a general description of the circulation over the inner sections of SDM and its connection to the SEC throughflow along the southern slopes in May 2018.

Materials and methods

Study area

The SDM is a large bank with a summit surface of about 350 km wide (Kara and Sivuka, 1990) and is located between latitudes 10-13°S and longitudes 59.30-62.30°E as shown in Figure 1a. The closest land, the Agalega Island, is approximately 300 km away. The bank is about 900 km and 700 km south of Mauritius and north of Seychelles, respectively. It is separated from the Nazareth Bank, in the south, by a 1100 m deep channel. The bank experiences relatively steady southeast trade winds. During the southern winter, the northern edge of the trade winds shifts northward and falls during the southern summer and autumn (Schott *et al.*, 2009). The precipitation in the region is around 100-200 mm/month during December, January and February and less than 50 mm/month during June, July and August (Schott *et al.*, 2009).

Survey approach

The field survey was undertaken on board the R/V Dr Fridtjof Nansen (Survey no. 2018406) (Bergstad *et al*., 2020) in May 2018 just before the onset of the southwest Monsoon season. The survey approach was derived primarily to characterize the marine ecosystem and morphology of SDM. It consisted of two legs as shown in Figure 1 (b and c). Leg 1 followed a pre-determined trajectory of eight parallel transects covering the whole bank. Each transect was separated by approximately 15 nautical miles from the other and covered the entire width of the bank from its western to its eastern edge, extending a few miles into the surrounding deep ocean. Leg 2 involved an intense sampling programme for habitat mapping at selected locations and did not follow a fixed transect grid. At the end of Leg 2, the vessel concluded the observations over the bank and departed southwards, crossing the SN sill towards the Nazareth Bank.

Ship-based ADCP data

Ocean current velocities and directions were recorded and measured continuously while the ship was underway with the vessel-mounted Ocean Surveyor 75 kHz and 150 kHz Acoustic Doppler Current Profiler (ADCP) by the Teledyne RD Instrument (RDI). The 75 kHz ADCP has a vertical resolution of 16 m and maximum depth of 800 m. The respective values for 150 kHz units were 8 m and 300 m.

CTD and wind data

The vertical profiles of temperature, salinity and dissolved oxygen were determined using the Seabird 911 plus Conductivity, Temperature and Depth (CTD) profiler. A total of 44 CTD stations covering the full depth of the water column were included in the survey, among which 30 were during Leg 1 (Fig. 1b) and 14 during Leg 2 (Fig. 1c).

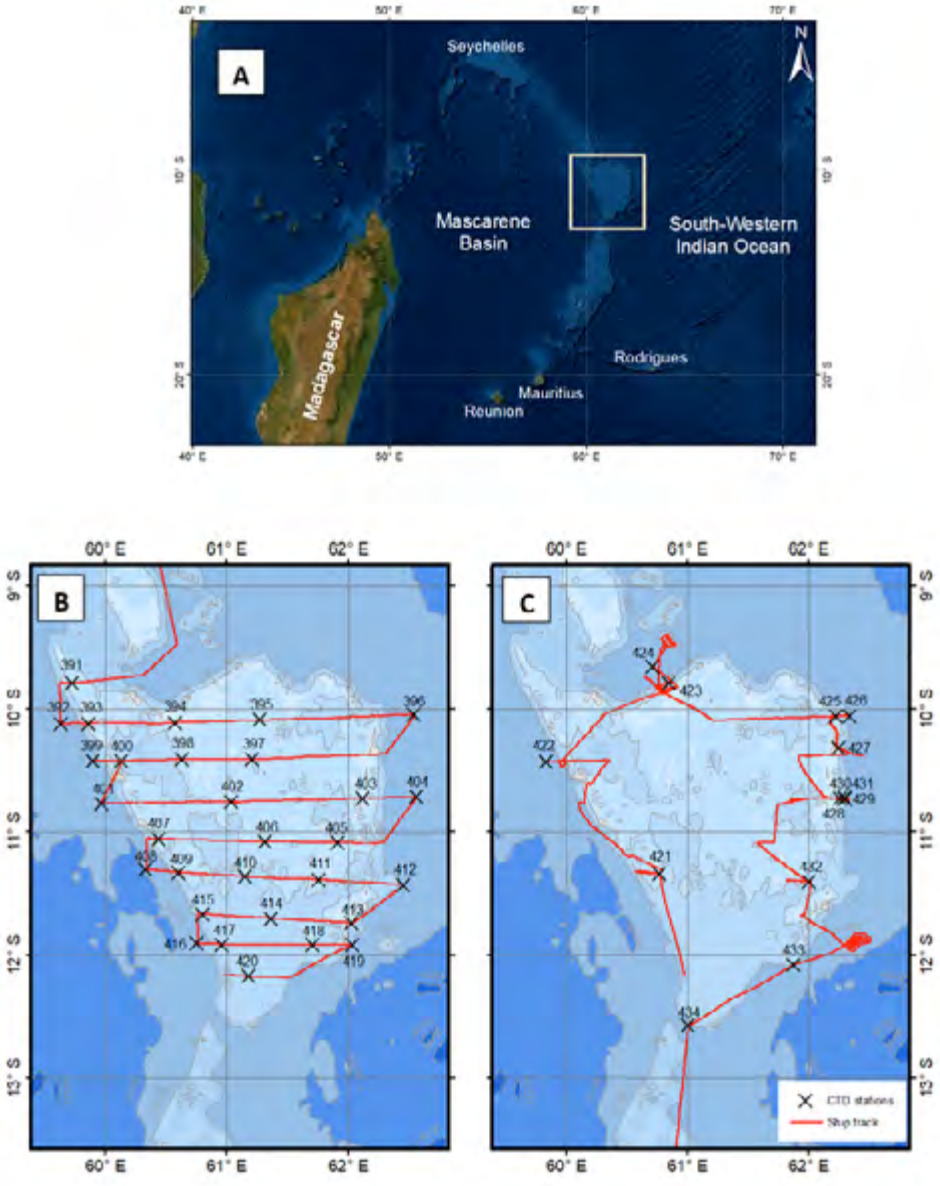

Figure 1. a) Region of the Mascarene Plateau surveyed in May 2018 (yellow box); b) Leg 1 of the survey (7-15 May 2018); and c) Leg 2 of the survey (15-25 May 2018) with their corresponding CTD stations undertaken over the Saya de Malha Bank.

Wind speed and direction data were collected with the vessel's Automated Weather Station (AWS) mounted 10 m above sea level with a sampling rate of 1 minute.

Bathymetry

The bathymetry of SDM was derived by merging the GEBCO 2021 atlas data (https://www.gebco.net) with the shallower depth *in situ* echo-sounding data (less

than 300 m deep) from 2008 (Stømme *et al*., 2009) and 2018 (Bergstad *et al*., 2020) Nansen expeditions.

Satellite data

The daily satellite data from the GlobCurrent product were used in this study. The images for the observational period from 7-27 May 2018 were accessed through the Copernicus Marine Service website (https://www.copernicus.eu/en), product MULTIOBS_GLO_PHY_REP_015_004. GlobCurrent combines altimetry-derived geostrophic currents and Ekman (wind-driven) currents (Cancet *et al.*, 2019). These data are distributed on a 0.25-degree grid.

Data analysis and techniques

The ADCP data were processed using a version of OSSI post processing software developed at GEOMAR (Fischer *et al.*, 2003) and adapted to the specifics of fishery surveys at the Institute of Marine Research, Norway [Ostrowski, personal communication]. The pre-processing involved removing erroneous data, bottom masking, and correcting the misalignment between the ship and the ADCP beam axis. The misalignment angle and its standard error were estimated to be -0.25° and 0.006° for the 150 kHz and 0.06° and 0.006° for the 75 kHz ADCP. As a result of this analysis, a time-averaged dataset with a 2-minute sampling step was obtained.

In this study, the 150 kHz data were used in the inner part of SDM, whereas the 75 kHz result was utilized exclusively to compute transports in the southern section of the bank and across the SN sill. The volume transport was computed using the following equation:

$$Volume\ transport = \iint v.dA$$

where v is the velocity and dA is the area normal to the velocity.

The vertical shear squared (Sh^2) of the horizontal velocity was computed using the following equation:

$$Sh^2 = (\frac{\partial u}{\partial z})^2 + (\frac{\partial v}{\partial z})^2$$

where $(\frac{\partial u}{\partial z})^2$ and $(\frac{\partial v}{\partial z})^2$ represent the contribution of the vertical shear associated with the zonal and meridional currents respectively.

The CTD data were quality checked and erroneous data and spikes were removed. The postprocessing was carried out using the Seasave software from Sea-Bird Scientific. The salinity and oxygen data were validated on-board by comparison with water bottle samples using the Guildline Portasal 8410A and the Winkler method (Langdon, 2010), respectively. The dual sensor configuration on the CTD probe secured the validation of temperature data.

The raw data of wind speed and direction displayed numerous gaps. After the removal of these gaps, the valid data sections were low-pass filtered using a 15-minute lag. Finally, the filtered dataset was regularised on a grid with a cell resolution of 10 x10 km to account for overlapping coverage when the ship was manoeuvring.

Results

Topographic features of Saya de Malha Bank

The overall topographic architecture of the bank can be divided into three main parts: a shallow submerged reef rim surrounding the eastern and northern part of the bank with a bathymetry of less than 40 m deep; an interior central lagoon (CL) of 70-150 m deep which opens up in the south shelf break ledge (SBL) of the bank at depths between 200 to 250 m; and a narrow southern tip (South Point - SP) with depth greater than 250 m. Moving from the west to east of the plateau (Fig. 2a), the water depth on the western part of the bank is around 70 m, in the lagoon (CL) 120 m and about 40 m in the eastern part (ES). This indicates that the plateau on the eastern side is more elevated than on the western side. Surrounding the eastern (ER) and northern rims (NR) are shallow areas of 40 to 100 m deep. The interior part of the bank consists of pinnacles and/or local highs protruding from the seafloor. One of them can also be seen on the western side, labelled western tower (WT) and stands about 75 m above the seafloor. Another similar pinnacle is located on the eastern side. It is a stand-alone seamount-type structure (hereafter referred to as the South Bank or SB). The main structures of the bank follows the description presented by Vortsepneva (2008) from the research work done in the 1980s.

Wind conditions

Steady southeasterly wind with velocities ranging between 10-12 m s^{-1} dominated throughout the survey period. The wind velocities however dropped to 7-8 m s^{-1} for a few hours on 14, 17, 20 and 22 May 2018 (not shown). The wind pattern observed on 8 May was an exception as the wind velocities reduced to 3-4 m s^{-1} with the wind direction being predominantly from the northeast. The overall wind conditions observed

over the SDM were consistent with the western Indian Ocean (WIO) wind climatology, characterized by the steady southeast trades south of 10°S (Schott and McCreary, 2001).

Water masses

Figure 3 presents temperature, salinity, and dissolved oxygen sections across the bank, in a north-south direction (Fig. 2b). All distributions showed the same vertical structure, consisting of the top layer of Topical Surface Water (TSW), characterized by uniform temperature (28.2-28.4°C), salinity (31.1-31.4 PSU) and oxygen (4.5-4.6 ml/L) ranges. This fresh TSW layer is transported by the SEC from the western Pacific region (New *et al.*, 2007; Vianello *et al.*, 2017) and was observed throughout the SDM region. The TSW varied across latitudes between depths of 40 to 70 m, with shallower depths in the northern part and deeper depths in the southern part of the bank. At the southern end of the section, the pycnocline was found at 60 m but appeared to shoal northwards. However, at the shallowest station, Sta. 395 located at the northern terrace, stratification was absent as the TSW layer extended to the bottom. Strong stratification separated the top TSW layer from colder, more saline and oxygen-deficient water masses below, identified as the Indonesian Throughflow Water (ITF) and the Subtropical Surface Water (STSW). The vertical profile of dissolved oxygen at Sta. 402 also displayed a low oxygen content (< 2 ml/L) in the Central Lagoon (CL) compared to the surrounding deep ocean, thus indicating higher production and decomposition rates in this region. Therefore, the local oceanographic conditions could be favourable to sustain regional productivity due to the topographic features of the bank. However, given the sparse CTD stations spacing over the Central Lagoon, the above observation is inconclusive.

Satellite observations – surface current pattern

Figure 4 presents streamlines of satellite-derived daily currents over the SDM and SN sill on the first and last day of the survey (on 7 and 27 May, 2018 respectively). The streamlines are overlaid on the shaded bathymetry. The location of the SEC core is manifested by the current velocities exceeding 40 cm s^{-1} (the green hue on the colour scale). Between the start and end of the survey, the flow patterns had evolved visibly. On 15 May 2018, on the eastern (upstream) side, the incident SEC flew in three separate cores (not shown). On 27 May 2018, in contrast, the upstream SEC reformed to a broad current extending from 10° to 14°S and further south. On both days (7 and 27 May 2018), the SEC streamlines behaved similarly – diverging into two branches on the upstream side of SDM; one branch swinging around the southern tip of the bank, the other following along the bank's northern edge. The two branches manifested topographic steering action where geostrophic flows must follow the bottom contours (Cushman-Roisin and Beckers, 2011). With a resolution of 0.25 degree, the GlobCurrent-derived streamlines presented in Figure 4 could only reproduce the largest-scale features of this process.

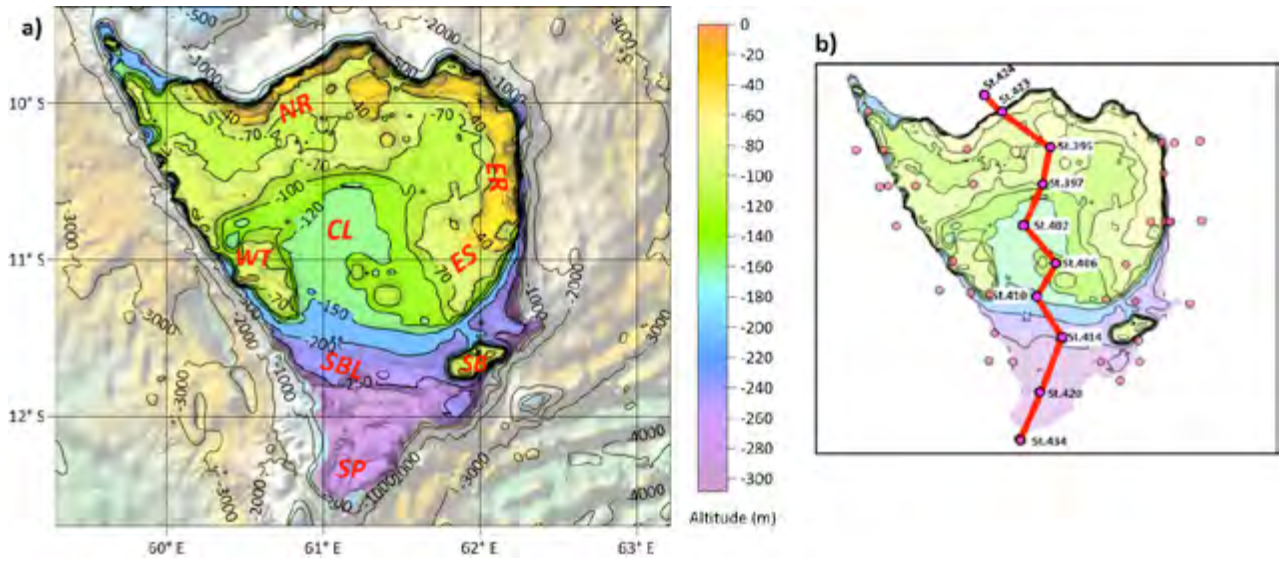

Figure 2. a) Bathymetry of the Saya de Malha Bank's shallow regions (above 300 m): NR – Northern Rim, ER – Eastern Rim, CL – Central Lagoon, ES – Eastern Slope, WT – West Tower, SB – South Bank, SBL – Shelf Break Ledge and SP – South Point; and b) Southbound section (red line) representing CTD stations used for the vertical distribution plots (pink dots represent all CTD stations).

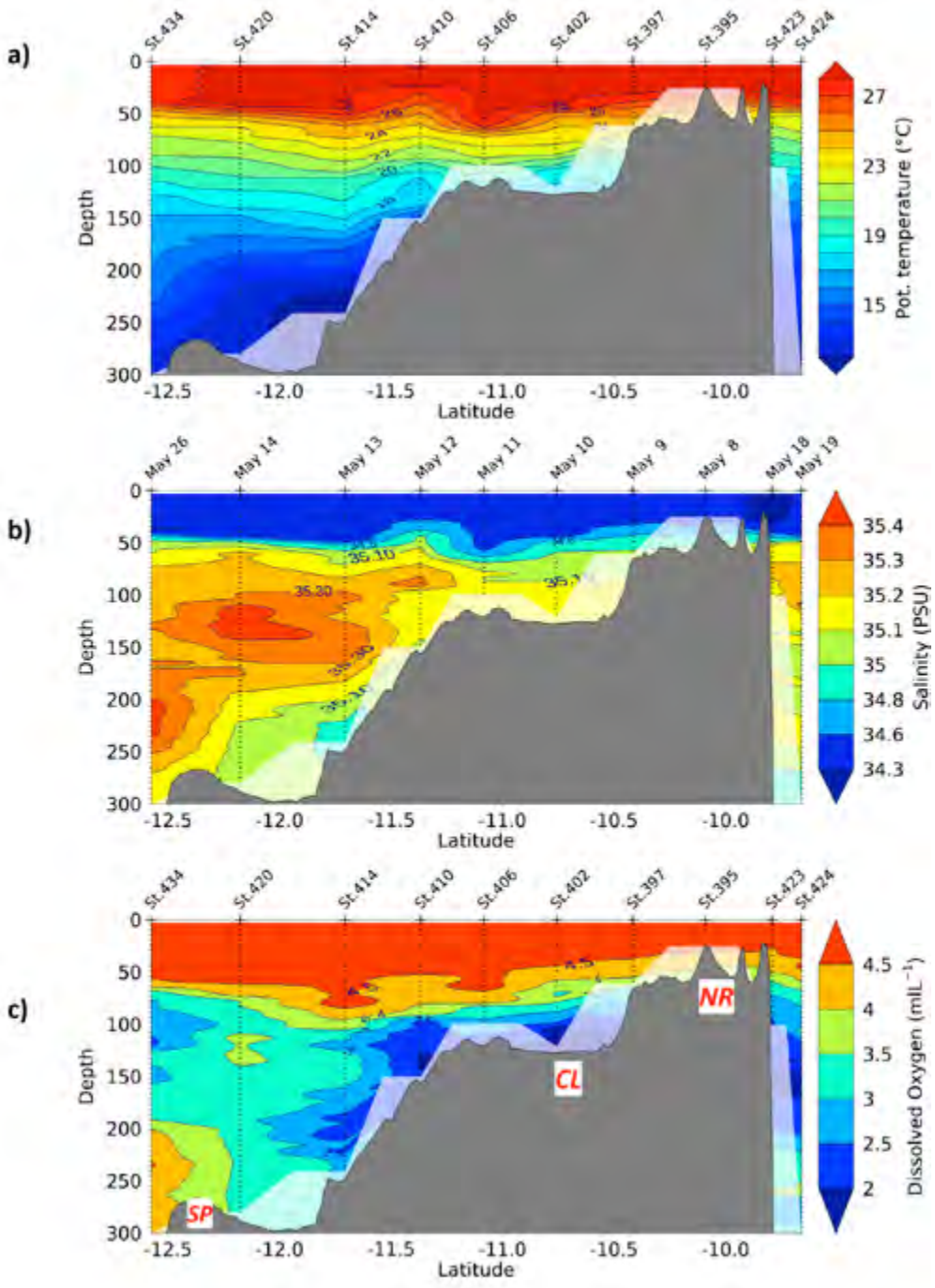

Figure 3. Latitudinal distribution of: a) Potential temperature (°C); (b) Salinity (PSU); and (c) Dissolved oxygen concentration (ml/L) across the Saya de Malha Bank.

ACDP currents

The ADCP data showed similar trend as previously described in the satellite observations; that is, upon reaching the eastern slopes of SDM, the SEC diverges into a northeastward and southwestward direction feeding the northern and southern part of the bank respectively. The ADCP currents revealed a general current pattern in the surface layer across the bank which flowed in a southwestward direction with velocities of 10-20 cm s^{-1} (Fig. 5a) and increasing intensity towards the south of the bank reaching velocities of 40-50 cm s^{-1} (Fig. 6). Furthermore, an eastward current was observed below the surface layer with velocities of 10-20 cm s^{-1}. This two-layered structure of the current was also apparent on the central region of the bank which demonstrates the complexity of the interaction of currents with the mountainous topography of SDM. The intensity of the SEC was found

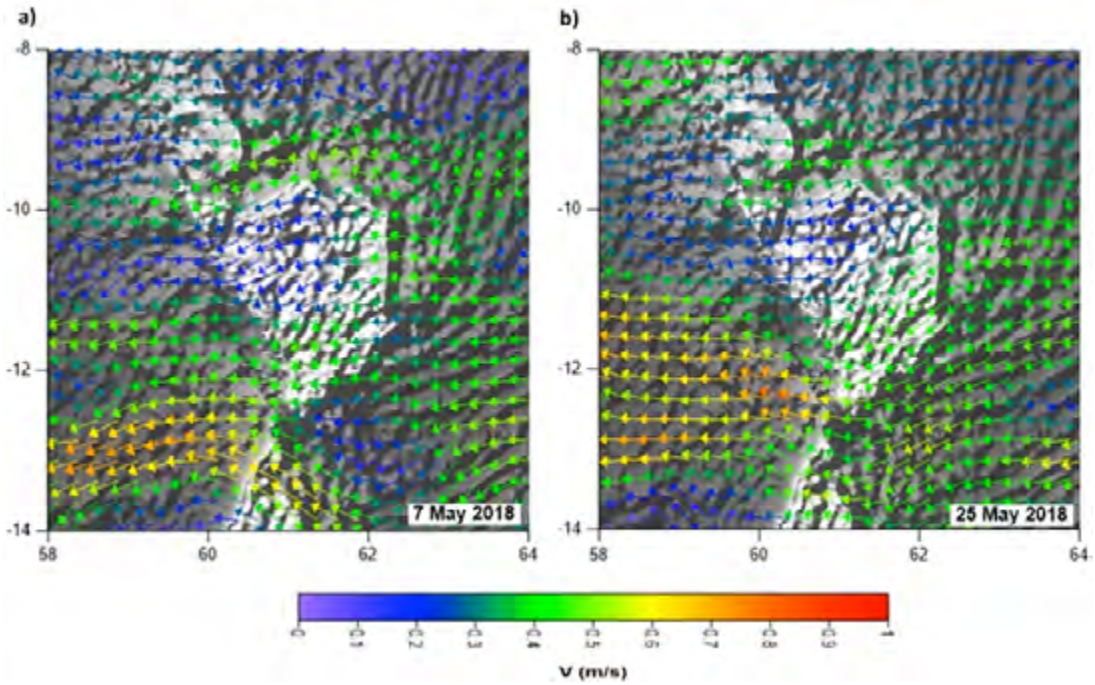

Figure 4. Streamlines of satellite-derived daily surface currents (m s^{-1}) over the Saya de Malha region for: a) 7 May 2018; and b) 25 May 2018.

to be greater at the northeastern and the southern regions of the bank. The southern branch of the current circumvented the Shelf Break Ledge (SBL) and continued westward, joining the SEC flow channelled through the SN sill. The current between latitudes 12° S to 14° S, in the SN sill, reached velocities of between 50-70 cm s^{-1}.

Figure 5 presents the horizontal currents measured over the inner part of SDM for two depth ranges: the 18-26 m, characterizing the top surface layer, TSW transport; and the 58-66 m, associated with the underlying layer, ITF/STSW. Figure 7 enhances this presentation by using the same data to show selected vertical sections of the meridional current component. The first impression from examining these figures is the randomness of the presented current vectors. This appears as a stark contrast to the smooth streamlines of the satellite-derived surface current shown in Figure 4, representing the mesoscale currents as compared to the resolution of the ADCP currents observed over the bank. However, similarities between both the satellite (Fig. 4) and ADCP currents (Fig. 5a) can be distinguished. Firstly, the TSW transport over the inner bank regions (CL, NR, ER; transects 2 to 5) and satellite-derived streamlines shared the same current speed range (10-20 cm s^{-1}) and, generally, the same, southwestward orientation. Moreover, towards the shelf break region (SBL, transect 6), on both figures, the current speed approximately doubled and assumed the direction of bathymetric contours (seawards of 200 m, cf. Fig. 5a and 6a) – manifesting the topographic steering of the SEC southern branch. Lastly, the bifurcation of the incident SEC into the southward and northward branches on the east side of the bank was present on both distributions. The reverse flows along the eastern slope of the bank were clearly identifiable at the ADCP transects 2 and 6 (Fig. 5a; Fig. 7a and c), while the satellite image demonstrated the same process of the SEC bifurcation on the bank's topography at a large scale. Comparing ADCP currents observed above and below the thermocline (Fig. 5a and b), the separation of the flows for the top layer and underlying layer was evident. The top TSW layer over the inner bank evidently followed the southern hemisphere Ekman layer dynamics, deflecting flow to the left of the wind direction. In contrast, the sub-thermocline layer appeared to recirculate around the Central Lagoon (Fig. 5b).

Figure 6a presents the horizontal distribution of ADCP currents from the 42-50 m, thus representing the current at the base of the thermocline (Fig. 3) for the southern region of the bank. The tendency of the flow to follow the 200 m depth contour across Line A and Line B is evident. Figure 6b presents the zonal current across these two lines. The surface-intensified zonal current dominated the observations in the downstream section (Line A, Fig. 6b). The zonal flow

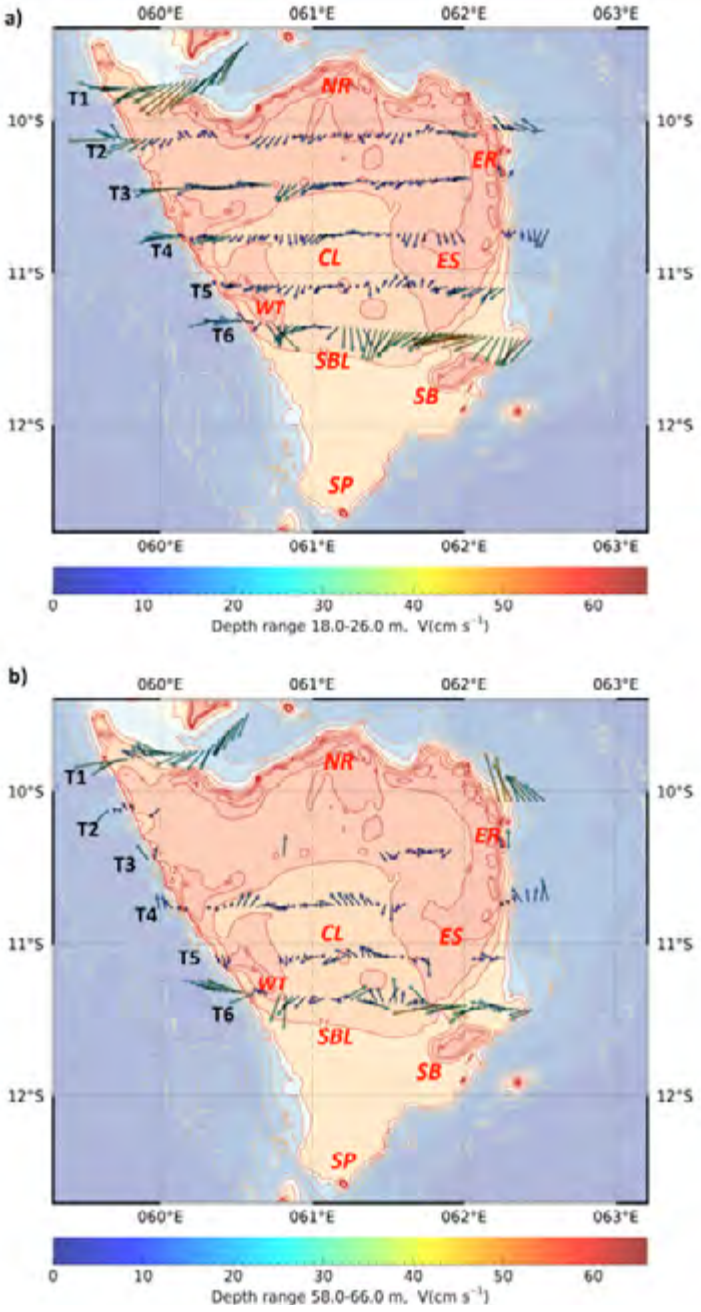

Figure 5. Distribution of ADCP-derived currents (cm s^{-1}) over the Central Plateau and northern perimeter of Saya de Malha Bank for the: a) Surface layer (18-26 m); and b) Sub-thermocline layer (58-66 m).

exceeded 50 cm s^{-1} in the upper layer and decreased gradually with the depth dropping to velocities of 10-20 cm s^{-1} below 200 m. This current flow velocity profile was also observed in the SN sill which was identified as a place of enhanced tidal currents that trigger internal solitary wave packets propagating onto SDM (Konyaev *et al.*, 1995; da Silva *et al.*, 2011, New *et al.*, 2013; da Silva *et al.*, 2015).

The upstream section (Line B, Fig. 6b) extended from the South Bank (SB) to the Eastern Slope (ES) and the shallow water of the Eastern Rim (ER) region. The zonal flow, initially barotropic to the south of the SB, over the shallow regions (ER) transformed into a two-layer current. The top and bottom currents were separated at the thermocline depth, hence entrained different water masses, TSW and ITF/STSW, respectively (Fig. 3). According to the presented vertical distribution, the two layers differed in the flow direction. Only the TSW layer displayed the westward zonal drift in contrast to the underlying ITF/STSW. Remarkably, the generally westward zonal current reversed abruptly to

eastward above the pinnacle on the northern side of the channel separating the SB from ES, suggesting a topography forced recirculation – the Taylor Column (Cushman-Roisin and Beckers, 2011).

Volume transport

Although applied to sub-optimal data (as the transects were not designed to provide accurate transport estimates), the volume transport was computed from Lines A and B (Fig. 6a) which produced a plausible result. A total volume transport of 3.88 Sv (Sv = 10^6 m^3 s^{-1}) and 3.44 Sv were computed from Lines A and B respectively. The volume transport for both lines substantiates the topographic steering of the SEC along the southern slope of SDM. The volume transport was also calculated from transect 6 (Fig. 7c) for the sub-thermocline layer resulting in 0.3 Sv (northwards) and -0.28 Sv (southwards) which supports the

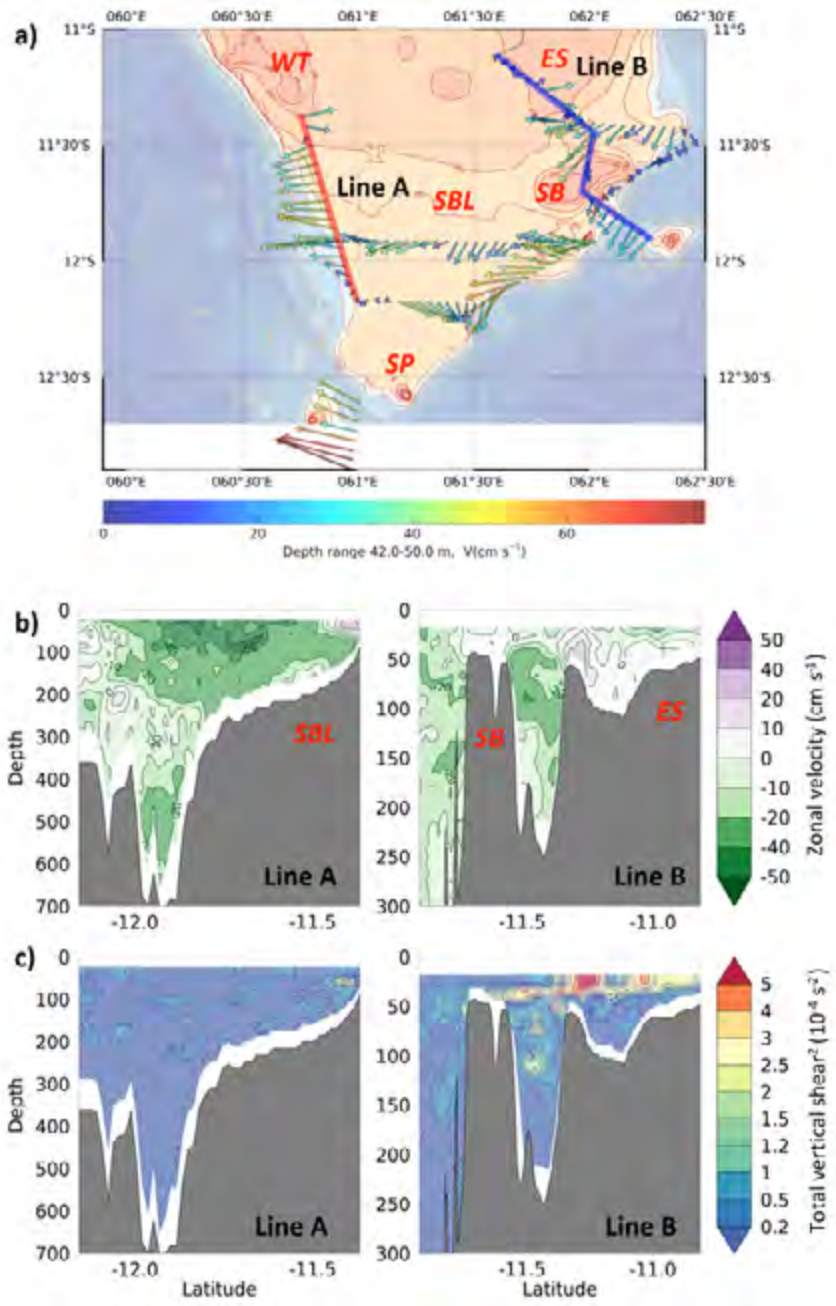

Figure 6. Distributions of ADCP-derived currents over the southern section of the Saya de Malha bank for: a) Horizontal currents (cm s^{-1}) observed in the 42-50 m layer; (b) Vertical distribution of the zonal velocity component (cm s^{-1}) computed from Line A (left) and Line B (right); and c) Total vertical shear squared distribution of horizontal velocity (10^{-4} s^{-2}) computed from Line A (left) and Line B (right).

hypothesis of the recirculation current pattern in the Central Lagoon region. By way of validation, the total SEC transport across the SN sill was computed, the region that was covered immediately after completing the observations over SDM (on 27 May). The result, using the 75 kHz ADCP (depth range 800 m) yielded 20.3 Sv, comparing well to previous studies with 23 Sv obtained from Lowered-ADCP (New *et al.*, 2007) and 14.41 Sv from ADCP 150 kHz (depth range 300 m) (Vianello *et al.*, 2017).

Vertical shear

Figure 6c presents the distribution of the vertical shear squared (Sh^2) of the horizontal velocity observed across Lines A and B. On the downstream of the SEC (Line A), the entire water column displayed a low shear ($< 1 \times 10^{-4}$ s^{-2}), manifesting a vertically rigid flow. On the upstream side (Line B), the vertical rigidity was confined to the deeper part (south of the SB). The Sh^2 increased visibly north of the SB, over the parts of the section characterized by the abrupt and shoaling topography.

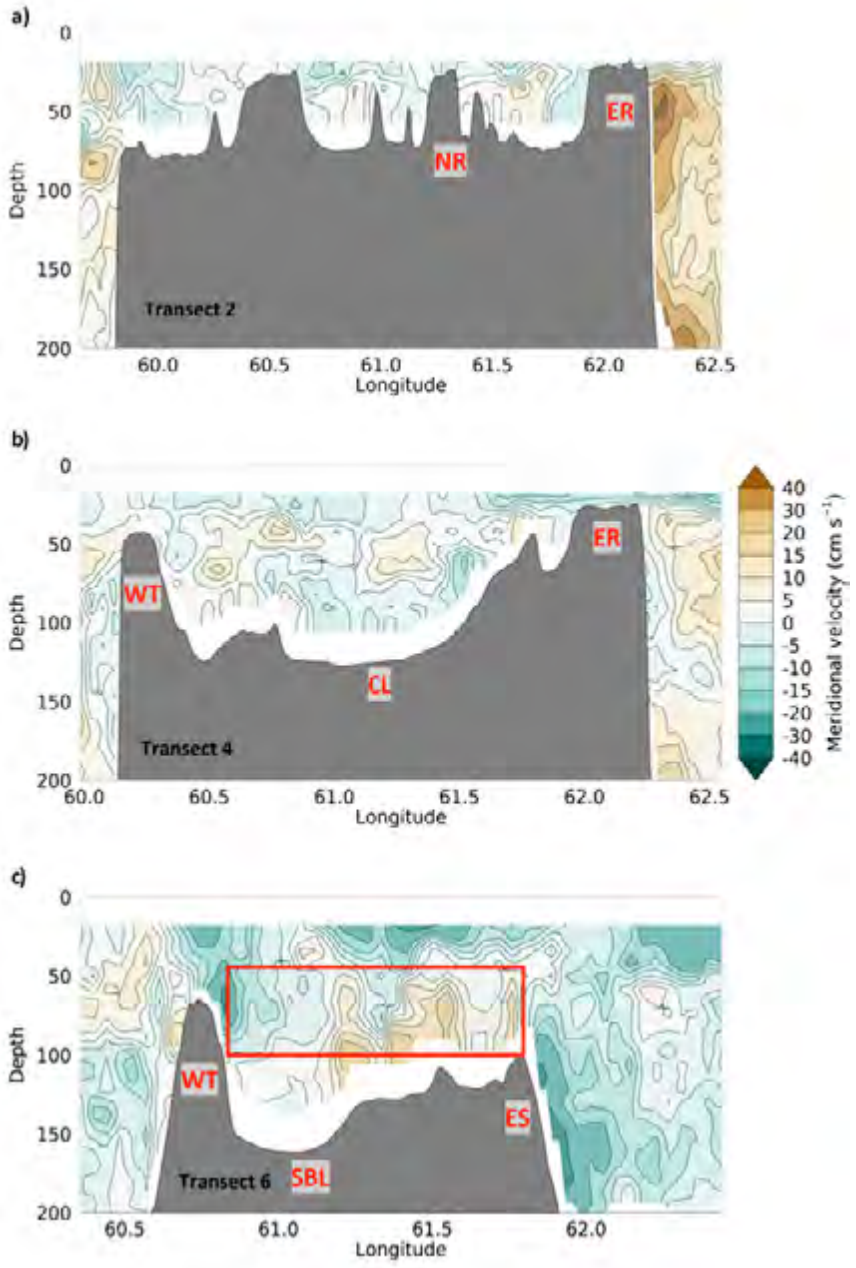

Figure 7. Meridional velocity (cm s^{-1}) component observed along the transect lines characteristic to the bathymetric regions of the Saya de Malha Bank for: a) Transect 2 – Northern Rim (NR); b) Transect 4 – Central Lagoon (CL); and c) Transect 6 – Shelf Break Ledge (SBL; the red box delimits the area used for the computation of volume transport in this region).

Strong shear (> 3 x 10^{-4} s^{-2}) was observed throughout this region, confined to the thermocline depth. However, the vertical shear tended to be more enhanced and expanded vertically over elevated topographic features of the bank. The vertical shear distribution pattern presented here characterized most of the ADCP data collected over slopes and the Central Lagoon (not shown). Strong shear was absent over the shallowest regions (NR and ER), coincident with the absence of stratification and TSW present near-bottom.

Discussion

This paper investigated the effect of the shallow bathymetry of SDM on the large circulation pattern of the SWIO; that is the westward propagating SEC, and consequently the down-scaled current pattern developed over the bank. The results presented in the previous section were congruent with the literature on the wind regime (southeast trade winds) established in the SWIO, leading to a westward propagating current, the SEC, and the topographic steering of the SEC along the slopes of the bank, resulting in the divergence of the SEC, feeding the northern and southern part of SDM. The surface current pattern was found to follow the wind-induced Ekman transport across the bank, flowing in a generally southwestward direction (10-20 cm/s) with increasing intensity in the southern region of the bank (40-50 cm/s). Moreover, the study revealed a two-layer structure of the current over the shallow bank; the top layer characterizing the TSW transport and the sub-thermocline layer appearing to recirculate over the central region of the bank. This two-layered current pattern was further corroborated by the vertical shear and volume transport analyses over the SDM region.

The mountainous-like topography of SDM clearly demonstrates the possibility of Internal Solitary Waves (ISWs) forming due to flow-topography interactions which are common occurrences in oceanography (Xie *et al.,* 2017). ISWs have been found to propagate over the SDM region and appeared to be originating from multiple sources which are generated by semi-diurnal tides, on both the western and southern slopes of the bank (New *et al*., 2013). Lee ISWs have also been observed at the SN sill and are considered as one of the largest known in the world (Konyaev *et al*., 1995; da Silva *et al*., 2011, New *et al*., 2013; da Silva *et al*., 2015). Packets of large ISWs propagating towards both a west-northwest and east-southeast direction from the SN sill near 12.5°S were recorded (da Silva *et al*., 2011). In the light of the findings on the role of tidal current and internal waves in the current dynamics of SDM (New *et al*., 2013; da Silva *et al*., 2015; da Silva *et al*., 2011), the hypothesis of a recirculating current in the sub-thermocline layer over the Central Lagoon may be oversimplified given the ISWs conditions established over the bank region.

A significant proportion of baroclinic tides propagate in a northeast direction (New *et al.*, 2013); thus over the region marked as SBL in this investigation. The activity of these wave packets explains large differences in the depth of the thermocline observed at the CTD stations occupied in this region (Stations 414, 410 and 406, Fig. 3). The prevailing northeast propagation direction implies that the shoaling eastern slope is the place for intense ISW breaking, therefore the location of strong turbulence, nutrient fluxes and, as New *et al.* (2013) pointed out, enhanced biological productivity. Furthermore, as the internal wave breaking induces longshore currents along isobaths (Zikanov and Slinn, 2001), the recirculation observed in Figure 5b is probably a manifestation of such currents.

The SEC is known to form a sharp boundary between the subtropical water masses from further north (nutrient-rich waters) and south (nutrient-poor waters) of the bank (New *et al*., 2007; Vortsepneva, 2008). The T/S profiles presented in New *et al.* (2007) showed little variations across the east-west profiles as compared to the north-south profiles. This could indicate that the topography along with the current dynamics enhance the mixing of water masses over the shallow bank (Pous *et al*., 2014). Additionally, this paper showed that the interaction of water masses with the bank differs strikingly. The TSW flows with the westward-flowing current (SEC) while the underlying STSW moves in a northward direction from the South Point and further interacts with the topography of the bank, establishing local oceanographic conditions. The pycnocline fluctuated strongly between Stations 414 to 406, manifesting the amplified ISW activity near the shelf-break as New *et al.* (2013) predicted. Underlying the pycnocline, water masses identified as ITW and STSW were present (New *et al.,* 2007; Vianello *et al.*, 2017). In the region of the topographically steered SEC flow, along the southern slope, the distributions of all three seawater properties were identical to those characterizing the SEC region upstream of the plateau (e.g. New *et al.*, 2007, in their Fig. 11 to 13]. The current dynamics such as the formation and propagation of ISWs over the shallow bank therefore plays a significant role in the distribution and mixing of water masses.

In the collected datasets, semi-diurnal tidal signal and minute-scale fluctuations from ISW motions were detected in both the ADCP and CTD analyses. For example, it was not unusual to observe a rise or fall of the thermocline by 40 m at the time of a CTD cast. However, to account for these tidally induced motions was beyond the scope of the observational programme adopted for this research survey. Further in-depth studies are therefore required to assess the role of the current dynamics developing over the shallow bank region.

Conclusion

This study provided a first synoptic outline of the current pattern developed over the shallow SDM resulting from the interaction of the SEC with the topography of the bank. The main observations derived from the ADCP and CTD datasets collected during the survey over the SDM are: (1) the vertically rigid flow over the southern slopes exposed to the SEC throughflow contrasting with the two-layered flow structure over the inner bank; (2) the top layer carrying the water mass, TSW, driven by the Ekman dynamics; as opposed to the (3) sub-thermocline currents, most likely controlled by the tidal and internal wave dynamics.

Acknowledgements

The underlying work was made possible with the support of the EAF-Nansen Programme "Supporting the Application of the Ecosystem Approach to Fisheries Management considering Climate Change and Pollution Impacts" executed by Food and Agriculture Organization of the United Nations (FAO) and funded by the Norwegian Agency for Development Cooperation (Norad). The authors are thankful to the FAO for funding and supporting the Indian Ocean research expedition 2018 (NORAD-FAO PROJECT GCP/INT/730/NOR) on the Saya de Malha Bank on board the R/V Dr Fridtjof Nansen. The authors are grateful to the Department for Continental Shelf, Maritime Zones Administration & Exploration (Prime Minister's Office, Republic of Mauritius) for coordinating and co-leading the expedition and for their continuous support towards the publication of this research study, and the Mauritius-Seychelles Joint Commission of the Extended Continental Shelf for their support and assistance and granting the necessary authorisations. Ms J Ramma is gratefully acknowledged for her contribution in collecting and conducting pre-analysis work of the physical oceanography data during the expedition. The authors are thankful to the participants of the expedition and the crew members for their work and contribution during the 2018 expedition cruise.

References

Bergstad OK, Bissessur D, Sauba K, Rama J, Coopen P, Oozeeraully Y, Seeboruth S, Audit- Manna A, Nicolas A, Reetoo N, Tabachnick K, Kuyper D, Gendron G, Hollanda S, Melanie R, Souffre A, Harlay J, Bhagooli R, Soondur M, Ramah S, Caussy L, Ensrud TM, Olsen M, Høines ÅS (2020) Regional resources and ecosystem survey in the Indian Ocean, Leg 2.1. Characterizing ecosystems and morphology of the Saya de Malha Bank and Nazareth Bank, 3 May - 4 June 2018. NORAD-FAO Programme GCP/GLO/690/NOR, Cruise reports Dr Fridtjof Nansen, EAF-Nansen/CR/2018/6.

Bergstad OK, Tabachnick K, Rybakova E, Gendron G, Souffre A, Bhagooli R, Ramah S, Olsen M, Høines SA, Dautova T (2021) Macro- and megafauna on the slopes of the Saya de Malha Bank of the Mascarene Plateau. Western Indian Ocean Journal of Marine Science, Special Issue 2/2021: 129-158

Cancet M, Griffin D, Cahill M, Chapron B, Johannessen J, Donlon C (2019) Evaluation of GlobCurrent surface ocean current products: A case study in Australia. Remote Sensing of Environment 220: 71-93 [doi:https://doi.org/10.1016/j.rse.2018.10.029]

Commission on the Limits of the Continental Shelf (CLCS) (2011) Summary of the recommendations of the commission on the limits of the continental shelf in regard to the joint submission made by Mauritius and Seychelles concerning the Mascarene Plateau region on 1 December 2008, CLCS/70 (11 May 2011). United Nations. 19 pp

Cushman-Roisin B, Beckers JM (2011) Introduction to geophysical fluid dynamics: physical and numerical aspects. Academic press. 875 pp

da Silva JCB, New AL, Magalhaes JM (2011) On the structure and propagation of internal solitary waves generated at the Mascarene Plateau in the Indian Ocean. Deep Sea Research, Part I: Oceanographic Research Papers 58 (3): 229-240 [doi:https://doi.org/10.1016/j.dsr.2010.12.003]

da Silva JCB, Buijsman MC, Magalhaes JM (2015) Internal waves on the upstream side of a large sill of the Mascarene Ridge: a comprehensive view of their generation mechanisms and evolution. Deep Sea Research Part I, 99: 87-104 [doi: 10.1016/j.dsr.2015.01.002]

Fischer J, Brandt P, Dengler M, Müller M, Symonds D (2003) Surveying the upper ocean with the ocean surveyor: a new phased array doppler current profiler. Journal of Atmospheric and Oceanic Technology 20: 742-751

Genin A (2004) Bio-physical coupling in the formation of zooplankton and fish aggregations over abrupt

topographies. Journal of Marine Systems 50 (1-2): 3-20 [doi:10.1016/j.jmarsys.2003.10.008]

Kara VI, Sivukha NM (1990) Marine geology: Geomorphology and recent development of the Central Mascarene Ridge. Oceanology 30 (2): 303-308

Konyaev KV, Sabinin KD, Serebryany AN (1995) Large-amplitude internal waves at the Mascarene Ridge in the Indian Ocean. Deep Sea Research, Part I: Oceanographic Research Papers 42 (11-12): 2075-2091

Langdon C, (2010) Determination of dissolved oxygen in seaweater by Winkler titration using amperometric technique. In: Hood EM, Sabine CL, Sloyan BM (eds) The GO-SHIP repeat hydrography manual: A collection of expert reports and guidelines, Version 1. 18 pp [doi: https://doi.org/10.25607/OBP-1350]

Lindhorst S, Appoo J, Artshwager M, Bialik O, Birkicht M, Bissessur D, Braga J, Budke L, Bunzel D, Coopen P, Eberhardt B, Eggers, D Eisermann JO, El Gareb F, Emeis K, Geßner A-L, Hüge F, Knaack-Völker H, Kornrumpf N, Lenz N, Lüdmann T, Metzke M, Naderipour C, Neziraj G, Reijmer J, Reolid J, Reule N, Rixen T, Saitz Y, Schäfer W, Schutter I, Siddiqui C, Sorry A, Taphorn B, Vosen S, Wasilewski T, Welsch A (2019) SONNE-Berichte, Saya de Malha Carbonates, Oceanography and Biogeochemistry (Western Indian Ocean). Cruise No. SO270, MASCARA (BMBF grant 03G0270A). 102 pp [https://doi.org/10.2312/cr_so270]

New AL, Stansfield K, Smythe-Wright D, Smeed DA, Evans AJ, Alderson SG (2005) Physical and biochemical aspects of the flow across the Mascarene Plateau in the Indian Ocean. Philosophical Transactions of the Royal Society A 363: 151-168 [doi: 10.1098/rsta.2004.1484]

New AL, Alderson S, Smeed D, Stansfield K (2007) On the circulation of water masses across the Mascarene Plateau in the South Indian Ocean. Deep Sea Research, Part I 54 (1): 42-74 [doi: 10.1016/j.dsr.2006.08.016]

New AL, Magalhaes JM, da Silva JCB (2013) Internal solitary waves on the Saya de Malha bank of the Mascarene Plateau: SAR observations and interpretation. Deep Sea Research, Part I 79: 50-61 [doi: 10.1016/j.dsr.2013.05.008]

Ostrowski M, da Silva JCB, Bazik-Sangolay B (2009) The response of sound scatterers to El Nino- and La Nina-like oceanographic regimes in the southeastern Atlantic. ICES Journal of Marine Science 66 (6): 1063-1072 [doi:https://doi.org/10.1093/icesjms/fsp102]

Payet R (2005) Research, assessment and management on the Mascarene Plateau: a large marine ecosystem perspective. Philosophical Transactions of the Royal Society A: Mathematical, Physical and Engineering Sciences 363 (1826): 295-307 [doi:10.1098/rsta.2004.1494]

Pous, S, Lazure P, Andre G, Dumas F, Halo I, Penven P (2014) Circulation around La Reunion and Mauritius islands in the south-western Indian Ocean: A modeling perspective. Journal of Geophysical Research: Oceans 119: 1957-1976 [doi:10.1002/2013JC009704]

Ramah S, Gendron G, Bhagooli R, Soondur M, Souffre A, Melanie R, Coopen P, Caussy L, Bissessur D, Bergstad OK (2022) Diversity and distribution of the shallow water (23 – 50 m) benthic habitats in the Saya de Malha Bank, Mascarene Plateau. Western Indian Ocean Journal of Marine Science, Special Issue 2/2021: 69-80

Schott FA, McCreary JP (2001) The monsoon circulation of the Indian Ocean. Progress in Oceanography 51 (1): 1-123 [doi: 10.1016/S0079-6611(01)00083-0]

Schott FA, Xie SP, McCreary JP (2009) Indian Ocean circulation and climate variability. Reviews of Geophysics 47 (1). 46 pp

Stømme T, Bjordal Å, Ansorge I, Balarin E, Ostrowski M, Francourt H, Bornman T, Plos A, Gibbons M, Cedras R, Bernard K, Kaehler S, Hill J, du Plessis S, Scott L, Tweddle D, Palmer R, Govinden R, Lucas V, Etienne M, McPhaden M, Kunze S, O'Donaghue K, Alvheim O, Zaera D, Mørk T, Sverre Fossheim O (2009) 2008 ASCLME Survey No 3, Cruise report No 7/2008, 8 October – 27 November 2008. Report No. EAF-N2008/7. Institute of Marine Research Bergen, Norway. 96 pp

Vianello P, Ansorge IJ, Rouault M, Ostrowski M (2017) Transport and transformation of surface water masses across the Mascarene Plateau during the Northeast Monsoon season. African Journal of Marine Science 39 (4): 453-466 [doi: 10.2989/1814232X.2017.1400999]

Vortsepneva E (2008) Saya de Malha Bank – an invisible island in the Indian Ocean. Geomorphology, oceanology, biology. Lighthouse Foundation. 44 pp

Xie X, Li M, Scully M, Boicourt WC (2017) Generation of internal solitary waves by lateral circulation in a stratified estuary. Journal of Physical Oceanography 47 (7):1789-1797

Zeng Z, Brandt P, Lamb KG, Greatbatch RJ, Dengler M, Claus M, Chen X (2021) Three-dimensional numerical simulations of internal tides in the Angolan upwelling region. Journal of Geophysical Research: Oceans 126 (2): p.e 2020JC016460

Zikanov O, Slinn D (2001) Along-slope current generation by obliquely incident internal waves. Journal of Fluid Mechanics 445: 235-261 [doi:10.1017/S0022112001005560]

Inorganic nutrient distribution at Saya de Malha and the eastern slope of the Nazareth Banks

Anishta Audit-Manna*, Reeya K. Oogarah, Yashvin Neehaul

Mauritius Oceanography Institute, Avenue des Anchois, Morcellement de Chazal, Albion 91005, Mauritius

* Corresponding author: aauditmanna@moi.intnet.mu

Abstract

The distribution of nutrients in the Mascarene Plateau is poorly studied due to limited data collected in the region. This study investigated the distribution of nutrients in the water column of the Saya de Malha and eastern slope of the Nazareth Banks. Water samples were collected at the Saya de Malha and eastern slope of Nazareth Banks during the scientific expedition on board the R/V Fridtjof Nansen in May 2018 and the vertical profiles of physical parameters were used to identify the different water masses. Phosphate, nitrate and silicate showed typical nutrient profiles along with the nutriclines. The dissolved oxygen and chlorophyll-*a* showed a correlation with nutrients. Most of the sampling stations on the Saya de Malha and Nazareth Banks showed high oxygen saturation above 92 % in the upper 75 m. Low chlorophyll-*a* values were recorded at both banks indicating an oligotrophic system. The nutrient results also reveal an increase in the concentration towards the northern part of the region due to the South Equatorial Current crossing the plateau.

Keywords: nutrients, Saya de Malha Bank, Nazareth Bank, South Equatorial Current, Western Indian Ocean, primary productivity

Introduction

The physical oceanography of the Southern Indian Ocean (SIO) remains poorly studied compared to the northern parts of the Indian Ocean or other ocean basins such as the South Atlantic (New *et al.,* 2005). This is due to limited research surveys carried out in the SIO region, resulting in less hydrographic data being available (Badal *et al.,* 2009; Stramma and Lutjeharms, 1997). The research surveys conducted have mainly been based on the currents, water masses or chlorophyll concentrations. Following the hydrographic survey of the RSS Charles Darwin in 2002, the presence of large-scale flow patterns and water masses which may affect part of the SIO was studied (New *et al.,* 2005). Little is known on the impact of flow on seasonal physical parameters such as temperature and chlorophyll concentrations (Badal *et al.,* 2009). A study on the dynamics of the flows in the region of the Mascarene Plateau has been conducted by Schott and McCreary (2001) who observed the occurrence of an Ekman divergence due to the north-east monsoon, previously described by Ragoonaden *et al*. (1987), as a divergence zone in the western part of the Plateau.

The subtropical Indian Ocean gyre is dominant in the region (Stramma and Lutjeharms, 1997). The South Equatorial Current (SEC) passes directly through the Mascarene Plateau near 60° E where the current continues and splits into two cores, i.e. the northern and southern core, towards the eastern coast of Madagascar (New *et al.,* 2007). The northern core passes across the Plateau through the channel between the Saya de Malha and Nazareth Banks which may be a significant obstacle to the flow below 200 m depth (New *et al.,* 2007) while the southern core passes through the south of Cargados-Carajdos Bank and north of Mauritius (Bhagooli and Kaullysing, 2019). However, there is sparse information on how the SEC crosses the Plateau or the impact of the flow on the biochemistry of the region (New *et al.,* 2007).

The biogeochemical cycles in the ocean are mainly controlled by biological processes in which nutrients play a major role as indicators for primary productivity. The Indian Ocean accounts for 15 – 20 % of the net primary productivity of the total ocean (Garcia *et al.,* 2018). The Southern Ocean usually receives

http://dx.doi.org/10.4314/wiojms.si2021.2.2

nutrients from the Antarctic Circumpolar Current where high concentrations of phosphate, nitrate and silicate can be found in the surface layer of the polar water; south of the subtropical convergence (Panassa *et al.,* 2018). However, since their primary production could be controlled by the availability of light and trace metals like iron (Fe), these waters show a small vertical gradient in nutrient concentrations (Garcia *et al.,* 2018; Panassa *et al.,* 2018; Grand *et al.,* 2015). The surface waters in most parts of the Indian Ocean are oligotrophic (Jena *et al.,* 2013; Schlüter *et al.,* 2011) due to the presence of a strong upper thermocline which prevents the supply of nutrients from the subsurface to the euphotic zone (Garcia *et al.,* 2018*;* Resplandy *et al.,* 2009; Gupta and Desa, 2001).

Limited studies on the nutrient distribution have been carried out in the southern Indian Ocean, most specifically on the Mascarene Plateau. The Plateau is considered to be the largest fishing bank (Munbodh, 2014) and major source of frozen fish for the Mauritian market, representing around 30 % of total fish consumption, where most fish are caught at a depth of 0 –100 m at Saya de Malha and Nazareth Banks (Bhagooli and Kaullysing, 2019; Degambur and Sólmundsson, 2005; Ardill, 1986). Thus, studies on the nutrient distribution in the water column on the Mascarene Plateau are of great importance.

The present study aimed at determining the distribution of nutrients across the Saya de Malha and Nazareth Banks. It was also attempted to correlate nutrient distribution with dissolved oxygen and chlorophyll-*a* (chl-*a*) at the Saya de Malha and eastern part of the Nazareth Banks.

Materials and methods

Study site

Data for this study were collected in May 2018 during an expedition on board the R/V Fridtjof Nansen (2018 EAF-Nansen programme) in the region of Saya de Malha and the eastern slope of the Nazareth Banks located in the SIO. The study area covers the region of Saya de Malha from 09°S to 12°S and 59°E to 62°E and the eastern slope of Nazareth Bank from 13°S to 15°S and 60°E to 61°E (Fig. 1). The Mascarene Plateau is a submarine plateau located in the Western Indian Ocean around 2300 km south of the equator (Fisher *et al.,* 1967; Payet, 2005); lying between Seychelles (4°S, 56°E) and Mauritius (20°S, 57°E). The Mascarene Plateau consists of chain of shallow banks (also known as shoals) that form a crescent-like feature from north to south, separated by deeper channels (Payet, 2005). The Saya de Malha Bank (North and South banks), located between 8°30'S - 12°0'S and 59°30'E - 62°30'E (Vortsepneva, 2008), is the largest fishing bank in the plateau with an area of 40,000 km² (Betzler *et al.,* 2021). The seabed is jointly managed by the Republic of Mauritius and the Republic of Seychelles by a Commission established under the United Nations Convention on the Law of the Sea. The southern bank is the focus of this study.

The Nazareth Bank is part of the Exclusive Economic Zone of 2.3 million km² (excluding the Saya de Malha bank) of the Republic of Mauritius and is situated south of the Saya de Malha Bank separated by a 100 km channel with a depth of around 1100 m (New *et al.,* 2007).

in situ measurement and sample collection

The vertical profiles of temperature, salinity and conductivity were obtained by a Seabird SBE 9 CTD probe. Twelve 10L-Niskin bottles attached to the CTD rosette were used to collect water at predefined depths along the hydrographical transects. The standard sampling depths were set at: 2000, 1700, 1500, 1200, 1000, 750, 500, 400, 300, 200, 100, 75, 50, 25 and 5 m (Table 1).

In total, 145 seawater samples at 27 CTD stations in Saya de Malha Bank and 21 seawater samples at 7 CTD stations in Nazareth Bank were collected in duplicates from the Niskin bottles for the measurement of nutrients. Once seawater samples were collected from the Niskin bottles, they were filtered through a nylon membrane syringe filter of pore size 0.2 µm in a PE tube (30 mL) and immediately stored at -20 °C during the cruise pending measurements.

The CTD was also equipped with sensors measuring chl-*a* (Chelsea Aquatracka III) and dissolved oxygen (SBE 43) in the water column.

Nutrient analyses

Nutrient analysis of seawater samples was carried out in the laboratory at the Mauritius Oceanography Institute. The concentration of nutrients (phosphate, PO_4^{3-}; nitrate, NO_3^-; nitrite, NO_2^-; ammonia, NH_4^+ and silicate, SiO_4^{4-}) in the water column was determined using standard colorimetric analysis (Grasshoff *et al.,* 2009) on an automated nutrient analyser equipped with a 5 cm absorbance reading unit (SYSTEA Easychem Plus) following recommended protocols supplied by the equipment manufacturer. Deionised water and filtered

seawater (low nutrient) were used for sample preparation and analyses. For reproducibility of nutrient measurements between analyses, in-house standards were used which were regularly compared with certified reference materials for nutrients in seawater.

Phosphate determination is based on the molybdenum blue method described by Murphy and Riley (1962). In acidic medium, phosphate present in the form a coloured azo dye complex; measured at 543nm (Strickland and Parsons 1968). The determination of ammonia employs an indophenol-blue reaction between ammonia, phenol and hypochlorite in an alkaline medium described by Grasshoff *et al.* (1972). The indophenol colorimetric reaction is modified by the introduction of the catalyst nitroprusside which accentuates the blue colour at room temperature where the absorbance is measured at 630 nm.

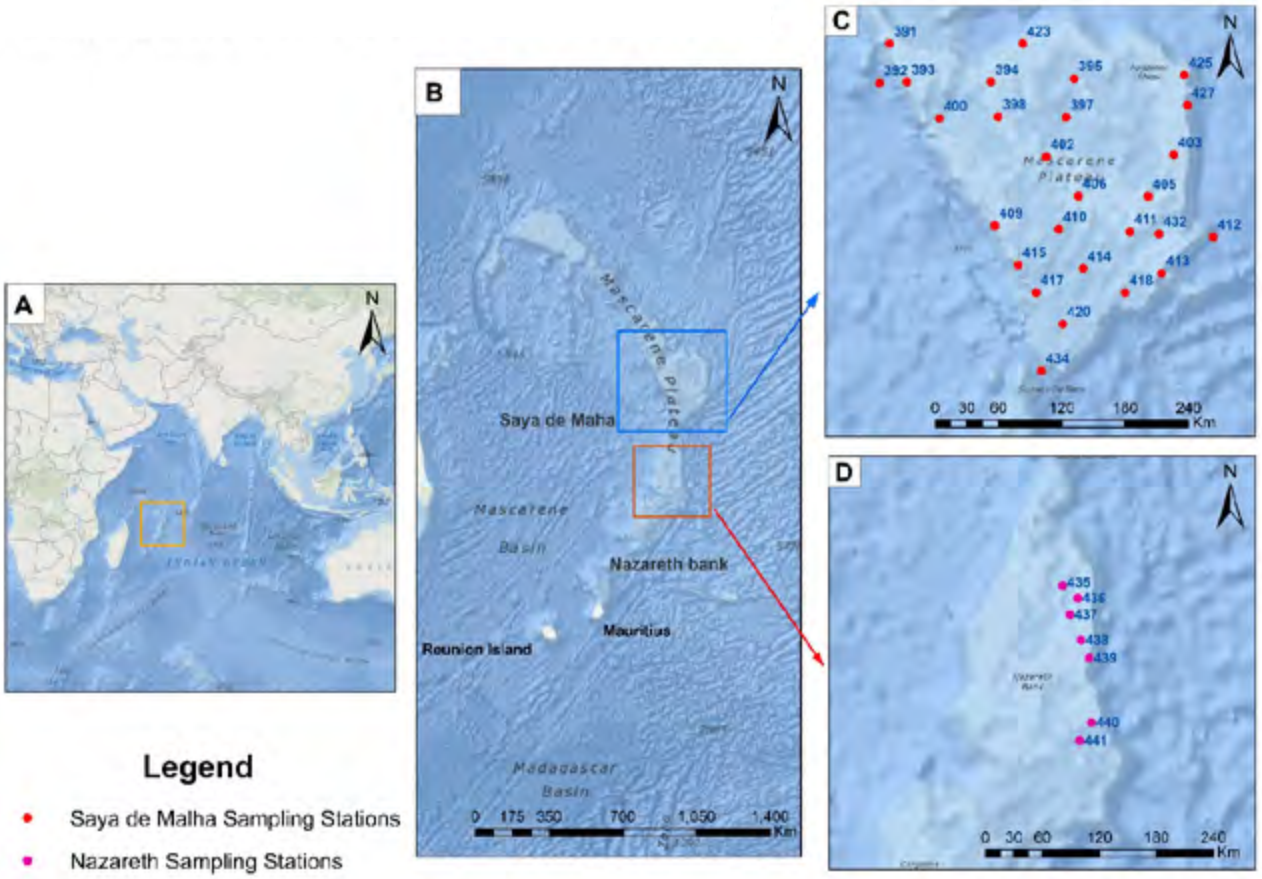

Figure 1. A: Map of the Indian Ocean showing location of the study; B: Study sites at Saya de Malha and Nazareth Banks; C: Sampling sites at Saya de Malha Bank; D: Sampling sites at Nazareth Bank.

samples reacts with ammonium molybdate and potassium antimony tartrate to form an antimony-phospho-molybdate complex which is further reduced to an intensely coloured molybdenum blue complex by ascorbic acid where it is measured at 880 nm.

Nitrate is determined by the reduction of nitrate to nitrite with a cadmium reduction column incorporated in the automated nutrient analyser. Nitrite reacts with sulfanilamide under acidic conditions to form a diazonium compound which in turn couples with N-(1-Naphthyl)-ethylenediamine dihydrochloride to

Silicate is determined by the reduction of silicate-molybdate by ascorbic acid in acidic medium based on the method described by Koroleff (1972). Oxalic acid is added before addition of ascorbic acid to prevent interference of phosphate in the samples.

Ammonia and nitrite concentrations were below detection limit. The relative error of duplicate sample measurements was on average below 2 % and the detection limit was < 0.2 µm for NH_4^+, < 0.1 µm for NO_2^-, < 0.05 µm for PO_4^{3-}, < 0.08 µm for NO_3^-, and < 0.07 µm for SiO_4^{4-}.

Table 1. Predefined depths down the water column at different bottom-depth stations on board the RV Fridtjof Nansen.

Stations	Defined depth for water sampling from sea surface
Shallow (bottom-depth < 30 m)	*5*, *25*
Intermediate (bottom-depth < 100 m)	100, *75*, *50*, *25*, *5*
Deep stations (bottom-depth < 500 m)	*500*, 400, 300, 200, 100, *75*, *50*, *25*, *5*
Extra deep (bottom-depth > 1000 m)	1000, *750*,*500*, 400, 300, 200, 100, *75*, *50*, *25*, *5*

Calculations, graphical plots and statistical analysis

Oxygen gas solubility was calculated as a function of *in situ* temperature, salinity and one atmospheric of total pressure using the equation of Garcia and Gordon (1992) and oxygen solubility coefficient values of Benson and Krause (1984). The oxygen saturation was calculated as percentage by dividing the concentration of oxygen in the samples by the oxygen solubility. Depth profiles were been built up for temperature, salinity, dissolved oxygen, nutrients and chl-*a* by calculating the average mean at each standard depth: *5*, *25*, *50*, *75*, 100, 200, 300, 400, *500*, *750*, 1000, 1500, 2000 m. The statistical analysis was carried out using GraphPad Prism version 8.4.3 software (San Diego, California, USA). For statistical analysis, the data was first tested for normality where non-normally distributed data were converted. The one-way ANOVA was used to determine any significant differences between the stations at Saya de Malha and Nazareth Banks, respectively, and two-way ANOVA was used to determine any significant differences with depth for

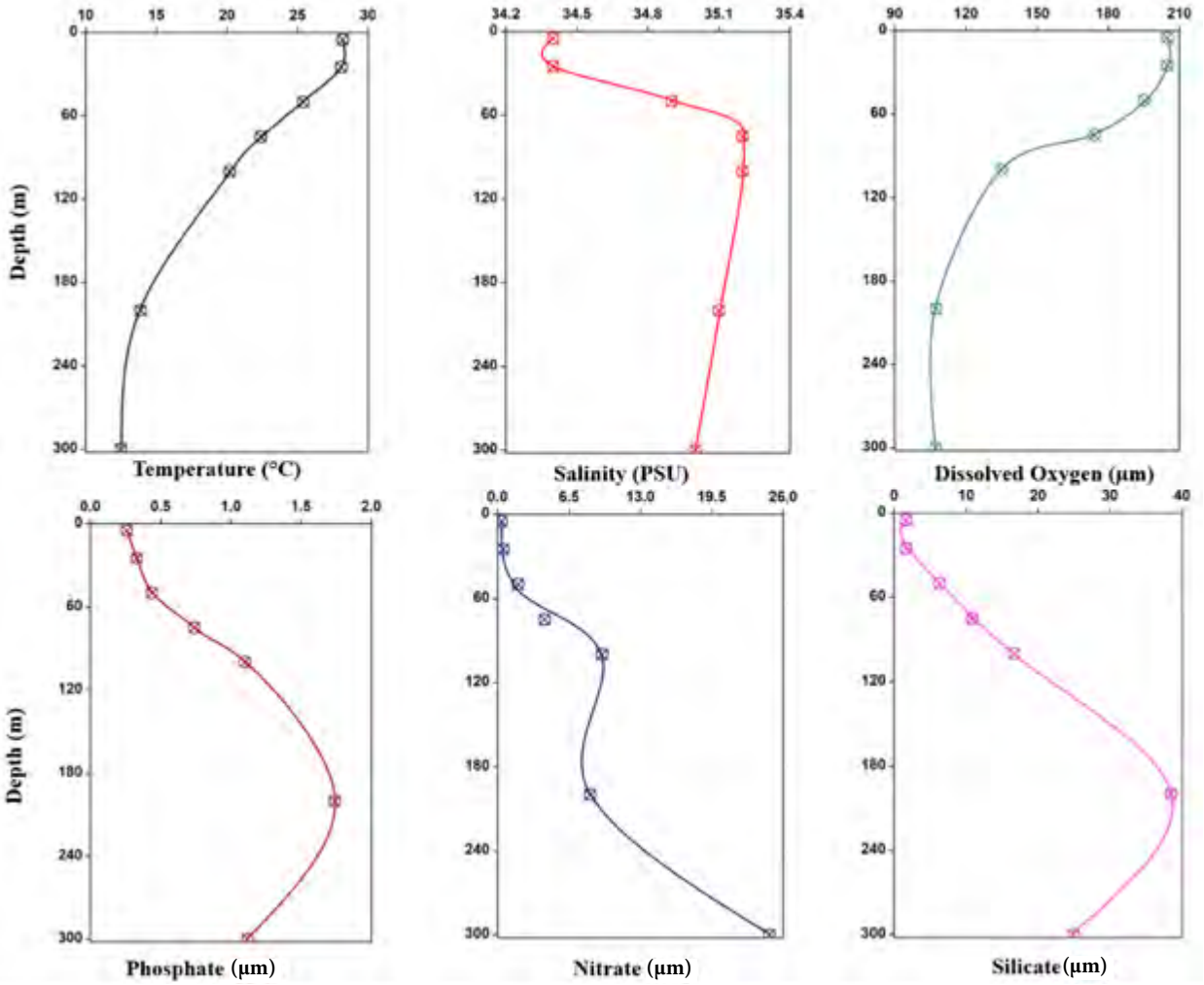

Figure 2. Vertical profiles at the Saya de Malha Bank illustrating the changes with depth of common parameters temperature, salinity, dissolved oxygen, phosphate, nitrate and silicate.

nutrients. Pearson's correlation coefficient was used to determine the correlation between the nutrients with dissolved oxygen and chl-*a*.

Results

The distribution of nutrients is usually affected by the physical dynamics of the ocean. The physical characteristics of the study regions were briefly studied in order to further understand the distribution of nutrients at the Saya de Malha and Nazareth Banks.

Concentration depth profile

Figures 2, 3 and 4 show the depth profiles of temperature, salinity, dissolved oxygen, phosphate, nitrate and silicate on the Saya de Malha and eastern slope of the Nazareth Banks. The bottom depths on the Saya de Malha plateau varied from 26 (CTD 403) to 380 m (CTD 432) at 24 sampling stations, and for the three sampling stations (CTD 392, 412 and 434) in deeper waters around the plateau, the bottom depths varied from 1068 to 2347 m. At the Nazareth Bank, the bottom depths ranged from 31 (CTD 437) to 242 m (CTD 441). The sampling depths at Saya de Malha ranged from 5 to 300 m, and for the deeper stations ranged from 5 to 2000 m, and 5 to 100 m for the Nazareth Bank.

On the Saya de Malha plateau, a surface temperature of 28 °C was observed in the upper 50 m which decreased down the water column to 12.5°C. The upper 25 m displayed a minimum salinity with values of 34.2 to 34.5 PSU which gradually increased to 35.0 PSU. The water column showed a stable stratification where the pycnocline occurred at around 30 to 50 m. The concentration of dissolved oxygen decreased gradually with increasing depth from 205 to 107.2 µm. Phosphate [PO_4^{2-}], nitrate [NO_3^-] and silicate [SiO_4^{4-}] showed the typical nutrient depth profile, with low concentrations on the surface which increases with depth. [PO_4^{2-}], [NO_3^-] and [SiO_4^{4-}] ranged from 0.26 to 1.12 µm, 0.14 to 24.74 µm and 1.56 to 29.94 µm

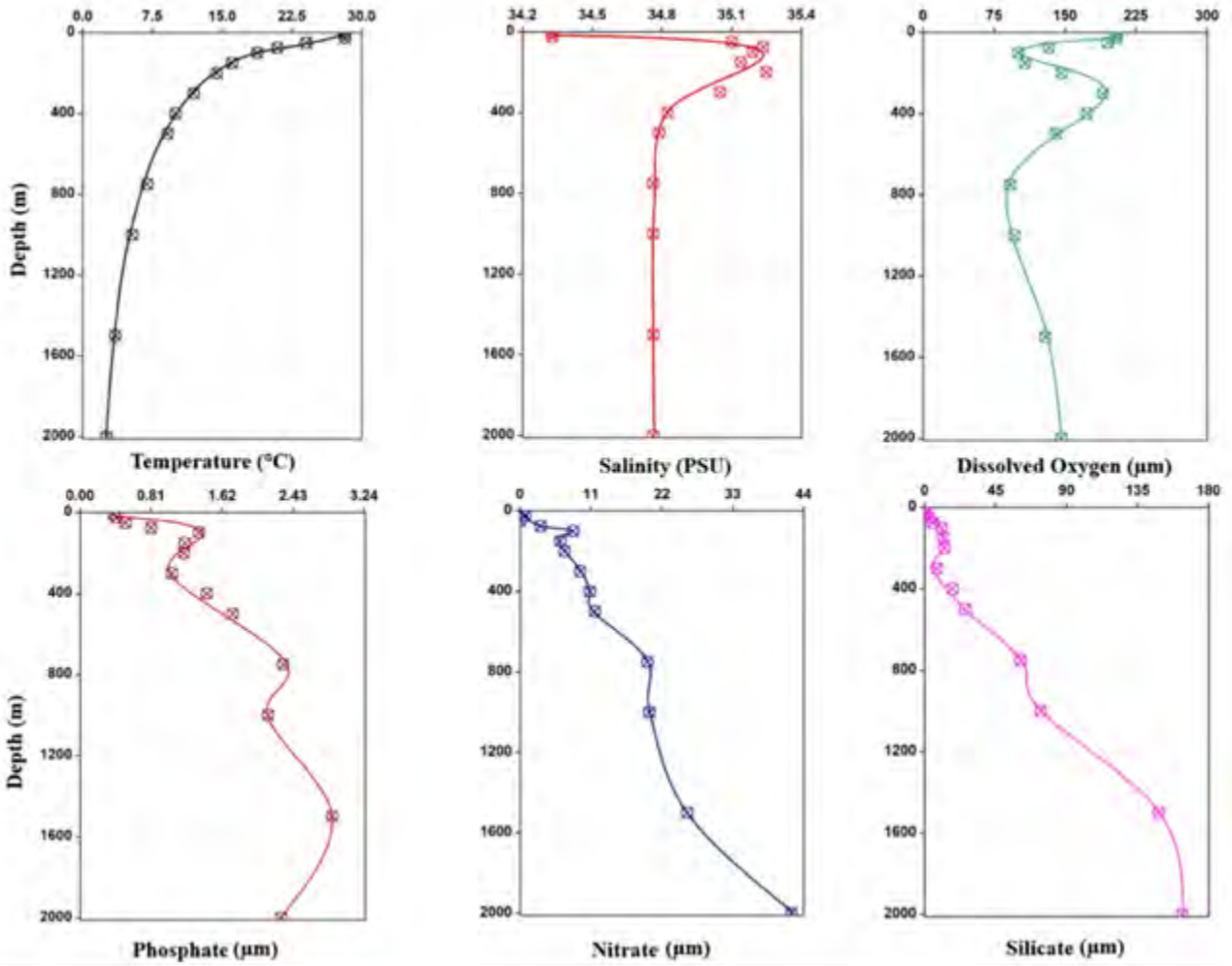

Figure 3. Vertical profiles in the deeper waters around the Saya de Malha plateau illustrating the changes with depth of temperature, salinity, dissolved oxygen, phosphate, nitrate and silicate.

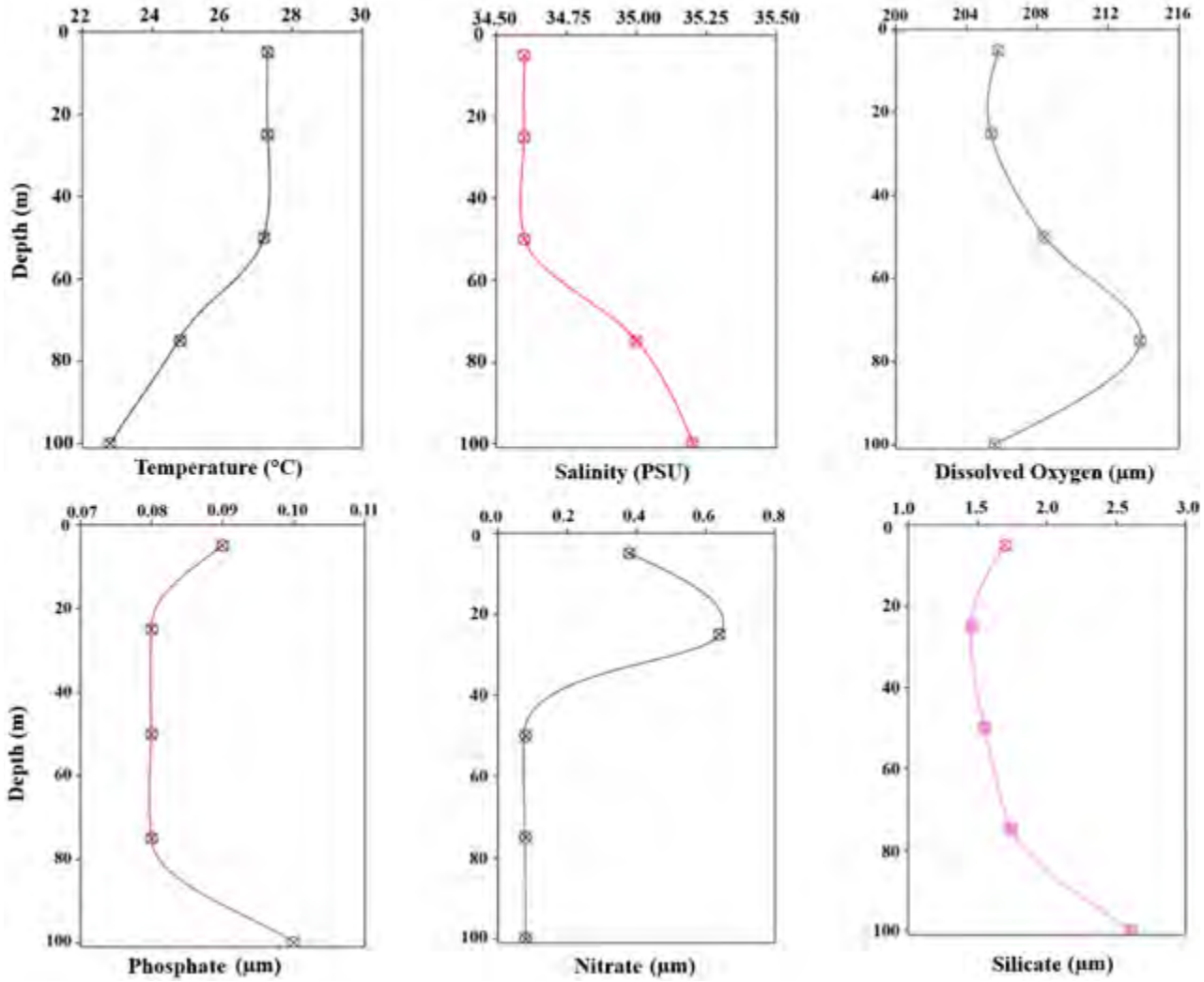

Figure 4. Vertical profiles at the eastern slope of Nazareth Bank illustrating the changes with depth of temperature, salinity, dissolved oxygen, phosphate, nitrate and silicate.

respectively. In general, the concentration of chl-*a* showed a decrease down the water column, ranging from 0.27 to 0.02 µg/l. However, an increase in chl-*a* (0.27 µg/l) was recorded at 50 m.

At the deeper stations, the surface temperature of 28 °C in the upper 50 m was also recorded depicting the presence of warm surface water, decreasing gradually to 2.6 °C. Salinity varied from 34.3 to 34.8 PSU, with an increase to 35.2 between 75 to 100 m. The pyncnocline at the deeper stations was observed between 50 to 150 m. The dissolved oxygen varied from 205.2 to 146.1 decreasing down the water column, but increased from 150 to 300 m, ranging from 107.9 to 190.3 µm. The oxygen minimum layer was found between 100 to 150 m. Similar to the plateau, the nutrients and chl-*a* follow the same pattern, i.e., increasing in with depth. Moreover, an increase of chl-*a* (0.4 µg/l) was also observed at 50 m. In comparison to the plateau, higher concentrations of nutrients and lower concentration of chl-*a* were observed in the deeper waters where the concentration of [PO_4^{2-}], [NO_3^-], [SiO_4^{4-}] and [chl-*a*] ranged from 0.4 to 2.3 µm, 0.4 to 42.1 µm, 0.6 to 163.6 µm, 0.6 to 0.2 µg/l, respectively.

On the eastern slope of Nazareth a small variation in temperature and salinity was found, gradually decreasing from 27.3 to 22.8°C and increasing from 34.6 to 35.2 PSU, respectively. The pycnocline was also observed at 50 m. The oxygen concentration was almost homogenous at different depths in the water column, ranging from 205.8 to 213.8 µm. The concentration of [PO_4^{2-}] was below the detection limit. [NO_3^-] and [SiO_4^{4-}] ranged from 0.2 to < 0.08 and 1.7 to 2.61 µm. The chl-*a* concentration varied from 0.05 to 0.17 µg/l down the depth, with an increase of 0.23 µg/l at 75 m. Overall, the eastern slope of Nazareth Bank exhibited lower concentrations compared to

Table 2A. Ranges of temperature, salinity, dissolved oxygen (DO), density, phosphate, nitrate, silicate and chlorophyll-*a* concentrations in the shallow water column of the Saya de Malha plateau.

Depth (m)	Temperature (°C)	Salinity (PSU)	DO (µm)	Density (kg/m³)	Phosphate (µm)	Nitrate (µm)	Silicate (µm)	Chl-a (µg/l)
5	28.0 - 28.5	34.2 - 34.5	201.5 - 208.0	21.7 - 22.0	0.1 - 0.7	0.1 - 0.4	0.1 - 2.9	0.0 - 0.1
25	28.0 - 28.5	34.2 - 34.5	201.0 - 207.3	21.7 - 22.0	0.1 - 0.8	0.1 - 1.6	0.1 - 3.4	0.0 - 0.2
50	22.7 - 28.1	34.2 - 35.2	172.5 - 223.6	21.8 - 24.2	0.1 - 1.3	0.1 - 7.4	0.1 - 7.5	0.0 - 0.5
75	20.7 - 23.7	35.1 - 35.3	131.5 - 212.5	23.8 - 24.7	0.1 - 1.5	0.1 - 7.4	1.6 - 13.1	0.2 - 0.3
100	18.4 - 21.7	35.1 - 35.4	104.6 - 176.3	24.4 - 25.4	0.3 - 2.4	0.1 - 16.4	2.3 - 18.9	0.1 - 0.2
200	13.9	35.1	107.4	26.3	1.7	8.4	38.5	0.03
300	12.5	35.0	107.2	26.5	1.1	24.7	24.9	0.02

Table 2B. Ranges of temperature, salinity, dissolved oxygen (DO), density, phosphate, nitrate, silicate and chlorophyll-*a* concentrations in the deeper water column around Saya de Malha plateau.

Depth (m)	Temperature (°C)	Salinity (PSU)	DO (µm)	Density (kg/m³)	Phosphate (µm)	Nitrate (µm)	Silicate (µm)	Chl-a (µg/l)
5	27.8 - 28.4	34.2 - 34.5	204.1 - 206.6	21.7 - 21.9	0.1 - 0.7	0.1 - 1.1	0.1 - 1.3	0.0 - 0.08
25	27.8 - 28.4	34.2 - 34.5	203.9 - 205.5	21.7 - 21.9	0.1 - 0.6	0.1 - 2.3	0.1 - 1.8	0.0 - 0.08
50	24	35.1	189.7 - 200.9	23.7	0.2 - 0.8	0.1	1.1 - 3.9	0.4
75	20.5 - 21.4	35.2 - 35.3	132.0 - 133.8	24.5 - 24.8	0.5 - 1.1	0.1 - 6.3	2.7 - 8.6	0.1 - 0.2
100	18.2 - 19.6	35.2	88.5 - 111.0	25.0 - 25.4	0.9 - 1.7	0.1 -16.9	3.3 - 15.7	0.1
150	15.3 - 16.8	35.0 - 35.2	84.3 - 131.5	25.7 - 26.0	0.6 - 1.8	0.1 - 12.5	7.4 - 16.7	0.02
200	13.4 - 15.6	35.1 - 35.4	104.5 - 187.3	26.2 - 26.4	0.4 - 1.9	0.08 - 11.6	4.2 - 26.1	0.0 - 0.02
300	11.9	35.0 - 35.1	183.4 - 197.2	26.6 - 26.7	0.8 - 1.3	0.08 - 18.6	2.4 - 13.1	0.0 - 0.01
400	9.7 - 10.3	34.8	152.7 - 192.6	26.8	0.5 - 2.0	0.08 - 20.5	4.5 - 31.6	0.0 - 0.02
500	9.1 - 9.3	34.8	119.7 - 163.1	26.9 - 27.0	0.6 - 2.3	0.3 - 22.4	10.9 - 40.5	0.02
750	6.6 - 7.4	34.7 - 34.8	87.0 - 94.7	27.2 - 27.3	1.6 - 3.0	0.7 - 31.7	19.6 - 92.1	0.02
1000	5.1 - 5.6	34.7 - 34.8	88.2 - 102.7	27.4 - 27.5	1.3 - 3.1	0.4 - 33.6	24.4 - 118.1	0.02
1500	3.5	34.8	129.2	27.7	2.9	26	148.4	0.02
2000	2.6	34.8	146.1	27.7	2.3	42.1	163.6	0.01

Table 2C. Ranges of temperature, salinity, dissolved oxygen (DO), density, phosphate, nitrate, silicate and chlorophyll-*a* concentrations in the water column of the eastern slope of Nazareth Bank.

Depth (m)	Temperature (°C)	Salinity (PSU)	DO (µm)	Density (kg/m³)	Phosphate (µm)	Nitrate (µm)	Silicate (µm)	Chl-a (µg/l)
5	27.2 - 27.3	34.5 - 34.6	202.8 - 209.1	22.3	< 0.1	< 0.08 - 0.2	1.5 - 1.8	0.0 - 0.1
25	27.2 - 27.3	34.5 - 34.6	202.4 - 208.9	22.3	< 0.1	< 0.08	0.9 - 1.7	0.0 - 0.1
50	27.1 - 27.2	34.6	207.6 - 209.3	22.3 - 22.4	< 0.1	< 0.08	1.2 - 1.9	0.07
75	25.3 - 24.4	34.9 - 35.1	210.1 - 217.5	23.2 - 23.6	< 0.1	< 0.08	1.4 - 2.1	0.2
100	23.0 - 22.6	35.2 - 35.3	204.4 - 206.8	24.1 - 24.3	< 0.1	< 0.08 - 0.1	1.9 - 3.3	0.2

the Saya de Malha Bank. Tables 2A-C show the range of temperature, salinity, dissolved oxygen and density, [PO_4^{2-}], [NO_3^-], [SiO_4^{4-}] and [chl-*a*] concentrations on the Saya de Malha plateau, deeper waters around Saya de Malha Bank and the eastern slope of the Nazareth Bank.

T-S profile

Figure 5 shows detailed temperature-salinity (T-S) profiles down the water column in the deeper waters at the deep CTD stations around the Saya de Malha plateau (Table 3), on the Saya de Malha plateau and Nazareth Bank.

The water mass distribution at the Saya de Malha Bank was characterised based on New *et al.,* (2007) and Emery (2005). Four water masses were identified in the upper 500 m. Low salinities ranging from 34.2 to 34.5 PSU and high temperatures ranging from 27.8 to 24.8 °C were observed in the surface water mass (Table 2B).

Table 3. Details of water samples collected with a CTD for nutrient analysis in the study areas.

Site	Station	Date	Time/UTC	GPS Location		Bottom Depth (m)	Nutrients	CTD
				Latitude (S)	Longitude (E)			
Saya de Malha plateau	391	7-May-18	14 00	09 47.50	059 43.90	131	√	√
	393	8-May-18	01 17	10 07.18	059 52.08	74	√	√
	394	8-May-18	10 00	10 06.79	060 34.51	27	√	√
	395	8-May-18	16 06	10 05.43	061 16.83	29	√	√
	397	9-May-18	11 20	10 24.88	061 12.75	68	√	√
	398	9-May-18	16 09	10 24.73	060 37.93	60	√	√
	400	10-May-18	01 42	10 25.62	060 08.38	51	√	√
	402	10-May-18	16 42	10 45.39	061 02.70	128	√	√
	403	11-May-18	02 42	10 43.91	062 07.79	26	√	√
	405	11-May-18	13 43	11 05.54	061 55.17	52	√	√
	406	11-May-18	19 22	11 04.98	061 19.39	120	√	√
	409	12-May-18	01 52	11 19.98	060 36.53	195	√	√
	410	12-May-18	13 53	11 21.96	061 09.33	156	√	√
	411	12-May-18	19 52	11 23.53	061 45.57	109	√	√
	413	13-May-18	06 35	11 44.65	062 02.11	284	√	√
	414	13-May-18	12 01	11 42.35	061 22.04	248	√	√
	415	13-May-18	17 48	11 40.49	060 48.52	265	√	√
	417	14-May-18	00 06	11 55.02	060 58.00	328	√	√
	418	14-May-18	06 21	11 55.02	061 42.86	265	√	√
	420	14-May-18	17 07	12 10.55	061 10.93	207	√	√
	423	18-May-18	21 23	09 47.46	060 51.07	110	√	√
	425	20-May-18	22 52	10 03.56	062 13.40	192	√	√
	427	21-May-18	18 07	10 19.17	062 14.73	215	√	√
	432	25-May-18	06 42	11 24.53	062 00.49	380	√	√
Deep Stations around Saya de Malha	392	7-May-18	21 20	10 07.55	059 38.10	2347	√	√
	396	9-May-18	00 31	10 02.80	062 32.99	2172	√	
	399	9-May-18	22:55	10 25.70	059 54.08	1204		√
	401	10-May-18	06 10	10 46.18	059 58.42	2129		√
	404	11-May-18	07 47	10 43.11	062 34.27	2125		√
	408	12-May-18	04 32	11 18.66	060 20.31	2700		√
	412	13-May-18	02 35	11 25.94	062 27.90	2068	√	√
	416	13-May-18	21 17	11 54.52	060 45.63	1309		√
	434	26-May-18	18 27	12 34.55	061 00.43	1068	√	√
Nazareth Bank	435	27-May-18	04 50	13 54.97	060 51.90	43	√	√
	436	27-May-18	06 24	14 02.27	061 00.74	36	√	√
	437	27-May-18	09 22	14 10.85	060 56.47	31	√	√
	438	27-May-18	12 33	14 24.87	061 02.64	32	√	√
	439	27-May-18	14 51	14 34.82	061 07.43	56	√	√
	440	29-May-18	08 03	15 10.42	061 08.64	170	√	√
	441	29-May-18	14 02	15 19.96	061 01.83	242	√	√

Three water masses were identified below the low salinity surface water (LSW), namely the Arabian Sea Water (ASW) found between 50 and 75 m, the Sub Tropical Surface Water (STSW) found at 150 m, and the South Indian Central Water (SICW), found between 300 and 400 m. The maximum temperature, salinity and density in these features occurred at around 20 °C to 23.5 °C, 34.7 PSU to 35.3 PSU, 24 kg/m³ to 24.5 kg/m³ for ASW, 15 °C to 18 °C, 35.1 PSU to 35.3 PSU, 26.0 kg/m³ for STSW, and 8 °C to 10 °C, 34.7 to 35.2 PSU, 26.5 kg/m³ to 27 kg/m³ for SICW, respectively.

The bottom or immediate layer (500 to 1500 m) had the same water mass properties as that of the Antarctic Intermediate Water (AIW) characterised with temperatures of 2.0 to 8.0 °C, salinity between 34.6 to 34.7 PSU and density at 27.25 kg/m³. From the T-S plot for the eastern part (Fig. 5c), an additional water mass was identified as the Indian Equatorial Water (IEW) with water characteristics of 8.0 °C to 23 °C, 34.6 PSU to 35.1 PSU, 24.0 kg/m³ to 26 kg/m³ in the upper waters. The T-S plot on the western part had similar water masses as in the overall deep stations (Fig. 5d).

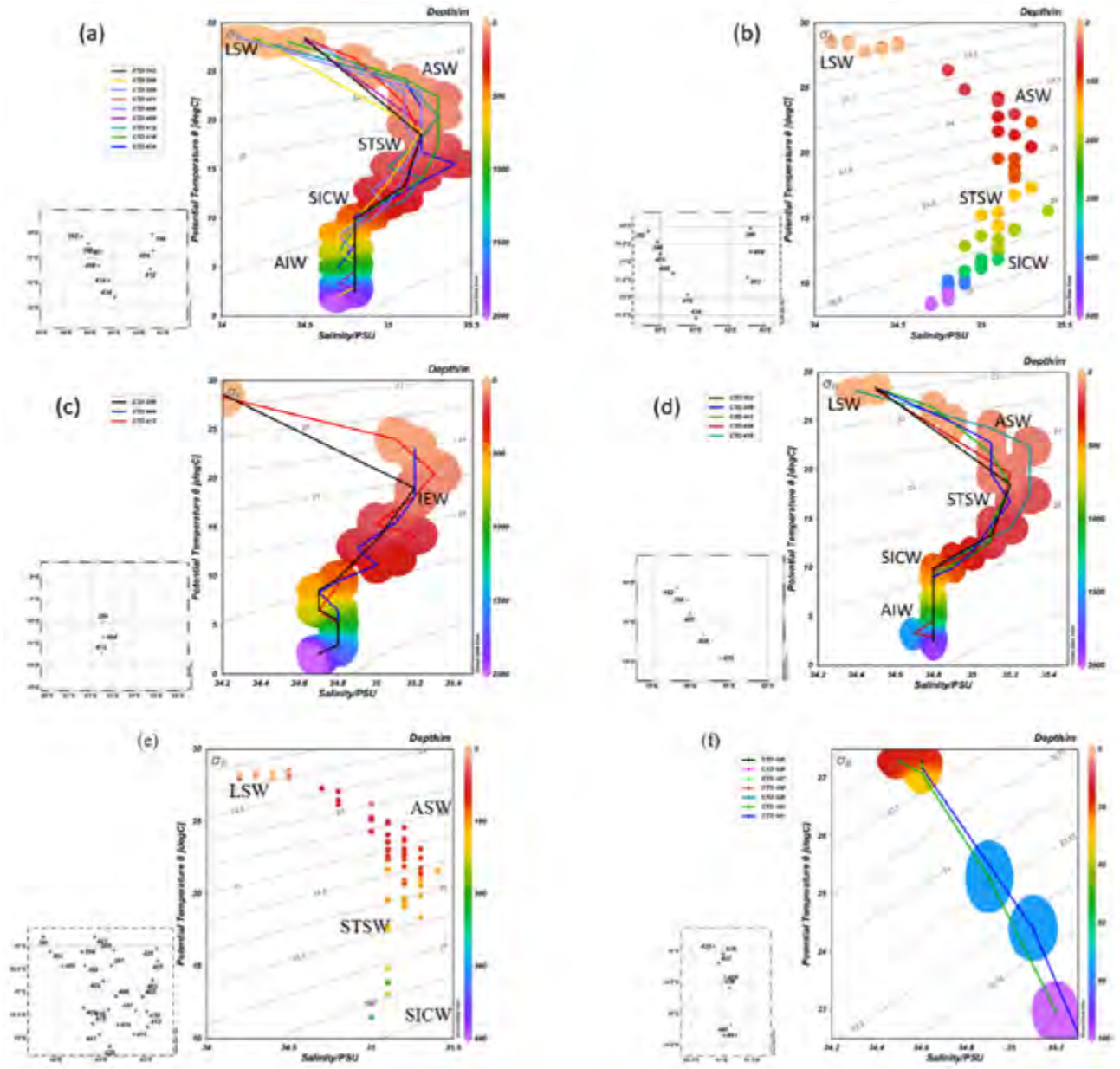

Figure 5. T-S diagram at (a) the deeper stations around the Saya de Malha Plateau, (b) upper 500 m of the deeper stations, (c) eastern part and (d) western part of the deep waters around Saya de Malha, (e) Saya de Malha plateau and (f) eastern slope of Nazareth Bank. Abbreviations are: LSW - Low Salinity Surface Water; ASW - Arabian Sea Water; STSW - Sub Tropical Surface Water; SICW - South Indian Central Water; AIW - Antarctic Intermediate Water; IEW - Indian Equatorial Water. The diagonal lines on the graphs show density in kg/m^3.

As for the Saya de Malha plateau (Fig. 5e), the water masses identified were ASW, STSW and SICW. At the Nazareth Bank (Fig. 5f), small variations in the water characteristics were observed due to insufficient data and the shallowness of the sampling stations. As such, the water mass(es) could not be identified.

Distribution of nutrients across Saya de Malha and Nazareth Banks

As mentioned above, [PO_4^{2-}], [NO_3^-] and [SiO_4^{4-}] show a typical nutrient depth profile which increases with depth. The concentration of phosphate (0.1 to 3.1µm) in general at the Saya de Malha and Nazareth Banks is lower as compared to nitrate (0.1 to 42.1 µm) and silicate (0.1 to 163.6 µm) as shown in Table 2. One-way ANOVA showed no significant differences among the CTD stations ($P > 0.05$). However, at different depths, strongly significant differences were observed for temperature, density, nutrients and chl-*a* ($p < 0.0001$). The nutricline on the Saya de Malha plateau was at around 50 m, similar to the pycnocline, indicating the presence of a mixed layer at that depth. The above mixing layer is depleted

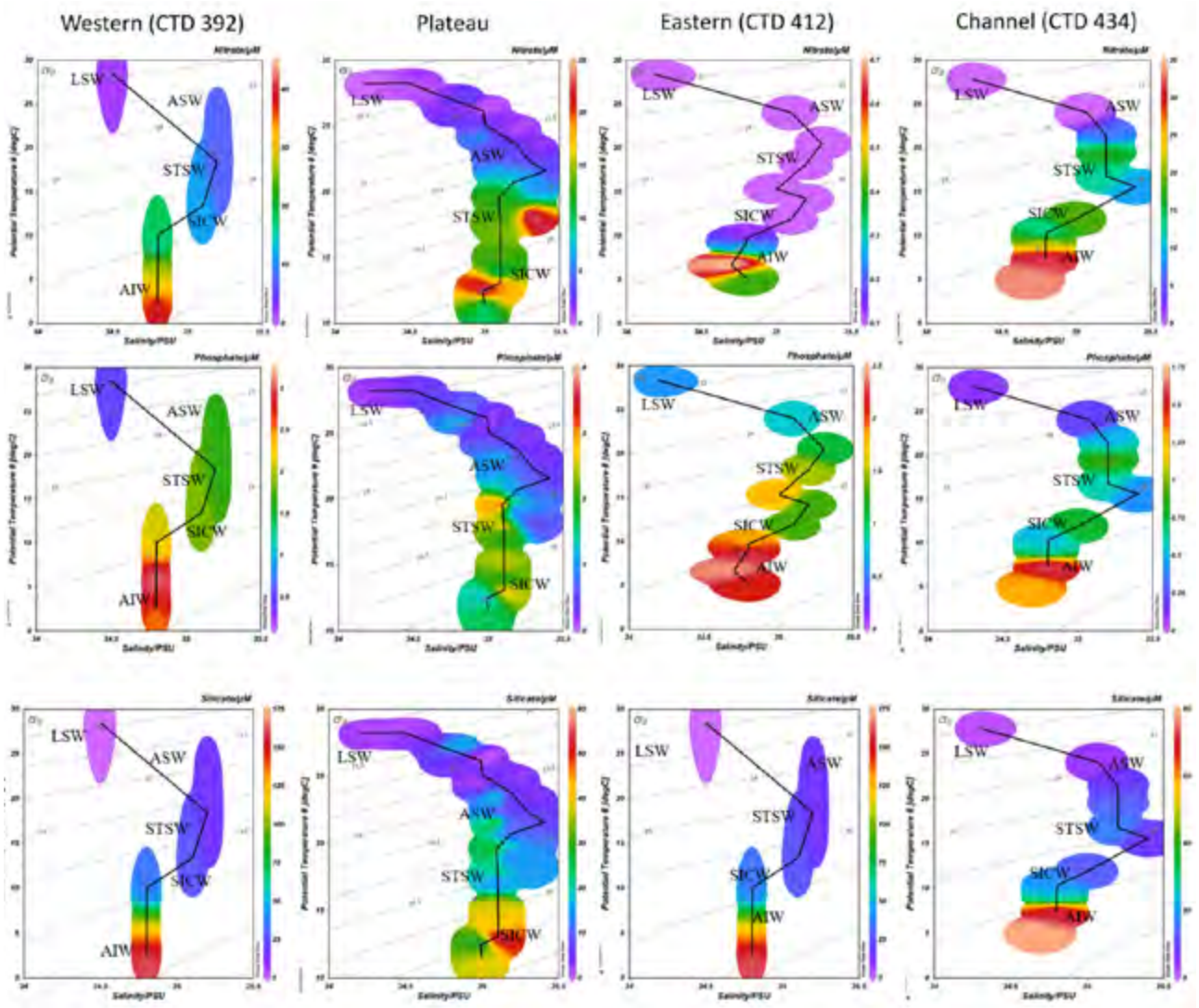

Figure 6. Profile of nutrients (phosphate, nitrate and silicate) at deep CTD stations 392, 412, 434 and Saya de Malha plateau with an overlay of the mass distribution. The diagonal lines on the graphs show density in kg/m^3.

in [PO_4^{2-}] (0.2 µm), [NO_3^-] (0.3 µm) and [SiO_4^{4-}] (2 µm) in the depth range of 34.5 to 34.8 PSU (Fig. 2).

In the deeper waters, the nutricline was observed at around 50 to 75 m. The concentration of [PO_4^{2-}] and [NO_3^-] was higher in the deep waters as compared to the plateau where the concentrations were around 1.6 µm and 10 µm. The concentration of [SiO_4^{4-}] was the same as for the plateau. Within the intermediate water (around 800 to 1000 m), phosphate and nitrate was within the range for typical deep waters with values > 30 µm and > 2 µm (Sarmiento and Gruber, 2006).

On the plateau, high concentrations of [PO_4^{2-}], [NO_3^-] and [SiO_4^{4-}], were observed in the STSW and SICW with the highest concentrations of [SiO_4^{4-}] and [NO_3^-] in the SICW, whereas the thermocline water was poor in nutrients (< 5 µm) in the same region. The LWS exhibited low nutrient concentrations of values less than 5 µm (Fig. 6). The northern part of the plateau also showed a higher concentration of nutrients than the southern part (Fig. 7). The different water masses are clearly seen in Figure 7. The concentrations of nutrients was more pronounced from 80 to 100 m on the northern part whereas in the southern part, an increase was seen from 100 to 120 m. The density surfaces seem to have an effect on the nutrients where high levels of nutrients were observed in surfaces denser than 25 kg/m^3. The western part of the plateau had higher nutrient concentrations than the eastern plateau.

Due to the shallowness of the plateau, it appeared that the nutrients from the deeper waters are brought to

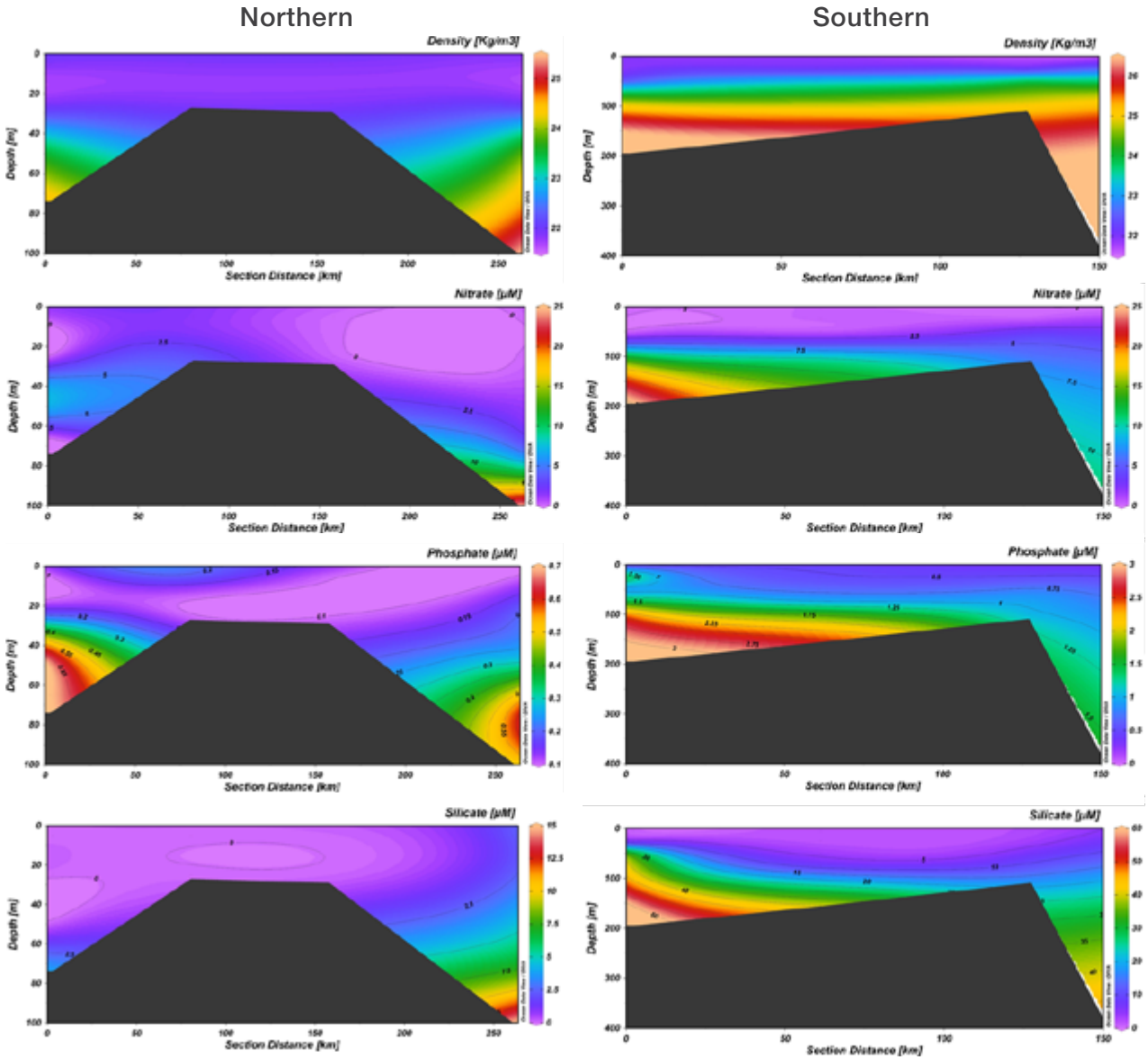

Figure 7. Section plot of nutrients and density from left (0 km) to right (150 km) on the northern and southern part of the Saya de Malha plateau. The northern transect comprised of CTD stations 393, 394, 395 and 425 and the southern transects of CTD stations 409, 410, 411, 432.

the upper waters on the plateau where the water layers on the western plateau are narrower and sharper than the eastern plateau (Fig. 8). The waters coming from the eastern part had much lower nutrient concentrations and a major difference could be seen in [NO_3^-] and [SiO_4^{4-}] with values 1.2 µm and 25 µm at 300 m passing through the plateau to the western part showing an increase to 3.0 µm and 60 µm respectively. This may be due to the upwelling of nutrients onto the plateau where the colder deep water could be seen to be brought to the surface as shown in Figure 8.

In the oceanic region, [SiO_4^{4-}] increased by almost 2.5 times towards the deepest depths (Fig. 6), being lowest in the LWS region to highest in the AIW region (~150 µm – Fig. 6). Similarly, high concentrations of [NO_3^-] were also seen at the western station and in the channel between Saya de Malha and Nazareth Banks. However, at the eastern station, [NO_3^-] was the lowest compared to the other deep stations and on the plateau. [PO_4^{2-}] was uniform in the deep waters and on the plateau. Figure 5 also displays a pattern in the nutrients at the deeper stations. CTD 392 (western) and CTD 412 (eastern) are located in the northern part of the Saya de Malha Bank while CTD 434 (channel) is found in the southern part of the Bank. The concentration of nutrients in the northern part at greater depths was higher than in the southern part. A notable increase was seen in [SiO_4^{4-}] where a major difference in concentrations could be found at

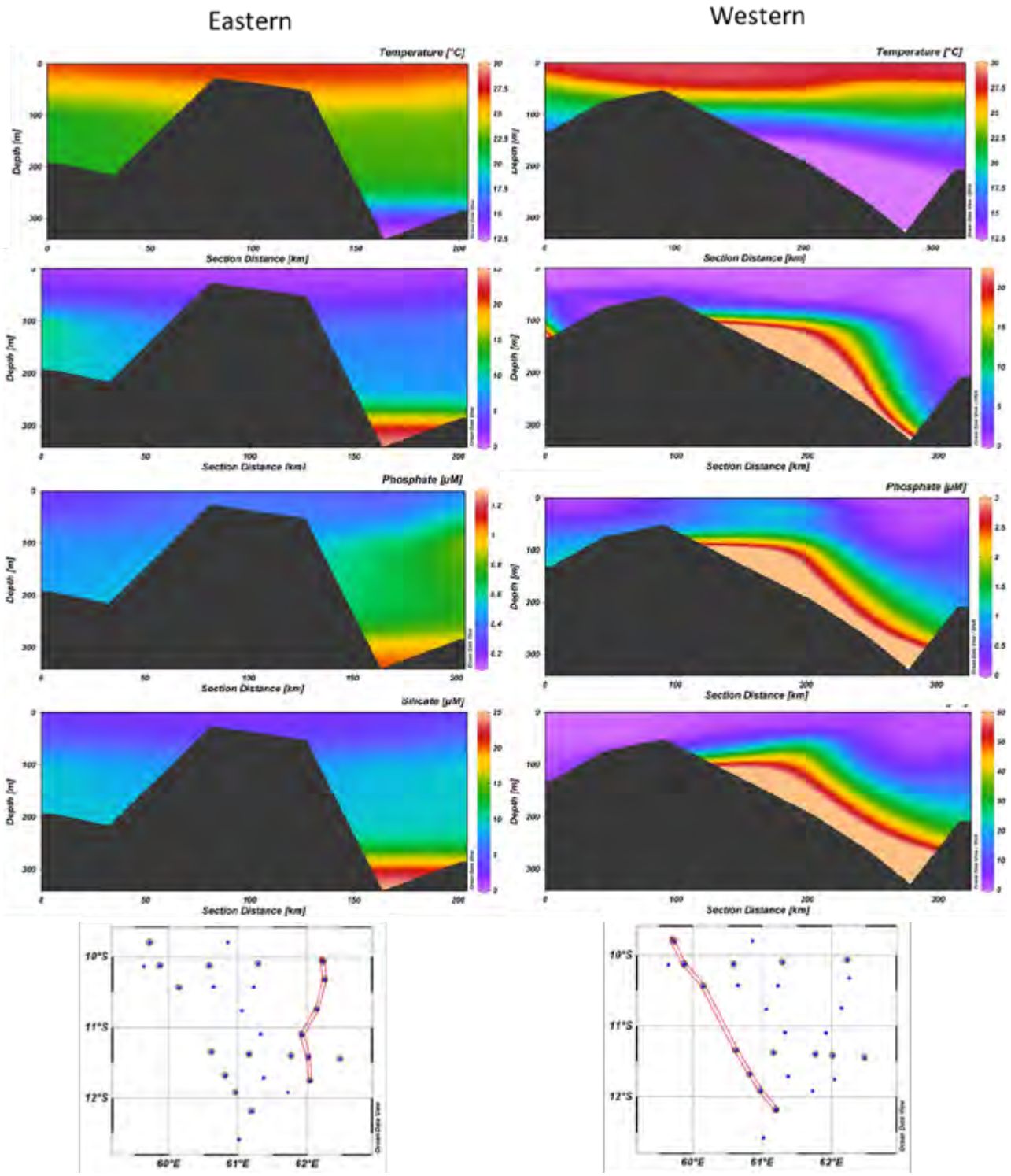

Figure 8. Section plot of nutrients and density from north (0 km) to south (300 km) on the eastern and western part of the Saya de Malha plateau. The eastern transect comprised of CTD stations 425, 427, 403, 405, 432 and 413 and the western transect of CTD stations 391, 393, 400, 409, 415, 417 and 420.

around 150 µm on the northern and 70 µm on the southern region.

At the Nazareth Bank, low concentrations of nutrients were observed as compared to the Saya de Malha Bank (Figs. 3 and 4).

Nutrients with dissolved oxygen and chl-*a*

The concentration of dissolved oxygen (DO) on the Saya de Malha plateau showed variation among the water masses and between transects (northern and southern), ranging between 75 to 220 µm/l. The highest concentrations were associated with LSW

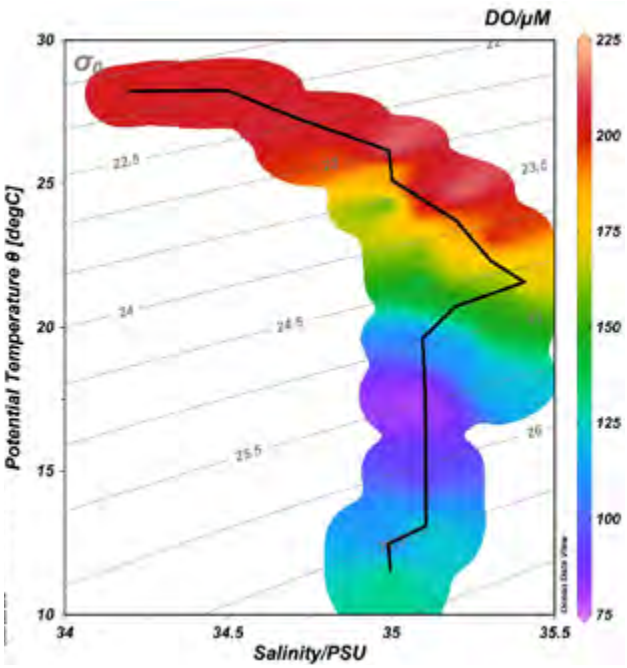

Figure 9. Profile of DO at the SDM plateau with an overlay of the mass distribution. The diagonal lines on the graphs show density in kg/m³.

and ASW in the upper 100 m and the lowest with the STSW (Figs. 5e and 9). High concentrations of DO was observed in the upper 50 m which decreased below the thermocline (Fig. 10e). The oxygen minimum layer could be observed at the deeper stations where the nutrient maximum is also the same at around 100 m (Fig. 3). The DO concentration (Fig. 10a-d) exhibited minor variations on the plateau and in comparison to the Nazareth Bank.

Correlation between DO along with oxygen saturation and nutrients showed negative R values where a strong correlation (R = -0.7) was observed with [PO_4^{2-}] and [NO_3^-] and a weak correlation with [SiO_4^{4-}]. [SiO_4^{4-}] is absorbed by diatoms; a type of phytoplankton that makes shell from SiO_4^{4-} (Gupta and Desa, 2001). The dissolution of frustules of diatoms attributing an increase in the [SiO_4^{4-}] in the deeper waters does not usually involve the consumption of oxygen (Gupta and Desa 2001; Gupta *et al.*, 1976). Considering the saturation of DO (%) on the plateau (Fig. 11a), most of the stations showed values higher than 92 % between

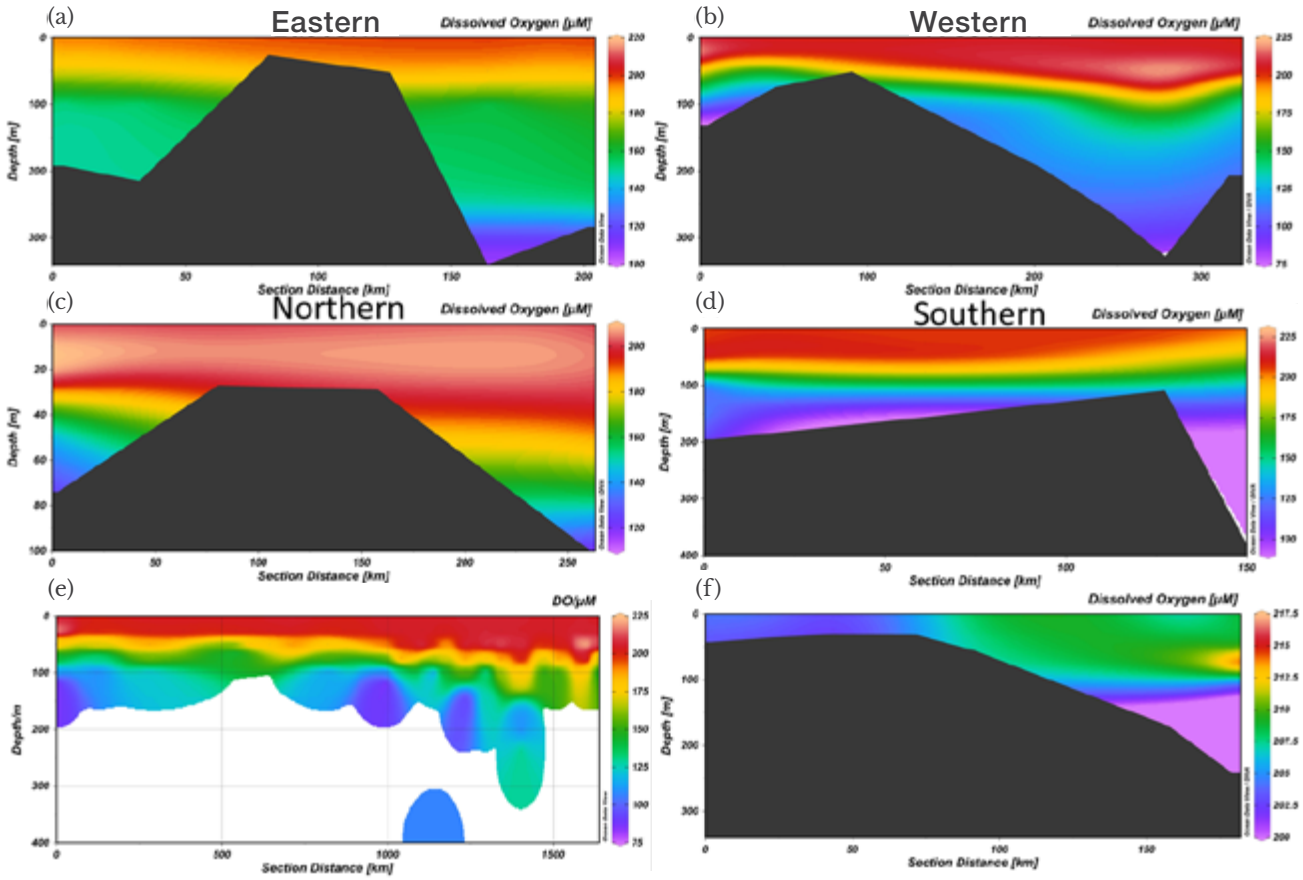

Figure 10. Section plot of dissolved oxygen (µm) on the (a) eastern, (b) western, (c) northern, (d) southern parts, and (e) overall dissolved oxygen distribution at the Saya de Malha plateau and (f) at Nazareth Bank.

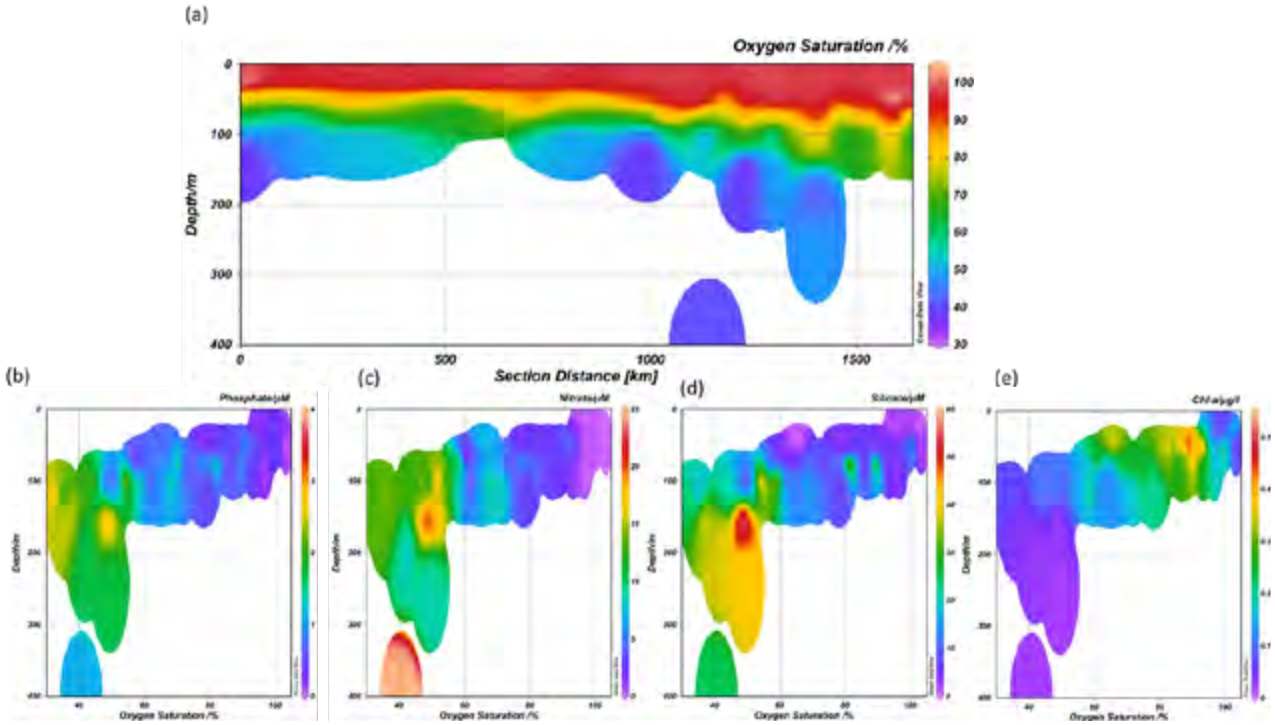

Figure 11. Section plot of oxygen saturation (%) on the plateau of Saya de Malha Bank and its correlation with (b) phosphate, (c) nitrate, (d) silicate and (e) chl-*a* in the water column.

5 to 75 m depth and values lower than 50 % between 100 to 400 m. At Nazareth Bank, the values at all the stations were higher than 94 %. High concentration of nutrients was observed at low - oxygen saturated water between 100 to 200 m (Fig. 11a-c); near the oxygen minimum layer which may be due to the decomposition of organic matter in that region.

Low chl-*a* values were recorded at Saya de Malha and Nazareth Bank where the mean value was found to be 0.13 µg/l and 0.09 µg/l respectively. The chl-*a* values are very low in comparison to the mean global ocean value of 193µg/l (Morel *et al.,* 2010). The low chl-*a* in the region confirms the region being oligotrophic. The deep chlorophyll maximum (DCM) is usually

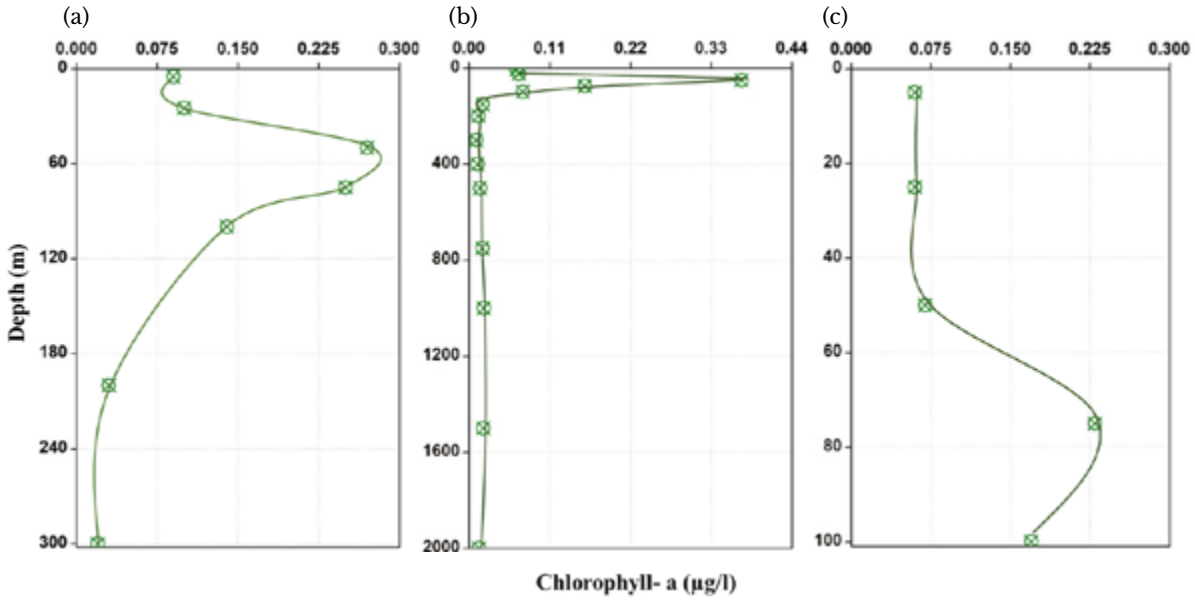

Figure 12. Chlorophyll-*a* profile at (a) Saya de Malha plateau (b) the deep station around Saya de Malha and (c) Nazareth Bank.

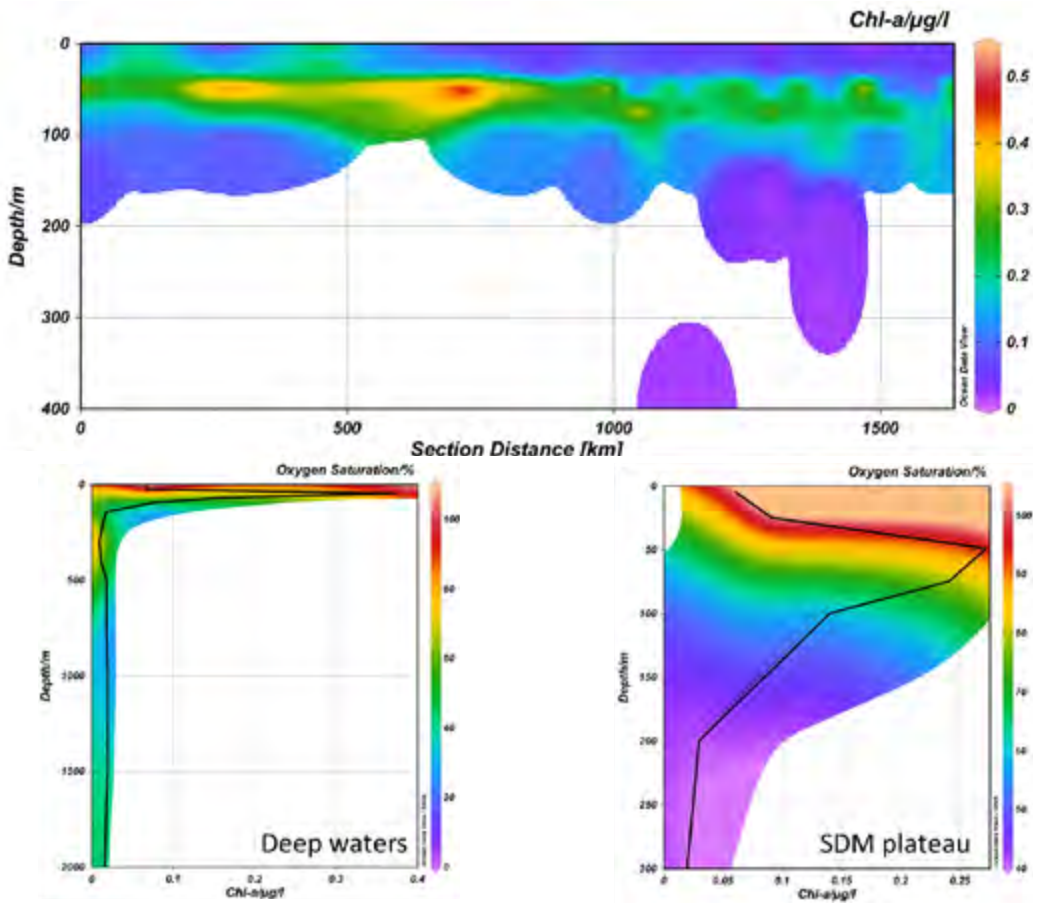

Figure 13. Section plot of Chl-*a* concentration at the Saya de Malha (SDM) plateau in the water column and its correlation with oxygen saturation at the deeper stations around the SDM and stations on the SDM plateau.

found between the upper water (nutrient deficient) and lower water layer (light limited) where it is characterised by high chl-*a* values, thus indicating high phytoplankton biomass (Latasa *et al*., 2017; Li *et al*., 2012). The DCM at the Saya de Malha Bank was found to be at 60 m and around 75 m at the Nazareth Bank where highest chl-*a* values were 0.3 to 0.35 µm and 0.23 µm respectively (Fig. 12).

Chl-*a* showed a correlation with negative R values (R =0.3) with the nutrients, indicating high concentration of chl-*a* present at low concentration of nutrients.

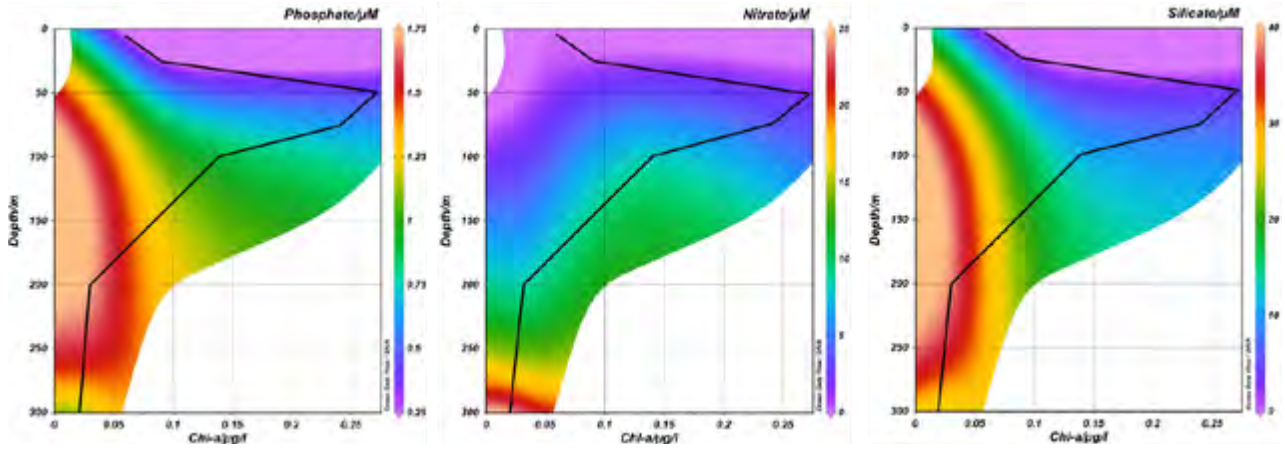

Figure 14. Relationship between nutrients and chl-*a* on the Saya de Malha plateau.

On the plateau, high chl-*a* values between 0.3 to 0.5 µg/l were found at 50 m in the upper layer (Fig. 13). Figure 13 clearly shows photosynthetic activity in the DCM where the oxygen saturation was 100 % and above at a high chl-*a* concentration.

The relationship of [PO_4^{2-}], [NO_3^-] and [SiO_4^{4-}] with chl-*a* followed a similar trend where high chl-*a* values were observed at low nutrient concentrations (Fig. 14). The low nutrient values at the DCM may be attributed to the fact that nutrients are utilised by phytoplankton for metabolic activities. Below 150 to 200 m, an increase in nutrient levels at low chl-*a* which may be attributed to the decomposition of organic matter, causes regeneration of nutrients into the water column and these sink into deeper waters.

Discussion

Phytoplankton are the primary producers of the marine food web where they depend entirely on sunlight and carbon dioxide for photosynthetic activities and are therefore found in the euphotic zone (Williams and Follows, 2003). Nutrients are depleted in the euphotic zone as they are utilised by phytoplankton and cyanobacteria (Riegman, 1995), explaining a decrease in the level of nutrients in the upper water column, especially at the DCM. These nutrients are regenerated into the water column through respiration and decomposition of marine organisms, mostly in deeper waters (Riegman 1995; Harrison 1992; Levitus *et al*., 1993) as confirmed in the results presented here. Nitrite, NO_3^-, is an immediate product of nitrification from a microbial-mediated oxidation of NH_4^+ which is also consumed and reduced by primary producers and certain microorganisms for building organic molecules (Zakem *et al.,* 2018); which explains the values of NH_4^+ and NO_3^- being below detection limits.

The survey area exhibited an oligotrophic system characterised by low chl-*a* concentration. Usually the lowest concentration of chl-*a* in the EEZ of Mauritius is recorded in the months of April to June (Ramchandur *et al.,* 2017) which may explain the low chl-*a* values obtained during sampling in May. The SEC is the most dominant current passing through the Mascarene Plateau (New *et al.,* 2005; New *et al.,* 2007). The Indonesian Throughflow contains fresh water (Talley, 2011) which flows through the Mascarene Plateau bringing nutrients from the eastern part of the Indian Ocean (Schott and McCreary, 2001) and diverges across the Saya de Malha and Nazareth Banks through the channel (CTD station 434). The southern Indian Ocean usually receives nutrients from Circumpolar Deep Water (1500 to bottom) which is rich in nutrients (Panassa *et al.,* 2018).

The results showed that nutrient levels increased westward from the eastern part of the plateau. The decrease in temperature and high [SiO_4^{4-}] levels in the STSW region on the plateau may be attributed to the shallowness of the plateau, with the nutrients from the AIW being brought up to the STSW and SICW water masses. New *et al.* (2005) showed that this is partly due to the Ekman upwelling of the density surfaces on the northern side of the SEC. The current study showed higher concentration of nutrients in the northern part in comparison to the southern part. Furthermore, the Southwest Monsoon starts to develop during April to May where weak winds close to shore occur off Somalia causing the concentrations of phosphate and nitrate to increase towards the northern part of the Indian Ocean (Schott and McCreary, 2001). This might explain the low concentration of nutrients on the Nazareth Bank located in the southern part of the Mascarene Plateau.

In general, the Indian Ocean has higher nutrients levels that the Atlantic Ocean (Levitus *et al*., 1993). However, the southern Indian Ocean is poor in nutrients unlike the northern part which may be due to the absence of a general equatorial upwelling mechanism in the Indian Ocean (Garcia *et al.,* 2018; Gupta and Desa, 2001).

Conclusion

This study is the first, to the author's knowledge, conducted in the region of Saya de Malha and Nazareth Banks showing the distribution of nutrients in the water column. In general, the nutrient levels increase down the water column. The Saya de Malha Bank has a higher concentration of nutrients than the Nazareth Bank. Due to the shallowness of the plateau, the nutrient-rich AIW water mass in the deep layer brings nutrients to the SICW found in the upper layer on the plateau through upwelling. At the DCM, low nutrient levels were observed with an increase in the oxygen saturation greater than 94 %, indicating high primary productivity in that region. In order to obtain a better understanding of the change in productivity and the nutrient distribution throughout the year, more information on the water masses, seasonal variation of the nutrients, and other physicochemical parameters are required which could not be achieved in this study since data were collected only during one season.

Nevertheless, this study can be used a a baseline for other studies on the Mascarene Plateau.

Acknowledgments

The authors are thankful to the Food and Agriculture Organization (FAO) for funding the expedition in the Saya de Malha under the EAF-Nansen Programme on board the R/V Dr Fridtjof Nansen, Department of Continental Shelf, Maritime Zones Administration & Exploration of Mauritius for co-leading and coordinating the scientific expedition and the Mauritius Oceanography Institute (MOI) for participation in the expedition and their never-ending support towards the research study. The participants of the expedition: OA Bergstad, D Bissessur, N Reetoo, A Audit-Manna, A Nicolas, K Sauba, J Rama, P Coopen, Y Oozeeraully, M Soondur, R Bhagooli, S Seeboruth, L Caussy, S Ramah, J Harley, A Souffre, G Gendron, S Hollanda, R Melanie, D Kuyper, TM Ensrud and M Singh from the MOI are gratefully acknowledged.

References

Ardill JD (1986) Current status of fisheries in Mauritius. Food and Agriculture Organization, United Nations. 31 pp

Badal MR, Rughooputh SD, Rydberg L, Robinson IS, Pattiaratchi C (2009) Eddy formation around South West Mascarene Plateau (Indian Ocean) as evidenced by satellite 'global ocean colour' data. Western Indian Ocean Journal of Marine Science 8 (2): 139-145 [doi: 10.4314/wiojms.v8i2.56969]

Benson BB, Krause Jr D (1984) The concentration and isotopic fractionation of oxygen dissolved in freshwater and seawater in equilibrium with the atmosphere. Limnology and Oceanography 29 (3): 620-32 [doi: 10.4319/lo.1984.29.3.0620]

Betzler C, Lindhorst S, Lüdmann T, Reijmer JJ, Braga JC, Bialik OM, Reolid J, Eisermann JO, Emeis K, Rixen T, Bissessur D (2021) Current and sea level control the demise of shallow carbonate production on a tropical bank (Saya de Malha Bank, Indian Ocean). Geology 49 (12): 1431-1435 [doi: 10.1130/G49090.1]

Bhagooli R, Kaullysing D (2019) Seas of Mauritius–Chapter 12. In: Sheppard CCR (eds) World seas: an environmental evaluation, 2nd Edition, Volume II: The Indian Ocean to the Pacific. Elsevier, Academic Press. pp 253-277

Dharmendra D, Sólmundsson J (2005) Stock assessment of the offshore Mauritian banks using dynamic biomass models and analysis of length frequency of the Sky Emperor (*Lethrinus mahsena*). Fisheries Training Program, The United Nations University. 61 pp

Emery WJ (2001) Water types and water masses. Encyclopedia of ocean sciences 1 (6): 3179-3187

Fisher RL, Johnson GL, Heezen BC (1967) Mascarene Plateau, Western Indian Ocean. Geological Society of America Bulletin 78 (10): 1247-1266.

Garcia HE, Gordon LI (1992) Oxygen solubility in seawater: Better fitting equations. Limnology and Oceanography 37 (6): 1307-1312 [doi: 10.4319/lo.1992.37.6.1307]

Garcia CA, Baer SE, Garcia NS, Rauschenberg S, Twining BS, Lomas MW, Martiny AC (2018) Nutrient supply controls particulate elemental concentrations and ratios in the low latitude eastern Indian Ocean. Nature Communications 9 (1): 1-10

Grand MM, Measures CI, Hatta M, Hiscock WT, Landing WM, Morton PL, Buck CS, Barrett PM, Resing JA (2015) Dissolved Fe and Al in the upper 1000 m of the eastern Indian Ocean: A high-resolution transect along 95° E from the Antarctic margin to the Bay of Bengal. Global Biogeochemical Cycles 29 (3): 375-396 [doi: 10.1002/2014GB004898]

Grasshoff K, Johannsen H (1972) A new sensitive and direct method for the automatic determination of ammonia in sea water. ICES Journal of Marine Science 34 (3): 516-521

Grasshoff K, Kremling K, Ehrhardt M (2009) Methods of seawater analysis. John Wiley & Sons. 419 pp

Gupta RS, Rajagopal, MD, Qasim, SZ (1976) Relationship between dissolved oxygen and nutrients in the north-western Indian Ocean. pp 201-211

Gupta RS, Desa E (eds) (2001) The Indian Ocean: A perspective (Vol. 2). CRC Press. 906 pp

Harrison WG (1992) Regeneration of nutrients. In: Falkowski PG, Woodhead AD, Vivirito K (eds) Primary productivity and biogeochemical cycles in the sea. Environmental Science Research 43. Springer, Boston, MA. pp 385-407

Jena B, Sahu S, Avinash, K, Swain D (2013) Observation of oligotrophic gyre variability in the south Indian Ocean: environmental forcing and biological response. Deep Sea Research Part I: Oceanographic Research Papers 80: 1-10

Koroleff F (1972) Determination of reactive silicate. ICES Cooperative Research Report Series A 29: 87-90

Latasa M, Cabello AM, Morán XA, Massana R, Scharek R (2017) Distribution of phytoplankton groups within the deep chlorophyll maximum. Limnology and Oceanography 62 (2): 665-85

Levitus S, Conkright ME, Reid JL, Najjar RG, Mantyla A (1993) Distribution of nitrate, phosphate and silicate in the world oceans. Progress in Oceanography 31 (3): 245-273

Li G, Lin Q, Ni G, Shen P, Fan Y, Huang L, Tan Y (2012) Vertical patterns of early summer chlorophyll a concentration in the Indian Ocean with special reference to the variation of deep chlorophyll maximum. Journal of Marine Biology 20 (2) [doi:10.1155/2012/801248]

Morel A, Claustre H, Gentili B (2010) The most oligotrophic subtropical zones of the global ocean: similarities and differences in terms of chlorophyll and yellow substance. Biogeosciences 7 (10): 3139-3151 [doi: 10.5194/bg-7-3139-2010]

Munbodh M (2014) An EAF baseline report for the fisheries of shallow water demersal fish species of the Saya de Malha and Nazareth Banks of Mauritius. In: Koranteng KA, Vasconcellos MC, Satia BP (eds) Preparation of management plans for selected fisheries in Africa. FAO, Rome. pp 118-155

Murphy JA, Riley JP (1962) A modified single solution method for the determination of phosphate in natural waters. Analytica Chimica Acta 27: 31-36

New AL, Stansfield K, Smythe-Wright, Smeed, DA, Evans AJ, Alderson SG (2005) Physical and biochemical aspects of the flow across the Mascarene Plateau in the Indian Ocean. Philosophical Transactions of the Royal Society A: Mathematical, Physical and Engineering Sciences, 363 (1826): 151-168

New A, Alderson SG, Smeed DA, Stansfield KL (2007) On the circulation of water masses across the Mascarene Plateau in the South Indian Ocean. Deep Sea Research Part I: Oceanographic Research Papers 54 (1): 42-74 [doi:10.1016/j.dsr.2006.08.016]

Panassa E, Santana-Casiano JM, González-Dávila M, Hoppema M, Van Heuven SM, Völker, C, Wolf-Gladrow D, Hauck J (2018) Variability of nutrients and carbon dioxide in the Antarctic Intermediate Water between 1990 and 2014. Ocean Dynamics 68 (3): 295-308

Payet R (2005) Research, assessment and management on the Mascarene Plateau: a large marine ecosystem perspective. Philosophical Transactions of the Royal Society A: Mathematical, Physical and Engineering Sciences 363 (1826): 295-307 [doi:10.1098/rsta.2004.1494]

Ragoonaden S, Babu VR, Sastry JS (1987) Physico-chemical characteristics and circulation of waters in the Mauritius-Seychelles Ridge zone, Southwest Indian Ocean. pp 184-191

Ramchandur V, Rughooputh SD, Boojhawon R, Motah BA (2017) Assessment of *chlorophyll-a* and sea surface temperature variability around the Mascarene Plateau, Nazareth Bank (Mauritius) using satellite data. Indian Journal of Fisheries 64 (4): 1-8

Resplandy L, Vialard J, Lévy M, Aumont O, Dandonneau Y (2009) Seasonal and intraseasonal biogeochemical variability in the thermocline ridge of the southern tropical Indian Ocean. Journal of Geophysical Research: Oceans 114 (C7) [doi: 10.1029/2008JC005246]

Riegman R (1995) Nutrient-related selection mechanisms in marine phytoplankton communities and the impact of eutrophication on the planktonic food web. Water Science and Technology 32 (4): 63-75

Sarmiento JL, Gruber N (2006) Ocean biogeochemical dynamics. Princeton University Press. 461 pp

Schlüter L, Henriksen P, Nielsen TG, Jakobsen HH (2011) Phytoplankton composition and biomass across the southern Indian Ocean. Deep Sea Research Part I: Oceanographic Research Papers 58 (5): 546-556

Schott FA, McCreary Jr JP (2001) The monsoon circulation of the Indian Ocean. Progress in Oceanography 51 (1): 1-123

Stramma L, Lutjeharms JR (1997) The flow field of the subtropical gyre of the South Indian Ocean. Journal of Geophysical Research: Oceans 102 (C3): 5513-5530

Strickland JD, Parsons TR (1972) A practical handbook of seawater analysis. Fisheries Research Board of Canada, Ottawa, Ontario. 310 pp

Talley LD (2011) Descriptive physical oceanography: an introduction. Academic Press. 577 pp

Vortsepneva E (2008) Saya de Malha Bank – an invisible island in the Indian Ocean. Geomorfology, Oceanology, Biology. Report to the Lighthouse Foundation, Moscow, Russia. 42 pp [https://lighthouse-foundation.org/Binaries/Binary1070/Saya-de-Malha-report-final.pdf]

Williams RG, Follows MJ (2003) Physical transport of nutrients and the maintenance of biological production. Ocean biogeochemistry. Springer, Berlin, Heidelberg. pp 19-51

Zakem EJ, Al-Haj A, Church MJ, van Dijken G, Dutkiewicz S, Foster SQ, Fulweiler RW, Mills MM, Follow MJ (2018) Ecological control of nitrite in the upper ocean. Nature Communications 9 (1):1-13

Spatial distribution of surface chlorophyll *a* and micro-phytoplankton density and diversity around two islands and at two banks of the Mascarene region

Mouneshwar Soondur[1,2]*, Sundy Ramah[1,3], Ravindra Boojhawon[4], Deepeeka Kaullysing[1,2], Ranjeet Bhagooli[1,2,5,6]

[1] Department of Biosciences and Ocean Studies, Faculty of Science & Pole of Research Excellence in Sustainable Marine Biodiversity, University of Mauritius, Réduit 80837, Republic of Mauritius

[2] The Biodiversity and Environment Institute, Réduit, Republic of Mauritius

[3] Albion Fisheries Research Centre, Ministry of Blue Economy, Marine Resources, Fisheries & Shipping, Albion, Petite Rivière 91001, Republic of Mauritius

[4] Department of Mathematics, Faculty of Science, University of Mauritius, Réduit 80837, Republic of Mauritius

[5] Institute of Oceanography and Environment (INOS), University Malaysia Terengganu, 21030 Kuala Terengganu, Terengganu, Malaysia

[6] The Society of Biology (Mauritius), Réduit, Republic of Mauritius

* Corresponding author: mouneshwar.soondur@gmail.com

Abstract

The present study validated the use of AquaMODIS sea surface chlorophyll *a* (Chl*a*) concentrations and investigated the spatial variation in density and diversity of micro-phytoplankton around two islands and two fishing banks of the Mascarene region. The study included areas around Mauritius (MRU) and Rodrigues (ROD) Islands, at Nazareth (NZ) Bank, and in the Joint Management Area (JMA) between the Republic of Mauritius and the Republic of Seychelles, more specifically at the Saya de Malha (SM) Bank. The AquaMODIS data were based on 67 match-up data points of *in-situ* against satellite Chl*a* concentrations. The micro-phytoplankton community structure was investigated by determining the density variation and using the Shannon Wiener (H') and Evenness (E_{var}) diversity indices. The satellite and *in-situ* Chl*a* data were significantly and positively correlated when pooled for the four sites studied (R^2 = 0.441; r = 0.642, $P < 0.01$), and when analysed separately for islands (R^2 = 0.480; r = 0.694), and banks (R^2 = 0.233; r = 0.483). However, the Chl*a* satellite values tended to be lower than the *in-situ* Chl*a* data. The highest densities of micro-phytoplankton were observed in the eastern and northern regions for MRU and ROD, respectively. The most dominant genera of micro-phytoplankton were *Coscinodiscus*, *Navicula, Chaetoceros* and *Ceratium*. The Shannon-Wiener diversity index values for diatoms were all above 2.5 with waters around the islands having higher diversity compared to the banks. Overall, the different micro-phytoplankton around the islands, except for the group of cyanobacteria at ROD Island, were more evenly distributed ($E_{var} > 0.6$) compared to the banks. This study indicated that AquaMODIS Chl*a* satellite data is valid and may be potentially used as a proxy for *in-situ* Chl*a* concentration on the Mascarene Plateau. The results of this study also provide detailed insight into the spatial variation in micro-phytoplankton density and diversity on the Mascarene Plateau in the Western Indian Ocean. Further long-term studies are warranted to thoroughly understand the temporal (including seasonal and inter-annual) variations in Chl*a* and micro-phytoplankton distribution for adequate and appropriate management of these ocean territories.

Keywords: Exclusive Economic Zone, Joint Management Area, micro-phytoplankton, fishing banks, AquaMODIS, Republic of Mauritius, Republic of Seychelles

http://dx.doi.org/10.4314/wiojms.si2021.2.3

Introduction

The Exclusive Economic Zone (EEZ), as defined by the United Nations Convention on the Law of the Sea (UNCLOS), is an area beyond and adjacent to the territorial sea of a coastal State having the sovereign rights for the purpose of exploring, exploiting, conserving and managing its natural resources. The EEZ of the Republic of Mauritius is vast (Fig. 1a). the Mascarene Plateau in the Western Indian Ocean is reputed for its fishing banks which have both economic and ecological importance (Sala *et al*., 2016). The Saya de Malha Bank (SM) (35,000 km^2), a jointly managed area by the Republic of Mauritius and Seychelles, is one of the major fishing banks of the world (WWF, 2011). Being a fairly challenging region to access by local scientists, the use of remote sensing for SM and Nazareth Bank (NZ) may prove to be a very convenient tool in providing important datasets over these vast sea areas (Shi and Wang, 2018).

Researchers all around the world are turning towards the use of satellite imaging to access biological and physical data of the ocean, especially for remote areas (Shi and Wang, 2018). Access to and acquisition of a vast range of scientific data (for instance, Chl*a* concentration, sea surface temperature and nutrients via modelling of reflectance data) (Wang *et al*., 2018), from any corner of the world has been possible using remote sensing (Colomina and Molina, 2014), even from regions that were previously inaccessible due to high traveling costs, dangers or other reasons (Zhu *et al*., 2018). Managing a vast area of the ocean can sometimes prove to be very costly and time-consuming. Hence, using remotely sensed data, for example to estimate sea surface Chl*a* concentration, can be used to predict the estimated productivity of a specific area of the ocean and monitor its change over time.

One of the most studied parameters in the ocean using remote sensing is Chl*a* concentration. Several studies on satellite-derived and *in-situ* chlorophyll distribution linked to phytoplankton density have been conducted. Numerous studies have indicated that the abundance of phytoplankton is directly proportional to the level of Chl*a* in the sea water (Felip and Catalan, 2000; Lyngsgaard *et al*., 2017) and this is explained by the fact that the Chl*a* molecule is present in all phytoplankton communities. Chl*a* as an estimate of phytoplankton abundance and temperature can be used as a sound basis to determine the productivity around fishing banks and other parts of the ocean (Townsend and Thomas, 2001). Generally, the higher the primary productivity, the higher will be the abundance of fish in an area (Capuzzo *et al*., 2018; Stock *et al*., 2017). Moreover, several studies have been conducted using various satellites such as MODIS-Aqua and SeaWiFS each having different accuracy levels, spatial and temporal resolutions, where the coefficient of determination (R^2 value) is usually used to determine the validity of the use of satellite Chl*a* concentrations (Deidun *et al*., 2011; Fleming and Korb, 2004; Wozniak *et al*., 2014) but requires ground truthing against *in situ* measurements. The aim of this study is to attempt the statistical comparison of MODIS ocean colour data, for a near-shore marine area off the north-east coastline of Malta, with *in situ* surface chlorophyll-a measurements, and to extract a twelve-month ocean colour data series for the same marine area. Peaks in surface chlorophyll-a concentration occurred in the January-February period, with lowest values being recorded during the early spring period. Log bias values indicate that the MODIS dataset under-estimates the surface chlorophyll-a values, whilst RMSD and R^2 values suggest that the match-up between satellite and *in situ* values is only partly consistent.". Around 60-78 % of the global ocean area has oligotrophic waters with Chl*a* concentrations of ≤0.25 mgm^{-3} (Armengol *et al*., 2019). A novel algorithm by Hu *et al*. (2012) has enabled scientists to use satellite extracted sea surface Chl*a* with an acceptable level of accuracy even if the waters are oligotrophic. It is now possible for scientists to determine the variability of ocean surface Chl*a* and to use this information as an index to determine primary productivity/phytoplankton biomass, both on small and large scales (Jacox *et al*., 2015; Lee *et al*., 2015).

In the Western Indian Ocean (WIO), Devassy and Goes (1991) assessed the variability of *in-situ* phytoplankton community assemblage in the EEZ of Mauritius through an oceanographic survey conducted almost two decades ago in September-October 1987. More recent micro-phytoplankton studies around MRU have also been conducted *in-situ* by Moodoosoodun *et al*. (2010) at a Marine Protected Area (MPA), Sadally *et al*. (2014a, 2015, 2016) and Sandooyea *et al*. (2020) at coral reefs and other coastal marine ecosystems, Sadally *et al*. (2014b) at a channel-based marine fish aquaculture site, and Armance *et al*. (2019) and Soondur *et al*. (2020) at a barachois-based oyster farm. Badal *et al*. (2009) used satellite global ocean color data to locate eddy formation in the South West

Mascarene Plateau while Ramchandur *et al*. (2017), using satellite data, documented the variability in Chl*a* and sea surface temperature at the NZ. However, very few studies have attempted to validate the use of satellite data by looking at *in-situ* and satellite Chl*a* and micro-phytoplankton density and diversity aspects simultaneously on the Mascarene Plateau in the WIO.

This study attempts to provide further data on Chl*a* and micro-phytoplankton from the Mascarene region which is known to be data deficient, though SM is an area of high ecological and economic importance. Therefore, the aim of this study was to validate satellite sea surface Chl*a* concentration data using *in-situ* Chl*a* data on the Mascarene Plateau. The objectives were to: (1) determine the in-situ sea surface Chl*a*

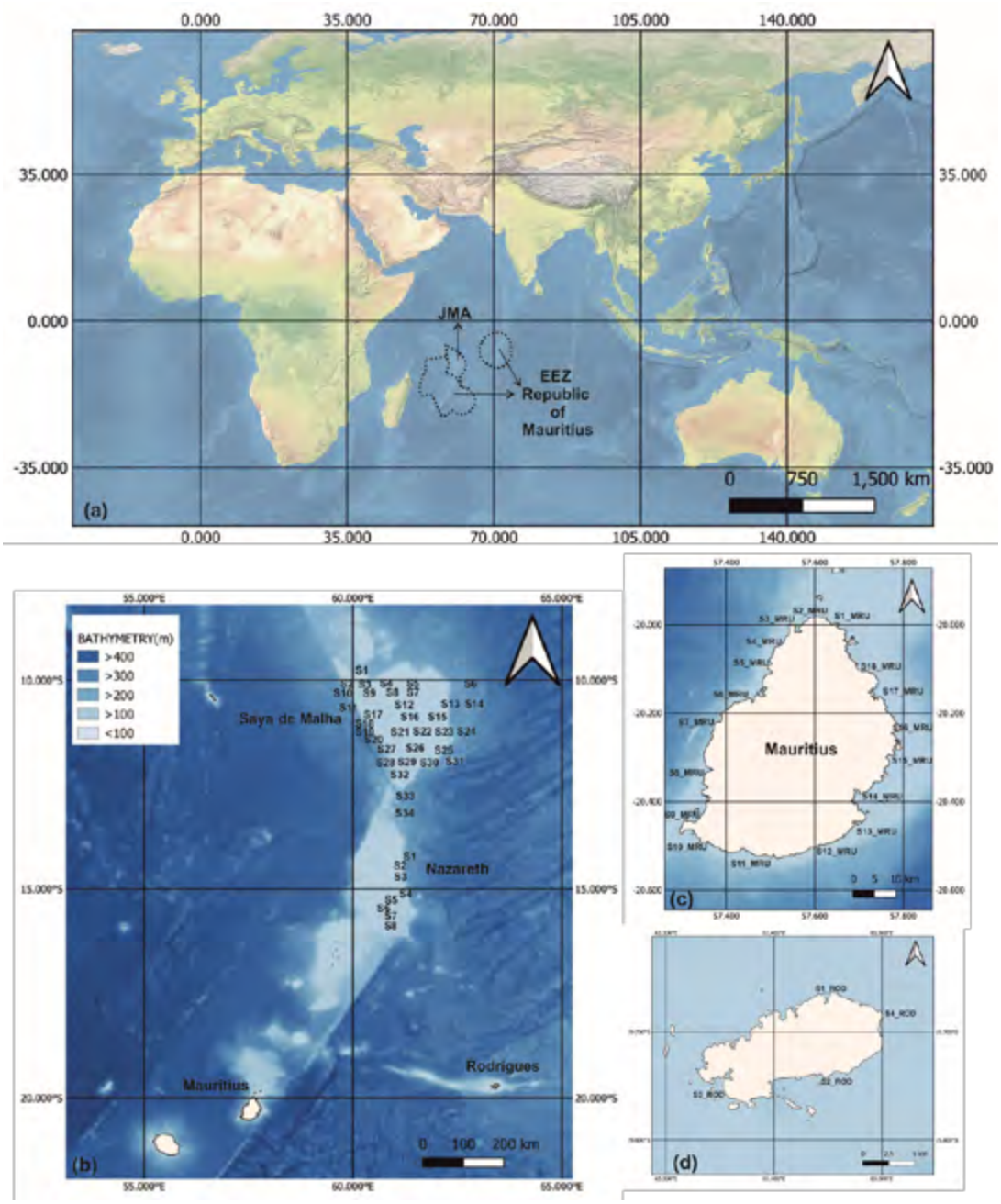

Figure 1. The world map indicating the EEZ (Exclusive Economic Zone) of the Republic of Mauritius and JMA (Joint Management Area) between the Republic of Mauritius and Republic of Seychelles. (a) EEZ and JMA boundaries; (b) the four study areas namely Saya de Malha (34 stations) and Nazareth (8 stations) Banks, Mauritius and Rodrigues Islands with indicative range of bathymetry data; (c) Mauritius Island (MRU) with the 18 stations and; (d) Rodrigues Island with 4 stations where station is referred to as "S".

concentration in four regions namely Maurituis Island (MRU), Rodrigues Island (ROD), Saya de Malha Bank (SM), and Nazareth Bank (NZ); (2) correlate *in-situ* Chl*a* data with AquaMODIS satellite sea surface Chl*a* concentrations; and (3) evaluate the density and diversity of micro-phytoplankton in the four studied regions.

Methodology

Site and stations

This study focused on four regions including MRU, ROD, and the two fishing banks SM and NZ were included in the study. ROD is located around 600 km from MRU, while SM and NZ are around 1175 km offshore from MRU. Eighteen stations (station is referred as 'S' throughout this paper) were established around MRU: S1_MRU - S18_MRU (Fig. 1c); 4 stations around ROD: S1_ROD - S4_ROD (Fig. 1d); 34 stations around SM: S1_SM - S32_SM (Fig. 1b); and 8 stations around NZ: S1_NZ - S8_NZ (Fig. 1b). A total of 67 sampling points from the 64 stations were covered, with an additional 3 samplings conducted at one of the stations at SM. Sampling was carried out during the month of April 2018 for coastal areas around MRU and ROD and during May 2018 for SM and NZ during the EAF-Nansen Indian Ocean Research Expedition 2018 on board the R/V Dr Fridtjof Nansen. The bathymetry map (Fig. 1b) gives an overview of the depth in the studied areas around the islands, where sampling was mostly done at depths less than 100 m, and at the banks where some stations were at depths greater than 400 m.

In-situ Chl*a* concentration analysis

Five hundred ml of surface seawater was collected in triplicate from each station to determine the *in-situ* Chl*a* concentration. Water samples were filtered using Whatman glass fiber filters of 0.45 µm pore size. Acetone (90% conc.) was used to extract the Chl*a* molecule from the filtrates. After 24 hrs, the extract was analyzed under a spectrophotometer at four different wavelengths (630, 647, 664 and 750 nm) (Sadally *et al.*, 2014a). The Chl*a* concentration was determined based on the formula:

$$\text{Chlorophyll } a = (11.85^{*} (E_{664} - E_{750}) - 1.54^{*} (E_{647} - E_{750}) - 0.08 (E_{630} - E_{750})) {}^{*}V_e/L^{*}V_f$$

Where: L = Cuvette light-path in centimeters; V_e = Extraction volume in milliliters; V_f = Filtered volume in liters; and concentrations in mgm^{-3} (Jeffrey and Humphrey, 1975) based on revised extinction coefficients of chlorophylls *a, b, c1* and *c2*. These equations may be used for determining chlorophylls *a* and *b* in higher plants and green algae, chlorophylls a and *c1* + *c2* in brown algae, diatoms and chrysomonads, chlorophylls a and *c2* in dinoflagellates and cryptomonads, and chlorophylls *a*, *b*, and *c1* + *c2* in natural phytoplankton.

Satellite Chl*a* concentration analysis

Satellite data for Chl*a* concentration was extracted from the AquaMODIS (Moderate Resolution Imaging Spectroradiometer) level 3, version MODISA_v2018.0, with 4 km spatial resolution from the "NASA Goddard Space Flight Center, Ocean Ecology Laboratory, Ocean Biology Processing Group, 2018". These level 3 images contain data of geophysical variables that have been derived and mapped onto a specific spatial grid for a well-defined lapse of time and atmospherically corrected. Satellite Chl*a* and temperature map data were extracted and processed on GIOVANNI Version 4.35 (https://giovanni.gsfc.nasa.gov/giovanni/). For oligotrophic waters such as those found in most regions of the Indian Ocean, the algorithm CI was used which is based on three-band reflectance (red, blue and green) using the formula of Hu *et al*. (2012):

The images were then processed using the software SeaDAS version 7.3.1 (Lacava *et al*., 2018; Pinkerton, 2003). For each specific site, five standard pixels in line with the *in-situ* area, encompassing the Chl*a*, were chosen at a resolution of 4 km each and the average calculated (Guḥmundsson *et al*., 2009). Black pixels were eliminated from the average as these were due to natural atmospheric disturbances such as cloud coverage (Carswell *et al*., 2017).

Micro-phytoplankton sample collection and processing

Ten litres of sea surface water was collected and filtered through a 5 µm plankton net and the residue was preserved using 1% Lugol's solution and stored at 4°C (Sadally *et al*., 2014a; Soondur *et al*., 2020; Zarauz and Irigoien, 2008) while keeping the maximum time lapse between sampling and fixation below 15 minutes. Centrifugation was done at 3500 rpm for 10 minutes to concentrate the sample into a 1 ml pellet (Sadally *et al*., 2014a). The samples were kept at 4°C until further processing (Mukherjee *et al*., 2014). Identification of micro-phytoplankton was done according to Tomas (1996) and Smith and Johnson (1996), and quantification was performed by loading the 1ml phytoplankton concentrate onto a Sedgwick Rafter counting chamber under a light microscope (Woelkerling *et al*.,

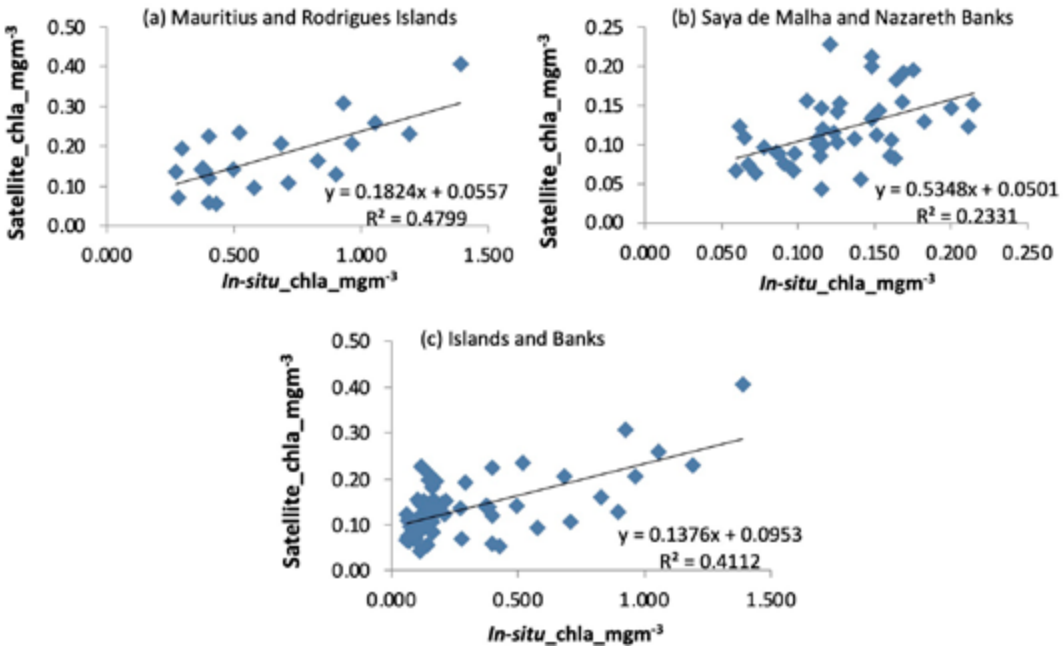

Figure 2. Scatter plot of average AquaMODIS satellite (average of 5 pixels for each data point) versus *in-situ* chlorophyll *a* (Chl*a*) data (3 replicates per data point). (a) Mauritius and Rodrigues Islands with 22 pairwise comparisons; (b) Saya de Malha and Nazareth Banks with 45 pairwise comparisons; and (c) Islands and Banks pooled to 67 pairwise comparisons.

1976; Devassy and Goes, 1991; Sadally *et al*., 2014a). The counting of micro-phytoplankton was conducted at magnifications x100, x200 and x400 and classified into three groups of diatoms, dinoflagellates, and cyanobacteria for the islands, and only two groups of diatoms and dinoflagellates at the banks. The groups were further classified into different genera. The density of micro-phytoplankton was calculated as cells L^{-1} whereby the total micro-phytoplankton density (TMPD) was taken as the sum of the different groups of micro-phytoplankton.

Data processing and statistics

The software PASW Statistics 18 was used to analyze the data. Data was first checked for normality. Non-normally distributed data was transformed via log10 or Arcsine, and one-way ANOVA, Pearson's Correlation and Tukey's HSD Post-Hoc tests were performed. Statistical tests were considered significant at $\alpha = 5\%$ level. Shannon-Wiener (*H'*) and Evenness (E_{var}) diversity indices were used to determine the variability of the different micro-phytoplankton genera. Principal Component Analysis (PCA) was conducted to determine the correlation coefficient for the different regions and the biological parameters such as Chl*a* concentration for satellite and *in-situ*, TMPD, diatom, dinoflagellate and cyanobacteria densities. The software SeaDAS version 7.3.1 was used to process the satellite data.

Results

Validation/trend in Chl*a* variation for *in-situ* and remotely-sensed data

The Chl*a* concentration variation among the 67 sampling points indicated an underestimation in the

Table 1. The regions studied with the respective number of comparisons made between *in-situ* chlorophyll *a* and satellite chlorophyll *a,* R^2 values, Pearson correlation, and the significance level.

Regions	No. of comparisons (satellite chl*a* vs In-situ class)	R^2 values	Pearson correlation, (r values)	Significance
Mauritius and Rodrigues Islands	22	0.480	0.694	*P < 0.01*
Saya de Malha and Nazareth Banks	45	0.233	0.483	*P < 0.01*
Islands and Banks	67	0.411	0.642	*P < 0.01*

satellite Chl*a* data as compared to the *in-situ* Chl*a* data (Fig. 2). A total of 22 pairwise comparison sets of data were used for the islands and 45 for the banks. The islands gave rise to a R^2 of 0.480 and a correlation of 0.694, while the banks had an R^2 of 0.233 and a correlation of 0.483. Both correlation values were significant at ($P < 0.01$). Combining both islands and banks, 67 comparisons with an R^2 of 0.411 and a correlation of 0.642 resulted (Table 1).

Additional data was extracted from GIOVANNI (https://giovanni.gsfc.nasa.gov/giovanni/) and the variations of AquaMODIS satellite sea surface Chl*a* and temperature were determined. The data on Chl*a* concentration in the WIO showed similar trends during the average months of March-April and May-June 2018. During April, SST around the islands was greater than 27.0°C (Fig. 3a) and during May, the temperature dropped below 27.0°C (Fig. 3b). The same scenario was apparent at the banks where in April SST was greater than 28.5°C (Fig. 3c) and during May, it dropped below 28.5°C (Fig. 3d). On average there was a difference of 1.5°C between the islands and the banks.

Micro-phytoplankton density variation Mauritius and Rodrigues Islands

At MRU, the one-way ANOVA revealed a strong spatial difference among the 18 stations (S1_MUR - S18_MUR) for the total micro-phytoplankton density (TMPD), as well as for the diatom, dinoflagellates and cyanobacteria densities ($P < 0.001$) (Table 2). Highest TMPD were recorded in the eastern regions at stations S14_MRU ($19.4 \pm 1.4 \times 10^4$ cells L^{-1}), S15_MRU ($19.8 \pm 0.6 \times 10^4$ cells L^{-1}) and S16_MRU ($20.0 \pm 1.4 \times 10^4$ cells L^{-1}), and the lowest densities were mainly in the western region at S5_MRU ($8.6 \pm 0.8 \times 10^4$cellsL^{-1}), S6_MRU ($9.4 \pm 1.3 \times 10^4$ cells L^{-1}) and S12_MRU ($7.7 \pm 0.8 \times 10^4$ cells L^{-1}) (Fig. 4). Diatoms contributed most to the TMPD followed by dinoflagellates and cyanobacteria. The highest and lowest densities of diatoms was recorded at the same

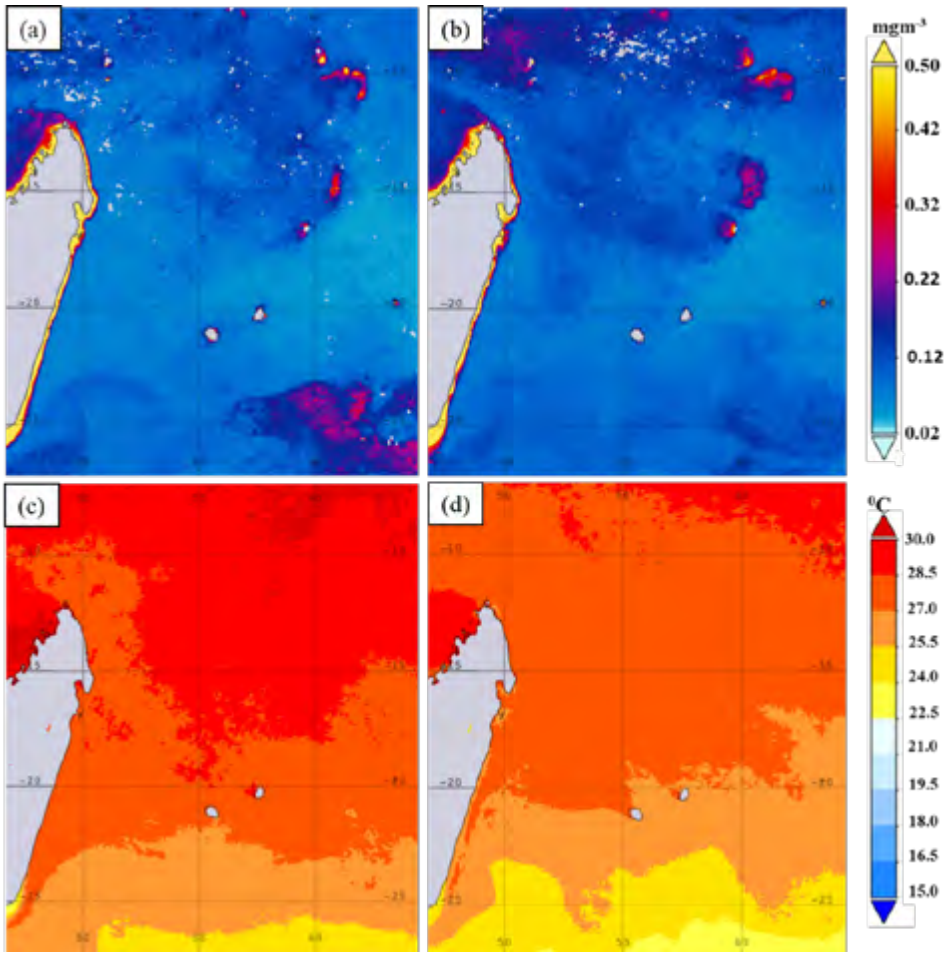

Figure 3. Average AquaMODIS satellite data: (a) Sea Surface Chl*a* concentration for April 2018; (b) Sea Surface Chl*a* concentration for May 2018; (c) Sea Surface Temperature for April 2018; and (d) Sea Surface Temperature for May 2018.

Table 2. One-way ANOVA for comparing the different densities of total micro-phytoplankton, diatom, dinoflagellates and cyanobacteria at different stations at the islands and banks.

Islands	**Mauritius**					**Rodrigues**				
Total micro-phytoplankton	SS	df	MS	F	P-value	SS	df	MS	F	P-value
Between Stations	12.136	19	0.639	49.949	***	2.215	3	0.738	99.115	***
Diatom										
Between Stations	3.439	19	0.181	25.711	***	0.626	3	0.209	24.889	***
Dinoflagellates										
Between Stations	1.125	19	0.059	18.108	***	0.253	3	0.084	37.679	***
Cyanobacteria										
Between Stations	0.416	19	0.022	10.658	***	0.055	3	0.018	15.803	***
Banks	**Saya de Malha**					**Nazareth**				
Total Phytoplankton	SS	df	MS	F	P-value	SS	df	MS	F	P-value
Between Stations	0.577	36	0.016	11.627	***	0.047	7	0.007	8.324	***
Diatom										
Between Stations	0.294	36	0.008	10.468	***	0.038	7	0.005	8.932	***
Dinoflagellates										
Between Stations	0.088	36	0.002	4.323	***	0.002	7	0.000	0.580	*NS*

*P < 0.001 = ***, P < 0.01 = **, P < 0.05= *, NS = Not Significant*

stations as the total micro-phytoplankton, and ranged between 4.0 ± 0.6 ×10⁴ cells L⁻¹ and 10.4 ± 1.0 ×10⁴ cells L⁻¹ (Fig. 4). Moreover, S14_MRU also recorded the highest density of dinoflagellates of 6.7 ± 0.9 ×10⁴ cells L⁻¹. S12_MRU, which recorded the lowest diatom density, also recorded the lowest density of dinoflagellates (2.7 ± 0.5 ×10⁴ cells L⁻¹) and cyanobacteria (1.0 ± 0.2 ×10⁴ cells L⁻¹), while S16_MRU had the highest density of cyanobacteria (3.4 ± 1.1 ×10⁴ cells L⁻¹) (Fig. 4). Out of the 18 stations around MRU, stations that recorded ≥ 50% dominance in diatoms were S1_MRU, S2_MRU, S3_MRU, S4_MRU, S7_MRU, S8_MRU, S9_MRU, S10_MRU, S11_MRU, S12_MRU, S15_MRU, S16_MRU, S17_MRU (Fig. 5).

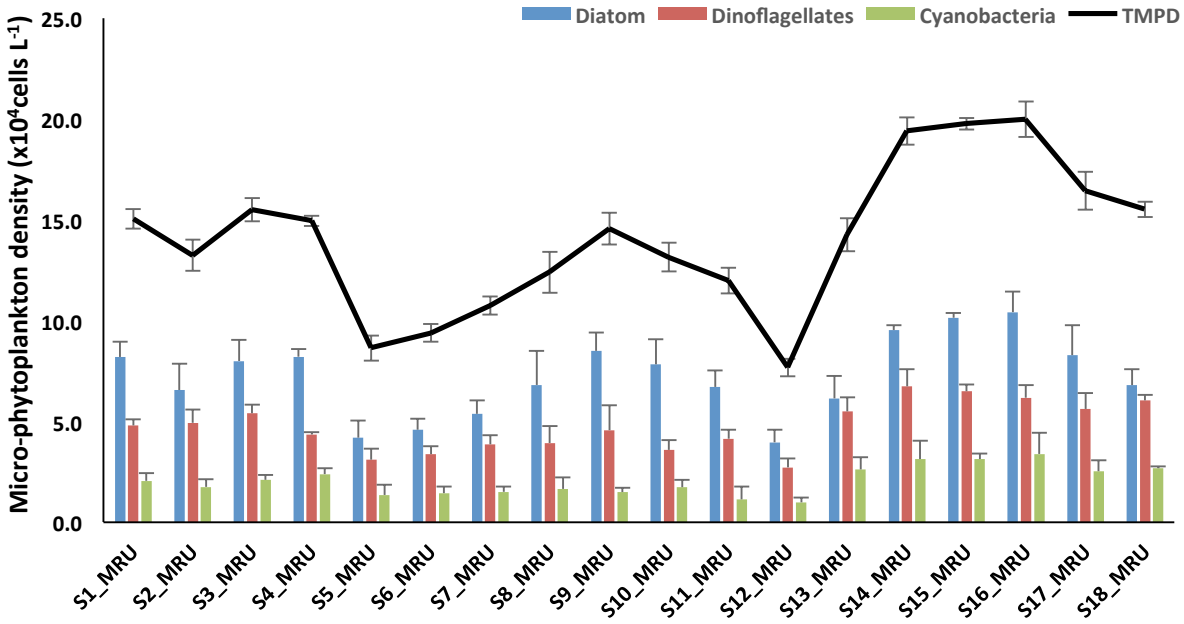

Figure 4. Densities of total micro-phytoplankton (TMPD), diatom, dinoflagellates and cyanobacteria around Mauritius Island (MRU) at 18 stations, where station is referred to as "S".

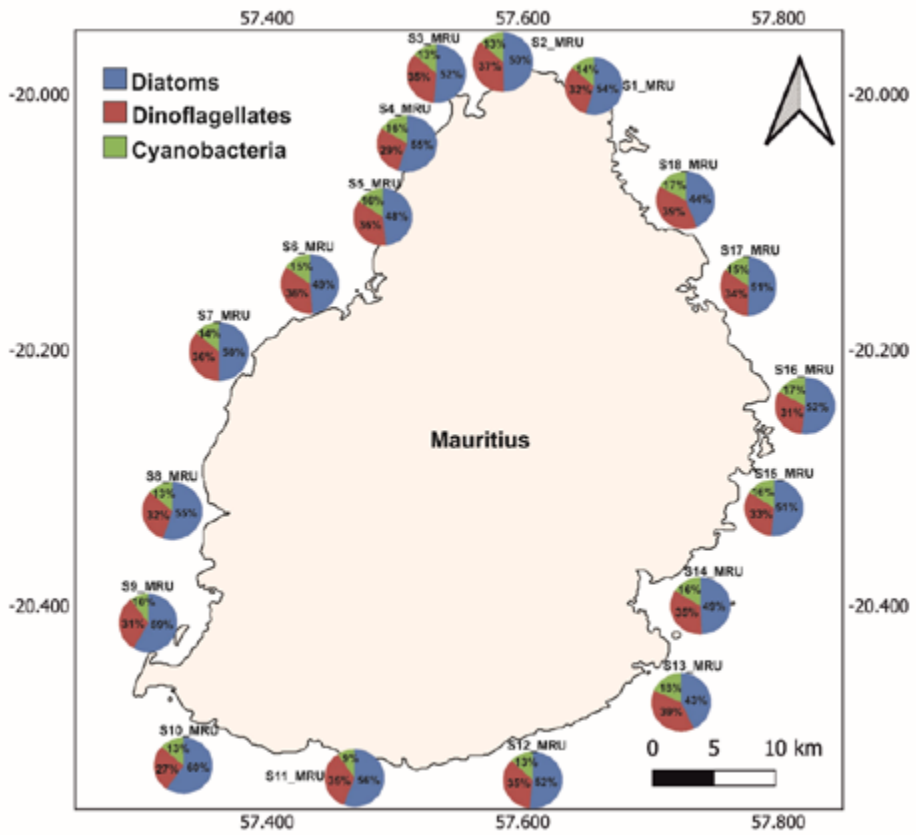

Figure 5. Percentage composition of the three groups of micro-phytoplankton (diatom, dinoflagellates and cyanobacteria) around Mauritius Island (MRU) where station is referred to as "S".

At ROD, the densities mainly followed the trend S1_ROD > S2_ROD > S4_ROD > S3_ROD. This trend was the same for the total micro-phytoplankton, diatom and dinoflagellates densities, except for the cyanobacteria where the lowest density was recorded at station S4_ROD. The total micro-phytoplankton ranged between 17.6 ± 1.2 × 10^4 cells L^{-1} and 8.8 ± 0.2 × 10^4 cells L^{-1}; diatoms between 9.1 ± 1.4 × 10^4 cells L^{-1} and 4.6 ± 0.5 × 10^4 cells L^{-1}; dinoflagellates between 6.0 ± 0.3 × 10^4 cells L^{-1} and 2.7 ± 0.5 ×10^4 cells L^{-1}; and cyanobacteria between 2.5 ± 0.3 × 10^4 cells L^{-1} and 1.5 ± 0.3 × 10^4 cells L^{-1} (Fig. 6). At the 4 stations around ROD, all recorded

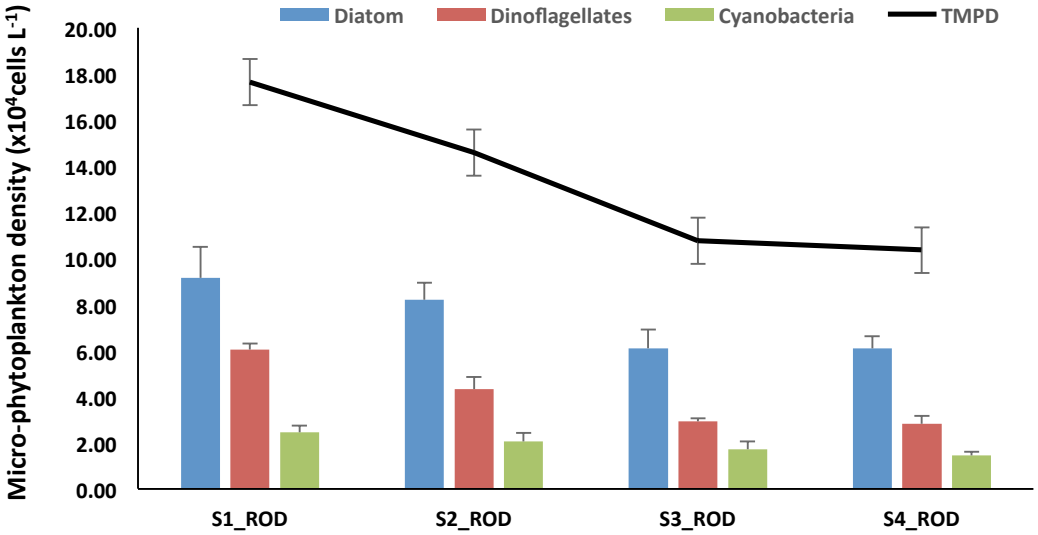

Figure 6. Densities of total micro-phytoplankton (TMPD), diatom, dinoflagellates and cyanobacteria around Rodrigues Island (ROD) at 4 stations, where station is referred to as "S".

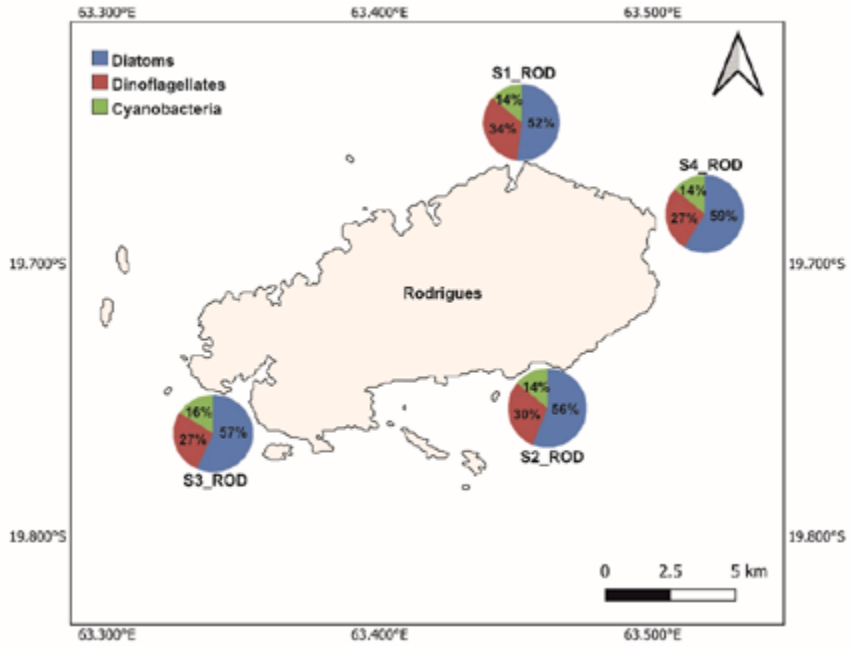

Figure 7. Percentage composition of the three groups of micro-phytoplankton (diatom, dinoflagellates and cyanobacteria) around Rodrigues Island (ROD) where station is referred to as "S".

≥ 50% dominance in diatoms (Fig. 7). Site-wise, for the different densities (total micro-phytoplankton, diatom, dinoflagellates and cyanobacteria), the one-way ANOVA test confirmed that there were strong significant differences at ($P < 0.001$) (Table 2).

Saya de Malha and Nazareth Banks

At SM the total micro-phytoplankton densities ranged between 3.0 - 4.0 x 10^4 cells L^{-1} for most stations except for S5_SM, S7_SM, S12_SM, S16_SM and S20_SM which had higher than 4.0 x 10^4 cells L^{-1} (Fig. 8). The highest diatom densities were recorded at station S5_SM, S7_SM, S12_SM and S16_SM which was above 3.0 x 10^4 cells L^{-1} (Fig. 8). For the rest of the stations, the densities were below 3.0 x 10^4 cells L^{-1}. The densities of dinoflagellates varied highly with the highest density recorded at station S12_SM (1.9 x 10^4 cells L^{-1}) and the lowest at S22_SM (0.8 x 10^4 cells L^{-1}) (Fig. 8). All the

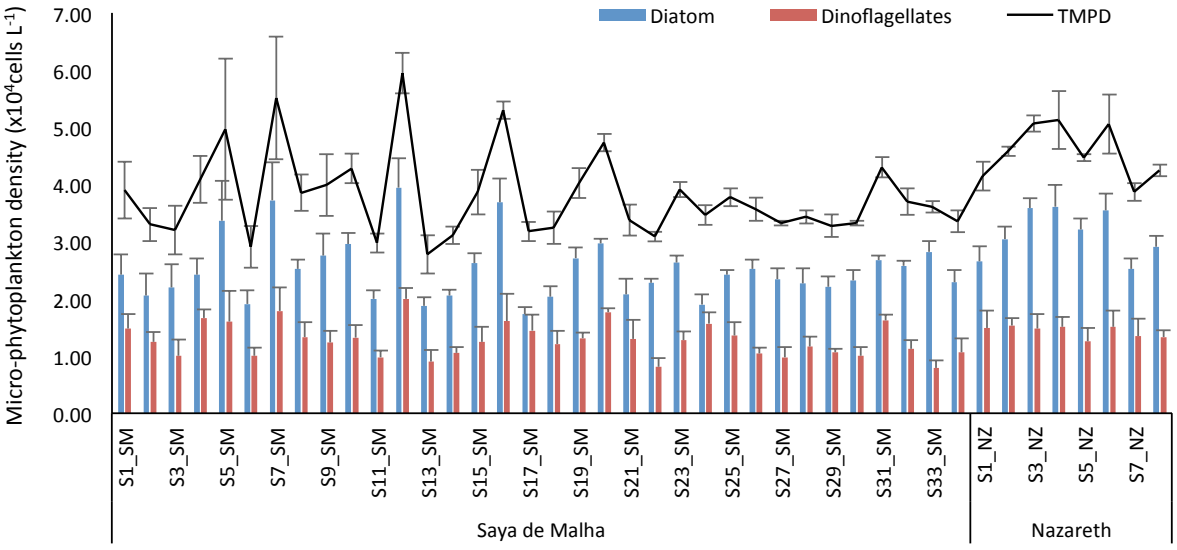

Figure 8. Densities of total micro-phytoplankton (TMPD), diatom and dinoflagellates in the Mascarene region at Saya de Malha (SM) and Nazareth (NZ) Banks where station is referred to as "S".

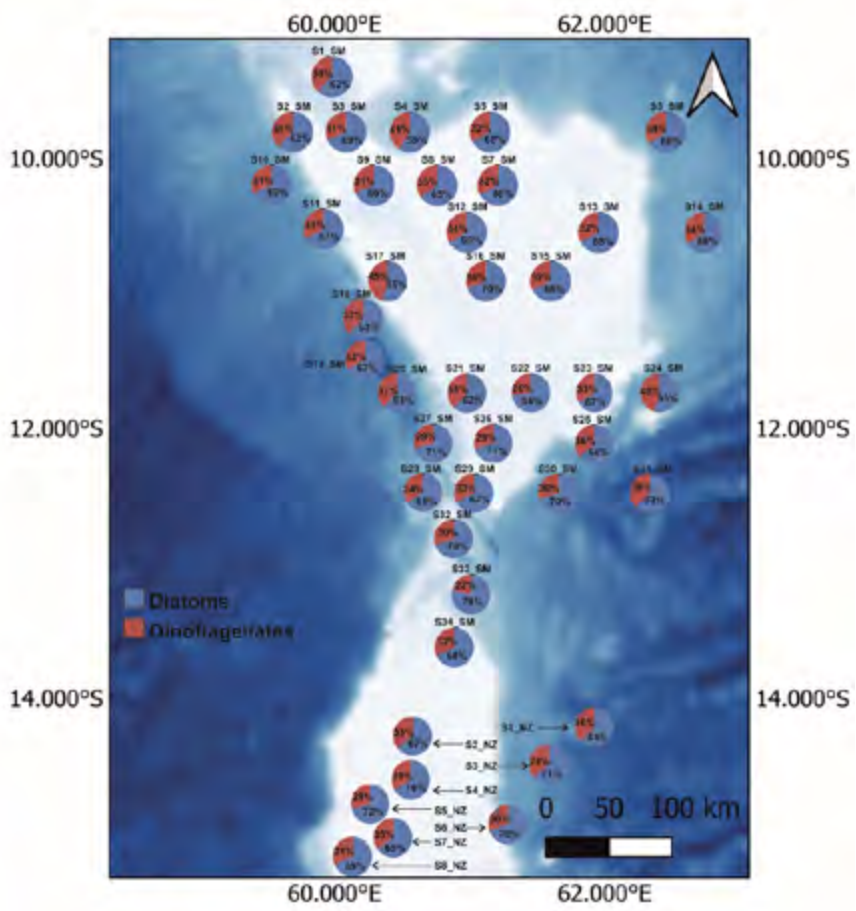

Figure 9. Percentage composition of the two groups of micro-phytoplankton (diatom and dinoflagellates) in the Mascarene region at Saya de Malha (SM) and Nazareth (NZ) Banks where station is referred to as "S".

34 stations recorded diatoms as the dominant group, and stations that showed diatom percentages ≥ 70% were S16_SM, S26_SM, S27_SM, S30_SM, S32_SM and S33_SM (Fig. 9). The one-way ANOVA showed the stations differed significantly ($P < 0.001$) for all the densities of total micro-phytoplankton, diatoms and dinoflagellates (Table 2).

At NZ, it was found that apart from station S6_NZ, all the other stations' total micro-phytoplankton densities were above 4.0 x 10^4 cells L^{-1}. The highest diatom densities were recorded at S2_NZ, S4_NZ and S6_NZ with over 1.5 x 10^4 cells L^{-1} and the lowest density was recorded at S7_NZ (1.2 x 10^4 cells L^{-1}) (Fig. 8). The densities of dinoflagellates at NZ did not differ a lot. Among the demarcations, the lowest density of dinoflagellates was recorded at station S5_NZ. The dominance of diatoms prevailed with diatom percentage ≥ 70% observed at S3_NZ, S4_NZ, S5_NZ, S6_NZ (Fig. 9). The one-way ANOVA showed the density of dinoflagellates between the stations did not differ significantly ($P > 0.05$) but for the total phytoplankton and diatom densities, the difference was significant at ($P < 0.001$) (Table 2).

Principal component analyses

The Principal Component Analysis (PCA) was performed with the data from the islands and banks separately. The parameters that were considered were the *in-situ* Chl*a*, satellite Chl*a*, and the densities of diatom, dinoflagellates, cyanobacteria, and total micro-phytoplankton. Around the islands, the PCA explained 85.50% of the total data variance where F1 had more influence with 72.33% (Eigen value = 4.340) compared to F2 with 13.47% (Eigen value = 0.790) (Fig. 10a). A similar trend was observed at the banks where F1 had more influence with 57.77% (Eigen value = 2.954) and F2 with 24.91% and a total of 82.68% (Eigen value = 1.219) (Fig. 10b). A high correlation between the satellite and *in-situ* Chl*a* concentration both at the islands and the banks was revealed (Fig 10). The PCA showed the highest correlation of TMPD with diatom and dinoflagellates followed by cyanobacteria for the islands. Compared to the islands, the banks had a

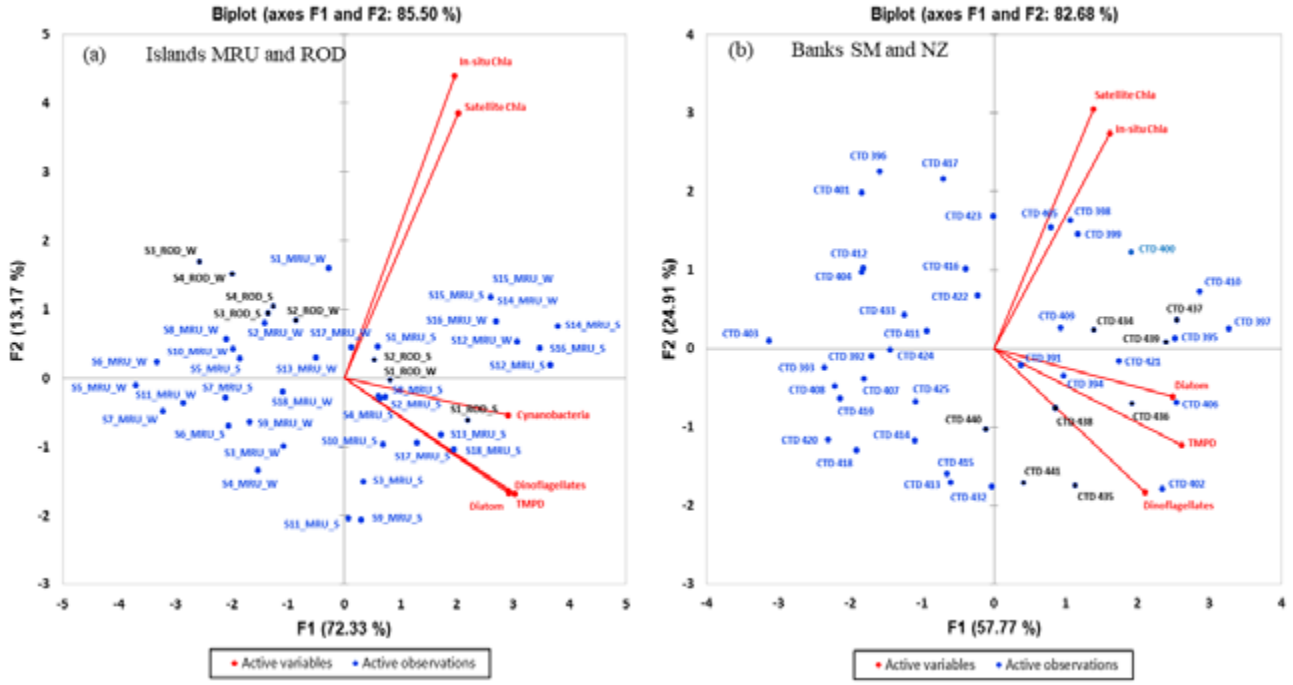

Figure 10. The Principal Component Analysis (PCA) representing correlation coefficient analysis for the different regions and the biological parameters of Chlorophyll *a* (Chl*a*) concentration for satellite and *in-situ*, Total Micro-Phytoplankton Density (TMPD), Diatom, Dinoflagellates and Cyanobacteria densities. (a) Mauritius Island (MRU) with 18 stations and Rodrigues Island (ROD) with 4 stations; and (b) Saya de Malha Bank (SM) with 32 stations and Nazareth Bank (NZ) with 8 stations.

higher positive correlation with the TMPD in diatoms compared to the dinoflagellates (Fig. 10).

Micro-phytoplankton diversity

The diversity of the micro-phytoplankton was investigated at 18 sites around MRU where 47 different genera were identified out of which 28 were diatoms, 12 dinoflagellates and 7 cyanobacteria. Around ROD (4 sites), 47 different genera of micro-phytoplankton were identified of which 28 were diatoms, 12 dinoflagellates and 7 cyanobacteria. On the Mascarene Plateau at the banks of SM and NZ, 23 diatoms and 11 dinoflagellates genera were identified. Figure 11 shows some of the common genera of micro-phytoplankton identified in the EEZ of the Republic of Mauritius.

On average at the four different sites the most dominant diatoms genera in terms of percentage in the community structure were *Coscinodiscus* (14.64%), *Navicula* (11.78%), *Nitzschia* (8.87%), *Chaetoceros* (8.27%), *Fragilaria* (5.68%) and *Licmorphora* (5.04%). *Coscinodiscus* and *Navicula* were the two diatom genera that were uniformly present at the four different sites. *Fragilaria* and *Licmorphora* were abundant around the islands (> 7.00%) compared to the banks (< 3.00%). For the dinoflagellates, *Ceratium* occupied the highest percentage accounting for 24.01%, followed by *Peridinium* (16.43%), *Oxyphysis* (13.09%), *Oxytoxum* (11.99%) and *Dinophysis* (8.24%). Out of the 5 dominant dinoflagellates genera, all showed consistency in percentage distribution. Cyanobacteria were identified only at the islands of MRU and ROD where the four most abundant genera were *Anabaena* (21.30%), *Lyngbya* (19.86%), *Nodularia* (19.30%) and *Oscillatoria* (17.77%). Some genera like *Actinoptuchus*, *Asteromphalus*, *Proboscia* and *Rhizosolenia* showed considerably higher densities at the banks compared to the islands (Table 3).

Shannon-Wiener and Evenness indices

The Shannon-Wiener diversity index revealed that the distribution of diatoms around MUR and ROD, and SM and NZ were all above H' > 2.5 with the islands having higher mean values compared to the banks. For the dinoflagellates, the H' was between 2 and 2.5 and for the cyanobacteria groups at MUR and ROD, the values ranged between 1.5 and 2 (Fig. 12a). The mean of the Evenness of dinoflagellates at SM was nearly the same as at NZ, but for the diatom, it was totally different. Overall, the different classes of micro-phytoplankton around the islands were more evenly distributed with a mean of the E_{var} > 0.6 compared to

Table 3. The percentage genera composition of different micro-phytoplankton at Mauritius (MRU), Rodrigues (ROD), Saya de Malha (SM) and Nazareth (NZ) Banks where the total percentage of each of micro-phytoplankton groups (diatom/dinoflagellates/cyanobacteria) made up 100%. Bold and highlighted cells indicate high percentages observed.

	Genera	MRU	ROD	SM	NZ	EEZ
Diatom	*Actinoptuchus*	1.70	2.26	4.93	3.94	3.21
	Asteromphalus	1.68	2.55	4.57	3.53	3.08
	Asterionellopsis	1.85	2.18	0.66	0.58	1.32
	Biddulphia	1.49	2.02	0.64	0.48	1.16
	Bleakeleya	1.87	1.81	0.00	0.00	1.84
	Chaetoceros	**7.40**	**5.96**	**9.94**	**9.77**	**8.27**
	Coscinodiscus	**14.27**	**11.81**	**15.95**	**16.55**	**14.64**
	Dactyliosolen	1.66	1.28	2.48	2.89	2.08
	Detonula	1.81	2.06	1.12	1.68	1.67
	Diploneis	2.03	1.69	0.00	0.00	1.86
	Eucampia	2.17	1.97	1.57	2.23	1.99
	Fragilaria	**7.71**	**11.93**	**1.92**	**1.17**	**5.68**
	Guinardia	2.27	2.18	1.17	1.17	1.70
	Haslea	1.71	2.06	0.00	0.00	1.88
	Hemiaulus	2.20	2.47	1.73	2.14	2.13
	Leptocylindrus	2.54	2.71	1.88	4.75	2.97
	Licmorphora	**7.55**	**8.14**	**1.47**	**2.98**	**5.04**
	Lioloma	2.06	1.60	0.00	0.00	1.83
	Melosira	1.74	1.11	1.36	1.08	1.32
	Odontella	1.88	2.02	0.00	0.00	1.95
	Proboscia	1.92	2.26	5.19	7.60	4.24
	Rhizosolenia	1.73	1.40	4.61	8.91	4.16
	Skeletonema	2.01	1.73	2.08	3.85	2.42
	Thalassiosira	2.11	2.34	0.32	0.93	1.43
	Navicula	**10.73**	**9.50**	**15.08**	**11.81**	**11.78**
	Nitzschia	**8.44**	**7.90**	**13.23**	**5.91**	**8.87**
	Pseudo_Nitzschia	3.16	2.71	3.45	3.49	3.20
	Thalassionema	2.29	2.34	4.63	2.56	2.96
Dinoflagellates	*Alexandrium*	2.72	3.24	2.37	2.38	2.68
	Amphidinium	5.26	5.94	3.46	4.63	4.82
	Ceratium	**24.89**	**22.48**	**23.73**	**24.92**	**24.01**
	Dinophysis	**7.88**	**7.36**	**8.28**	**9.42**	**8.24**
	Gonyaulax	3.98	5.06	5.17	6.02	5.06
	Gymnodinium	2.58	3.92	3.66	5.02	3.80
	Oxyphysis	**10.45**	**10.53**	**16.59**	**14.79**	**13.09**
	Oxytoxum	**10.67**	**10.47**	**12.76**	**14.08**	**11.99**
	Peridinium	**19.71**	**19.24**	**14.63**	**12.15**	**16.43**
	Polykriskos	3.47	3.78	5.40	3.44	4.02
	Prorocentrum	3.53	3.78	0.00	0.00	3.65
	Pyrocystis	4.86	4.19	3.94	3.15	4.03
Cyanobacteria	*Anabaena*	**23.07**	**19.54**	0.00	0.00	**21.30**
	Lyngbya	**19.10**	**20.62**	0.00	0.00	**19.86**
	Nodularia	**19.60**	**19.00**	0.00	0.00	**19.30**
	Oscillatoria	**17.23**	**18.32**	0.00	0.00	**17.77**
	Phormidium	10.58	7.73	0.00	0.00	9.16
	Snowella	5.43	8.55	0.00	0.00	6.99
	Spirulina	5.01	6.24	0.00	0.00	5.62

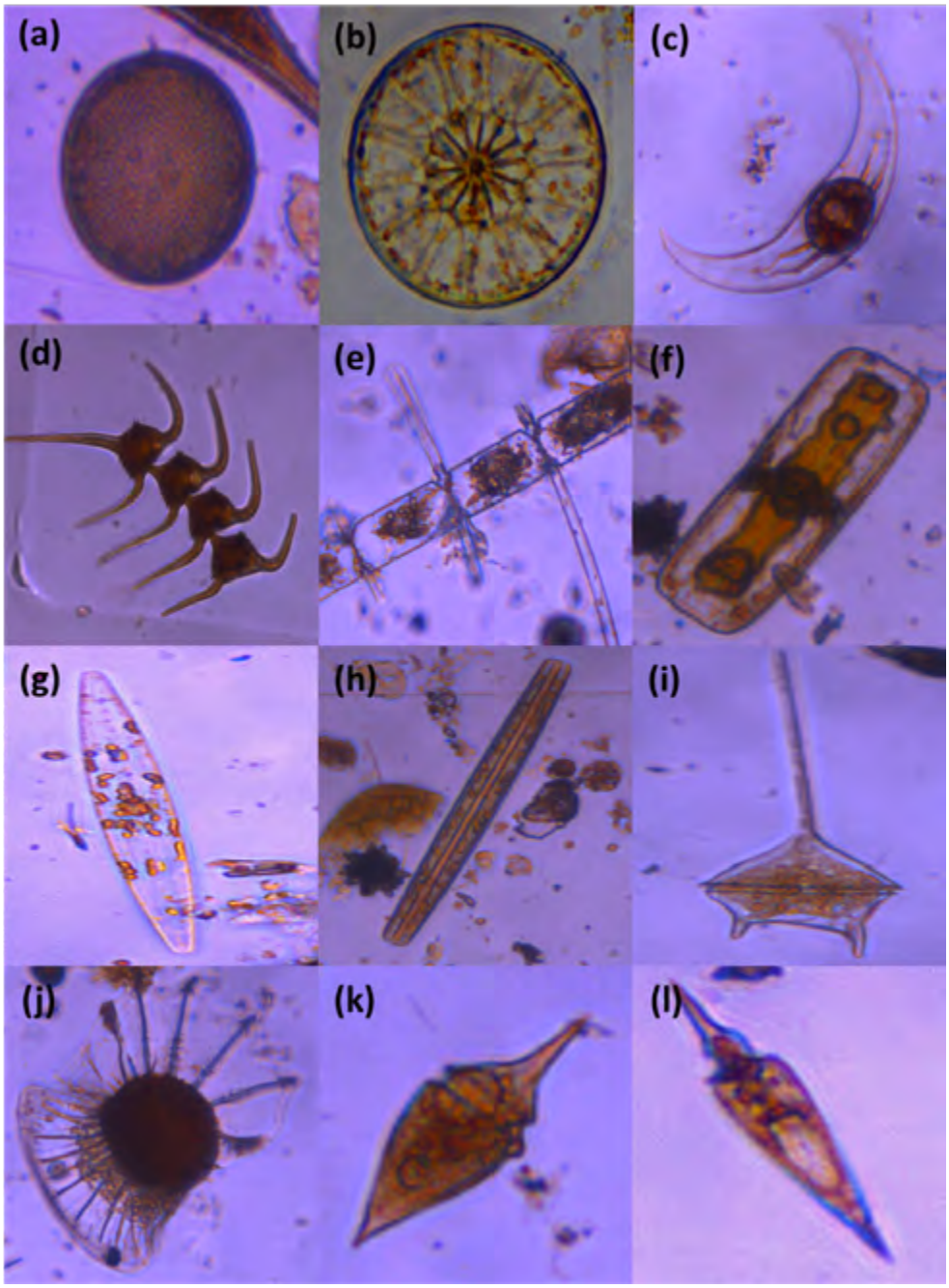

Figure 11. Common micro-phytoplankton genera in the EEZ of the Republic of Mauritius and the Joint Management Area (JMA) between the Republic of Mauritius and Republic of Seychelles. a) *Coscinodiscus*; b) *Asteromphalus*; c) *Pyrocystis*; d) *Ceratium sp1*; e) *Chaetoceros*; f) *Navicula*; g) *Nitzschia*; h) *Thalassionema*; i) *Ceratium sp2*; j) *Dinophysis*; k*) Oxyphysis*; l) *Oxytoxum.*

the fishing banks with a mean E_{var} < 0.6, except for the group of cyanobacteria around ROD which had a mean of E_{var} < 0.6 (Fig. 12b). Overall, the diatom had higher genera variability followed by dinoflagellates and cyanobacteria. The Shannon-Wiener indices revealed that the highest biodiversity was among the genera of diatoms. A high Evenness value showed that the number of individual genera of micro-phytoplankton was fairly equal.

Discussion

Oligotrophic waters are categorized as being exceptionally clear due to very low concentrations of chlorophyll and low levels of chromophoric dissolved organic matter. Furthermore, these waters have low concentration of nutrients and phytoplankton biomass which depict low primary productivity (Jena *et al*., 2013). In this study, satellite data indicated low concentrations of Chl*a* in the Indian Ocean waters

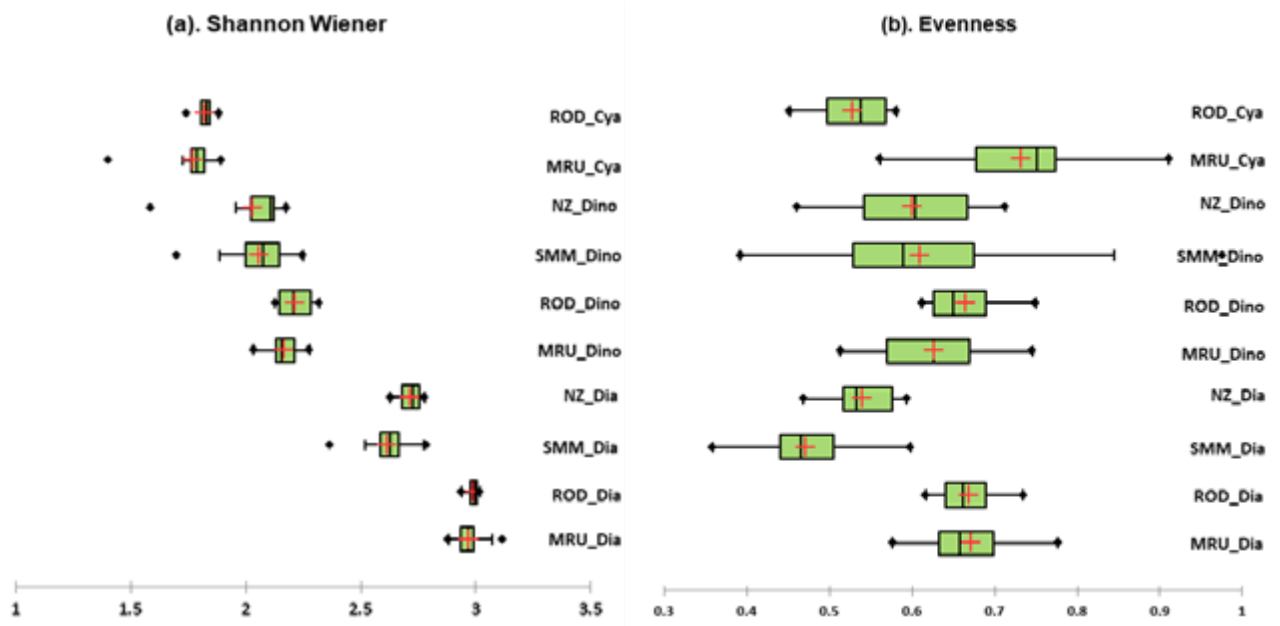

Figure 12. The representation of box plots for the diversity indices of the biological parameters Diatom (Dia), Dinoflagellates (Dino), and Cyanobacteria (Cya) at the islands of Mauritius (MRU) and Rodrigues (ROD) and the banks of Saya de Malha (SM) and Nazareth (NZ) where (a) is the Shannon Wiener (H') and (b) is Evenness (E_{var}).

around the islands of MRU and ROD, and the Mascarene Plateau. This observation corroborated studies that reported the Southern Indian Ocean as having oligotrophic waters (Morel *et al*., 2010). Using the algorithm developed by Hu *et al*. (2012), the AquaMODIS Chl*a* satellite was effectively used in oligotrophic waters where the concentration of Chl*a* is ≤ 0.25 mg m^{-3}. Several studies worldwide have supported the use of satellite data (Gregg and Rousseaux, 2014; Mudgal *et al*., 2009; Tilstone *et al*., 2013).

Several studies have investigated the relationship between satellite and *in-situ* Chl*a* data and the strength of R^2 values were found to be variable. A study conducted by Gregg and Casey (2004) reported a fairly low R^2 value for the regression between satellite and *in-situ* Chl*a* concentration data in regions near the Equatorial Indian Ocean, whereas the southern Indian Ocean had a higher value. Low R^2 values (0.168 and 0.116) for satellite verses *in-situ* Chl*a* data were found in Maltese coastal waters (Deidun *et al*., 2011) but requires ground truthing against in situ measurements. The aim of this study is to attempt the statistical comparison of MODIS ocean colour data, for a near-shore marine area off the north-east coastline of Malta, with in situ surface chlorophyll-a measurements, and to extract a twelve-month ocean colour data series for the same marine area. Peaks in surface chlorophyll-a concentration occurred in the January-February period, with lowest values being recorded during the early spring period. Log bias values indicate that the MODIS dataset under-estimates the surface chlorophyll-*a* values, whilst RMSD and R^2 values suggest that the match-up between satellite and in situ values is only partly consistent. and it was attributed to the low set of matchup comparisons. In the present study lower R^2 values were recorded at SM and NZ (nearer the Equatorial Indian Ocean) compared to those around MRU and ROD Islands (in the southern Indian Ocean). It is noteworthy that even with a relatively low number of pairwise comparison data sets (67) obtained during April and May 2018, there was a significant correlation (R^2 of 0.411; 0.642; $P < 0.01$) between satellite and *in-situ* Chl*a* concentration, explaining about half of the variance in the *in-situ* values. This suggests that satellite Chl*a* data from the AquaMODIS sensor may act as a relatively good potential predictor of spatial trends in the EEZ of the Republic of Mauritius and in the JMA. A larger number of comparative data points for the satellite and *in-situ* Chl*a* would probably minimize the scatter in the relationship and the margin of bias and error (Clerici *et al*., 2008; Fleming and Korb, 2004). Additional data points at different times of the season and for several years would generate a more robust dataset for appropriate assessments of seasonal and inter-annual variations, and may increase the confidence of this validation and yield a higher R^2 value.

The inhabited Islands of MRU and ROD are expected to be affected by anthropogenic activities as compared

to the remote regions of the Mascarene Plateau like SM and NZ (Ramessur, 2002). Thus, the higher density of micro-phytoplankton recorded around both islands compared to the two banks may be attributed to the Island Mass Effect (IME) being higher at the islands, linked to anthropogenic influences, compared to the remote Mascarene regions. Elliott *et al*. (2012) and eddies on the downstream side of the island that form in both tidal and steady currents. In some cases, runoff from the island and/or exchange with a lagoonal system can enhance nearshore production. Phytoplankon blooms in otherwise oligotrophic systems have the potential to increase nearshore zooplankton abundance. Greater availability of nearshore zooplankton may help reefs cope with stressors such as bleaching events. Palardy *et al.* (2008) used remote sensing to confirm an IME around MRU and ROD. The IME tends to boost primary productivity more around oceanic islands compared to the adjacent waters. Several physical factors drive the IME including tidal change, runoff of freshwater with its associated nutrient loading, coastal upwelling due to wind velocity coupled with mass water flow, wave actions, and Ekman transport (Jena, 2016). Tidal changes that occur four times in a diel cycle promote the mixing of the different water layers which may enhance primary productivity and an increase in phytoplankton biomass (Blauw *et al*., 2012) we analyzed fluctuations in coastal phytoplankton concentration in relation to the tidal cycle. Time series of chlorophyll fluorescence, suspended particulate matter (SPM).

Around MRU, higher total micro-phytoplankton density was recorded in the south-east region, and the lowest in the extreme south region. The south-east region of Mauritius is characterized by many river discharges and highly turbid waters (Turner and Klaus, 2005) having high organic matter content which is converted to nutrients by bacterial recycling and enhances phytoplankton growth. Furthermore, there are mangrove areas in these specific regions (Appadoo, 2003) which promote the growth of phytoplankton (Saifullah *et al*., 2016). The southern region of MRU is characterized by high wave action and there is an absence of high reef barriers on certain parts of the coast (Elliott *et al*., 2018; Turner and Klaus, 2005). This potentially leads to a higher mixing rate of the water which in turn leads to a decrease in the phytoplankton density.

Sadally *et al*. (2014a) reported a low density of phytoplankton at certain sites around MRU, especially around the reef zone where there is high levels of water flushing. Furthermore, the southeast trade winds probably enhance coastal upwelling and give a boost to primary productivity in the eastern region of MRU (González-Rodríguez *et al*., 2012) a highly productive area off the western coast of the Baja California Peninsula, is examined for five successive years (2003-2007). In the northern and southern parts of ROD, the presence of mangrove ecosystems explains the higher density of micro-phytoplankton compared to the eastern and western zones. ROD most probably faces the impacts of anthropogenic activities as does MRU together with the input of nutrients from runoff to promote the growth of phytoplankton. The rate of runoff at ROD may be greater as it is a more mountainous island.

The plankton dynamics around the Mascarene Plateau is mainly influenced by natural environmental drivers such as wave action, upwelling, mass water flow, and climate change. This region may be least affected by direct anthropogenic activities owing to its distant location from the inhabited islands of MRU and ROD, and subsequent inaccessibility. Badal (2003) highlighted that a mini-monsoon had enhanced the primary productivity on the Mascarene Plateau. The high productivity in the region of the Mascarene Plateau can be attributed to the shallowness of the fishing banks of SM and NZ that may cause accumulation of nutrients rising to the upper layer of the water through upwelling (Vortsepneva, 2008). Lower phytoplankton density on the Mascarene Plateau may be attributed to the open ocean circulation that may impact both density and diversity.

This study revealed that the islands of MRU and ROD, and the SM and NZ of the Mascarene region had higher diatom density compared to dinoflagellates. This trend has been observed in several studies (Aubry *et al*., 2006; Devassy and Goes, 1991; Sadally *et al*., 2014). Diatoms are known to be more robust and adaptive to changes in environmental conditions such as temperature and salinity. The reproductive rate of diatoms is very high (Chepurnov *et al*., 2004). The dominant species in this study, *Navicula* and *Coscinodiscus,* were also reported to be abundant in many other studies. *Fragilaria* was most abundant at sites near freshwater rivers. The genera *Fragilaria* has been reported to be highly abundant in some freshwater ecosystems (Almeida *et al*., 2016).

Conclusion

Satellite-derived sea surface Chl*a* concentrations in the Mascarene Plateau region and the EEZ of Mauritius may be used as a good proxy for *in-situ* Chl*a*, with a fair level of confidence. These data may potentially serve as a basis to better determine areas of high productivity and eventually contribute towards achieving sustainability in the fisheries sector. Variable micro-phytoplankton density and diversity was found at the studied stations and regions. Densities were higher around the islands compared to the open sea on the Mascarene Plateau, though the micro-phytoplankton communities tended to be dominated by similar genera. It is important to explore the existing limited data set so that future studies may advance this field of study through further data collection and analyses, especially in the data-deficient Mascarene region. Further research is warranted in order to thoroughly capture the intra- and inter-annual variations in Chl*a* and micro-phytoplankton distribution on the Mascarene Plateau.

Acknowledgements

The underlying work was made possible with the support of the EAF-Nansen Programme "Supporting the Application of the Ecosystem Approach to Fisheries Management considering Climate Change and Pollution Impacts" executed by Food and Agriculture Organization of the United Nations (FAO) and funded by the Norwegian Agency for Development Cooperation (Norad). The authors are thankful to FAO for funding and supporting the Indian Ocean research expedition 2018 on the Saya de Malha Bank and Nazareth Bank with the R/V Dr Fridtjof Nansen, the Department of Continental Shelf, Maritime Zones Administration & Exploration of Mauritius for co-leading and coordinating the scientific expedition, the Mauritius-Seychelles Joint Commission of the Extended Continental Shelf for their support and assistance and granting the necessary authorisations, the Ministry of Blue Economy, Marine Resources, Fisheries and Shipping for granting the permits for sampling, and the University of Mauritius for logistic support and laboratory facilities. The authors also gratefully acknowledge the fellow participants on the expedition: OA Bergstad, D Bissessur, K Sauba, J Rama, P Coopen, Y Oozeeraully, S Seeboruth, A Audit-Manna, A Nicolas, N Reetoo, D Kuyper, G Gendron, A Souffre, S Hollanda, R Melanie, J Harlay, M. Soondur, L Caussy, K Tabachnick, M Olsen and TM Ensrud. The authors are grateful to the anonymous reviewers for their insightful comments that significantly improved the manuscript.

References

Armance M, Mattan-Moorgawa S, Bhagooli R (2019) Micro-phytoplankton density and diversity at a pilot oyster culture barachois site of Mauritius Island. Ocean Life 3 (1): 1-12

Almeida PD, Morales A, Wetzel CE, Ector L, Bicudo DDC (2016) Two new diatoms in the genus *Fragilaria lyngbye* (Fragilariophyceae) from tropical reservoirs in Brazil and comparison with type material of *F. tenera*. Phytotaxa 246: 163-183 [https://doi.org/10.11646/phytotaxa.246.3.1]

Appadoo C (2003) Status of mangroves in Mauritius. Journal of Coastal Development (7): 1-4

Armengol L, Calbet A, Franchy G, Rodríguez-Santos A, Hernández-León S (2019) Planktonic food web structure and trophic transfer efficiency along a productivity gradient in the tropical and subtropical Atlantic Ocean. Scientific Report (9): 2044 [https://doi.org/10.1038/s41598-019-38507-9]

Aubry F, Acri F, Bastianini M, Bianchi F, Cassin D, Pugnetti A, Socal G (2006) Seasonal and interannual variations of phytoplankton in the Gulf of Venice (Northern Adriatic Sea). Chemistry and Ecology 22: 71-91 [https://doi.org/10.1080/02757540600687962]

Badal R (2003) Enhanced primary production on the Mascarene Plateau caused by a mini-monsoon: a satellite perspective. In: Frouin RJ, Yuan Y, Kawamura H (eds) Proceedings of the Third International Asia-Pacific Environmental Remote Sensing Conference: Remote Sensing of the Atmosphere, Ocean, Environment, and Space. Hangzhou, China. 305 pp [https://doi.org/10.1117/12.466781]

Badal MR, Rughooputh S, Rydberg L, Robinson IS, Pattiaratchi C (2009) Eddy formation around South West Mascarene Plateau (Indian Ocean) as evidenced by satellite 'global ocean colour' data. Western Indian Ocean Journal of Marine Science (8): 139-144

Blauw AN, Benincà E, Laane RWPM, Greenwood N, Huisman J (2012) Dancing with the tides: Fluctuations of coastal phytoplankton orchestrated by different oscillatory modes of the tidal cycle. PLoS ONE 7 [https://doi.org/10.1371/journal.pone.0049319]

Capuzzo E, Lynam CP, Barry J, Stephens D, Forster RM, Greenwood N, McQuatters-Gollop A, Silva T, van Leeuwen SM, Engelhard GH (2018) A decline in primary production in the North Sea over 25 years, associated with reductions in zooplankton abundance and fish stock recruitment. Global Change Biology 24: e352-e364 [https://doi.org/10.1111/gcb.13916]

Carswell T, Costa M, Young E, Komick N, Gower J, Sweeting R (2017) Evaluation of MODIS-Aqua atmospheric correction and chlorophyll products of Western

North American coastal waters based on 13 years of data. Remote Sensing 9 [https://doi.org/10.3390/rs9101063]

Chepurnov VA, Mann DG, Sabbe K, Vyverman W (2004) Experimental studies on sexual reproduction in diatoms. International Review of Cytology: 91–154 [https://doi.org/10.1016/S0074-7696(04)37003-8]

Clerici M, Melin F, Hoepffner N (2008) Assessment of global ocean colour products against *in-situ* datasets. EUR 23357 EN. OPOCE, Luxembourg (Luxembourg): JRC45007 [https://publications.jrc.ec.europa.eu/repository/handle/JRC45007]

Colomina I, Molina P (2014) Unmanned aerial systems for photogrammetry and remote sensing: A review. ISPRS Journal of Photogrammetry and Remote Sensing 92: 79-97 [https://doi.org/10.1016/j.isprsjprs.2014.02.013]

Deidun A, Drago A, Gauci A, Galea A, Azzopardi J, Mélin F (2011) A first attempt at testing correlation between MODIS ocean colour data and in situ chlorophyll-a measurements within Maltese coastal waters. Presented at the SPIE Remote Sensing, Prague, Czech Republic: 81750J [https://doi.org/10.1117/12.896189]

Devassy VP, Goes JI (1991) Phytoplankton assemblages and pigments in the exclusive economic zone of Mauritius (Indian Ocean). Indian Journal of Marine Sciences 20: 163-168

Elliott J, Patterson M, Gleiber M (2012) Detecting 'Island Mass Effect' through remote sensing. Proceedings of the 12th International Coral Reef Symposium, 9-13th July 2012, Cairns, Queensland, Australia

Elliott JA, Patterson MR, Staub CG, Koonjul M, Elliott SM (2018) Decline in coral cover and flattening of the reefs around Mauritius (1998–2010). PeerJ 6: e6014 [https://doi.org/10.7717/peerj.6014]

Felip M, Catalan J (2000) The relationship between phytoplankton biovolume and chlorophyll in a deep oligotrophic lake: decoupling in their spatial and temporal maxima. Journal of Plankton Research 22: 91-106

Fleming AH, Korb RE (2004) A comparison of satellite and cruise chlorophyll-a measurements in the Scotia Sea, Antarctica. IEEE International Geoscience and Remote Sensing Symposium. *5*: 3485-3486 [https://doi.10.1109/IGARSS.2004.1370458.].

González-Rodríguez E, Trasviña-Castro A, Gaxiola-Castro G, Zamudio L, Cervantes-Duarte R (2012) Net primary productivity, upwelling and coastal currents in the Gulf of Ulloa, Baja California, México. Ocean Science 8: 703-711 [https://doi.org/10.5194/os-8-703-2012]

Gregg WW, Casey NW (2004) Global and regional evaluation of the SeaWiFS chlorophyll data set. Remote Sensing of Environment 93: 463-479 [https://doi.org/10.1016/j.rse.2003.12.012]

Gregg WW, Rousseaux CS (2014) Decadal trends in global pelagic ocean chlorophyll: A new assessment integrating multiple satellites, *in situ* data, and models. Journal Geophysical Research Oceans 119: 5921-5933 [https://doi.org/10.1002/2014JC010158]

Guḥmundsson K, Heath MR, Clarke ED (2009) Average seasonal changes in chlorophyll a in Icelandic waters. ICES Journal of Marine Science 66: 2133-2140

Hu C, Lee Z, Franz B (2012) Chlorophyll a algorithms for oligotrophic oceans: A novel approach based on three-band reflectance difference: A novel ocean chlorophyll a algorithm. Journal Geophysical Research [https://doi.org/10.1029/2011JC007395]

Jacox MG, Edwards CA, Kahru M, Rudnick DL, Kudela RM (2015) The potential for improving remote primary productivity estimates through subsurface chlorophyll and irradiance measurement. Deep Sea Research Part II: Topical Studies in Oceanography 112: 107-116 [https://doi.org/10.1016/j.dsr2.2013.12.008]

Jeffrey SW, Humphrey GF (1975) New spectrophotometric equations for determining chlorophylls a, b, c_1 and c_2 in higher plants, algae and natural phytoplankton. Biochemie und Physiologie der Pflanzen 167: 191-194 [https://doi.org/10.1016/S0015-3796(17)30778-3]

Jena B, Sahu S, Avinash K, Swain D (2013) Observation of oligotrophic gyre variability in the south Indian Ocean: Environmental forcing and biological response. Deep Sea Research Part I: Oceanographic Research Papers 80: 1-10 [https://doi.org/10.1016/j.dsr.2013.06.002]

Jena B (2016) Satellite remote sensing of the island mass effect on the Sub-Antarctic Kerguelen Plateau, Southern Ocean. Frontiers in Earth Science 10: 479-486 [https://doi.org/10.1007/s11707-016-0561-8]

Lacava T, Ciancia E, Di Polito C, Madonia A, Pascucci S, Pergola N, Piermattei V, Satriano V, Tramutoli V (2018) Evaluation of MODIS–Aqua chlorophyll-a algorithms in the Basilicata Ionian coastal waters. Remote Sensing 10: 987 [https://doi.org/10.3390/rs10070987]

Lee YJ, Matrai PA, Friedrichs MAM, Saba VS, Antoine D, Ardyna M, Asanuma I, Babin M, Bélanger S, Benoît-Gagné M, Devred E, Fernández-Méndez M, Gentili B, Hirawake T, Kang S.-H, Kameda T, Katlein C, Lee SH, Lee Z, Mélin F, Scardi M, Smyth TJ, Tang S, Turpie KR, Waters KJ, Westberry TK (2015) An assessment of phytoplankton primary productivity in the Arctic Ocean from satellite ocean color/*in situ* chlorophyll- a based models: Arctic primary productivity round robin. Journal of Geophysical

Research: Oceans 120: 6508-6541 [https://doi.org/10.1002/2015JC011018]

Lyngsgaard MM, Markager S, Richardson K, Møller EF, Jakobsen HH (2017) How well does chlorophyll explain the seasonal variation in phytoplankton activity? Estuaries and Coasts 40: 1263-1275 [https://doi.org/10.1007/s12237-017-0215-4]

Morel A, Claustre H, Gentili B (2010) The most oligotrophic subtropical zones of the global ocean: similarities and differences in terms of chlorophyll and yellow substance. Biogeosciences 7: 3139-3151 [https://doi.org/10.5194/bg-7-3139-2010]

Moodoosoodun K, Appadoo C, Oocheetsing S (2010) An investigation on the phytoplankton and zooplankton abundance and diversity at the Balaclava Marine Protected Area in the North West coast of Mauritius. Journal of Environmental Research and Development 5 (2): 366-374

Mudgal R, Dash MK, Pandey PC (2009) Seasonal and inter-annual variability of chlorophyll-a in the Arabian Sea from SeaWiFS Data 10: 21-32

Mukherjee A, Das S, Bhattacharya T, De M, Maiti T, Kumar De T (2014) Optimization of phytoplankton preservative concentrations to reduce damage during long-term storage. Biopreservation and Biobanking 12: 139–147 [https://doi.org/10.1089/bio.2013.0074]

NASA Goddard Space Flight Center, Ocean Ecology Laboratory, Ocean Biology Processing Group (2017) Sea-viewing Wide Field-of-view Sensor (SeaWiFS) Ocean Color Data, NASA OB.DAAC

Pinkerton MH (2003) Validation of SeaWiFS ocean color satellite data using a moored databuoy. Journal of Geophysical Research [https://doi.org/10.1029/2002JC001337]

Ramchandur V, Rughooputh SDDV, Boojawon R, Motah BA (2017) Assessment of chlorophyll-a and sea surface temperature variability around the Mascarene Plateau, Nazareth Bank (Mauritius) using satellite data. Indian Journal Fisheries [https://doi.org/10.21077/ijf.2017.64.4.71978-01]

Ramessur R (2002) Anthropogenic-driven changes with focus on the coastal zone of Mauritius, south-western Indian Ocean. Regional Environmental Change 3: 99-106 [https://doi.org/10.1007/s10113-002-0045-0

Sadally S, Taleb-Hossenkhan N, Bhagooli R (2014a). Spatio-temporal variation in density of microphytoplankton genera in two tropical coral reefs of Mauritius. African Journal of Marine Science 36: 423-438 [https://doi.org/10.2989/1814232X.2014.973445]

Sadally S, Nazurally N, Taleb-Hossenkhan N, Bhagooli R (2014b). Micro-phytoplankton distribution and biomass in and around a channel-based fish farm: implications for sustainable aquaculture. Acta Oceanologica Sinica 33: 180-191 [https://doi.org/10.1007/s13131-014-0577-4]

Sadally S, Taleb-Hossenkhan N, Casareto BE, Suzuki Y, Bhagooli R (2015) Micro-tidal dependent micro-phytoplankton C-biomass dynamics of two shallow tropical coral reefs. Western Indian Ocean Journal of Marine Science 14 (1-2): 53-72

Sadally S, Taleb-Hossenkhan N, Bhagooli R (2016) Microalgal distribution, diversity and photo-physiological performance across five tropical ecosystems around Mauritius Island. Western Indian Ocean Journal of Marine Science 15 (1): 49-68

Saifullah ASM, Kamal AHM, Idris MH, Rajaee AH, Bhuiyan MdKA (2016) Phytoplankton in tropical mangrove estuaries: role and interdependency. Forest Science and Technology 12: 104-113 [https://doi.org/10.1080/21580103.2015.1077479]

Sandooyea S, Ave H, Soondur M, Kaullysing, D, Bhagooli R (2020) Variations in the density and diversity of micro-phytoplankton and micro-zooplankton in summer months at two coral reef sites around Mauritius Island. Journal of Sustainable Science Management 15: 18-33 [https://doi.org/10.46754/jssm.2020.06.003]

Sala E, Costello C, De Bourbon Parme J, Fiorese M, Heal G, Kelleher K, Moffitt R, Morgan L, Plunkett J, Rechberger KD, Rosenberg AA, Sumaila R (2016) Fish banks: An economic model to scale marine conservation. Marine Policy 73: 154-161 [https://doi.org/10.1016/j.marpol.2016.07.032]

Shi W, Wang M (2018) Ocean dynamics observed by VIIRS day/night band satellite observations. Remote Sensing [https://doi.org/10.3390/rs10010076]

Smith DL, Johnson KB (1996) A guide to marine coastal plankton and marine invertebrate larvae, 2nd edition. Kendall/Hunt Publishing Company, Iowa

Soondur M, Kaullysing D, Boojhawon R, Lowe R, Casareto B, Yoshimi S, Bhagooli R (2020) Diel variations in density and diversity of micro-phytoplankton community in and around a barachois-based oyster culture farm. Journal of Sustainable Science and Management 15: 2–17 [https://doi.org/10.46754/jssm.2020.06.002]

Stock CA, John JG, Rykaczewski RR, Asch RG, Cheung WW, Dunne JP, Friedland KD, Lam VW, Sarmiento JL, Watson RA (2017) Reconciling fisheries catch and ocean productivity. Proceedings of the National Academy of Sciences 114: 1441-1449

Tilstone GH, Lotliker AA, Miller PI, Ashraf PM, Kumar TS, Suresh T, Ragavan BR, Menon HB (2013) Assessment of MODIS-Aqua chlorophyll-a algorithms in coastal and shelf waters of the eastern Arabian Sea. Continental Shelf Research 65: 14-26 [https://doi.org/10.1016/j.csr.2013.06.003]

Tomas CR (ed) (1996) Identifying marine diatoms and dinoflagellates. Academic Press, San Diego

Townsend DW, Thomas AC (2001) Winter-spring transition of phytoplankton chlorophyll and inorganic nutrients on Georges Bank. Deep Sea Research Part II: Topical Studies in Oceanography 48: 199-214

Turner J, Klaus R (2005) Coral reefs of the Mascarenes, Western Indian Ocean. Philosophical Transactions: Mathematical, Physical and Engineering Sciences 363: 229-250.

Vortsepneva E (2008) Saya de Malha Bank–an invisible island in the Indian Ocean. Moscow State University, Moscow, Russia. Journal Geomorphology, Oceanology, biology 3-42.

Wang D, Cui Q, Gong F, Wang L, He X, Bai Y (2018) Satellite retrieval of surface water nutrients in the coastal regions of the East China Sea. Remote Sensing [https://doi.org/10.3390/rs10121896]

Woelkerling WJ, Kowal RR, Gough S.B (1976) Sedgwick-rafter cell counts: a procedural analysis. Hydrobiologia 48: 95-107 [https://doi.org/10.1007/BF00040161]

Wozniak M, Bradtke KM, Krezel A (2014) Comparison of satellite chlorophyll a algorithm for the Baltic Sea. Journal Applied Remote Sensing 8 [https://doi.org/10.1117/1.JRS.8.083605]

WWF (2011) The Saya de Malha Banks factsheet. WWF Madagascar Marine Programme

Zarauz L, Irigoien X (2008) Effects of Lugol's fixation on the size structure of natural nano-microplankton samples, analyzed by means of an automatic counting method. Journal of Plankton Research 30: 1297-1303 [https://doi.org/10.1093/plankt/fbn084]

Zhu L, Suomalainen J, Liu J, Hyyppä J, Kaartinen H, Haggren H (2018) A review: Remote sensing sensors. In: Rustamov RB, Hasanova S, Zeynalova MH (eds) Multi-purposeful application of geospatial data. InTech [https://doi.org/10.5772/intechopen.71049]

Variations in abundance, diversity, photo-physiology and estimated productivity of micro-phytoplankton with depth at the Saya de Malha Bank, Mascarene Plateau

Mouneshwar Soondur[1,2]*, Sundy Ramah[1,3], Ravindra Boojhawon[4], Deepeeka Kaullysing[1,2], Ranjeet Bhagooli[1,2,5,6]

[1] Department of Biosciences and Ocean Studies, Faculty of Science & Pole of Research Excellence in Sustainable Marine Biodiversity, University of Mauritius, Réduit 80837, Republic of Mauritius

[2] The Biodiversity and Environment Institute, Réduit, Republic of Mauritius

[3] Albion Fisheries Research Centre, Ministry of Blue Economy, Marine Resources, Fisheries & Shipping, Albion, Petite Rivière 91001, Republic of Mauritius

[4] Department of Mathematics, Faculty of Science, University of Mauritius, Réduit 80837, Republic of Mauritius

[5] Institute of Oceanography and Environment (INOS), University Malaysia Terengganu, 21030 Kuala Terengganu, Terengganu, Malaysia

[6] The Society of Biology (Mauritius), Réduit, Republic of Mauritius

* Corresponding author: mouneshwar.soondur@gmail.com

Abstract

The variations in micro-phytoplankton abundance, diversity, photo-physiology, chlorophyll *a* (Chl*a*) concentration and estimated productivity were assessed at depth ranges of 0-4, 5-10, and 11-29 m with 100, 28 and 11% of irradiance, respectively, in Saya de Malha waters. The total micro-phytoplankton abundance (TMPA) differed significantly ($P < 0.001$) with depth ranges, and between day and night samples. Out of the 34 genera identified, 27 showed a decrease in abundance of over 40% with depth. *Chaetoceros*, *Coscinodiscus*, *Navicula*, *Nitzschia* and *Ceratium* were most dominant. The Shannon-Wiener (H') diversity index did not differ among depth ranges and between samples collected during day and night, but diatoms were more diverse than dinoflagellates. The effective quantum yield (Φ_{PSII}) and the light-use efficiency factor (α) tended to decrease, while the maximum relative electron transport rate ($rETR_{max}$), the photo-inhibitory factor (β) and the maximum non-photochemical quenching (NPQ_{max}) varied insignificantly from morning to afternoon sampling points at all depth ranges studied. The estimated productivity, $rETR_{max}$ and Chl*a* concentration decreased with depth ranges. The higher diversity of diatoms, better photosynthetic performance in the morning hours and higher near-surface estimated productivity provide new insights into micro-phytoplankton dynamics and productivity in Saya de Malha waters.

Keywords: estimated productivity, micro-phytoplankton, photo-physiology, water column, Saya de Malha, Mascarene Plateau

Introduction

Phytoplankton form the base of the marine food chain and are one of the most important biological components that regulate life in the ocean. In the open ocean, there are several parameters that influence the diversity, distribution and photo-physiological state of phytoplankton. The variation of phytoplankton is less affected by anthropogenic activities in the open ocean compared to the coastal regions. The abundance and distribution of phytoplankton in the open ocean is mostly governed by mixing processes, more specifically vertical mixing which eventually promotes changes in the light and nutrient availability, and influence the growth performance of the micro-algae

http://dx.doi.org/10.4314/wiojms.si2021.2.4

(Diehl, 2002). At a depth where there is limited light, even if there is high nutrient flux from the deeper waters, the phytoplankton density will remain low due to the lower photosynthetic activity (Bode *et al*., 1996). Moreover, species-wise, Margalef (1978) demonstrated that resilient vertical mixing is more advantageous for diatom dominance compared to dinoflagellates where the dinoflagellates were found to choose to migrate towards more stratified water columns. The locomotive advantage of the dinoflagellates provides them with the ability to swim to zones rich in nutrients and light (Glibert, 2016; Smayda and Reynolds, 2003).

Being a primary producer, the phytoplankton is consumed by the zooplankton. During night-time, there is absence of light and thus, the primary productivity decreases and zooplankton tends to move to the upper water layer to graze on the free floating phytoplankton (Roman *et al*., 1988). This migration of zooplankton, which is at the same time an escape from larger predators in the deep waters, has been well studied by Shaw and Robinson (1998). The grazing capacity of the zooplankton will impact the density and abundance of certain species of phytoplankton. Moreover, Goldyn and Kowalczewska-Madura (2007) have demonstrated that a high density of zooplankton tends to cause a significant decrease in the phytoplankton community.

The photo-physiological state of all photosynthetic organisms depends mainly on the availability of irradiance. McMinn *et al*. (2003) reported the dependence of the variability of maximum relative electron transport rate ($rETR_{max}$) on irradiance, but at the same time stated that the observation varied due to the changing weather conditions in the Antarctica, and in the natural environment, the change in intensity of light is not consistent. Excess irradiance causes harm to the photosystem of photosynthetic organisms (Aro *et al*., 1993). In order to prevent this damaging effect, photosynthetic organisms have established a defense mechanism which disperses excess light energy as heat. This process is called non-photochemical quenching (NPQ) which is identified as a decrease in chlorophyll fluorescence (Guidi *et al*., 2019; Krause and Weis, 1991). The diatom dissipates thermal energy via the xanthophyll cycle (Kashino and Kudoh, 2003). This is why diatoms have rapidly-inducible NPQ, and sustain high photochemical activities through a wide range of light intensities (Buck *et al*., 2019; Derks and Bruce, 2018). The Western Indian Ocean is among the regions that have been least studied during the past years with very few studies conducted on phytoplankton (Armance *et al*., 2019; Sadally *et al*., 2012; Sadally *et al*., 2014a, 2014b; Sadally *et al*., 2015; Sadally *et al*., 2016; Sandooyea *et al*., 2020; Schlüter *et al*., 2011; Soondur *et al*., 2020).

Studies on phytoplankton and their photo-physiology are limited in the Saya de Malha region, which is a fishing bank that is considered to be among the world's largest fishing areas covering over 44,130 km², and is conjointly managed by the Republic of Mauritius and the Republic of Seychelles. An indicative decrease in total fish catch from 2010 to 2011 of nearly 6 tonnes has been reported at the bank. In 2011, around 1,472 tonnes of frozen fish were caught from the region of Saya de Malha which highlights its importance for the fisheries sector. Over 80% of fish are caught from depths of 15-50 m (Bhagooli and Kaullysing, 2019). Given the known relationship between productivity and fish catch, studies on productivity and micro-phytoplankton in the water column of this region are imperative. The present study aimed at determining the change in species composition and abundance of micro-phytoplankton and their photo-physiological features, together with the estimated productivity across different depth ranges in the Saya de Malha region. The objectives were to: 1) investigate the spatial and depth variation of micro-phytoplankton abundance and diversity; 2) compare the abundance of micro-phytoplankton between samples collected during the day and night; and 3) investigate the general trend in the variation of Chl*a*, estimated productivity and photo-physiological parameters in response to different depth ranges for samples collected during the day.

Methodology

Study site, stations and sampling strategy

This study was conducted in May 2018, during the southern hemisphere winter which is a low rainfall period, on board the R/V Dr Fridtjof Nansen during the Indian Ocean Research Expedition 2018l in the region of the Saya de Malha Bank located in the Southern Indian Ocean (Fig. 1a). A CTD was used for seawater sample collection and sensors to record light intensity. For the determination of the micro-phytoplankton density and abundance, *in-situ* Chl*a* concentration and estimated productivity, samples were collected at three different depth ranges: 0-4 m; 5-10 m; and 11-29 m at seven stations during the day (391, 394, 397, 400, 401, 404 and 408) and six stations during the night (393, 396, 398, 403, 412 and 416) (Fig. 1b). All samples were collected in triplicates. Level 3 satellite sea surface Chl*a* (MODIS-Aqua

MODISA_L3m_Chl*a*_8d_4km vR2019.0) and sea surface temperature (MODIS-Aqua MODISA_L3m_SST_8d_4km vR2019.0) data were extracted from AquaMODIS and processed on GIOVANNI version 4.35 (https://giovanni.gsfc.nasa.gov/giovanni/).

Micro-phytoplankton and Chl*a* sampling, preservation and analysis

The CTD was deployed at each station and samples were collected from the Niskin bottles at respective depths, and 10 L of sea water were filtered through a plankton net of 5 µm mesh size. The filtrate containing the micro-phytoplankton was then preserved using 1% Lugol's solution and stored at 4°C on board the vessel. The samples were later processed in the laboratory where they were centrifuged at 3500 rpm for 10 min-

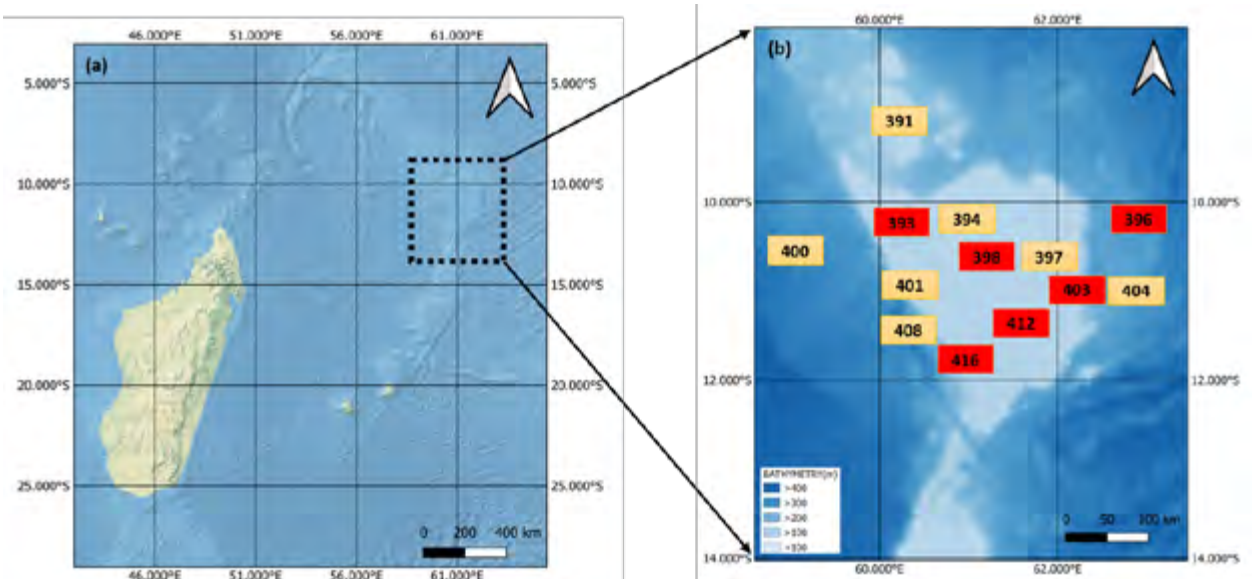

Figure 1. (a) Southern Indian Ocean; and (b) Region of Saya de Malha with yellow and red boxes indicating daytime and night-time sampling stations, respectively, and the blue color indicating the bathymetry data in meters. The CTD station numbers are shown in the boxes.

utes to further concentrate the sample to 1 ml (Mukherjee *et al*., 2014; Sadally *et al*., 2014; Zarauz and Irigoien, 2008). The samples were analysed according to Woelkerling *et al.* (1976). The 1 ml micro-phytoplankton sample was loaded on a Sedgwick Rafter counting chamber and quantification was carried out under a light microscope (Devassy and Goes, 1991; Sadally *et al*., 2014). Furthermore, the species and genera of the micro-phytoplankton were identified according to Tomas (1996).

The sea water samples for Chl*a* analysis were collected from the CTD at respective depths and stations. From the Niskin bottle, 500 ml of water were filtered through Whatman® glass fiber filters of pore size 0.45 µm using an electrical pump. Then, Chl*a* pigment extraction was conducted in 10 ml of 90% acetone. The extract in the liquid acetone was read under a spectrophotometer (Spectronic® GenesysTM 8) at wavelengths 630, 647, 664 and 750 nm after 24 hours. The Chl*a* concentration was determined using the formula:

$$\text{Chlorophyll } a = (11.85^{*} (E_{664} - E_{750}) - 1.54^{*} (E_{647} - E_{750}) - 0.08 (E_{630} - E_{750})) {}^{*}V_e/L^{*}V_f$$

Where, L = Cuvette light-path in centimeters; V_e = Extraction volume in milliliters; V_f = Filtered volume in liters; and concentrations were in mgm^{-3} (Jeffrey and Humphrey, 1975).

Photo-physiology and estimated productivity

The photo-physiology and estimated productivity were assessed only for samples that were collected during daytime. The Diving Pulse Amplitude Modulator (D-PAM) fluorometer (Submersible Photosynthesis Yield Analyzer, Walz, Germany) was used to assess the photo-physiology of micro-phytoplankton by measuring the fluorescence of Chl*a*, thus determining the relative electron transport rate (rETR) and non-photochemical quenching (NPQ) when exposed to a series of rapidly (10 s) changing light climates (RLC) (McMinn *et al*., 2005, 2012). Phytoplankton were adsorbed on filter papers by filtering seawater samples collected using the CTD at different depths

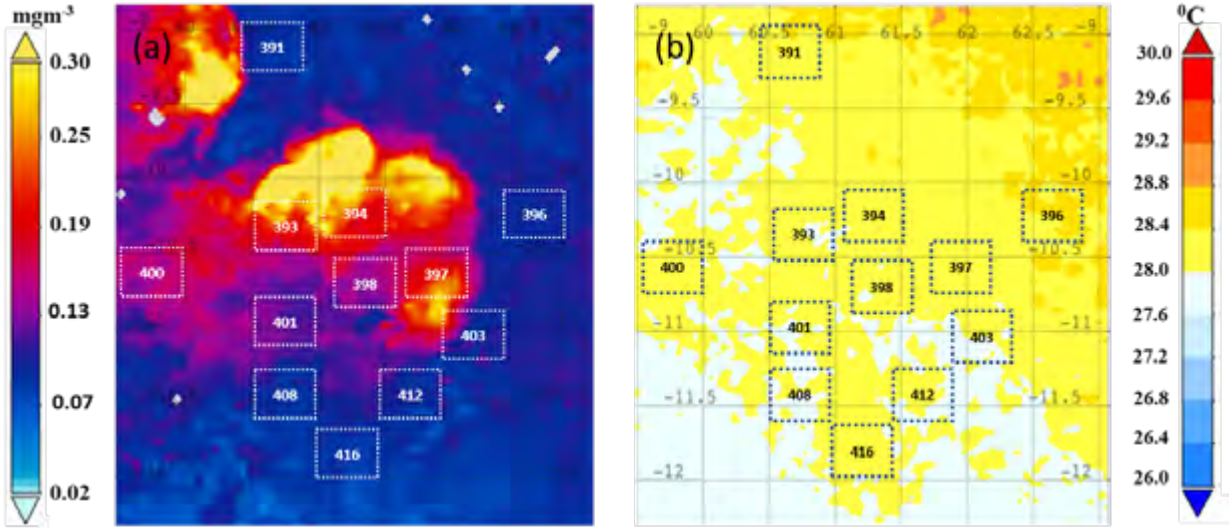

Figure 2. Average satellite AquaMODIS data for: (a) sea surface Chl*a* concentration and (b) sea surface temperature for the region of Saya de Malha for May 2018. The CTD numbers indicated in white colour represent the sampling locations.

through the Whatman® glass fiber filters of pore size 0.45 µm, and immediately analyzed using the D-PAM on-board the research vessel (Bhagooli and Hidaka, 2003; Bhagooli, 2010; Bhagooli *et al.*, 2021). Using the RLCs, the rETR and NPQ were estimated at each irradiance. At each irradiance, the respective relative electron transport rate (rETR) was calculated using the formula rETR= 0.5 x Φ_{PSII} x PAR, where PAR is the photosynthetically active radiance. The different PAR used were 110, 150, 300, 400, 500, 800, 1000 and 1325. The NPQ was calculated based on the formula NPQ = (F_m-F_m')/F_m'. The maximum rETR and NPQ WERE calculated using sigma plots (Platt and Jassby, 1976). Furthermore, other photophysiology parameters calculated were Ek ($rETR_{max}/\alpha$) which is the minimum saturating irradiance, and α (light-use efficiency factor measured as the initial slope of the light curve before the onset of saturation) and β (the slope of the light curve beyond the onset of photo-inhibition) was determined from the rETR curve. Estimated relative productivity for each sample at respective sites was calculated using the formula for Estimated productivity, P, defined as P = ($rETR_{max}$× Chl*a*) (McMinn and Hegseth, 2004; McMinn *et al.*, 2005; McMinn *et al.*, 2010).

Statistical analysis

The software PASW Statistics 18 was used to analyze the data. The data was first tested for normality before any further statistical analyses. Non-normally distributed data were transformed via $\log_{10}$ or Arcsine. The one-way ANOVA was used to determine any significant differences between the CTD stations, and two-way ANOVA was used to determine significant differences for the micro-phytoplankton in terms of depth and time. Moreover, a Principle Correspondence Analysis (PCA) was generated to reveal the relationship between all the different parameters analyzed. Shannon-Wiener, Equitability, and Evenness diversity indices were used to determine the variability of the different micro-phytoplankton genera at different depth ranges.

Results

AquaMODIS sea surface Chl*a*, sea surface temperature, light variation with depth, and associated hydrographic data

The average sea surface Chl*a* concentration for the period May 2018 to early June 2018 revealed the oligotrophic characteristic of the region of Saya de Malha. The satellite Chl*a* showed an average concentration below 0.3 mgm^{-3}. Using the Chl*a* concentration as an index for phytoplankton biomass, the highest biomass was around stations CTD 393, CTD 394, CTD 397, CTD 400 and CTD 401 (Fig. 2a). The variation in sea surface temperature was low, where CTD 396 showed the highest temperature (> 28.8°C), while lower temperatures were apparent (< 28.0°C) at CTD 408, CTD 412 and CTD 416 (Fig. 2b).

Samplings at stations CTD 391, CTD 400 and CTD 401 were carried out on cloudy days resulting in low absolute light intensity with the highest values recorded at CTD 404 and CTD 408 (Fig. 3a). The average absolute light intensity was highest at the 0-4 m surface layer (236.2 ± 211.9 µmol quanta m^{-2} s^{-1}) followed by 5-10 m (75.4 ± 69.0 µmol quanta m^{-2} s^{-1}) and by 11-29 m (30.8 ± 30.4 µmol quanta m^{-2} s^{-1}). Considering the near-surface

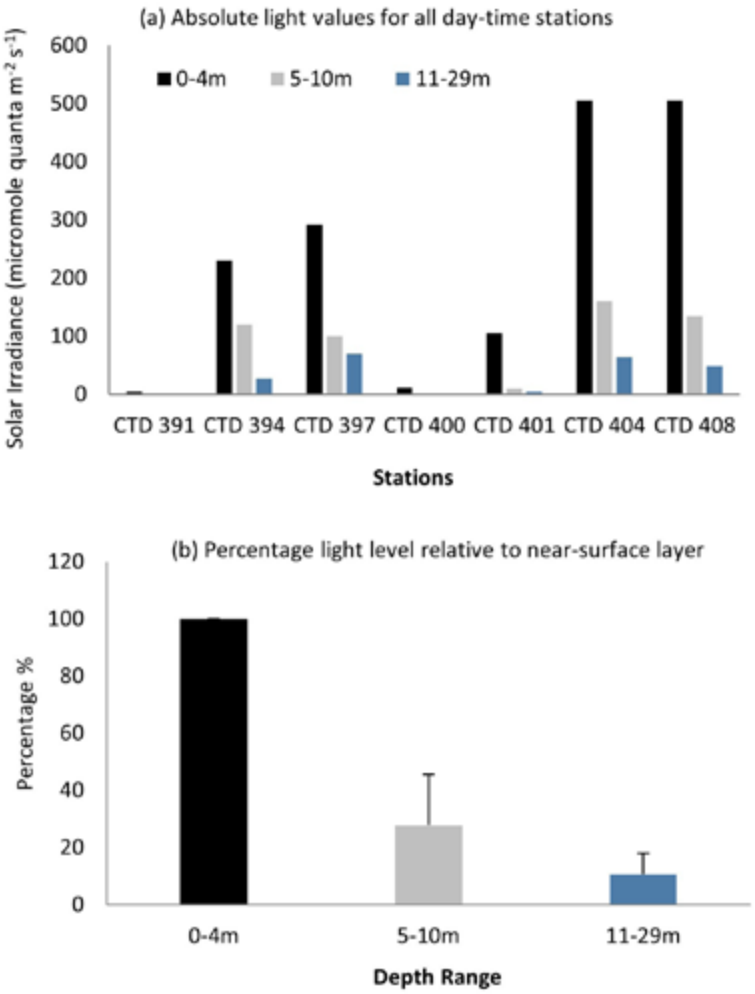

Figure 3. Absolute light values (a), and percentage light level relative to near-surface layer (b) for all daytime stations.

layer of 0-4 m to have 100% of solar irradiance, then the layer of 5-10 m had around 28% light which was a decrease of 72%. At a depth range of 11-29 m, the solar irradiance was 11% which was a decrease of 89% from the 0-4 m layer (Fig. 3b). Thus, there was a noticeable decrease in the light intensity reaching the layers between 5 and 29 m depth. Additionally, Table 1 gives an overview of the maximum depth at each station with minimum depth at stations CTD 403 (29 m) and maximum depth at CTD 396 (2172 m).

Table 1. Time, CTD station, and maximum depth at respective stations where samples were collected.

Sampling time	CTD Station	Max depth (m)
Day	391	135
	394	31
	397	68
	400	51
	404	2123
	408	-
Night	393	79
	396	2172
	398	60
	403	29
	412	2068
	416	1309

Micro-phytoplankton abundance at different depth ranges

The highest TMPA during daytime was recorded at CTD 397 (5.51 ± 0.54 × 10^4 cells L^{-1}) and at night-time at CTD 398 (3.86 ± 0.21 × 10^4 cells L^{-1}) at a depth range of 0-4 m. These two CTD stations also maintained their highest abundances of TMP at depth ranges of 5-10 m and 11-29 m among the stations. During daytime, the highest TMPA was 3.12 ± 0.12 × 10^4 cells L^{-1} at CTD 397 at depth 5-10 m, and at depth 11-29 m the highest TMPA was also at CTD 397 with an abundance of 1.88 ± 0.18 × 10^4 cells L^{-1}. For the night-time, the abundance was 1.30 ± 0.80 × 10^4 cells L^{-1} at CTD 398 at depth 5-10 m, and at depth 11-29 m, it was 1.03 ± 0.25 × 10^4 cells L^{-1}. The lowest abundances of TMP during daytime was recorded at CTD 401 (1.20 ± 0.11 × 10^4 cells L^{-1}) and for night-time, at CTD 416 (0.84 ± 0.21 × 10^4 cells L^{-1}) (Fig. 4a). The highest and lowest diatom abundances followed the same trend at the same CTD stations (CTD 397 and CTD 398) as the

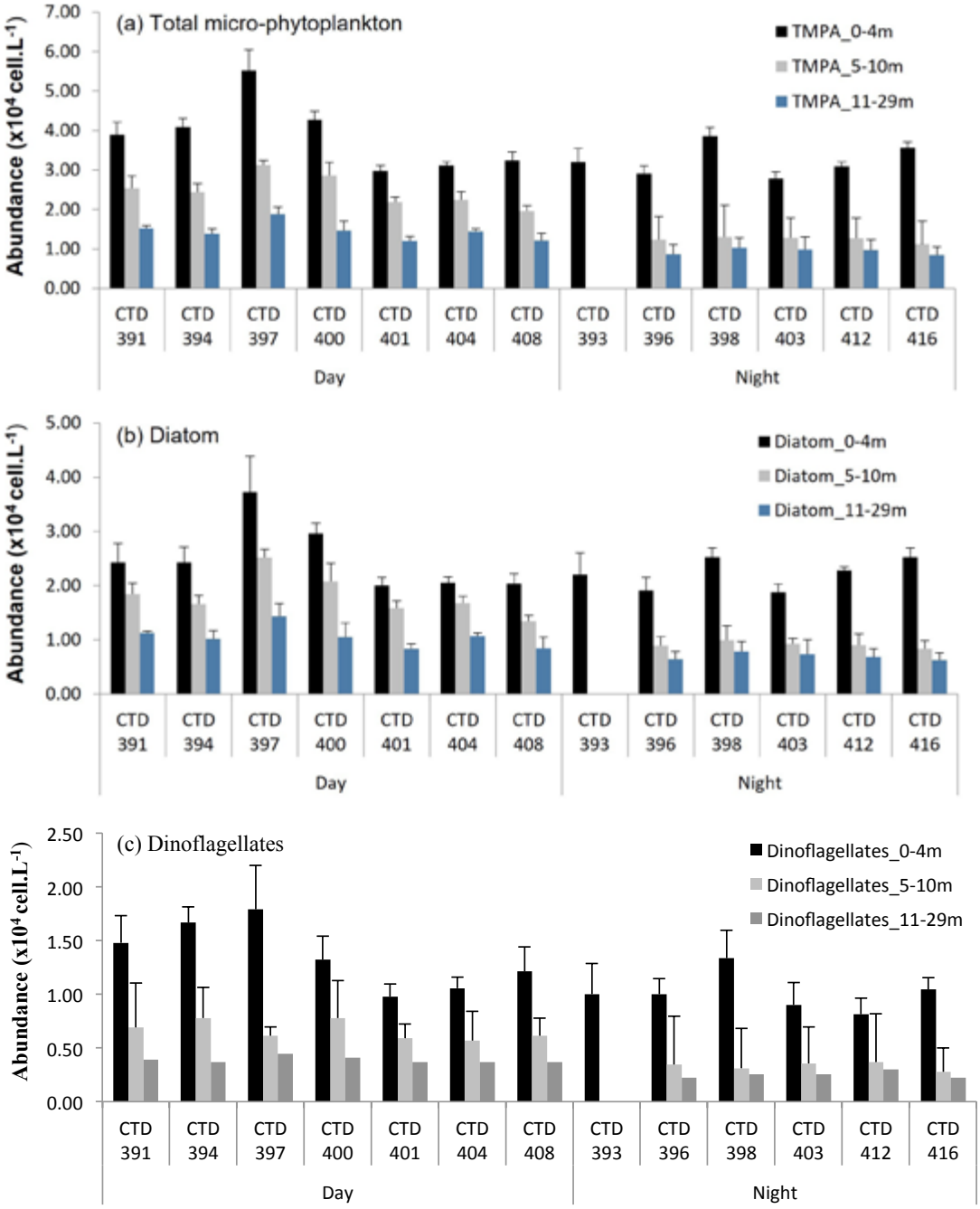

Figure 4. Abundance of total micro-phytoplankton (a), diatom (b), and dinoflagellates (c) during day- and night-time at different CTD stations at three depth ranges of 0-4 m, 5-10 m and 11-29 m.

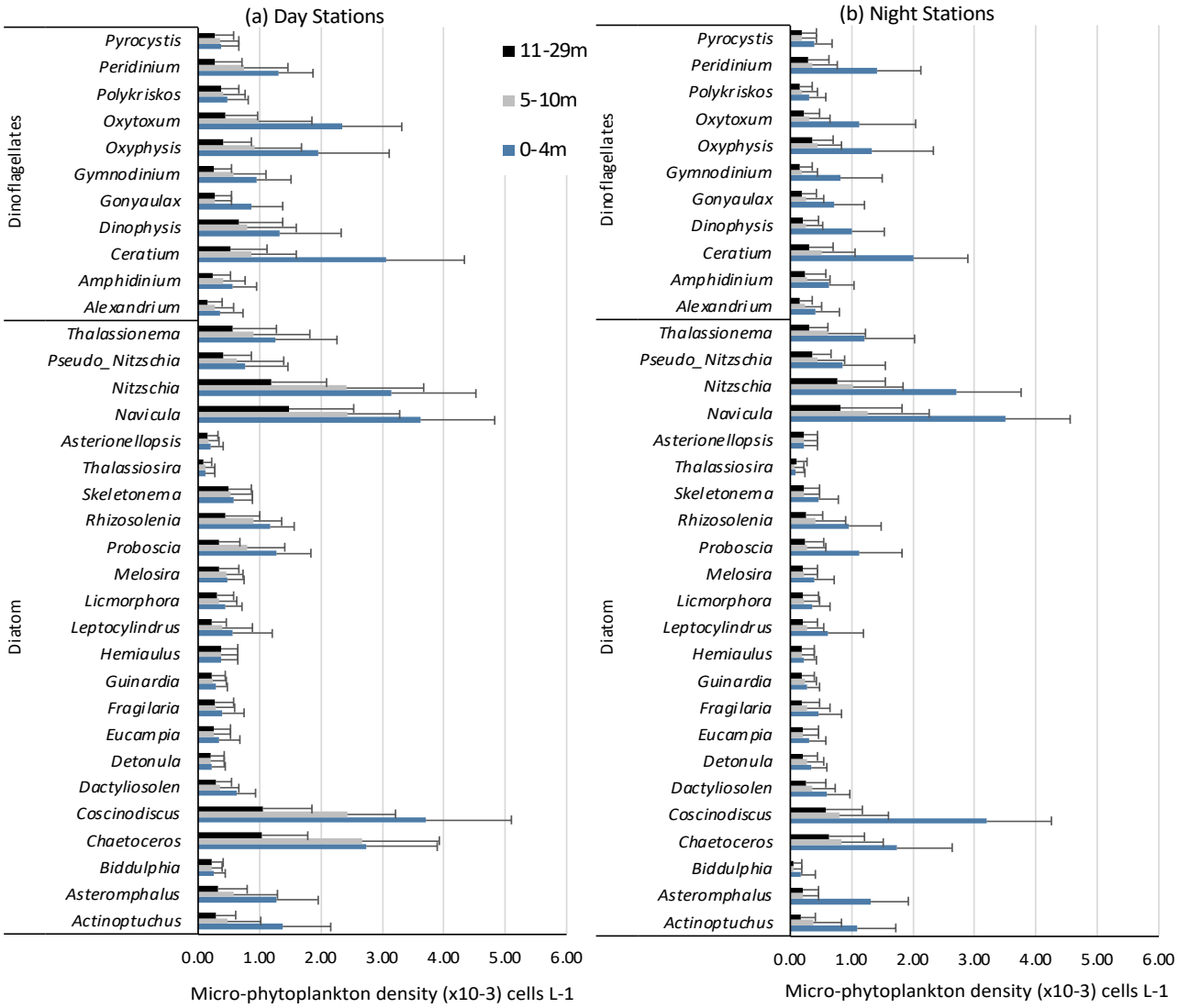

Figure 5. Average micro-phytoplankton abundance of different genera for samples collected during (a) day, and (b) night.

TMPA at all the studied depth ranges (Fig. 4b). For dinoflagellates, a similar trend was followed only for the depth 0-4 m. At 5-10 m, during daytime the highest dinoflagellates abundance was at CTD 394 and CTD 400 and lowest at CTD 401, and during night-time the highest was at CTD 412 and lowest at CTD 416. Moreover, at 11-29 m during daytime the highest dinoflagellates abundance was at CTD 397, and lowest abundances at CTD 394, CTD 401, CTD 404 and CTD 408, and during night-time the highest was at CTD 412 and lowest at CTD 396 and CTD 416. One-way ANOVA test revealed no significant differences among the different CTD stations ($P > 0.05$). Among the different depths, there were strong significant differences for diatoms, dinoflagellates and TMPA ($P < 0.001$). Significant difference was also revealed between daytime and night-time abundances of the different groups of micro-phytoplankton. When the parameters of depth and time were combined, the difference was not significant ($P > 0.05$).

The TMPA had the highest percentage decrease (-61.15%) during night-time and it was between the depth ranges 0-4 m and 5-10 m. This trend was also observed for the diatom subgroup (-58.52%) and dinoflagellates (-66.18%). For depths between 5-10 m and 11-29 m, the highest decrease was noted during daytime for TMPA (-41.67%) and diatoms (-41.70%) followed by dinoflagellates (40.55%).

Micro-phytoplankton diversity

Thirty-four genera of micro-phytoplankton were identified out of which 23 were diatoms and 11 were dinoflagellates. Moreover, 5 genera revealed consistency in terms of percentage dominance at all the studied depths. These were *Chaetoceros* (range: 5.38-10.78%),

Coscinodiscus (range: 6.24-9.91%), *Navicula* (range: 8.85-10.82%), *Nitzschia* (range: 8.11-9.75%) and *Ceratium* (range: 3.42-7.91%). The lowest percentage dominance was exhibited by the genera *Biddulphia, Thalassiosira*, *Alexandrium,* and *Pyrocystis*.

The highest decrease in the abundance of genera was noted during the night-time at the depth change of 0-4 m to 5-10 m, where 27 out of the 34 genera revealed a decrease in abundance of over 40%. During the day-time, the highest decrease was between the depth changes of 5-10 m to 11-29 m where 15 of the 34 genera decreased by at least 40%. During daytime at a depth change of 0-4 m to 5-10 m, two genera (*Hemiaulus* and *Thalassiosira*) revealed no change in abundances, while from 5-10 to 11-29 m, five genera (*Biddulphia, Detonula, Eucampia, Hemiaulus,* and *Gonyaulax*) maintained their abundances (Fig. 5a). Moreover, during night-time at a depth change of 0-4 m to 5-10 m, one genus (*Asterionellopsis*) revealed no change in abundance, and at 5-10 to 11-29 m, seven genera revealed no change (*Asteromphalus, Biddulphia, Eucampia, Hemiaulus, Skeletonema, Asterionellopsis,* and *Pyrocystis*) (Fig. 5b). Among all the different depths and during day/night-time, *Hemiaulus* showed the lowest decrease of 16.67%.

The Shannon-Wiener (H') diversity index showed that the diatom subgroup had higher diversity values (H' > 2.5) compared to the dinoflagellates (H' < 2.5), irrespective of depth range and day/night-time (Fig. 6a). An increase in Equitability (E_H) values was noted when moving from 0-4 m to depth range of 11-29 m. For the dinoflagellates, there was an increase in E_H from 0-4 m to 5-10 m, and a decrease from 5-10 m to 11-29 m (Fig. 6b). The Evenness (E_{var}) revealed highest values during night-time for all the depth ranges for both diatom and dinoflagellates, and overall, the dinoflagellates tended to have higher E_{var} than diatoms (Fig. 6c).

Photo-physiology of micro-phytoplankton

The effective quantum yield (Φ_{PSII}) varied mostly below 0.4 with not much difference with respect to depth changes. At the depth range 0-4 m and 11-29 m, Φ_{PSII} revealed a decrease with time-scale reaching 15:00 pm with R^2 of 0.034 and 0.721, respectively. At the depth range of 5-10 m, an increase with R^2 = 0.597 was apparent. The highest mean Φ_{PSII} was recorded at 11-29 m (0.32 ± 0.11) and the lowest at 5-10 m (0.21 ± 0.06) (Fig. 7a). As for $rETR_{max}$, an increasing trend was noted at both the depth ranges 0-4 m and 5-10 m, whereas a decreasing trend was revealed at 11-29 m through the time scale 5:00 am to 15:00 pm. Highest mean $rETR_{max}$ was recorded at 0-4 m (6.27 ± 2.97) and lowest at 5-10 m (4.57 ± 2.33) (Fig. 7b). The value of α (Fig. 7c) showed a decreasing trend throughout all the different depth ranges with high R^2 values of 0.686, 0.426 and 0.562, and on the contrary, the values of β (Fig. 7d) showed increasing trends with lower R^2 values (0.390, 0.262 and 0.077). Moreover, α had slightly higher values at depth 11-29 m. The NPQ_{max} depicted an increasing trend at the depth range of 0-4 m and decreasing trends in the other depth ranges with low R^2 values. In terms of means, the higher NPQ_{max} was at a depth range 0-4 m (3.38 ± 1.85) and lowest at 11-29 m (2.04 ± 2.23) (Fig. 7d). Finally, E_k revealed decreasing trends at all the different depth ranges with highest

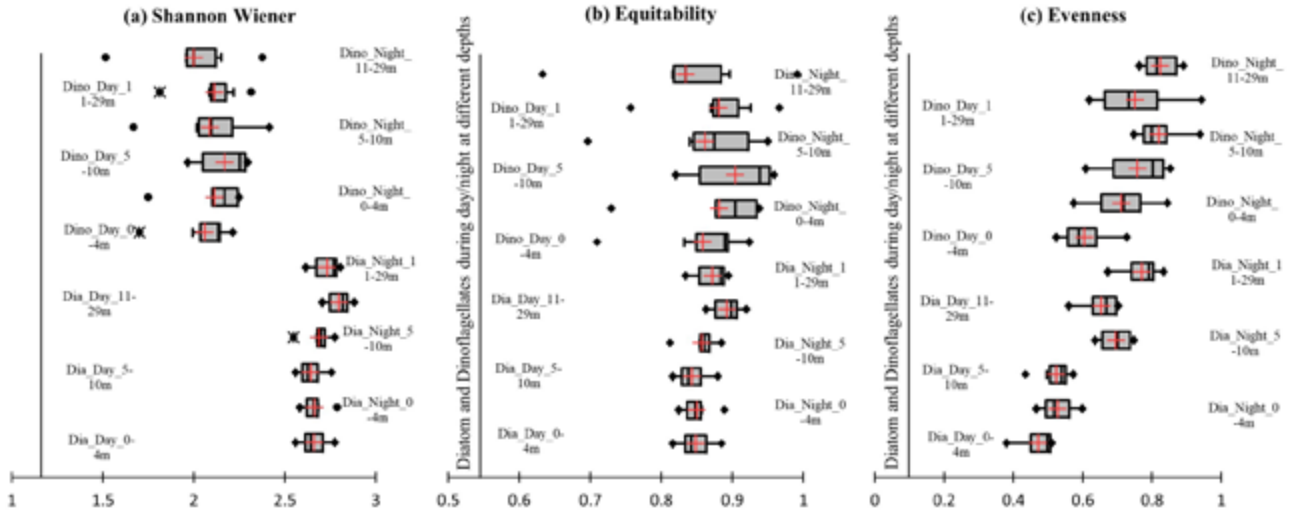

Figure 6. The diversity indices (a) Shannon Wiener (H'), (b) Equitability (E_H) and (c) Evenness (E_{var}) for the diatom and dinoflagellates at different depth ranges and time (day/night).

mean at 0-4 m (240.67 ± 322.89 µmol photons m^{-2} s^{-1}) and lowest at 11-29 m (101.73 ± 106.83 µmol photons m^{-2} s^{-1}) (Fig. 7e). For all the different photo-physiological parameters, there was no significant differences with depth, where P > 0.05.

It is noteworthy that the photo-physiological parameters of the micro-phytoplankton at the three studied water depths varied differentially with the time of the day. Φ_{PSII} at 0-4, 5-10 and 11-29 m exhibited no clear trend, slight linear decline and a clear gradual

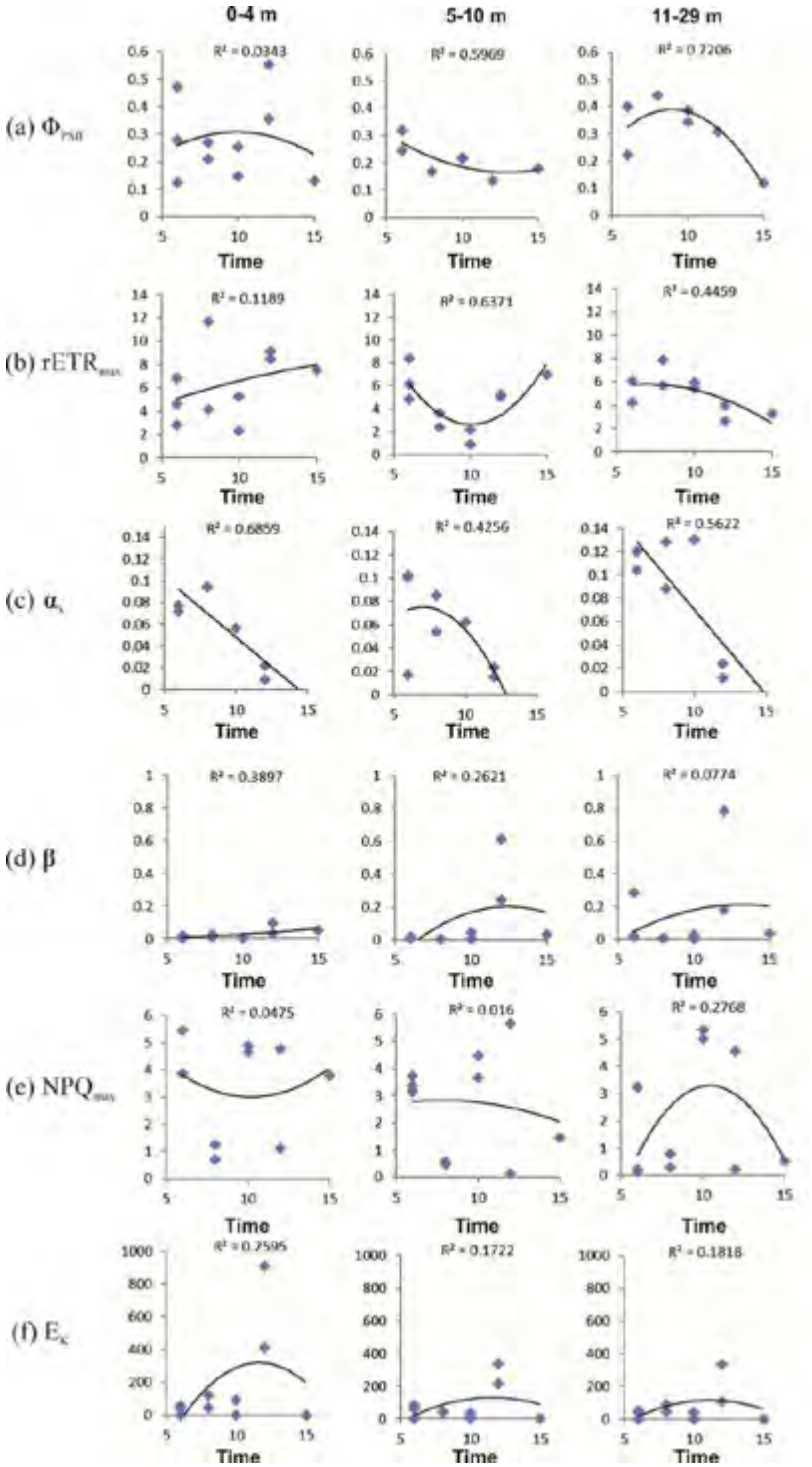

Figure 7. Physiological parameters (y-axis) (a) Effective quantum yield (Φ_{PSII}), (b) $rETR_{max}$, (c) α, (d) β, (e) NPQ_{max} and (f) E_k at three depth ranges of 0-4 m, 5-10 m and 11-29 m where the x-axis represents the time scale from 5:00 am to 15:00 pm, and the y-axis is the scale for the different parameters.

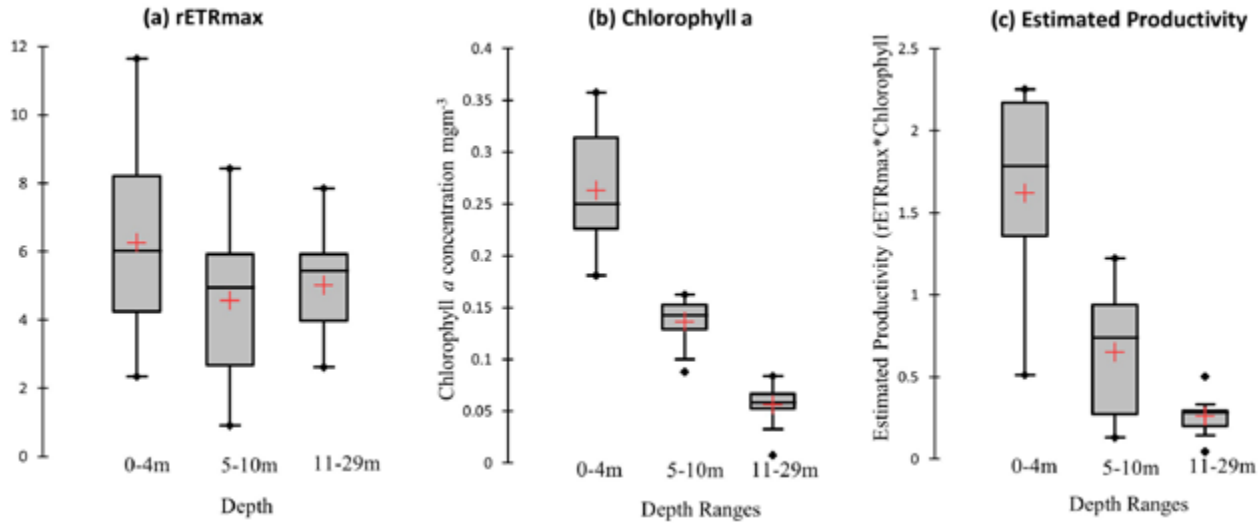

Figure 8. rETR$_{max}$ (a), Chl*a* concentration (b) and Estimated productivity (c) at depth ranges of 0-4 m, 5-10 m and 11-29 m at Saya de Mlaha Bank

decline (Fig. 7a), respectively, with the time of the day. The lowest ΦPSII occurred at around noon and 15:00 for 0-4 and 11-29 m, respectively. As for rETR$_{max}$, a very weak linear increase for 0-4 m, a U-shaped curve for 5-10 m and a gradual linear decrease for 11-29 m were recorded (Fig. 7b). For α and β, clear opposite trends were observed where α linearly decreased (Fig. 7c) and β linearly increased (Fig. 7d) with the time of the day. For NPQ$_{max}$ and E$_k$, a bell-shaped trend was observed for depths 11-29 m (Fig. 7e) and 0-4 m (Fig. 7f), respectively.

rETRmax, Chl*a* concentration and estimated productivity

Mean highest rETR$_{max}$ was recorded at the surface from 0-4 m and decreased at depth range 5-10 m and then increased slightly in the deeper water of 11-29 m (Fig. 8a). Both the Chl*a* concentration and estimated productivity were inversely proportional to the depth range of the water column. The Chl*a* concentration varied from the lowest at depth 11-29 m (0.05 ± 0.02 mgm^{-3}) to the highest of 0.26 ± 0.06 mgm^{-3} at 0-4 m (Fig. 8b). This trend was followed by estimated productivity where the lowest (0.23 ± 0.15 mgm^{-2}) was at the deeper depth range and the highest (1.62 ± 0.67 mgm^{-2}) at 0-4 m (Fig. 8c). Both the Chl*a* concentration and estimated productivity differed significantly among the depth ranges studied.

Principle Component Analysis

The Principle Component Analysis (PCA) showed the separation of the photo-physiological parameters from the biological parameters such as micro-phytoplankton densities, but not with Chl*a*. PCA explained 66.13% of the total data variance whereby F1 had more influence with 40.89% compared to F2 at 25.25%. It was clear that the station with highest density of micro-phytoplankton was at CTD 397 at the depth 0-4 m. Moreover, Chl*a* at depth 5-10 m showed the highest positive correlation with the TMPA and also with the subgroups of diatoms and dinoflagellates. The highest Φ_{PSII} (Yield) was at station CTD 404 in the near-surface layer of 0-4 m. In terms of stations, there were two cluster groupings; firstly CTD 401, 404 and 408 which had stronger correlation with the photo-physiology parameters, and a second cluster comprising of CTD 391, CTD 397 and 400 which correlated strongly with micro-phytoplankton abundance (Fig. 9).

Discussion

In oceanic waters, the abundance and growth performance of phytoplankton in the water column is partially dependent on vertical mixing as this process brings nutrients to the upper photic zone and thus boosts primary productivity (Diehl, 2002; Huisman *et al.*, 2004). Moreover, as highlighted by Bode *et al.* (1996), light plays an important role in the biomass of phytoplankton such that, if there are high nutrient levels, the absence of sufficient light will hinder phytoplankton growth.

In the present study, the highest abundance of micro-phytoplankton was recorded in the near-surface layer of the water column. The study was conducted during the winter season and thus, the high abundance may possibly be explained by upwelling where cold deeper nutrient rich water tends to mix with photic layers which eventually results in an increased abundance

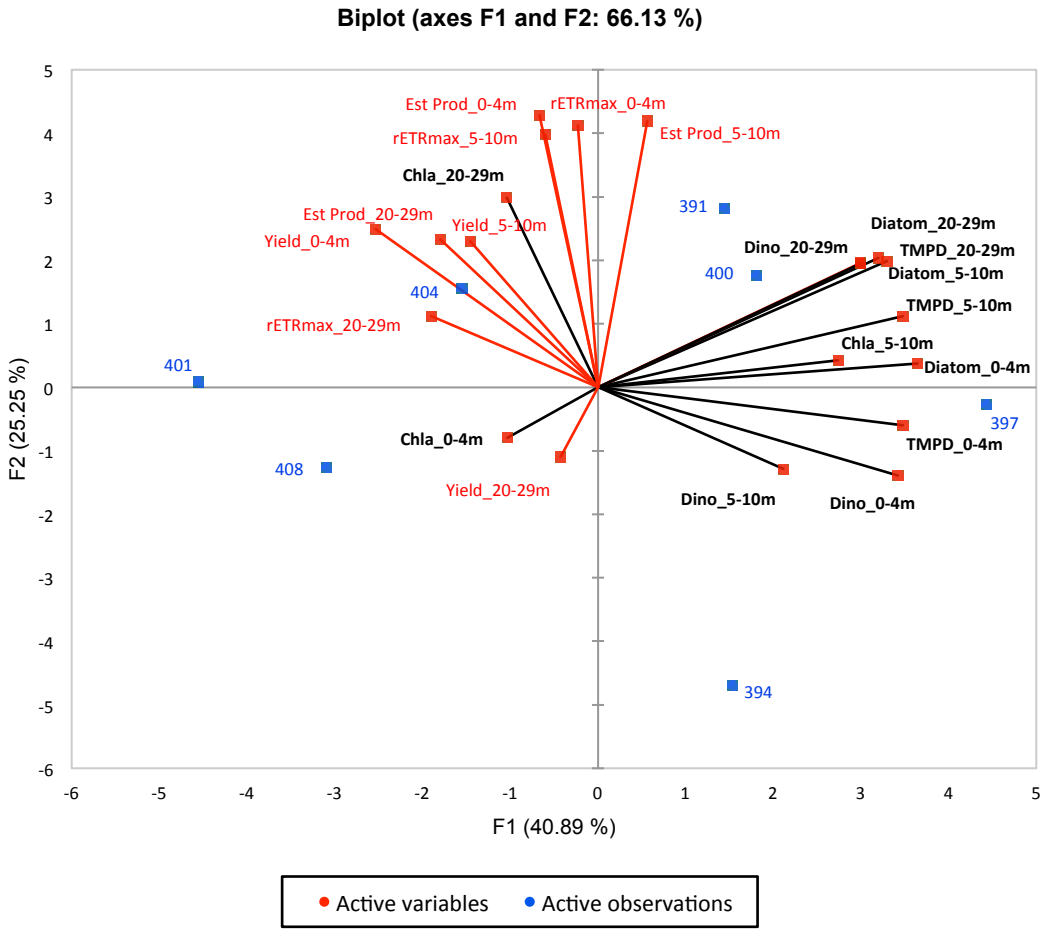

Figure 9. The Principal Component Analysis (PCA) representing correlation coefficient analysis for the different CTD stations with the photophysiology parameters, namley, Φ_{PSII} (Yield), $rETR_{max}$, Estimated productivity (Est Prod), and biological parameters such as Chl*a* concentration, and the abundances of Diatom, Dino (Dinoflagellates) and Total Micro-phytoplankton (TMP) at the studied depth ranges of 0-4 m, 5-10 m and 11-29 m.

of phytoplankton (Pitcher *et al.*, 2011; Yoder *et al.*, 1983). Water depth and abundance of phytoplankton displayed inverse proportionality. The highest difference in the abundance of micro-phytoplankton occurred between the near-surface layer of 0-4 m and the depth of 5-10 m at night. This may be partially attributed to the migration of zooplankton to the upper water layers in search of food while at the same time escaping predators at deeper depths. Goldyn and Kowalczewska-Madura (2007) demonstrated that a high abundance of zooplankton tends to cause a significant decrease in the phytoplankton abundance. The growth of phytoplankton decreases at night due to the absence of light, and coupled with the grazing activity by zooplankton, results in lower abundance of phytoplankton (Roman *et al.*, 1988; Shaw and Robinson, 1998).

Moreover, throughout the study period, diatoms were more dominant compared to dinoflagellates, irrespective of depth ranges, time of sampling and stations (Bazin *et al.*, 2014; Bernardi Aubry *et al.*, 2006). This may be explained by their ability to thrive under varying environmental conditions such as temperature or even light availability (Kokfelt *et al.*, 2009). Margalef (1978) found that strong vertical mixing favors the dominance of diatoms and that dinoflagellates more likely preferred stratified water columns where they are able to compete advantageously over other groups of phytoplankton due to their ability of locomotion which helps greatly in reaching light and nutrient rich water zones (Glibert, 2016; Smayda and Reynolds, 2003). It is also noteworthy that dinoflagellates are ecologically diverse with different species specifically adapted to different levels of nutrients, mixing and euphotic zone depth (Smayda and Reynolds, 2003). Other studies have confirmed the higher abundance of diatoms over dinoflagellates in intensely turbulent mixed waters (Irigoien, 2000; Jones and Gowen, 1990) aligning with the findings from Saya de Malha. The study conducted by Barlow *et al.* (2004) indicated that in oligotrophic waters, there was dominance of pico-plankton over micro and nano-plankton. Further

studies on pico- and nano-plankton are therefore warranted to obtain a thorough understanding of the variations in and dominance of different groups of phytoplankton at the Saya de Malha bank.

The genera that were recorded as having the highest percentage contribution in the current study were *Chaetoceros* (range: 5.38%-10.78%), *Coscinodiscus* (range: 6.24%-9.91%), *Navicula* (range: 8.85%-10.82%), *Nitzschia* (range: 8.11%-9.75%) and *Ceratium* (range: 3.42%-7.91%). These results are in accordance with the findings of Savidge and Lennon (1987) where the authors showed the numerical dominance of *Chaetoceros* in the planktonic community in oceanic Scottish waters. Similarly, Yang *et al*. (2014) reported a dominance of *Chaetoceros* from 1959 to 2009 in the Changjiang River Estuary and pointed out that the seasonal succession of *Chaetoceros* by *Coscinodiscus* could be attributed to the seasonal variation of nutrient level and water stability. Recently, Park *et al*. (2020) conducted a study around the Korean islands and reported the abundance of *Navicula*, among other genera. Muñiz *et al*. (2019) reported a high number of *Ceratium* in the Bay of Biscay. Kopczynska *et al*. (1986) documented the dominance of *Nitzschia* in the Antarctic Ocean. Thus, ample studies have in fact confirmed the common prevalence of the genera *Chaetoceros*, *Coscinodiscus*, *Navicula, Nitzschia* and *Ceratium* throughout oceanic waters, ranging from temperate to cold regions. Globally, the species diversity of phytoplankton is driven by temperature in the tropical regions coupled with different environmental conditions (Righetti *et al*., 2019).

Furthermore, photo-physiological studies by Li *et al*. (2016) and McMinn and Hegseth (2004) indicated higher Φ_{PSII} at deeper depths, which corroborates with the findings in the present study where high Φ_{PSII} tended to occur at a depth of 11-29 m. A plausible explanation for this may be that high nutrient availability at such depths may have boosted the photosynthetic rate. In the upper layer of water, even if the water is nutrient rich, lower Φ_{PSII} could indicate photo-inhibition and photo-protection (Barlow *et al*., 2017; Oliver *et al*., 2003). The Φ_{PSII} increased with depth in concurrence with the findings of Yuan *et al*. (2019). In addition, Silsbe *et al*. (2015) showed that light had a greater influence on the Φ_{PSII} compared to different nutrient regimes. In the near-surface layer of 0-4 m, the micro-phytoplankton faced high light intensity and responded by making optimal use of this light and eventually dissipating the excess. Higher $rETR_{max}$ values indicated that the micro-phytoplankton has higher acclimatization potential and thus a higher light saturation point (Ralph and Gademann, 2005; Wagner *et al*., 2006).

Micro-phytoplankton in the near-surface layer of 0-4 m had lower α compared to the depth range of 11-29 m. This showed that the micro-phytoplankton in the near-surface layer had higher acclimatization potency to high irradiance and explained the lower light usage efficiency (α). In contrast, the micro-phytoplankton at the depth of 11-29 m revealed higher light utilization efficiency maintaining a high photosynthetic rate even when there is lower light level. These results corroborate those of Yuan *et al*. (2019) and are indicative of the photo-adaptive strategies of the micro-phytoplankton in this under-explored region of the Saya de Malha. Higher dissipation of excess light at PSII (NPQ_{max}) was observed in the near-surface layer of 0-4 m compared to the depth range of 11-29 m; in line with the findings of Kashino *et al*. (2002) who reported an increase in NPQ_{max} of phytoplankton when exposed to high light regimes. Such responses in dissipating excess light is natural in micro-phytoplankton exposed to high light as a high level of NPQ may act as a safety valve to photo-protect its PSII, which is indicated by lower Φ_{PSII}. The minimum saturating irradiance, E_k, tended to be highest in the near-surface layer of 0-4 m and this was also the case in the study conducted by Yuan *et al*. (2019).

It is noteworthy that the trend in photochemical efficiency in terms of Φ_{PSII}, $rETR_{max}$ and NPQ_{max} with the time of the day was not clear in the micro-phytoplankton at any of the studied depths, as compared to dinoflagellates harbored by sedentary cnidarians, which show clear depressions in Φ_{PSII}, and increases in $rETR_{max}$ and NPQ_{max} around mid-day (Brown *et al*., 1999; Hoegh-Guldberg and Jones, 1999). The fact that micro-phytoplankton are in the water column, and not fixed to the seafloor and exposed to high light environments like the shallow sedentary corals, may likely explain the absence of a clear similar diurnal trend in photochemical efficiency. In laboratory-based experiments differential photochemical efficiency responses to variable light climates among diatoms (Lavaud and Lepetit, 2013) and dinoflagellates (Islabão *et al*., 2016) have been reported. The light-induced photochemical efficiency trends in micro-phytoplankton, when measured in communities, may mask the responses among the species present and thus, lead to poor detection of a clear trend in the overall response. Additional investigations using microscopy-PAM to look at the photo-physiology of individual cells from the different micro-phytoplankton species may help

to better understand their respective photo-physiological contributions and adjustments to diurnal variations in light regimes. On the other hand, the light usage efficiency (α) and photo-inhibition (β, the slope of the light curve beyond the onset of photo-inhibition) of the micro-phytoplankton at all studied depths exhibited clear decreasing and increasing trends, respectively, with the time of the day. This may be indicative of the micro-phytoplankton in the water column being collectively more sensitive in terms of α and β, as dynamic diurnal responses to photo-acclimate with the changes in light during the day.

Both the Chl*a* concentration and the estimated productivity decreased with depth. The fairly oligotrophic waters could be the reason behind the low level of Chl*a* in the waters surrounding Saya de Malha Bank (Jena *et al*., 2013). Bergstad *et al*. (2019) reported that surface salinity varied from 34.1 PSU to 34.6 PSU and the oligotrophic waters were characterized by phosphate levels of less than 0.5 µM, silicate levels of less than 0.05 µM, and ammonia levels below detectable range (< 0.01 µM) at the Saya de Malha Bank. Even though the $rETR_{max}$ might have shown a declining trend with the decrease in light, the low Chl*a* concentration contributed to the decrease in the estimated productivity (Bot, 1996). It should, however, be highlighted that estimated productivity deduced from Chl*a* biomass and the photo-physiological parameter, $rETR_{max}$, are rapid, relative measures and are only indicative of the changes with depth. Further studies using conventional methods of determining absolute productivity would be necessary to thoroughly understand productivity changes with depth.

Conclusion

This study presents additional data on spatial variation in micro-phytoplankton abundance and diversity, and the first photo-physiological assessment of micro-phytoplankton with depth and time of the day at the Saya de Malha Bank. Micro-phytoplankton abundance varied among the studied stations and decreased with depth. The most dominant micro-phytoplankton group was the diatoms at the Saya de Malha Bank. The photo-physiological assessments revealed that the Φ_{PSII}, $rETR_{max}$, NPQ_{max} did vary with the time of the day without clear general trends with respect to depth, while α and β exhibited clear opposite trends with the time of the day at all studied depths. The significant decline in estimated productivity with depth was mainly due to a significant decrease in Chl*a* as the $rETR_{max}$ only tended to diminish with depth. Further studies on other classes of phytoplankton like picoflagellate prokaryotes (*Prochlorococcus* and *Synechococcus*) and nanoflagellates (Haptophytes, Pelagophytes, Prasinophytes), and photochemical efficiency of important and dominant genera of micro-phytoplankton are necessary to thoroughly understand their contributions and their potentially depth-dependent photosynthetic functioning in relation to oceanic primary production in the Mascarene Plateau.

Acknowledgments

The underlying work was made possible with the support of the EAF-Nansen Programme "Supporting the Application of the Ecosystem Approach to Fisheries Management considering Climate Change and Pollution Impacts" executed by Food and Agriculture Organization of the United Nations (FAO) and funded by the Norwegian Agency for Development Cooperation (Norad). The authors are thankful to FAO for funding and supporting the Indian Ocean research expedition 2018 on the Saya de Malha Bank and Nazareth Bank with the R/V Dr Fridtjof Nansen, the Department of Continental Shelf, Maritime Zones Administration & Exploration of Mauritius for co-leading and coordinating the scientific expedition, the Mauritius-Seychelles Joint Commission of the Extended Continental Shelf for their support and assistance and granting the necessary authorisations, the Ministry of Blue Economy, Marine Resources, Fisheries and Shipping for granting the permits for sampling, and the University of Mauritius for logistic support and laboratory facilities. The research cruise leaders' Dr Odd Aksel Bergstad and Dr Dass Bissessur, and the participating researchers and cruise crew are also kindly acknowledged for their kind support. The authors also gratefully acknowledge the fellow participants on the expedition: K Sauba, J Rama, P Coopen, Y Oozeeraully, S Seeboruth, A Audit-Manna, A Nicolas, N Reetoo, D Kuyper, G Gendron, A Souffre, S Hollanda, R Melanie, J Harlay, L Caussy, K Tabachnick, M Olsen and TM Ensrud. The authors are indebted to the anonymous reviewers for their insightful comments that significantly improved the manuscript.

References

Armance M, Mattan-Moorgawa S, Bhagooli R (2019) Micro-phytoplankton density and diversity at a pilot oyster culture barachois site of Mauritius Island. Ocean Life 3 (1): 1-12

Aro EM, Virgin I, Andersson B (1993) Photoinhibition of photosystem II. Inactivation, protein damage and turnover. Biochimica et Biophysica Acta (BBA) - Bioenergetics 1143: 113-134 [https://doi.org/10.1016/0005-2728(93)90134-2]

Barlow R, Lamont T, Gibberd MJ, Airs R, Jacobs L, Britz K (2017) Phytoplankton communities and acclimation in a cyclonic eddy in the southwest Indian Ocean. Deep Sea Research Part I: Oceanographic Research Papers 124: 18-30 [https://doi.org/10.1016/j.dsr.2017.03.013]

Bazin P, Jouenne F, Friedl T, Deton-Cabanillas AF, Le Roy B, Véron B (2014) Phytoplankton diversity and community composition along the estuarine gradient of a temperate macrotidal ecosystem: combined morphological and molecular approaches. PLoS ONE 9: e94110 [https://doi.org/10.1371/journal.pone.0094110]

Bergstad OA, Bissessur D, Sauba K, Rama J, Coopen V, Oozeeraully V, Seeboruth S, Audit-Manna A, Nicolas A, Reetoo N, Tabachnick K, Kuyper D, Gendron G, Hollanda S, Melanie R, Souffre A, Harlay J, Bhagooli R, Soondur M, Ramah S, Caussy L, Ensrud TM, Olsen M, Høines ÅS (2019) Cruise reports RV Dr Fridtjof Nansen survey of regional resources and ecosystem of the Indian Ocean, leg 2.1: Characterizing ecosystems and morphology of the Saya de Malha Bank and Nazareth Bank. Survey No. 2018406, Seychelles and Mauritius, 3 May-3 June 2018. 144 pp

Bernardi Aubry F, Acri F, Bastianini M, Bianchi F, Cassin D, Pugnetti A, Socal G (2006) Seasonal and interannual variations of phytoplankton in the Gulf of Venice (Northern Adriatic Sea). Chemistry and Ecology 22: S71-S91 [https://doi.org/10.1080/02757540600687962]

Bhagooli R, Hidaka M (2003) Comparison of stress susceptibility of *in hospite* and isolated zooxanthellae among five coral species. Journal of Experimental Marine Biology and Ecology 291: 181-197

Bhagooli R (2010) Photosystem II responses to thermal and/or light stresses of distinct endosymbiotic ITS2 *Symbiodinium* types isolated from marine animal hosts. Journal of Environmental Research and Development *5* (1): 117-133

Bhagooli R, Kaullysing D (2019) Seas of Mauritius – Chapter 12. In: Sheppard CCR (ed) World seas: An environmental evaluation, 2nd Edition, Volume II: The Indian Ocean to the Pacific. Elsevier. Academic Press. pp 253-277 Paperback ISBN: 9780081008539, 912p [http://10.1016/B97-0-08-100853-9.00016-6]

Bhagooli R, Mattan-Moorgawa S, Kaullysing D, Louis YD, Gopeechund A, Ramah S, Soondur M, Pilly SS, Beesoo R, Wijayawanti DP, Bachok ZB, Monrás VC, Casareto BE, Suzuki Y, Baker AC (2021) Chlorophyll fluorescence - a tool to assess photosynthetic performance and stress photo-physiology in symbiotic marine invertebrates and seaplants. Marine Pollution Bulletin 165 [https://doi.org/10.1016/j.marpolbul.2021.112059]

Bode A, Casas B, Fernandez E, Maran E, Serret P, Varela M (1996) Phytoplankton biomass and production in shelf waters off NW Spain: spatial and seasonal variability in relation to upwelling. Hydrobiologia 341: 225-234 [https://doi.org/10.1007/BF00014687]

Bot, P (1996) A method for estimating primary production from chlorophyll concentrations with results showing trends in the Irish Sea and the Dutch coastal zone. ICES Journal of Marine Science *53*: 945-950 [https://doi.org/10.1006/jmsc.1996.0116]

Brown BE, Fitt WK, Dunne R.P, Gibb SW, Cummings DG, Ambarsari I, Warner ME (1999) Diurnal changes in photochemical efficiency and xanthophyll concentrations in shallow water reef corals: evidence for photoinhibition and photoprotection. Coral Reefs 18: 99-105 [https://doi.org/10.1007/s003380050163]

Buck JM, Sherman J, Bártulos CR, Serif M, Halder M, Henkel J, Falciatore A, Lavaud J, Gorbunov MY, Kroth PG, Falkowski PG, Lepetit B (2019) Lhcx proteins provide photoprotection via thermal dissipation of absorbed light in the diatom *Phaeodactylum tricornutum*. Nature Communication 10: 4167 [https://doi.org/10.1038/s41467-019-12043-6]

Derks AK, Bruce D (2018) Rapid regulation of excitation energy in two pennate diatoms from contrasting light climates. Photosynthesis Research 138: 149–165 [https://doi.org/10.1007/s11120-018-0558-0]

Devassy VP, Goes JI (1991) Phytoplankton assemblages and pigments in the exclusive economic zone of Mauritius (Indian Ocean). Indian Journal of Marine Sciences 20: 163-168

Diehl S (2002) Phytoplankton, light, and nutrients in a gradient of mixing depths: Theory 83: 13

Glibert M (2016) Margalef revisited: A new phytoplankton mandala incorporating twelve dimensions, including nutritional physiology. Harmful Algae *55*: 25–30 [https://doi.org/10.1016/j.hal.2016.01.008]

Goldyn R, Kowalczewska-Madura K (2007) Interactions between phytoplankton and zooplankton in the hypertrophic Swarzedzkie Lake in western Poland. Journal of Plankton Research 30: 33-42 [https://doi.org/10.1093/plankt/fbm086]

Guidi L, Lo Piccolo E, Landi M (2019) Chlorophyll fluorescence, photoinhibition and abiotic stress: Does it make any difference the fact to be a C3 or C4 species? Frontier Plant Science 10: 174 [https://doi.org/10.3389/fpls.2019.00174]

Hoegh-Guldberg O, Jones R (1999) Photoinhibition and photoprotection in symbiotic dinoflagellates from reef-building corals. Marine Ecology Progress Series 183: 73-86 [https://doi.org/10.3354/meps183073]

Huisman J, Sharples J, Stroom JM, Visser PM, Kardinaal WEA, Verspagen JMH, Sommeijer B (2004) Changes in turbulent mixing shift competition for light between phytoplankton species. Ecology 85: 2960-2970 [https://doi.org/10.1890/03-0763]

Irigoien, X, Harris, RP, Head, RN, Harbour, D (2000) North Atlantic Oscillation and spring bloom phytoplankton composition in the English Channel. Journal of Plankton Research 22 (12): 2367-2371

Islabão CA, Mendes CRB, Russo ADPG, Odebrecht C (2016) Effects of irradiance on growth, pigment content and photosynthetic efficiency on three peridinin-containing dinoflagellates. Journal of Experimental Marine Biology and Ecology 485: 73-82 [https://doi.org/10.1016/j.jembe.2016.08.012]

Jena B, Sahu S, Avinash K, Swain D (2013) Observation of oligotrophic gyre variability in the south Indian Ocean: Environmental forcing and biological response. Deep Sea Research Part I: Oceanographic Research Papers 80: 1-10 [https://doi.org/10.1016/j.dsr.2013.06.002]

Jones KJ, Gowen RJ (1990) Regime on summer phytoplankton composition in coastal and shelf seas of the British Isles 11: 557-567

Kashino Y, Kudoh S, Hayashi Y, Suzuki Y, Odate T, Hirawake T, Satoh K, Fukuchi M (2002) Strategies of phytoplankton to perform effective photosynthesis in the North Water. Deep-Sea Research II 49: 5049-5061 [https://doi.org/10.1016/S0967-0645(02)00177-7]

Kashino Y, Kudoh S (2003) Concerted response of xanthophyll-cycle pigments in a marine diatom, *Chaetoceros gracilis*, to shifts in light condition 6: 168-172

Kokfelt U, Struyf E, Randsalu L (2009) Diatoms in peat – dominant producers in a changing environment? Soil Biology and Biochemistry 41: 1764-1766 [https://doi.org/10.1016/j.soilbio.2009.05.012]

Kopczynska EE, Weber LH, El-Sayed SZ (1986) Phytoplankton species composition and abundance in the Indian sector of the Antarctic Ocean. Polar Biology 6: 161–169 [https://doi.org/10.1007/BF00274879]

Krause GH, Weis E (1991) Chlorophyll fluorescence and photosynthesis: the basics. Annual Review of Plant Biology 42: 313-349

Lavaud J, Lepetit B (2013) An explanation for the inter-species variability of the photoprotective non-photochemical chlorophyll fluorescence quenching in diatoms. Biochimica et Biophysica Acta (BBA) 1827: 294-302 [https://doi.org/10.1016/j.bbabio.2012.11.012]

Li J, Sun X, Zheng S (2016) *In situ* study on photosynthetic characteristics of phytoplankton in the Yellow Sea and East China Sea in summer 2013. Journal of Marine Systems 13: 94-106

Margalef M (1978) Life forms of phytoplankton as survival alternatives in an unstable environment. Oceanology Acta 4: 493-509

McMinn A, Ryan K, Gademann R (2003) Diurnal changes in photosynthesis of Antarctic fast ice algal communities determined by pulse amplitude modulation fluorometry. Marine Biology 143: 359-367 [https://doi.org/10.1007/s00227-003-1052-5]

McMinn A, Hegseth E.N (2004) Quantum yield and photosynthetic parameters of marine microalgae from the southern Arctic Ocean, Svalbard. Journal of the Marine Biological Association of the UK 84: 865-871

McMinn A, Hirawake T, Hamaoka T, Hattori H, Fukuchi M (2005) Contribution of benthic microalgae to ice covered coastal ecosystems in northern Hokkaido, Japan. Journal of Marine Biological Association UK 85: 283-289

McMinn A, Pankowskii A, Ashworth C, Bhagooli R, Ralph PJ, Ryan K (2010) *In situ* net primary productivity and photosynthesis of Antarctic sea ice algal, phytoplankton and benthic algal communities. Marine Biology 157 (6): 1345-1356

McMinn, A, Ashworth C, Bhagooli R, Martin A, Salleh A, Ralph P, Ryan K (2012) Antarctica coastal microalgal primary production and photosynthesis. Marine Biology 159(12):2827-2837

Mukherjee A, Das S, Bhattacharya T, De M, Maiti T, Kumar De T (2014) Optimization of phytoplankton preservative concentrations to reduce damage during long-term storage. Biopreservation and Biobanking 12: 139-147 [https://doi.org/10.1089/bio.2013.0074]

Muñiz O, Revilla M, Rodríguez J.G, Laza-Martínez A, Fontán A (2019) Annual cycle of phytoplankton community through the water column: Study applied to the implementation of bivalve offshore aquaculture in the southeastern Bay of Biscay. Oceanologia 61: 114-130 [https://doi.org/10.1016/j.oceano.2018.08.001]

Oliver RL, Whittington J, Lorenz Z, Webster IT (2003) The influence of vertical mixing on the photoinhibition of variable chlorophyll a fluorescence and its inclusion in a model of phytoplankton photosynthesis. Journal of Plankton Research 25: 1107-1129

Park J, Bergey EA, Han T, Pandey LK (2020) Diatoms as indicators of environmental health on Korean islands. Aquatic Toxicology 227: 105594 [https://doi.org/10.1016/j.aquatox.2020.105594]

Pitcher GC, Figueiras FG, Hickey BM, Moita M (2011) The physical oceanography of upwelling systems and the development of harmful algal blooms. Progress Oceanography 57: 5-32

Platt T, Jassby AD (1976) The relationship between photosynthesis and light for natural assemblages of coastal marine phytoplankton. Journal of Phycology 12: 421-430

Ralph PJ, Gademann R (2005) Rapid light curves: A powerful tool to assess photosynthetic activity. Aquatic Botany 82: 222-237 [https://doi.org/10.1016/j.aquabot.2005.02.006]

Righetti D, Vogt M, Gruber N, Psomas A, Zimmermann NE (2019) Global pattern of phytoplankton diversity driven by temperature and environmental variability. Science Advance 5: 6253 [https://doi.org/10.1126/sciadv.aau6253]

Roman MR, Ashton KA, Gauzens AL (1988) Day/night differences in the grazing impact of marine copepods. Hydrobiologia 167: 21-30 [https://doi.org/10.1007/BF00026291]

Sadally SB, Taleb-Hossenkhan N, Bhagooli R (2012) Micro-phytoplankton distribution and biomass at two lagoons around Mauritius Island. Special Issue on Sustainable Marine Environment, University of Mauritius Research Journal 18A: 54-87

Sadally SB, Taleb-Hossenkhan N, Bhagooli R (2014a) Spatio-temporal variation in density of microphytoplankton genera in two tropical coral reefs of Mauritius. African Journal of Marine Science 36: 423-438 [https://doi.org/10.2989/1814232X.2014.973445]

Sadally SB, Nazurally N, Taleb-Hossenkhan N, Bhagooli R (2014b) Micro-phytoplankton distribution and biomass in and around a channel-based fish farm: implications for sustainable aquaculture. Acta Oceanologica Sinica 33: 180-191 [https://doi.org/10.1007/s13131-014-0577-4]

Sadally SB, Taleb-Hossenkhan N, Casareto BE, Suzuki Y, Bhagooli R (2015) Micro-tidal dependent micro-phytoplankton C-biomass dynamics of two shallow tropical coral reefs. Western Indian Ocean Journal of Marine Science 14 (1-2): 53-72

Sadally SB, Taleb-Hossenkhan N, Bhagooli R (2016) Microalgal distribution, diversity and photo-physiological performance across five tropical ecosystems around Mauritius Island. Western Indian Ocean Journal of Marine Science 15 (1): 49-68

Sandooyea S, Avé H, Soondur M, Kaullysing D, Bhagooli R (2020) Variations in the density and diversity of micro-phytoplankton and micro-zooplankton in summer months at two coral reef sites around Mauritius Island. Journal of Sustainability Science and Management 15: 18-33 [https://doi.org/10.46754/jssm.2020.06.003]

Savidge G, Lennon HJ (1987) Hydrography and phytoplankton distributions in north-west Scottish waters. Continental Shelf Research 7: 45-66 [https://doi.org/10.1016/0278-4343(87)90063-X]

Schlüter L, Henriksen P, Nielsen TG, Jakobsen HH (2011) Phytoplankton composition and biomass across the southern Indian Ocean. Deep Sea Research Part I: Oceanographic Research Papers 58: 546-556 [https://doi.org/10.1016/j.dsr.2011.02.007]

Shaw W, Robinson C (1998) Night versus day abundance estimates of zooplankton at two coastal stations in British Columbia, Canada. Marine Ecology Progress Series 175: 143-153 [https://doi.org/10.3354/meps175143]

Silsbe GM, Smith REH, Twiss MR (2015) Quantum efficiency of phytoplankton photochemistry measured continuously across gradients of nutrients and biomass in Lake Erie (Canada and USA) is strongly regulated by light but not by nutrient deficiency. Canadian Journal of Fisheries and Aquatic Sciences 72: 1-45

Smayda TJ, Reynolds CS (2003) Strategies of marine dinoflagellate survival and some rules of assembly. Journal of Sea Research 12: 91-106

Soondur M, Kaullysing D, Boojhawon R, Lowe R, Casareto B, Yoshimi S, Bhagooli R (2020) Diel variations in density and diversity of micro-phytoplankton community in and around a barachois-based oyster culture farm. Journal Sustainable Science and Management 15: 2-17 [https://doi.org/10.46754/jssm.2020.06.002]

Tomas CR (ed) (1996) Identifying marine diatoms and dinoflagellates. Academic Press, San Diego.

Wagner H, Jakob T, Wilhelm C (2006) Balancing the energy flow from captured light to biomass under fluctuating light conditions. New Phytologist 169: 95-108 [https://doi.org/10.1111/j.1469-8137.2005.01550.x]

Yang S, Han X, Zhang C, Sun B, Wang X, Shi X (2014) Seasonal changes in phytoplankton biomass and dominant species in the Changjiang River Estuary and adjacent seas: General trends based on field survey data 1959–2009. Journal Ocean University China 13: 926-934 [https://doi.org/10.1007/s11802-014-2515-7]

Yoder JA, Atkinson LP, Stephen Bishop S, Hofmann EE, Lee TN (1983) Effect of upwelling on phytoplankton productivity of the outer southeastern United States continental shelf. Continental Shelf Research 1: 385-404 [https://doi.org/10.1016/0278-4343(83)90004-3]

Yuan C, Xu Z, Zhang X, Wei Q, Wang H, Wang Z (2019) Photosynthetic physiologies of phytoplankton in the eastern equatorial Indian Ocean during the spring inter-monsoon. Acta Oceanologica Sina 38: 83-91 [https://doi.org/10.1007/s13131-018-1218-0]

Zarauz L, Irigoien X (2008) Effects of Lugol's fixation on the size structure of natural nano-microplankton samples, analyzed by means of an automatic counting method. Journal of Plankton Research 30: 1297-1303 [https://doi.org/10.1093/plankt/fbn084]

Diversity and distribution of the shallow water (23-50 m) benthic habitats on the Saya de Malha Bank, Mascarene Plateau

Sundy Ramah[1,4]*, Gilberte Gendron[2,3], Ranjeet Bhagooli[4,5,6,7], Mouneshwar Soondur[4,5], Andrew Souffre[8], Rodney Melanie[8], Priscilla Coopen[9], Luvna Caussy[1], Dass Bissessur[9], Odd A. Bergstad[10]

[1] Albion Fisheries Research Centre, Ministry of Blue Economy, Marine Resources, Fisheries & Shipping, Albion, Petite-Riviere, 91001, Republic of Mauritius

[2] Island Biodiversity & Conservation Centre, University of Seychelles, PO Box 1348, Anse Royale, Mahé, Seychelles

[3] Seychelles National Parks Authority, PO Box 1240, Orion Mall, Victoria, Mahé, Seychelles

[4] Department of Biosciences & Ocean Studies, Faculty of Science & Pole of Research Excellence in Sustainable Marine Biodiversity, Réduit 80837, University of Mauritius, Republic of Mauritius

[5] The Biodiversity and Environment Institute, Réduit, Republic of Mauritius

[6] Institute of Oceanography and Environment (INOS), University Malaysia Terengganu, 21030 Kuala Terengganu, Terengganu, Malaysia

[7] Society of Biology (Mauritius), Réduit, Republic of Mauritius

[8] Seychelles Fishing Authority, Fishing Port, PO Box 149, Victoria, Mahé, Seychelles

[9] Department for Continental Shelf, Maritime Zones Administration and Exploration, Prime Minister's Office, Belmont House 2nd Floor, Intendance Street, Port Louis, 11328, Republic of Mauritius

[10] Institute of Marine Research (IMR), PO Box 1870 Nordnes, N-5817 Bergen, Norway

* Corresponding author: sundy.ramah@gmail.com

Abstract

The Saya de Malha Bank (SMB) is one of the largest and least studied marine banks on the Mascarene Plateau. This study aimed to examine the diversity and distribution of the main benthic habitats in the shallow waters of the SMB (23 to 50 m). The survey was carried out in May 2018 during the EAF-Nansen Indian Ocean Research Expedition using a Remotely Operated Vehicle (ROV) deployed at 15 stations. Four main benthic habitats were investigated and their relative abundance determined during the survey. The 143,110 m² surveyed area revealed proportional benthic habitat cover of 43.6 ± 22.4, 24.5 ± 21.9, 21.2 ± 27.8, and 10.5 ± 12.6 % for seaweed, abiotic substrate, seagrasses and corals, respectively. The seaweed habitat (43.6 %) was mainly composed of *Halimeda* spp. It represented up to 77 % of the habitats observed at SS34 (4553 m²). Even though seaweeds are considered seasonal, their dominance at all stations creates an important habitat structure for many organisms. The seagrass habitat (21.2 %) was dominated by *Thalassodendron ciliatum*. This habitat covered up to 93 % of the area investigated at SS38 (5950 m²) and was found mainly on the eastern side of the bank. The live hard coral habitat (10.5 %) was the highest at SS36-2 (35% of 9819 m²) and was more homogenously spread within the shallow areas. The unstable and the stable bare bottom substrate habitat (24.7 %) characterized as abiotic habitat was mainly composed of bedrock, sand, and rubble. It dominated at SS42 where it constituted 72.5 % of the 5114 m² investigated and was recorded at all stations. Further research is warranted to better understand the diversity and the distribution of benthic habitats within the shallow waters of the SMB, along with collection of targeted benthic organisms for identification at higher taxonomic levels, to better formulate conservation and management measures and strategies.

Keywords: Saya de Malha Bank, shallow water, benthic habitat, distribution, diversity, ROV

http://dx.doi.org/10.4314/wiojms.si2021.2.5

Introduction

The Saya de Malha Bank (SMB) forms part of the Mascarene Plateau, an aseismic ridge that extends from Mauritius to the Seychelles and is comprised of the SMB, the Nazareth Bank, and the Cargados Carajos Bank. It is one of the largest submerged ocean banks in the world, with the closest land approximately 300 km to the west known as Agalega (Bhagooli and Kaullysing, 2019). The bank covers an area of approximately 40,808 km^2 and is subsequently divided into two regions: the north, also known as the Ritchie Bank; and the south which is known to be the largest area of the SMB (Vierros, 2009). The bank consists of a series of narrow shoals, with depths ranging from 17 to 29 m on the rim, and slopes on all sides of the bank. Some areas of the bank are shallow, with the shallowest point (8 m) known as the Poydenot Rock (New *et al.,* 2013). The shallow areas of the SMB are covered with seagrass and sparsely distributed small coral reefs (Obura *et al.,* 2012). Due to its remote location, limited studies on its benthic habitats have been carried out. Most of the studies conducted were between the 1960's and 1990's, mostly by the Russian expedition, principally targeting physical oceanography and fishery research (Vortsepneva, 2008) or seabed mineral resources and bathymetry studies (Shor and Pollard, 1963; Meyerhoff and Kamen-Kaye, 1981; Gershanovich and Dubinets, 1991; Badal, 2003; Rogers, 2012; Seamounts Project, 2013; Lindhorst *et al.,* 2019).

Since 2012, the SMB has been jointly managed by the Republic of Mauritius and the Republic of Seychelles through the Mauritius-Seychelles Joint Management Area (JMA) Commission (CLCS, 2011), where the Commission has exclusive rights to explore, exploit, conserve and manage natural resources such as minerals, petroleum, and benthic resources found on the seabed and subsoil. Benthic habitats are diverse as are the biological communities inhabiting and shaping them (Henseler *et al.,* 2019). However, only a few comprehensive major benthic habitat (corals, seagrass, seaweed, and bare substrate) studies are available to date (Rosen, 1971; Fredericq *et al.,* 1999; Hagan and Robinson, 2001; Hilbertz and Goreau, 2002; and Milchakova *et al.,* 2005). In February 2021, the SMB was the target of an expedition led by Greenpeace with the Arctic Sunrise vessel (Drozdovskiy, 2021). It aimed at documenting the biodiversity and threats to the bank. However, no data has been made available on the area to date following that expedition. Consequently, an assessment of the benthic habitat making up the SMB is urgently needed to better understand the potential marine resources it hosts and the sensitivity of the area.

The bank has been used as an illustration of a likely Ecologically or Biologically Significant Area (EBSA), satisfying four out of the seven criteria: it's uniqueness or rarity; special importance for life history stages of species; importance for threatened, endangered or declining species and/or habitats; and for its biological productivity (Obura *et al.,* 2012). Another analysis by the World Wildlife Fund (WWF) further emphasized the significance of Saya de Malha through satisfying three other EBSA criteria such as: vulnerability, fragility, sensitivity, or slow recovery; biological diversity; and naturalness, and the bank was selected as a priority seascape of global significance for its ecoregional conservation strategy (Christiansen, 2010). Due to the importance of some areas in the SMB, Hilbertz and Goreau made two expeditions to the bank in 1997 and 2002 with the aim of creating an artificial island using electricity to accrete the minerals in sea water onto a metal structure (Hilbertz and Goreau, 2002) on the Ritchie Bank (northern region).

Scientific research on the underlying seafloor of the SMB has become critical to help both the Republic of Mauritius and the Republic of Seychelles in the future management and development of effective conservation strategies within the JMA using science-based evidence. As such, in May 2018, an Indian Ocean Research Expedition was carried out on the SMB on board the RV Dr Fridtjof Nansen under the EAF-Nansen Programme Science Plan Theme 7 'Habitat mapping' - facilitating collection of baseline data on a range of benthic habitats. The expedition surveyed the shallow plateau of the SMB as well as the rim and upper slopes. For this study, particular attention has been given to the most important shallow water benthic habitats found on SMB at depths between 23 – 50 m, while areas of the plateau deeper than 50 m were considered by Bergstad *et al.* (2021, *in press*). The aim of this study was to supplement earlier studies and characterise the major marine benthic habitats (biotic and abiotic) found within the shallow waters of SMB. The present survey used a non-destructive methodology; that is, visual observations by using high-definition videos taken from a remotely operated vehicle (ROV), as compared to the use of benthic samplers and trawls used in previous surveys (Hilbertz and Goreau, 2002; Vortsepneva, 2008). The objective was to develop the first map of the SMB characterising the diversity and

the distribution of its major benthic biotic and abiotic habitats found within its shallow water areas.

Materials and methods

Study sites

The Saya de Malha Bank (SMB) is located between 8°30' – 12°00'S and 59°30' – 62°30'E and is the largest bank of the Mascarene Plateau with an area of approximately 40,000 km^2. The shallow waters of the SMB were investigated during the EAF-Nansen Indian Ocean Research Expedition on board the RV Dr Fridtjof Nansen, within the 23 to 50 m depth range. Two high-resolution Multi Beam Echo Sounders (MBES), Kongsberg EM 710 and EM 302 (operation depth 3 to 2000 m and 10 to 7000 m, respectively) helped with mapping the seafloor to adequately select the studied stations. Fifteen stations (SS4, SS9, SS13, SS34, SS36-1, SS36-2, SS37-1, SS37-2, SS38, SS39-1, SS39-2, SS39-3, SS39-4, SS40 and SS42) were within the targeted depth range and were therefore selected for the survey (Fig. 1). SS36, SS37 and SS39 were split into different stations but were found within the same area.

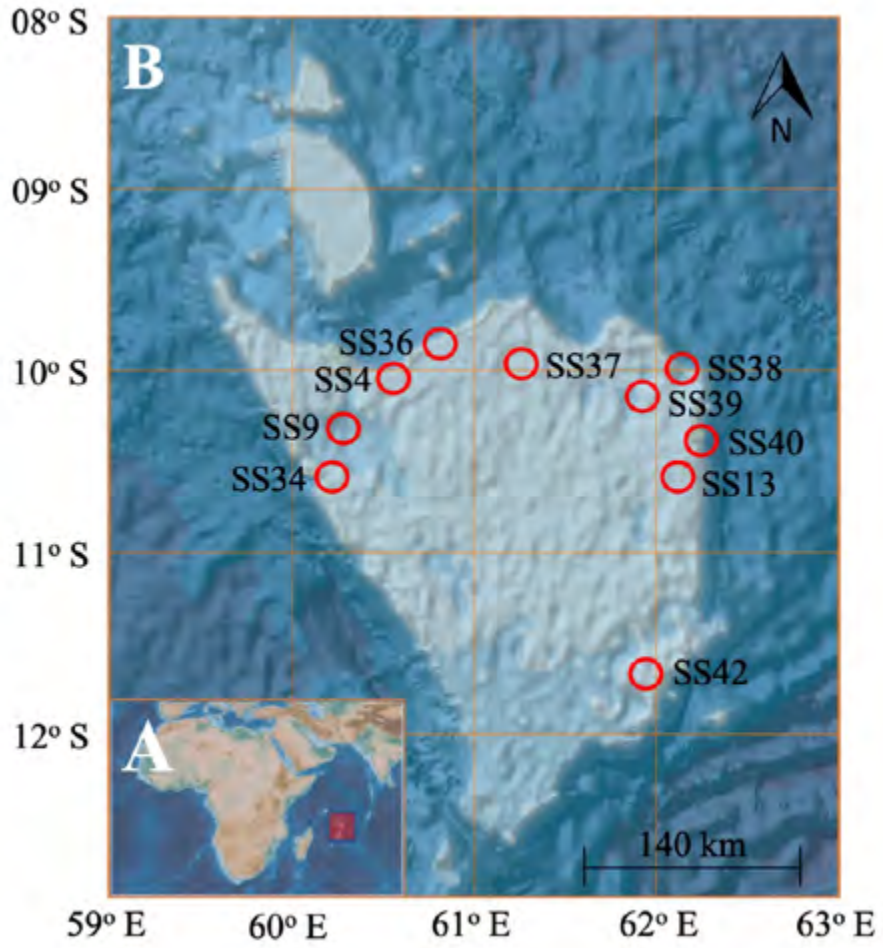

Figure 1. Map of the Saya de Malha Bank indicating the surveyed stations. A: Western Indian Ocean region map showing the location of Saya de Malha Bank in the red box. B: Map showing the 15 shallow surveyed stations (SS) in red circles. SS36 represents both stations SS36-1 and SS36-2l, SS37 represents both stations SS37-1 and SS37-2 and SS39 represents stations SS39-1, SS39-2, SS39-3 and SS39-4. The maps were prepared using the General Bathymetric Chart of the Ocean (EBCO) Bathymetry Grid layer data 2020.

Video transect data collection

In-situ visual data collection was carried out using the HD camera of a tethered ROV, able to operate at depth between 20 – 1000 m, attached to a Video-assisted Multi-sampler (VAMS), a tubular cage hosting the ROV (Serigstad *et al.,* 2015). The ROV attached to the VAMS was used to carry out the video transect survey in two modes: 1) as a point sampler where the VAMS was deployed on the seabed allowing the ROV to explore the immediate 15 m vicinity in four directions (north, east, south and west); and 2) in a towed

Table 1. Percentage cover of the biotic (seagrass, seaweed and live hard coral) and the abiotic (sand, rubble and bedrock) habitats, depth range of each station, GPS locations and total area surveyed at each station.

ROV Operation Modes	Station N°	Latitude (S)	Longitude (E)	Total Surface Explored by ROV per dive (m^2)	Depth Range (m)	Biotic Category			Abiotic Category
						Seagrass (%)	Seaweed (%)	Live Hard Coral (%)	Bottom Substrate (Unstable & Stable) (%)
Mode 1	SS4	-10.113192	60.575226	703	29 - 32	20	51.8	5.2	23
	SS9	-10.427421	60.140288	703	45 - 50	0	30	0	70
	SS13	-10.732368	62.130394	703	28 - 31	52	47	0	1
	SS34	-10.625219	60.199550	4553	44 - 46	1	77	0	22
	SS36-1	-9.831724	60.762377	12228	46 - 50	0	72.4	23.3	4.3
	SS36-2	-9.859240	60.791336	9819	23 - 30	13.9	23.1	35	28
	SS37-1	-10.094556	61.221217	11674	37 - 42	11.1	71.2	4.3	13.4
	SS37-2	-10.092485	61.242757	13330	32 - 35	19.6	52.5	4.2	23.7
Mode 2	SS38	-10.062541	62.183355	5950	26 - 30	93	5	1	1
	SS39-1	-10.382314	62.078151	13070	39 - 43	1.2	71.3	13.8	13.7
	SS39-2	-10.381302	62.093671	10211	31 - 33	0	33.3	33.3	33.4
	SS39-3	-10.379792	62.123875	4143	24 - 26	65	21	9	5
	SS39-4	-10.377526	62.204940	14600	33 - 43	22.6	26.2	25	26.2
	SS40	-10.736205	61.945050	36309	38 - 50	18.8	48	0.2	33
	SS42	-11.676877	61.948717	5114	47 - 50	0	25	2.5	72.5

mode whereby the vessel towed the VAMS at 5 m above the seabed along pre-determined transects perpendicular to isobaths at 0.1-0.4 knots while the ROV, attached to the VAMS, explored the underlying seabed. The distance between the ROV camera and the seabed was kept at 2 m, with a lens' swarth width of 15 m during steady passage, depending on the environment and sea condition. As a first exploratory survey, several stops were made along the transects in order to capture close-up videos for record and identification of certain benthic organisms. The video records were logged with data on GPS position to calculate the distance covered by the ROV along the transect, dive time and depth using the CAMPOD Logger software, a camera-based data collection software designed by the Institute of Marine Science of Norway (IMR) that is used with the ROV. The CAMPOD Logger uses the same principle as the Coral Point Count with Excel extension (CPCe) Software (Kohler and Gill, 2006). The data was further analysed after the cruise.

Video data analyses

The video records were further analysed during a workshop organised in August 2019 in Mauritius that brought together various experts. From the footage obtained at the different stations, focus was placed on the four main benthic habitats: live hard corals; seagrass; seaweed; and bare substrate (stable and unstable). The abiotic bottom substrate cover was calculated when no other biotic benthic habitat was present, and it was further sub-categorised into sand and rubble, which represented the unstable substrate, and bedrock, which represented the stable substrate. The sub-category 'sand' was used for fine and coarse substrates, where typically ripple marks were present comprising of small fossil gastropod and bivalve shells and dead calcareous seaweed leaves (e.g., *Halimeda* spp.). The 'rubble' sub-category was used for broken corals, small pebbles, broken gravel, and stones while the 'bedrock' sub-category was used to describe substrates involving basalt, limestone, cemented sand, and/or boulders, including when covered by a thin superficial layer of soft sediment. The percentage habitat cover was determined by dividing the area covered by each habitat category recorded along the transect by the total area of the transect at each station and multiplied by 100. The area of one habitat category was calculated using the distance moved by the ROV over the transect, calculated using the GPS coordinates at the point where a specific habitat category started and ended, multiplied by the ROV lens' swarth of 15 m.

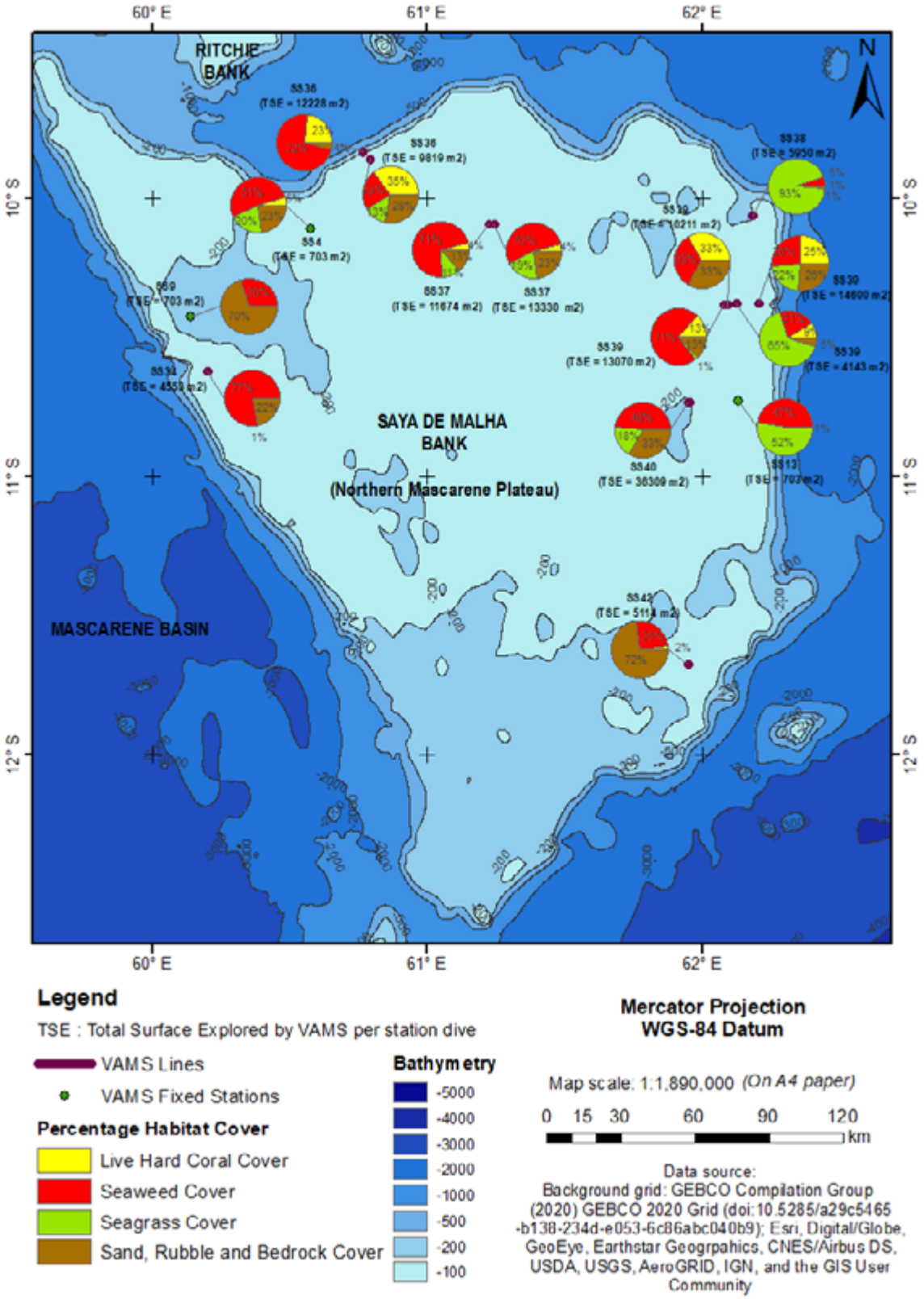

Figure 2. Percentage habitat cover for the total shallow-water seafloor area explored by the ROV (VAMS) in the shallow water of Saya de Malha Bank. Total habitat cover represented by live hard coral cover (yellow), seaweed cover (red), seagrass cover (green) and bottom substrate (sand, rubble and bedrock) cover (brown). Total number of stations = 15. Map Data Source: Background grid – GEBCO Compilation Group (2020) GEBCO 2020 Grid (doi:10.5285/a29c5465-b138-234d-e053-6c86abc040b9); Esri,Digital/Globe, GeoEYe, Earthstar Geographics, CNES/Airbus DS, USDA, USGS, AeroGrid, IGN, and the GIS User Community. Mercator Projection WGS-84 Datum.

Results

Live hard coral cover and diversity

The highest percentage of live hard corals was recorded at station SS36-2 (35 % in 9819 m²), at depths ranging from 44.5 - 46.8 m. The lowest percentage of live hard coral cover was recorded at station SS40 with 0.2 % in an area of 36309 m². No live hard corals were recorded during the survey at stations SS4, SS9 and SS13 (Table 1 and Fig. 2). Shallow waters harboured a range of hard live coral colonies such as branching and massive *Porites, Acropora* spp., *Heliopora* sp., *Turbinaria* spp., *Danafungia* spp., *Herpolitha* spp., *Favites* spp., *Dipsastraea* spp., *Goniastrea* spp., *Lobophyllia* spp., *Seriatopora* spp., and *Goniopora* spp. (Fig. 3 and Table 2).

Seagrass cover and diversity

The highest seagrass cover was recorded at station SS38 with 93 % per 5959 m². This station had an abiotic substrate cover (1 %) comprised of rubble and sand. These are suitable substrates for *Thalassodendron ciliatum* which was abundant at those stations. The lowest seagrass percentage cover was observed at station SS34 with 1 % per 4553 m², while no seagrass was observed at stations SS9, SS36-1, SS39-2 and SS42 (Table 1 and Fig. 2). Another species of seagrass observed during the survey was *Halophila decipiens* (Table 2 and Fig. 4) observed to occur as deep as 50 m, but in small, isolated patches. These mainly occurred at stations SS34, SS37 and SS40 where sand was abundant. Seagrass, consisting primarily of *T. ciliatum,* occurred from 38 m in depth and formed large meadows as depth became shallower.

Seaweed cover and diversity

The highest percentage cover for seaweed was found at SS34 (77 % in 4553 m²) while the lowest percentage cover was observed at SS38 (5 % in 5950 m²) (Table 1

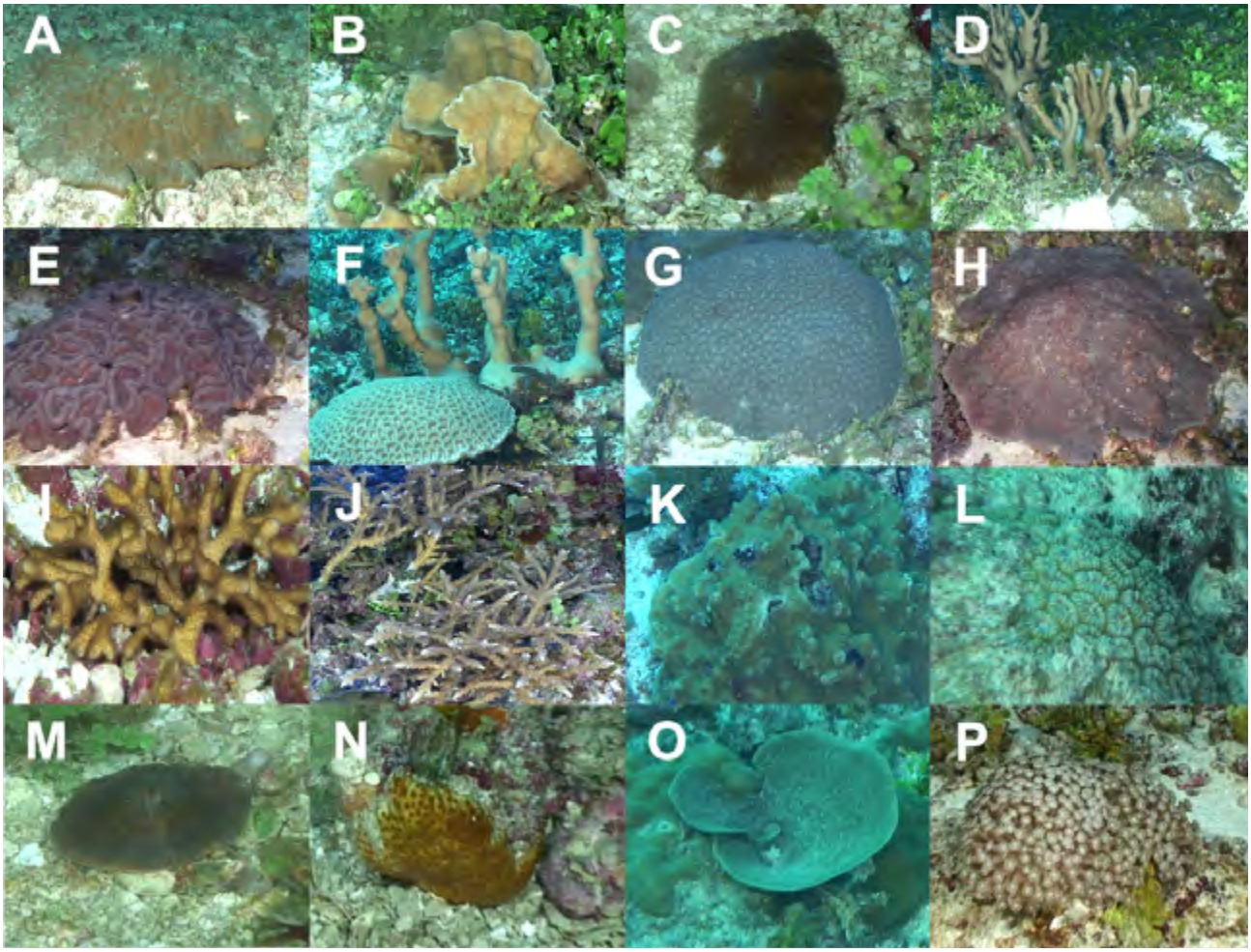

Figure 3. Common coral genera found in the shallow waters of Saya de Malha Bank. A: *Porites* sp. at SS4 (32 m); B: *Turbinaria* sp. at SS36 (38 m); C: *Herpolitha* sp. at SS36 (38 m); D: *Heliopora* sp. and *Platygyra* sp. at SS36 (38 m); E: *Lobophyllia* sp. at SS39 (39 m); F: *Porites* sp. and *Goniastrea* sp. at SS39 (33 m); G: *Favites* sp. at SS39 (37 m); H: *Leptoria* sp. at SS39 (43 m); I: *Seriatopora* sp. at SS42 (49 m); J: *Acropora* sp. at SS39 (35 m); K: *Echinopora* sp. at SS36 (25 m); L: *Dipsastraea* sp. at SS36 (25 m); M: *Danafungia* sp. at SS36 (42 m); N: *Cyphastrea* sp. at SS36 (38 m); O: *Pachyseris* sp. at SS36 (25 m); and P: *Goniopora* sp. at SS37 (39 m).

Table 2. List of recorded biotic habitat genera at each station (SS) and depth range (m).

Station N°	Depth Range (m)	Biotic habitat category		
		Seagrass genera	Seaweed genera	Live Hard Coral genera
SS4	29 - 32	*Thalassodendron ciliatum*	*Halimeda* spp., *Lithothamnion* spp.	*Heliopora* sp., *Porites* spp., *Favites* spp.
SS9	45 - 50	Nil	*Lithothamnion* spp.	Nil
SS13	28 - 31	*T. ciliatum*	*Lithothamnion* spp., *Caulerpa cuppresoides, Udotea* spp.,	Nil
SS34	44 - 46	*Halophila decipiens*	*Lithothamnion* spp., *Halimeda* spp., *Udotea* sp.	Nil
SS36-1	46 - 50	Nil	*Lithothamnion* spp., *Halimeda* spp.	Unk. Encrusting coral, *Galaxea* sp., *Danafungia* sp., *Acropora* spp., *Porites* spp., *Turbinaria* sp., *Herpolitha* sp., *Dipsastraea* sp., *Heliopora* sp., *Astreopora* sp., *Pocillopora* sp., *Platygyra* sp., *Cyphastrea* sp.
SS36-2	23 - 30	*T. ciliatum*	*Lithothamnion* spp., *Halimeda* spp.	*Acropora* spp., *Porites* spp., *Turbinaria* sp., *Herpolitha* sp., *Dipsastraea* sp., *Heliopora* sp, *Pocillopora* sp., *Millepora* sp., *Echinopora* sp., *Pachyseris* sp.
SS37-1	37 - 42	*T. ciliatum*	*Lithothamnion* spp., *Halimeda* spp., *Udotea* spp.	*Heliopora* sp., *Porites* spp., *Favites* spp., *Turbinaria* sp., *Herpolitha* sp., *Dipsastraea* spp., *Acropora* spp., *Goniopora* sp.
SS37-2	32 - 35	*T. ciliatum*	*Lithothamnion* spp., *Caulerpa cuppresoides, Udotea* spp.,	*Porites* spp., *Goniopora* sp., *Dipsastraea* spp., *Turbinaria* spp., *Acropora* spp., *Acanthastrea* spp.
SS38	26 - 30	*T. ciliatum*	*Lithothamnion* spp., *Caulerpa cuppresoides, Halimeda* spp.	*Acropora* spp.
SS39-1	39 - 43	*T. ciliatum, H. decipiens*	*Lithothamnion* spp., *Halimeda* spp., *Caulerpa cuppresoides, Udotea* spp.,	*Turbinaria* sp., *Porites* spp., *Acropora* spp., *Dipsastraea* spp., *Heliopora* sp., *Lobophyllia* sp., *Favites* spp.
SS39-2	31 - 33	Nil	*Lithothamnion* spp., *Halimeda* spp., *Caulerpa taxifolia*	*Heliopora* sp., *Porites* spp., *Dipsastraea* spp., *Goniastrea* sp.
SS39-3	24 - 26	*T. ciliatum*	*Lithothamnion* spp., *Udotea* spp., *Caulerpa cuppresoides, Halimeda* spp.	*Porites* spp., *Heliopora* sp.,
SS39-4	33 - 43	*T. ciliatum*	*Lithothamnion* spp., *Halimeda* spp., *Udotea* spp., *Caulerpa taxifolia*.,	*Porites* spp., *Acropora* spp., *Platygyra* spp., *Heliopora* sp., *Goniopora* spp., *Dipsastraea* spp., *Turbinaria* spp., *Danafungia* spp., *Pavona* spp., *Seriatopora* spp., *Stylophora* sp., *Lobophyllia* sp., *Goniastrea* sp., *Leptoria* sp.
SS40	38 - 50	*H. decipiens*	*Lithothamnion* spp., *Caulerpa cuppresoides, Caulerpa taxifolia*., *Udotea* spp., *Halimeda* spp.,	*Heliopora* sp., *Stylophora* sp.
SS42	47 - 50	Nil	*Lithothamnion* spp.	*Acropora* spp., *Seriatopora* spp.

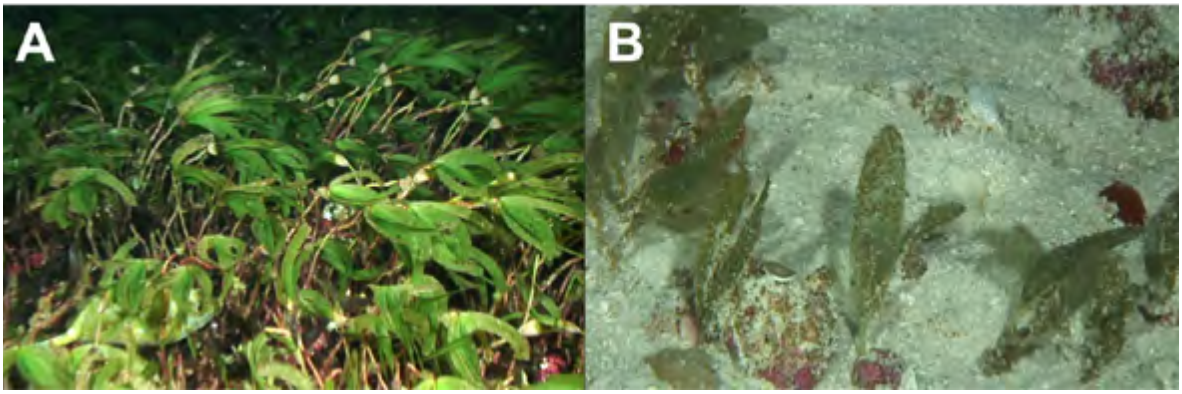

Figure 4. Seagrass species found in the shallow waters of the Saya de Malha Bank. A: *Thalassodendron ciliatum* at SS38 (28.8 m); and B: *Halophila decipiens* at SS40 (45.5 m).

and Fig. 2). Five main seaweeds were observed in the shallow water of SMB, namely *Halimeda* spp., *Lithothamnion* spp., *Caulerpa cupressoides, C. taxifolia* and *Udotea* spp. (Table 2 and Fig. 5), with *Halimeda* spp. being the most dominant at all stations except for SS42 where only *Lithothamnion* spp. occurred (25 % in an area of 5114 m²). At all the stations where *Halimeda* spp. cover was found to be high, the upper layer of the sediment seemed to consist of the dead calcareous leaves of this species. The seaweed *Caulerpa cupressoides* was observed forming clusters within *T. ciliatum* seagrass meadows, while the seaweed *Udotea* spp. and *Caulerpa taxifolia* were also observed to occur in small isolated patches.

Bottom substrate cover and characteristics

The highest bottom substrate percentage cover (consisting of either one of sand, rubble and bedrock or a mixture of the three) was observed at station SS42 with 72.5 % over an area of 5114 m². The lowest percentage substrate cover was at SS13 and SS38 with 1 % over an area of 703 m² and 5950 m², respectively. Most of the cover at the stations varied between sand and rubble while the presence of bedrock was recorded at stations SS36, SS37 and SS39 only. Station SS39 had the highest percentage of bedrock cover recorded while at stations SS34, SS38, SS40 and SS42 the bottom substrate was composed of sand and/or rubble.

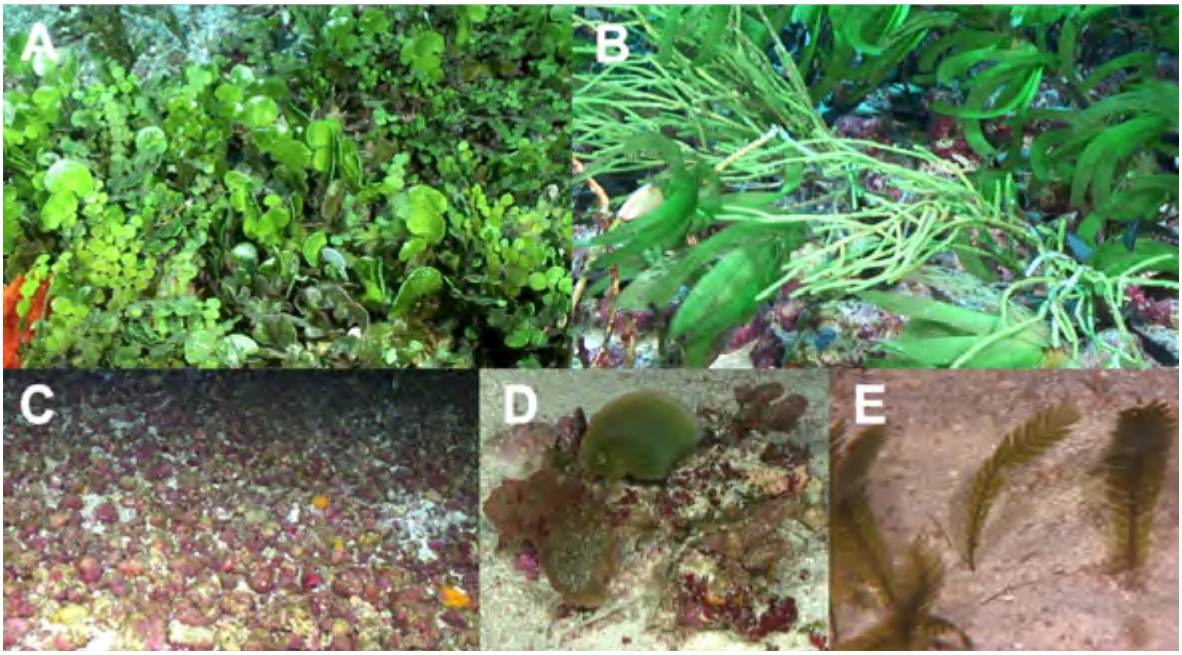

Figure 5. Seaweed in the shallow waters of the Saya de Malha Bank. A: *Halimeda* spp. at SS36 (38 m); B: *Caulerpa cupressoides* at SS13 (31 m); C: *Lithothamnion* spp. at SS42 (49 m); D: *Udotea* spp. at SS37 (34 m); and E: *Caulerpa taxifolia* at SS40 (50 m).

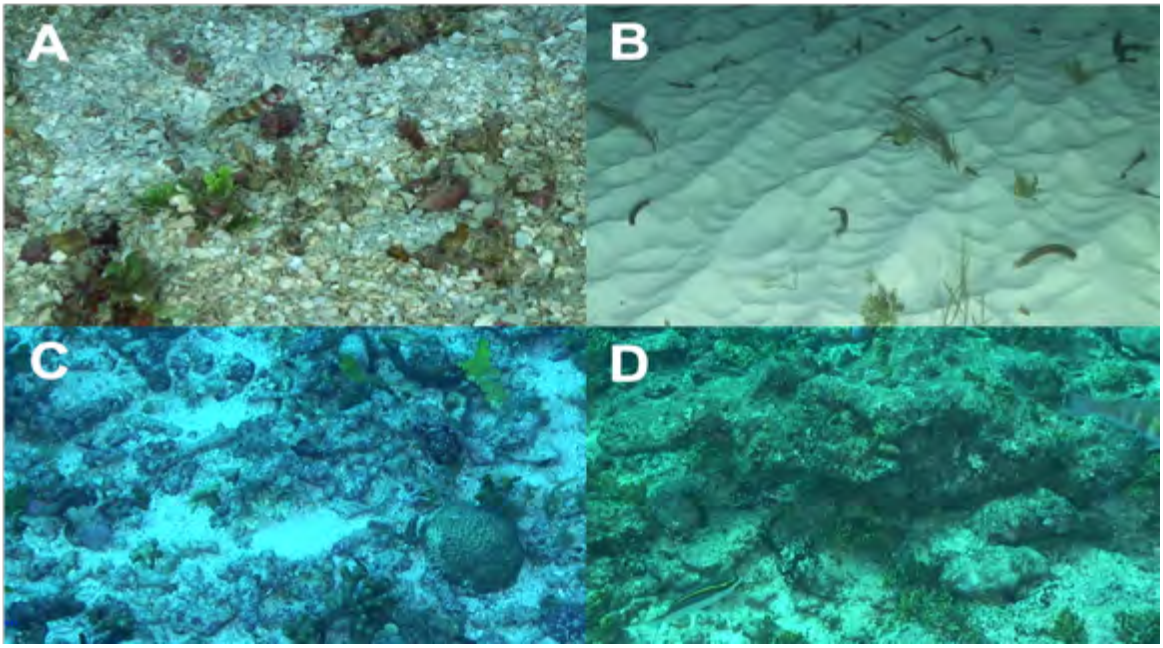

Figure 6. The four main bottom substrate habitats present within the Saya de Malha Bank. A: Sand made from calcified *Halimeda* spp. at SS38 (36 m); B: Fine sand at SS37 (32 m); C: Rubble at SS36 (24 m); and D: Bedrock at SS39 (26 m).

Discussion

The present study from the 2018 Nansen research expedition covered 3.6 x 10^{-4} % (1.4 x 10^{-1} out of about 40,000 km²) of the SMB area which was calculated along a transect assuming the swath width of the camera lens to be 15 m. The 143,110 m² surveyed area revealed the benthic habitat cover of 43.64 ± 22.36, 24.48 ± 21.85, 21.21 ± 27.77, and 10.46 ± 12.55 % for seaweed, abiotic substrate, seagrasses and corals, respectively. These findings indicate the presence of significant biotic benthic habitats in the shallow areas between 23-50 m on the SMB. One of the most striking observations made on the bank was the dominance of seaweed at almost all the stations (notably *Halimeda* spp.) even though other species of seaweed were also recorded in lower abundance. However, this abundance is highly relative to season and the dominance of this species may alter over time (Spalding *et al.,* 2019). Vortsepneva (2008) reported that red calcareous coralline algae and *Halimeda* were more frequent than corals in the shallow waters with beds (mainly rhodolith) that extended over 80-90 % of the fringing reef area. In the present study green calcareous algae (*Halimeda* spp.) were the most abundant among the seaweeds and probably constitutes the main source of unstable substrate (sand) dominating the stations surveyed. *Halimeda* spp. are known to be important and rapidly growing primary producers which are known to sometimes be associated with coral reefs (Vogel *et al.,* 2015). They act as suitable habitat for many important invertebrates (Fukunaga, 2008) such as communities of the sea cucumber *Thelenota ananas* that were observed in this study. Moreover, they also contribute considerably to carbonate production and sediment formation due to their calcium carbonate skeleton and are considered important for establishing the substrate needed for other species to develop (e.g. seagrasses), in addition to their role in carbon sequestration (Rees *et al.,* 2007).

Current knowledge suggests that the SMB supports the largest contiguous seagrass beds in the world (Obura *et al.,* 2012) with 80–90 % of shallow surfaces being covered by seagrasses and dominated almost exclusively by *T. ciliatum* up to depths of 30–40 m, with additional records of *H. decipiens* and *Enhalus acoroides*. (Obura *et al.,* 2012; Klaus, 2014). This expedition confirmed the presence of two species of seagrass, where *T. ciliatum* was dominant and formed large meadows principally at SS38. No *E. acoroides* was observed during the expedition. However, *E. acoroides* may be present in the shallower areas of Saya de Malha as this expedition did not investigate stations shallower than 23 m deep (Hilbertz and Goreau, 2002; Vortsepneva, 2008). Seagrass beds are among the most productive aquatic ecosystems. They are important as nursery grounds, foraging areas, and predation refuges for numerous vertebrates and invertebrates (Hilbertz and Goreau, 2002; Klaus, 2014). The large seagrass beds found within the SMB are also considered to provide

great benefits for commercial, subsistence and recreational fisheries. The clear water observed during the survey may be attributed to the complex architecture of the leaf canopy in combination with the dense network of roots and rhizomes, allowing seagrass beds to stabilize bottom sediments and serve as effective hydrodynamic barriers reducing wave energy and current velocity, thereby reducing turbidity (Burnett *et al.,* 2001; Hagan and Robinson, 2001; Gullstrom *et al*., 2002; Milchakova *et al*., 2005; GOBI, 2009). Further, seagrass beds trap large amounts of nutrients and organic matter in the bottom sediment through microbial decomposition, and seagrass biomass may enter the marine food web as detritus and support productivity through recycling of nutrients and carbon (Lindhorst *et al.,* 2019). This makes SMB a hot spot for blue carbon sequestration within the region and worldwide. Due to their high productivity, they are often a food source for animals resident in adjacent ecosystems such as coral reefs and may increase the biodiversity in these systems (Sala *et al.,* 2016).

The shallow water of the SMB also supported several coral. New *et al.* (2013) reported coral reefs on the SMB to occur on rocky patches and outcrops, while Gershanovich and Dubinets (1991) found the corals to be on the edges of the bank forming an atoll ring with a lagoon and intra-lagoon reefs. Thirteen genera of corals have previously been recorded from the shallow areas of the SMB (Rosen, 1971). At the north bank, however, an entirely different coral ecosystem was found, dominated by large stands of a single species of branching *Acropora* corals (Hagan and Robinson, 2001). *Acropora, Pocillopora, Montipora*, *Porites* and *Heliopora* sp. were the most common genera (Sirenko, 1993 in Vortsepneva, 2008) which is in concurrence with records from the present study, with several other common genera recorded such as *Danafungia*, *Favites*, *Dipsastraea*, *Seriatopora* and possibly *Stylophora* amongst others. In this study the highest live coral cover was observed at station 36-2 with 35 % over an area of 9819 m^2 in a depth range 23 – 30 m on the south bank. All the studies previously carried out on the corals of the SMB have targeted the north bank mainly due to its shallowness, with no focus on the south bank (Rosen, 1971; Hilbertz and Goreau, 2002; Vortsepneva, 2008). The current study fills some of these gaps and provides a stronger basis for future studies on corals in this region. In addition, Vortsepneva (2008) estimated a 5 % rate of endemism in the area which corroborates with this study where coral genera such as *Seriatopora* and *Stylophora* were observed.

Although the present study gave a good indication of the diversity and distribution of the benthic habitats in the shallow waters (23-50 m) of the SMB, several limitations such as the inaccuracy of the existing bathymetry maps prevented the survey from being carried out in shallower waters. All dives were carried out during daytime and the technical crew was only available for 8-12 hours per day, hence limiting operation time. Another major setback that made the identification process difficult was the inability to carry out targeted collection of samples to confirm identification from videos. Accordingly, most of the marine organisms were identified to family and/or genus levels as compared to previous studies where SCUBA diving (Hilbertz and Goreau, 2002) and bottom trawling (Vortsepneva, 2008) allowed sample collection. This limitation may be considered in future explorations in order to more extensively uncover the relative importance of the habitats documented to the diversity and productivity of the area, especially with regards to their blue carbon capacity.

Conclusions

This study presents a first documentation of the diversity and distribution of the main biotic and abiotic habitats present in the shallow waters (23 – 50 m) of the SMB. Though the SMB is renowned for being one of the largest banks in the world with extensive seagrass beds, the present study indicates that seaweeds, in particular the coralline green algae (*Halimeda* spp.), were more dominant than the seagrasses and corals at the surveyed shallow-water (23-50 m) stations during the survey period. This study therefore brings forth new data and further adds to the limited information present on the diversity and distribution of benthic habitats in the shallow water areas of the SMB which may be used to contribute to the better management of the bank. It is however worth carrying out further in-depth research in the shallower waters (less than 23 m) of the SMB to obtain a better understanding of the diversity and distribution of its benthic habitats.

Acknowledgments

The underlying work was made possible with the support of the EAF-Nansen Programme “Supporting the Application of the Ecosystem Approach to Fisheries Management considering Climate Change and Pollution Impacts” executed by Food and Agriculture Organization of the United Nations (FAO) and funded by the Norwegian Agency for Development Cooperation (Norad). The authors are thankful to FAO for

funding and supporting the Indian Ocean research expedition 2018 on the Saya de Malha Bank and Nazareth Bank with the R/V *Dr Fridtjof Nansen*, the Department of Continental Shelf, Maritime Zones Administration & Exploration of Mauritius for co-leading and coordinating the scientific expedition, the Mauritius-Seychelles Joint Commission of the Extended Continental Shelf for their support and assistance and granting the necessary authorisations, the Ministry of Blue Economy, Marine Resources, Fisheries & Shipping for hosting and spearheading the Habitat Mapping Workshop in Mauritius and for granting necessary authorization to carry out research in the Nazareth Bank; the Institute of Marine Research, Norway for leading the expedition and providing the technical and logistic support. The authors also thank the participating scientists, the crew members and the VAMS / Argus ROV technicians for their work and contribution during the expedition and to the anonymous reviewers for their insightful comments which have significantly improved the manuscript.

References

Badal RM (2003) Enhanced primary production on the Mascarene Plateau caused by a mini-monsoon: a satellite perspective. In: Frouin RJ, Yuan Y, Kawamura H (eds) Abstract in report from the Third International Asia-Pacific Environmental Remote Sensing of the Atmosphere, Ocean, Environment, and Space Conference, Hangzhou, China. pp 305 [doi: https://doi.org/10.1117/12.466781]

Bergstad OK, Tabachnick K, Rybakova E, Gendron G, Souffre A, Bhagooli R, Ramah S, Olsen M, Høines SA, Dautova T (2021) Macro- and megafauna on the slopes of the Saya de Malha Bank of the Mascarene Plateau, Western Indian Ocean. Western Indian Ocean Journal of Marine Science, Special Issue 2/2021: 103-132

Bhagooli R, Kaullysing D (2019) Seas of Mauritius. World seas: An environmental evaluation. pp 253-277 [doi:10.1016/b978-0-08-100853-9.00016-6]

Burnett JC, Kavanagh JS, Spencer T (eds) (2001) Shoals of Capricorn Programme field report 1998–2001: marine science, training and education in the Western Indian Ocean. Royal Geographical Society, London/ Institute of British Geographers: 507-535

Christiansen S (2010) Saya de Malha Banks – A potential MPA. World Wildlife Foundation Briefing. 7 pp

Commission on the Limits of the Continental Shelf (CLCS) (2011) Summary of the recommendations of the commission on the limits of the continental shelf in regard to the joint submission made by Mauritius and Seychelles concerning the Mascarene plateau region on 1 December 2008. United Nations Convention on the Law of the Sea (UNCLOS). 33 pp

Drozdovskiy A (2021) Saya de Malha Research Expedition. Global Mapping Hub by Greenpeace. [https://maps.greenpeace.org/project/saya-de-malha-research-expedition/]

Fredericq S, Freshwater DW, Hommersand MH (1999) Observations on the phylogenetic systematics and biogeography of the Solieriaceae (Gigartinales, Rhodophyta) inferred from rbcL sequences and morphological evidence. Hydrobiologia 398/399: 25-38

Fukunaga A (2008) Invertebrate community associated with the macroalga *Halimeda kanaloana* meadow in Maui, Hawaii. International Review of Hydrobiology, 93: 328-341

Gershanovich DY, Dubinets GA (1991) Geomorphology of Indian Ocean seamounts. International Geology Review 33: 903-913

GOBI (2009) Saya de Malha Banks—Case study [http://www.gobi.org/Our%20Work/rare-1]

Gullstrom M, de la Torre Castro M, Bandeira SO, Bjork M, Dahlberg M, Kautsky N, Ronnback P, Ohman MC (2002) Seagrass ecosystems in the Western Indian Ocean. Ambio 31 (7): 588-596

Hagan A, Robinson J (2001) Benthic habitats of the Saya de Malha Bank. Marine Science, training, and education in the western Indian Ocean. Royal Geographical Society, London/30 Reefs Symposium of the Zoological Society of London 28: 26-27

Henseler C, Nordström MC, Törnroos A, Snickars M, Pecuchet L, Lindegren M, Bonsdorff E (2019) Coastal habitats and their importance for the diversity of benthic communities: A species- and trait-based approach. Estuarine, Coastal and Shelf Science 226: 106272

Hilbertz W, Goreau T (2002) Saya de Malha Expedition report. Lighthouse Foundation Project. 101 pp

Klaus R (ed) (2014) Coral reef atlas and outlook -Southwestern Indian ocean islands. Report to the Indian Ocean Commission ISLANDS Project. 277 pp

Kohler KE, Gill SM (2006) Coral Point Count with Excel extensions (CPCe): A Visual Basic program for the determination of coral and substrate coverage using random point count methodology. Computers and Geosciences 32 (9): 1259-1269

Lindhorst S, Appoo J, Artschwager M, Bialik O, Birkicht M, Bissessur D, Braga J-C, Budke L, Bunzel D, Coopen P, Eberhardt B, Eggers D, Eisermann JO, El Gareb F, Emeis K, Geßner A-L, Hüge F, Knaack-Völker H, Kornrumpf N, Lenz N, Lüdmann T, Metzke M,

Naderipour C, Neziraj G, Reijmer J, Reolid J, Reule N, Rixen T, Saitz Y, Schäfer W, Schutter I, Siddiqui C, Sorry A, Taphorn B, Vosen S, Wasilewski T, Welsch A (2019) Saya de Malha carbonates, oceanography and biogeochemistry (Western Indian Ocean). SONNE-Berichte Cruise No. SO270. 210 pp

Meyerhoff AA, Kamen-Kaye M (1981) Petroleum prospects of Saya de Malha and Nazareth Banks, Indian Ocean. American Association of Petroleum Geologists Bulletin 65: 1344-1347

Milchakova NA, Phillips RC, Ryabogina VG (2005) New data on the locations of seagrass species in the Indian Ocean. Atoll Research Bulletin 537: 177-188

New AL, Magalhaes JM, da Silva JCB (2013) Internal solitary waves on the Saya de Malha bank of the Mascarene Plateau: SAR observations and interpretation. Deep Sea Research Part I: Oceanographic Research Papers 79: 50-61 [doi:10.1016/j.dsr.2013.05.008]

Obura DO, Church JE, Gabrié C (2012) Assessing marine world heritage from an ecosystem perspective: the Western Indian Ocean. World Heritage Centre, United Nations Education, Science and Cultural Organization (UNESCO). 124 pp

Rees SA, Opdyke BN, Wilson PA, Henstock TJ (2007) Significance of *Halimeda* bioherms to the global carbonate budget based on a geological sediment budget for the Northern Great Barrier Reef, Australia. Coral Reefs 26: 177-188

Rogers AD (2012) Ocean. Volume 1—Overview of seamount ecosystems and biodiversity. IUCN, Gland. pp 18+ii

Rosen B (1971) The distribution of reef coral genera in the Indian Ocean. Regional variation in Indian Ocean coral reefs. Symposium of the Zoological Society of London No. 28: 263-299

Sala E, Costello C, De Bourbon PJ, Fiorese M, Heal G, Kelleher K, Moffitt R, Morgan L, Plunkett J, Rechberger KD, Rosenberg AA, Sumaila R (2016) Fish banks: An economic model to scale marine conservation. Marine Policy 73: 154-161 [doi: https://doi.org/10.1016/j.marpol.2016.07.032]

Seamounts Project (2013) An ecosystem approach to management of seamounts in the southern Indian Ocean. IUCN, Gland, Switzerland. 60 pp

Serigstad B, Ensrud TM, Olsen M, Ostrowski M, Adu-Kumi S, Akoto L, Aggrey-Fynn J, Blazewicz-Paszkowycz M, Jozwiak P, Pabis K, Siciński J (2015) Environmental monitoring Ghana 2012, chemical and biological analysis. NORAD – FAO Project GCP/003/NOR Survey Report R/V Dr Fridtjof Nansen EAF – N/2012/7. 163 pp

Spalding HL, Amado-Filho GM, Bahia RG, Ballantine DL, Fredericq S, Leichter JJ, Nelson WA, Slattery M, Tsuda RT (2019) Chapter 29-Macroalgae. In: Loya Y, Puglise KA, Bridge TCL (eds) Coral reefs of the world mesophotic, Coral Ecosystems 21: 507-536

Shor GG, Pollard DD (1963) Seismic investigations of Seychelles and Saya de Malha Banks, Northwest Indian Ocean. Science 142: 48-49 [doi:10.1126/science.142.3588.48]

Vierros, M (2009) The Saya de Malha Banks. GOBI illustration case study. pp 1-6 [http://openoceansdeepseas.org/Our%20Work/rare-1/at_download/pdf.]

Vogel N, Fabricius KE, Strahl J, Noonan SHC, Wild C, Uthicke S (2015) Calcareous green alga *Halimeda* tolerates ocean acidification conditions at tropical carbon dioxide seeps. Limnology and Oceanography 60: 263-275

Vortsepneva E (2008) Review: Saya de Malha Bank – an invisible island in the Indian Ocean. Geomorphology, Oceanology, Biology. Lighthouse Foundation. 44 pp

Grain size analysis and total organic matter and carbonate contents of sediments on Saya de Malha and Nazareth Banks

Arnaud Nicolas*, Rohinee Bhiwajee

Mauritius Oceanography Institute, Albion, Mauritius

* Corresponding author: anicolas@moi.intnet.mu

Abstract

The Mascarene Plateau is one of the least studied regions of the Western Indian Ocean. The aim of this paper is to describe the qualitative grain size characteristics and the total organic matter and carbonate contents of sediments on the two underwater banks known as the Saya de Malha and Nazareth Banks. Sediment samples were collected during the R/V Dr Fridtjof Nansen expedition in 2018, using a Video-Assisted Multi-Sampler (VAMS). Sieving techniques and GRADISTAT software were used for granulometric analysis and grain size statistics, respectively. Total organic matter and carbonate contents were determined with the sequential weight loss on ignition method. Grain size parameters from 15 stations (depths ranging from 37 to 381 m) are reported in this study. The results showed that sand was the dominant grain size on both banks. Eleven of the 15 stations had a mean grain size of coarse sand, three stations had a mean size of medium sand and one station had fine sand. The average total organic matter and carbonate contents on the Banks ranged from 2.1 to 7.7 % and from 53.9 to 58.3 %, respectively. This study provides baseline information that will help to classify benthic habitats and better understand the ecosystem functioning and dynamics on of the Saya de Malha and Nazareth Banks.

Keywords: grain size analysis, total organic matter, carbonate content, Saya de Malha Bank, Nazareth Bank, Western Indian Ocean

Introduction

The Saya de Malha (SDM) Bank is situated in the Western Indian Ocean on the Mascarene Plateau and covers an area of about 40, 000 km^2. It is considered as the world's largest underwater Bank and is subdivided into a northern section, the North Bank or Ritchie Bank and a southern section known as the South Bank. South of the SDM Bank lies the smaller Nazareth Bank, covering an area of about 22, 000 km^2. Due to very few *in situ* studies conducted on the SDM and Nazareth Banks, their respective geological compositions are poorly described. A core of 3264 m deep drilled on the northwest area of the South Bank in 1975 revealed that the bottommost 832 m of sediment were composed of volcanic basalts, the intermediate section was limestone and the uppermost 1249 m were reported as "reef carbonates" (Meyerhoff and Kamen-Kaye, 1981). Another core of 1716 m was drilled from the Nazareth Bank indicating shallow bank limestones overlaid the bottom volcanic basalts (Meyerhoff and Kamen-Kaye, 1981).

The remoteness of the SDM Bank makes it one of the least studied shallow tropical marine ecosystems on earth. Based on a study on the Ritchie Bank, Hilbertz *et al.* (2002) put forward that sandy areas occupy less than 5 % of the seafloor, corals cover around 10-20 %, and seagrass meadows about 80-90 % of the SDM Bank. Two earlier studies investigating the sediment composition from different areas on the Bank reported the occurrence of stone-like pebbles, coral gravels, *Acropora* spp. fragments, silt (consisting of foraminifera shells, pteropods and calcium carbonate flakes), coral sand (comprising of calcareous algae fragments (10-15 %), sponge spicules and detritus) and mollusks and globigerina shells (Fedorov and Danilov, 1979; Ingole *et al*., 1992). On the Ritchie Bank, Hilbertz *et al*. (2002) found that the sediments

http://dx.doi.org/10.4314/wiojms.si2021.2.6

consisted primarily of rhodoliths, described as spherical layered concretions from a few centimeters to decimeters in diameter that are formed by calcareous encrusting red algae growing around a nucleus. Rhodoliths were mostly found in areas predominantly affected by strong currents that prevent the accumulation of sand or fine-grained sediments (Hilbertz *et al.*, 2002).

The SDM Bank lies directly in the path of the South Equatorial Current (SEC) which is the dominant current in the western Indian Ocean. A large portion of the SEC is forced through the deep narrow channel

Granulometric distributions provide important information on sediment origin, transport dynamics and depositional conditions (Benavente *et al.*, 2005; Bui *et al.*, 1989; Folk and Ward, 1957). Grain size analysis has been commonly employed to statistically investigate spatial changes in sediment size properties. The common techniques employed in grain size analysis include direct measurement, dry and wet sieving, sedimentation, use of particle-size analysers, such as laser granulometers and Coulter particle counters (Blott and Pye, 2001). The classical sieving method is the most used technique in the case of sand and gravel (Blatt *et al.*, 1972).

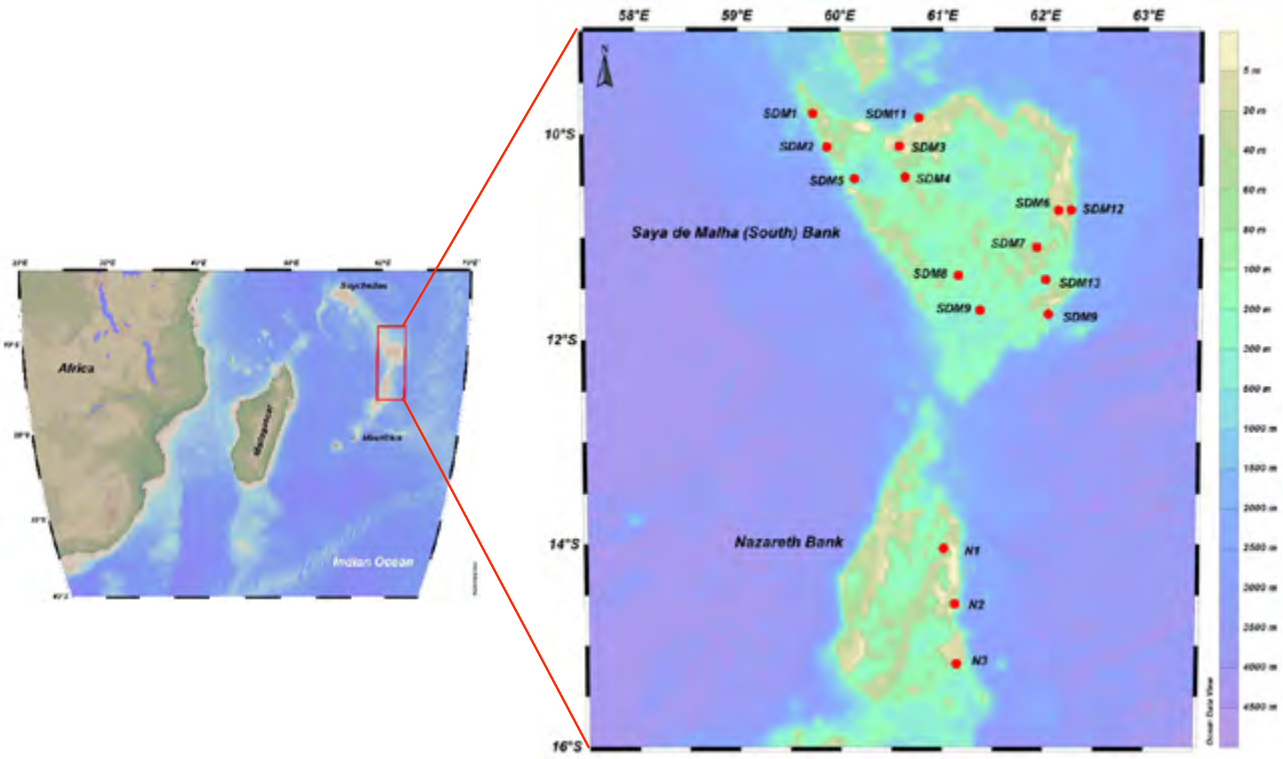

Figure 1. Sampling locations on Saya de Malha (South) and Nazareth Banks.

(1100 m deep, 8-10 km wide) separating the SDM and Nazareth Banks (New *et al.*, 2005). The SEC also feeds the SDM Bank with waters high in nutrients through mixing and upwelling, which enhances the primary productivity over the area (New *et al.*, 2005). The prevailing bottom water currents are believed to have an influence on the physical properties of sediments on the seafloor and the benthic cover assemblages (Hilbertz *et al.*, 2002).

Grain size analysis is an important tool for categorizing different sedimentary environments (Anfuso and Gracia, 2005; Folk and Ward, 1957; Shepard, 1954).

Sediment is also the major site for organic matter which is decomposed mainly by bacteria and thus mixing nutrients with overlying waters. The origin of organic matter content of sediments in the open ocean is mainly derived from the settling of biogenic material which originates from marine primary production. The quantity and nature of organic matter deposited in marine sediments are closely linked to the environmental conditions of deposition (Trask, 1955). The wet oxidation, sequential weight loss on ignition (WLOI) and gas chromatographic analysis are a few of the techniques employed to estimate organic carbon in sediments (Byers *et al.*, 1978). The sequential WLOI

is a simple, cost-effective, commonly used method to determine the organic matter and carbonate content of sediments (Bengtsson and Enell, 1986; Dean, 1974; Heiri *et al.*, 2001; Wang *et al.*, 2011).

There are a very few publications (Fedorov and Danilov, 1979) that briefly described the sediment characteristics and composition on the SDM Bank. However, no investigations on the sediment grain-size distribution and organic matter and carbonate contents have been undertaken so far. This study aimed at qualitatively describing the sediment grain size characteristics on the SDM and the eastern part of the Nazareth Banks. Furthermore, the total organic matter (% TOM) and the carbonate content (% CC) of sediments were determined. This granulometric data could shed further light on the prevailing water current conditions and help better understand the ecosystem dynamics on the world's largest underwater bank.

Materials and methods

The present study is based on sediment samples collected by the Research Vessel Dr Fridjof Nansen from the 3rd May 2018 to the 3rd June 2018, with the scientific expedition entitled 'Leg 2.1: Characterizing ecosystems and morphology of the Saya de Malha and Nazareth Banks'. Sediment samples were collected on 16 selected stations at depths ranging from 37 to 381 m based on the pre-planned cruise track on the banks (Fig.1; Table 1). Due to insufficient amount of sediment collected at station N2, granulometric analysis was not undertaken and only the % TOM and % CC were measured.

Sediment samples were collected from different depths during the cruise using the five hydraulic-operated Van Veen grabs mounted on a Video Assisted Multi Sampler (VAMS) system. Depending on the amount of sediment sampled by the grabs, at least two sediment samples were collected per station and kept frozen until granulometric analysis and TOM and CC examination. Coral rubbles and rhodoliths greater than 5 cm in length, collected commonly from the shallow stations, were discarded as most of them were fouled by encrusting algae and were still being used by seagrasses and macroalgae as a medium to attach their roots (Fig. 7).

For the granulometric analysis, the sediment samples from 15 stations were washed, dried and sieved for 10 min (Román-Sierra *et al.*, 2013) through a sieve-shaker consisting of six different sieve mesh sizes of 2000,

Table 1. Sampling depths and coordinates of the 16 stations on the SDM and Nazareth Banks.

Station name	Sampling depth (m)	Coordinates	
		Latitude	Longitude
Saya de Malha Bank			
SDM1	132	-9.7917	59. 7317
SDM2	74	-10.1197	59.8680
SDM3	30	-10.1132	60.5752
SDM4	62	-10.4122	60.6322
SDM5	55	-10.4270	60.1397
SDM6	28	-10.7318	62.1298
SDM7	55	-11.0923	61.9195
SDM8	160	-11.3660	61.1555
SDM9	288	-11.7442	62.0352
SDM10	251	-11.7058	61.3673
SDM11	37	-9.8340	60.7648
SDM12	73	-10.7302	62.2540
SDM13	381	-11.4088	62.0077
Nazareth Bank			
N1	38	-14.0378	61.0128
N2*	58	-14.5803	61.1260
N3	133	-15.1732	61.1422

**Note: Due to limited availability of sediment, grain size analysis has not been carried out for station N2. Only TOM/CC results are available.*

1000, 500, 250, 125 and 63 µm. The weight of the sediment retained in each sieve was noted and the material passing through the 63 µm sieve was retained in the pan and recorded as silt. Grain size distributions were processed through the GRADISTAT Version 9.1 software package (Blott and Pye, 2001) to obtain grain size classifications according to Wentworth (1922) and grain size statistics [Median grain size (d_{50}), Mean grain size (Mz), Standard deviation (σI), Skewness (SK) and Kurtosis (KG)] according to Folk and Ward (1957). The grain-size parameters were expressed in terms of phi (ϕ) units with the formula: $\phi = -\log_2 d$, where d is the grain diameter in millimeters.

The median grain size (d_{50}) is the midpoint value of the sediment distribution, which means that half of the mass of the sediment grains are smaller than this value and the other half is higher. The mean grain size (Mz) refers to the average grain size of the sediment distribution and provides an indication of the dominant grain character. The mean size can also be employed to differentiate between areas influenced by high and low current velocities (Nordstrom, 1977). The standard deviation (σI) describes the variation of the grain sizes in sediment sample and the inclusive graphic standard deviation is used to evaluate the sorting of sediments (Folk and Ward, 1957). Skewness (SK) provides an indication of the symmetry of the grain size distribution. Skewness indicates the level of mixing of the different fractions within a sample and can also describe the energy conditions in a depositional area. The inclusive graphic skewness values are used to classify the sediment distribution (Folk and Ward, 1957). A symmetrical distribution has a skewness value of 0.00. A positively skewed curve has a fine-particle 'tail' whereas a negatively skewed curve has a coarse-particle 'tail'. Kurtosis (KG) measures the 'peakedness' in the grain size distribution curve and evaluates the ratio between sorting in the tail of the distribution and that in the central portion. A normal distribution with a kurtosis of 1.00 will have the sorting in the tails equal to the sorting in the central part. A curve is leptokurtic (excessively peaked) when better sorting is observed in the central part compared to the tails. If a curve shows better sorting in the tails than in the central part, then it is platykurtic (flat peaked). Kurtosis ranges from very platykurtic to leptokurtic with values from 0.51 to 1.30. The average value is 0.83 which indicates platykurtic conditions.

For the sequential WLOI method, sediment subsamples (5-10 g) were placed in crucibles and the weights were recorded. The weight loss was measured after oven-drying the sediment samples overnight at 105 °C and burned in a furnace at 550 °C for 4 h to oxidize organic matter to carbon dioxide and ash and then at 1000 °C for 2 hours to remove the carbonates, leaving oxide (Dean, 1974; Heiri *et al.*, 2001). The percentage of total organic matter (% TOM) and carbonate content (% CC) were estimated by loss on ignition (LOI) at 550 and 1000 °C using the following equations (weights are in grams) adapted from Dean (1974) and Heiri *et al*. (2001):

LOI_{550} = [pre-ignition weight (105 °C) - post-ignition weight (550 °C)] / pre-ignition weight (105 °C) * 100

LOI_{1000} = [post-ignition weight (550 °C) - weight after 1000 °C burn out] / pre-ignition weight (105 °C) * 100

The % TOM is equivalent to the % LOI_{550} and is twice the organic carbon content (Dean, 1974). The amount of carbonate content (% CC) in a sample is calculated as 1.36 x LOI_{1000}, with the assumption that ignition follows a stoichiometric relationship and the percentage total inorganic carbon (% TIC) is determined as 0.273 x LOI_{1000} (Dean, 1974; Heiri *et al*., 2001).

Results and discussion

Granulometric analysis

The descriptive statistics of the different grain size parameters are represented in Table 2. The average sediment composition for each location is illustrated in Figure 2. Sand was found to be the dominant grain size representing an average of 98.12 % for the 15 locations on the two underwater Banks. Based on videos captured by the VAMS system and from sediment samples brought on board with the grabs (Bergstad *et al.*, 2018) and descriptions from previous studies (Hilbertz *et al.*, 2002), it was observed that the shallow banks provide habitats to a plethora of carbonate producers namely hermatypic corals such as *Porites* and *Acropora* spp., *Halimeda* spp., molluscs, large benthic foraminifera and sponges amongst others. Post-mortem, these organisms release their carbonate structures into the surrounding sediments which are broken down to smaller fragments and almost fully constitute the sand fraction in the range of -1 to 4 ϕ.

Bivariate relationships between grain size parameters

Bivariate plots provide important information that helps to differentiate between different depositional settings. This technique has been commonly

Table 2. Descriptive statistics of grain size parameters from 13 stations from SDM Bank and 2 stations from Nazareth Bank.

Station name	Mean size (Mz)	Mean Sand type	Standard deviation (σI)	Sorting type	Skewness (SK)	Skewness type	Kurtosis (KG)	Kurtosis type
Saya de Malha Bank								
SDM1	0.469±0.09	CS	1.00±0.02	PS	0.129±0.05	FS	0.977±0.08	MK
SDM2	1.62±0.15	MS	1.27±0.05	PS	-0.100±0.07	S	0.980±0.03	MK
SDM3	0.876±0.02	CS	1.35±0.03	PS	0.091±0.06	S	0.510±0.03	VP
SDM4	0.796±0.10	CS	1.14±0.02	PS	0.05±0.04	S	0.862±0.10	P
SDM5	0.322±0.14	CS	1.07±0.13	PS	0.370±0.21	VFS	0.605±0.01	VP
SDM6	0.993±0.01	CS	1.31±0.05	PS	-0.150±0.05	CS	0.550±0.12	VP
SDM7	0.165±0.34	CS	0.833±0.02	MS	0.244±0.13	FS	0.555±0.23	VP
SDM8	0.580±0.03	CS	1.02±0.02	PS	0.550±0.02	VFS	0.555±0.01	VP
SDM9	1.45±0.03	MS	0.885±0.04	MS	-0.012±0.02	S	1.16±0.05	L
SDM10	0.864±0.04	CS	0.986±0.01	MS	0.03±0.01	S	0.975±0.05	MK
SDM11	0.200±0.01	CS	1.13±0.02	PS	1.53±0.01	VFS	1.13±0.02	L
SDM12	1.50±0.21	MS	1.59±0.08	PS	-0.01±0.01	S	0.785±0.10	P
SDM13	2.13±0.02	FS	1.43±0.02	PS	-0.286±0.03	CS	1.30±0.01	L
Nazareth Bank								
N1	0.124±0.13	CS	0.870±0.11	MS	1.29±0.32	VFS	0.882±0.13	P
N3	0.888±0.24	CS	1.49±0.17	PS	0.349±0.02	VFS	0.622±0.05	VP

Mean sand type: CS= Coarse Sand, MS= Medium Sand, FS= Fine Sand. Sorting type: PS= Poorly Sorted, MS= Moderately sorted. Skewness type: FS= Fine Skewed, S= Symmetrical, VFS= Very Fine Skewed, CS=Coarse Skewed, FS= Fine Skewed. Kurtosis type: MK= Mesokurtic, VP= Very Platykurtic, P= Platykurtic, L= Leptokurtic.

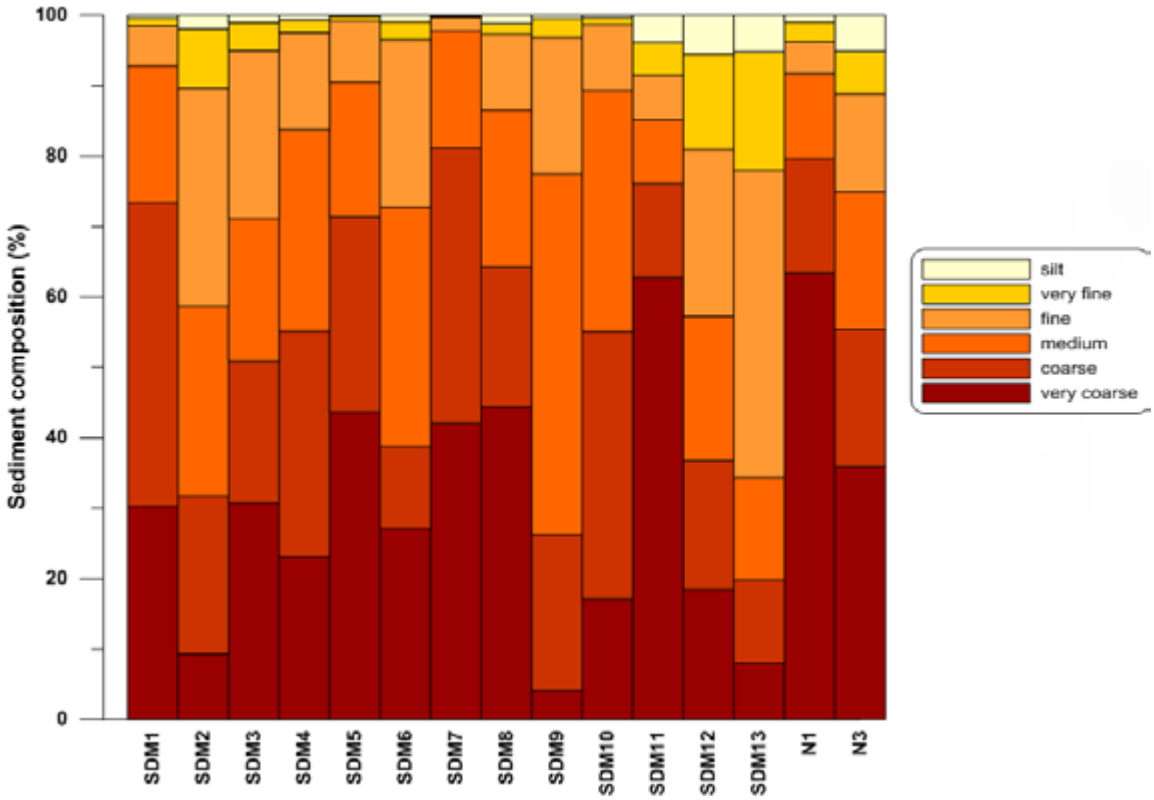

Figure 2. Percentage sediment composition of different grain sizes for 13 locations on SDM Bank and two locations on Nazareth Bank.

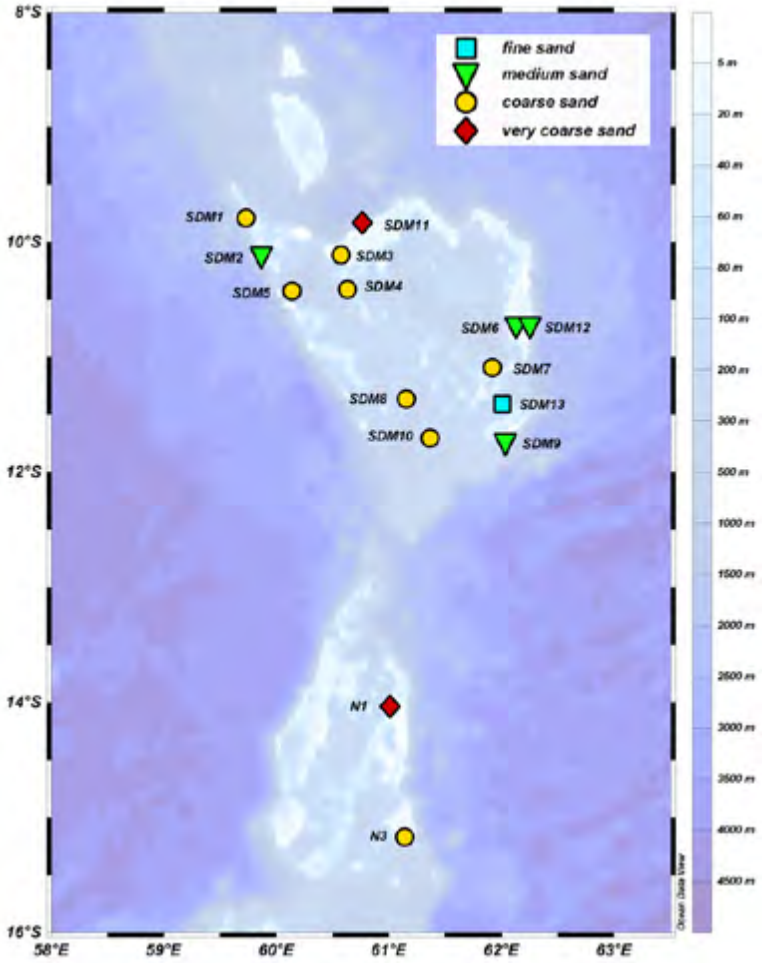

Figure 3. Median (d_{50}) values of sediment at different sampling locations.

employed to determine differences among beach sediment samples to elucidate transportation and deposition mechanisms and determine the governing energy conditions in these environments (Azidane *et al.*, 2020; Nordstrom, 1977; Rajganapathi *et al.*, 2013). To better understand the depositional environments prevailing at the different stations on the submerged banks, bivariate plots of mean versus standard deviation, mean versus skewness and mean versus kurtosis were computed.

Median grain size (d_{50})

The median size values of sediment samples from 13 locations on SDM Bank and 2 locations on Nazareth Bank are illustrated in Figure 3. The median size results revealed that 8 out of 15 stations had coarse grain-size and were mostly located in the inner and outer areas of the Banks. Medium grain-size sediment was found at four stations on the outer edge of the Saya de Malha Bank. The two shallowest stations (< 40 m) on the Banks had very coarse sediment grain-size. The deepest station of 381 m was located at the bottom of the 'Nansen sinkhole' (further described hereunder) on the Saya de Malha Bank and was characterized as fine grain-size sediment. A low positive relationship (y=64.142x+70.756, R^2 = 0.2749) was noted between median grain size and depth, where median sizes (ϕ) seemed to increase (towards finer grain size) with increasing depths. A Spearman's rank correlation coefficient demonstrated that the correlation was however, not significant (r' = 0.40, n = 15, α=0.05 and p > 0.05).

Mean grain size (Mz)

Eleven of the 15 stations had a mean size of coarse sand (0 -1 ϕ), three stations had medium sand (1 -2 ϕ) and one station (SDM13) had fine sand (2 -3 ϕ) (Table 2). The percentage composition of coarse sand varied from 11.5 to 43.1 % for the 11 stations with an average mean value of 0.57 ϕ. Medium sand ranged from 20.5 to 51.2 % for the three stations with an average mean value of 1.52 ϕ. The percentage composition of fine sand at SDM13 was 43.6 % with a mean size of 2.13 ϕ. It is suggested that the predominance of mean size in the coarse sand category may be due to the influence

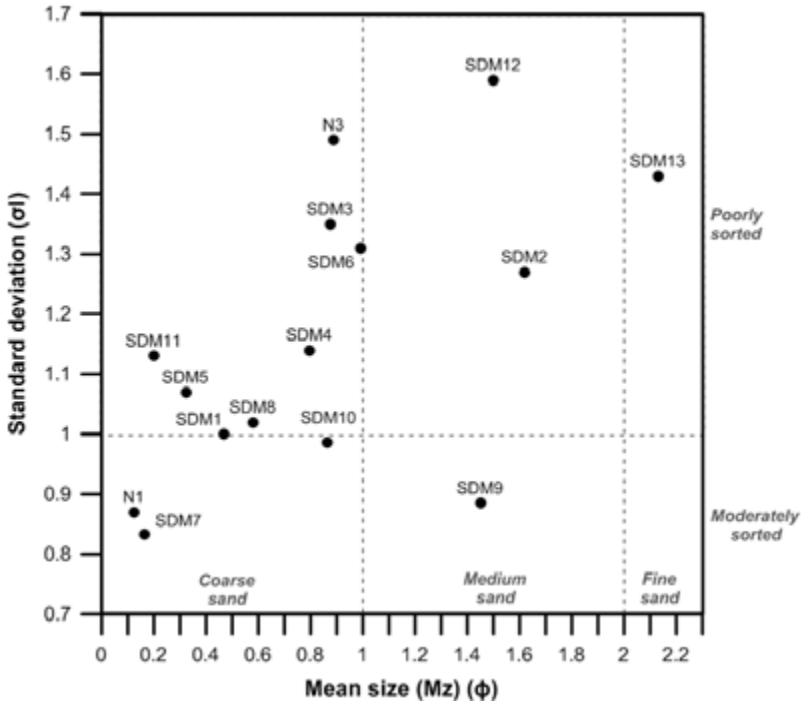

Figure 4. Bivariate relationship between mean size (Mz) and standard deviation (σI).

of the westward currents over the Banks that winnow away the smaller grain sizes, leaving behind higher proportions of coarser grains. At a depth of 50 m, a general strong westward current of 25 cm/s flows on the eastern side of the Banks, which then increases to 50 cm/s between the gap between the SDM and Nazareth Banks and which emerges again as a broad current with a speed of 30 cm/s (New *et al.*, 2005). Preliminary results from this cruise indicated the occurrence of westward currents of 10 and 30 cm/s on the Bank along latitude 10.5 °S and on the eastern slope along latitude of 11.5 °S, respectively (Bergstad *et al.*, 2018). The sudden changes in topography along the outer slopes and over the banks lead to changes in the zonal and meridional current velocities which further generated strong vertical shear over the top of the eastern slope (Bergstad *et al.*, 2018). The westward current of 10 cm/s measured over the bank along latitude 10.5 °S might be strong enough to cause erosion and movement of fine bottom sediments and possibly leaving behind the coarser fractions. This could explain why 11 of the 15 stations on the Banks had mean grain sizes in the coarse sand category.

Standard deviation (σI)

The values of the sediments varied between 0.83 and 1.59 ϕ (moderately sorted to poorly sorted) for the 15 stations. The average value is 1.16 ϕ which indicated poorly sorted grains. Eleven of the 15 stations had poorly sorted grains, while the remaining four stations exhibited moderately sorted grains (Table 2). The scatter graph of mean size versus standard deviation indicated that the sediment samples were mainly clustered in coarse sand size within the poorly sorted category (Fig. 4). Both mean size and standard deviation were influenced by hydrological conditions and the best-sorted sediments usually had the mean size of fine sand (Griffiths, 1967). None of the sediment samples in this study was in the 'very well sorted' range. The poorly sorted values observed at the majority of the stations may suggest the influence of high current velocities that could be constantly changing the sediment compositions with varying degrees of sediment influx to these sites over time. The predominance of mean size as coarse sand at eight stations exhibiting poorly sorted values could further indicate that high sorting values might be linked to occurrence of large grain sizes in the samples.

Skewness (SK)

Skewness values varied between -0.286 and 1.53 (coarsely skewed to very fine skewed), with an average value of 0.271 (fine skewed). Six stations with coarse sand as mean size showed symmetrical distribution, which indicates that coarse and fine sediments are distributed more or less equally. Five and two stations were very fine skewed and fine skewed, respectively. Only two stations were coarsely skewed (Table 2). Figure 5 illustrates the correlation between mean size and skewness. Most of the stations are clustered

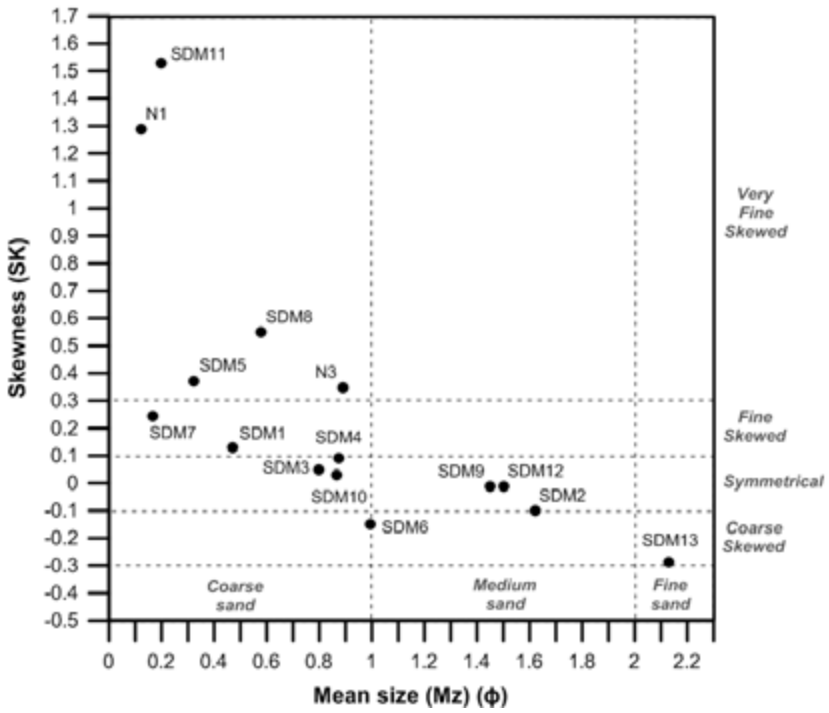

Figure 5. Bivariate relationship between mean size (Mz) and skewness (SK).

in the symmetrical to very fine skewed range. Only stations SDM13 and SDM6 with mean sizes in the fine and coarse sand categories respectively were coarsely skewed. An area affected by low current velocities is usually characterized with fine sediment grains which are poorly sorted and showed positive skewness. In contrast, an area influenced by high current velocities will have coarse sediment grains with good sorting and show either positive or negative skewness (Kim *et al.*, 2018). All the seven sites showing very fine to fine skewness (positively skewed) had mean size in the coarse sand category which indicate that they could be located in areas affected by strong currents.

Kurtosis (KG)

Six of the 15 stations were clustered in the very platykurtic category with mean size as coarse sand. Three stations exhibited platykurtic distribution, three stations showed sediment samples with mesokurtic distribution and three others indicated leptokurtic conditions (Fig. 6). Extreme values of kurtosis (leptokurtic to very leptokurtic) were usually observed when sediments are sorted in low or high energy environments (Folk and Ward, 1957). Two of the three stations exhibiting leptokurtic sediments are SDM11 (mean size=coarse sand, poorly sorted, depth=37 m) and SDM13 (mean size=fine sand, poorly sorted, depth=381 m). These results suggest that SDM11 might be influenced by high current velocities at shallower depth whereas SDM13 is located in a low energy environment. Platykurtic distribution usually occurs when a sediment distribution is poorly sorted and the three stations with platykurtic sediments were found to be moderately to poorly sorted. Skewness and Kurtosis values provide important clues of how closely a grain-size distribution fits a normal Gaussian probability curve. Pronounced skewness and kurtosis occur when the sediment distribution consists of different grain sizes, as observed for some sediment samples in this study.

Contribution of *Halimeda* spp. to sediments on the Banks

Sites SDM11 and N1 were comprised predominantly of very coarse sand (-1 to 0 ϕ) with compositions of 62.7 % and 63.3 %, respectively. Sites SDM11 and N1 were relatively shallow (< 40 m) and their sediment compositions consisted mostly of plates of the calcifying green macroalgae *Halimeda* spp. Video images from the VAMS indicated that *Halimeda* spp. plants thrived in high densities at these shallow depths. The plants consisted of several leaf-like calcareous segments and once dead, these calcified segments were shed into the surrounding sediments as individual plates. These calcified plates initially formed part of coarse sand to gravel size fractions and then with time disintegrated into mud-grade carbonate sediment as needles and nanograins (Ford and Kench, 2012; Neumann and Land, 1975). The contribution of

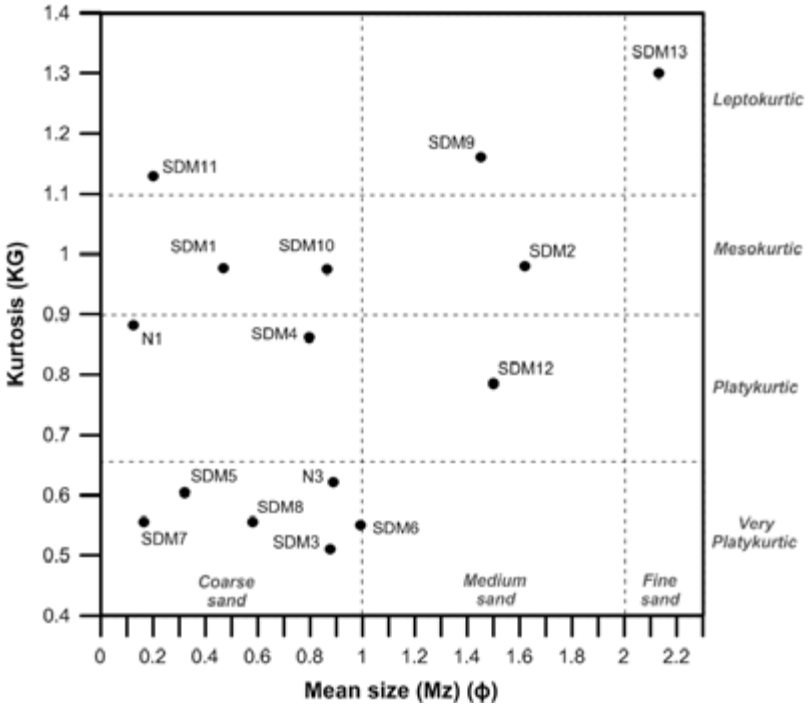

Figure 6. Bivariate relationship between mean size (Mz) and kurtosis (KG).

Halimeda spp. to the various sediment size fractions is considerably important in tropical shallow reef systems (Hewins and Perry, 2006) and further provides substrates and habitats (Jinendradasa and Ekaratne, 2002) for other reef communities. Rhodoliths were also observed on both Banks and were more abundant in areas influenced by strong currents, which prevented the accumulation of finer grain-size sediments. This general observation was also reported on the Ritchie Bank by Hilbertz *et al.* (2002), but the abundance or percentage composition of rhodoliths for the sampling stations on the SDM and Nazareth Banks were not assessed in this present study. At site N1 on the Nazareth Bank, rhodoliths were observed to occur in association with calcified plates of *Halimeda* spp. and coral rubbles (Fig. 7). Altogether, they provide substrate for seagrasses and other macroalgae to anchor their roots to the seafloor.

Figure 7. Intact grab sample for station N1.

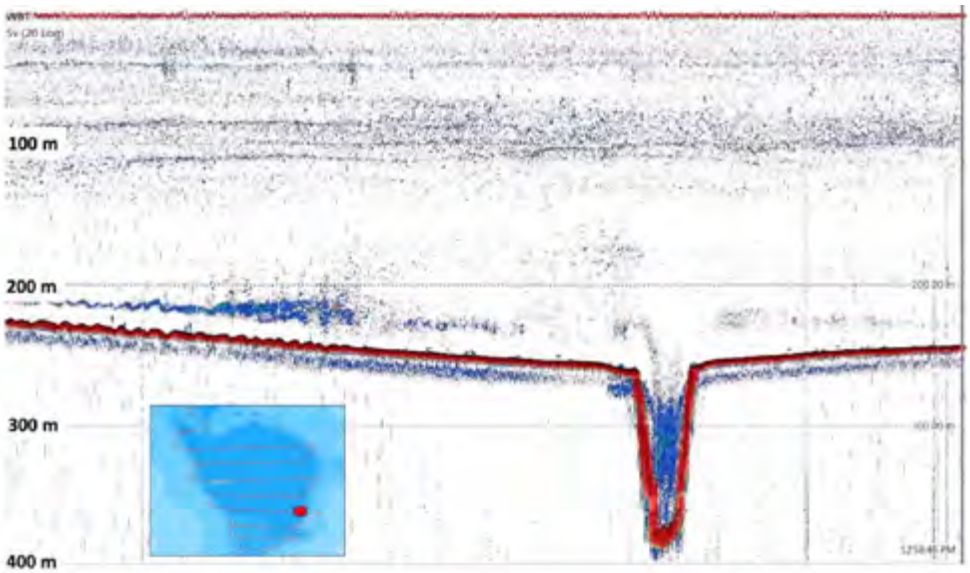

Figure 8. Station SDM13 known as the "Nansen Sinkhole". Depth profile from EK 80, 38 KHz. Picture taken from cruise report (Bergstad *et al.*, 2018).

Dominance of fine sediment at the bottom of 'Nansen Sinkhole'

Contrary to the shallow sites SDM11 and N1 where 62.7-63.3 % of the sediment composition fell in the very coarse range, the sediment collected from the deepest station SDM13 (381 m) was composed predominantly of finer grain size where 60.4 % of sediment was found in the range of fine to very fine sand (-3 to -1 ϕ). This station was provisionally called as the "Nansen Sinkhole" and was a prominent hole with a conical shape with more or less vertical walls on the sides (Bergstad *et al.,* 2018). The opening of the hole started at 260 m deep and the bottom depth reached approximately 385 m deep, which gave the cone a depth of 125 m (Fig. 8). The sediment accumulated at the bottom comprised of 43.5 % fine sand, 16.9 % very fine sand, 5.2 % silt, 14.5 % medium sand, 11.8 % coarse sand and 8.0 % very coarse sand. Little coral debris was observed at the bottom which was presumed to have fallen from the top edges of the hole and it was suggested that this debris be categorized as coarse to very coarse sand. The higher proportion of finer grain size accumulating at the bottom of the 'Nansen Sinkhole' can be explained by fine sediments in suspension and biogenic materials that have slowly settled to the bottom with time. The influence of currents was less pronounced inside the hole of 125 m deep, which could allow the settling and accumulation of fine sediments on the bottom.

Total organic matter and carbonate contents

The TOM of sediment samples on the SDM and Nazareth Banks varied from 2.09±0.40 to 7.70±0.03 %. The lowest TOM value of 2.09±0.40 % was reported at SDM9 at a depth of 288 m. The highest TOM values of 7.59±0.18 and 7.70±0.18 % were found at SDM7 and N2, respectively, at corresponding depths of 55 and 58 m (Fig. 9). A TOM of 3.17 % was recorded on the Kenyan shelf at a depth of 78 m (Mohamed *et al.*, 2018) and similar values in the range of 2.6±0.64-8.1±7.01 % were found in Mida Creek in Kenya (Wafula *et al.*, 2020). The TOM measured on the SDM and Nazareth Banks are therefore in the same range as TOC values from coastal waters bordering land areas. A low negative relationship (y=-30.358x+237.54, R^2 = 0.201) existed between TOM and depth, where TOM values seemed to increase with decreasing depths. A significant Spearman's rank correlation was observed between TOM contents and depth (r' = 0.40, n = 16, α=0.05 and p < 0.05). This can further be explained by the fact that shallower areas have higher primary production compared to deeper zones. Remineralization of organic matter occurs in the water column as it sinks and this process can also explain the occurrence of low TOC values in the deeper zones.

The relationship between TOM and grain size was described to be positively correlated with the fine grain size category in comparison with coarser grain sizes (Mohamed *et al.*, 2018; Secrieru and Oaie, 2009). However, it was observed that SDM13 with mean size as fine sand had a low TOM value of 3.18±0.04 % and SDM7 with a mean size in the coarse sand range having a relatively high TOM value of 7.59±0.18 %. With the exception of SDM7, all sediment samples in the coarse sand range were clustered between TOM values of 2.67±0.04 and 4.82±0.40 %.

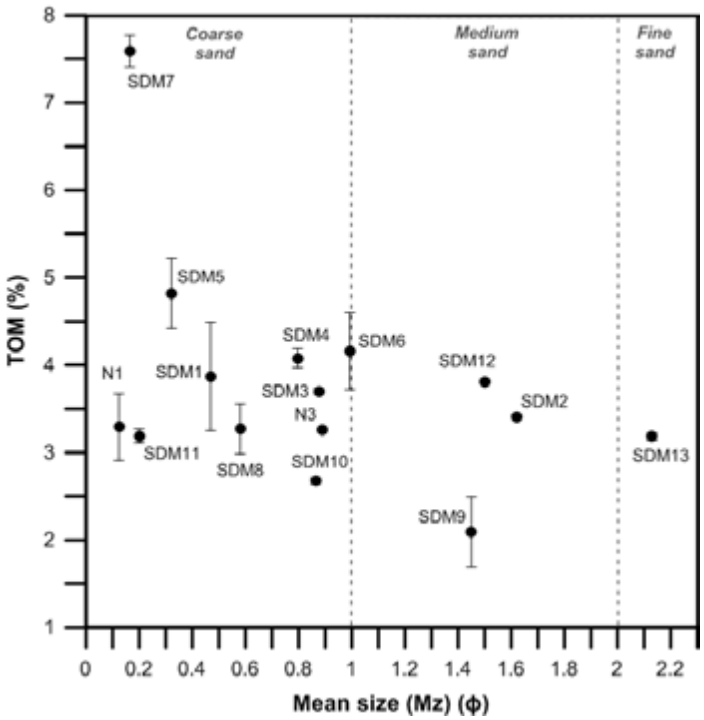

Figure 9. Scatter plot of mean size (Mz) versus Total Organic Matter (TOM (%)).
Note: N2 is not shown in plot.

The high TOM content reported from SDM7 could be due to the presence of calcareous biogenic materials that can additionally contain organic carbon which could be released slowly into the nearby sediment. However, Krumgalz (1989) reported high concentrations of organic matter content in the medium and coarse sediment categories (> 2 ϕ) that have been formed from clusters of the smaller particles. This phenomenon can also potentially explain the anomalously high concentrations of TOC in the

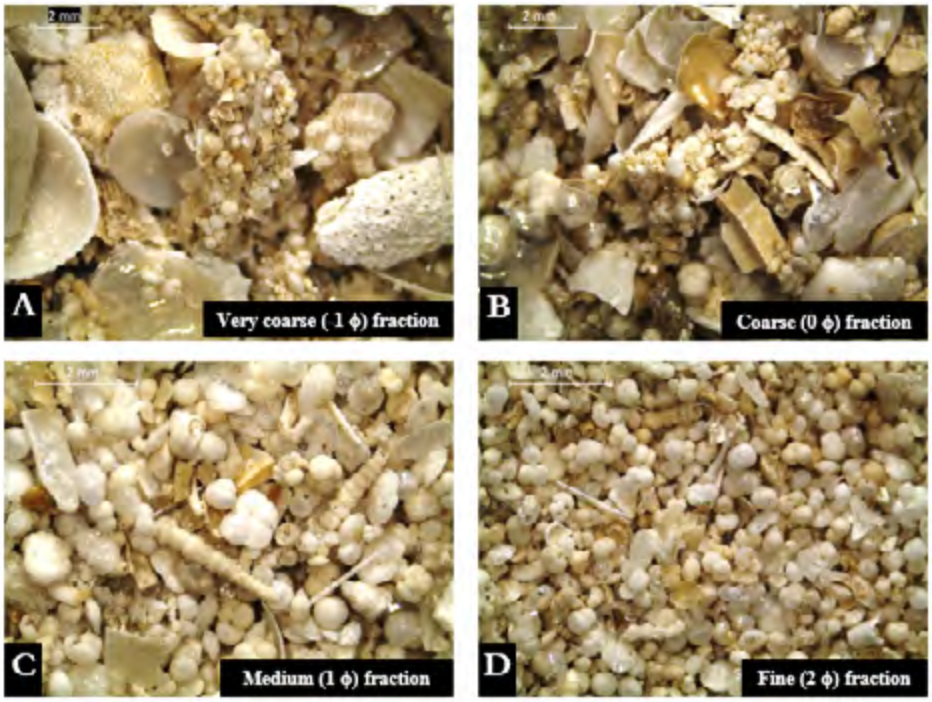

Figure 10. Micrographs of sediment fractions from SDM10. (A) very coarse (-1 ϕ), (B) coarse (0 ϕ), (C) medium (1 ϕ), and (D) fine (2 ϕ) fractions. Agglomerates are observed in (A) and (B).

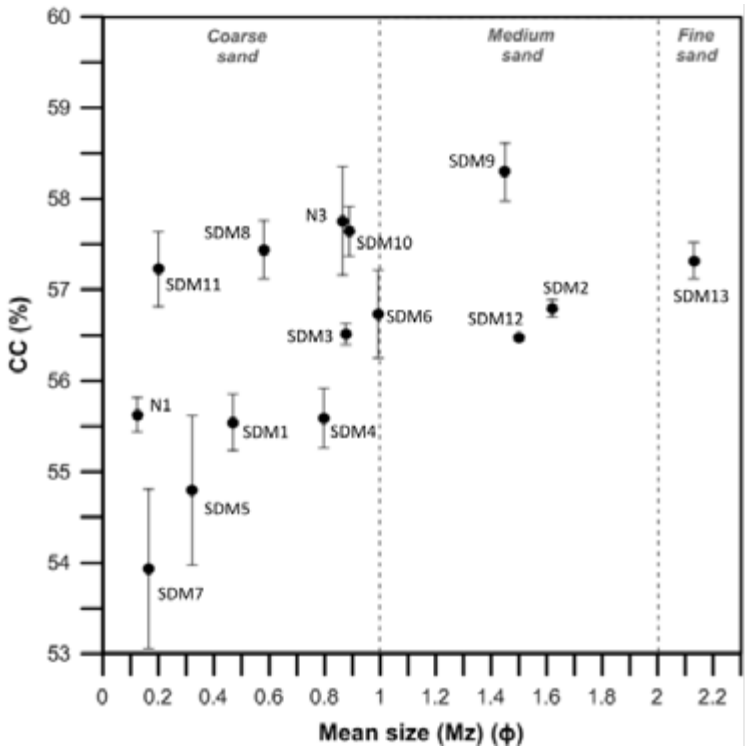

Figure 11. Scatter plot of mean size (Mz) versus Carbonate Content (CC (%))

coarser sand fractions on the Banks. The large agglomerates could be formed during the drying procedures without any prewashing step of the sediments. Therefore, during drying of unwashed sediment samples, sea salts or dissolved organic matter from calcareous biogenic materials present in the sediments cement the small sediment particles together to form these agglomerates and might affect the TOM measurements. It is suspected that the high TOM in the coarse sand category could be due to the presence of these agglomerates as confirmed by micrographs (Fig. 10) in the very coarse to coarse fractions (-1 to 0 ϕ) of sediment samples from SDM10, which had a relatively low TOM of 2.67 %. If such agglomerates were observed in a sediment sample with mean size of coarse sand with relatively low TOM, it is suggested that more such agglomerates should be present in SDM7 sample, which had a higher TOM value. The findings showed that standard mechanical sieving might be insufficient to break apart the agglomerates that had been developed. When designing standard methods for sediment analysis, the risk of large agglomerates forming from smaller particles should be taken into consideration.

Figure 11 illustrates the % CC in the sediment samples. CC values vary from 53.9 ±0.88 to 58.3 ±0.32 %. From the micrographs in Figure 10, it was observed that the sediments consisted mainly of remains of carbonate producers such as bivalve shells, coral rubble and foraminifera shells amongst others, which explain the moderate CC results. SDM9 with a mean size of medium sand had the highest CC with a value of 58.3±0.32 %. Siesser and Rogers (1971) reported that carbonate contents from 36 marine sediment samples varied from 40.2 to 98.0 % when employing a weight-loss method. This method however provides a rough approximation of the true carbonate value in marine sediments, but is widely employed due to its simplicity and cost-effectiveness (Siesser and Rogers, 1971).

Conclusion

This study has provided new information on the physical characteristics of sediments and their TOM and CC on the SDM and Nazareth Banks. It was revealed that sand was the dominant grain size with an average composition of 98.12 %. The majority of the stations (11 out of 15) had a mean grain size of coarse sand, three stations had medium sand range and only one station had fine sand.

The average TOM and CC on the Banks ranged from 2.1 to 7.7 % and from 53.9 to 58.3 %, respectively. The TOM estimated from sediments on the Banks falls in the same range of values as reported from the coastal

waters of Kenya (Mohamed *et al.*, 2018; Wafula *et al.*, 2020). However, it is suspected that high TOM values > 7 % in the coarse sand range might be due to the formation of agglomerates during the drying procedures of sediments without any prewashing step.

Sediment grain size characteristics were found to be mostly influenced by the prevailing bottom water currents and possibly by the type of nearby living carbonate producers, which then integrate into the sediment composition. Rate of sand production seemed therefore to be high at shallow depths where the calcareous macroalgae *Halimeda* spp grows in high abundance. These newly generated data on the physical characteristics of sediments will provide baseline information that will help to classify benthic habitats in the different sedimentary environments and help to better understand the ecosystem functioning and dynamics on these two major underwater banks.

Acknowledgments

The authors wish to acknowledge the Food and Agriculture Organization (FAO) for funding the expedition in the Saya de Malha under the EAF-Nansen Programme on board the R/V Dr Fridtjof Nansen and the Department of Continental Shelf, Maritime Zones Administration & Exploration of Mauritius for co-leading and coordinating the scientific expedition. We are grateful to the Mauritius Oceanography Institute (MOI) for their continuous support during this study, M Singh for guidance and help in improving the quality of the manuscript, and B Mugun and L Harree-Somah for their invaluable support for laboratory analysis. We also express our gratitude to all the participants of the expedition and the scientific team who assisted in the sampling of sediments onboard.

References

Anfuso G, Gracia FJ (2005) Morphodynamic characteristics and short-term evolution of a coastal sector in SW Spain: implications for coastal erosion management. Journal of Coastal Research 21 (6): 1139-1153

Azidane H, Michel B, Bouhaddioui ME, Haddout S, Magrane B, Benmohammadi A (2020) Grain size analysis and characterization of sedimentary environment along the Atlantic Coast, Kenitra (Morocco). Marine Georesources & Geotechnology 39 (5): 569-576

Benavente J, Gracia FJ, Anfuso G, Lopez-Aguayo F (2005) Temporal assessment of sediment transport from beach nourishments by using foraminifera as natural tracers. Coastal Engineering 52 (3): 205-219

Bengtsson L, Enell M (1986) Chemical analysis. In: Berglund BE (ed) Handbook of holocene palaeoecology and palaeohydrology. Wiley & Sons, Chichester. pp 423-451

Bergstad OA, Bissessur D, Sauba K, Rama J, Coopen P, Oozeeraully Y, Seeboruth S, Audit-Manna A, Nicolas A, Reetoo N, Tabachnick K, Kuyper D, Gendron G, Hollanda S, Melanie R, Souffre A, Harlay J, Bhagooli R, Soondur M, Ramah S, Caussy L, Ensrud TM, Olsen M, Høines ÅS (2018) Regional resources and ecosystem survey in the Indian Ocean, Leg 2.1. Characterizing ecosystems and morphology of the Saya de Malha Bank and Nazareth Bank. In: Norad-FAO Programme GCP/GLO/690/NOR, Cruise Reports Dr Fridtjof Nansen. EAF-Nansen/Cr/2018/6

Blatt H, Middleton GV, Murray RC (1972) Origin of sedimentary rocks. Englewood Cliffs, Prentice-Hall, NJ. 782 pp

Blott SJ, Pye K (2001) GRADISTAT: a grain size distribution and statistics package for the analysis of unconsolidated sediments. Earth Surface Processes and Landforms 26 (11): 1237-1248

Bui E, Mazzullo J, Wilding L (1989) Using quartz grain size and shape analysis to distinguish between aeolian and fluvial deposits in the Dallol Bosso of Niger (West Africa). Earth Surface Processes and Landforms 14 (2): 157-166

Byers SC, Mills EL, Stewart PL (1978) A comparison of methods of determining organic carbon in marine sediments, with suggestions for a standard method. Hydrobiologia 58 (1): 43-47

Dean WE (1974) Determination of carbonate and organic matter in calcareous sediments and sedimentary rocks by loss on ignition; comparison with other methods. Journal of Sedimentary Research 44 (1): 242-248

Fedorov V, Danilov I (1979) Investigations of relief of central region Mascarene Plateau. Geomorphology 4: 75-81 (In Russian)

Folk RL, Ward WC (1957) Brazos River bar: a study in the significance of grain size parameters. Journal of Sedimentary Research 27 (1): 3-26

Ford MR, Kench PS (2012) The durability of bioclastic sediments and implications for coral reef deposit formation. Sedimentology 59 (3): 830-842

Griffiths JC (1967) Scientific method in analysis of sediments. McGraw-Hill, New York. 508 pp

Heiri O, Lotter A.F, Lemcke G (2001) Loss on ignition as a method for estimating organic and carbonate content in sediments: reproducibility and comparability of results. Journal of Paleolimnology 25 (1): 101-110

Hewins M, Perry C (2006) Bathymetric and environmentally influenced patterns of carbonate sediment accumulation in three contrasting reef settings, Danjugan Island, Philippines. Journal of Coastal Research 22 (4): 812-824

Hilbertz W, Gutzeit F, Goreau T (2002) Saya de Malha Expedition Report. Lighthouse Foundation. 107 pp

Ingole B, Ansari Z, Parulekar A (1992) Benthic fauna around Mauritius Island, southwest Indian Ocean. Indian Journal of Marine Sciences 21: 268-268

Jinendradasa S, Ekaratne S (2002) Composition and monthly variation of fauna inhabiting reef-associated *Halimeda*. Proceedings of the Ninth International Coral Reef Symposium, Bali 2: 1059-1063

Kim S, Ahn J, Kim H, Kwon H, Kim G, Shin D, Yang D (2018) The distribution characteristics of grain size and organic matters of surface sediments from the Nakdong-Goryeong mid-watershed. Journal of Environmental Science International 27 (6): 411-423

Krumgalz BS (1989) Unusual grain size effect on trace metals and organic matter in contaminated sediments. Marine Pollution Bulletin 20 (12): 608-611

Meyerhoff A, Kamen-Kaye M (1981) Petroleum prospects of Saya de Malha and Nazareth Banks, Indian Ocean. AAPG Bulletin 65 (7): 1344-1347

Mohamed, HS, Muthumbi, A, Githaiga J, Okondo J (2018) Sediment macro-and meiobenthic fauna distribution along the Kenyan continental shelf. Western Indian Ocean Journal of Marine Science 17 (2): 103-116

Neumann AC, Land LS (1975) Lime mud deposition and calcareous algae in the Bight of Abaco, Bahamas: a budget. Journal of Sedimentary Research 45 (4): 763-786

New AL, Stansfield K, Smythe-Wright, D, Smeed D, Evans A, Alderson S (2005) Physical and biochemical aspects of the flow across the Mascarene Plateau in the Indian Ocean. Philosophical Transactions of the Royal Society A (363): 151-168

Nordstrom KF (1977) The use of grain size statistics to distinguish between high-and moderate-energy beach environments. Journal of Sedimentary Research 47 (3): 1287-1294

Rajganapathi V, Jitheshkumar N, Sundararaja M, Bhat K, Velusamy S (2013) Grain size analysis and characterization of sedimentary environment along Thiruchendur coast, Tamilnadu, India. Arabian Journal of Geosciences 6 (12): 4717-4728

Román-Sierra J, Muñoz-Perez JJ, Navarro-Pons M (2013) Influence of sieving time on the efficiency and accuracy of grain-size analysis of beach and dune sands. Sedimentology 60 (6): 1484-1497

Secrieru D, Oaie G (2009) The relation between the grain size composition of the sediments from the NW Black Sea and their Total Organic Carbon (TOC) content. Geo-Eco-Marina 15: 5-11

Shepard FP (1954) Nomenclature based on sand-silt-clay ratios. Journal of Sedimentary Research 24 (3): 151-158

Siesser WG, Rogers J (1971) An investigation of the suitability of four methods used in routine carbonate analysis of marine sediments. Deep-Sea Research 18: 135-139

Trask PD (1955) Organic content of recent marine sediments. In: Trask PD (ed) Recent marine sediments. American Association of Petroleum Geologists. pp 428-453

Wafula M, Muthumbi AW, Wangondu V, Kihia C, Okondo J (2020) Nematodes as bio-indicators of physical disturbance of marine sediments following polychaete bait harvesting. Western Indian Ocean Journal of Marine Science 19 (2): 117-130

Wang Q, Li Y, Wang Y (2011) Optimizing the weight loss-on-ignition methodology to quantify organic and carbonate carbon of sediments from diverse sources. Environmental Monitoring and Assessment 174 (1): 241-257

Wentworth CK (1922) A scale of grade and class terms for clastic sediments. The Journal of Geology 30 (5): 377-392

Variable photo-physiological performance of macroalgae and seagrasses from Saya de Malha and Nazareth Banks, Mascarene Plateau

Ranjeet Bhagooli[1,2,3,4*], Mouneshwar Soondur[1,2], Sundy Ramah[1,5], Arvind Gopeechund[1,2], Deepeeka Kaullysing[1,2]

[1] Department of Biosciences and Ocean Studies, Faculty of Science & Pole of Research Excellence in Sustainable Marine Biodiversity, University of Mauritius, Réduit 80837, Republic of Mauritius

[2] The Biodiversity and Environment Institute, Réduit, Republic of Mauritius

[3] Institute of Oceanography and Environment (INOS), University Malaysia Terengganu, 21030 Kuala Terengganu, Terengganu, Malaysia

[4] The Society of Biology (Mauritius), Réduit, Republic of Mauritius

[5] Albion Fisheries Research Centre, Ministry of Blue Economy, Marine Resources, Fisheries & Shipping, Albion, Petite Rivière 91001, Republic of Mauritius

* Corresponding author: r.bhagooli@uom.ac.mu

Abstract

The photosynthetic performance of macroalgae and seagrasses related to their body parts, depth and colours from the poorly-studied Saya de Malha and Nazareth Banks on the Mascarene Plateau was investigated in this study. Two seagrass (*Thalassodendron ciliatum* and *Halophila decipiens*) and seven macroalgae species (*Caulerpa cupressoides, Acrosorium ciliolatum*, *Dictyosphaeria cavernosa*, *Halimeda opuntia*, *Ulva* sp., *Udotea orientalis* and *Udotea palmetta*) were collected using the five Van Veen grabs attached to the Video-Assisted Multi-Sampler (VAMS) from 29-79 m depths in May during the FAO EAF-Nansen Research Programme 2018. The photosynthetic performance was measured using a Diving-Pulse-Amplitude-Modulated (D-PAM) fluorometer and the parameters included effective quantum yield at photosystem II (PSII) (Φ_{PSII}), relative maximum electron transport rate ($rETR_m$), photosynthetic efficiency (α), photoinhibition (β), saturating light level (E_k), and maximum non-photochemical quenching (NPQ_{max}). All photo-physiological parameters varied significantly in *T. ciliatum* and *C. cupressoides* across their body parts. However, variation with seawater depths was not significant for NPQ_{max} and β in the seagrass, and Φ_{PSII}, $rETR_m$ and β in the macroalgae. Photo-physiological functioning of the leaf of *T. ciliatum* was optimal at 40 m. The photosynthetic performance of the frond and stolon of *C. cupressoides* decreased and remained unchanged, respectively, at 79 m when compared to that at 29 m. The whitish lobes of *H. opuntia* at 31 m exhibited significantly lower photosynthetic performance, in terms of Φ_{PSII}, $rETR_m$, α and E_k, than the greenish lobes. These findings provide a first insight of seaplant body parts-, depth- and colour-related photo-physiological performance from the Mascarene Plateau.

Keywords: macroalgae, Nazareth, PAM, photo-physiology, Saya de Malha, seagrass

Introduction

Seagrasses and macroalgae from the Saya de Malha and Nazareth Banks on the Mascarene Plateau have received very little scientific attention to date (Fredericq *et al*., 1999; Hagan and Robinson, 2001; Gullstrom *et al*., 2002; Hilbertz and Goreau, 2002; Milchakova *et al*., 2005; Vortsepneva, 2008). Three species of seagrasses, namely, *Thalassodendron ciliatum*, *Halophila decipiens* and *Enhalus acroides* have been reported at the Saya de Malha Bank (Hilbertz and Goreau, 2002; Vortsepneva, 2008). Reported macroalgae include species of Rhodophyta *Kappaphycus cottonii*, *Neogoniolithon*,

http://dx.doi.org/10.4314/wiojms.si2021.2.7

Hydrolithon, *Sporolithon*, *Mesophyllum*, *Lithophyllum* (Fredericq *et al*., 1999 cited in Vortsepneva, 2008), and calcareous encrusting and branching red algae, soft green alga *Microdictyon* sp. and calcareous green alga *Halimeda opuntia* from the Ritchie Bank (Hilbertz and Goreau, 2002). These are important primary producers which exhibit photo-physiological plasticity with respect to the prevailing light regimes.

Though light is essential for photosynthesis to take place, light limitation or excess irradiance may trigger multiple responses in photosynthetic marine organisms. Responses to light limitation in seagrasses usually include increased photosynthetic efficiency, lowered maximum electron transport rate, and a decline in the saturating irradiance (Ralph, 1999; Ralph and Gademann, 2005), while responses to increased irradiance entail decreased effective and maximum quantum yield at photosystem II (Durako and Kunzelman, 2002; Ralph and Gademann, 2005). In contrast, no photosynthetic responses to change in light regime or along a light gradient have been reported (Major and Dunton, 2000; Olesen *et al*., 2002). Solar irradiation, in particular short wavelengths (UVB, 280-315 nm), may change photo-physiological performance and protective mechanisms in plants (Bischof *et al*., 2006) and cause DNA damage (van de Poll *et al*., 2001), which in turn slows growth (Aguilera *et al*., 2002). Elevated light levels enhance the production of reactive oxygen species, which if not soaked up by antioxidant activities, may cause cellular damage and photosynthetic dysfunctioning. Phenolic compounds, such as coumarins, with their high UV absorption properties, prevent light-induced damage in green macroalgae such as *Caulerpa* and *Dasycladus* (Aguilera *et al*., 2002; Bischof *et al*., 2006). Macroalgae in the intertidal environment adapt physically and physiologically to changing irradiance, and thus optimise their photosynthetic performance (Davison and Pearson, 1996). Similarly, light-induced stress leads to reduced photosynthetic activity as a photo-physiological adaptation to elevated irradiance (Schagerl and Möstl, 2011). Seagrasses and macroalgae occurring in the waters of the Mascarene Plateau at depths greater than 20 m may be more likely exposed to a light-limited environment and more so on their different body parts, like stem or stolon, thus warranting investigation of the photo-physiological responses of their different photosynthetically active body parts.

Although the leaves of seagrasses or fronds of macroalgae have mainly been used in photosynthetic investigations, other body parts like the stem and stolon are yet to be photo-physiologically explored. The different body parts of some seagrass and macroalgal species appear green in colour, potentially indicating the presence of the green photosynthetic pigment, and consequently may be photosynthetically active. Several plants have either specialized/modified or different body parts that perform photosynthesis. Examples include the roots of the epiphytic orchids, *Taeniophyllum* (Chinese Herbs Healing, 2020), the roots of the flowering plant, *Podostemon* (Cook and Rutishauser, 2007), the adventitious roots and succulent stem of the aquatic plant, *Tecticornia pergranulata* (Rich *et al*., 2008), and the leaves and roots of water chestnut *Trapa bispinosa* Roxb (Ishimaru *et al*., 1996). It is noteworthy that re-oxygenation effectiveness in marine plant tissues in different body parts may be reduced due to the lower solubility and about a thousand-fold slower oxygen diffusion rate in water than in air (Grable, 1966). Though the photosynthetic adventitious roots in some aquatic plants like *Tecticornia pergranulata* occur in very light-limited environment, they may reduce the internal oxygen deficit (Rich *et al*., 2008). Similarly, the different body parts of seagrasses and marine macroalgae may possibly avoid internal oxygen deficit through limited photosynthetic activities despite occurring in low light regimes or in deeper waters. Given these possibilities, future investigations may be necessary; first exploring the photo-physiological activities and any photo-acclimatory capacity in seagrass and macroalgal body parts using non-destructive chlorophyll fluorescence techniques. A similar approach may also be applied to investigate the decolouration process in green coralline macroalga like *Halimeda*, which usually whitens and degrades to produce sand.

Apart from light, temperature, substratum type and hydrodynamics act as major determinants of marine macrophytes spatial distribution (Riss and Hawes, 2003; Koch *et al*., 2006; Infantes *et al*., 2011). Seagrasses and macroalgae attach firmly to consolidated substrata such as rocks, which provide a stable and non-motile surface, and colonise unconsolidated substrata like sand, which requires root-like structures to stabilize unstable and mobile surface. Seagrases have true roots while some macroalgae have root-like rhizoids to colonise sediment particles on unconsolidated substrata, which may be mobilized by waves and currents leading to erosion or accretion and thus negatively impacting marine macrophytes through uprooting or burial (Fonseca and Kenworthy, 1987; Cabaco *et al*., 2008).

Though most macroalgae colonise consolidated substratum, some species of order Caulerpales grow on unconsolidated substrata, where the creeping stolons have rhizoids that may bind with sediment particles (Taylor, 1960; Chisholm and Moulin, 2003) and thus anchor in sandy sediments (Klein and Verlaque, 2008). *Caulerpa* species may inhabit both consolidated and unconsolidated substrata (Thibaut *et al*., 2004). Some *Caulerpa* species appear to tolerate sediment deposition and burial to a certain extent (Glasby *et al*., 2005; Piazzi *et al*., 2005) as reflected by macroalgae cover persistence (Infantes *et al*., 2011). However, photo-physiological tolerance of the creeping stolon to temporary burial by sandy sediment has yet to be investigated.

However, photo-physiological variations among species of macroalgae and seagrasses, and in relation to environmental gradients such as depth, are uncharted on the Saya de Malha and Nazareth Banks, Mascarene Plateau. This study aimed at investigating the variations in the photo-physiological performance, using a diving fluorometer, in two seagrass and seven macroalgae species. The variability in photo-physiological performance of selected seaplants with respect to their body parts, whitening, seawater depth and sand burial was assessed.

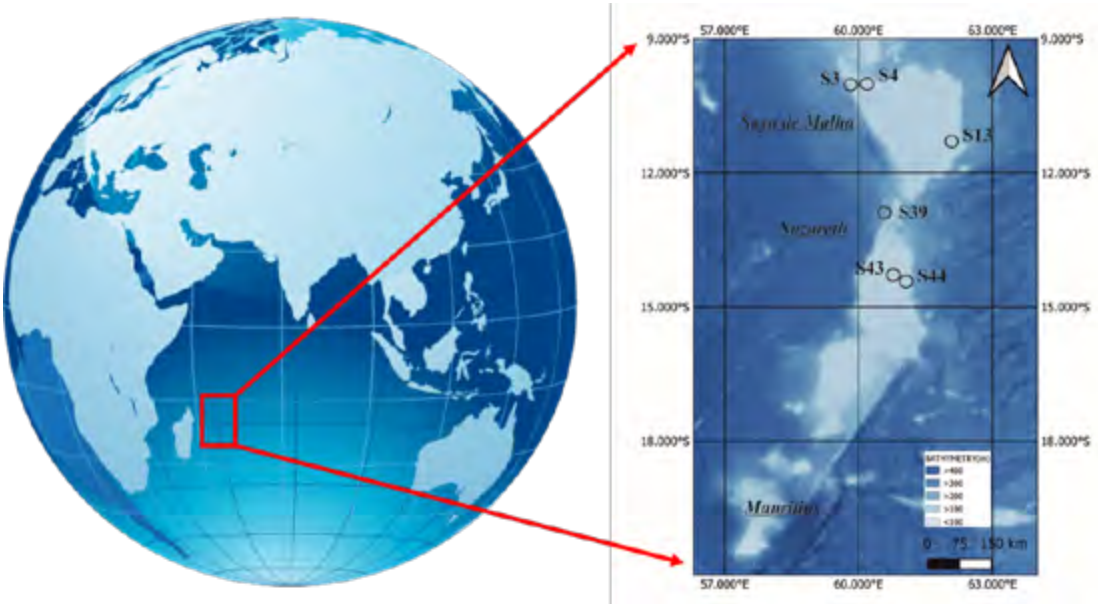

Figure 1. Map of Mascarene Plateau indicating the sampling locations at Saya de Malha (S3, S4, S13 and S39) and Nazareth Banks (S43 and S44).

Rapid light curves (RLCs) generated by Pulse-Amplitude-Modulated (PAM) fluorometry (Beer and Bjork, 2000; Beer *et al*., 2000; Beer and Axelsson, 2004; Campbell *et al*., 2008) provide chlorophyll *a* fluorescence parameters such as effective quantum yield at photosystem II (Φ_{PSII}), initial slope (α), photoinhibition (β), maximum relative electron transport rate ($rETR_m$), and maximum non-photochemical quenching (NPQ_{max}). These act as a proxy indicating natural variations and stress responses in marine plants including seagrasses and macroalgae (Li *et al*., 2010, 2014; Bhagooli *et al*., 2021). Diving-PAM fluorometry is a non-destructive method to estimate photosynthetic activities in seaplants (Beer *et al*., 2001) and symbiotic marine invertebrates (Bhagooli *et al*., 2021).

Material and methods

Study sites

Grab sites for this study included S3, S4, S13 and S39 at the Saya de Malha Bank, and at S43 and S44 at the Nazareth Bank (Fig. 1). Sampling was conducted in the month of May 2018 during the Nansen research expedition to the Mascarene Plateau. The seagrass and macroalgal samples were collected using Van Veen grabs on the Video-Assisted Multi-Sampler (VAMS) deployed at respective study sites. The samples were kept in seawater from the respective sites and the chlorophyll fluorescence measurements were performed within 1-1.5 hours following collection.

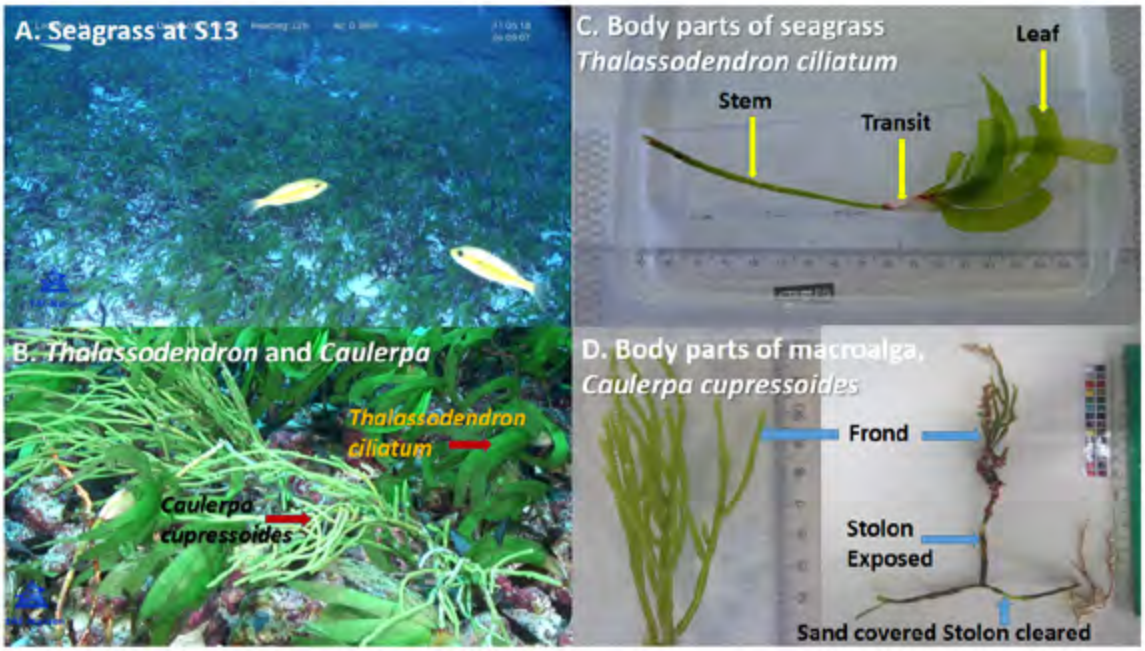

Figure 2. A. Seagrass at SMB location S13 at a depth of 29 m. B. Close up image of the seagrass, *Thalassodendron ciliatum* and the macroalga, *Caulerpa cupressoides,* both indicated by red arrows. C. Stem, transit and leaf body parts of the seagrass, *Thalassodendron ciliatum* (indicated by yellow arrows) for measurement of chlorophyll fluorescence. D. Frond, Exposed stolon and cleared stolon covered with sand as body parts of the macroalga *Caulerpa cupressoides* (indicated by blue arrows) for measurement of chlorophyll fluorescence.

Light intensity, salinity and temperature measurements at study sites

CTDs were deployed at all study sites, except for S39. Light intensity and salinity were recorded through the CTD at depths of 66 m, 22.2 m, 21 m, and 25 m for S3, S4, S13, and S43/44, respectively. For temperature measurements, records from the VAMS were used for the specific collection depths.

Seagrass and macroalgae identification

Seagrasses and macroalgae were identified based on morphological features related to their leaves, stems and roots, and the thallus/fronds, respectively (Oliveira *et al*., 2005).

Photo-physiology of seagrass and macroalgae – Chlorophyll *a* fluorescence measurement

Following collections using the Van Veen grabs, the seagrasses and macroalgae were kept shaded to provide dark conditions for a maximum of one hour prior to being exposed to saturating pulses using a Diving-PAM fluorometer (WALZ, Germany) for measurement of chlorophyll fluorescence parameters such as effective quantum yield at photosystem II (Φ_{PSII}), relative electron transport rate (rETR), photosynthetic efficiency (α), photoinhibition (β), saturating light level (E_k). ETR_m and NPQ_{max} were determined from the rapid light curves. rETR was computed as half the product of photosynthetically active radiation (PAR) and Φ_{PSII}. The effective quantum yield, $\Delta F/F_m'$ (Φ_{PSII}), which is unitless, was determined as the ratio of change in maximum fluorescence (F_m') and minimum fluorescence (F) to F_m', where F and F_m' were measured by applying a weak and saturating light, respectively (Genty *et al*., 1989; Serôdio *et al*., 2007). NPQ was calculated as $(F_m - F_m')/F_m'$ (Bilger and Bjorkman, 1990). Samples were exposed to a series of rapidly (10 s) increasing light climates (0, 110, 150, 300, 400, 500, 800, 1000, 1325 µmol quanta m^{-2} s^{-1}) from the D-PAM to generate the Rapid Light Curves (RLCs) (Ralph *et al*., 1999). Using the RLCs the rETR and NPQ were estimated at each irradiance. The ETR and NPQ curve fitting was done using the equation of Platt *et al*. (1980) on SigmaPlot 12.0 (Systat Software Inc, USA) to determine $rETR_m$ (µmol electron m^{-2} s^{-1}) and NPQ_{max}, α and β, which are unitless. E_k (µmol quanta m^{-2} s^{-1}) was determined as $rETR_m/\alpha$. Gain was set to 3 for all samples, except for the cleaned sand-covered stolons of *C. cupressoides* and the whitish lobes of *Halimeda opuntia* whereby gains were set to 6 and 12, respectively, to get reliable fluorescence signals.

For the seagrass, *Thalassodendron ciliatum* (Fig. 2A, B), the photo-physiological performance of three different parts of the plant were measured: 1) leaf; 2) transition part between leaf and stem (transit); and 3) stem (Fig. 2C). For the other seagrasses tested, measurements

were taken on the leaves only. In the case of the macroalga *Caulerpa cupressoides* (Fig. 2B), chlorophyll fluorescence measurements were carried out at two parts: 1) frond; and 2) stolon (Fig. 2D). For the *C. cupressoides* stolons, exposed and sand-covered were also compared, with the sand on the stolon physically removed prior to measurements (Fig. 2D). Upon collection, some stolons were exposed (not-covered) and others were covered by sand. Prior to PAM measurements, sand-covered stolons were cleaned after collection and thus both exposed and sand-covered (but cleaned) stolons were measured in a similar manner for reliable comparison. For the other macroalgae studied, measurements were taken on the frond. For the macroalga *Halimeda*, measurements were taken on the green and white lobes to test the effect of discolouration.

Statistical analyses

Photo-physiological parameters such as Φ_{PSII}, $rETR_m$, NPQ_{max}, α, β, and E_k were analysed using the software PASW Statistics 18. The data was expressed as mean±SD from three replicates (n=3). The raw data was Arcsine square root transformed prior to ANOVA tests. The two-way ANOVA was employed to test the effect of seawater depth on body parts in terms of photo-physiological parameters in *T. ciliatum* and *C. cupressoides*. The one-way ANOVA was used to test for the effect of exposure of stolon (exposed vs covered with sand) on photo-physiological parameters in *C. cupressoides* and the effect of colour (greenish vs whitish) on photo-physiological parameters in *H. opuntia*.

Results and discussion

Seagrass and macroalgae identification

Two seagrass species, namely, *Thalassodendron ciliatum* and *Halophila decipiens*, and seven macroalgae species, namely, *Caulerpa cupressoides*, *Acrosorium ciliolatum*, *Dictyosphaeria cavernosa*, *Halimeda opuntia*, *Udotea orientalis, Udotea palmetta*, and *Ulva* sp. were collected from different depths (Table 1).

Photo-physiology of different parts of *T. ciliatum* and *C. cupressoides*

T. ciliatum and *C. cupressoides* from S13 and S39 at Saya de Malha and S44 at Nazareth, respectively, were used for assessing the variation in photo-physiology of the parts of these seaplants. All the photo-physiological parameters investigated differed significantly across the body parts for *T. cilatum* (Table 2). The mean Φ_{PSII}, $rETR_m$, NPQ_{max}, α, β and E_k of the seagrass *T. ciliatum* ranged from 0.77 to 0.84, 4.81 to 28.31, 0.44 to 1.07, 0.27 to 0.96 0.02 to 0.05 and 18.31 to 74.43, respectively (Fig. 3A-F). Φ_{PSII} was highest in the leaf of *T. ciliatum* (Fig. 3A), while the $rETR_m$ was highest in the transit part at NZB and in the stem at SMB (Fig. 3B). The NPQ_{max} was highest in leaf part of *T. ciliatum* (Fig. 3C). Photosynthetic efficiency (α) was higher in transit and stem for SMB, while it was lowest in the transit part at NZB (Fig. 3D). Photo-inhibition (β) was highest in the transit part in samples from NZB (Fig. 3E). The light saturation (E_k) was highest in transit and stem parts for NZB and SMB samples, respectively (Fig. 3F).

Both the frond and stolon of the macroalga *C. cupressoides* exhibited significantly variable photosynthetic performance (Table 3). The mean Φ_{PSII}, $rETR_m$, NPQ_{max}, α, β and E_k ranged from 0.55 to 0.81, 3.68 to 13.60, 0.09 to 7.37, 0.10 to 0.99, 0.00 to 0.47 and 3.72 to 25.77, respectively (Fig. 4A-F).

Table 1. Species of seagrasses and macroalgae collected from Saya de Malha and Nazareth Banks and used for chlorophyll fluorescence measurements. For light and salinity, data were available at the specified depths in brackets at respective locations.

Location	Depth of collection (m)	Temp (oC)	Light (µmol quanta m-2 s-1)	Salinity (PSU)	Seagrass species	Macroalgal species
SMB-S3	79.0	23.3	10.81 (at 66 m)	35.1 (at 66 m)	-	*Caulerpa cupressoides, Acrosorium ciliolatum*
SMB-S4	31.0	28.4	27.2 (at 22 m)	34.4 (at 22 m)	-	*Dictyosphaeria cavernosa; Halimeda opuntia*
SMB-S13	29.0	28.3	21.1 (at 21 m)	34.3 (at 21 m)	*Thalassodendron ciliatum*	*Caulerpa cupressoides*
SMB-S39	33.0	28.1	-	-	-	*Caulerpa cupressoides*
NB- S43	44.0	27.3	15.1 (at 25 m)	34.3 (at 25 m)	*Halophila decipiens*	*Udotea orientalis, Udotea palmetto, Caulerpa cupressoides*
NB-S44	40.0	27.1	15.0 (at 25 m)	34.1 (at 25 m)	*Thalassodendron ciliatum*	*Udotea orientalis, Ulva* sp.

Table 2. Two-way ANOVA for the effect of depth (29 m and 40 m) and plant parts (leaf, transit and stem) on photo-physiological features of *Thalassodendron ciliatum*. Asterisks ***, ** and * represent significant differences at *P<0.001*, *P<0.01* and *P<0.05*, respectively.

	Source of Variation	SS	df	MS	F	P-value
Φ_{PSII}	Depth	0.008	1	0.008	25.570	0.000***
	Plant parts	0.042	2	0.021	65.698	0.000***
	Depth x Plant parts	0.014	2	0.007	21.723	0.000***
rETR$_m$	Depth	0.001	1	0.001	8.821	0.012*
	Plant parts	0.003	2	0.002	10.326	0.002**
	Depth x Plant parts	0.021	2	0.011	62.398	0.000***
NPQ$_{max}$	Depth	0.003	1	0.003	0.864	0.371
	Plant parts	0.029	2	0.015	5.033	0.026*
	Depth x Plant parts	0.003	2	0.002	0.591	0.569
α	Depth	0.976	1	0.976	58.198	0.000***
	Plant parts	0.496	2	0.248	14.774	0.001**
	Depth x Plant parts	0.642	2	0.321	19.128	0.000***
β	Depth	0.055	1	0.055	4.198	0.063
	Plant parts	0.242	2	0.121	9.246	0.004**
	Depth x Plant parts	0.231	2	0.115	8.814	0.004**
E$_k$	Depth	0.018	1	0.018	52.740	0.000***
	Plant parts	0.025	2	0.013	35.801	0.000***
	Depth x Plant parts	0.052	2	0.026	74.496	0.000***

These results suggest that the leaf, transit part and stem of the seagrass *T. ciliatum* and the frond and stolon of the macroalga *C. cupressoides* were comparably photosynthetically competent. This study highlights the photo-physiological performance of the stem of *T. ciliatum* and the stolon of *C. cupressoides* as also being photosynthetically active and functional. Studies on photo-physiology of seagrasses and macroalgae using the chlorophyll fluorescence technique focus mostly on the leaves and the fronds, respectively, and the conventional methods may use leaves or fronds or parts of entire seaplant communities enclosed in bottles (Beer and Bjork, 2000; Beer *et al*., 2001; Beer and Axelsson, 2004). Further studies on the relative photosynthetic contributions of the different parts of seagrasses and macroalgae to the whole respective

Table 3. Two-way ANOVA for the effect of depths (29 m, 44 m, and 79 m) and plant parts (frond and stolon) on photo-physiological features of *Caulerpa cupressoides*. Asterisks ***, ** and * represent significant differences at *P<0.001*, *P<0.01* and *P<0.05*, respectively.

	Source of Variation	SS	df	MS	F	P-value
Φ_{PSII}	Plant parts	0.111	2	0.055	42.426	0.000***
	Depth	0.000	1	0.000	0.359	0.560
	Plant parts x Depth	0.026	2	0.013	9.933	0.003**
rETR$_m$	Plant parts	0.007	2	0.004	27.511	0.000***
	Depth	0.000	1	0.000	3.623	0.081
	Plant parts x Depth	0.003	2	0.001	11.194	0.002**
NPQ$_{max}$	Plant parts	0.968	2	0.484	180.613	0.000***
	Depth	0.423	1	0.423	157.847	0.000***
	Plant parts x Depth	0.707	2	0.353	131.847	0.000***
α	Plant parts	2.003	2	1.001	153.223	0.000***
	Depth	1.867	1	1.867	285.747	0.000***
	Plant parts x Depth	0.670	2	0.335	51.260	0.000***
β	Plant parts	0.528	2	0.264	40.562	0.000***
	Depth	0.026	1	0.026	3.965	0.070
	Plant parts x Depth	0.443	2	0.222	34.056	0.000***
E$_k$	Plant parts	0.032	2	0.016	36.752	0.000***
	Depth	0.048	1	0.048	109.678	0.000***
	Plant parts x Depth	0.019	2	0.010	22.203	0.000***

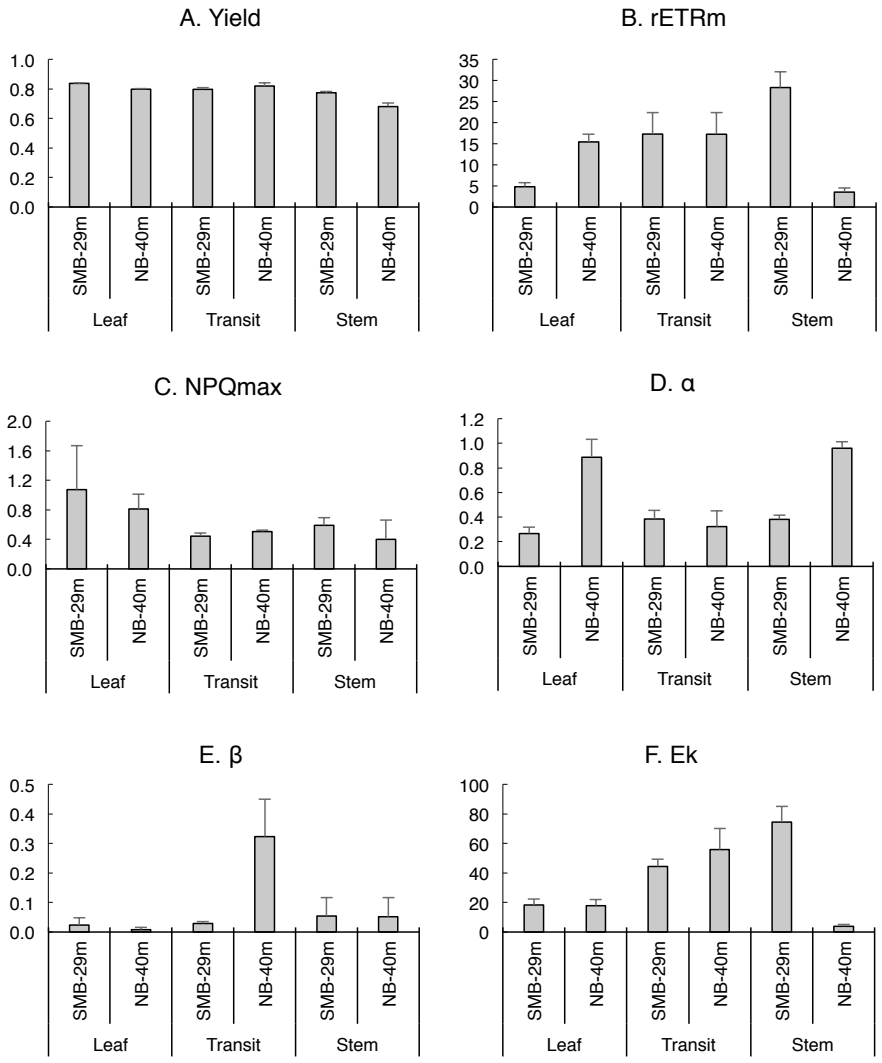

Figure 3. Photo-physiological performance of the seagrass *Thalassodendron ciliatum* from Saya de Malha (SMB) and Nazareth Banks (NB) at 29 m (white bars - S13) and 40 m (black bars - S44), respectively. A. Yield (unitless); B. rETRm (µmol electron m^{-2} s^{-1}); C. NPQmax (unitless); D. α (unitless); E. β (unitless); F. Ek (µmol quanta m^{-2} s^{-1}). Three parts of the plant were measured: 1) leaf; 2) transit part between leaf and stem; and 3) stem. Bars represent Mean±SD (n=3).

individual would help understand these primary producers more thoroughly.

It is noteworthy that there is a tendency to consider mostly the leaves of seagrasses and fronds of macroalgae as being involved in photo-physiological studies. For instance, Campbell *et al*. (2007) using the chlorophyll fluorescence to study photo-physiological variations in seagrasses such as *Thalasodendron ciliatum* and *Halophila decipiens* among other species in tropical Queensland at depths of 2-7 m reported values within the range found for the parameters used in this study. The mean values of Φ_{PSII}, $rETR_m$, α and E_k for *T. ciliatum* were 0.66, 103.9, 0.30, and 365.5 at 2 m and 0.65, 42.6, 0.20, 221.6, respectively. In the case of *H. decipiens*, the mean values of Φ_{PSII}, $rETR_m$, α and E_k were 0.59, 58.5, 0.22 and 294.9, respectively. Olsen *et al*. (2017) documented photo-physiology of macroalgae, in particular *Halimeda* and *Caulerpa* species at depths of 3-5 m around Browse Island off the north-western coast of Western Australia. In October 2017 the mean Φ_{PSII}, $rETR_m$, α, and E_k for *Halimeda* sp. were 0.546, 34.8, 0.36, and 101.1, while for *Caulerpa* sp. the mean values were 0.687, 80.8, 0.41, and 203 for respective parameters. Driscoll (2004) reported photo-physiological performance of three *Caulerpa* species, namely *C. racemosa*, *C. sertularioides*, and *C. mexicana*, at less than 15 m depth from Florida Keys and Tampa Bay, South Florida. For *in-situ C. racemosa* the mean $rETR_m$, NPQ, α, and E_k reported were 4.0-4.4, 0.083-0.098, 0.370-.390, and 27.9-28.4, while

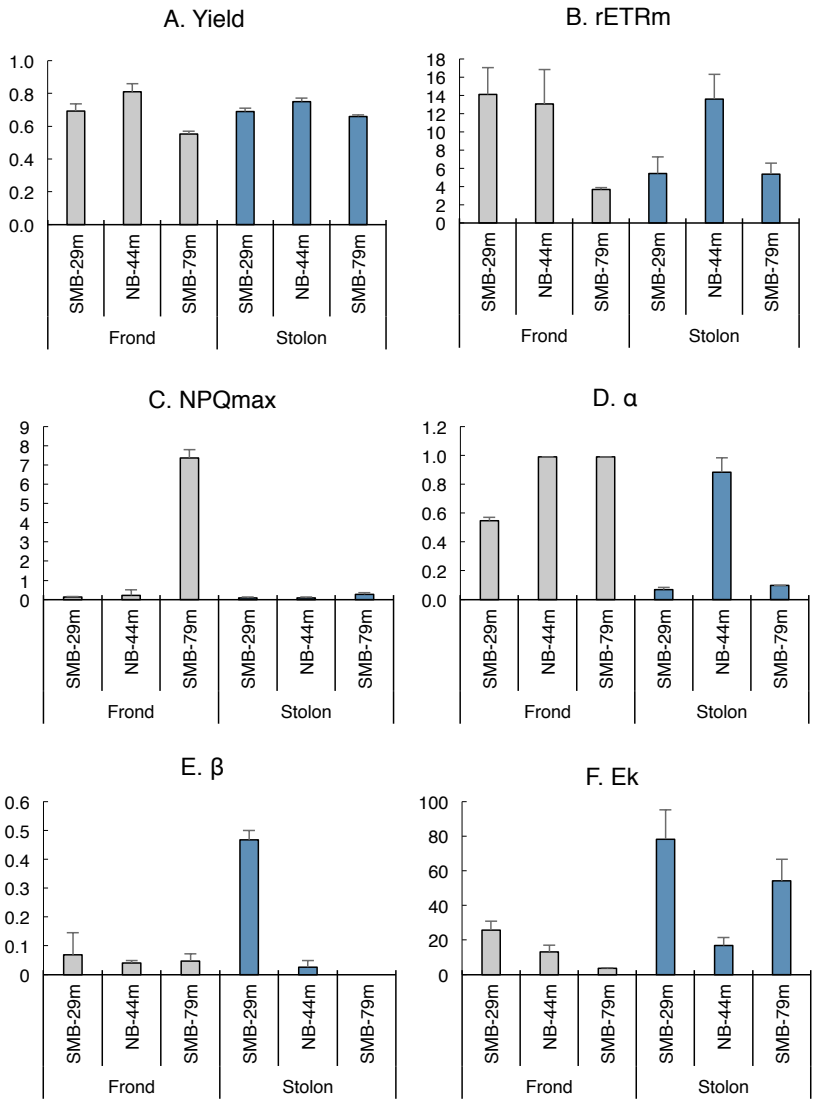

Figure 4. Photo-physiological performance of the macroalgae *Caulerpa cupressoides* from Saya de Malha (SMB) at 29 m (white bars - S13) and 79 m (black bars - S3) and Nazareth (NZB) Banks at 44 m (blue bars - S43). A. Yield (unitless); B. rETRm (µmol electron m^{-2} s^{-1}); C. NPQmax (unitless); D. α (unitless); E. β (unitless); F. Ek (µmol quanta m^{-2} s^{-1}). Two parts of the macroalga were measured: 1) frond; and 2) stolon. Bars represent Mean±SD (n=3).

for *in situ C. sertularioides* the mean values for $rETR_m$, α, and E_k were 7.2-12.8, 0.217-0.257, and 30.3-56.8, respectively. The range of values for the chlorophyll fluorescence parameters seem to be within similar range for the macroalgae tested in the present study. Due to the environmental variability in which these seagrasses and macroalgae were studied and the variability in the values of chlorophyll fluorescence parameters tested, it is difficult to make direct comparison of these values among studies. The present study adds the first report of chlorophyll fluorescence photo-physiological features of seagrasses and macroalgae at depths of ≥29 m deep, with new insights into the photosynthetic performance of the different body parts, including leaf, stem, frond and stolon.

Variation in photo-physiology of *T. ciliatum* and *C. cupressoides* with depth

Availability of samples of the seagrass *T. ciliatum* from depths of 29 m at SMB-S13 and 40 m at NB-S44 (Fig. 3), and macroalga *C. cupressoides* from depths of 29 m at SMB-S13, 44 m at NB-S43 and 79 m at SMB-S3 (Fig. 4) allowed for depth-related photo-physiological performance comparison for the seagrass and macroalga. Significant variation in photo-physiology with seawater depth was noted except for NPQ_{max} and β for the seagrass (Table 2), and Φ_{PSII}, rETR*m* and β for the macroalga (Table 3). It is noteworthy that the interaction between depth and body parts was found to be significant (Table 2). The depth at which samples were collected did reflect variations in light levels (Table 1)

and thus different body parts of *T. ciliatum* and *C. cupressoides* may have differential photo-acclimatory capacities. However, in this study pigment analyses were not conducted and this aspect warrants future investigation.

In the case of *T. ciliatum* (Fig. 3A-F), the leaf had slightly reduced Φ_{PSII}, higher $rETR_m$ and α, and similar β and E_k at 40 m in comparison to 29 m, suggesting higher photosynthetic activity at 40 m. The transit part between leaf and stem (transit) exhibited slightly higher Φ_{PSII} and E_k, higher β and similar $rETR_m$ and NPQ_{max} at 40 m relative to 29 m, implying similar photosynthetic activity at these two depths. The stem had a significantly lower Φ_{PSII}, $rETR_m$ and E_k, similar NPQ_{max} and higher α at a depth of 40 m compared to those parameters at 29 m. This may be indicative of reduced photosynthetic activity and lower light saturation levels. Thus, these results generally indicate that the photosynthetic activity increased in the leaf, decreased in the stem and was similar in the transit part of *T. ciliatum* in deeper waters. One possible explanation for this may be that leaves are the most important photosynthetic part of the seagrass and may adjust to lower light levels at a depth of 40 m. In other words, the conditions at this depth may be optimal for photosynthesis in the leaf part of *T. ciliatum*.

For *C. cupressoides* (Fig. 4A-F), with reference to the values at 29 m in the frond, the Φ_{PSII} increased at 44 m but decreased at 79 m; $rETR_m$ was similar at 44 m but decreased at 79 m; NPQ_{max} was similar at 44 m and increased at 79 m; α increased at both 44 m and 79 m; β remained similar, and E_k decreased with depth. In the stolon part, Φ_{PSII} increased at 44 m but decreased at 79 m; $rETR_m$ increased at 44 m but remained unchanged at 79 m; NPQ_{max} remained unchanged at 44 m but increased slightly at 79 m; α increased at 44 m but remained unchanged at 79 m; β decreased with depth; and E_k decreased at a higher level at 44 m. The results may indicate that the frond of *C. cupressoides* may perform equally well photosynthetically at 44 m but not at 79 m when compared to that at 29 m. While the stolon of *C. cupressoides* may perform equally well photo-physiologically at 79 m and better at 44 m compared to that at 29 m.

Photo-physiology of *C. cupressoides* stolons exposed vs covered by sand

The stolon covered by sand and that not covered by sand was compared At S39. The covered stolon had significantly lower $rETR_m$ (Table 4) and slightly lower Φ_{PSII}, similar NPQ_{max} and β but slightly higher β (Fig. 5A-F). This indicates that the stolon of *C. cupressoides* that burrowed under the sand may be slightly affected in terms of electron transport rate and was not chronically damaged, implying the possibility of maintaining its photo-physiological functioning though temporarily covered by sand at this station.

Photo-physiology of greenish and whitish *Halimeda opuntia* lobes

Both greenish and whitish lobes of *H. opunitia* from 31 m deep from S39 at Saya de Malha Bank were examined for their photo-physiological functioning (Fig. 6). The whitish lobes of *H. opuntia* at 31 m exhibited significantly lower photosynthetic performance, in terms of Φ_{PSII}, $rETR_m$, α and E_k, than the greenish lobes. The Φ_{PSII} and E_k almost halved; $rETR_m$ decreased seven-fold; NPQ_{max} increased about 40-fold; α decreased by about six-fold; and β increased six-fold in the whitish compared to the greenish lobes. These results suggest that in the whitish condition, the photo-physiology of *H. opuntia* lobes declined drastically. The whitish lobes may be due to either of two processes, namely, sexual reproduction and/or chloroplast movement. It is understood that when *Halimeda* segments reproduce, the edges become whitish while the reproductive cells expel the protoplasmic contents of their spores through a process called holocarpy (Drew and Abel, 1988). These segments die and disintegrate after turning white. The photo-physiology of *Halimeda* under these

Table 4. One-way ANOVA for the effect of exposed or covered stolon on photo-physiological features of *Caulerpa cupressoides*. Asterisk (*) represents significant difference at *P<0.05*.

Parameters	SS	df	MS	F	P-value
Φ_{PSII}	0.013	1	0.013	2.479	0.190
$rETR_m$	0.002	1	0.002	8.547	0.043*
NPQ_{max}	5.386E-06	1	5.386E-06	0.041	0.849
α	0.001	1	0.001	1.733	0.258
β	0.033	1	0.033	1.619	0.272
E_k	0.024	1	0.024	3.342	0.142

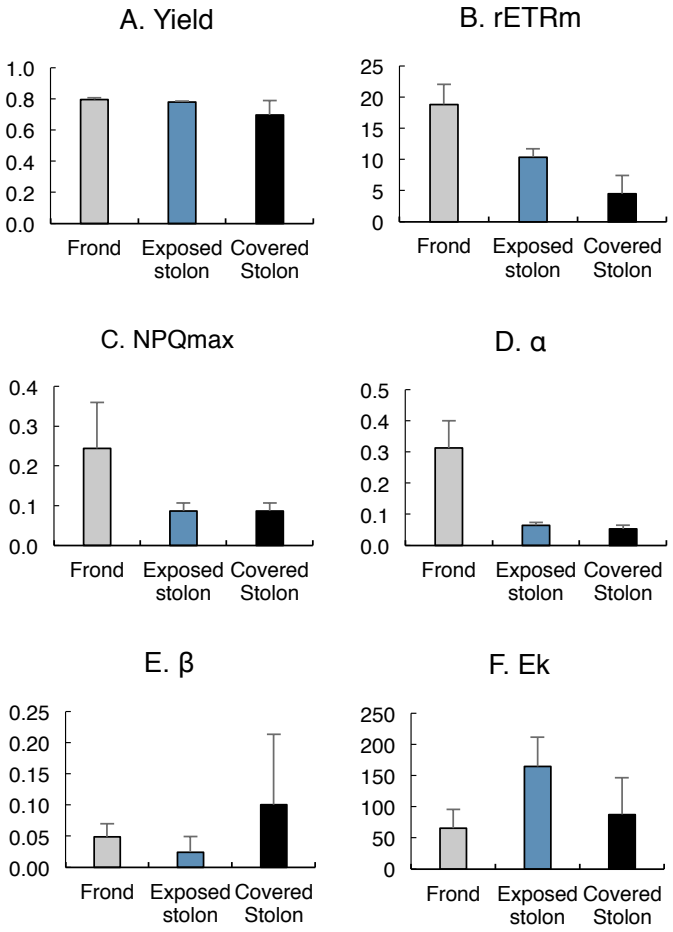

Figure 5. Photo-physiological performance of the macroalgae *Caulerpa cupressoides* from Saya de Malha (SMB) at 33 m (S39). A. Yield (unitless); B. rETRm (µmol electron m^{-2} s^{-1}); C. NPQmax (unitless); D. α (unitless); E. β (unitless); F. Ek (µmol quanta m^{-2} s^{-1}). The parts of the macroalga measured were: 1) frond (white bars); and 2) exposed stolon (not burrowed under sand – blue bars); and 3) covered stolon (mostly burrowed under sand – black bars). Bars represent Mean±SD (n=3).

conditions is not known. The gametogenesis process is known to occur seasonally in *Halimeda* spp. on the Great Barrier Reef (Drew and Abel, 1988).

Chloroplast redistribution in *Halimeda* leads to changes from a greenish to a whitish colour. This occurs because *Halimeda* is coenocytic, where the branching filamentous structure lacks crosswalls, and thus allows mass movement of the chloroplasts into the medullary filaments below the calcium carbonate deposits from the utricles at the segment surface (Drew and Abel, 1990). Mass migration of chloroplasts in *Halimeda* has been shown to be rhythmic (Drew and Abel, 1992). The photo-physiology of *Halimeda* under these migrations conditions is not thoroughly understood. However, the photo-physiology of greening in *Halimeda*

Table 5. One-way ANOVA for the effect of greenish or whitish conditions on photo-physiological features of *Halimeda opuntia*. Asterisks ***, ** and * represent significant differences at *P<0.001*, *P<0.01* and *P<0.05*, respectively.

Parameters	SS	df	MS	F	P-value
Φ_{PSII}	0.182	1	0.182	597.553	0.000***
$rETR_m$	235.978	1	235.978	45.855	0.002**
NPQ_{max}	6.045	1	6.045	1.629	0.271
α	0.175	1	0.175	24.036	0.008**
β	0.014	1	0.014	0.904	0.396
E_k	471.263	1	471.263	8.900	0.041*

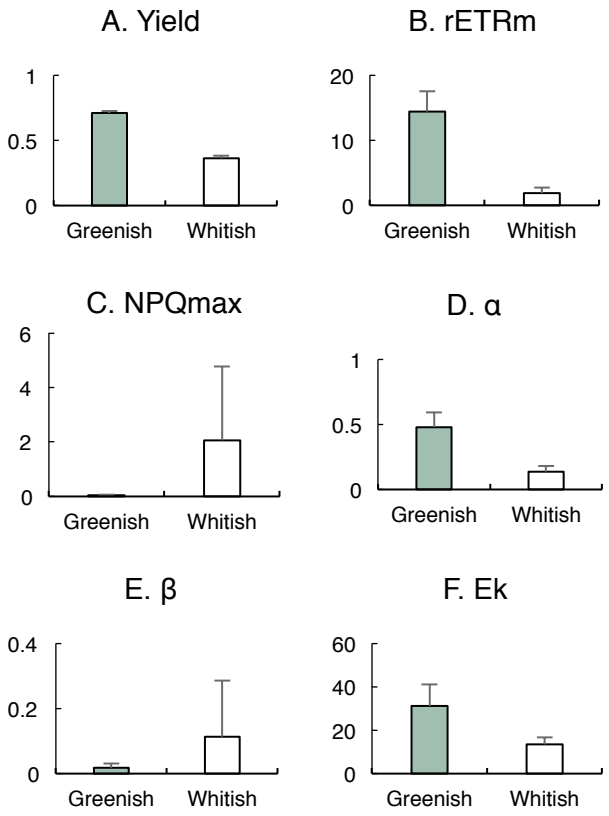

Figure 6. Photo-physiological performance of the greenish (green bars) and whitish (white bars) lobes of the macroalga *Halimeda opuntia* from a depth of 31 m at S4 at Saya de Malha. A. Yield (unitless); B. rETRm (µmol electron m^{-2} s^{-1}); C. NPQmax (unitless); D. α (unitless); E. β (unitless); F. Ek (µmol quanta m^{-2} s^{-1}). Bars represent Mean±SD (n=3).

Table 6. Photo-physiological performance of other seagrass (leaf) and macroalgal (frond) species collected from Saya de Malha Bank (SMB) and Nazareth Bank (NZB).

Species	Bank-Location-depth (m)	Photo-physiological parameters					
		Φ_{PSII}	$rETR_m$	NPQ_{max}	α	β	E_k
Seagrass							
Thalassodendron ciliatum	SMB-S13-29	0.84±0.00	4.81±1.00	1.07±0.60	0.27±0.03	0.02±0.03	18.31±4.00
	NZB-S44-40	0.80±0.00	15.42±1.79	0.81±0.20	0.89±0.15	0.01±0.01	17.84±4.33
Halophila decipiens	NZB-S43-44	0.63±0.00	2.94±0.43	0.46±0.12	0.99±0.00	0.01±0.01	2.97±0.43
Macroalgae							
Caulerpa cupressoides	SMB-S13-29	0.96±0.04	14.11±2.92	0.14±0.02	0.55±0.02	0.06±0.08	25.77±5.20
	NZB-S43-44	0.81±0.50	13.06±3.78	0.22±0.30	0.99±0.00	0.04±0.01	13.20±3.81
	SMB-S3-79	0.55±0.02	3.68±0.21	7.37±0.42	0.99±0.00	0.05±0.02	78.23±0.21
Halimeda opuntia	SMB-S39-31 (green lobes)	0.71±0.01	14.42±3.08	0.05±0.01	0.49±0.11	0.02±0.01	31.23±9.79
	SMB-S39-31 (white lobes)	0.36±0.02	1.88±0.89	2.06±2.72	0.14±0.04	0.11±0.17	13.50±3.18
Acrosorium ciliolatum	SMB-S3-79	0.36±0.04	11.19±1.21	0.13±0.08	0.07±0.01	0.00±0.00	161.09±8.18
Dictyosphaeria cavernosa	SMB-S4-31	0.73±0.04	46.77±33.61	0.61±0.09	0.34±0.08	0.04±0.05	127.38±66.91
Udotea orientalis	NZB-S44-40	0.68±0.00	10.25±2.35	0.15±0.02	0.98±0.01	0.05±0.02	10.48±2.50
Ulva sp.	NZB-S44-40	0.67±0.05	28.84±10.46	0.06±0.10	0.54±0.39	0.03±0.01	79.95±54.51
Udotea orientalis	NZB-S43-44	0.73±0.01	5.53±0.67	0.17±0.02	0.99±0.00	0.06±0.01	5.58±0.68
Udotea palmetto	NZB-S43-44	0.75±0.00	25.75±7.84	0.31±0.10	0.48±0.27	0.15±0.22	64.24±6.56

macroloba, where rapid mass movement of chloroplasts occurs in newly formed fronds during the night, has been captured progressively by an Imaging-PAM (Larkum *et al*., 2011).

Variation in photo-physiology in the other seagrass and macroalgae studied

The other seagrass studied here, *Halophila decipiens*, and macroalgae, including *Acrosorium ciliolatum*, *Dictyosphaeria cavernosa*, *Ulva* sp., *Udotea orientalis*, and *Udotea palmetta* exhibited variable photo-physiological performances (Table 6). These could be potentially used as baseline data for future works, though these measurements and chlorophyll fluorescence-derived parameters are relative values and may not be directly used for comparative purposes.

Conclusions

This is the first study to document the photo-physiology of two seagrass and seven macroalgal species from the Saya de Malha and Nazareth Banks, Mascarene Plateau. *Thalassodendron ciliatum* and *Caulerpa cupressoides* exhibited variable photo-physiology among their body parts and with depths. The photosynthetic activity increased in the leaf, decreased in the stem and was similar in the transit part between the leaf and the stem of *T. ciliatum* at 40 m compared to 29 m depth. Photo-physiological functioning of the leaf of *T. ciliatum* was optimal at 40 m. The photosynthetic performance of the frond of *C. cupressoides* was similar at 44 m but decreased at 79 m when compared to that at 29 m, while the stolon of *C. cupressoides* performed equally well at 79 m and better at 44 m compared to that at 29 m. The photosynthetic performance of the whitish lobes of *H. opuntia* at 31 m was poorer compared to the greenish ones. Variable photo-physiology among the other studied seagrass and macroalgae were also documented. These results provide a first insight into the plant part-, seawater depth- and colour-related photo-physiological performance of seaplants from the Mascarene Plateau. Future research on photo-physiology of other seagrass and macroalgal species from this region would further shed light on their photosynthetic features and their biological and ecological importance on the Mascarene Plateau.

Acknowledgments

We are grateful to the Food and Agriculture Organization (FAO) EAF-Nansen programme for supporting participation in the Indian Ocean Research Expedition 2018 (NORAD-FAO PROJECT GCP/INT/730/NOR) to the Saya de Malha and Nazareth Banks on board the "R/V Dr Fridtjof Nansen", the Department for Continental Shelf, Maritime Zones Administration & Exploration of Mauritius for co-leading and coordinating the scientific expedition, the Joint Management Commission for their support and assistance, the Ministry of Blue Economy, Marine Resources, Fisheries and Shipping for granting the permits for sampling and the University of Mauritius for logistic support. RB is thankful to the Mauritius Research and Innovation Council for funding (K0460 and K0461) studies on macroalgae of the Republic of Mauritius. We also acknowledge the support of our fellow participants on the expedition: OA Bergstad, D Bissessur, K Sauba, J Rama, P Coopen, Y Oozeeraully, S Seeboruth, A Audit-Manna, A Nicolas, N Reetoo, D Kuyper, G Gendron, A Souffre, S Hollanda, R Melanie, J Harlay, L Caussy, K Tabachnick, M Olsen and TM Ensrud. The authors are grateful to the anonymous reviewer/s for insightful comments that have significantly improved the manuscript.

References

Aguilera J, Bischof K, Karsten U, Hanelt D, Wiencke C (2002) Seasonal variation in ecophysiological patterns in macroalgae from an Arctic fjord. II. Pigment accumulation and biochemical defence systems against high light stress. Marine Biology 140 (6): 1087-1095

Beer S, Bjork M (2000) A comparison of photosynthetic rates measured by pulse amplitude modulated (PAM) fluorometry and O_2 evolution in two tropical seagrasses. Aquatic Botany 66: 69-73

Beer S, Larsson C, Poryan O, Axelsson L (2000) Photosynthetic rates of *Ulva* (Chlorophyta) measured by pulse amplitude modulated (PAM) fluorometry. European Journal of Phycology 35: 69-74

Beer S, Björk M, Gademann R, Ralph P (2001) Measurements of photosynthetic rates in seagrasses. In: Short FT, Coles R (eds) Global seagrass research methods. Elsevier Publishing, The Netherlands. pp 183-198

Beer S, Axelsson L (2004) Limitations in the use of PAM fluorometry for measuring photosynthetic rates of macroalgae at high irradiance. European Journal Phycology 39 (1): 1-7

Bhagooli R, Mattan-Moorgawa S, Kaullysing D, Louis YD, Gopeechund A, Ramah S, Soondur M, Pilly SS, Beesoo R, Wijayawanti DP, Bachok ZB, Monrás VC, Casareto BE, Suzuki Y, Baker AC (2021) Chlorophyll fluorescence - a tool to assess photosynthetic performance and stress photo-physiology in symbiotic marine invertebrates and seaplants. Marine Pollution Bulletin 165 [https://doi.org/10.1016/j.marpolbul.2021.112059]

Bilger W, Bjorkman O (1990) Role of the xanthophyll cycle in photoprotection elucidated by measurements of light-induced absorbance changes, fluorescence and photosynthesis in leaves of *Hedera canariensis*. Photosynthesis Research 25 (3): 173-185

Bischof K, Gómez I, Molis M, Hanelt D, Karsten U, Lüder U, Wiencke C (2006) Ultraviolet radiation shapes seaweed communities. In: Life in extreme environments. Springer, Dordrecht, Netherlands. pp 187-212 [https://doi.org/10.1007/978-1-4020-6285-8_12]

Cabaço S, Santos R, Duarte CM (2008) The impact of sediment burial and erosion on seagrasses: a review. Estuarine, Coastal and Shelf Science 79: 354-366

Campbell SJ, McKenzie LJ, Kerville SP, Bite´ JS (2007) Patterns in tropical seagrass photosynthesis in relation to light, depth and habitat. Estuarine, Coastal and Shelf Science 73: 551-562

Campbell SJ, Kerville SP, Short F (2008) Photosynthetic responses of subtidal seagrasses to a daily light cycle in Torres Strait: A comparative study. Continental Shelf Research 28 (16): 2275-2281

Chinese Herbs Healing (2020) Plastids in root of *Taeniophyllu*m. [https://www.chineseherbshealing.com/rain-forest/roots.html]

Chisholm JRM, Moulin P (2003) Stimulation of nitrogen fixation in refractory organic sediments by *Caulerpa taxifolia* (Chlorophyta). Limnology and Oceanography 48: 787-794

Cook CDK, Rutishauser R (2007) Podostemaceae. In: Kubitzki K (ed) Flowering plants · Eudicots. The families and genera of vascular plants, vol 9. Springer, Berlin, Heidelberg. [https://doi.org/10.1007/978-3-540-32219-1_40]

Davison IR, Pearson GA (1996) Stress tolerance in intertidal seaweeds. Journal of Phycology 32 (2): 197-211

Drew EA, Abel KM (1988) Studies on *Halimeda* II. Reproduction, particularly the seasonality of gametangia formation, in a number of species from the Great Barrier Reef Province. Coral Reefs 6: 207-218

Drew EA, Abel KM (1990) Studies on *Halimeda*. III. A daily cycle of chloroplast migration within segments. Botanica Marina 33: 31-45

Drew EA, Abel KM (1992) Studies on *Halimeda.* IV. An endogenous rhythm of chloroplast migration in the siphonous green alga, *H. distorta*. Journal of Interdisiplinary Cycle Research 23 (2): 128-135

Driscoll MD (2004) Effects of hydrodynamic regime on photosynthesis in the green alga *Caulerpa*. Graduate Theses and Dissertations. University of South Florida. 87 pp

Durako MJ, Kunzelman JI (2002) Photosynthetic characteristics of *Thalassia testudinum* Banks ex König measured *in situ* by pulse amplitude modulated (PAM). Aquatic Botany 73: 173-185

Fonseca MS, Kenworthy WJ (1987) Effects of current on photosynthesis and distribution of seagrasses. Aquatic Botany 27: 59-78

Fredericq S, Freshwater D W, Hommersand MH (1999) Observations on the phylogenetic systematics and biogeography of the Solieriaceae (Gigartinales, Rhodophyta) inferred from rbcL sequences and morphological evidence. Hydrobiologia 398/399: 25-38

Genty B, Briantais J-M, Baker NR (1989) The relationship between the quantum yield of photosynthetic electron transport and quenching of chlorophyll fluorescence. Biochimica et Biophysica Acta 990 (1): 87-92

Glasby TM, Gibson PT, Kay S (2005) Tolerance of the invasive marine alga *Caulerpa taxifolia* to burial by sediment. Aquatic Botany 82: 71-81

Grable AR (1966) Soil aeration and plant growth. Advances in Agronomy 18: 57-106

Gullstrom M, de la Torre Castro M, Bandeira SO, Bjork M, Dahlberg M, Kautsky N, Ronnback P, Ohman MC (2002) Seagrass ecosystems in the Western Indian Ocean. Ambio 31 (7): 588-596

Hagan A, Robinson J (2001) Benthic habitats of the Saya de Malha Bank. Marine Science, training, and education in the western Indian Ocean. 30 Reefs, Symposium of the Zoological Society of London 28. pp 26-27

Hilbertz W, Goreau T (2002) Saya de Malha Expedition report. Lighthouse Foundation Project. 101 pp

Infantes E, Terrados J, Orfila A (2011) Assessment of substratum effect on the distribution of two invasive *Caulerpa* (Chlorophyta) species. Estuarine, Coastal and Shelf Science 91: 434-441

Ishimaru K, Kubota F, Saitou K, Nakayama M (1996) Photosynthetic response and carboxylation activity of enzymes in leaves and roots of water chestnut *Trapa bispinosa* Roxb. Journal of the Faculty of Agriculture, Kyushu University 41: 57-65

Klein J, Verlaque M (2008) The *Caulerpa racemosa* invasion: a critical review. Marine Pollution Bulletin 56: 205-225

Koch EW, Ackerman JD, Verduin J, van Keulen M (2006) Fluid dynamics in seagrass ecology - from molecules to ecosystems. In: Larkum AWD, Orth RJ, Duarte CM (eds) Seagrasses: Biology, ecology and conservation. Springer, Netherlands. pp 193-224

Larkum AWD, Salih A, Kuhl M (2011) Rapid mass movement of chloroplasts during segment formation of the calcifying siphonalean green alga, *Halimeda macroloba*. PLoS ONE 6 (7): e20841 [doi:10.1371/journal.pone.0020841]

Li W, Park J, Park SR, Zhang X, Lee K (2010) Chlorophyll a fluorescence as an indicator of establishment of *Zostera marina* transplants on the southern coast of Korea. Algae 25 (2): 89-97

Li XM, Zhang QS, Tang YZ, Yu YQ, Liu HL, Li LX (2014) Highly efficient photoprotective responses to high light stress in *Sargassum thunbergii* germlings, a representative brown macroalga of intertidal zone. Journal of Sea Research 85: 491-498

Major KM, Dunton KH (2000) Photosynthetic performance in *Syringodium filiforme*: seasonal variation in light-harvesting characteristics. Aquatic Botany 68: 249-264

Milchakova NA, Phillips RC, Ryabogina VG (2005) New data on the locations of seagrass species in the Indian Ocean. National Museum of Natural History Smithsonian Institution. Washington, DC, USA. Atoll Research Bulletin 537: 178-187

Olesen B, Enríquez S, Duarte CM, Sand-Jensen K (2002) Depth acclimation of photosynthesis, morphology and demography of *Posidonia oceanica* and *Cymodocea nodosa* in the Spanish Mediterranean Sea. Marine Ecology Progress Series 236: 89-97

Oliveira EC, Osterlund K, Mtolera MSP (2005) In: Sporrong N, Bjork M (eds) Marine plants of Tanzania. A field guide to the seaweeds and seagrasses. Botany Department, Stockholm University, Sweden. 267 pp

Olsen YS, Bessey C, McLaughlin J, Keesing J (2017) 2017 Annual Report: Patterns in primary producers, herbivory and reef metabolism around Browse Island. Australian Institute of Marine Science and Shell Development (Australia) Pty Ltd (Shell) and INPEX Operations Australia Pty Ltd. Shell/INPEX ARP7-2 Milestone 2017 Report #2. 69 pp

Piazzi L, Balata D, Ceccherelli G, Cinelli F (2005) Interactive effect of sedimentation and *Caulerpa racemosa* var. cylindracea invasion on macroalgal assemblages in the Mediterranean Sea. Estuarine, Coastal and Shelf Science 64: 467-474

Platt T, Galleoos CL, Harrison WG (1980) Photoinhibition of photosynthesis in natural assemblages of marine photoplankton. Journal of Marine Research 38: 687-701

Ralph PJ (1999) Light-induced photoinhibitory stress responses of laboratory-cultured *Halophila ovalis*. Botanica Marina 42 (1): 11-22

Ralph PJ, Gademann R (2005) Rapid light curves: a powerful tool for the assessment of photosynthetic activity. Aquatic Botany 82: 222-237

Rich SM, Ludwig M, Colmer TD (2008) Photosynthesis in aquatic adventitious roots of the halophytic stem-succulent *Tecticornia pergranulata* (formerly *Halosarcia pergranulata*). Plant, Cell and Environment 31: 1007-1016

Riis T, Hawes I (2003) Effect of wave exposure on vegetation abundance, richness and depth distribution of shallow water plants in a New Zealand lake. Freshwater Biology 48: 75-87

Schagerl M, Möstl M (2011) Drought stress, rain and recovery of the intertidal seaweed *Fucus spiralis*. Marine Biology 158 (11): 2471-2479

Serôdio J, Vieira S, Cruz S, Coelho H (2007) Rapid light-response curves of chlorophyll fluorescence in microalgae: relationship to steady-state light curves and non-photochemical quenching in benthic diatom-dominated assemblages. Photosynthesis Research 90 (1): 29-43

Taylor WR (1960) Marine algae of the eastern tropical and subtropical coasts of the Americas. University of Michigan Press, Ann Arbor. 870 pp

Thibaut T, Meinesz A, Coquillard P (2004) Biomass seasonality of *Caulerpa taxifolia* in the Mediterranean sea. Aquatic Botany 80: 291-297

van De Poll WH, Eggert A, Buma AGJ, Breeman AM (2001) Effects of UV-B-induced DNA damage and photoinhibition on growth of temperate marine red macrophytes: habitat-related differences in UV-B tolerance. Journal of Phycology 37 (1): 30-38

Vortsepneva E (2008) Saya de Malha Bank – an invisible island in the Indian Ocean. Geomorphology, Oceanology, Biology. Moscow State University, Moscow, Russia. 44 pp

Photo-physiology of healthy and bleached corals from the Mascarene Plateau

Ranjeet Bhagooli[1,2,3,4]*, Mouneshwar Soondur[1,2], Sundy Ramah[1,5], Arvind Gopeechund[1,2], Sruti Jeetun[1,2], Deepeeka Kaullysing[1,2]

[1] Department of Biosciences and Ocean Studies, Faculty of Science & Pole of Research Excellence in Sustainable Marine Biodiversity, University of Mauritius, Réduit 80837, Republic of Mauritius

[2] The Biodiversity and Environment Institute, Réduit, Republic of Mauritius

[3] Institute of Oceanography and Environment (INOS), University Malaysia Terengganu, 21030 Kuala Terengganu, Terengganu, Malaysia

[4] The Society of Biology (Mauritius), Réduit, Republic of Mauritius

[5] Albion Fisheries Research Centre, Ministry of Blue Economy, Marine Resources, Fisheries & Shipping, Albion, Petite Rivière 91001, Republic of Mauritius

* Corresponding author: r.bhagooli@uom.ac.mu

Abstract

This study presents the first report of variable photo-physiology of healthy-looking and bleached corals from the upper mesophotic waters of the Mascarene Plateau. In May 2018, during the FAO EAF-Nansen research expedition cruise, coral bleaching was visually observed. Five coral species from Saya de Malha Bank, namely *Heliopora coerulea, Favites* sp. and *Porites* sp. from 27 m and *Acropora* sp. and *Lithophyllon repanda* from 30 m, and three coral species from the Nazareth Bank, namely *Acropora* sp. and *Galaxea fascicularis* from 36 m and *Stylophora*-like species from 58 m were studied using the Video-Assisted Multi-Sampler (VAMS) and collected using a Van Veen grab. Chlorophyll *a* fluorescence parameters such as effective quantum yield at photosystem II (Φ_{PSII}), relative maximum electron transport rate ($rETR_m$), photosynthetic efficiency (α), photoinhibition (β), saturating light level (E_k), and maximum non-photochemical quenching (NPQ_m) were measured using a Diving-Pulse-Amplitude-Modulated (D-PAM) fluorometer to study variable photo-physiology in bleached and non-bleached corals. All photo-physiological parameters varied significantly among coral species tested and between coral conditions, except for β. The interaction between species and coral conditions was only significant in the case of β, but generally not significant. A two-way ANOVA indicated significant effects of depth and coral conditions in *Acropora* sp. on almost all photo-physiological parameters, except for β, and the effect of depth on $rETR_{max}$ and α, and the effect of depth along with its interaction with coral conditions on E_k. Φ_{PSII} did not differ in bleached and healthy-looking coral parts of *Porites* and *Lithophyllon* from 27 m, *Galaxea* and *Acropora* from 36 m while it decreased significantly in *Heliopora* and *Favites* at 27 m, *Acropora* from 30 m, and *Stylophora*-like at 58 m. NPQ_m did not change for *Porites*, *Acropora* (30 m) and *Galaxea* but it tended to increase for *Heliopora*, *Acropora* (36 m), *Lithophyllon*, *Galaxea*, and decrease for *Favities*, *Acropora* (30 m) and *Stylophora*-like. The thermally tolerant coral *Porites* exhibited normal photo-physiology even in bleached conditions while the bleached parts of *Favites*, *Acropora* (30 m) and *Stylophora*-like corals exhibited photo-physiological dysfunctioning. This study revealed that the seven studied corals from the upper mesophotic waters of the Mascarene Plateau are not spared from the bleaching phenomenon and exhibit variable photo-physiology in bleached and non-bleached conditions. Further studies are warranted to thoroughly understand the coral bleaching patterns and severity during summer periods at the Saya de Malha and Nazareth Banks.

Keywords: coral bleaching, Nazareth, PAM, photo-physiology, Saya de Malha, VAMS

http://dx.doi.org/10.4314/wiojms.si2021.2.8

Introduction

Coral bleaching has become more frequent and severe worldwide (Hoegh-Gulberg *et al*. 1999; Hughes *et al*. 2018) with variable impacts on reefs (Darling *et al*., 2019). Coral bleaching events have not spared the Western Indian Ocean region (Obura *et al*. 2017) including the Islands of the Mascarene Plateau (Bhagooli and Taleb-Hossenkhan, 2012; Mattan-Moorgawa *et al*., 2012, 2018; Bhagooli and Kaullysing, 2019; McClanahan and Muthiga, 2020). Under environmentally stressful conditions, mainly elevated sea temperature and high solar irradiance, corals bleach, whereby they lose either their symbiotic zooxanthellae (Hoegh-Guldberg and Smith, 1989; Brown, 1997; Le Tissier and Brown, 1996) or their photosynthetic pigments, or both (Kleppel *et al*. 1989), and appear white. If corals do not regain their symbiont-associated pigmentation in due course, they succumb. Sea surface temperature-based models indicate that some reefs would suffer from "local extinctions" (Sheppard, 2003; Bhagooli and Sheppard, 2012).

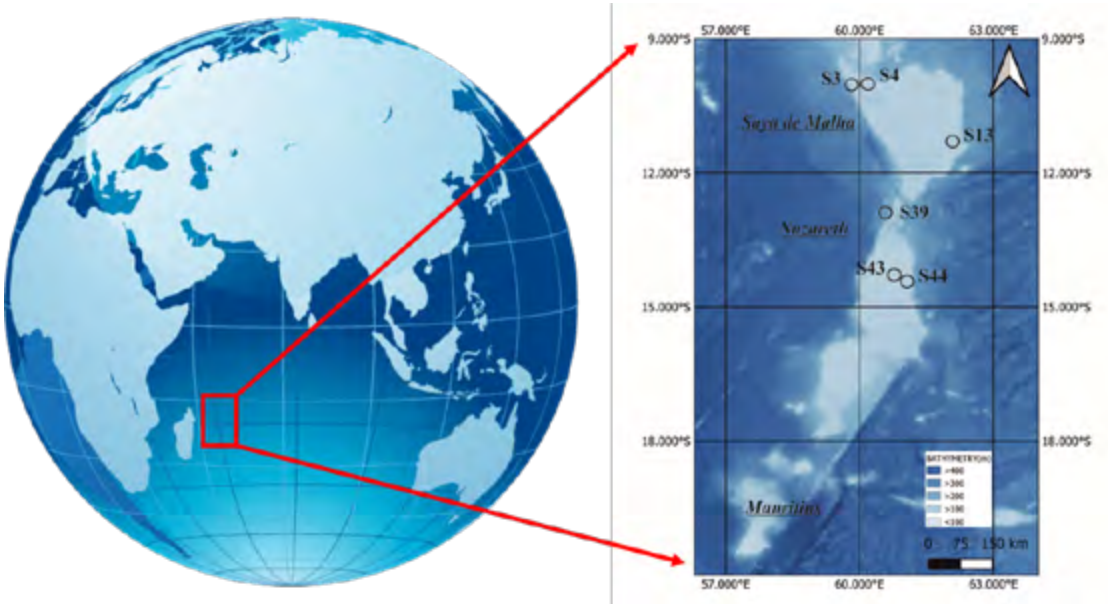

Figure 1. A. Mascarene Plateau on the global map. B. Map of Mascarene Plateau indicating the sampling locations for corals at Saya de Malha (S4 and S39) and Nazareth Banks (S44 and S47).

Several studies have suggested that damage to the zooxanthellar photosynthetic apparatus and/or its repair (Jones *et al*., 1998; Warner *et al*. 1999; Takahashi *et al*., 2004; Bhagooli, 2013) is implicated in the bleaching process. This has led to the increased use of chlorophyll *a* fluorescence techniques to study the normal and stress photo-physiology of the endosymbiont dinoflagellates, commonly called zooxanthellae, in corals (Bhagooli *et al*., 2021). Several studies have indicated that different zooxanthellae species (LaJeunesse *et al*., 2018) have variable photo-physiological thermal tolerance (Rowan, 2004; Sampayo *et al*., 2008). However, other studies have shown that thermal bleaching may occur without thermally-induced dysfunctioning of the photosystem II as photosynthetically competent zooxanthellae are released under stress (Ralph *et al*., 2001; Bhagooli and Hidaka, 2004). Observations of photosynthetic functioning of zooxanthellae indicated a decline in photochemical efficiency in some stressed corals (Rodrigues *et al*., 2008) and variable changes for some corals in the field (Mattan-Moorgawa *et al*., 2012, 2018). These stress photo-physiological studies have focused mostly on shallow-water corals while the thermal stress photo-physiology of deep water corals is not well documented.

Ample evidence documenting differential bleaching patterns among coral taxa (Marshall and Baird, 2000; Loya *et al*., 2001; Bhagooli and Yakovleva, 2004; Mattan-Moorgawa *et al*., 2012) and depths (Glynn, 1996; Lesser, 2009; Bongaerts *et al*., 2010; Muir *et al*., 2017) exist. However, with increasing frequency and severity of coral bleaching events recently, it appears that coral genera that were previously tolerant and/or resilient to bleaching in both shallow and deep waters may become vulnerable to increasing thermal anomaly severity

(McClanahan and Muthiga, 2020), and deep water mesophotic coral ecosystems from the Caribbean and Great Barrier Reef, for example, may not act as potential climate refugia (Smith *et al*., 2016; Frade *et al*., 2018). Though Frade *et al*. (2018) documented variable bleaching susceptibilities among deep water coral species, their stress photo-physiology is almost unchartered.

This study, therefore, aimed at a snap-shot investigation of the variable photo-physiological performance, using a Diving-Pulse Amplitude Modulated (D-PAM) fluorometer, in seven coral species collected from the upper mesophotic waters of the Saya de Malha and Nazareth Banks on the Mascarene Plateau, Western Indian Ocean, a region that has been very poorly studied. The objectives were to 1) qualitatively observe bleaching in corals, and 2) assess the photo-physiological performance of i) healthy-looking corals, and ii) their conspecific bleached corals from depths >25 m at the Saya de Malha and Nazareth Banks.

Methodology

Sample collection from studied locations

The studied locations were within the Saya de Malha Bank, an area jointly managed by the Republic of Mauritius and Seychelles, and the Nazareth Bank, which is within the Exclusive Economic Zone of the Republic of Mauritius. The samples of the symbiotic cnidaria were collected using the van Veen grabs on the VAMS at station S4 at Saya de Malha Bank on 8th May 2018 at a depth of 27 m, and at S39 at Nazareth Bank on 22nd May 2018 at a depth of 30 m. At the Nazareth Bank, stations included S44 at a depth of 36 m and S47 at a depth of 58 m and collection was carried out on 27th May 2018 (Fig. 1). Live coral samples were preliminarily identified on the research vessel and used for photo-physiological studies onboard. Chlorophyll fluorescence measurements were conducted between 09:00 and 14:00 hrs at the studied locations. Samples were frozen at -20 °C for further detailed identification at a later stage.

Coral morphological identification

Corals (cnidarian) were collected and preliminarily identified onboard. After close-up pictures were taken, samples were frozen at -20°C for later laboratory identification. Advanced identification of corals was done using skeletal morphological methods such as light and scanning electron microscopy (SEM). Corals were identified from external morphologies using Corals of the World (Veron, 2000) and relevant papers documenting scanning electron micrographs.

For SEM analyses, the coral samples were treated with 10 % sodium hypochlorite, washed with water, and air-dried prior to SEM. The coral fragments were cut into smaller pieces to fit on the SEM stub. The coral samples were mounted on the stub using carbon tape and sputter coated with a thin layer of gold/platinum. SEM observations were performed with a Vega Tescan microscope (Stefani *et al*., 2011).

Photo-physiology of corals – Chlorophyll *a* fluorescence measurement

The Diving-PAM fluorometer (Submersible Photosynthesis Yield Analyzer, Walz, Germany) was used to assess the photo-physiology of collected corals by measuring, in triplicates, the fluorescence of chlorophyll *a* on-board the ship immediately after collection. In a non-dark-adapted sample, the initial fluorescence (F) and the maximal fluorescence (F_m') were measured by applying pulses of weak red light (< 1 µmol quanta m^{-2} s^{-1}) and a saturating pulse (4000 µmol quanta m^{-2} s^{-1}, 0.8 s duration), respectively. The ratio of the change in fluorescence ($\Delta F = F_m' - F$) caused by the saturating pulse to the maximal fluorescence (F_m'), in a light adapted sample can be considered as a proxy for the effective maximum quantum yield of the photosystem II (PSII) (Genty *et al*., 1989). The chlorophyll fluorescence parameters included the effective quantum yield ($\Delta F/F_m'$, Φ_{PSII}), the relative electron transport rate (rETR) and non-photochemical quenching (NPQ) when exposed to a series of rapidly (10 s) changing light climates (Rapid Light Curves, RLCs) (Ralph *et al*. 1999; Bhagooli and Yakovleva, 2004). The irradiance levels were 0, 110, 150, 300, 400, 500, 800, 1000 and 1325 µmol quanta m^{-2} s^{-1}. Using the RLCs the rETR and NPQ were estimated at each irradiance.

At each irradiance, the respective relative electron transport rate (rETR) was calculated as the product of 0.5 x Φ_{PSII} x PAR, where PAR is the photosynthetically active radiance. Non-photochemical quenching (NPQ), determined by the ratio of F_m-F_m' to F_m', is the process by which oxygenic photoautotrophs harmlessly dissipate excess light absorbed as heat and fluorescence. When light energy absorption exceeds the capacity for utilization, there is a need to dissipate the energy to protect the light harvesting structures from photo-oxidative damage. The maximum rETR and NPQ were determined using sigma plots (Platt and Jassby, 1976). The initial slope of the light curve prior to the onset of saturation (α) and the slope of the light curve beyond the onset of photo-inhibition (β), representing the light-use efficiency and photo-inhibitory

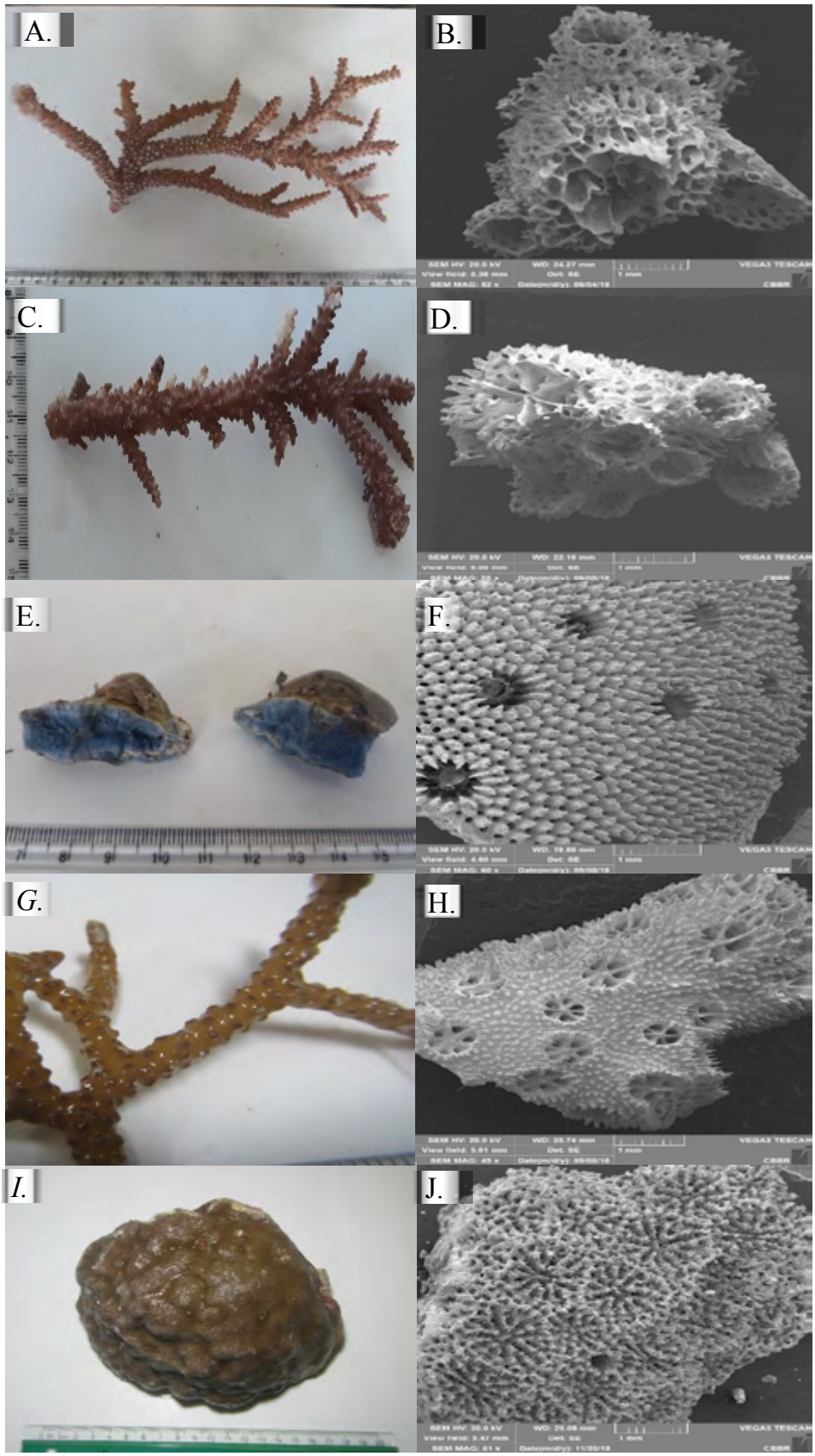

Figure 2. Fragments and scanning electron micrographs of the studied corals from Saya de Malha (SMB) and Nazareth (NB) Banks. A and B – *Acropora* sp. from SMB; C and D – *Acropora* sp. from NB; E and F – *Heliopora coerulea* from SMB; G and H – *Stylophora*-like sp. from NB; and I and J – *Porites* sp. from SMB.

factors, respectively, were determined through curve fitting of the RLC. The E_k was calculated as $rETR_{max}/\alpha$ and represents the minimum saturating irradiance. Chlorophyll fluorescence measurements were done in three replicates (n=3). Based on visual observations prior to chlorophyll fluorescence measurements, corals were grouped into three categories: healthy-looking; bleached (whitish); and pale (intermediate between the former two). Not all coral species studied could be categorised into all three conditions and thus some had data collection for only two categories.

Statistical analyses

Φ_{PSII}, $rETR_m$, NPQ_{max}, α, β, and E_k were statistically analysed using the software PASW Statistics 18. The data was expressed as mean±SD from three replicates (n=3). The raw data was Arcsine square root transformed prior to ANOVA tests. The two-way ANOVA was employed to test the effect of species and coral conditions in seven coral species. Since *Acropora* sp. were found at two depths (30 m and 36 m) the two-way ANOVA was run twice: 1) with *Acropora* sp. from 30 m; and 2) with *Acropora* sp. from 36 m. A separate two-way ANOVA was conducted to test for the effects of depths and coral condition in *Acropora* sp. The Tukey post hoc significance difference test was used for multiple comparison of means at $P<0.05$.

Results and discussion

Coral identification

At Saya de Malha Bank, the corals at S4 included *Heliopora coerulea*, *Favites* sp., and *Porites* sp. from a depth of 27 m, while at S39, *Acropora* sp. and *Lithophyllon repanda* were recorded from a depth of 30 m. At Nazareth Bank, the corals recorded at S44 from a depth of 36 m were *Acropora* sp. and *Galaxea fascicularis*, and at S47 *Stylophora-like* sp. From the colony and fragment morphologies, and scanning electron micrographs, the same *Acropora* sp. was observed at both Saya de Malha S39 (Fig. 2A, B) and Nazareth S44 (Fig. 2C, D). *H. coerulea* at S4 was confirmed through their colony and fragment morphologies, and scanning electron micrograph (Fig. 2E, F). At S47, the colony/fragment morphologies and the SEM analysis revealed a *Stylophora*-like sp. (Fig. 2G, H). At S4, the massive coral was confirmed to be a *Porites* sp. based on the colony morphology and scanning

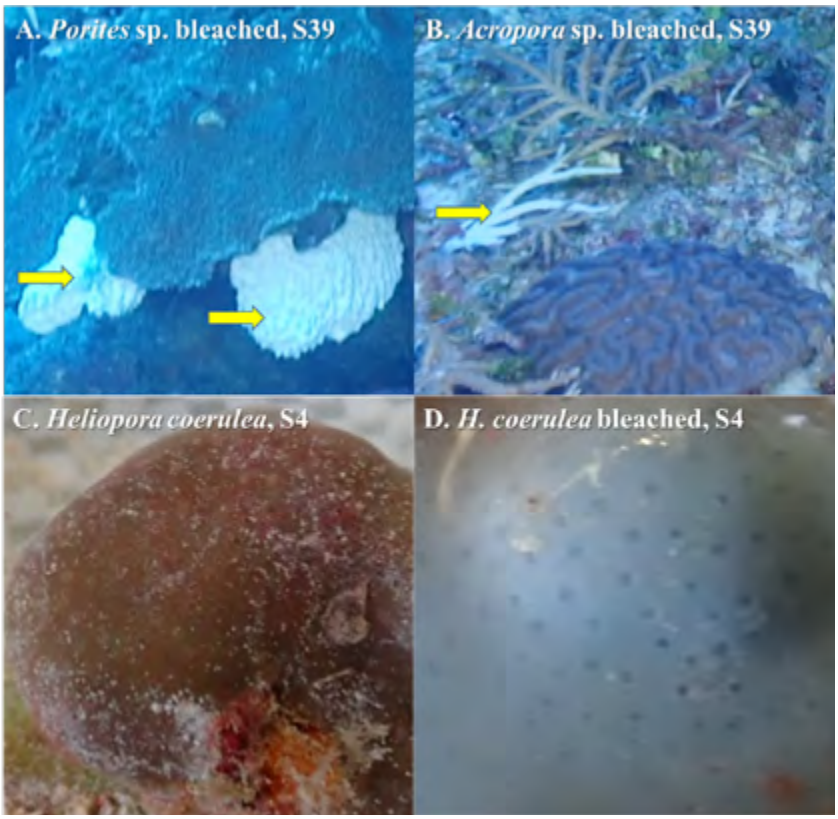

Figure 3. Healthy-looking and bleached conditions of corals. A. *Porites* sp. (EAF-Nansen, 2018), and B. *Acropora* sp. healthy and bleached colonies observed via the VAMS in the field at study location S39 at Saya de Malha (EAF-Nansen, 2018). The yellow arrows indicate the bleached corals in the field; C. Healthy and D. Bleached *Heliopora coerulea* post-collection observation following sampling from S4 at Saya de Malha.

micrograph (Fig. 2I, J). The morphology of the *Acropora*, *Stylophora*-like and *Porites* species looks quite different from their genera reported around Mauritius (Moothien-Pillay *et al*. 2002; Bhagooli *et al*. 2017) and Rodrigues (Fenner *et al*., 2004), though these reports did not use SEM. The SEM analyses done in this study indicated clear fine micro-level details in these coral specimens, but they could not be identified clearly at the species level. Further molecular level identification work is required to be able to reveal the species level identity of these specimens.

Field- and post-collection observed bleaching conditions

The VAMS used in the study allowed for qualitative observations. Several coral colonies belonging to the genera *Porites* (Fig. 3A) and *Acropora* (Fig. 3B) could be observed *in situ* through the videos of the VAMS. Post-collection, the grabs attached and operated through the VAMS provided samples of *Heliopora* (Fig 3C, D), *Porites*, *Acropora*, *Galaxea fascicularis*, *Lithophyllon repanda, and Stylophora*-like species in healthy and bleached-conditions. Variable levels of bleaching

Table 1. Two-way ANOVA for the effect of species (*Heliopora coerulea, Favites* sp., *Porites* sp., *Acropora* sp., *Lithophyllon repanda*, *Galaxea fascicularis* and *Stylophora*-like species) and coral condition (healthy-looking and bleached) on photo-physiological features of test corals. Since *Acropora* sp. was found at 30 m and 36 m, the ANOVA test was run with *Acropora*-30m and *Acropora*-36m, separately. Asterisks (***) represent significant differences at *P<0.001*.

	Parameters	Source of Variation	SS	df	MS	F	P-value
With *Acropora* at 30 m	Φ_{PSII}	Species	0.702	6	0.117	17.675	0.000***
		Condition	0.234	1	0.234	35.394	0.000***
		Species x Condition	0.290	6	0.048	7.303	0.000***
	$rETR_m$	Species	0.070	6	0.012	35.601	0.000***
		Condition	0.062	1	0.062	190.857	0.000***
		Species x Condition	0.021	6	0.004	10.893	0.000***
	NPQ_{max}	Species	0.060	6	0.010	18.997	0.000***
		Condition	0.056	1	0.056	106.523	0.000***
		Species x Condition	0.033	6	0.005	10.254	0.000***
	α	Species	0.322	6	0.054	13.077	0.000***
		Condition	0.198	1	0.198	48.179	0.000***
		Species x Condition	0.252	6	0.042	10.221	0.000***
	β	Species	0.140	6	0.023	9.033	0.000***
		Condition	0.000	1	0.000	0.082	0.777
		Species x Condition	0.033	6	0.006	2.136	0.080
	E_k	Species	0.292	6	0.049	24.453	0.000***
		Condition	0.042	1	0.042	21.199	0.000***
		Species x Condition	0.112	6	0.019	9.368	0.000***
With *Acropora* at 36 m	Φ_{PSII}	Species	0.774	6	0.129	19.928	0.000***
		Condition	0.181	1	0.181	27.896	0.000***
		Species x Condition	0.320	6	0.053	8.230	0.000***
	$rETR_m$	Species	0.071	6	0.012	35.778	0.000***
		Condition	0.057	1	0.057	172.034	0.000***
		Species x Condition	0.020	6	0.003	10.188	0.000***
	NPQ_{max}	Species	0.103	6	0.017	32.238	0.000***
		Condition	0.044	1	0.044	82.959	0.000***
		Species x Condition	0.024	6	0.004	7.669	0.000***
	α	Species	0.370	6	0.062	13.728	0.000***
		Condition	0.186	1	0.186	41.487	0.000***
		Species x Condition	0.253	6	0.042	9.378	0.000***
	β	Species	0.173	6	0.029	10.257	0.000***
		Condition	0.001	1	0.001	0.185	0.670
		Species x Condition	0.034	6	0.006	2.029	0.095
	E_k	Species	0.294	6	0.049	24.929	0.000***
		Condition	0.035	1	0.035	18.012	0.000***
		Species x Condition	0.106	6	0.018	8.973	0.000***

were observed in these coral species but no quantitative assessments were undertaken. It is noteworthy that in other shallow-water locations of the Mascarene Plateau, both intra- and inter-species variable bleaching observations have been made; for example by Hilbertz and Goreau (2002) at the Ritchie Bank of the northern Saya de Malha, Bhagooli and Taleb-Hossenkhan (2012), Mattan-Moorgawa *et al*. (2012, 2018) and McClanahan and Muthiga (2020) around Mauritius Island, and Hardman *et al*. (2004, 2008) around Rodrigues Island. These studies in general indicated that *Porites* and *Galaxea* are more tolerant to bleaching than some *Acropora* species. The present study, for the first time, reports qualitative bleaching observations from the Mascarene Plateau at depths of 27 and 36 m. Further quantitative studies on bleaching vulnerability observations in the Saya de Malha and Nazareth Banks are necessary to understand the bleaching status of corals on the Mascarene Plateau.

Photo-physiological performance of healthy-looking and bleached corals

All photo-physiological parameters varied significantly among coral species tested and between coral conditions, except for β, irrespective of the analysis including *Acropora* sp. from 30 m or 36 m (Table 1). The interaction between species and coral condition was not significant; only in the case of β. The two-way ANOVA indicated significant effects of depth and coral condition in *Acropora* sp. on almost all photo-physiological parameters, except for β, and the effect of depth on $rETR_{max}$ and α, and the effects of depth along with its interaction with coral condition on E_k (Table 2).

The effective quantum yield at PSII did not differ in bleached and healthy samples for *Porites* and *Lithophyllon* from 27 m, *Galaxea* and *Acropora* from 36 m, while it decreased significantly in *Heliopora* ($P<0.05$) and *Favites* ($P<0.01$) at 27 m, *Acropora* ($P<0.001$) from 30 m, and *Stylophora*-like ($P<0.001$) at 58 m (Fig. 4A). $rETR_m$ decreased ($P<0.05$) or tended to decrease in all bleached species except for *Porites* where it tended to increase (Fig. 4B). NPQ_m did not change ($P>0.05$) for *Porites*, *Acropora* (30 m) and *Galaxea*, while it tended to increase for *Heliopora*, *Acropora* (36 m) ($P<0.05$), *Lithophyllon*, *Galaxea*, and decrease for *Favities*, *Acropora* (30 m), *Stylophora*-like ($P<0.05$), respectively (Fig. 4C). Usually, under thermal stress conditions, there is a tendency for effective yield at PSII and $rETR_m$ to decrease and NPQ_m to increase as a sign of coping with thermal stress, and a decrease in all these parameters indicates damage to the photosynthetic apparatus of the zooxanthellae in the corals. The thermally tolerant coral, *Porites*, exhibited no change in PSII effective yield and NPQ_m and a tendency to have an increased $rETR_m$ in bleached conditions, which is in accordance with Bhagooli and Yakovleva (2004). Conversely, *Favites, Acropora* (30 m) and *Stylophora*-like corals showed a clear decrease in effective yield at PSII, $rETR_m$ and NPQ_m suggesting some level of damage to

Table 2. Two-way ANOVA for the effect of depth (30 m and 36 m) and coral condition (healthy-looking and bleached) on photo-physiological features of *Acropora* sp. Asterisks ***, ** and * represent significant differences at *P<0.001, P<0.01* and *P<0.05*, respectively.

Parameters	Source of Variation	SS	df	MS	F	P-value
Φ_{PSII}	Depth	0.021	1	0.021	25.012	0.001**
	Condition	0.012	1	0.012	14.649	0.005**
	Depth x Condition	0.012	1	0.012	14.886	0.005**
$rETR_m$	Depth	0.001	1	0.001	10.017	0.013*
	Condition	0.025	1	0.025	250.848	0.000***
	Depth x Condition	0.000	1	0.000	4.560	0.065
NPQ_{max}	Depth	0.012	1	0.024	59.341	0.000***
	Condition	0.046	1	0.039	97.033	0.000***
	Depth x Condition	0.001	1	0.003	6.460	0.035*
α	Depth	0.007	1	0.012	5.682	0.044*
	Condition	0.002	1	0.046	21.931	0.002**
	Depth x Condition	0.000	1	0.001	0.285	0.608
b	Depth	0.007	1	0.007	1.269	0.293
	Condition	0.002	1	0.002	0.333	0.580
	Depth x Condition	0.000	1	0.000	0.042	0.843
E_k	Depth	0.000	1	0.000	0.012	0.916
	Condition	0.040	1	0.040	27.522	0.001**
	Depth x Condition	0.001	1	0.001	0.725	0.419

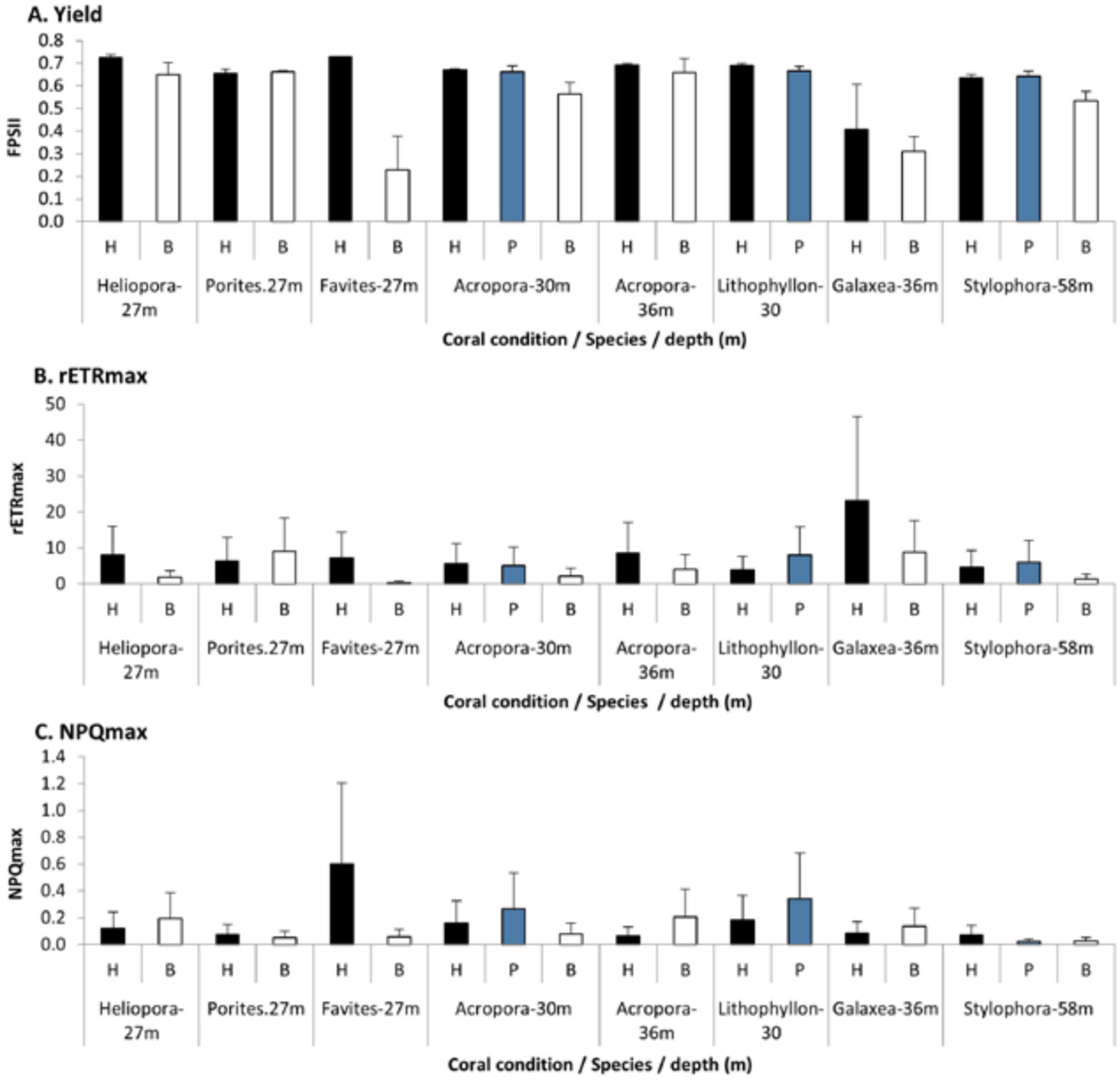

Figure 4. Photo-physiological parameters of healthy-looking and bleached parts of corals. A. Effective quantum yield at PSII (Φ_{PSII}); B. Maximum relative electron transport rate ($rETR_m$); and C. Maximum non-photochemical quenching (NPQ_{max}). H-Healthy-looking, P-Pale, and B-bleached. Bars represent Mean±SD (n=3).

the photosynthetic capacity of their symbiotic zooxanthellae. The other studied corals showed variable responses in these tested chlorophyll fluorescence parameters. These findings indicate that *Porites* symbionts may be photosynthetically thermally tolerant but still bleach to a certain degree, while *Favites*, *Acropora* (30 m) and *Stylophora*-like symbionts are photosynthetically thermally susceptible and bleach. It is noteworthy that Ralph *et al*. (2001) and Bhagooli and Hidaka (2004) showed that photosynthetically competent symbionts were released when corals like *Galaxea fascicularis* and *Pocillopora damicornis* were exposed to elevated temperature. Other studies have proposed that the photosynthetic machinery of the symbionts broke down or their repair mechanisms are affected and thus corals bleached (Jones *et al*., 1998; Warner *et al*., 1999; Takahashi *et al*., 2004; Bhagooli, 2013). Mattan-Moorgawa *et al*. (2012) studied eight shallow-water coral species and indicated a decline in PSII activity of four bleached corals that are usually susceptible to thermal bleaching, and out of the four thermally tolerant corals only pale *Pocillopora* and *Galaxea* showed a declining tendency in their PSII activities.

The E_k tended to decrease in bleached samples in most studied corals, except for *Galaxea* and *Stylophora*-like

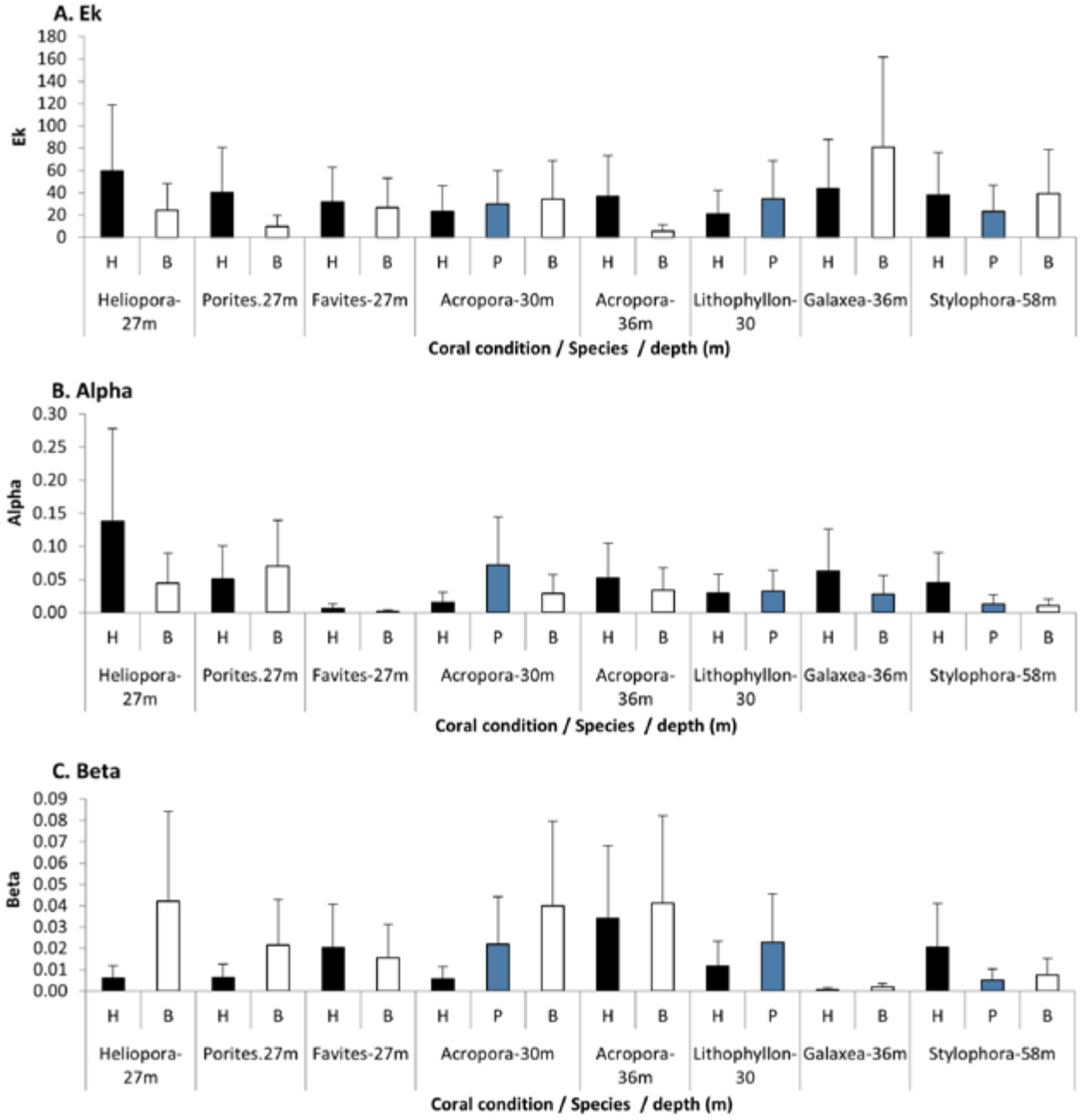

Figure 5. Photo-physiological parameters of healthy-looking and bleached parts of corals. A. Alpha (α, initial slope of the light curve prior to onset of saturation); B. Beta (β, the slope of the light curve beyond the onset of photo-inhibition); and C. E_k (the minimum saturating irradiance). H-Healthy-looking, P-Pale, and B-bleached. Bars represent Mean±SD (n=3).

samples (Fig. 5A), implying a lowering of the light saturation level. Alpha declined in bleached samples of *Heliopora*, and *Stylophora*-like only (Fig. 5B), suggesting a decline in the slope of the photosynthetic rate. Beta increased in bleached samples of *Heliopora*, *Porites* and *Acropora*-30 m (Fig. 5C), indicating increased photo-inhibition of photosynthesis in the symbionts of these corals. These chlorophyll fluorescence parameters were variable and not many studies have used these parameters in studies on photosynthetic marine invertebrates, including corals, and sea plants (Bhagooli *et al*., 2021).

This is the first study to document *Stylophora*-like species at Nazareth Bank, and variable bleaching observations and their photo-physiological features in healthy and bleached conditions from both the Saya de Malha and Nazareth Banks. The qualitative field observations indicated that bleaching was readily spotted through the VAMS video for corals like *Porites*

and *Acropora*, while for other small-colony forming corals such as *Favites*, *Galaxea*, *Heliopora*, *Lythophyllon*, *Stylophora*-like, grab collections revealed their bleaching conditions. For the bleached conditions, the well-known thermally tolerant coral *Porites* exhibited normal photo-physiology, while *Favites*, *Acropora* (30 m) and *Stylophora*-like showed some level of photo-physiological dysfunctioning. The water temperatures were 27.5, 26.8, 27 and 26 °C at S4, S39, S44 and S47, respectively. These were snap-shot measurements available from the ROV and are inadequate for explaining the intra- and inter-species variability in bleaching susceptibility at these studied depths on the Mascarene Plateau. It is noteworthy that Frade *et al*. (2008) has reported that *Madracis* spp. from the southern Caribbean region exhibit depth-dependent photo-physiological features in some species. Additional vertical profiling data or depth-specific data of temperature and light intensity for longer periods during summer, as done by Frade *et al*. (2008, 2018), would be needed to appropriately determine the influence of these parameters on coral bleaching patterns and photo-physiological functioning of corals in this part of the world. Further detailed studies undertaken prior- and post-field bleaching events at the Banks along with a thermal stress experiment may provide insights into the photo-physiology of bleaching tolerance and susceptibility of these corals at Saya de Malha and Nazareth Banks. Additionally, determination of the symbiont genetic types will provide important information related to the bleaching vulnerabilities among these corals from the Mascarene Plateau.

Acknowledgments

The authors are grateful to the Food and Agriculture Organization (FAO) EAF-Nansen programme for supporting their participation in the Indian Ocean Research Expedition 2018 (NORAD-FAO PROJECT GCP/INT/730/NOR) in the Saya de Malha and Nazareth Banks on board the "R/V Dr Fridtjof Nansen", the Department for Continental Shelf, Maritime Zones Administration & Exploration of Mauritius for co-leading and coordinating the scientific expedition, the Joint Management Commission for their support and assistance, the Ministry of Blue Economy, Marine Resources, Fisheries and Shipping for granting the permits for sampling and the University of Mauritius for logistic support. RB and SJ are thankful to the Higher Education Commission for funding (T0721) studies on corals of the Republic of Mauritius. The authors also acknowledge the support of the participants, the cruise members and the VAMS technicians during the expedition. The authors are thankful to the anonymous reviewers for insightful comments that have improved the manuscript.

References

Bhagooli R, Hidaka M (2004) Release of zooxanthellae with intact photosynthetic activity by the coral *Galaxea fascicularis* in response to temperature stress. Marine Biology 145: 329-337

Bhagooli R, Yakovleva I (2004) Differential bleaching susceptibility and mortality patterns among four corals in response to thermal stress. Symbiosis 37: 121-136

Bhagooli R, Sheppard CCR (2012) Prediction of recurrences of mass coral bleaching / mortality and vulnerability of reef-building corals to climate change in Mauritian and Japanese waters. Sustainable Marine Environment, University of Mauritius Research Journal, Special Issue 18A: 105-121

Bhagooli R, Taleb-Hossenkhan N (2012) Thermal spatial heterogeneity and coral bleaching: implications for habitat refuges. Proceedings of the 12th International Coral Reef Symposium 2012. Cairns, Australia. 6 pp [http://www.icrs2012.com/proceedings/manuscripts/ICRS2012_9D_1.pdf]

Bhagooli R (2013) Inhibition of Calvin-Benson cycle suppresses the repair of photosystem II in *Symbiodinium*: Implications for coral bleaching. Hydrobiologia 714: 183-190

Bhagooli R, Ramah S, Kaullysing D, Mattan-Moorgawa S, Taleb-Hossenkhan N, Gopeechund A, Soondur M, Flot J-F (2017) Field observation of five *Stylophora pistillata*-like morphotypes near Mauritius Island. Western Indian Ocean Journal of Marine Science, Special Issue 1/ 2017: 51-53

Bhagooli R, Kaullysing D (2019) Seas of Mauritius – Chapter 12. In: Sheppard CCR (ed.) World seas: An environmental evaluation, 2nd edition, volume II: The Indian Ocean to the Pacific. Elsevier. Academic Press. pp 253-277 [Paperback ISBN: 9780081008539, 912p]

Bhagooli R, Mattan-Moorgawa S, Kaullysing D, Louis YD, Gopeechund A, Ramah S, Soondur M, Pilly SS, Beesoo R, Wijayawanti DP, Bachok ZB, Monrás VC, Casareto BE, Suzuki Y, Baker AC (2021) Chlorophyll fluorescence - a tool to assess photosynthetic performance and stress photo-physiology in symbiotic marine invertebrates and seaplants. Marine Pollution Bulletin. 165 [https://doi.org/10.1016/j.marpolbul.2021.112059]

Bongaerts P, Ridgway T, Sampayo EM, Hoegh-Guldberg O (2010) Assessing the 'deep reef refugia' hypothesis: focus on Caribbean reefs. Coral Reefs 29: 309-327

Brown BE (1997) Coral bleaching: causes and consequences. Coral Reefs 16, Suppl. S: 129-138

Darling, ES, McClanahan, TR, Maina, J *et al*. (77 more authors) (2019) Social–environmental drivers inform strategic management of coral reefs in the Anthropocene. Nature Ecology and Evolution 3: 1341-1350

Fenner D, Clark TH, Turner JR, Chapman B (2004) A checklist of the corals of the island state of Rodrigues, Mauritius. Journal of Natural History 38: 3091–3102

Frade PR, Bongaerts P, Winkelhagen AJS, Tonk L, Bak RPM (2008) *In situ* photobiology of corals over large depth ranges: A multivariate analysis on the roles of environment, host, and algal symbiont. Limnology and Oceanography 53 (6): 2711-2723

Frade PR, Bongaerts P, Englebert N, Rogers A, Gonzalez-Rivero M, Ove Hoegh-Guldberg O (2018) Deep reefs of the Great Barrier Reef offer limited thermal refuge during mass coral bleaching. Nature 9: 3447 [doi: 10.1038/s41467-018-05741-0]

Genty B, Briantais JM, Baker NR (1989) The relationship between the quantum yield of photosynthetic electron transport and quenching of chlorophyll fluorescence. Biochimica et Biophysica Acta 990: 87-92

Glynn PW (1996) Coral reef bleaching: facts, hypotheses and implications. Global Change Biology 2: 495-509

Hardman ER, Meunier MS, Turner JR, Lynch T, Taylor M, Klaus R (2004) The extent of coral bleaching in Rodrigues, 2002. Journal of Natural History 38: 3077-3089

Hardman ER, Thoma J, Stampfli NS, Desiré MS,Perrine S (2008) Small-scale variations in the effects of coral bleaching in Rodrigues. Proceedings of the 11th International Coral Reefs Symposium. pp 742-746

Hilbertz W, Goreau T (2002) Saya de Malha expedition, March 2002. 101 pp

Hoegh-Guldberg O, Smith GJ (1989) The effect of sudden changes in temperature, light and salinity on the population density and export of zooxanthellae from the reef corals *Stylophora pistillata* Esper and *Seriatopora hystrix* Dana. Journal of Experimental Marine Biology and Ecology 129: 279-303

Hoegh-Guldberg O (1999) Climate change: coral bleaching and the future of the world's coral reefs. Marine and Freshwater Research 50: 839-866

Hughes TP, Anderson KD, Connolly SR, Heron SF, Kerry JT, Lough JM, Baird AH, Baum JK, Berumen ML, Bridge TC, Claar DC (2018) Spatial and temporal patterns of mass bleaching of corals in the Anthropocene. Science 359: 80-83

Jones RJ, Hoegh-Guldberg O, Larkum AWD, Schreider U (1998) Temperature-induced bleaching of corals begins with impairment of the CO_2 fixation mechanism in zooxanthellae. Plant, Cell and Environment 21: 1219-1230

Kleppel GS, Dodge RE, Reese CJ (1989) Changes in pigmentation associated with the bleaching of stony corals. Limnology and Oceanography 34: 1331-1335

LaJeunesse TC, Parkinson JE, Gabrielson PW, Jeong HJ, Reimer JD, Voolstra CR, Santos SR (2018) Systematic revision of Symbiodiniaceae highlights the antiquity and diversity of coral endosymbionts. Current Biology 28: 2570-2580

Le Tissier MDA, Brown BE (1996) Dynamics of solar bleaching in the intertidal reef coral *Goniastrea aspera* at Ko Phuket, Thailand. Marine Ecology Progress Series 136: 235-244

Lesser MP, Slattery M, Leichter JJ (2009) Ecology of mesophotic coral reefs. Journal of Experimental Marine Biology and Ecology 375: 1-8

Loya Y, Sakai K, Yamazato K, Nakano J, Sambi H, van Woesik R (2001) Coral bleaching: the winners and the losers. Ecology Letters 4: 122-131

Marshall PA, Baird AH (2000) Bleaching of corals on the Great Barrier Reef: differential susceptibilities among taxa. Coral Reefs 19: 155-163

Mattan-Moorgawa S, Bhagooli R, Rughooputh SDDV (2012) Thermal stress physiology and mortality responses in scleractinian corals of Mauritius. Proceedings of the 12th International Coral Reef Symposium 2012. Cairns, Australia. 6pp [http://www.icrs2012.com/proceedings/manuscripts/ICRS2012_9A_6.pdf]

Mattan-Moorgawa S, Rughooputh SDDV, Bhagooli R (2018) Variable PSII functioning and bleaching conditions of tropical scleractinian corals pre-and post-bleaching event. Ocean Life 2: 1-10

McClanahan TR and Muthiga NA (2020) Oceanic patterns of thermal stress and coral community degradation on the island of Mauritius. Coral Reefs. [https://doi.org/10.1007/s00338-020-02015-4]

Moothien-Pillay R, Terashima H, Venkatasami, A, Uchida H (2002) Field guide to corals of Mauritius. Albion Fisheries Research Centre (AFRC), Japan International Cooperation Agency (JICA). 334 pp

Muir PR, Marshall PA, Abdulla A, Aguirre JD (2017) Species identity and depth predict bleaching severity in reef-building corals: shall the deep inherit the reef? Proceedings of the Royal Society B: Biological Sciences 284: 20171551

Obura DO, Gudka M, Abdou Rabi F, Bacha Gian S, Bigot L, Bijoux J, Freed S, Maharavo J, Munbodhe

V, Mwaura J, Porter S, Sola E, Wickel J, Yahya S, Ahamada S (2017) Coral reef status report for the Western Indian Ocean. Global Coral Reef Monitoring Network (GCRMN)/International Coral Reef Initiative (ICRI). 144 pp [https://www.icriforum.org/sites/default/files/COI%20REEF%20LR%20F2.compressed.pdf]

Platt T, Jassby AD (1976) The relationship between photosynthesis and light for natural assemblages of coastal marine phytoplankton. Journal of Phycology 12: 421-430

Ralph PJ, Larkum AWD, Gademann R, Schreiber U (1999) Photosynthetic responses of coral reef endosymbionts. Marine Ecology Progress Series 180: 139-147

Ralph PJ, Gademann R, Larkum AWD (2001) Zooxanthellae expelled from bleached corals at 33 °C are photosynthetically competent. Marine Ecology Progress Series 220: 163-168

Rodrigues LJ, Grottoli AG, Lesser MP (2008) Long-term changes in the chlorophyll fluorescence of bleached and recovering corals from Hawaii. Journal of Experimental Biology 211: 2502-2509

Rowan R (2004) Coral bleaching: thermal adaptation in reef coral symbionts. Nature 430: 742

Sampayo EM, Ridgway T, Bongaerts P, Hoegh-Guldberg O (2008) Bleaching susceptibility and mortality of corals are determined by fine-scale differences in symbiont type. Proceedings of the National Academy of Science USA 105 (30): 10444-10449

Sheppard CRC (2003) Predicted recurrences of mass coral mortality in the Indian Ocean. Nature 245: 294-297

Smith TB, Gyory J, Brandt ME, Miller WJ, Jossart J, Nemeth RS (2016) Caribbean mesophotic coral ecosystems are unlikely climate change refugia. Global Change Biology 22: 2756-2765

Stefani F, Benzoni F, Yang SY, Pichon M, Galli P, Chen CA (2011) Comparison of morphological and genetic analyses reveals cryptic divergence and morphological plasticity in *Stylophora* (Cnidaria, Scleractinia). Coral Reefs 30 (4): 1033

Takahashi S, Nakamura T, Sakamizu M, Van Woesik R, Yamasaki H (2004) Repair machinery of symbiotic photosynthesis as the primary target of heat stress for reef building corals. Plant and Cell Physiology 45: 251-255

Veron JE (2000) Corals of the world, Volumes 1-3. Australian Institute of Marine Science, Townsville. 1410 pp

Warner ME, Fitt WK, Schmidt GW (1999) Damage to photosystem II in symbiotic dinoflagellates: A determinant of coral bleaching. Ecology Proceedings of the National Academy of Science USA 96: 8007-8012

Marine mollusc (Mollusca: Gastropoda and Bivalvia) diversity of the Saya de Malha and Nazareth Banks, Mascarene Plateau

Sundy Ramah[1,2]*, Deepeeka Kaullysing[2,3], Ranjeet Bhagooli[2,3,4,5]

[1] Albion Fisheries Research Centre, Ministry of Blue Economy, Marine Resources, Fisheries & Shipping, Albion, Petite-Rivière, Republic of Mauritius

[2] Department of Biosciences and Ocean Studies, Faculty of Science & Pole of Research Excellence in Sustainable Marine Biodiversity, University of Mauritius, Réduit 80837, Republic of Mauritius

[3] The Biodiversity and Environment Institute, Réduit, Republic of Mauritius

[4] Institute of Oceanography and Environment (INOS), University Malaysia Terengganu, 21030 Kuala Terengganu, Terengganu, Malaysia

[5] The Society of Biology (Mauritius), Réduit, Republic of Mauritius

* Corresponding author: sundy.ramah@gmail.com

Abstract

Marine molluscs are among the largest assemblages of the animal kingdom and inhabit the marine environment from the intertidal zone to the deep sea. This study reports the diversity of marine molluscs (Gastropoda and Bivalvia) collected from sediments at 19 stations (SS) at the Saya de Malha and Nazareth Banks during the EAF-Nansen expedition in May 2018. Sampling was carried out using the five hydraulic Van Veen grabs mounted on a Video-Assisted Multi-Sampler (VAMS). The mollusc shells were morphologically identified using established procedures and published guides. Shannon-Wiener diversity (*H'*) and Pielou's evenness (*J*) indices were used to assess the diversity of the molluscs at each station. A total of 56 genera of marine gastropods belonging to 34 families, and 40 genera of bivalves from 16 families were recorded. The SS8 station at the Saya de Malha Bank had the highest diversity at a depth of 79 m for Gastropoda and Bivalvia, while SS1 harbored the highest overall molluscan diversity. At the Nazareth Bank, highest gastropod diversity was recorded at SS44, while SS43 had the highest bivalve and overall molluscan diversity. This study provides new information on the molluscan diversity at the Saya de Malha and Nazareth Banks.

Keywords: Gastropoda, Bivalvia, diversity, Saya de Malha Bank, Nazareth Bank, VAMS

Introduction

The Saya de Malha and Nazareth Banks are submerged banks on the Mascarene Plateau, Western Indian Ocean (WIO), hosting a diversity of marine organisms, including molluscs. The molluscan diversity around the easily accessible islands of the Plateau are better documented as compared to the remote banks. One such study to document marine molluscs was carried out around Rodrigues Island by Oliver *et al.* (2004) where 17 new species of cryptic bivalves were reported, and Schwabe (2004) provided descriptions for seven species of Polyplacophora with a new description of the bivalve *Cryptoconchus oliveri*, while the survey by Sheppard (1984) confirmed 384 mollusc species representing 282 gastropods and 99 bivalves in the Chagos Archipelago. Lorenz and Chiapponi (2012) reported two new gastropods from the Cargados Carajos Shoal - *Bistolida nanostraca* and *Ficus dandrimonti*, while Monsecour (2016) reported one new species of giant clam, *Tridacna lorenzi.*

Michel (1985) carried out preliminary works on marine molluscs in Mauritius reporting some species based on morphological features. More recently, Kaullysing *et al.* (2017a) reported the presence of a higher number of mollusc species (16) at a sheltered intertidal zone (east

http://dx.doi.org/10.4314/wiojms.si2021.2.9

coast) in Mauritius as compared to an exposed zone (7) with relatively stronger wave action (south coast), highlighting the suitability of calmer zones for mollusc settlement. Coral-eating gastropods *Drupella* spp. have been found in high densities on corals (Kaullysing *et al*., 2016; 2017b; 2020). Furthermore, the presence of species of marine molluscs such as the ectoparasitic gastropods *Coralliophila erosa* and *C. radula* on coral hosts, and the giant clams *Tridacna maxima* and *T. squamosa* have been recorded in the coastal waters of Mauritius, with the identification having been confirmed using morphological and as well as molecular tools (Kaullysing *et al*., 2019; Ramah *et al*., 2017; 2019).

Despite the efforts to document the marine molluscan diversity from the Mascarene Plateau by Mackie *et al*. (2003) in the Seychelles, Bourmaud *et al.* (2005) and Drivas and Jay (2001) in Reunion Island, Oliver *et al.* (2004) in Rodrigues, and Kaullysing *et al.* (2019) and Michel (1985) in Mauritius, many of the molluscan taxa remain understudied or unreported (Fedosov and Puillandre, 2005), especially in remote and less frequented areas such as the Saya de Malha and Nazareth Banks (Federov *et al*., 1980; Sirenko and Scarlato, 1991; Sirenko, 1993; Nesis, 1993; Vortsepneva, 2008; Fauvelot *et al.*, 2020), leading to a potential drastic underestimation of the extant molluscan assemblage in this part of the world. The present study therefore aimed at providing additional information on the diversity of molluscs found within the waters of the Saya de Malha and Nazareth Banks, Mascarene Plateau.

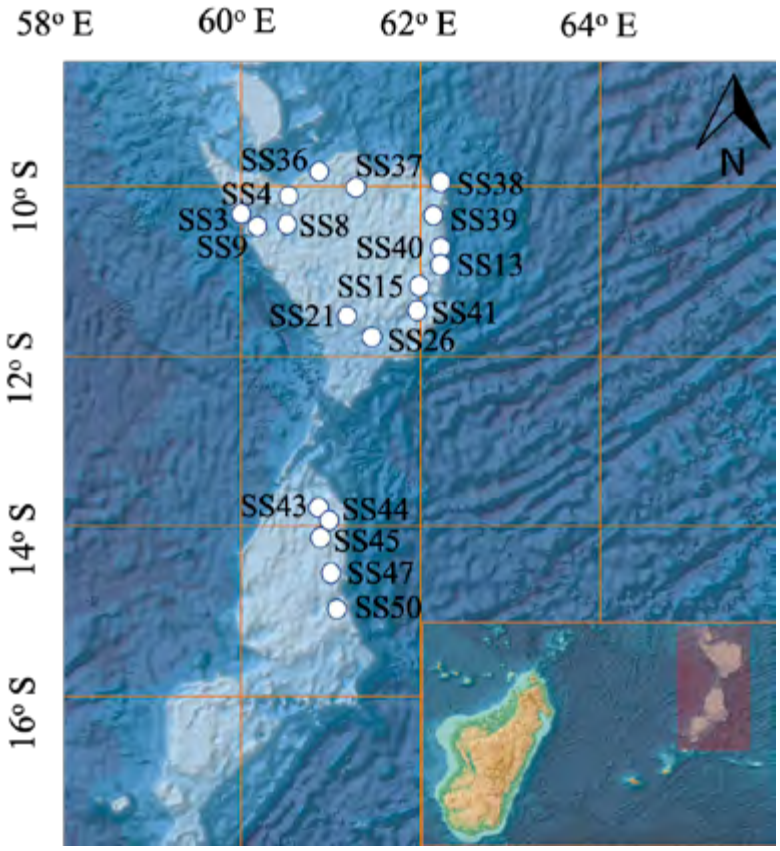

Figure 1. Map of the Saya de Malha and Nazareth Banks indicating the 19 sampling stations (SS). The map was prepared using the GEBCO Bathymetry Grid layer data 2020.

Materials and methods

Survey sites

This study focused on the Saya de Malha and Nazareth Banks on the Mascarene Plateau. The survey took place in May 2018 during the EAF-Nansen Indian Ocean Expedition on board the F/V Dr. F. Nansen. Nineteen stations were surveyed, namely, SS3, SS4, SS8, SS9, SS13, SS15, SS21, SS26, SS36, SS37, SS38, SS39, SS40 and SS41 on Saya de Malha Bank, and SS43, SS44 SS45, SS47 and SS50 on Nazareth Bank, inclusive of shallow, deep and slope areas (Fig. 1).

Sampling

Sampling of bottom sediments was conducted using the five hydraulic Van Veen grabs mounted on the Video-Assisted Multi-Sampler (VAMS) at the 19 stations - 14 stations at the Saya de Malha Bank and 5 stations at the Nazareth Bank. Once the grabs were brought on the deck, the surface water was drained, and the sediment was passed through a sieve of 5 mm mesh size to collect the mollusc shells. They were then cleaned and washed with freshwater and stored for further identification.

Morphological identification

Identification of the collected shells to the family and genus levels was carried out based on their morphological features using published identification manuals and guides, namely Michel (1985), Oliver (1992), Jarrett (2000), Abbott and Dance (2000), Drivas and Jay (2001), Dandrimont (2008), Richmond (2011), Wilson (2016), and Harasewych and Moretzsohn (2017). Species-level identification was difficult to achieve due to some of the shells being eroded and degraded.

Diversity Index

Shannon-Wiener diversity index (*H'*) (Shannon and Wiener, 1949) and Pielou's evenness index (*J*) (Pielou, 1966) were used to assess molluscan diversity at each station at the banks.

Results and discussion

Fifty-six genera of gastropods belonging to 34 families, and 40 genera of bivalves belonging to 16 families were recorded from the 19 stations on the Saya de Malha and Nazareth Banks. At the Saya de Malha Bank, 51 genera of gastropods from 30 families, and 38 genera of bivalves from 15 families were recorded, while at the Nazareth Bank, 12 genera of gastropods from 12 families, and 13 genera of bivalves from 7 families were found (Table 1). While this study recorded fewer families of gastropods as compared to the compilation by Vortsepneva (2008), it has reported a higher number of bivalve families (16) comprising of 40 genera, as compared to four families (5 genera) from Vortsepneva (2008) and adds 13 new gastropod families to the existing list for Saya de Malha Bank. New data on molluscs is also presented for the first time from the Nazareth Bank as no published literature is available on molluscs from this specific bank.

The broader WIO region is known to host approximately 2,500 species of molluscs out of which 75 families are from the Gastropoda class, 667 species from 49 families of the Bivalvia, and 39 species from 6 families of the Polyplacophora (Vortsepneva, 2008). The findings of this study complement the only record available from Saya de Malha Bank from the previous Russian expedition reporting a total of 142 species of molluscs, out of which 102 species were from 36 families of gastropods, 32 species from 10 families of cephalopods and 8 species from 3 families of bivalves (compiled in Vortsepneva, 2008).

At the Saya de Malha Bank, SS8 harboured the highest diversity of gastropods (H' = 2.56) and bivalves (H' = 2.40). In terms of total molluscan population at this bank, the highest diversity was also recorded at SS3 (H' = 3.14) (Fig. 2). At the Nazareth Bank, the highest diversity of gastropods was recorded at SS44 (H' = 1.61), while the highest bivalve and total molluscan diversity were recorded at SS43, with H' values of 1.79 and 2.30, respectively (Fig. 2). Pielou's evenness (J) values were comparable at all the stations for gastropods, bivalves and overall molluscan population, ranging from 0.93 to 1.00, implying an equally distributed molluscan assemblage at all the studied stations at the Saya de Malha and Nazareth Banks. In this study, the highest number of genera was recorded from the Strombidae and Cypraeidae families (four genera in both) for gastropods, and in the Cardiidae and Veneridae families (nine genera in both) for bivalves.

As compared to the only available list of molluscs from the Saya de Malha Bank (compiled by Vortsepneva, 2008), the high diversity may be explained by the difference in the collection depth and methodology. Sirenko and Scarlato (1991; 1993) carried out their collection at depths of 12-15 m, 70 m and 200 m only by using trawls. This study used the Van Veen grabs that were able to collect a deeper profile of the bottom sediment. However, the sediment collected by the grabs were composed of only dead molluscs shells, ranging from 0.5 cm to 2.0 cm, while no live molluscs were recorded.

Conclusion

This expedition to the Saya de Malha and Nazareth Banks presents new records of gastropod and bivalve families in addition to the compilation made by Vortsepneva (2008). Records from previous expeditions and the records from this expedition indicate the possibility of a substantial infauna residing in these areas. However, mollusc species diversity of the Saya de Malha and Nazareth Banks may be underestimated, and further collections are required to provide a clearer picture of the situation in these areas.

Table 1. List of molluscan families and genera recorded during the May 2018 EAF-Nansen Indian Ocean Expedition at the Saya de Malha and Nazareth Banks. √ = genus present, (n) = number of species recorded under the genus.

Sites		**Saya de Malha Bank**														**Nazareth Bank**				
Stations (SS)		**3**	**4**	**8**	**9**	**13**	**15**	**21**	**26**	**36**	**37**	**38**	**39**	**40**	**41**	**43**	**44**	**45**	**47**	**50**
Depth (m)		**79**	**32**	**60**	**57**	**30**	**56**	**160**	**251**	**36**	**32**	**23**	**30**	**70**	**381**	**43**	**37**	**32**	**58**	**53**
Family	**Genus**																			
Class: Gastropoda																				
Ancillariidae	*Ancilla*							√ (1)												
	Amalda													√ (1)						
Bullidae	*Bulla*									√ (1)										
Bursidae	*Bursa*						√ (1)													
	Marsupina	√ (1)																		
Calliostomatidae	*Calliostoma*	√ (1)		√ (1)			√ (1)													
Cassidae	*Casmaria*									√ (1)										
Cerithiidae	*Cerithium*			√ (1)													√ (1)			
Columbellidae	*Columbella*																√ (1)			
Conidae	*Conus*	√ (1)				√ (1)		√ (2)	√ (1)	√ (1)									√ (1)	√ (2)
Costellariidae	*Vexillum*	√ (1)	√ (1)	√ (3)	√ (1)															
	Gyrineum		√ (1)	√ (1)																
Cymatiidae	*Monoplex*					√ (2)														
	Cymatium													√ (1)						
	Staphylaea		√ (1)																	
Cypraeidae	*Cypraea*		√ (1)				√ (1)	√ (1)	√ (1)	√ (1)				√ (1)		√ (1)				√ (1)
	Ipsa									√ (1)										
	Naria									√ (1)										
Drilliidae	*Fusiturricula*								√ (1)											
Epitoniidae	*Epitonium*								√ (1)											
	Janthina								√ (1)						√ (1)					
	Peristernia	√ (1)	√ (1)												√ (1)					
Fasciolariidae	*Fusinus*	√ (1)										√ (1)	√ (1)							
	Latirus		√ (1)							√ (1)										
Fissurellidae	*Fissurella*										√ (1)									
Haminoeidae	*Aliculastrum*								√ (1)											
Littorinidae	*Littorina*		√ (1)			√ (1)		√ (1)									√ (1)	√ (1)		
Marginellidae	*Volvarina*	√ (1)																		
	Marginella	√ (1)		√ (1)																
	Mitra	√ (1)								√ (1)			√ (1)							
Mitridae	*Neocancilla*			√ (1)			√ (1)								√ (1)					
	Cancilla														√ (1)					
Muricidae	*Murex*							√ (1)				√ (1)								
	Siratus							√ (1)									√ (1)			
	Nassarius			√ (2)				√ (1)												√ (1)
Nassariidae	*Bullia*							√ (1)												
	Phos							√ (1)												
Naticidae	*Neverita*	√ (1)		√ (1)				√ (1)			√ (1)			√ (1)						
	Polinices							√ (1)	√ (1)											
Olividae	*Oliva*						√ (1)		√ (1)											
Patellidae	*Patella*				√ (1)	√ (1)														
Phasianellidae	*Phasianella*															√ (1)		√ (1)		
Siliquariidae	*Tenagodus*																√ (1)			
Strombidae	*Strombus*	√ (1)		√ (1)			√ (1)			√ (1)									√ (1)	
	Lambis	√ (1)																		
	Dolomena			√ (1)																
	Persististrombus									√ (1)										
Tegullidae	*Tectus*															√ (1)				
Terebridae	*Terebra*	√ (2)		√ (1)			√ (1)		√ (1)											
Triviidae	*Trivia*			√ (1)				√ (1)												

Sites		**Saya de Malha Bank**														**Nazareth Bank**				
Stations (SS)		**3**	**4**	**8**	**9**	**13**	**15**	**21**	**26**	**36**	**37**	**38**	**39**	**40**	**41**	**43**	**44**	**45**	**47**	**50**
Depth (m)		**79**	**32**	**60**	**57**	**30**	**56**	**160**	**251**	**36**	**32**	**23**	**30**	**70**	**381**	**43**	**37**	**32**	**58**	**53**
Family	**Genus**																			
Class: Gastropoda																				
Trochidae	*Stomatolina*				√ (1)															
Turbinidae	*Turbo*			√ (1)																
	Bolma					√ (1)														
Turridae	*Gemmula*			√ (1)					√ (1)				√ (1)		√ (1)					
	Turris							√ (1)												
Tonnidae	*Tonna*															√ (1)				
Total number of species recorded		14	7	17	3	6	7	14	10	10	2	2	3	4	5	**4**	**5**	**2**	**2**	**4**
Class: Bivalvia																				
Arcidae	*Arca*	√ (2)		√ (2)	√ (1)		√ (2)	√ (1)				√ (1)								
	Anadara			√ (1)				√ (1)												
	Barbatia							√ (1)												
	Lunulicardia		√ (1)																	
	Fulvia		√ (1)						√ (1)				√ (1)		√ (1)					
	Nemocardium			√ (1)		√ (1)			√ (1)											√ (1)
	Ctenocardia	√ (1)			√ (1)		√ (1)	√ (1)												√ (1)
	Fragum						√ (1)	√ (1)		√ (1)										
	Trachycardium									√ (1)		√ (1)		√ (1)						√ (1)
	Lyrocardium						√ (1)									√ (1)				
	Tridacna									√ (1)							√ (1)			
Carditidae	*Cardita*				√ (1)			√ (1)												
Chamidae	*Chama*	√ (1)																		
Donacidae	*Donax*			√ (1)			√ (2)													
Glossidae	*Meiocardia*							√ (1)												
Glycymerididae	*Glycymeris*	√ (1)		√ (1)	√ (2)		√ (2)											√ (1)		√ (2)
Limidae	*Lima*					√ (1)						√ (1)						√ (1)		√ (1)
	Limaria												√ (1)							
Lucinidae	*Ctena*	√ (1)																		
	Anodontia		√ (1)																	√ (1)
	Miltha			√ (1)																
	Divaricella				√ (1)															
Mactridae	*Mactra*	√ (1)																		
Mytilidae	*Perna*								√ (1)											
Pectinidae	*Aequipecten*	√ (1)		√ (2)	√ (2)		√ (2)	√ (1)												
	Chlamys	√ (1)	√ (1)	√ (4)	√ (2)	√ (1)			√ (1)	√ (2)	√ (1)					√ (1)				
	Pecten		√ (1)	√ (3)			√ (2)			√ (2)					√ (1)	√ (1)	√ (1)			
Pinnidae	*Pinna*					√ (1)														
Semelidae	*Semele*	√ (2)																		
Spondylidae	*Spondylus*															√ (1)				
Tellinidae	*Tellina*						√ (2)					√ (1)								
	Pitar	√ (1)			√ (1)			√ (1)												
	Dosinia	√ (1)		√ (2)			√ (2)	√ (1)	√ (1)	√ (1)	√ (1)			√ (2)		√ (1)				
	Antigona			√ (5)	√ (2)															
	Marcia			√ (2)																
Veneridae	*Circomphalus*			√ (1)	√ (1)	√ (1)														
	Paphia				√ (1)		√ (1)													
	Chionella					√ (1)														
	Globivenus															√ (1)				
	Humilaria						√ (1)													
Total number of species recorded		**13**	**5**	**26**	**15**	**6**	**19**	**10**	**5**	**8**	**2**	**4**	**2**	**3**	**2**	**6**	**2**	**2**	**0**	**7**

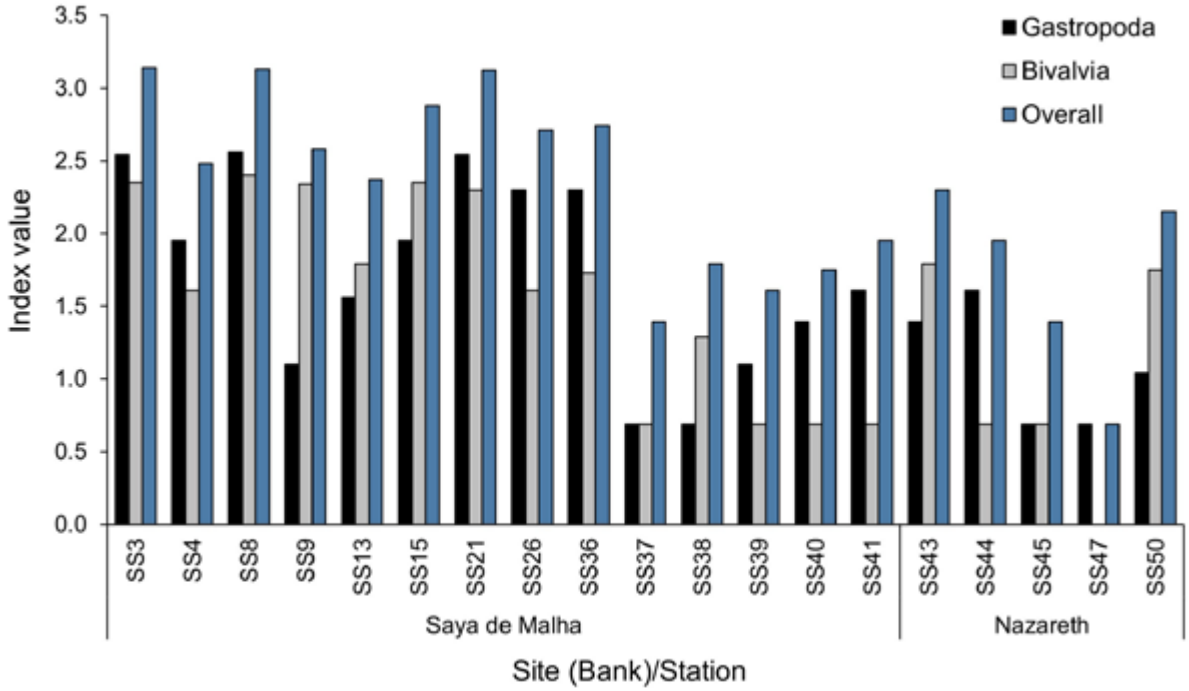

Figure 2. Shannon-Wiener diversity index (*H'*) indicating the molluscan diversity at the Saya de Malha and Nazareth Banks at each station (SS).

Acknowledgements

The underlying work was made possible with the support of the EAF-Nansen Programme "Supporting the Application of the Ecosystem Approach to Fisheries Management considering Climate Change and Pollution Impacts" executed by Food and Agriculture Organization of the United Nations (FAO) and funded by the Norwegian Agency for Development Cooperation (Norad). The authors are thankful to FAO for funding and supporting the Indian Ocean research expedition 2018 on the Saya de Malha Bank and Nazareth Bank with the R/V *Dr Fridtjof Nansen*, the Department of Continental Shelf, Maritime Zones Administration & Exploration of Mauritius for co-leading and coordinating the scientific expedition, the Mauritius-Seychelles Joint Commission of the Extended Continental Shelf for their support and assistance and granting the necessary authorisations, the Ministry of Blue Economy, Marine Resources, Fisheries & Shipping for hosting and spearheading the Habitat Mapping Workshop in Mauritius and for granting necessary authorization to carry out research in the Nazareth Bank; the Institute of Marine Research, Norway for leading the expedition and providing the technical and logistic support. The authors also thank the participating scientists, the crew members and the VAMS / Argus ROV technicians for their work and contribution during the expedition and to the anonymous reviewers for their insightful comments which have significantly improved the manuscript.

References

Abbott RT, Dance SP (2000) Compendium of seashells: a color guide to more than 4,200 of the world's marine shells, 4th edition. Odyssey Publishing, California. 421 pp

Bourmoud CAF, Abouidane A, Boissier P, Leclere L, Mirault E, Pennober G (2005) Coastal and marine biodiversity of la Reunion. Indian Journal of Marine Science 34 (1): 98-103

Dandrimont T (2008) Coquillages de L'Ile Maurice. Database CD-ROM version

Drivas J, Jay M (2001) Coquillages de la Réunion et de l'Île Maurice. Les Editions du Pacifique. Times Media Private Ltd. Singapore. 159 pp

Fauvelot C, Zuccon D, Borsa P, Grulois D, Magalon H, Riquet F, Andrefouet S, Berumen ML, Sinclair-Taylort TH, Gelin P, Behivoke P, Johan Ter Poorten J, Strong EE, Bouchet P (2020) Phylogeographical patterns and a cryptic species provide new insights into Western Indian Ocean giant clams phylogenetic relationships and colonization history. Journal of Biogeography 00: 1-20

Fedorov VV, Rubinstein IG, Danilov IV, Lanin VI (1980) Bottom landscapes of the Saya de Malha Bank (the Indian Ocean). Okeanologia 20: 660-668

Fedosov AE, Puillandre N (2012 Phylogeny and taxonomy of the Kermia–Pseudodaphnella (Mollusca: Gastropoda: Raphitomidae) genus complex: A remarkable radiation via diversification of larval development. Systematics and Biodiversity 10: 447-477

Harasewych MG, Moretzsohn F (2017) The book of shells: A lifesize guide to identifying and classifying six hundred shells. The IVY Press, United Kingdom. 656 pp

Jarrett AG (2000) Marine shells of the Seychelles. Carole Green Publishing, Cambridge. 172 pp

Kaullysing D, Gopeechund A, Mattan-Moorgawa S, Taleb-Hossenkhan N, Kulkarni B, Bhagooli R (2016) Increased density of the corallivore *Drupella cornus* on *Acropora muricata* colonies overgrown by *Padina boryana*. Proceedings of the 13th International Coral Reef Symposium, Honolulu. pp 288-304

Kaullysing D, Taleb-Hossenkhan N, Kulkarni BG, Bhagooli R (2017a) A comparison of the density and diversity of intertidal benthic molluscs at a sheltered and an exposed tropical coast around Mauritius Island. Western Indian Ocean Journal of Marine Science, Special Issue 1/2017: 31-41

Kaullysing D, Taleb-Hossenkhan N, Kulkarni BG, Bhagooli R (2017b) A first field report of various coral-eating gastropods and associated infestations around Mauritius Island, Western Indian Ocean. Western Indian Ocean Journal of Marine Science, Special Issue 1/2017: 73-75

Kaullysing D, Taleb-Hossenkhan N, Kulkarni BG, Bhagooli R (2019) Variations in the density of two ectorapasitic gastropods (*Coralliophila* spp.) on scleractinian corals on a coast-reef scale. Symbiosis 78: 65-71

Kaullysing D, Mehrotra R, Arnold S, Ramah S, Allchurch A, Haskin E, Taleb-Hossenkhan N, Bhagooli R (2020) Multiple substrates chosen in mass *in-situ* egg deposition by *Drupella* in Mauritius, a first record for the Western Indian Ocean waters. Journal of Molluscan Studies 86: 427-430

Lorenz F, Chiapponi M (2012) A new species of *Bistolida* (Gastropoda: Cypraeidae). Schriften zur Malakozoologie 27: 3-16

Mackie ASY, Oliver PG, Darbyshire T, Mortimer K (2005) Shallow marine benthic invertebrates of the Seychelles Plateau: high diversity in a tropical oligotrophic environment. Philosophical Transactions of the Royal Society A 363: 203-228

Michel C (1985) Marine molluscs of Mauritius. World Wildlife Fund/International Union for Conservation of Nature and Natural Resources. Editions de l'Océan Indien. 83 pp

Monsecour K (2016) A new species of giant clam (Bivalvia: Cardiidae) from the Western lndian Ocean. Conchylia 46: 1-4

Nesis KN (1993) Cephalopods from the Saya de Malha Bank, Indian Ocean. Transactions of the PP Shirshov Institute of Oceanology 128: 26-39

Oliver PG (1992) Bivalved seashells of the Red Sea, Verlage Christa Wiesbaden, Germany. 333 pp

Oliver PG, Holmes AM, Killeen IJ, Light JM, Wood H (2004) Annotated checklist of the marine Bivalvia of Rodrigues. Journal of Natural History 38: 3229-3272

Pielou EC (1966) Ecological diversity. Wiley, New York. 165 pp

Ramah S, Taleb-Hossenkhan N, Bhagooli R (2017) Differential substrate affinity between two giant clam species, *Tridacna maxima* and *Tridacna squamosa,* around Mauritius. Western Indian Ocean Journal of Marine Science, Special Issue 1/2017: 13-20

Ramah S, Taleb-Hossenkhan N, Todd PA, Neo ML, Bhagooli R (2019) Drastic decline in giant clams (Bivalvia: Tridacninae) around Mauritius Island, Western Indian Ocean: implications for conservation and management. Marine Biodiversity 49: 815-823

Richmond MD (2011) A field guide to the seashores of the Eastern Africa and the Western Indian Ocean Islands. Sida/WIOMSA. 464 pp

Schwabe E (2004) The Polyplacophora (Mollusca) collected during the First International Marine Biodiversity Workshop for Rodrigues (western Indian Ocean), with the description of a new species. Journal of Natural History 38: 3143-3173

Shannon CE, Wiener W (1949) The Mathematical theory of communication. University of Illinois Press, Urbana. 125 pp

Sheppard ALS (1984) The molluscan fauna of Chagos (Indian Ocean) and an analysis of its broad distribution patterns. Coral Reefs 3: 43-50

Sirenko BI, Scarlato OA (1991) *Tridacna rosewateri*: a new species from the Indian Ocean. La Conchiglia 22: 4-9

Sirenko BI (1993) On the fauna of shell-bearing mollusks in the Saya de Malha Bank, Indian Ocean (part I & II). La Conchiglia/Shell, International Shell Magazine. 275 pp

Vortsepneva E (2008) Review: Saya de Malha Bank – an invisible island in the Indian Ocean. Geomorphology, Oceanology, Biology. Lighthouse Foundation. 44 pp

Wilson B (2016) A handbook to Australia seashells. Louise Egerton, Australia. 185 pp

Macro- and megafauna on the slopes of the Saya de Malha Bank of the Mascarene Plateau

Odd A. Bergstad[1]*, Konstantin Tabachnick[2], Elena Rybakova[2], Gilberte Gendron[3,4], Andrew Souffre[5], Ranjeet Bhagooli[6], Sundy Ramah[6,7], Magne Olsen[1], Åge S. Høines[1], Tatjana Dautova[8]

[1] Institute of Marine Research (IMR), PO Box 1870 Nordnes, N-5817 Bergen, Norway

[2] Shirshov Institute of Oceanology, Russian Academy of Sciences, Moscow, Russia

[3] Seychelles National Parks Authority, PO Box 1240, Orion Mall, Victoria, Mahe, Seychelles

[4] Island Biodiversity & Conservation Centre, University of Seychelles, P.O. Box 1348, Anse Royale, Mahé, Seychelles

[5] Seychelles Fishing Authority, Fishing Port, PO Box 149, Victoria, Mahé, Seychelles

[6] Department of Biosciences & Ocean Studies, Faculty of Science & Pole of Research Excellence in Sustainable Marine Biodiversity, University of Mauritius, Reduit 80837, Republic of Mauritius

[7] Albion Fisheries Research Centre, Ministry of Blue Economy, Marine Resources, Fisheries & Shipping, Albion, Petite-Riviere, Republic of Mauritius

[8] AV Zhirmunsky Institute of Marine Biology, National Scientific Center of Marine Biology, Far Eastern Branch of Russian Academy of Sciences, Vladivostok, Russia

* Corresponding author: oabergstad@gmail.com

Abstract

A first characterization of the distribution and composition of benthic and demersal macro- and megafauna was derived based on video records sampled along five pre-determined transects up the slope on the western, northern and eastern sides of the Saya de Malha Bank on the Mascarene Plateau, starting at a maximum depth of 1000 m. Abundance was highest in the upper parts of eastern slope locations, primarily reflecting a relatively higher abundance of black corals (Antipatharia) than in other locations. A consistent feature of several transects, but most prominent in eastern and northern slopes, was the occurrence of patchy coral and sponge aggregations along the margin where the substrate was mostly hard. In some cases, these aggregations might be considered 'gardens' but reefs were not observed. Higher-level taxonomical composition of the fauna is presented. Demersal fish were widespread but not abundant, and within the depth range studied, there was a transition from a marginal shallow fish assemblage to a deepwater assemblage. Fishes were in most cases only assigned to family level, and 49 families were recorded. To thoroughly assess the biodiversity and abundance of fauna of the slopes of Saya de Malha Bank, further studies conducting more detailed video transects and sampling of specimens are warranted.

Keywords: benthos, fish, oceanic, bank slope, abundance, composition, Mascarene, Saya de Malha

Introduction

This paper presents first visual observations of benthic and demersal macro- and megafauna and substrates on the upper slopes of the Saya de Malha Bank, the more prominent amongst several shallow banks of the Mascarene Plateau in the Western Indian Ocean (Fig. 1). The paper is one in a series generated by an investigation of the Saya de Malha ecosystem facilitated by the FAO EAF-Nansen Programme and the RV *Dr Fridtjof Nansen*. In a separate account the benthos of the shallower parts of the bank, i.e. shallower than 50 m is described (Ramah *et al*., this issue). The present paper explores macro- and megafauna and habitats from the margin of the shallow bank plateau downslope

http://dx.doi.org/10.4314/wiojms.si2021.2.10

from approximately 50 m to 1000 m. Together these two accounts add significant new information to the relatively sparse older data on macro- and megabenthos in the area. The Saya de Malha Bank plateau is roughly triangular in shape and mostly less than 200 m deep. Its margin is characterised by steep slopes and Spiridonov, 2008 and papers cited therein; Strømme *et al.*, 2009). From the Russian accounts there are extensive species lists, and distributions and composition of faunal assemblages were compiled, mainly for the plateau (Vortsepneva and Spiridonov, 2008), but not for the slopes. The current study aimed

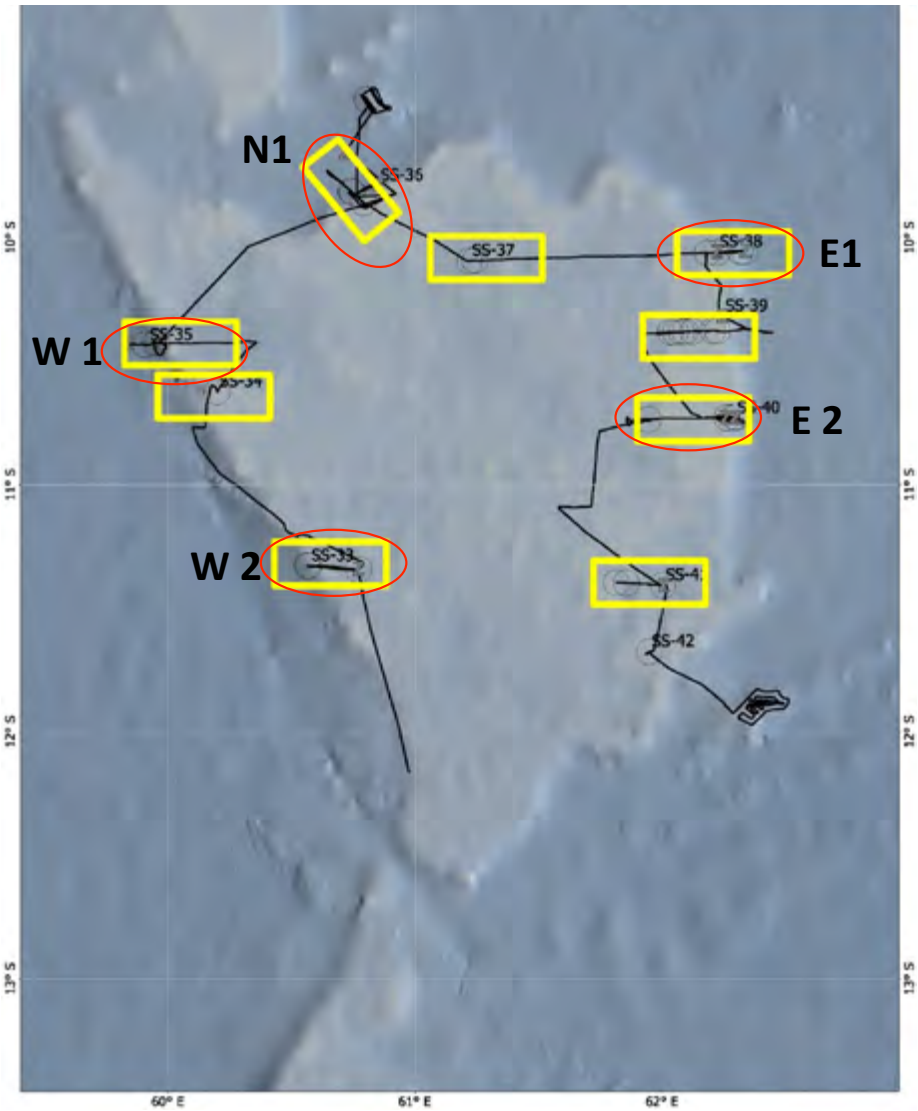

Figure 1. Survey track of the vessel, locations of targeted studies (Superstations, yellow rectangles). The five slope locations considered in this study are encircled in red. In these locations the VAMS vehicle was towed along transects to explore macro-and megafauna near and on the seabed. Saya de Malha Bank study 2018, RV *Dr Fridtjof Nansen, Leg II*.

that ends in the surrounding abyssal depths except at the saddle that connects it to the Nazareth Bank at depth of around 1200 m.

The few previous studies of fauna and flora on Saya de Malha primarily targeted the shallow bank areas, and mostly used benthic samplers and trawls (Vortsepneva

to provide additional information using visual observations by video.

The targeting of macro- and megafauna reflected the special attention paid to occurrence of deepwater fish and taxa regarded as indicators of Vulnerable Marine Ecosystems (VMEs *sensu* FAO (2009)). VME-taxa

expected in the area were sponges and corals that might form especially vulnerable assemblages such as sponge bed and coral gardens or reefs. These are features susceptible to significant adverse impacts of bottom fishing, should such fisheries develop in the area. Prior to this study no information was available on deepwater fish or the occurrence of VME-taxa in the Saya de Malha slope areas.

The data for the present paper were collected during the May 2018 expedition to Saya de Malha on the RV *Dr Fridtjof Nansen*. Serving multiple project objectives, the aim of the cruise was to characterize the ecosystem and morphology of the Saya de Malha Bank for the benefit of Seychelles and Mauritius that are sharing the management of the 'Joint Management Area' encompassing the major portion of the Saya de Malha Bank.

Saya de Malha waters are oceanic and oligotrophic (Kyewalyanga, 2015), and the bank is exposed to major regional ocean currents, with the eastern slope upstream and the western slope downstream of the westward flowing South Equatorial Current (Schott *et al.*, 2009; Vianello *et al.*, 2017). A working hypothesis for the study was that the composition of the fauna on the slopes would vary by depth and substrate character, but also with the regional circulatory influence with eastern and perhaps northern slopes being more exposed than the western slopes. Bio-physical coupling around shallow seamounts in the South Western Indian Ocean have been studied nearby (e.g. Harris *et al*. 2020), but not on the Saya de Malha Bank which is a more extensive feature than the isolated seamounts targeted elsewhere.

The objective and scope of this study was to develop a first characterization of the distribution and composition of benthic fauna and substrates derived from a visual census on the upper slope. Working within the bank margin to 1000 m depth, the approach was to carry out sampling along pre-determined transects up the slope on the western, northern and eastern sides of the Saya de Malha. Along these transects, fauna and substrate information was collected with a high-definition video camera operated from a Remotely Operated Vehicle (ROV).

Material and methods

The main vehicle used to collect data for this study was the Video Assisted Multisampler (VAMS) described in detail by Serigstad *et al.* (2015) and illustrated in Buhl-Mortensen *et al.* (2017). This vehicle consists of a tubular instrument cage connected to the vessel by a 2500 m optical cable. The vehicle has five remotely operated 0.1 m^2 van Veen grabs, and a tethered lightweight (75 kg) ROV with a HD camera for collecting video data in a radius of approx. 30 m around the cage. In all the slope locations selected for studying substrate, geomorphology, fauna and flora, the VAMS was used in towed transect mode where the vessel towed the VAMS cage along pre-determined paths at a speed of 0.1-0.4 knots while the ROV explored the underlying seabed. The operational depth range of the VAMS was 20-1000 m. For this study, slope transects running perpendicular to isobaths were run starting at 780-1000 m and moving up to the outer rim of the bank plateau. All dives were made during daytime and technical crew was only available for 8-12 hours per day.

The distance between the seabed and the ROV camera varied depending on conditions but was kept at 1-2 m during steady passage. The study was exploratory and there was frequently a need to stop to identify and enumerate organisms at or near the seabed. The vehicle was thus not moved with a constant speed along the transect. The amount of time spent focusing on specific targets was assumed roughly equal in the different locations and sampling periods.

Initial identification and counting of benthos and fish were carried out onboard the vessel, to be followed by land-based post-processing. Video records were achieved by continuous recording by skilled observers during the VAMS operations. Records were logged with data on time, position, depth, and substrate in a dedicated logging software developed by the Institute of Marine Research, Norway. The videos were revisited after the dives had been completed and again in several dedicated sessions after the cruise. Overlooked observations were added and erroneous/uncertain records amended accordingly. For each taxon, number of individuals or number of colonies appearing within the field of view was recorded, taking care not to record each more than once.

The VAMS and ROV was not equipped with megabenthos samplers, hence organisms could only be identified from the video footage and still images derived from the videos. Few taxa could consistently be identified to species or low taxonomic levels, hence the analyses in this paper were based on records at high taxonomical levels, usually class and in some cases order. The taxonomical categories used

were the same for all transects. Fishes could normally be assigned to family. Some taxa could, however, be identified to genera and species and records of such cases were used to identify what appeared as prominent members of the slope assemblages.

Bathymetry mapping guided the work with the VAMS. The RV *Dr Fridtjof Nansen* is equipped with two Multi Beam Echo Sounders (MBES), Kongsberg EM 710 and EM 302. The operational depth of the EM 710 is 3 to 2000 m, and for the EM302 it is 10 to 7000 m. Both MBES can achieve a swath width of 5.5 times the water depth with high resolution and accuracy. Continuous seabed mapping using the EM 302 was carried out throughout the expedition whereas the EM 710 was used only when in water depths less than 1500 m, mainly on the Saya de Malha Bank plateau. The recorded data was viewed on Seafloor Information System (SIS), Kongsberg real time software designed to be the user interface and the real time data processing system for its hydrographic instruments, and on Olex, the onboard navigation planning system. The single-beam acoustics also provided data on bottom profiles and the SIMRAD EK80 Scientific Split Beam Echo Sounders with 18, 38, 70, 120, 200 and 333 kHz transducers mounted in a drop keel was run continuously.

The substrate characterization used in this fauna study was mainly based on video images, hence a crude classification distinguishing between 'sand', 'gravel', and 'rock' was chosen. There are transitions between sand and gravel. 'Sand' was used for fine, apparently homogeneous substrates, where typically ripple marks and tracks of crawling and digging animals occurred. 'Gravel' ranged from coarse sands with scattered small pebbles and stones, to coarse gravel beds such as found in e.g. *Lithothamnion* beds on the rim of the bank. 'Rock' encompassed bedrock of various character, e.g. basalt, limestone, cemented sand, but also boulders. In many areas, the seabed appeared as rock covered with only a superficial and uneven layer of soft sediment (i.e. mostly sand, but also gravel). In rocky areas and locations with sand and gravel, sampling with grabs to obtain sediment samples and samples of flora and fauna was impossible, hence the substrate classification was based on the video imagery.

Sampling and data

The track of the vessel during Leg 2 of the 2018 Saya de Malha study is shown in Figure 1. Yellow rectangles were locations selected for targeted studies, including transects using the VAMS and ROV. The slope transects were run in the two western (W1, W2), one northern (N1), and two eastern (E1, E2) rectangles encircled by a red eclipse. The remaining rectangles are shallow bank locations and not considered here. Within each rectangle, referred to as 'Superstations', several activities were carried out including VAMS dives, CTDs, plankton and fish sampling, among others.

At each of the five locations (W1-2, N1, E1-2) one or more VAMS dives were conducted, together forming a transect from maximum 1000 m up the slope to the plateau of the bank (Table 1a). For this account focused on slope assemblages, data from depths shallower than 60 m were disregarded. Due to various technical constraints and the inability to work the ROV around the clock, some transects had to be interrupted and were not completely sampled.

In some of the descriptions and analyses, the slope transects were split into four depth zones; 1. <100 m, 2. 100-249 m, 3. 250-499 m, 4. >499 m. Zone 1 represents the outer margin of the bank where there is a rather sharp break between the inner parts of the bank and the steeper outer slope. Zones 2, 3 and 4 were on the slope. Since the maximum range of the vehicle was 1000 m, all the three zones are 'upper slope' depth strata. Sampling levels in the different locations varied (Table 1b), and the E2 and W1 sites have the most complete and continuous sampling. The time spent in different depth zones is given in Table 1 b.

In order to facilitate comparisons between locations and depth zones, the recorded numerical abundances were standardized by observation time. This resulted in a matrix of standardized numbers for each taxon vs. depth zones, scaled to 100 hours of observation time. The standardized numerical abundance data were used in descriptions and exploratory analyses of abundance and taxonomical composition patterns.

Results

Thirteen successful VAMS dives with a total of 1462 minutes of observation time with the ROV was conducted on the upper slope and margin of the Saya de Malha Bank. Details on the sampling effort by four depth zones in each of five study locations is provided in Table 1. Video observations of substrate and organism numbers derived from video records formed the basis of accounts for individual slope locations and inter-location comparisons.

Table 1. List of VAMS locations with associated information on ROV dives, grabs and other observations. Saya de Malha Bank survey 2018, *RV Dr Fridtjof Nansen*. a) dive list and depth ranges., b) duration of observations in each of four depth zones, and the depth ranges actually observed.

a)

Location	Superstation	VAMS & grab st. number	Depth range (max.-min.), m	Hydrography station a.o.	Date
W1	35	19	1006-741	CTD #422 and LADCP 2000m	17.05.2018
		20	495-462		17.05.2018
		21	400-100		18.05.2018
W2	33	13	515-250		15.05.2018
		14	780-494		15.05.2018
		15	80-77	CTD #421 at 72m	15.05.2018
N1	36	22	1013-848		18.05.2018
		23	843-56 (38)	CTD #423 at 110m	19.05.2018
E1	38	27 (interrupted, no data)	1000	CTD #426 at 1418m	21.05.2018
		28	510-285		21.05.2018
		29	192-62		21.05.2018
E2	40	38	1000-410	CTD #429 at 1008m	23.05.2018
		39	420-233		23.05.2018
		40	145-73		23.05.2018

b)

Location	Depth zones	Observation time (mins)	Depth ranges observed, m
W1	>499 m	88	1000-741
	499-250	56	495-461, 400-255
	299-100	54	239-100
	<100	-	-
W2	>499 m	105	781-500
	499-250	89	491-250
	299-100	-	-
	<100	40	80-77
N1	>499 m	264	1027-848, 843-500
	499-250	56	499-250
	299-100	29	249-100
	<100	28	99-56
E1	>499 m	3	512-500
	499-250	107	499-285
	299-100	71	192-100
	<100	53	99-62
E2	>499 m	115	1000-500
	499-250	184	499-250
	299-100	62	145-100
	<100	58	99-73

Characterization of the locations on western, northern and eastern slopes

Western slope

The two locations W1 and W2 on the western slope were studied for 198 and 234 mins, respectively. The start depth of the dives was different, i.e. 1006 m and 781 m. Sandy substrate occurred at the beginning of the transects and some distance up the slope. In W1 there was sand from the start until 741 m, and then again when the transect was resumed at 490 m. In W2 the substrate was sandy from the start at 791 m until about 490 m.

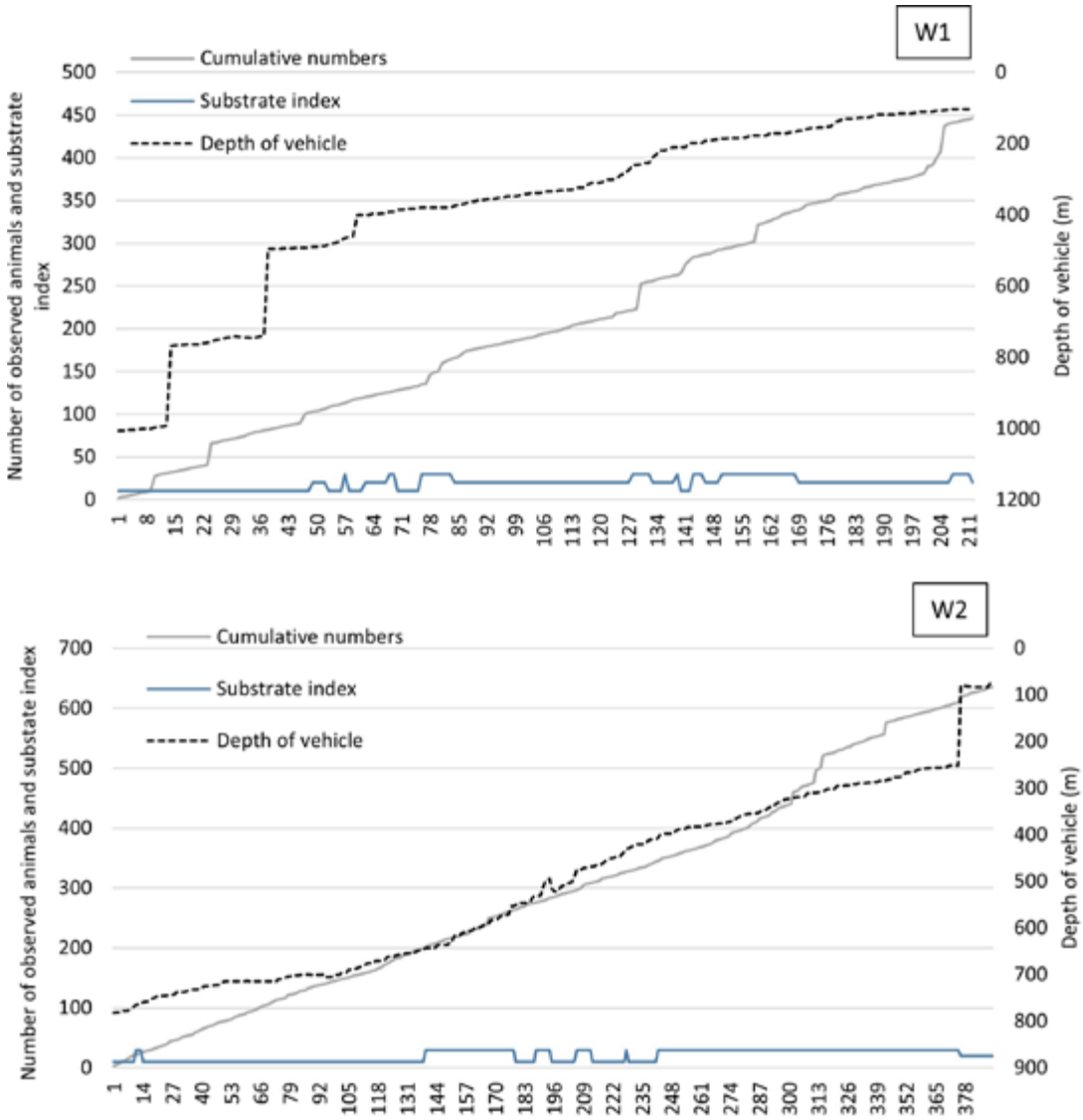

Figure 2. Cumulative numbers of animals observed by video along transects up the slope of the Saya de Malha Bank, RV *Dr Fridtjof Nansen*, 2018. Observations from the western W1 (upper) and W2 (lower) slope locations. The depth of the vehicle as the records were made (hatched line), and cumulative number of animals (solid line) are shown. Grey line indicates substrate associated with each record: 10=sand, 20=gravel and 30=rock. Vertical drops in the depth curve reflect interruptions in the dives and movement to a shallower location, not real depth changes along the transects.

Sandy patches also occurred at shallower depths where harder substrates dominated. Gravel was predominant, with several rocky outcrops. The rock appeared as cemented biogenic sand and gravel. Encrusting red algae, *Lithothamnion*, appeared for the first time at 151 m in W1 and patches of *Lithothamnion* gravel bed, also with brachiopods, was observed until the end of the transect at 100 m. In W2, *Lithothamnion* gravel beds was the habitat at 80-77 m but may have occurred deeper in the unsampled area between 250 and 80 m.

There was a steady accumulation of animal records along the two depth transects, indicating no pronounced patchiness or aggregation related to depth or substrate changes (Fig. 2). W2 had a higher number of animal records than W1, but the observation time was also appreciably higher in that transect.

In the W1 transect broken off seagrass leaves (*Thalassodendron ciliatum*) was observed as deep as 103 m. Live foliate green macroalgae (Ulvophyceae) occurred at the upper end of W2 at around 80 m.

Mesopelagic fishes were observed near the seabed in both transects (but were not recorded amongst benthic fauna). In W1, where abundance appeared highest, they occurred between 491 and 300 m, i.e. beneath the margin of the bank.

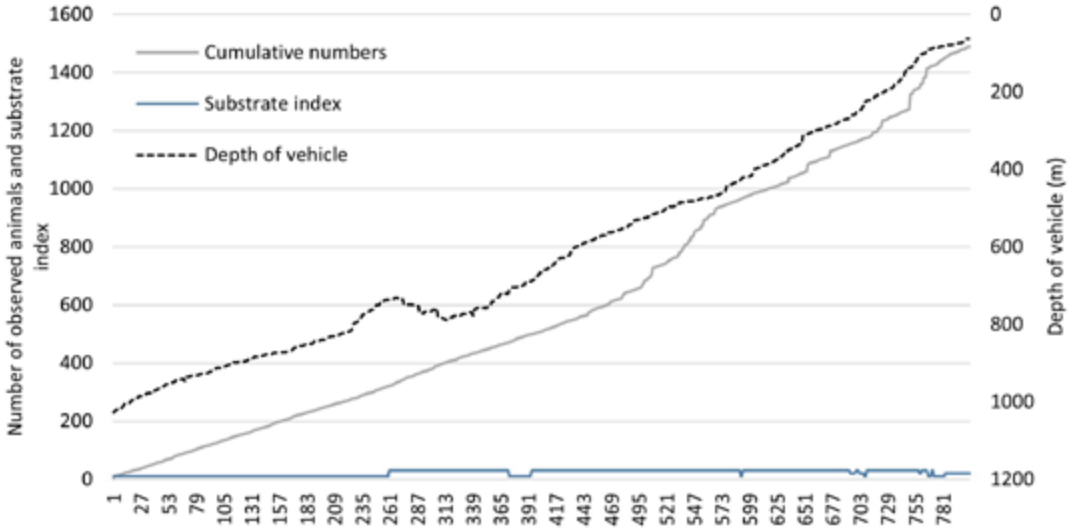

Figure 3. Cumulative numbers of animals observed by video along transects up the slope of the Saya de Malha Bank, RV *Dr Fridtjof Nansen*, 2018. Observations from the N1 northern slope location. The depth of the vehicle as the records were observed (hatched line), and cumulative number of animals (solid line) are shown. Grey line indicates substrate associated with each record: 10=sand, 20=gravel and 30=rock. Vertical drops in the depth curve reflect interruptions in the dives and movement to a shallower location, not real depth changes along the transects.

Northern slope

The single northern slope location was sampled for 377 minutes along a continuous transect from 1027-56 m.

The substrate was sand between the start and 732 m, whereas the shallower portion had boulders, bedrock and only small patches of soft sediments. The rock was variably appearing as cemented biogenic sand and more consolidated limestone. *Lithothamnion* was first observed at 158 m, and from about 140 m there was a transition from rather bare rocky substrate to rock and gravel with significantly more biota. This is reflected in a somewhat stepwise steepening of the cumulative number of animal numbers towards the end of the transect (Fig. 3).

At around 100 m a prominent rocky habitat with a coral and demospongian 'garden' occurred. At shallower depths extensive *Lithothamnion* beds were observed, and at 67 m the first foliate green algae appeared. At 57 m more and more calcified green algae was seen on the gravel beds. Scattered seagrass (*Thalassodendron ciliatum*) leaves were observed from 768m and throughout the depth range of the transect.

Mesopelagic fish were noted across a wide depth range from 920-300 m.

Eastern slope

The two eastern slope locations E1 and E2 were sampled for 234 and 419 minutes, respectively. At E1 a dive at 1000 m generated no data since it had to be interrupted due to high current speeds. The E2 transect was a near continuous transect from 1000-73 m.

The E2 transect had rocky substrate from the beginning until the end, only interrupted by very few patches of sand and some more extensive gravel areas toward the shallower end (Fig. 4). At the deep end the bedrock appeared as basalt, and further up the slope there was basaltic outcrops and walls, but also what appeared as limestone and cemented sand. The northeastern location, sampled from 512 m and up the slope, had a similar substrate distribution with rock until about 250 m and a mixture of rock and softer substrates towards the shallower end. In both these eastern transects, sandy patches were small, and the rocky habitats had only a thin layer of sediment, if any. *Lithothamnion* occurred on gravel beds from 186 m in E1 and 131 m of E2, and towards the shallower end of the transects encrusting algae (including calcified green algae, *Halimeda* sp.) were dominating in gravel beds where foliate green algae were also prominent.

The cumulative abundance curves suggested even abundance until about 100 m after which a pronounced increase was observed. This increase predominantly reflected elevated numbers of coral colonies, and this pattern was particularly pronounced in E2 where the abundance of corals was the highest. At depths shallower than 100 m patches of particularly

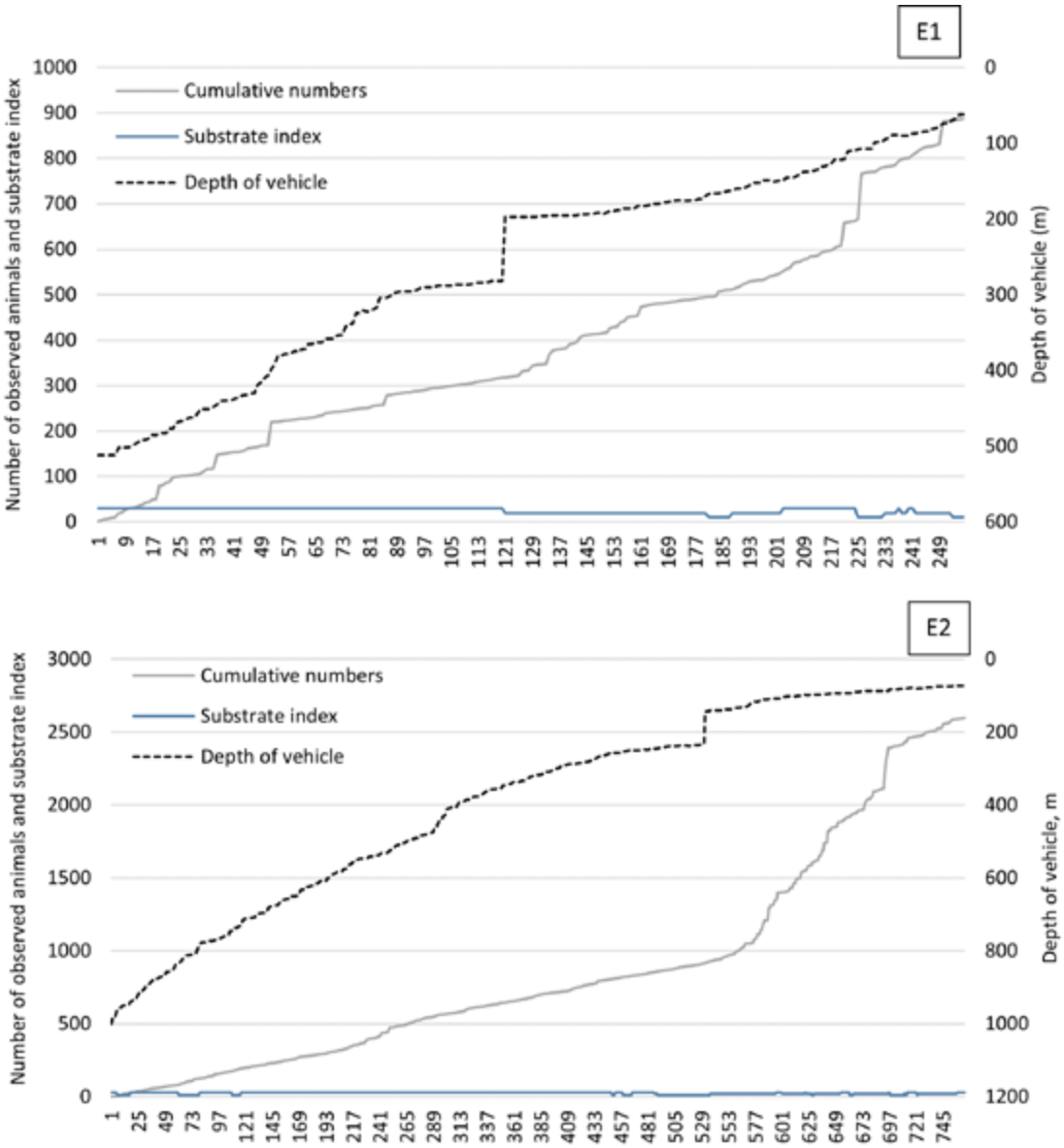

Figure 4. Cumulative numbers of animals observed by video along transects up the slope of the Saya de Malha Bank, RV *Dr Fridtjof Nansen*, 2018. Observations from the eastern E1 (upper) and E2 (lower) slope locations. The depth of the vehicle as the records were made (hatched line), and cumulative number of animals (solid line) are shown. Grey line indicates substrate associated with each record: 10=sand, 20=gravel and 30=rock. Vertical drops in the depth curve reflect interruptions in the dives and movement to a shallower location, not real depth changes along the transects.

high density occurred that would likely qualify as 'coral gardens' defined as 'a relatively dense aggregation of colonies or individuals of one or more coral species' (*sensu* OSPAR, www.ospar.org).

Foliate green algae occurred for the first time at 86 and 93 m in E1 and E2, respectively. Broken off seagrass leaves (*Thalassodendron ciliatum*) occurred at 186 m in E1 and scattered live seagrass appeared at 69 and 73 m and shallower in E1 and E2, respectively.

Mesopelagic fish were observed in E2 from around 750-300 m, with apparently highest numbers at around 400 m. Relatively high abundance was also noted at the beginning of the E1 transect at 510-500 m.

Numbers and composition of animals

Numbers of animals observed, standardized to 100 hours of observation time, by the four depth zones showed no obvious pattern other than the marked higher abundance in the two shallower depth zones in the eastern slope location E2 (Fig. 5). The elevated abundance in E2 mostly reflected a higher abundance of Antipatharia. The western slope locations seemed to have somewhat lower numbers than the northern and eastern locations, but differences were small and not

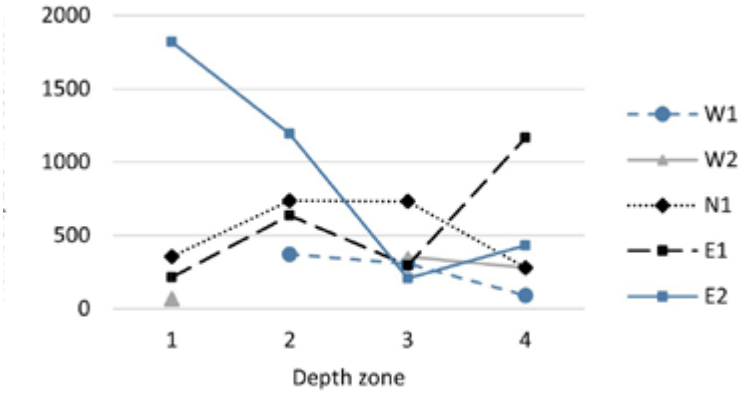

Figure 5. Abundance of megafauna at Saya de Malha western (W1-2), northern (N1) and eastern (E1-2) slope locations as observed by video imagery, RV *Dr Fridtjof Nansen*, 2018. Summed standardized abundance by depth zones: 1- <100 m, 2-100-249 m, 3-250-499 m, 4->499 m.

Table 2. Saya de Malha Bank, RV *Dr Fridtjof Nansen* 2018. Numbers of organisms observed by video in locations W1-2, N1, E1-2 and Depth zones 1-4. Numbers are standardized to 100 hours of observation time. Plants were excluded and fishes identified to families were pooled as 'Pisces'.

Location	W2	W2	W2	W2	W1	W1	W1	W1	N1	N1	N1	N1	E1	E1	E1	E1	E2	E2	E2	E2
Depth zone	1	2	3	4	1	2	3	4	1	2	3	4	1	2	3	4	1	2	3	4
Demospongiae	7.5		27.0	0.0		44.4	62.5	0.0	39.3	262.1	30.4	1.1	28.3	8.5	29.0	0.0	150.0	46.8	9.2	5.2
Hexactinellida	0.0		11.2	21.0		0.0	17.9	53.4	0.0	0.0	62.5	35.2	0.0	8.5	16.8	266.7	19.0	24.2	25.0	132.2
Ctenophora	0.0		6.7	0.0		3.7	0.0	0.0	0.0	0.0	0.0	0.0	0.0	0.0	0.0	0.0	0.0	0.0	0.0	0.0
Actiniaria	5.0		6.7	0.0		14.8	12.5	0.0	0.0	0.0	5.4	9.8	3.8	4.2	0.9	0.0	6.9	19.4	2.7	13.0
Alcyonacea	0.0		57.3	21.9		42.6	23.2	2.3	67.9	17.2	26.8	30.7	11.3	74.6	96.3	200.0	132.8	159.7	68.5	67.8
Ceriantharia	5.0		0.0	0.0		0.0	0.0	2.3	0.0	0.0	0.0	0.0	0.0	1.4	0.0	0.0	0.0	0.0	0.0	0.0
Hydrozoa	0.0		61.8	9.5		29.6	23.2	1.1	0.0	124.1	175.0	37.5	9.4	71.8	33.6	333.3	37.9	45.2	16.3	29.6
Pennatulacea	7.5		2.2	0.0		0.0	0.0	0.0	0.0	0.0	0.0	0.0	0.0	4.2	2.8	66.7	6.9	1.6	0.0	0.0
Scyphozoa	0.0		0.0	0.0		0.0	0.0	0.0	0.0	0.0	0.0	0.0	0.0	1.4	0.0	0.0	0.0	0.0	0.0	0.0
Scleractinia	0.0		3.4	0.0		0.0	0.0	0.0	0.0	17.2	23.2	0.4	0.0	7.0	9.3	0.0	0.0	14.5	12.5	2.6
Zoantharia	0.0		1.1	97.1		0.0	0.0	3.4	0.0	0.0	126.8	36.4	0.0	0.0	0.0	0.0	0.0	0.0	0.5	29.6
Antipatharia	0.0		19.1	0.0		61.1	7.1	0.0	0.0	113.8	3.6	0.8	115.1	77.5	28.0	166.7	882.8	724.2	2.7	7.8
Platyhelminthes	0.0		7.9	0.0		0.0	0.0	0.0	0.0	0.0	0.0	0.0	0.0	0.0	0.0	0.0	0.0	0.0	6.0	0.9
Bivalvia	0.0		0.0	0.0		0.0	0.0	0.0	0.0	0.0	0.0	0.0	0.0	0.0	0.0	0.0	172.4	0.0	0.0	0.0
Cephalopoda	0.0		1.1	0.0		1.9	0.0	0.0	0.0	0.0	0.0	1.1	0.0	0.0	0.0	0.0	0.0	0.0	0.0	0.0
Gastropoda	0.0		0.0	0.0		13.0	0.0	0.0	0.0	0.0	0.0	0.4	0.0	1.4	0.0	0.0	0.0	9.7	0.5	2.6
Scaphopoda	0.0		0.0	0.0		0.0	0.0	0.0	0.0	0.0	0.0	0.0	0.0	1.4	0.0	0.0	0.0	0.0	0.0	0.0
Brachiopoda	0.0		0.0	0.0		9.3	10.7	0.0	0.0	0.0	0.0	0.4	0.0	0.0	0.0	0.0	0.0	0.0	0.5	7.0
Annelida	0.0		1.1	0.0		0.0	0.0	0.0	0.0	0.0	0.0	0.0	0.0	0.0	0.0	0.0	0.0	0.0	0.0	0.0
Polychaeta	0.0		0.0	0.0		1.9	10.7	2.3	0.0	0.0	0.0	0.4	0.0	0.0	0.0	0.0	86.2	6.5	0.5	0.0
Pycnogonida	0.0		0.0	0.0		0.0	0.0	0.0	0.0	0.0	0.0	0.4	0.0	0.0	0.0	0.0	0.0	0.0	0.0	0.0
Achelata	0.0		0.0	0.0		0.0	0.0	0.0	0.0	0.0	1.8	0.0	0.0	0.0	0.0	0.0	1.7	0.0	1.6	0.0
Anomura	0.0		6.7	2.9		1.9	32.1	1.1	0.0	3.4	10.7	4.5	0.0	1.4	0.9	33.3	0.0	0.0	0.5	14.8
Astacidea	0.0		0.0	1.0		0.0	0.0	0.0	0.0	0.0	0.0	0.0	0.0	0.0	0.0	0.0	0.0	0.0	0.0	0.0
Brachyura	2.5		1.1	2.9		0.0	3.6	0.0	0.0	0.0	0.0	1.9	0.0	0.0	0.9	33.3	0.0	0.0	0.0	0.9
Caridea	2.5		14.6	48.6		1.9	17.9	12.5	3.6	10.3	139.3	51.9	0.0	2.8	3.7	33.3	0.0	3.2	4.9	32.2
Cirripedia	0.0		0.0	0.0		0.0	0.0	0.0	0.0	0.0	0.0	0.0	0.0	2.8	0.0	0.0	0.0	0.0	0.0	0.0
Isopoda	0.0		0.0	1.0		0.0	0.0	0.0	0.0	0.0	0.0	0.0	0.0	0.0	0.0	0.0	0.0	0.0	0.0	0.0
Asteroidea	5.0		25.8	2.9		27.8	5.4	0.0	7.1	6.9	16.1	1.1	5.7	14.1	14.0	0.0	3.4	11.3	12.5	6.1
Crinoidea	0.0		1.1	0.0		0.0	0.0	1.1	0.0	0.0	3.6	0.8	0.0	145.1	5.6	0.0	72.4	3.2	2.2	1.7
Echinoidea	25.0		4.5	0.0		66.7	8.9	1.1	157.1	10.3	12.5	4.2	0.0	2.8	11.2	0.0	129.3	38.7	7.1	0.9
Holothuroidea	0.0		0.0	0.0		0.0	0.0	1.1	3.6	10.3	23.2	7.6	0.0	1.4	0.0	0.0	13.8	0.0	1.1	1.7
Ophiuroidea	0.0		6.7	3.8		1.9	3.6	0.0	0.0	0.0	21.4	6.4	0.0	1.4	0.9	33.3	0.0	3.2	8.7	3.5
Bryozoa	0.0		3.4	1.9		7.4	5.4	0.0	0.0	0.0	0.0	0.4	0.0	7.0	0.0	0.0	0.0	0.0	0.0	0.0
Ascidiacea	0.0		0.0	0.0		0.0	0.0	0.0	0.0	0.0	0.0	0.0	0.0	0.0	0.0	0.0	0.0	0.0	0.0	1.7
Pisces	5.0	0.0	83.1	65.7	0.0	40.7	64.3	10.2	78.6	162.1	50.0	47.7	43.4	197.2	43.0	0.0	105.2	80.6	21.7	68.7
Total numbers recorded	65.0	0.0	353.9	280.0	0.0	370.4	308.9	92.0	357.1	737.9	732.1	281.0	217.0	638.0	297.2	1166.7	1820.7	1191.9	205.4	430.4

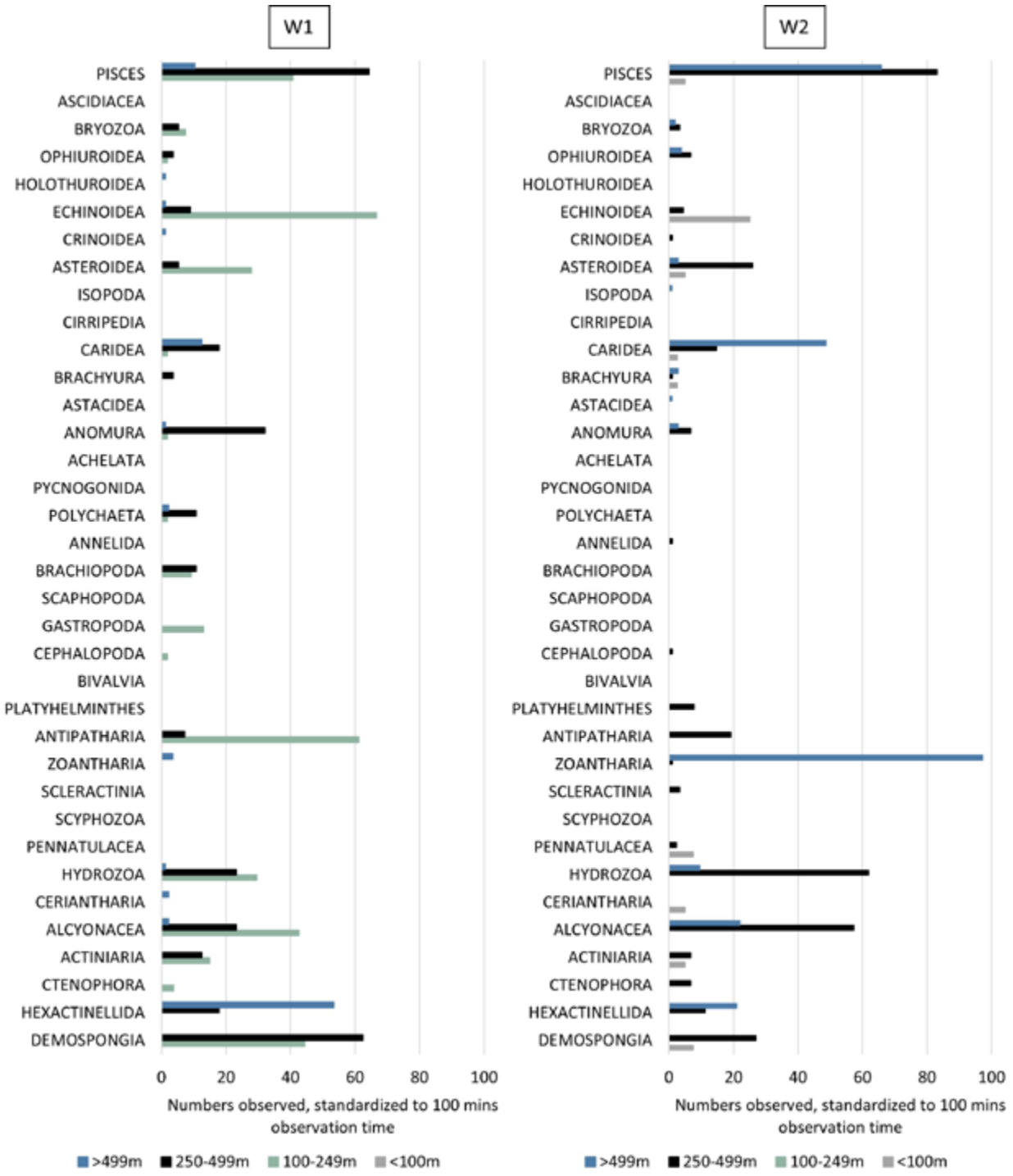

Figure 6. Higher-level taxonomical composition of the fauna recorded by video imagery on the western slope of Saya de Malha Bank, Locations W1 (left) and W2 (right). RV *Dr Fridtjof Nansen*, 2018. Note that two depth zones were not sampled: <100 m in W1, and 100-249 m in W2.

entirely consistent between depth zones (and data were missing in two depth zones). The data from the two locations that were sampled best, i.e. N1 and E1 with near continuous sampling of the entire transects, the patterns of abundance by depth were not very different.

The higher-level taxonomical composition of the animal assemblages observed, by location and depth zones, can be extracted from Table 2 and is further illustrated in Figure 6, 7 and 8.

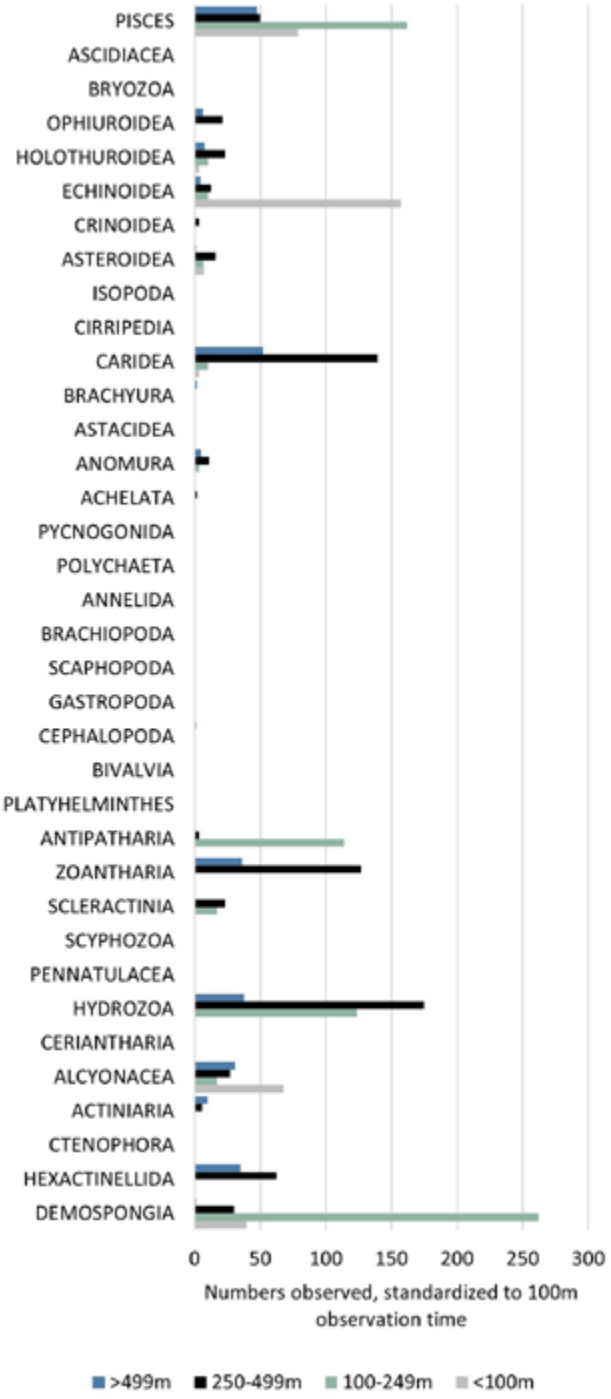

Figure 7. Higher-level taxonomical composition of the fauna recorded by video imagery on the northern slope of Saya de Malha Bank, Location N1. RV *Dr Fridtjof Nansen*, 2018.

Of the 35 categories used, the ten taxa with highest overall numbers were (from highest to lowest) Antipatharia, Pisces, Alcyonacea, Hydrozoa, Demospongiae, Hexactinellida, Echinoidea, Caridea, Zoantharia and Crinoidea. Cnidaria were important and diverse, and Antipatharia, Alcyonacea and Hydrozoa were prominent in all locations but particularly abundant in E2 where the already mentioned increased abundance was observed in the two shallower depth zones. Zoantharia mostly occurred as colonies attached to the hexactinellid sponge *Hyalonema* and was widespread (and possibly underestimated) with highest abundance on the western and northern slopes. Fish and shrimps/prawns were widespread but seldom very abundant. Amongst Porifera, Demospongiae occurred mainly in shallow strata, whereas Hexactinellida were more prominent in the deepest areas. Echinoderms were also common and diverse, with crinoids and echinoids as the more numerous groups.

Notes on individual taxa

Cnidaria

Amongst the overall most abundant taxa were cnidarians in class Anthozoa (orders Antipatharia and Alcyonacea and Zoantharia) and the class Hydrozoa. Actiniaria were frequent but not abundant, and some were species associated with hermit crabs. Common examples of each are illustrated in Appendix Figure A a).

The antipatharian occurring in greatest numbers was *Cirrhipathes* sp. of the family Antipathidae and the few other antipatharians observed were not identifiable from images. The highest densities were observed in Depth zone 1 and 2 but scattered colonies also occurred in deep areas. In some locations the spiral-shaped single strand *Cirrhipathes* sp. formed aggregations.

Thirteen genera of Alcyonacea were recorded (Table 3) across the depth range studied, but this was very probably only a subset of the genera occurring in the area. Some contributed to coral gardens and were more significant in deep than in shallow gardens. Pennatulacea were uncommon and only three genera were recognized (Table 3, Fig. A a). Solitary Scleractinia were infrequent and only one genus was identified, *Caryophyllia* sp.

Hydrozoa were ubiquitous in several locations as small white colonies Fig. A a), primarily in the Depth zones 3 and 4 on soft and rocky substrates. The genera *Errina* (*capensis*?), *Stylaster* (*subviolacea*?), *Conopora* (*tenuiramus*?), and *Sertularella* (*diaphana*?) were recognized. Most of the Hydrozoa were small and not well recorded from videos, hence numbers of colonies as presented above and diversity of taxa were probably underestimated.

On sandy and gravelly substrate at >500 m, the zoantharian *Epizoanthus* was very common and widespread with

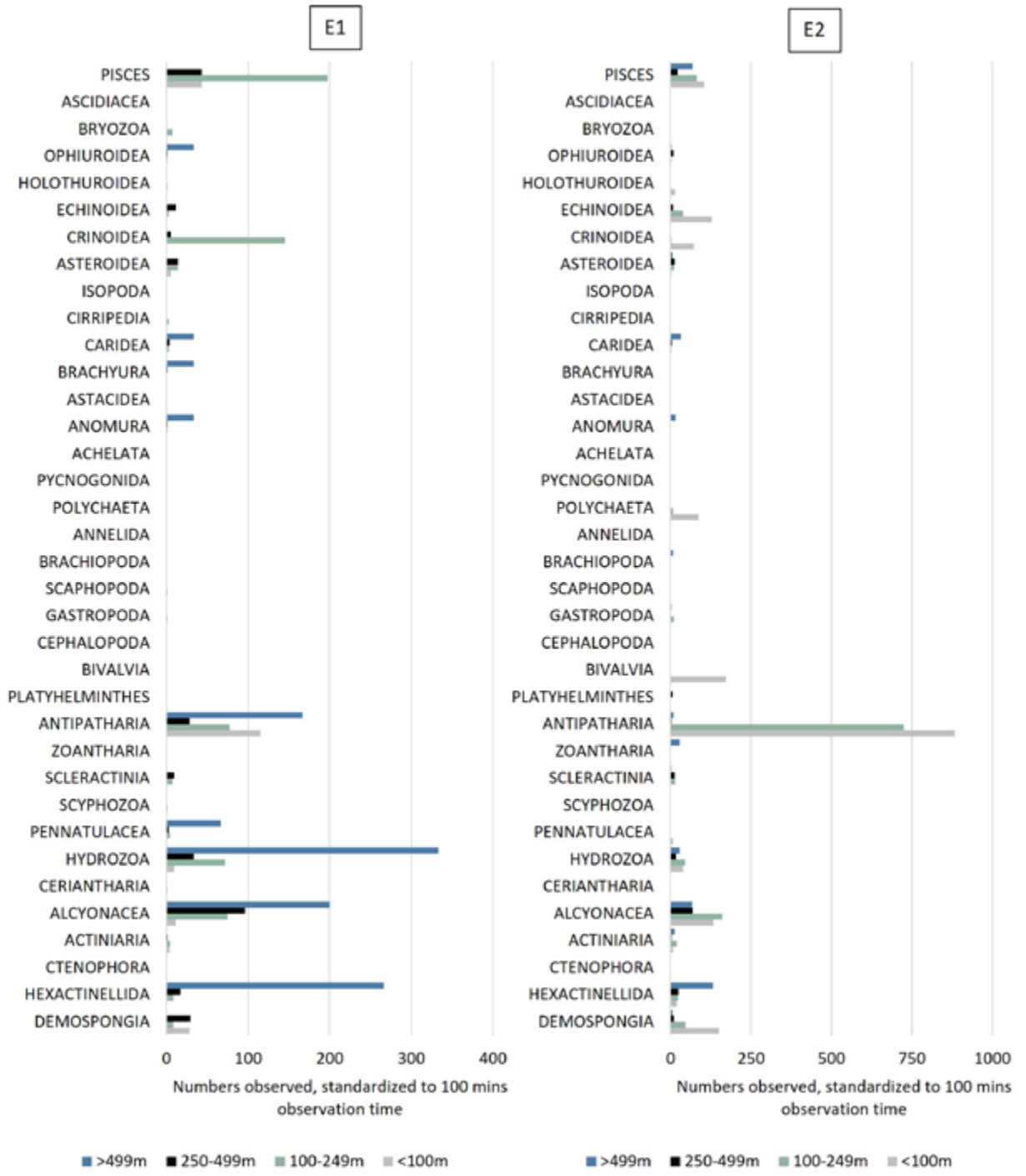

Figure 8. Higher-level taxonomical composition of the fauna recorded by video imagery on the eastern slope of Saya de Malha Bank, Locations E1 (left) and E2 (right). RV *Dr Fridtjof Nansen*, 2018. Note different scales on the numbers axes.

colonies occupying the anchorate spicules of the hexactinellid sponge *Hyalonema (Cyliconema) apertum.*

Seven of the Actiniaria were identified to genus (*Stephanauge* sp., *Dofleinia* sp., *Exocoelactis* sp., *Actinernus* sp., *Sicyonis* sp., *Hormathia* sp., *Paracalliactis* sp.) but several more to family level (e.g. two morphospecies in Hormathidiidae).

On the eastern and northern margins of the bank (Locations N1, E1 and 2), the density of corals (and sponges) was particularly high along the rim facing the deeper slope. The aggregations were multispecies assemblages typically observed at 75-120 m. Examples from Location E1 and E2, including aggregations of the antipatharian genus *Cirrhipathes* sp., are shown in Figure 9.

Table 3. Records of corals in the orders Alcyonacea, Pennatulacea and Scleractinia from Saya de Malha Bank. Identities and depth records of taxa for which good images were extracted from videos. RV *Dr Fridtjof Nansen*, 2018.

Order and family	Genus or species	Location and depth of observation, m				
		SS33	SS35	SS36	SS38	SS40
Alcyonacea:						
Nephtheidae	*Dendronephthya* sp.			83		
Acanthogorgiidae	*Acanthogorgia* sp.					88
Alcyoniidae	*Alcyonium* sp.					107
Nephtheidae	*Dendronephthya* sp.		111			
Ellisellidae	*Ctenocella* sp.				136	
Alcyoniidae	*Anthomastus* sp.				151	
Plexauridae	*Menella* sp.		168			
Alcyoniidae	*Anthomastus* sp.					237
Acanthogorgiidae	*Acanthogorgia* sp.					249
Acanthogorgiidae	Acanthogorgia sp. ?				285	
Primnoidae	*Callogorgia* sp.	294				
Alcyoniidae	*Anthomastus* sp.	383				
Acanthogorgiidae	*Acanthogorgia* sp.			463		
Acanthogorgiidae	*Acanthogorgia* sp.					657
Primnoidae	*Narella* sp.					710
Isididae	*Isidella* sp.			751		
Primnoidae	*Narella* sp.					774
Chrysogorgiidae	*Iridogorgia* sp.					806
Chrysogorgiidae	*Radicipes* sp.			821		
Chrysogorgiidae	*Chrysogorgia* sp.					848
Chrysogorgiidae	*Radicipes* sp.			878		
Pennatulacea:						
Pennatulidae	*Pennatula* sp.					75
Pennatulidae	*Pteroeides* sp.	82				
Pennatulidae	*Pennatula* sp.					84
Pennatulidae	*Pennatula* sp.				164	
Kophobelemnidae	*Kophobelemnon* sp.			757		
Kophobelemnidae	*Kophobelemnon* sp.			814		
Scleractinia:						
Caryophylliidae	*Caryophyllia* sp.				180	

Coral aggregations also occurred in deeper areas, mainly associated with rocky outcrops. Examples from Location E1, where such features were best developed, are shown in Figure 10. Similar observations were made in N1 and E2, but not in the western slope locations. Alcyonacean corals appeared to be prominent in these deep gardens.

Porifera

Multiple Demospongiae were observed in the two shallower depth zones where they were substrate-forming together with many other taxa. In deeper slope areas, fewer Demospongiae were observed and aggregations that might be classified as 'gardens' or 'sponge beds' were infrequent. The only example was the one shown in Figure 11 from the northeastern location E1 (SS 38) at 284 m. The sponges observed were Tetractinomorpha (Fig. A b).

Hexactinellida (Fig. A b) were common in all locations and some could be identified to genus and species level. On the western slope *Semperella schulzei* (600-800 m) and *Hyalonema (Cyliconema) apertum* (400-1000 m), and *Euplectella* sp. (400-500 m), possessing anchorate

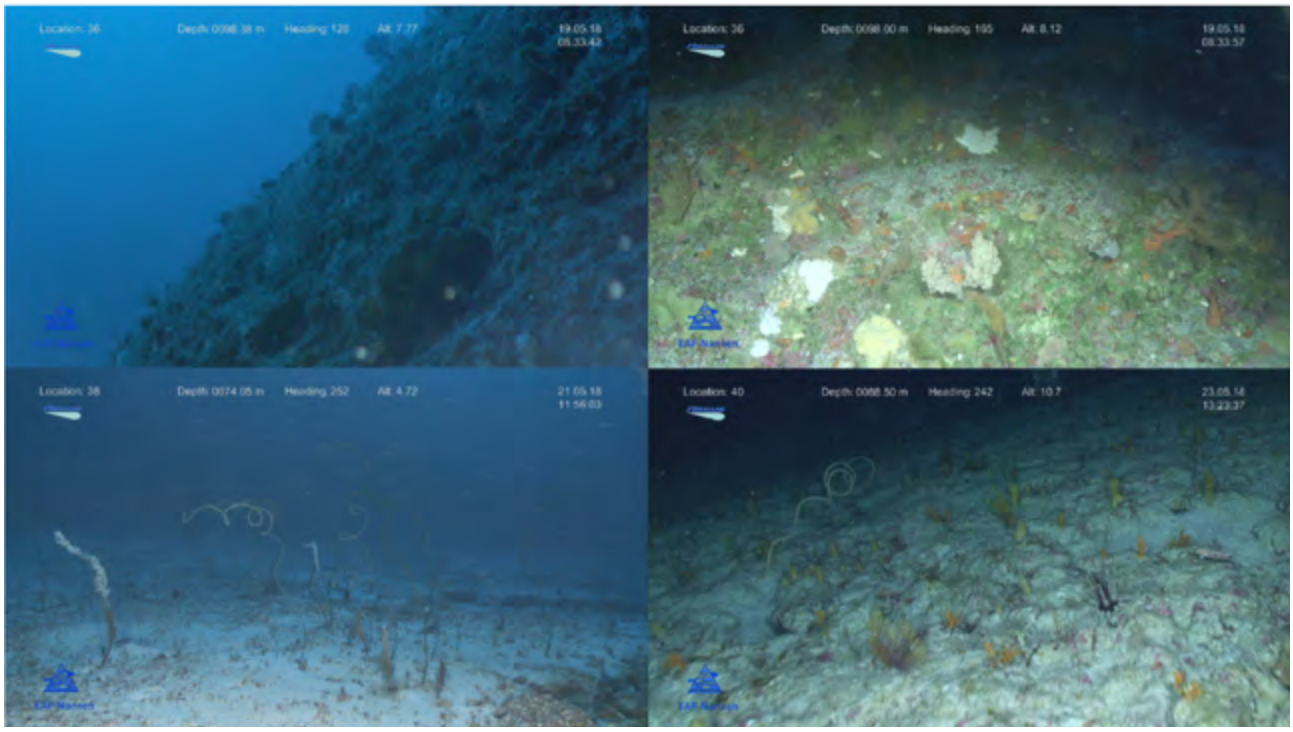

Figure 9. Examples of multispecies coral and sponge gardens observed on margin of Saya de Malha Bank, in the eastern Locations denoted E1 and E2. Images are from 74 and 98 m. RV *Dr Fridtjof Nansen*, 2018.

spicules on the sand were present. Several representatives of Hexactinosida: *Aphrocallistes* (dead skeletons) and, likely *Farrea,* and several genera of Euretidae, were observed on bedrock habitats. These attach to the bottom directly by their base. Several specimens of *Pheronema* were also observed on both sandy and rocky substrata, and these have a wide tuft of anchorate spicules.

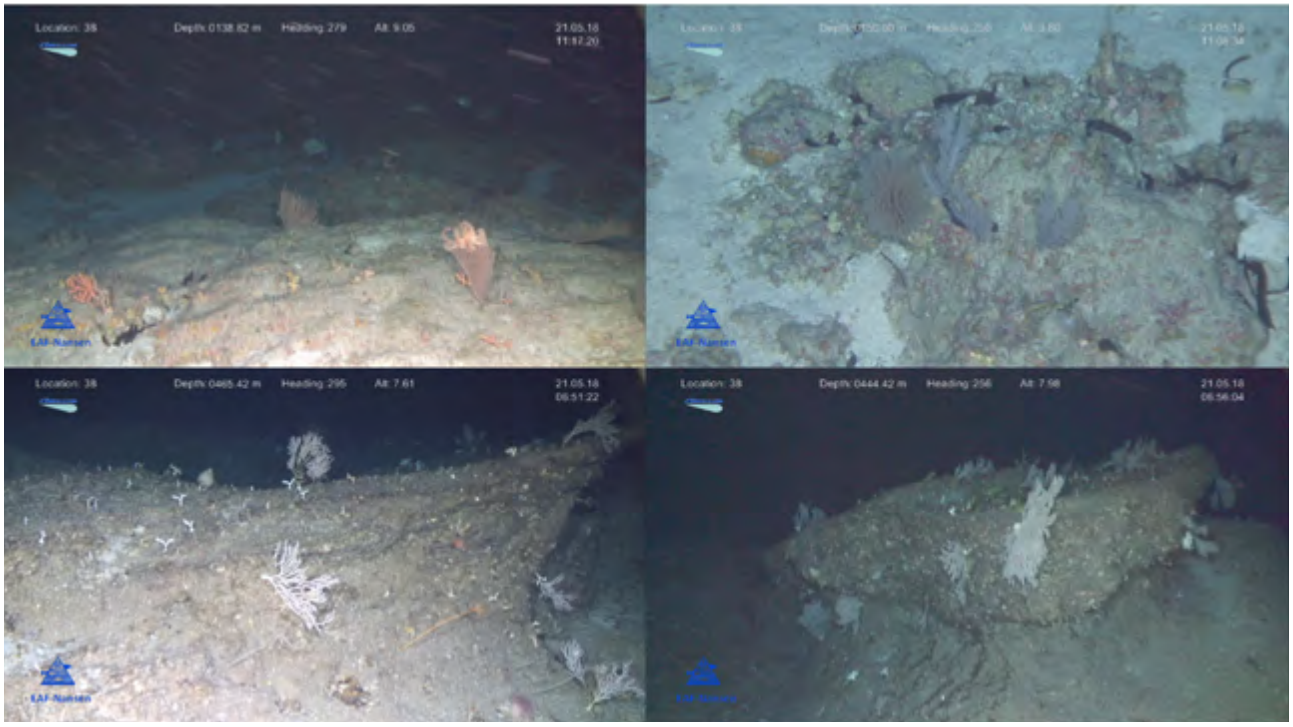

Figure 10. Examples of deep coral gardens observed on the slope of Saya de Malha Bank, in the Location denoted E1. The images are from 138 and 150 m (upper) and 465 and 444 m (lower). RV *Dr Fridtjof Nansen*, 2018.

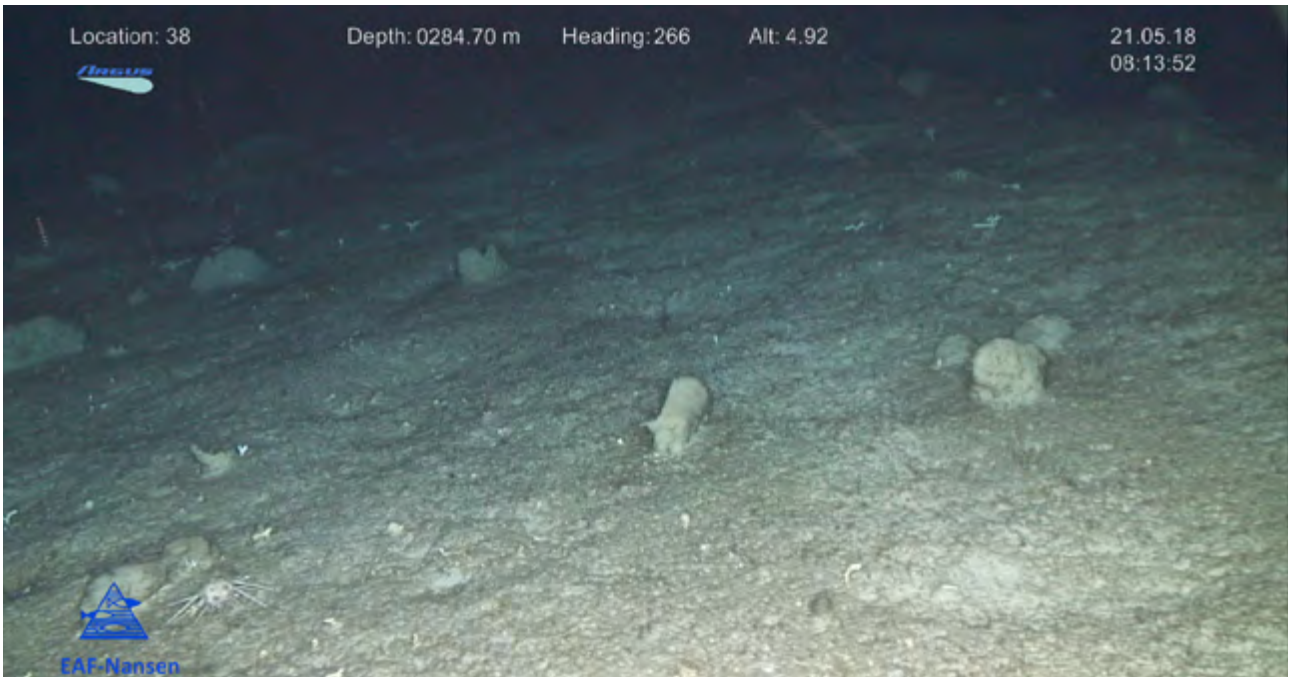

Figure 11. Aggregation of Demospongiae observed at 285 m on gravelly substrate in the northeastern slope location (E1, SS 38) on Saya de Malha Bank. RV *Dr Fridtjof Nansen*, 2018.

On the eastern slope, no reliable observations were made of hexactinellids adopted for life on sands. The specimens living on hard substrata were more diverse; numerous specimens of live *Aphrocallistes* together with *Farrea* and several genera of Euretidae at depth of 200-1000 m, Corbitellinae (likely *Corbitella*) at about 200 m, representatives of the family Rossellidae at <400 m. The only hexactinellids with anchorate type of fixation observed was *Pheronema* at about 200 m.

Echinodermata

Echinoidea and Crinoidea featured among the ten more frequently observed taxa, but Asteroidea and Holothuroidea were also common. Images of some of the echinoderms observed are provided in Figure A.

Table 4 lists taxa of holothurians, asteroids and echinoids identified to lowest possible level from best images and associated depth records. These data do not reflect abundance, only best identities of recurring taxa. All the crinoids observed were stalkless and identified as Comatulidae and at least two morphospecies occurred in the area.

Crustacea

Shrimps provisionally assigned to Caridea ranked amongst the ten most abundant taxa. It is probable, however, that these records included both Caridea and Penaoidea. Images of recurring morphospecies are shown in Figure A d). Less common taxa were Anomura (hermit crabs, squat lobsters, and lithodoid crabs) and Brachyura (primarily specimens noted as *Chaceon* sp.). Only four burrowing lobsters were observed, three Achelata and one Astacidea (Fig. A e).

Mollusca

Bivalvia were not prominent in the observations other than in one location, i.e. the E2 (SS40) where an aggregation was seen at 87 m (Fig. A f). At least three morphospecies of cephalopods occurred (Fig. A f).

Ctenophora

The sessile ctenophore *Lyrocteis* sp. occurred in the two western slope locations attached to the seabed and various erect organisms (e.g. hexactinellid sponges, alcyonaria) (Fig. A f). The depth range of the records was 220-285 m.

Pisces

Fish occurred in all depth zones and locations, and representatives of 49 families were observed. However, about 40 % of the records could not confidently be assigned to a family, mainly because they were not examined closely enough or occurred too briefly to be identified. All the fish not assigned to family were teleosts and recorded as 'unidentified Teleostei'.

Cartilaginous fishes were uncommon and contributed 5.3 % to the standardised abundance records for all

Table 4. Echinodermata records from Saya de Malha Bank. Identities and depth records of taxa for which good images were extracted from videos. RV *Dr Fridtjof Nansen*, 2018.

Order	Family	Species	Location and depth of observation, m				
Holothuriodea:			**SS33**	**SS35**	**SS36**	**SS38**	**SS40**
Synallactida	Stichopodidae	Stichopus sp. (*Stichopus pseudohorrens*?)			*55*		
Holothuriida	Holothuriidae	*Holothuria (Halodeima) edulis?)*					73
Holothuriida	Holothuriidae	*Actinopyga obesa?*					74
Holothuriida	Holothuriidae	*Holothuria (Halodeima) edulis*?)					74
Holothuriida	Holothuriidae	*Actinopyga ?*					*75*
Holothuriida	Holothuriidae	*Holothuria (Halodeima) edulis*?)					82
Holothuriida	Holothuriidae	*Holothuria (Halodeima) signata?)*					88
Holothuriida	Holothuriidae	*Holothuria* sp.					293
Synallactida	Synallactidae	Synallactidae gen. sp.1			*573*		
Synallactida	Deimatidae	*Oneirophanta* sp.?			608		
Synallactida	Synallactidae	Synallactidae gen. sp.2		759			
Synallactida	Deimatidae	*Oneirophanta* sp.?			797		
Elasipodida	Pelagothuriidae	*Enypniastes eximia*			884		
Persiculida		*Benthothuria* sp.			906		
Asteroidea:							
Valvatida	Ophidiasteridae	Ophidiasteridae gen. sp.	82				
Valvatida	Goniasteridae	Goniasteridae gen. sp.1		126			
Forcipulatida	Asteriidae	*Coscinasterias* sp.?		136			
Brisingida		Brisingida fam. Ind.1				136	
Forcipulatida	Pedicellasteridae			157			
Brisingida		Brisingida fam. Ind.1				158	
Valvatida	Oreasteridae?	Oreasteridae gen.sp.?		169			
Forcipulatida	Asteriidae	*Coscinasterias* sp.?				170	
Forcipulatida	Asteriidae	*Coscinasterias* sp.?				*175*	
Brisingida				198			
Notomyotida	Benthopectinidae	Benthopectinidae gen.sp.					243
Paxillosida	Astropectinidae	Astropectinidae gen. sp.	268				
Velatida	Pterasteridae	*Hymenaster* sp.	292				
Forcipulatida	Asteriidae	*Coscinasterias* sp.?		300			
Spinulosida	Echinasteridae	*Henricia* sp.					772
Echinoidea:							
Spatangoida					77		
Cidaroida					81		
Cidaroida							88
Cidaroida							89
Cidaroida							93
Cidaroida							94
Cidaroida							97
Cidaroida							100
subclass Euechinoidea				102			
Cidaroida	Cidaridae	*Prionocidaris ?*		102			
Cidaroida							102
Cidaroida	Cidaridae	*Prionocidaris ?*		103			
Superorder Echinacea				106			
Cidaroida				117			
Cidaroida				118			
Diadematoida	Diadematidae	*Astropyga radiata*		126			
Cidaroida						192	
Clypeasteroida	Clypeasteridae	*Clypeaster ?*			260		
Cidaroida						287	
Cidaroida							293
Cidaroida				348			
Cidaroida						358	
Cidaroida						440	
Echinothurioida	Echinothuriidae				798		
Echinothurioida	Phormosomatidae	*Phormosoma bursarium*			886		
Echinothurioida	Echinothuriidae	*Sperosoma* sp.			909		

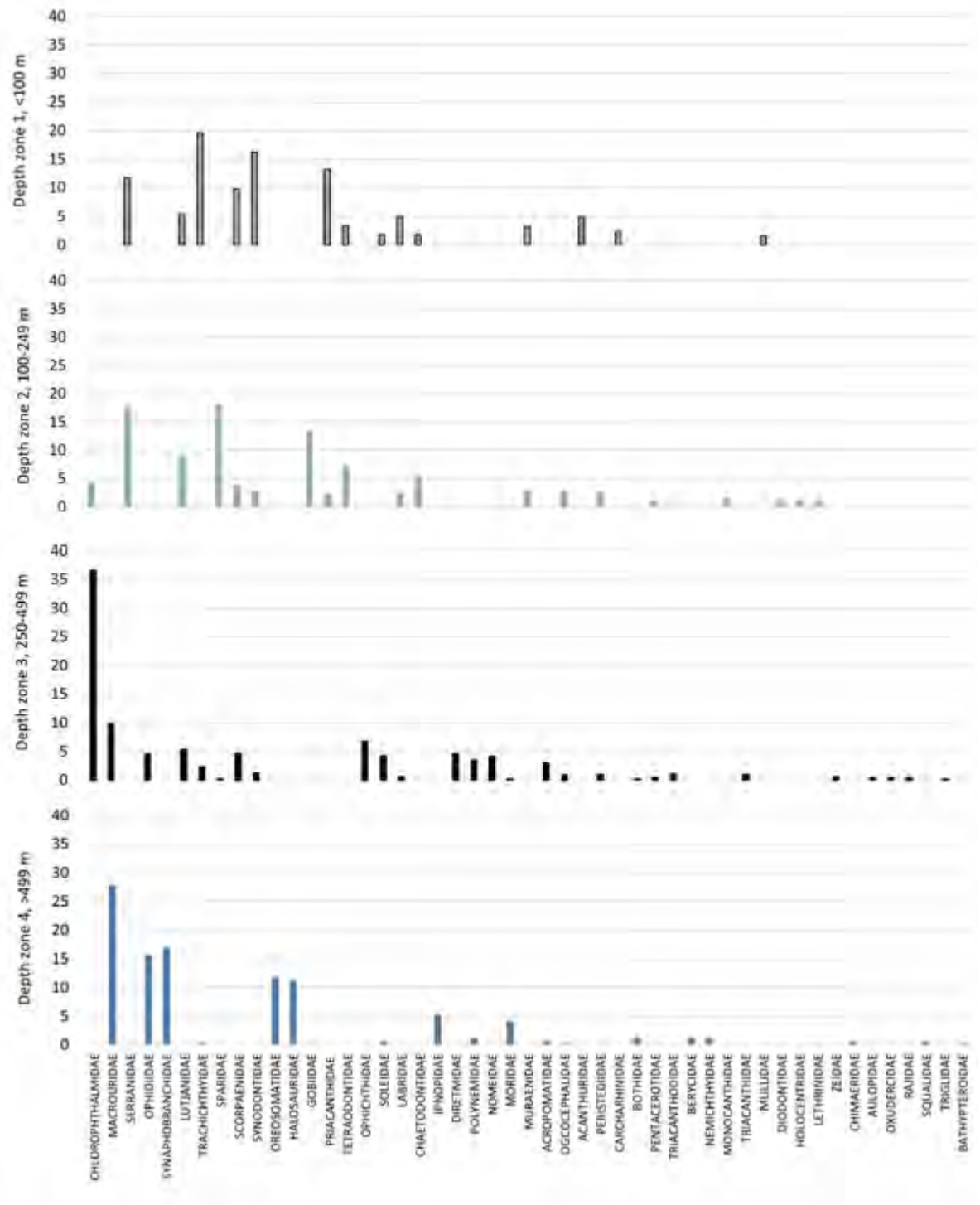

Figure 12. Fish families observed by ROV on the upper slopes of the Saya de Malha Bank, by depth zones. Compositions were derived by summing for each depth zone across the five study locations the standardised numbers observed, disregarding observations assigned to 'Unidentified Teleost'. Families are ordered from left to right according to declining total abundance in the entire study area. RV *Dr Fridtjof Nansen*, 2018.

depth zones and locations, reflecting sharks assigned to Squalidae and Carcharhinidae and some not assigned to family, a single Rajidae, and a single Chimaeridae. Apart from the single carcharhinid specimen, which was probably a silvertip shark (*Carcharhinus albimarginatus*) observed in Depth zone 1 (Location W2) at 77 m, all other observations of cartilaginous fishes were made in Depth zones 3 and 4.

Amongst the 45 teleost families, Chlorophthalmidae and Macrouridae were the most abundant with 70 and 64 records (12 and 11 % of the fish records identified

to family, respectively). Families with 20-35 records were Serranidae, Ophidiidae, Synaphobranchidae, Lutjanidae, Trachichthyidae, Sparidae, Scorpaenidae, Synodontidae and Oreosomatidae. Some additional deepwater families such as Moridae, Halosauridae, and Ipnopidae were relatively frequently observed in the deepest areas.

The data were too sparse to compare fish abundance or family composition between the five slope locations. Pooling the data for all locations, some depth-related patterns emerged (Fig. 12). Macrourids were confined to Depth zones 3 and 4, and the Chlorophthalmidae to Depth zones 2 and 3. Figure 12 suggests that there may be a transition from the shallow plateau-associated fish assemblage, to a 'shelf-break' assemblage where the Chlorophthalmidae are prominent, and then to a deepwater fish assemblage from about 500 m with Macrouridae and other deep-sea families.

Images of some of the fishes observed are provided in Appendix Figure A f)-j) with, when available, more details on identity. The images were sorted by depth of occurrence from shallow to deep. While abundance appeared low at all depths, fish were consistently present in all habitats. Schooling Carangidae were observed in a few instances, as was aggregations of Sparidae associated with crevices. The Chlorophthalmidae were widespread and abundant and likely to be *Chlorophthalmus agassizi*.

In the two deepest depth zones representing the upper slope of the bank, at least seven morphospecies of Macrouridae were observed, probably two Ipnopidae, and one or more Moridae, Ophidiidae, Synaphobranchidae and Halosauridae. Only very few and seemingly solitary specimens of Trachichthyidae, probably *Hoplostethus atlanticus*, and Oreostomatidae, probably *Neocyttus acanthorhynchus,* were observed. Meso-and bathypelagic families were not included here because they were not recorded consistently.

Discussion

This study constitutes a first attempt to characterize the macro- and megafauna of the upper slopes of the Saya de Malha Bank, and it was not exhaustive. The VAMS vehicle used could only collect van Veen grab samples, and trawling was not permitted in the area. By reducing the influence of vessel motion and waves, the vehicle used in towed mode proved a good platform for lightweight ROV operations. However, using video imagery as the sole source of information constrained the study in several ways. Identification of organisms are tentative based on images alone, hence the taxonomical resolution remained low. The lack of scaling lasers on the ROV prevented recording of sizes of organisms, and it was also difficult to fully control key observation parameters such as distance to seabed, speed, and direction influencing observation volume and area. The investigation should therefore be regarded as an initial exploration. Specifically, the information provided on abundance patterns, standardized only by observation time, is therefore only indicative. Some main patterns of taxonomical composition and abundance still emerged but should be investigated in greater detail and with improved quantification methods in future studies.

Substrates were characterized visually and this may be acceptable for hard-bottom areas but less so for soft substrates. Studies of grab samples are needed to characterize soft substrates and to provide more insight into mineralization and consolidation processes. The impression from video data and scattered attempts to sample soft substrates was that the slopes had relatively little soft substrates. What appeared as sand may be rather consolidated sands with little loose material. Muddy areas were not observed on the slopes.

As expected, the abundance of organisms declined somewhat with depth and there was also a rather clear change in the composition of fauna (and flora) with depth from the deepest to shallowest areas observed. The deep occurrence of seagrass leaves down the slope illustrates an import of material from the adjacent inner parts of the bank which have extensive seagrass meadow patches. The occurrence of coral gardens and *Lithothamnion* beds along the margin, most pronounced in the eastern and northern transects, was a prominent feature. Demospongiae beds were uncommon, but in deeper areas hexactinellid sponges were ubiquitous and conspicuous.

The northern and eastern transects had more bare rock and consolidated sandy substrate that the western locations, and the abundance of suspension-feeding taxa was also highest in the east and north. This is an indication that the conditions for suspension feeders are better in areas most exposed to the main westwards-flowing prevailing currents.

Based on trawl data from depths shallower than the 500 m isobath collected in 1976 and 1977, Vortsepneva and Spiridonov (2008) provided a few comments on upper slope features. It is difficult to compare

species lists between trawls and video observations. They noted that "Immovable sestonfeeders as a spongy, bryozoans and tunicate dominate in the slopes. East slope inhabits horny coral (Gorgonaria) that needs strong current. Abrupt change of assemblage can be observed on the border between slope and bottom." Although the data cannot be compared directly, these comments based on catch records correspond to some degree with the video observations from the present study.

The diversity of organisms was considerable but probably not high except in the shallowest slope locations. Conclusions on diversity are obviously tentative due to the low taxonomical resolution of the observations. The prominence of a few key taxa such as cnidarians, fish, echinoids and shrimps/prawns is probably not unexpected. It was somewhat surprising that 49 fish families occurred in the area, and the diversity may be quite high, partly reflecting the sampling of a range of assemblages from the margin of the bank to 1000 m depth.

Future studies should apply more quantitative approaches to study abundance patterns in greater detail and with higher confidence. Methods facilitating improved taxonomical resolution will be needed, also technology to obtain physical samples of organisms. That would permit stronger analyses and conclusions on abundance and diversity patterns. The videos and data from this investigation are kept by the EAF-Nansen contract partner (the Joint Management Area Commission), and by the Norwegian Marine Data Centre of the Institute of Marine Research. The results and data will contribute to future biodiversity assessments.

Acknowledgements

The paper is a contribution to the project entitled "Characterizing the Marine Ecosystem and Morphology of the Saya de Malha Bank" submitted to the FAO EAF-Nansen Programme in February 2017 by the Department for Continental Shelf, Maritime Zones Administration & Exploration, Prime Minister's Office, Mauritius on behalf of the Joint Management Area Commission. The project is referred to as NORAD-FAO PROJECT GCP/INT/730/NOR, and co-operating partners were multiple institutions in Mauritius and the Seychelles and the Institute of Marine Research, Norway, operating the RV *Dr Fridtjof Nansen*. The project is particularly grateful to the Benthos Laboratory of the PP Shirshov Institute of Oceanology, Moscow, for liaising with experts on selected taxa: Nadezhda and Karen Sanyaman (Kamchatka Branch of Pacific Geographical Institute, Far-Eastern Branch of the Russian Academy of Sciences, Petropavlovsk-Kamchatsky, Russia), Yves Samyn (Royal Belgian Institute of Natural Sciences, Brussels, Belgium), Dhugal Lindsay (Japan Agency for Marine-Earth Science and Technology, JAMSTEC). Peter Psomadakis at FAO assisted with fish identification. We thank the crew and VAMS technicians on the RV *Dr Fridtjof Nansen* for excellent efforts during the 2018 expedition. The following participants on the expedition are gratefully acknowledged: D Bissessur, K Sauba, J Rama, P Coopen, Y Oozeeraully, S Seeboruth, A Audit-Manna, A Nicolas, N Reetoo, D Kuyper, S Hollanda, R Melanie, J Harlay, M. Soondur, L Caussy and TM Ensrud.

References

Buhl-Mortensen L, Serigstad B, Buhl-Mortensen P, Olsen MN, Ostrowski M, Błażewicz-Paszkowycz M, Appoh E (2017) First observations of the structure and megafaunal community of a large *Lophelia* reef on the Ghanaian shelf (the Gulf of Guinea). Deep Sea Research Part II: Topical Studies in Oceanography 137: 148-156

FAO (Food and Agriculture Organization of the United Nations) (2009) International guidelines for the management of deep-sea fisheries in the high seas. FAO Fisheries Department, Rome. [http://www.fao.org/fishery/topic/166308/en]

Kyewalyanga M (2015) Phytoplankton and primary production. pp 213-230 in: UNEP-Nairobi Convention and WIOMSA. The Regional State of the Coast Report: Western Indian Ocean. UNEP and WIOMSA, Nairobi, Kenya. 546 pp

Harris SA, Noyon M, Francis M, Vianello P, Roberts MJ (2020) Ichthyoplankton assemblages at three shallow seamounts in the South West Indian Ocean. In: Payne A, Roberts M, Marsac F, Noyon M, Ternon J-F (eds) Bio-physical coupling around three shallow seamounts in the South Western Indian Ocean, with regional comparisons based on modelling, remote sensing and observational studies. Deep-Sea Research Part II: Topical Studies in Oceanography 176, art: 104809, 1-15 ISSN 0967-0645

Strømme T, Ansorge I, Bornman T, Kaehler S, Ostrowski M, Tweddle D, Alvheim O (2009). 2008 ASCLME SURVEY NO. 3 FAO PROJECT CCP/INT/003/NOR Cruise reports "Dr. Fridtjof Nansen" EAF-N2008/7. 58 pp

Serigstad B, Ensrud TM, Olsen M, Ostrowski M, Adu-Kumi S, Akoto L, Aggrey-Fynn J, Blazewicz-Paszkowycz M, Jozwiak P, Pabis K, Siciński J (2015) Environmental monitoring Ghana 2012, chemical and biological analysis. NORAD – FAO PROJECT

GCP/003/NOR SURVEY REPORT R/V Dr. FRIDTJOF NANSEN EAF – N/2012/7. 163 pp

Schott FA, Shang-Ping X, McCreary Jr JP (2009) Indian Ocean circulation and climate variability. Reviews in Geophysics 47: RG1002 [doi:10.1029/2007RG000245]

Vianello P, Ansorge IJ, Rouault M, Ostrowski M (2017) Transport and transformation of surface water masses across the Mascarene Plateau during the Northeast Monsoon season. African Journal of Marine Science 39: 453-466

Vortsepneva E, Spiridonov V (2008) Saya de Malha –an invisible island in the Indian Ocean. Review of historical surveys of environmental conditions and biodiversity. Report to the Lighthouse Foundation, Moscow, Russia. 42 pp

Appendix

Figure A. Selected images of invertebrates and fish extracted from video records from Saya de Malha Bank. SS-superstation. RV *Dr Fridtjof Nansen*, 2018. a) Cnidaria (from left to right, top to bottom): Zoantharia, possibly genus *Epizoanthus* (SS33, 728 m), Hydrozoa *Stylaster cf. subviolacea* (SS40, 877 m), Hydrozoa (top white colony) and Alcyonacea (with crab) (SS35, 379 m), Alcyonacea *Narella* sp. (SS40, 774 m), Alcyonacea *Anthomastus* sp. (SS40, 237 m), Scleractinia *Caryophyllia* sp. (SS38, 180 m), Alcyonacea *Chrysogorgia* sp. (SS40, 848 m), Alcyonacea *Acanthogorgia* sp. (SS40, 657 m), Alcyonacea *Alcyonium* sp. (SS40, 107 m), Pennatulacea *Pennatula* sp. (SS40, 75m), Antipatharia, *Cirripathes* sp. (two images from SS40, 271 and 108 m), Actiniaria *Sicyonis* sp. (SS40, 620 m), Actiniaria *Exocoelactis* sp. (SS40, 235 m), Hormathiidae (?) associated with hermit crab. (SS35, 400 m).

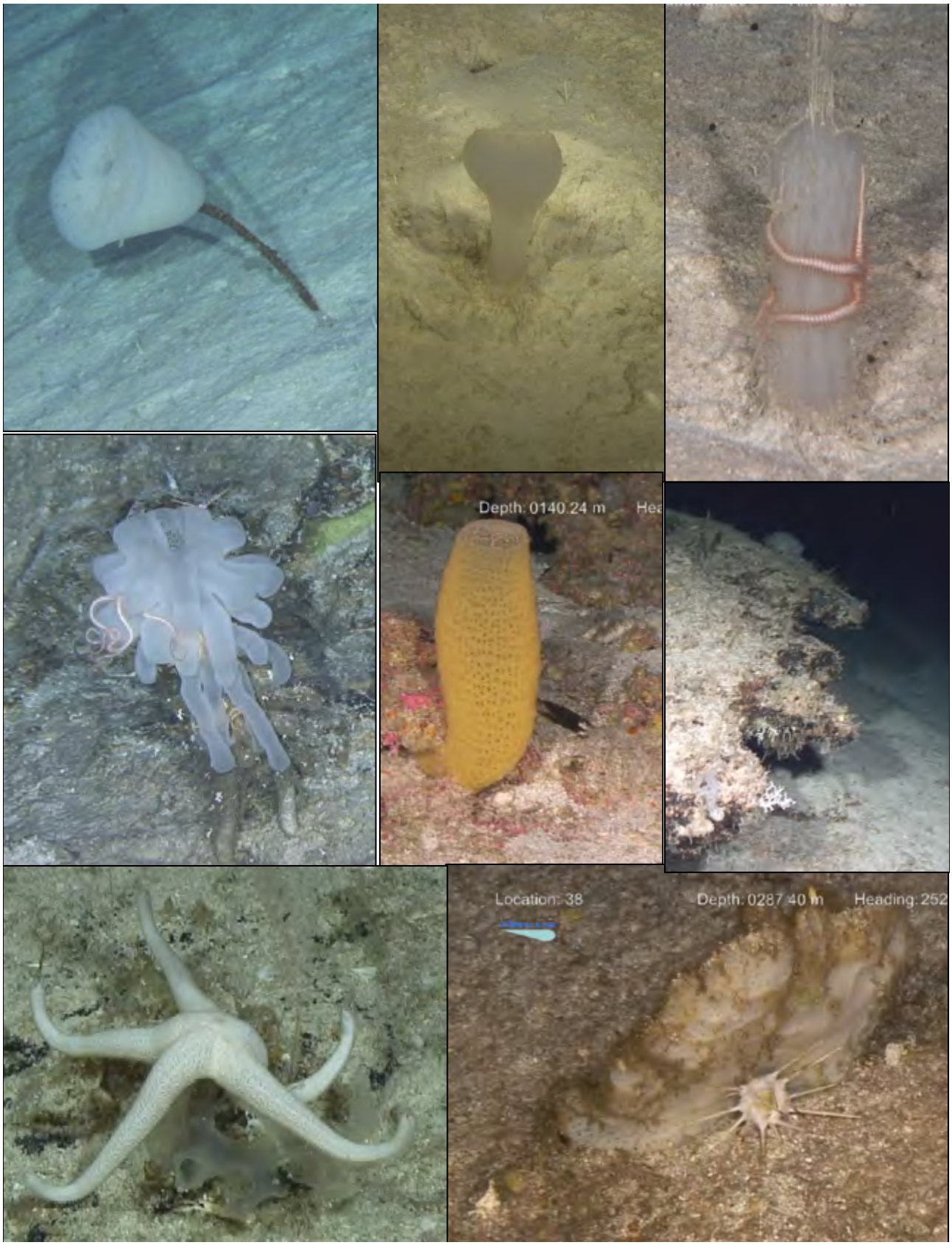

b) Porifera: hexactinellid sponge *Hyalonema* with zoantharia on anchorate spicules (SS 35, 765 m), hexactinellid, probably *Plathylistrum platessa* (SS 35, 995 m), hexactinellid, Pheronematidae (SS36, 990 m) with ophuiroid, hexactinellid, *Aphrocallistes beatrix* (SS38, 464 m), hexactinellid *Corbitellinae* (SS38, 140 m), hexactinellid *Farraea* (SS40, 710 m), asteroid (*Henricia* sp.) climbing on the hexactinellid *Farrae* (SS40, 772 m), Demospongiaa, Tetractinomorpha (SS38, 287 m).

c) Echinodermata: Asteroidea: *Hymenaster* (?) (SS33, 292 m), Astropectinidae (SS33, 268 m), Ophidiasteridae (SS33, 82 m), *Coscinasterias* sp.(?) (SS35,136 m), *Coscinasterias* sp. (?) (SS35, 136 m), Benthopectinidae (SS40, 243 m), Brisingida (SS35, 198 m), Brisingida (SS38, 136 m); Crinoidea: Order Comatulida (SS40, 74 m), Comatulida (SS40, 302 m), Comatulida (SS40, 80 m); Holothuroidea: Synallactidae (SS35, 760 m), juv. Stichopodidae? (SS40, 74 m), *Oneirophanta* sp.? (SS36, 797 m), *Enypniastes eximia* (SS36, 884 m).

d) Echinodermata continued, and Crustacea: Echinoids of order Cidaroida (SS35, 349m), order Cidaroida (SS35, 117 m), order Cidaroida, *Prionocidaris* (SS35, 103 m), *Astropygia radiata* (SS35, 127 m), *Phormosoma bursarium* (SS36, 886 m), superorder Echinacea (SS35, 106 m), *Sperosoma* sp. (SS36, 909 m), order Spatangoida (SS36, 77 m), Clypeaster (?)(SS36, 260 m); Ophiuroidea: indet. (SS35,304 m); Crustacea: Decapod shrimps (Dendrobranchiata and Pleocyemata) from SS 35 (751, 381 m), SS33 (705 m, 670 m), SS36 (873 m, 926 m).

e) Crustacea, Decapoda: Astacidea, Nephropoidea (*Acanthacaris* sp.?) (SS33, 757 m), Achelata (Palinuridae) (SS40, 94 m), Brachyura *Chaceon* sp. (SS38, 512 m and SS 36, 895 m), Anomura, Lithodoidea (SS33, 758 m and SS40, 624 m), Anomura, Paguroidea (SS35, 309 m), Anomura, Galatheoidea (SS35, 382 m).

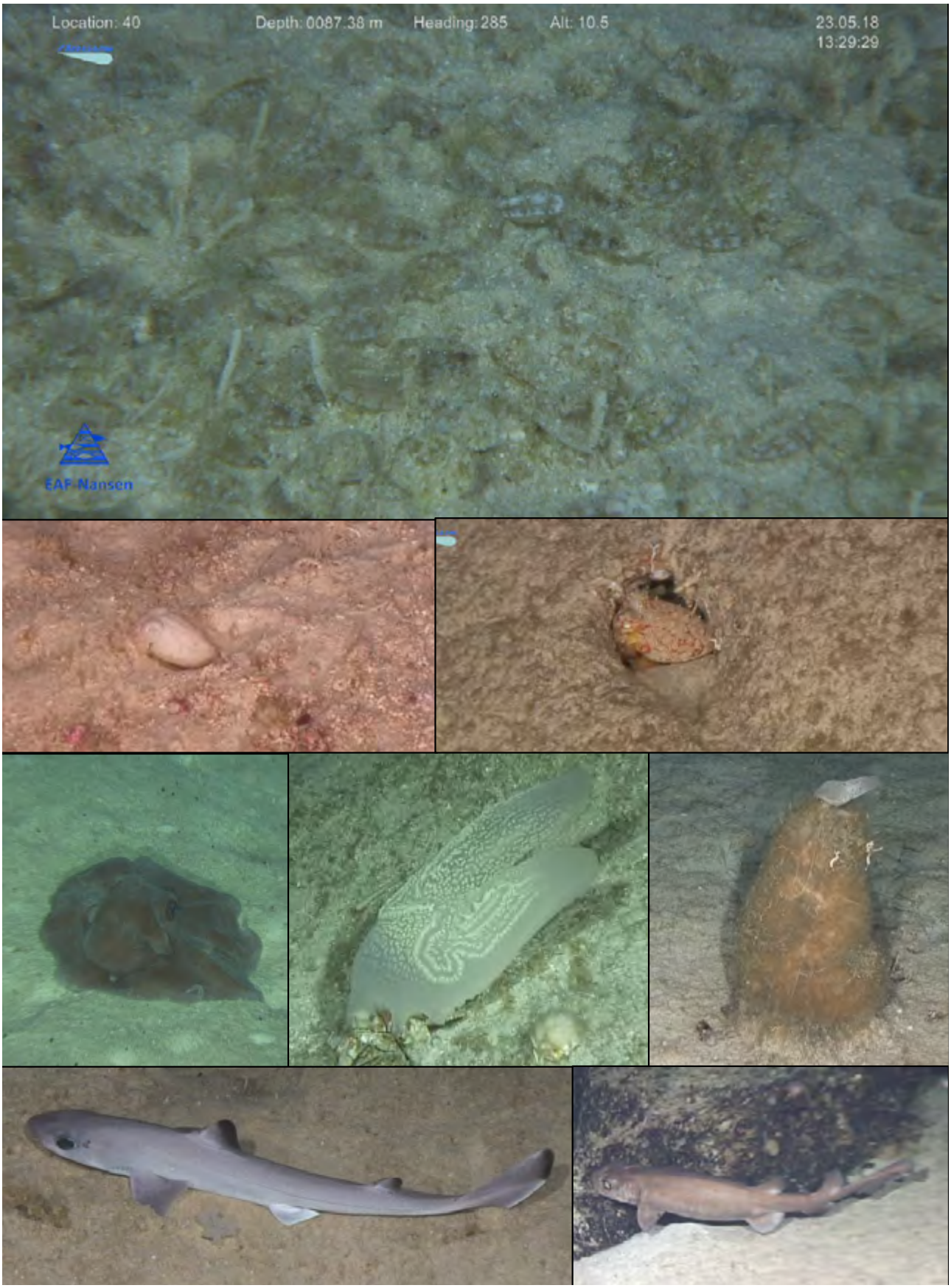

f) Mollusca: Bivalvia (SS40, 87 m), Cephalopod1 (SS40, 67m), Cephalopod2 (SS33, 274 m), Cephalopod3 (SS36, 904 m); Ctenophora: *Lyrocteis* sp. (SS35, 238 m), Ctenophora on top of hexactinellid sponge (SS33, 285 m); Pisces: Squalidae (SS40, 519 m) and indet. (SS40, 651 m).

g) Pisces continued: Sparidae, *Polysteganus* sp. (SS35, 198 m), Sparidae (SS36, 100 m), Peristediidae (SS35, 183 m), Peristediidae (SS36, 376 m), Muraenidae (SS35, 186 m), Tetraodontidae (SS38, 196 m), Tetraodontidae (SS40, 74 m), Mullidae (SS40, 74 m), Priacanthidae (SS38, 190 m), Serranidae, *Epinephelus aenus* (?) (SS38, 146 m).

h) Pisces continued: Carangidae, *Seriola rivoliana* (SS38, 107 m), Priacanthidae (SS40, 97 m), Lutjanidae (SS38, 72 m), Scorpaenidae (SS 40, 79 m), Scorpaenidae (SS40, 83 m), Synodontidae (SS40, 104 m), Chlorophthalmidae, *Chlorophthalmus* sp. (SS35, 384 m); same from SS35, 352 m; same from SS35, 356 m, Acropomatidae (SS38, 342 m), Ophichtiidae (SS33, 449 m), Bothidae (SS 33, 500 m).

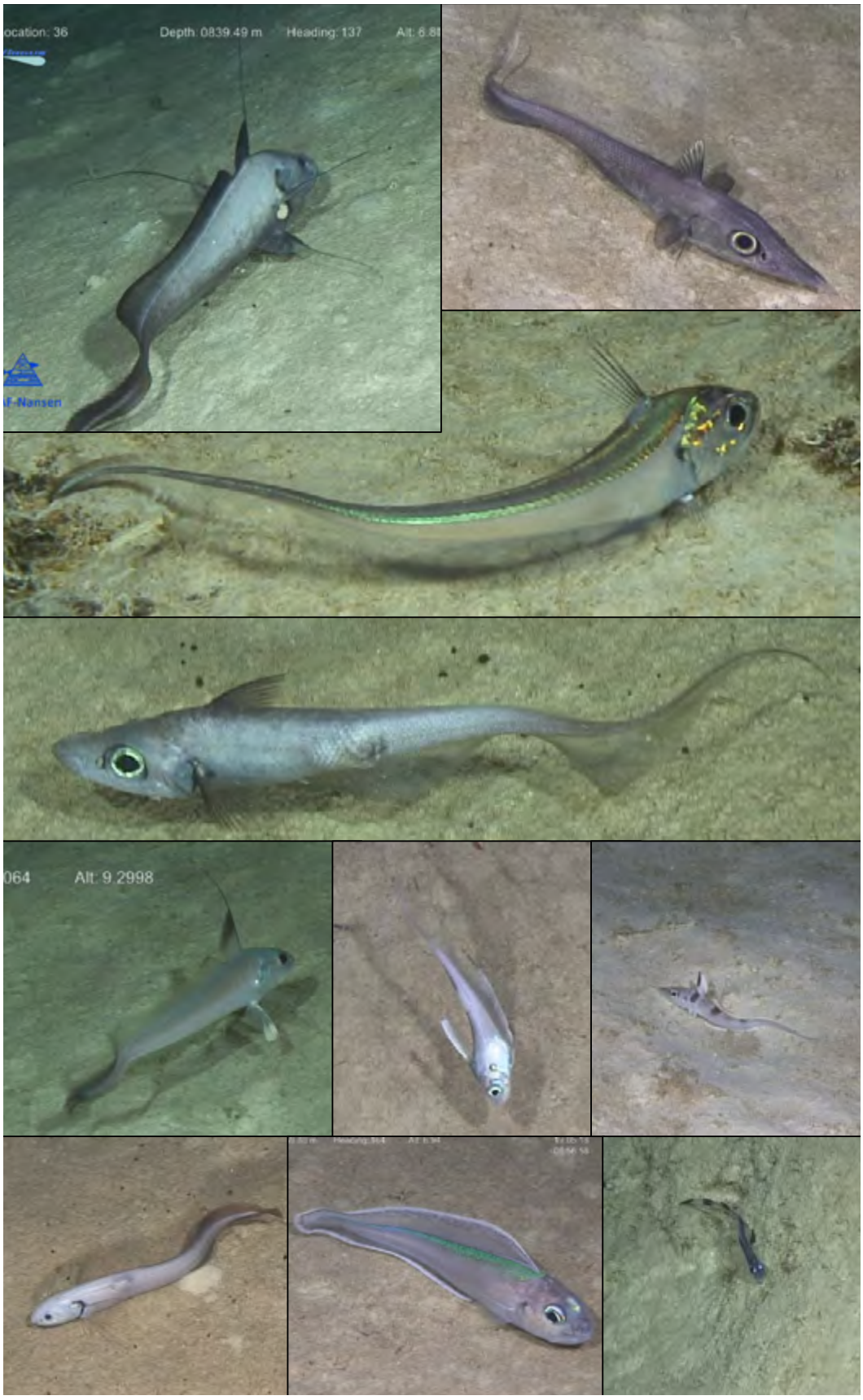

i) Pisces continued, deepwater assemblage: Macrouridae1 (SS36, 840 m), Macrouridae2 (SS33, 657 m), Macrouridae3 (SS36, 890 m), Macrouridae4 (SS36, 526 m), Macrouridae5 (SS33, 701 m), Macrouridae6 (SS36, 557 m), Macrouridae7 (SS33, 505 m), Moridae (SS36, 872 m), Ophidiidae (SS36, 559 m), Ophidiidae (SS36, 501 m).

j) Pisces continued, deepwater assemblage: Synaphobranchidae (SS36, 734 m; SS36, 870 m), Halosauridae (SS36, 930 m; SS36, 833 m), Trachicthyidae, probably *Hoplostethus atlanticus* (SS36, 567 m), Oreostomatidae, *Neocyttus acanthorhynchus* ? (SS36, 785 m), Ogcocephalidae (SS36, 663 m), Ipnopidae (SS36, 940 m), Ipnopidae (SS33, 710 m).

Pelagic and demersal fish diversity of the Saya de Malha and Nazareth Banks, Mascarene Plateau

Luvna Caussy[1]*, Rodney Melanie[2], Andrew Souffre[2], Stephanie Hollanda[2], Magne Olsen[3], Gilberte Gendron[4,5], Sundy Ramah[1,6]

[1] Albion Fisheries Research Centre, Ministry of Blue Economy, Marine Resources, Fisheries & Shipping, Albion, Petite-Rivière, 91001, Republic of Mauritius

[2] Seychelles Fishing Authority, Fishing Port, PO Box 149, Victoria, Mahé, Seychelles

[3] Institute of Marine Research (IMR), PO Box 1870 Nordnes, N-5817 Bergen, Norway

[4] Island Biodiversity & Conservation Centre, University of Seychelles, PO Box 1348, Anse Royale, Mahé, Seychelles

[5] Seychelles National Parks Authority, PO Box 1240, Orion Mall, Victoria, Mahé, Seychelles

[6] Department of Biosciences & Ocean Studies, Faculty of Science & Pole of Research Excellence in Sustainable Marine Biodiversity, University of Mauritius, Reduit 80837, Republic of Mauritius

* Corresponding author: luvna_caussy@yahoo.com

Abstract

The Saya de Malha (SMB) and Nazareth Banks (NB) are the main offshore locations where fishing activities are carried out by the Republic of Mauritius, targeting mainly shallow water Lethrinids, deep-water snappers and groupers. A multi-disciplinary survey was carried out on the two banks in May 2018 on-board the R/V Dr. Fridtjof Nansen with the objective of studying the diversity of fish on both banks using pelagic trawls, bottom trawls, basket traps and video using a Remotely Operated Vehicle (ROV). Analysis of data showed that the main fish family recorded in the pelagic waters of SMB, using pelagic trawl, was Myctophidae while the bottom trawls on NB showed the presence of fishes from the families Gobiidae, Triglidae and Synodontidae, mainly at depths between 200 and 300 m. The ROV video analysis highlighted principally the presence of demersal fishes of the family Lethrinidae and other reef-associated and commercial families recorded between 20 and 50 m. The main catch from the basket traps set at the SMB was *Lethrinus mahsena*, caught at a depth of 21 m. While previous studies focussed mainly on commercial fishes, this study brings forth new information on other fish families, contributing to the knowledge of the fish community that exists at these two banks.

Keywords: fish diversity, Saya de Malha Bank, Nazareth Bank, trawls, VAMS, basket traps

Introduction

The Republic of Mauritius, being a coastal state, has an Exclusive Economic Zone (EEZ) that extends from the islands of Mauritius, Rodrigues, Cargados Carajos Shoals, Agalega, Tromelin and Chagos Archipelago (United Nations, 1993), covering a total surface area of 2.3 million km^2. In March 2011, the United Nations Commission on the limits of the Continental Shelf conferred upon the Republic of Mauritius and the Republic of Seychelles an extended continental shelf, of area 396,000 km^2, also known as the Mauritius-Seychelles Joint Management Area (United Nations, 2018a, 2018b). The Saya de Malha Bank (SMB) and the Nazareth Bank (NB) are situated some 650 km and 1050 km from Mauritius island, respectively (Samboo and Mauree, 1987). NB is characterised by a shallow central part of about 50-60m deep with a sandy bottom, and surrounded by a sloping rim to around 150 m followed by an abrupt outer slope (Mees, 1996), while SMB consists of narrow shoals (depths range between 17 to 29 m on the rim) and slopes on all side of the bank (New *et al.,* 2013).

Fishery resource exploitation in the shallow waters of the SMB and NB occurs mainly from industrial refrigerated vessels (length range of vessel: 35-50 m) and

http://dx.doi.org/10.4314/wiojms.si2021.2.11

semi-industrial boats (length range of boats: 13-24 m) at depths of around 20-50 m (Ministry of Fisheries and Rodrigues, 2011). In 2018, there were four active industrial fishing vessels and 23 active semi-industrial fishing boats operating on both banks (AFRC, 2018; unpublished data). About 90% of the fish catch from the shallow waters of the banks comprises of the sky emperor *Lethrinus mahsena* (Forsskål, 1775), while the rest consists mainly of other shallow water demersal fishes such as Serranids and other Lethrinids (Samboo, 1983; Samboo and Mauree, 1987; Mees, 1996, Degambur and Sólmundsson, 2005; Munbodh, 2012). Fishing activities are also carried out on the slopes of the banks, targeting mainly deep-water snappers and groupers, at a depth of 150 to 300 m (Degambur and Korsbrekke, 2011).

Marine survey expeditions have been carried out in the past mainly by the Russians to investigate the fishery resources and the oceanography aspects of the SMB during the 1960s and 1970s (Vortsepneva, 2008), while limited attention has been given to the NB. One such survey was carried out between 1975 and 1977 on-board the Research Vessel Professor Mesyatsev by the Food and Agriculture Organization (FAO) and the Ministry of Fisheries of the Soviet Union to investigate the pelagic and demersal fish resources on SMB and NB, (Birkett, 1979). The main pelagic species encountered on SMB during the survey were species of Carangidae including *Decapterus kiliche* (Cuvier, 1833), *Decapterus macarellus* (Cuvier, 1833) and *Trachurus indicus* Nekrasov, 1966. The main demersal species included *Etelis carbunculus* Cuvier, 1828 (Lutjanidae) from NB, and *Polysteganus* spp (Sparidae), *Saurida undosquamis* (Richardson, 1848), and *Nemipterus* spp.

In Vortsepneva's (2008) review of the Russian expeditions on SMB, the presence of ten families of fish were recorded from 10 to 1300 m depth; namely Carangidae, Trachichthyidae, Lethrinidae, Stromateoidei, Synodontidae, Nemipteridae, Sparidae, Chlorophthalmidae, Macrouridae and Chimaeridae. A British survey, the Percy Sladen Trust Expedition, was carried out in the Indian Ocean in 1905, and according to the report by Regan (1908), resulted in the description of 10 new fish species from the SMB, from families Macrouridae (described as Macruridae in the report), Oreosomatidae (described as Cyttidae in the report), Bothidae and Cynoglossidae (described as Pleuronectidae in the report), Synanceiidae (described as Scorpaenidae in the report), Hoplichthyidae, Triglidae, Ogcocephalidae (described as Malthidae in the report) and Tetraodontidae (described as Tetrodontidae in the report).

In 2006, through the Technical Cooperation Programme between the Government of Mauritius and the FAO, an acoustic survey was carried out on the slopes of St Brandon and Nazareth Bank. The aims of the survey programme were to determine the presence of deep-water demersal fishery resources, and the abundance and productivity of the resources (Boyer *et al*., 2006). The survey highlighted the presence of snappers and groupers, namely *Polysteganus baissaci* Smith 1978, *Etelis coruscans* Valenciennes, 1862, *Pristipomoides argyrogrammicus* (Valenciennes, 1832), *Pristipomoides auricilla* (Jordan, Evermann and Tanaka, 1927) and *Epinephelus morrhua* (Valenciennes, 1833). The results of the above surveys led to the regular exploitation of the deep-water resources at St Brandon and on the NB.

Most of the research carried out on fish diversity is dated and mainly limited to commercial fishery resources, while little is known about diversity of other fishes and their occurrence within these two banks. An expedition was carried out on-board the R/V Dr Fridtjof Nansen in May 2018, focusing on the regional resources and ecosystems of the Indian Ocean, with the main objective of characterizing the ecosystems and morphology of the SMB and NB (Bergstad *et al.,* 2018). This study is focussed on the pelagic and demersal fish diversity of the SMB and NB. While previous studies on fishery resources used bottom trawls as the main sampling method, this study brings forth additional data using four different sampling methods to determine diversity and occurrence at both banks.

Materials and methods

Study sites

The SMB and NB are both part of the Mascarene Plateau with the SMB being the larger bank with an area of approximately 40,000 km^2. The SMB is composed of two structures; the main Saya the Malha Bank in the south and the smaller bank in the north, also known as the Ritchie Bank. Data on fish was collected using the four methods of pelagic trawls, bottom trawls, basket traps and underwater video footage using a Video-Assisted Multi Sampler (VAMS) attached to a Remotely Operated Vehicle (ROV). Pelagic trawls were carried out at 10 stations at the SMB; namely PTS 1, PTS 2, PTS 3, PTS 4, PTS 5, PTS 6, PTS 7, PTS 8, PTS 9 and PTS 10, and two stations at NB; namely PTS 11 and PTS 12. Four bottom trawls were carried out at the NB only (BTS 1, BTS 2, BTS 3 and BTS 4). Basket traps were deployed at two stations at SMB; BT 1 and BT 2. Video seafloor exploration by the ROV in depths from

23-50 m was carried out at 10 predetermined stations on SMB; SS 4, SS 9, SS 13, SS 34, SS 36, SS 37, SS 38, SS 39, SS 40 and SS 42. (Table 1 and Fig. 1). Being large stations, SS 36, SS 37 and SS 39 were subdivided into SS 36-1, SS 36-2, SS 37-1, SS 37-2, SS 39-1, SS 39-2, SS 39-3 and SS 39-4, respectively.

mounted in a drop keel. The raw data from the EK80 was primarily obtained from the 38 kHz transducer and was treated with the KORONA software to reduce noise influence. Trawls were deployed to collect fish samples to identify scattering layers observed on echograms from the EK80 multi-frequency echo-

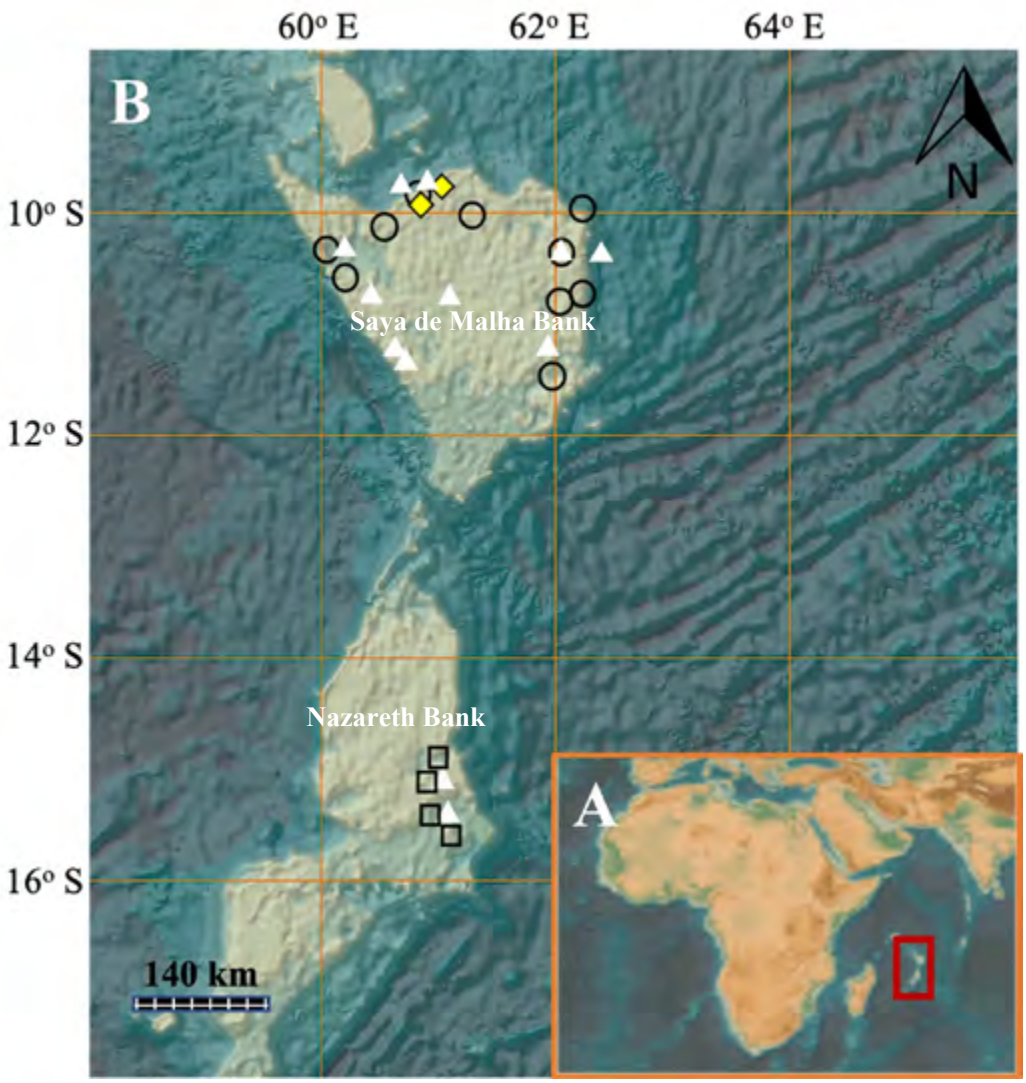

Figure 1. Map showing locations of stations for fish data collection from pelagic trawls (defined by △), bottom trawls (defined by □), basket traps (defined by ◇) and video ROV (defined by ○) from the Saya de Malha (SMB) and Nazareth Banks (NB). A: Western Indian Ocean map showing locations of Saya de Malha and Nazareth Banks within the red outlined rectangle. B: Map showing the 12 stations for pelagic trawls, four stations for bottom trawls, two stations for basket traps and the ROV stations. The map was generated using GEBCO Bathymetry Grid layer data 2020.

Sampling and identification

Pelagic and bottom trawling

The instrument used for observing sound-scatters within the water column was a single-beam multi-frequency sounder, namely the SIMRAD EK80 Scientific Split Beam Echo Sounders with 6 different transducers (18, 38, 70, 120, 200 and 333 kHz) sounder and were carried out on an ad-hoc basis due to scarcity of indications from echograms. Each trawl catch was first sorted to the lowest possible taxonomic level, and numbers and bulk weight of each taxon recorded. When the sorted catches were large, a sample of the catch was weighed and the number of specimens in the taxon recorded. This was then

Table 1. Station details for the pelagic trawls (PTS), bottom trawls (BTS), basket traps (BT) and Video (VAMS: Video-Assisted Multi Sampler) at Saya de Malha Bank (SMB) and Nazareth Bank (NB).

Bank	Fish Data Collection Method	Station	Latitude	Longitude
	Pelagic trawl	PTS 1	-10.7645	60.439667
	Pelagic trawl	PTS 2	-10.766333	61.086667
	Pelagic trawl	PTS 3	-11.216167	60.583667
	Pelagic trawl	PTS 4	-11.202667	60.507833
	Pelagic trawl	PTS 5	-10.422333	60.3475
	Pelagic trawl	PTS 6	-9.7503333	60.659333
	Pelagic trawl	PTS 7	-9.7955	60.825667
	Pelagic trawl	PTS 8	-10.383833	62.4235
	Pelagic trawl	PTS 9	-10.384167	62.0065
	Pelagic trawl	PTS 10	-11.091	61.677167
	Basket Trap	BT 1	-9.8771667	60.797333
	Basket Trap	BT 2	-9.8245	60.918167
	VAMS	SS 4	-10.113192	60.575226
Saya de Malha (SMB)	VAMS	SS 9	-10.427421	60.140288
	VAMS	SS 13	-10.732368	62.130394
	VAMS	SS 34	-10.625219	60.199550
	VAMS	SS 36-1	-9.831724	60.762377
	VAMS	SS 36-2	-9.859240	60.791336
	VAMS	SS 37-1	-10.094556	61.221217
	VAMS	SS 37-2	-10.092485	61.242757
	VAMS	SS 38	-10.062541	62.183355
	VAMS	SS 39-1	-10.382314	62.078151
	VAMS	SS 39-2	-10.381302	62.093671
	VAMS	SS 39-3	-10.379792	62.123875
	VAMS	SS 39-4	-10.377526	62.204940
	VAMS	SS 40	-10.736205	61.945050
	VAMS	SS 42	-11.676877	61.948717
	Pelagic Trawl	PTS 11	-15.243833	61.0465
	Pelagic Trawl	PTS 12	-15.491833	61.0215
	Bottom Trawl	BTS 1	-15.1835	61.146
Nazareth (NB)	Bottom Trawl	BTS 2	-15.348	61.023833
	Bottom Trawl	BTS 3	-15.508167	61.030667
	Bottom Trawl	BTS 4	-15.665333	61.018

extrapolated to obtain the estimated number (N) of individuals caught using the formula below:

$$N_i = \frac{W_i}{w_i}(n_i),$$

Where W_i is the total weight of the sorted species *i* obtained from the catch, w_i is the weight of the sample taken from species *i*, and n is the number of individuals obtained in the sample.

Preliminary identification of fish species was carried out through examination of morphometric and meristic characteristics using identification guides (e.g., FAO Identification sheets for fishery purposes: Western Indian Ocean Fishing Area 51, Food and Agriculture Organization, 1984). Species were identified to the lowest taxon possible and data from each trawl were inputted in the NANSIS Survey Information System, with corresponding catches. The catch rate per hour was expressed as weight/hour (W/hr) and as number of individuals caught per hour (N/hr):

$$W/hr = \frac{W_i}{t_i}(60)$$

$$N/hr = \frac{N_i}{t_i}(60),$$

Where t is the duration of the trawling activity in minutes.

Table 2. Gear depths, catch rate (kg/hr) and number of families obtained from each pelagic trawl station (PTS) on the Saya de Malha Bank (SMB) and Nazareth Bank (NB).

Bank	Trawl Station No.	Gear Depth (m)	Weight (kg)/hour	No. of families identified
Saya de Malha (SMB)	PTS 1	10 - 60	2.1	10
	PTS 2	0 - 30	520.6	7
	PTS 3	0 - 5	38.9	10
	PTS 4	0	41.5	14
	PTS 5	0	74.4	8
	PTS 6	150 - 420	11.3	10
	PTS 7	0 - 6	89.9	8
	PTS 8	0	91.3	12
	PTS 9	0	5.2	8
	PTS 10	0	37.1	8
Nazareth (NB)	PTS 11	0 - 10	0.5	2
	PTS 12	20 - 50	0.0	0

Basket traps

Bottom trawls were not allowed on the SMB. Attempts were therefore made to obtain data on demersal fish using different methods. A set of three collapsible traps were deployed at two stations in the shallow waters of SMB at 20 and 21 m deep within a seagrass and sandy bottom substrate. The set of traps were left for approximately six hours. The traps were then hauled and the catch was sorted and identified.

Remotely Operated Vehicle (ROV) videos

Video data was collected with the ROV which was attached to a video-assisted multi sampler (VAMS). Two exploration modes were used to record videos of the bottom environments. In the first method, the ROV was deployed in four directions (North, South, East and West), each covering a distance of 15 m from the VAMS. In the second method, the VAMS was towed by the vessel along pre-determined paths, while the ROV recorded the bottom habitats along the transect. The video footages recorded at depths from 23 to 50 m on SMB were analysed and the fish specimens observed along the transects were identified to Family level and the maximum number of individuals encountered in a frame was calculated. Fish individuals that could not be identified was categorised as 'Unidentified'. The percentage composition of a given family (% F_i) was calculated for each station as follows:

$$\% F_i = \frac{Nf_i}{Nmax} \; x \; 100$$

Where Nf_i is the total number of individuals calculated for Family i; Nmax is the total number of fish encountered per Station.

Results and discussion

Pelagic fish

The catch rates from the pelagic trawls varied from 2 kg from PTS 1 to 520 kg from PTS 2. All trawls were carried out within depths of 0 to 60 m, except for PTS 6, where the trawl was done at a depth of 150 to 420 m. A total of 38 families were identified from the pelagic trawl catches. The station with the highest number of different families recorded was PTS 4, with 14 families; while the lowest was PTS 2, with seven families (Table 2). The main fish family encountered during the pelagic trawl surveys was Myctophidae which were recorded at five (PTS 3, PTS 4, PTS 6, PTS 8 and PTS 9) out of 10 stations. This family was obtained from 0 to 420 m deep and the species are characterised by the presence of photophores along the body. Samples from stations PTS 1 and PTS 5 consisted mainly of unidentified fish larvae, collected between the sea surface to 60 m. Diodontidae was found mainly at PTS 2 (10-30 m) with the main species identified as *Diodon holocanthus* Linnaeus, 1758. Juvenile fish were the main catch at PTS 9 and PTS 11 from 0 - 10 m. The PTS 10 catch consisted mainly of Carangids *Selar crumenophthalmus* (Bloch, 1793) and *Decapterus* sp., and Scombrid *Euthynnus affinis* (Cantor, 1849). No catch was obtained from station PTS 12 (20-50m) at the NB (Table 3). Most of the families identified during this study have also been recorded in the waters of Reunion Island (Durville *et al.*, 2009b; Durville *et al.*, 2021). The resource survey carried out by the R/V 'Professor Mesyatsev' from 1975 to 1977 on the SMB showed concentrations of *Decapterus kiliche*, *Trachurus indicus* (both Carangidae) and *Saurida undosquamis* (Synodontidae) which were detected by acoustic surveys and sampled using bottom trawls (Birkett, 1979). Both families

Table 3. Percentage composition of families of fish obtained from pelagic trawls (PT) on the Saya de Malha (SMB) and Nazareth Banks (NB). The main family identified from each station is highlighted in gray.

Location	Saya de Malha Bank										Nazareth Bank	
Pelagic Trawl Station / Family	PTS 1 (10-60m)	PTS 2 (0-30m)	PTS 3 (0-5m)	PTS 4 (0m)	PTS 5 (0m)	PTS 6 (150-420m)	PTS 7 (0-6m)	PTS 8 (0m)	PTS 9 (0m)	PTS 10 (0m)	PTS 11 (0-10m)	PTS 12 (20-50m)
Acanthuridae	-	-	-	-	-	-	-	0.3	65.2	9.5	-	
Alepocephalidae	-	-	-	-	-	1.1	-	-	-	-	-	
Balistidae	-	-	-	<0.1	-	-	0.5	-	-	-	-	
Barbourisiidae	-	-	-	<0.1	-	0.2	-	-	-	-	-	
Belonidae	-	<0.1	-	-	-	-	-	-	-	-	-	
Bothidae	-	-	-	-	-	-	-	0.5	-	-	-	
Bramidae	-	-	-	-	-	-	-	0.1	-	-	-	
Bregmacerotidae	-	-	0.1	-	-	-	-	-	0.8	-	-	
Caesionidae	-	-	0.2	-	4.2	-	-	-	-	-	-	
Carangidae	30.2	15.6	0.1	<0.1	10.2	-	0.6	-	3.8	23.8	-	
Carcharhinidae	-	-	-	-	-	-	-	-	-	4.8	-	
Champsodontidae	-	0.1	10.5	0.1		-	-	-	-	-	-	
Cynoglossidae	0.4	-	-	-	-	-	-	-	-	-	-	
Dactylopteridae	0.1	-	-	-	-	-	-	-	-	-	-	
Diodontidae	<0.1	82.9	14.2	0.9	0.6	-	-	-	-	9.5	-	
Diretmidae	-	-	-	-	-	2.0	-	-	-	-	-	
Echeneidae	-	-	-	-	0.1	-	-	-	2.3	19.1	-	
Exocoetidae	-	-	-	-	-	-	-	-	-	4.8	-	
Gempylidae	-	-	-	-	-	-	0.1	0.3	-	-	-	
Gonostomatidae	-	-	-	-	-	5.7	-	-	-	-	-	No catch
Hemiramphidae	-	-	0.1	<0.1	-	-	-	0.3	0.8	-	-	
Holocentridae	-	-	<0.1	0.1	-	-	-	-	-	-	-	
Melamphaidae	-	-	-	-	-	2.7	-	-	-	-	-	
Mobulidae	-	-	-	-	-	-	-	-	-	4.8	-	
Myctophidae	-	-	73.9	98.0	-	63.0	82.6	84.7	-	-	-	
Nemichthyidae	-	-	-	-	-	14.3	-	-	-	-	-	
Nomeidae	0.6	-	-	0.6	-	1.6	-	4.2	-	-	-	
Ogcocephalidae	0.1	-	-	-	-	-	-	-	-	-	-	
Ophichthidae	0.2	-	0.1	<0.1	-	-	4.9	8.2	-	-	5.4	
Ostraciidae	-	-	-		-	-		0.1	0.8	-	-	
Paralepididae	-	-	-	0.1	-	-	2.7	-	-	-	-	
Scombridae	0.2	<0.1	-	<0.1	13.0	-	-	0.2	-	23.8	-	
Sphyraenidae	-	-	-	<0.1	2.3	-	<0.1	-	3.0	-	-	
Sternoptychidae	-	-	-	-	-	1.1	-	-	-	-	-	
Stomiidae	-	-	-	-	-	8.4	-	-	-	-	-	
Synodontidae	5.2	1.4	0.7	<0.1	1.0	-	8.3	0.8	12.9	-	-	
Tetraodontidae	<0.1	<0.1	-	-	0.1	-	-	-	-	-	1.4	
Zanclidae	-	-	-	-	-	-	-	0.4	-	-	-	
Unidentified Fish Larvae	61.7	-	0.2	-	68.5	-	-	-	9.9	-	-	
Unidentified fish juvenile	1.1	-	-	<0.1	-	-	0.30	-	0.8	-	93.2	
Total No. of families identified	10	7	10	14	8	10	8	12	8	8	2	-
Total No. of individuals caught /hr	4684	13229	6664	24864	1435	559	2957	8554	132	21	74	-

Table 4. Gear depths, catch rate (kg/hr) and number of families recorded from bottom trawls (BT) from the Nazareth Bank (NB).

Bank	Trawl Station No.	Gear Depth (m)	Weight (kg)/hour	No. of families recorded
Nazareth (NB)	BTS 1	213-214	26.6	9
	BTS 2	240-242	9.2	10
	BTS 3	276-288	50.4	24
	BTS 4	288-290	45.8	18

Table 5. Percentage composition of families of fish obtained from bottom trawls on the Nazareth Bank (NB). The main family identified from each station is highlighted in gray.

Location	Nazareth Bank (NB)			
Bottom Trawl Station / Family	BTS 1 (213-214m)	BTS 2 (240-242m)	BTS 3 (276-288m)	BTS 4 (288-290m)
Ariommatidae	-	-	-	0.3
Bothidae	4.8	-	0.6	0.3
Caproidae	2.4	-	12.046	1.5
Carangidae	2.4	4.3	5.6	0.2
Cepolidae	-	-	0.2	-
Champsodontidae	2.4	3.8	0.4	35.2
Chaunacidae	-	-	0.6	0.1
Chlorophthalmidae	-	-	1.9	0.3
Cynoglossidae	-	-	0.7	0.1
Diodontidae	-	8.7	0.5	-
Emmelichthyidae	-	-	0.1	0.1
Exocoetidae	-	-	-	0.1
Gempylidae	-	-	0.1	-
Gobiidae	4.8	61.4	39.3	57.9
Malacanthidae	-	0.5	0.1	-
Mullidae	-	0.9	-	-
Ogcocephalidae	2.4	-	1.0	0.1
Ophichthidae	-	0.9	0.9	-
Peristediidae	-	-	0.1	0.1
Pristiophoridae	-	-	-	0.1
Rhinobatidae	-	-	0.1	-
Serranidae	-	-	-	0.1
Sparidae	-	4.3	0.1	-
Squatinidae	7.2	-	-	-
Synodontidae	55.4	2.2	39	1.2
Tetraodontidae	18.1	-	0.4	-
Triancanthidae	-	-	0.4	-
Trichiuridae	-	-	0.1	-
Triglidae	-	13.0	29.6	2.2
Uranoscopidae	-	-	0.9	0.1
Unidentified	-	-	0.18	-
Total No. of families identified	9	10	25	18
Total No. of individuals caught /hr	83	446	2201	4701

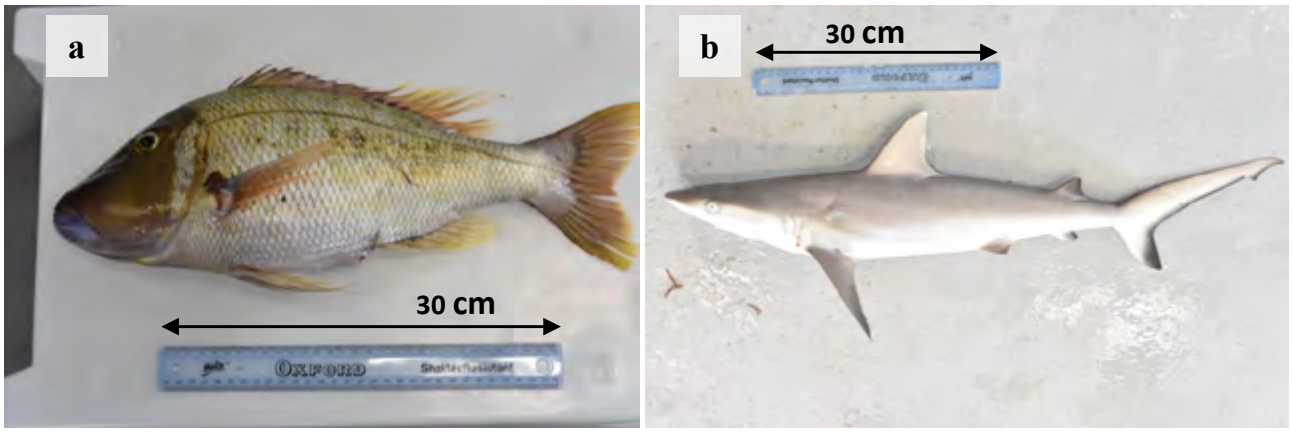

Figure 2. Catch from basket traps set at the Saya de Malha Bank (SMB) at 21 m depth. a) *Lethrinus mahsena*; and b) *Carcharhinus amblyrhynchos.*

were encountered during this study and were present at most of the stations. However, unlike the survey carried out in 1975-1979 which made use of bottom trawls on the SMB, records of this study were obtained from pelagic trawls.

Demersal fish

Bottom trawl

The bottom trawls carried out in the deep-water of the eastern slopes of NB at the four stations between 200 and 300 m (BTS 1, BTS 2, BTS 3 and BTS 4) resulted in catch rates of 26.6 kg/hr, 9.2 kg/hr, 50.4 kg/hr and 45.8 kg/hr, respectively. The total number of families obtained from BTS 1, BTS 2, BTS 3 and BTS 4 were 9, 10, 24 and 18, respectively (Table 4). A total of 30 families were identified from the bottom trawls. The fish family with highest percentage composition was Gobiidae and was obtained from BTS 2, BTS 3 and BTS 4. The main fish family recorded was Synodontidae (*Synodus* spp.) at BTS 1 while other families such as the Champsodontidae (*Champsodon* spp.) and Triglidae (*Lepidotrigla* sp. and *Trigla* sp.) were also prevalent (Table 5). *Polysteganus* sp. (Sparidae) were also collected from the trawls and this coincides with the results of Boyer *et al*. (2006) and Iwatsuki and Heemstra (2011; 2015) where this species was collected at the same depths on the NB. *Polysteganus* sp. is an important commercial deepwater demersal fish from the slopes of the NB (Degambur and Korsbrekke, 2011). An exploration of the deep waters of Reunion Island showed similarities with families encountered in this study such as Caproidae, Carangidae, Gobiidae, Mullidae, Serranidae, Synodontidae, Tetraodontidae, and Trichiuridae (Durville *et al*., 2009a)

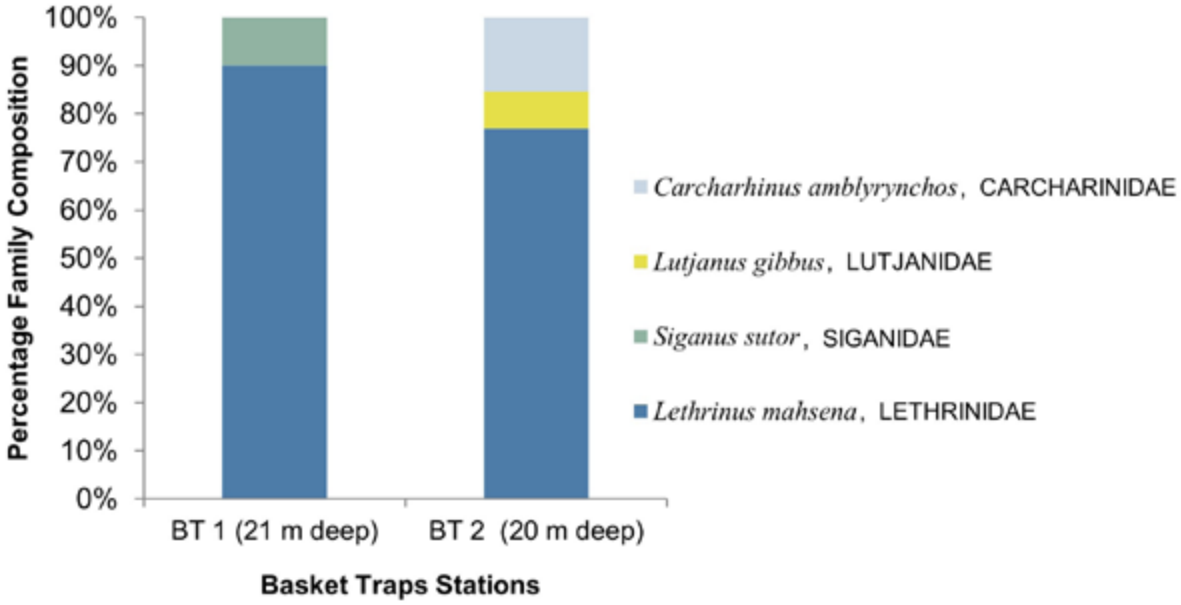

Figure 3. Percentage composition of families of fish obtained from basket traps (BT) on the Saya de Malha Bank (SMB). The main species identified from each station is indicated.

Table 6. Percentage composition of fish families encountered at the VAMS (Video-Assisted Multi Sampler) stations from video footage. The main family encountered from each station is highlighted in gray.

Family	SS 4	SS 9	SS 13	SS 34	SS 36-1	SS 36-2	SS 37-1	SS 37-2	SS 38	SS 39-1	SS 39-2	SS 39-3	SS 39-4	SS 40	SS 42
Acanthuridae	-	-	-	-	3.8	48.6	20.7	5.1	-	19.2	22.5	-	20.1	-	-
Apogonidae	-	-	-	5.0	10.2	-	-	3.4	-	14.4	0.7	-	-	-	-
Balistidae	-	-	-	2.5	-	0.9	3.0	-	-	1.0	-	3.3	1.0	2.3	-
Callionymidae	-	5.9	-	-	-	-	-	-	-	-	-	-	-	-	-
Carangidae	-	-	-	37.5	-	-	14.8	20.3	94.3	2.9	-	-	-	36.4	-
Chaetodontidae	-	-	-	-	2.7	3.7	-	-	-	-	2.8	1.6	1.9	-	-
Dasyatidae	-	-	-	-	0.5	-	-	-	-	-	-	-	-	2.3	-
Diodontidae	-	-	-	-	-	-	-	-	-	1.0	-	-	-	4.6	-
Echeneidae	-	-	-	2.5	-	-	-	-	-	-	-	-	-	-	-
Fistulariidae	-	-	-	-	-	-	-	-	-	-	-	-	-	2.3	25.0
Gobiidae	-	29.4	-	-	1.1	-	0.6	-	-	-	-	-	0.5	-	-
Haemulidae	-	-	-	-	-	-	15.4	-	-	-	-	1.6	-	-	-
Holocentridae	-	-	-	2.5	-	-	6.5	17.0	-	28.9	10.6	-	7.2	-	-
Labridae	12.9	-	2.9	-	15.6	3.7	16.0	-	-	12.5	9.9	18.0	17.2	-	-
Lethrinidae	80.7	-	71.4	2.5	1.6	14.0	-	28.8	1.9	-	-	42.6	21.5	34.1	-
Lutjanidae	-	-	2.9	-	-	-	1.2	-	-	-	21.8	-	0.5	-	-
Monacanthidae	-	-	2.9	-	-	-	-	-	-	-	-	-	-	-	-
Mullidae	-	-	-	5.0	3.2	-	1.2	-	-	-	-	-	-	-	-
Muraenidae	-	-	-	-	0.5	-	0.0	-	-	-	-	-	-	-	25.0
Nemipteridae	-	-	11.4	5.0	-	4.7	-	10.2	1.9	-	2.8	-	4.3	-	-
Ophichthidae	-	-	-	-	-	-	-	-	-	-	-	-	0.5	-	-
Ostraciidae	-	-	-	2.5	-	-	-	-	-	-	-	-	0.5	4.6	-
Pegasidae	-	5.9	-	-	-	-	-	-	-	-	-	-	-	-	-
Plotosidae	-	-	-	12.5	-	-	-	-	-	-	-	-	-	-	-
Pomacanthidae	-	-	-	-	0.5	-	0.6	-	-	1.9	-	-	1.0	-	-
Pomacentridae	1.6	-	-	2.5	7.0	2.8	11.8	6.8	-	12.5	2.1	26.2	20.1	-	-
Priacanthidae	-	-	-	-	-	-	-	1.7	-	-	0.7	-	-	-	-
Pseudochromidae	-	-	-	5.0	-	-	-	-	-	-	-	-	-	-	-
Rhinidae	-	-	-	2.5	-	-	-	-	-	-	-	-	-	-	-
Scaridae	-	-	-	-	-	7.5	1.8	-	-	-	20.4	1.6	-	-	-
Scorpaenidae	-	-	-	2.5	-	-	1.2	-	-	-	-	-	-	4.6	-
Serranidae	-	-	-	-	2.7	-	2.4	-	-	-	0.7	-	0.5	-	-
Siganidae	-	-	-	-	-	-	-	-	1.9	-	-	-	-	-	-
Syngnathidae	-	5.9	-	2.5	-	-	-	-	-	-	-	-	-	-	-
Synodontidae	-	23.5	-	-	-	-	-	1.7	-	-	-	-	-	-	-
Tetraodontidae	-	11.8	-	2.5	-	-	-	3.4	-	-	-	-	-	2.3	-
Trichonotidae	-	17.7	-	-	-	-	-	-	-	-	-	-	-	-	-
Zanclidae	-	-	-	-	-	-	1.2	-	-	4.8	0.7	-	-	-	-
Unidentified	4.8	-	8.6	5.0	50.5	14.0	1.8	1.7	-	1.0	4.2	4.9	3.4	6.8	50.0
Total no. of families identified	3	7	5	16	12	5	15	10	4	10	12	7	14	9	2
Total no. of individuals encountered	62	17	35	40	186	107	169	59	53	104	142	61	209	44	4

Basket traps

The main species caught in the traps was the sky emperor *Lethrinus mahsena* (Fig. 2a) with nine individuals caught at BT 1, and ten individuals at BT 2. Other species caught in the traps were one *Siganus sutor* (Valenciennes, 1835) at BT 1 and two specimens of *Carcharhinus amblyrhynchos* (Bleeker, 1856) (Fig. 2b) and one *Lutjanus gibbus* (Forsskål, 1775) at BT 2. Station BT 1 yielded 2 families while BT 2 yielded three families (Fig. 3). All specimens were caught at around 20 m depth.

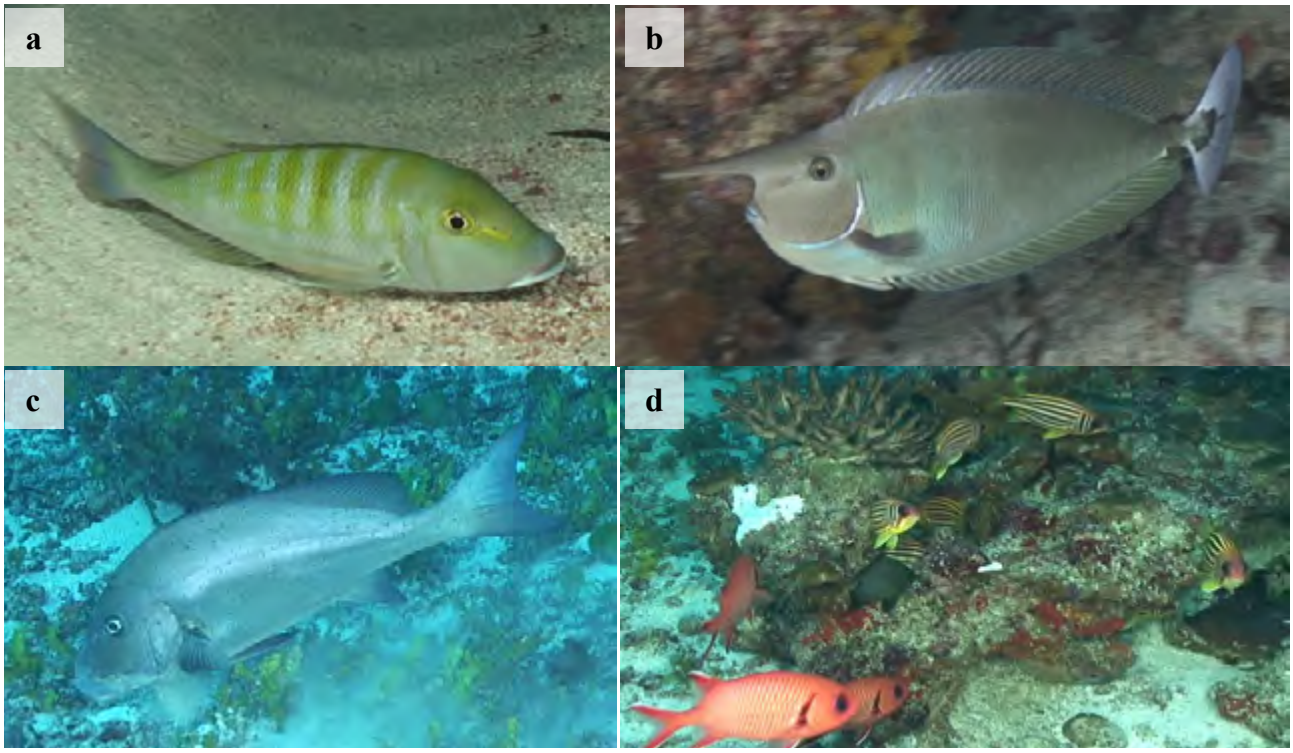

Figure 4. Species captured on videos from the shallow waters of the Saya de Malha Bank: a) *Lethrinus mahsena*, Lethrinidae at 35 m deep; b) *Naso brevirostris* (Cuvier, 1829), Acanthuridae at 33 m deep; c) *Diagramma labiosum* Macleay, 1883, Haemulidae at 39 m deep; d) *Myripristis* and *Sargocentron* spp, Holocentridae and *Dascyllus trimaculatus* (Rüppell, 1829), Pomacentridae at 38 m deep.

Remotely Operated Vehicle (ROV) videos

A total of 37 families of bony fish and one family of cartilaginous fish (Rhinidae) were encountered from the 10 stations. The number of families identified per station ranged from two (SS 42) to 16 for SS 34 which showed the highest family diversity recorded. In terms of fish abundance, the highest number of fish encountered was 209, from SS 39-4. The least diverse and least abundant station was SS 42, with a total of four fish individuals encountered, of which two were unable to be identified due to blurred video footage. The main families that occurred were Lethrinidae, Acanthuridae and Carangidae. Other families identified included several commercial families such as Serranidae, Scaridae, Holocentridae (Table 6 and Fig. 4). Some of the commercial fish encountered during the video transects are the same species recorded during fishing activities within the shallow waters of SMB (Ministry of Fisheries and Rodrigues, 2011; Munbodh, 2012). As described by Munbodh (2012), the main catch from the shallow water fishery is *Lethrinus mahsena*, along with some other species from the Lethrinidae and Serranidae. Though other commercial fish were encountered during this survey, such as from the families Acanthuridae, Scaridae and Siganidae, those species are not targeted by the banks fishery industry. This is attributed to the fact that fishermen make use of handlines for fishing at the SMB (Degambur and Korsbrekker, 2011). Handlines are highly selective fishing gears for carnivorous fish, and target mainly Lethrinids and some Serranids. Other herbivorous species like rabbit fish (Siganidae), parrot fish (Scaridae) or unicorn fish (Acanthuridae) are not caught by this fishing method (Mees, 1996). Carangidae, though a family of commercial importance, do not appear in commercial catches. This is because the carangids from the fishing banks have been categorised as toxic by the 'Fisheries and Marine Resources (Toxic Fish) Regulations' of Mauritius since 2004 and the regulations prohibit the fishing and landing of these fishes.

Conclusions

This study highlighted the presence of several fish families that occur in the pelagic and demersal waters of the Saya de Malha and Nazareth Banks. Since the information on the composition of the fish fauna of these two banks was previously based only on catch data, this study provides new data that expands the current knowledge of fish diversity in this region using four different fishing gears. Further in-depth studies are however warranted to obtain a better understanding of fish diversity and occurrence on these two banks and the Mascarene Plateau in general.

Acknowledgments

The authors are grateful to the Food and Agriculture Organization (FAO) for funding the research expedition as part of the Indian Ocean NORAD-FAO PROJECT GCP/INT/730/NOR) in the Saya de Malha and Nazareth Banks, on-board the 'R/V Dr. Fridjof Nansen' and for funding of the Habitat Mapping Workshop in Mauritius in August 2019. The authors are thankful to the Ministry of Blue Economy, Marine Resources, Fisheries and Shipping for authorising the bottom trawling in the Nazareth Bank and for hosting the Habitat Mapping Workshop; to the Department for Continental Shelf, Maritime Zones Administration & Exploration (Prime Minister's Office) for co-leading and coordinating the expedition and to the Institute of Marine Research in Norway for leading the expedition and providing all logistic supports. The authors are also thankful to the fellow scientists, crew members and the VAMS / ROV operators during the expedition.

References

Bergstad OA, Bissessur D, Sauba K, Rama J, Coopen P, Oozeeraully Y, Seeboruth S, Audit- Manna A, Nicolas A, Reetoo N, Tabachnick K, Kuyper D, Gendron G, Hollanda S, Melanie R, Souffre A, Harlay J, Bhagooli R, Soondur M, Ramah S, Caussy L, Ensrud TM, Olsen M, Høines ÅS (2018) Regional resources and ecosystem survey in the Indian Ocean, Leg 2.1. Characterizing ecosystems and morphology of the Saya de Malha Bank and Nazareth Bank, 3 May - 4 June 2018. NORAD-FAO Programme GCP/GLO/690/NOR, Cruise Reports Dr Fridtjof Nansen, EAF-Nansen/CR/2018/6. 206 pp

Birkett L (1979) Western Indian Ocean resources survey report on the cruises of R/V "Professor Mesyatsev", December 1975 - June 1976 and July 1976 - December 1977. FAO/UNDP, Rome Indian Ocean Programme, IOP/Technical Report 26. 96 pp

Boyer D, Nelson J, Hampton I, Soule M, Soondron V, Degambur D (2006) Acoustic survey of the slopes of St Brandon and Nazareth Banks - Distribution and relative abundance of deepwater snappers and groupers. FAO/EU. TCP/MAR/3001. 53 pp

Degambur D, Korsbrekke K (2011) Fisheries on the fishing banks of Mauritius – A description of the fishery, its monitoring, and scientific sampling and recommendations. Ministry of Fisheries/NORAD. 26 pp

Degambur D, Sólmundsson J (2005) Stock assessment of the offshore Mauritian Banks using dynamic biomass models and analysis of length frequency of the sky emperor *(Lethrinus mahsena)*. Thesis (Fisheries Training Programme). United Nations University. 61 pp

Durville P, Mulochau, T, Alayse J-P, Barrière A, Bigot L, Troadec R (2009a) Exploration sous-marine à l'aide d'un engin de type ROV sur les reliefs profonds de l'Île de la Réunion Expedition Abyssea. Revue Écologique (Terre Vie) 64: 293-304

Durville P, Mulochau T, Barrere A, Quod JP, Spitz J, Quero JC, Ribes S (2009b) Inventaires des poissons récoltés lors de l'éruption volcanique d'Avril 2007 du Piton de la Fournaise (Île de la Réunion). Annales de la société de sciences naturelles de la Charente-Maritime 9(9): 948-956

Durville P, Mulochau T, Quod JP, Pinault M, Ballesta L (2021) Premier inventaire ichthyologique du mont sous-marin La Pérouse, Île de la Réunion, sud-ouest Océan Indian. Annales de la société de sciences naturelles de la Charente-Maritime 11(3): 305-327

Food and Agriculture Organization (1984) FAO Species identification sheets for fishery purposes: Western Indian Ocean: Fishing Area 51. Volumes I - V. Rome: FAO. 1473 pp

Iwatsuki Y, Heemstra PC (2011) *Polysteganus mascarensis*, a new sparid fish species from Mascarene Islands, Indian Ocean. Zootaxa 3018: 13-20

Iwatsuki Y, Heemstra PC (2015) Redescription of *Polysteganus coeruleopuncatus* (Klunzinger, 1870) and *P. lineopunctatus* (Boulenger, 1903), with two new species from Western Indian Ocean. Zootaxa 4059 (1): 133-150

Mees CC (1996) The Mauritian banks fishery – A review and spatial analysis. MRAG, London. 61 pp

Ministry of Fisheries and Rodrigues (2011) Annual Report 2011 – Fisheries Division. Mauritius: Government Printing Department. 103 pp

Munbodh M (2012) Baseline report for the development of a fisheries management plan for the shallow water demersal fish species of the Saya de Malha and Nazareth banks of Mauritius. Ministry of Fisheries/SWIOFP/EAF Nansen Project. 75 pp

New AL, Magalhaes JM, da Silva JCB (2013) Internal solitary waves on the Saya de Malha bank of the Mascarene Plateau: SAR observations and interpretation. Deep Sea Research Part I: Oceanographic Research Papers 79: 50–61 [doi:10.1016/j.dsr.2013.05.008]

Regan CT (1908) No. XIV Report on the marine fishes collected by Mr J Stanley Gardiner in the Indian Ocean. The Transactions of the Linnean Society of London. Second Series. Zoology 12 (3): 217-255; 23-32

Samboo CR (1983) An appraisal of the banks fishery in Mauritius. Ministry of Agriculture and Natural Resources. Report No.1 RD(F)/SU/83/1. 17 pp

Samboo CR, Mauree D (1987) Summary of fisheries and resources information for Mauritius. Proceedings of the workshop on the assessment of the fishery

resources in the Southwest Indian Ocean, 14-27 September 1987, Albion. FAO, Rome. pp 62-79

United Nations (1993) The law of the sea: National legislation on the Exclusive Economic Zone. United Nations, New York. 403 pp

United Nations (2018a) Treaty No. 49782: Treaty concerning the joint exercise of sovereign rights over the continental shelf in the Mascarene Plateau region between the Government of the Republic of Seychelles and the Government of the Republic of Mauritius. United Nations Treaty Series2847. pp 277 – 306 [https://treaties.un.org/doc/Publication/UNTS/Volume%202847/v2847.pdf].

United Nations (2018b) Treaty No. 49783: Treaty concerning the joint management of the continental shelf in the Mascarene Plateau region between the Government of the Republic of Seychelles and the Government of the Republic of Mauritius. United Nations Treaty Series 2847.pp307 – 344 [https://treaties.un.org/doc/Publication/UNTS/Volume%202847/v2847.pdf].

Vortsepneva E (2008) Saya de Malha Bank - An invisible island in the Indian Ocean. Geomorphology, Oceanology, Biology. University of Moscow, Russia [https://lighthouse-foundation.org/Binaries/Binary1070/Saya-de-Malha-report-final.pdf]

Rhodolith beds (Corallinaceae, Rhodophyta): An important marine ecosystem of the Saya de Malha and Nazareth Banks

Sundy Ramah[1,2]*, Ranjeet Bhagooli[2,3], Deepeeka Kaullysing[2], Odd A. Bergstad[4]

[1] Albion Fisheries Research Centre, Ministry of Blue Economy, Marine Resources, Fisheries & Shipping, Albion, Petite-Rivière, 91001, Republic of Mauritius

[2] Department of Biosciences and Ocean Studies, Faculty of Science & Pole of Research Excellence in Sustainable Marine Biodiversity, University of Mauritius, Réduit 80837, Republic of Mauritius

[3] Institute of Oceanography and Environment (INOS), University Malaysia Terengganu, 21030 Kuala Terengganu, Terengganu, Malaysia

[4] Institute of Marine Research (IMR), PO Box 1870 Nordnes, N-5817 Bergen, Norway

* Corresponding author: sundy.ramah@gmail.com

Rhodoliths are unattached marine benthic crustose coralline red algae (Corallinaceae, Rhodophyta) nodules which are the foundation species of the rhodolith beds (Bruno and Bertness, 2001). These coralline red algae are formed by precipitating calcium carbonate ($CaCO_3$) within their cell walls (Foster, 2001). Rhodoliths depend strongly on water motion (currents) to enable their periodic rotation which allows them to be exposed to light on both sides (to photosynthesize) and to remain unburied by sediment (Hinojosa-Arango *et al*., 2009). These rhodolith beds (RBs) represent a key habitat worldwide and form an important ecosystem themselves (Schubert *et al*., 2019), and are associated with other tropical or polar benthic organisms such as sponges, corals, molluscs, seagrass, bryozoans and macroalgae, among others (Grall and Glemarec, 1997; Steller *et al*., 2003; Amado-Filho *et al*., 2012; Foster *et al*., 2013; Vilas-Boas *et al*., 2014; Ordines *et al*., 2015; Riosmena-Rodríguez *et al*., 2017). RBs also form part of the largest recognized macrophyte-dominated benthic communities, consisting of coralline algal reef, seagrass and kelp beds (Amado-Filho *et al*., 2012; Pena *et al*., 2014). They have been mainly reported around islands, capes, on submarine plateaus, seamounts, marine terraces, channels and banks (Basso *et al*., 2017).

While in-depth research on rhodoliths has mainly been concentrated in the Mediterranean, North Atlantic, and Pacific regions (Foster, 2001; Amado-Filho *et al*., 2012; Harvey *et al*., 2017), the only mention of these coralline algae from Saya de Malha (reported as red-pink *Lithothamnium*) was in Vortsepneva's review on previous expeditions carried out at this particular bank (Vortsepneva, 2008). Despite the fact that RB habitats are considered as a hotspot of biodiversity providing an array of ecosystem goods and services, such as fishery resources, soil conditioning, carbon trapping and climate regulation, among others (Jacquotte, 1962; Hall-Spencer *et al*., 2003; Cavalcanti *et al*., 2014; Basso *et al*., 2016; Krayesky-Self *et al*., 2017; Coletti *et al*., 2017; Schubert *et al*., 2020), not many studies have been conducted to properly understand their overall contribution to ocean ecology.

The Indian Ocean EAF-Nansen research expedition survey cruise in May 2018 helped to gather new information on RBs from the Saya de Malha and Nazareth Banks. With the help of a Remotely Operated Vehicle (ROV), RBs were mainly observed at eight locations within the Saya de Malha Bank namely SS4, SS34, SS36, SS37, SS38, SS39, SS40 and SS42 at depths ranging from 20-80 m and at three locations within the Nazareth Bank namely SS49, SS50 and SS52 at depths ranging from 53-126 m (Fig. 1). Rhodolith ball sizes ranged from approximately 0.5 to 4 cm. RBs have been reported to mostly occur at depths ranging between 30-75 m (Foster *et al*., 2013), but have also been recorded from as deep as 150 m (Aguilar *et al*., 2009) and forming beds of up to 10 m in thickness (Harvey *et al*., 2017). Although rhodoliths are most likely to occur in photic to mesophotic areas, they

http://dx.doi.org/10.4314/wiojms.si2021.2.12

are acclimated to survive in restricted light ranges in deeper waters as well (Figueiredo *et al*., 2012). RBs are considered as a rich and important habitat harbouring high diversity and density of echinoderms and many other associated species (Steller *et al*., 2003; Gondim *et al*., 2014; Moura *et al*., 2021).

The study showed that RBs found on both banks provided a benthic substrate to sustain other organisms such as echinoderms, asteroids, sea cucumbers, as a niche for echinoderm assemblages, while the other locations show the importance of RBs for the sustainability of many other organisms at the banks.

In addition to their structural complexity and their importance to continental shelf biodiversity, RBs are considered as important carbonate factories (Amado-Filho *et al*., 2012). This is similar to coral reefs which have been reported to be a major coastal $CaCO_3$ manufacturers (Spalding and Grenfell, 1997;

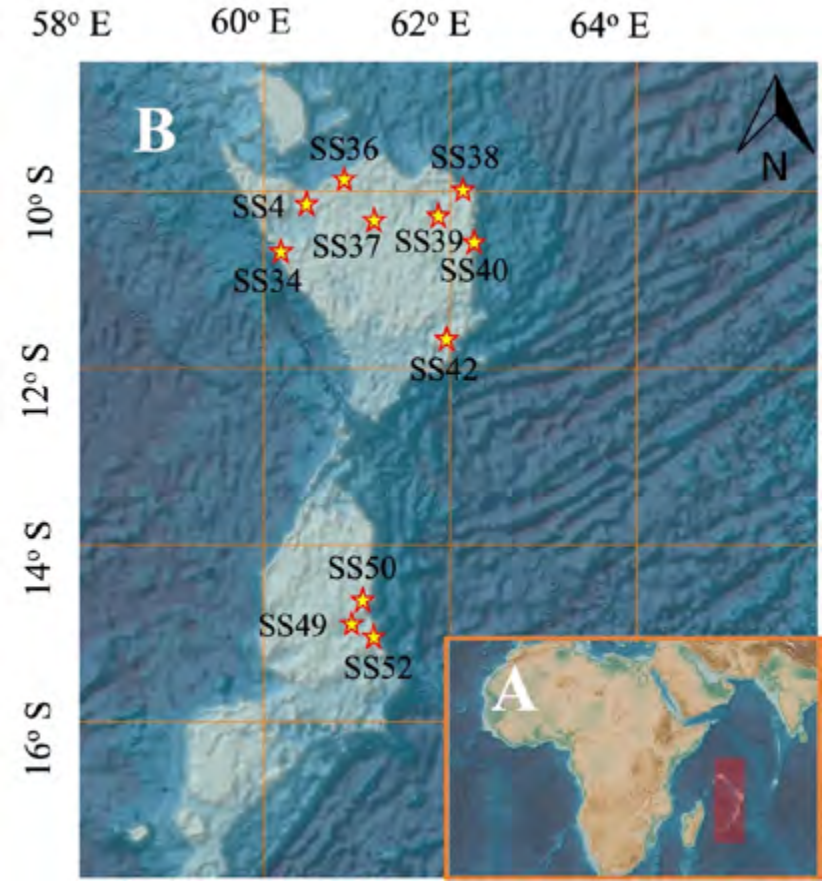

Figure 1. Map showing the locations of the rhodolith beds. A: Western Indian Ocean map showing the location of Saya de Malha and Nazareth Banks in the red-shaded box. B: Map showing the 11 locations (indicated by yellow and red border stars) where rhodolith beds were observed using the ROV. Map prepared using the GEBCO Bathymetry Grid layer data 2020.

sponges, corals, seagrass, fish, and seaweed (Fig. 2B-D, F-H and Fig. 3C-H). Studies in the Gulf of California demonstrated that sea urchins help rhodoliths by turning them, in a process called bioturbation, during feeding and movement, which contributes to bed integrity (James, 2000). RBs provide a safe and important ground for juvenile echinoderms (Riosmena-Rodriguez and Medina-Lopez, 2010). The RBs at location SS42 (Fig. 2B) on the Saya de Malha Bank and location SS50 (Fig. 3D) at the Nazareth Bank may be considered

Vecsei, 2000, 2004a, b) through evidence built on their global distribution (Spalding and Grenfell, 1997; Vecsei, 2000, 2004a, b) estimations of their mineralization rates (Kinsey and Hopley, 1991; Milliman, 1993; Milliman and Droxler, 1996; Kleypas, 1997). Similarly, RBs contribute considerably to continental shelf ecosystem $CaCO_3$ cycles owing to their high community $CaCO_3$ production and dissolution rates (Foster, 2001; Martin *et al*., 2007; Martin and Gattuso, 2009). Ample evidence indicates that the capture and

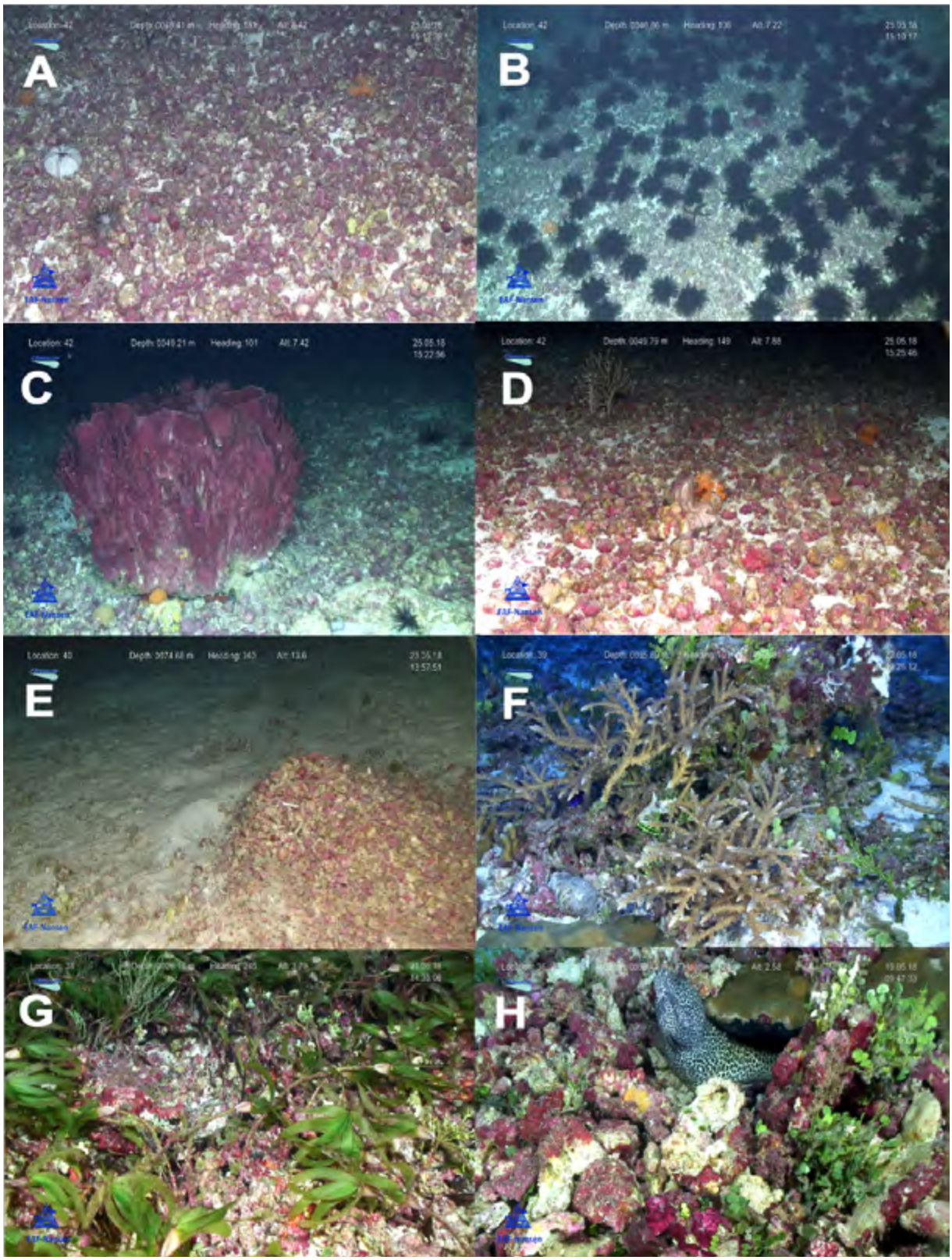

Figure 2. Rhodolith beds (RBs) at Saya de Malha Bank. A. Location 42 at a depth of 48.41 m - Sponge and echinoderms on RB; B. Location 42 at a depth of 46.86 m – Group of echinoderms on RB.; C. Location 42 at a depth of 49.21 m – Demospongia growing on RB; D. Location 42 at depth of 49.79 m – Octocoralia, soft corals and sponge growing on RB; E. Location 40 at a depth of 74.66 m – Rhodoliths clustered forming a mount; F. Location 39 at a depth of 35.89 m - *Acropora* sp. and *Porites* sp. growing on rhodoliths; G. Location 38 at a depth of 26.16 m – Seagrass *Thalassodendron ciliatum* growing on RB; H. Location 36 at a depth of 38.44 m - Moray eel (*Gymnothorax* sp.) using rhodoliths as habitat. Photos were taken using the Argus Remotely Operated Vehicle (ROV) during the expedition.

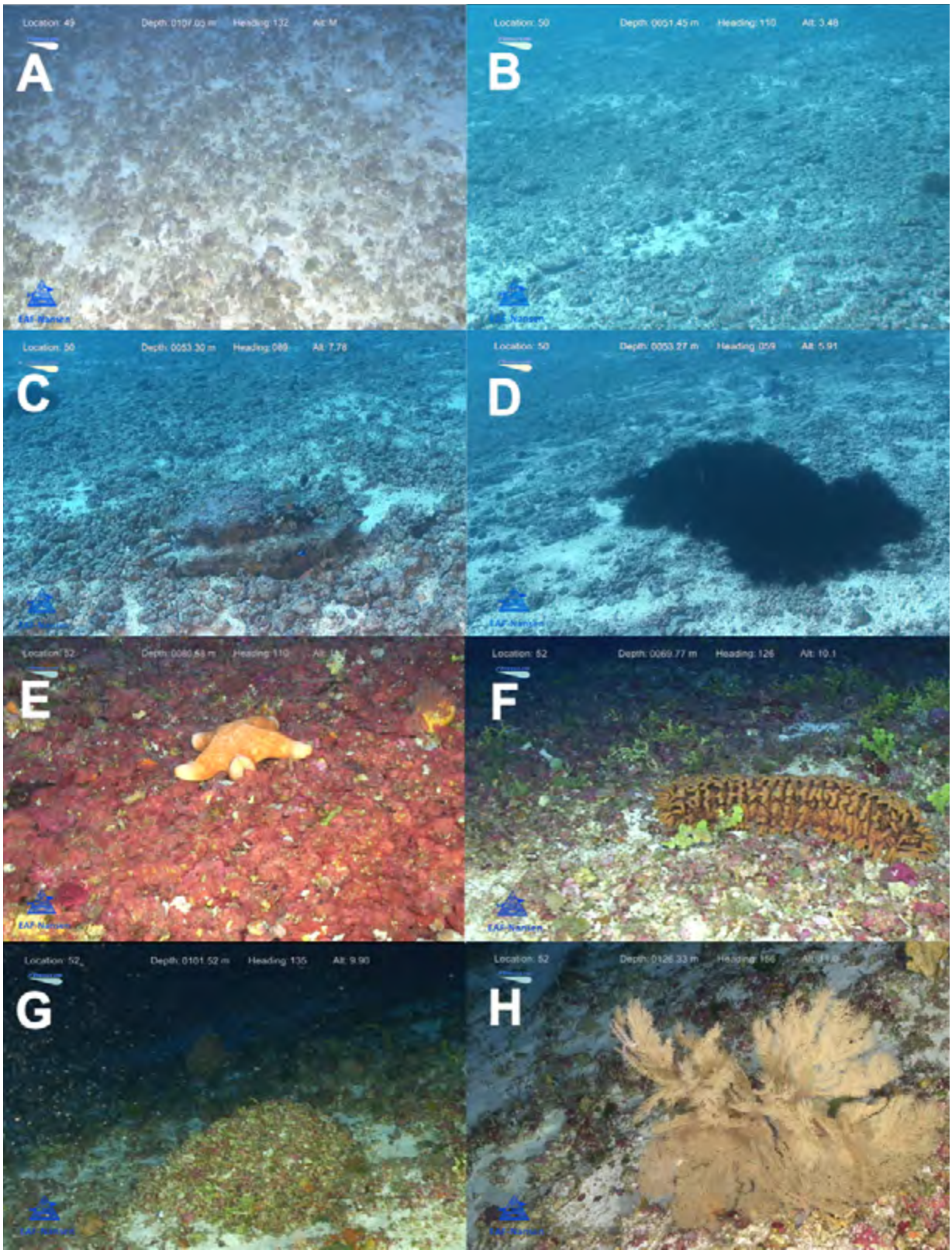

Figure 3. Rhodolith beds (RBs) at Nazareth Bank. A. Location 49 at a depth of 107.05 m – RB overview; B. Location 50 at a depth of 51.45 m – RB overview; C. Location 50 at a depth of 53.30 m – Coral (Tabular *Acropora* sp.) growing on RB; D. Location 50 at a depth of 53.27 m – Group of echinoderms on RB; E. Location 52 at a depth of 80.58 m – cushion seastar on RB; F. Location 52 at a depth of 69.77 m – Sea cucumber (*Thelenota ananas*) on RB; G. Location 52 at a depth of 101.52 m – Rhodoliths clustered forming a mount with coralline algae (*Halimeda* sp.) colonising the mount; H. Location 52 at a depth of 126.33 m – Gorgonian sea fan growing on RB. Photos were taken using the Argus Remotely Operated Vehicle (ROV) during the expedition.

storage of atmospheric carbon dioxide by RBs over time are comparable, both in efficiency and area, to those of coral reefs (Amado-Filho *et al*., 2012). Studies have shown that the RB on the Abrolhos Shelf (approximate area of 200,000 km^2) was able to produce a total of 0.025 Gt yr^{-1} (1.060.7 kg m^{-2} yr^{-1}) of $CaCO_3$ (Amado-Filho *et al*., 2012), almost equivalent to the yearly total $CaCO_3$ produced by Caribbean coral reefs (0.04-0.08 Gt yr^{-1} or 1.3-2.7 kg m^{-2} yr^{-1}) (Vecsei, 2004a, b) and the estimated mean calcification rate of 1.5 kg m^{-2} yr^{-1} produced by global coral reefs (Andersson *et al*., 2005). RBs are however at risk from disturbances such as climate change, global warming, and associated ocean acidification, as well as from other disturbances with anthropogenic sources such as sedimentation, and fishery trawling (Foster *et al*., 2013; Harvey *et al*., 2017; Schubert *et al*., 2019). Rhodoliths grow only a few millimeters per year (Foster *et al*., 2013) and these disturbances affect their recruitment, development, health, and survival rate which may lead increased competition from space competitors such as fleshy algae (Martin and Hall-Spencer, 2017; Carvalho *et al*., 2020) in shallower areas.

This first documentation of RBs from the Saya de Malha and Nazareth Banks provides the basis for future research and conservation work on RBs in this part of the world. RBs at the two banks may be considered as marine biodiversity hotspots that function as seedbanks, habitat, nursery grounds, refugia and areas of high carbonate production. The vast number of organisms that RBs host, including sponges and other macroalgae, may also provide new opportunities for bioprospecting in the future. However, there is a need for directed research to fully understand the physical integrity, ecological balance and community structure of RBs over time in order to better conserve and protect these important, yet poorly studied and understood ecosystems on the Saya de Malha and Nazareth Banks.

Acknowledgements

The underlying work was made possible with the support of the EAF-Nansen Programme "Supporting the Application of the Ecosystem Approach to Fisheries Management considering Climate Change and Pollution Impacts" executed by Food and Agriculture Organization of the United Nations (FAO) and funded by the Norwegian Agency for Development Cooperation (Norad). The authors are thankful to FAO for funding and supporting the Indian Ocean research expedition 2018 on the Saya de Malha Bank and Nazareth Bank with the R/V *Dr Fridtjof Nansen*, the Department of Continental Shelf, Maritime Zones Administration & Exploration of Mauritius for co-leading and coordinating the scientific expedition, the Mauritius-Seychelles Joint Commission of the Extended Continental Shelf for their support and assistance and granting the necessary authorisations, the Ministry of Blue Economy, Marine Resources, Fisheries & Shipping for hosting and spearheading the Habitat Mapping Workshop in Mauritius and for granting necessary authorization to carry out research in the Nazareth Bank; the Institute of Marine Research, Norway for leading the expedition and providing the technical and logistic support. The authors also thank the participating scientists, the crew members and the VAMS / Argus ROV technicians for their work and contribution during the expedition and to the anonymous reviewers for their insightful comments which have significantly improved the manuscript.

References

Aguilar R, Pastor X, Torriente A, Garcia S (2009) Deep-sea coralligenous beds observed with ROV on four seamounts in the western Mediterranean. In: Proceedings of the 1st Mediterranean Symposium on the Conservation of the Coralligenous and Other Calcareous Bio-Concretions, Tabarka, Tunis, 15-16 January 2009. pp 147-149

Amado-Filho GM, Moura RL, Basto AC, Salgado LT, Sumida P, Guth AZ, Francini-Fihlo R. B, Pereira-Filho GH, Abrantes DP, Brasileiro PS, Bahia RG, Leal RN, Kaufman L, Kleypas FA, Farina M, Thompson FL (2012) Rhodolith beds are major $CaCO_3$ biofactories in the tropical South West Atlantic. PLoS One 7: e35171

Andersson AJ, Mackenzie FT, Lerman A (2005) Coastal ocean and carbonate systems in the high CO_2 world of the anthropocene. American Journal of Science 305: 875-918

Basso D, Babbini L, Kaleb S, Bracchi V, Falace A (2016) Monitoring deep Mediterranean rhodolith beds. Aquatic Conservation 26: 549-561

Basso D, Babbini L, Ramos-Esplá AA, Salomidi M (2017) Mediterranean Rhodolith Beds. In: Riosmena-Rodríguez R, Nelson W, Aguirre J (eds) Rhodolith/Maërl beds: A global perspective. Coastal Research Library. Springer: Cham, Switzerland. pp 230-237

Bruno JF, Bertness MD (2001) Habitat modification and facilitation in benthic marine communities. In: Bertness MD, Gaines SD, Hay ME (eds) Marine community ecology. pp 201-218

Carvalho VF, Silva J, Kerr R, Anderson AB, Bastos EO, Cabral D, Gouvêa LP, Peres L, Martins CDL,

Silveira-Andrade VM, Sissini MN, Horta PH (2020) When descriptive ecology meets physiology: a study in a South Atlantic rhodolith bed. Journal of the Marine Biological Association of the United Kingdom: 1-14

Cavalcanti GS, Gregoraci GB, Santos EO, Silveira CB, Meirelles PM, Longo L, Gotoh K, Nakamura S, Iida T, Sawabe T (2014) Physiologic and metagenomic attributes of the rhodoliths forming the largest $CaCO_3$ bed in the South Atlantic Ocean. International Society for Microbial Ecology Journal 8: 52-62

Coletti G, Basso D, Frixa A (2017) Economic importance of coralline carbonates. In: Riosmena-Rodríguez R, Nelson W, Aguirre J (eds) Rhodolith/Maërl beds: A global perspective. Coastal Research Library. Springer: Cham, Switzerland. pp. 87-101

Figueiredo MAO, Coutinho R, Villas-Boas AB, Tâmega FTS, Mariath R (2012) Deep-water rhodolith productivity and growth in the southwestern Atlantic. Journal of Applied Phycology 24: 487-493

Foster MS (2001) Rhodoliths: between rocks and soft places. Mini-review. Journal of Phycology 37: 659-667

Foster MS, Filho GMA, Kamenos KA, Riosmena-Rodríguez R, Steller DL (2013) Rhodoliths and rhodolith beds. In: Research and discoveries: The revolution of science through SCUBA. American Academy of Underwater Sciences: Mobile, AL, USA. pp 143-155

Gondim AI, Dias TLP, Duarte RCS, Riul P, Lacouth P, Christoffersen ML (2014) Filling a knowledge gap on the biodiversity of Rhodolith-associated Echinodermata from northeastern Brazil. Tropical Conservation Science 7: 87-99

Grall J, Glemarec M (1997) Biodiversite des fonds de maërl en Bretagne: Approache fonctionnelle et impacts anthropogeniques. Vie Milieu 47: 339-349

Hall-Spencer JM, Grall J, Moore PG, Atkinson RJA (2003) Bivalve fishing and maerl-bed conservation in France and the UK-retrospect and prospect. Aquatic Conservation 13: S33-S41

Harvey AS, Harvey RM, Merton E (2017) The distribution, significance and vulnerability of Australian rhodolith beds: A review. Marine and Freshwater Resources 68: 411-428

Hinojosa-Arango G, Maggs CA, Johnson MP (2009) Like a rolling stone: the mobility of maerl (Corallinaceae) and the neutrality of the associated assemblages. Ecology 90: 517-528

Jacquotte R (1962) Etude des fonds de maerl de Méditerranée. Recueil Travaux Station Marine d'Endoume 26: 141-216

James DW (2000) Diet, movement, and covering behavior of the sea urchin *Toxopneustes roseus* in rhodolith beds in the Gulf of California, Mexico. Marine Biology 137: 913-923

Kinsey DW, Hopley D (1991) The significance of coral reefs as global carbon sink-response to greenhouse. Palaeogeographical Palaeoclimatology and Palaeoecology 89: 363-377

Kleypas J (1997) Modeled estimates of global reef habitat and carbonate production since the last glacial maximum. Paleoceanography, 12: 533-545

Krayesky-Self S, Schmidt W, Phung D, Henry C, Sauvage T, Camacho O, Felgenhauer BE, Fredericq S (2017) Eukaryotic life inhabits rhodolith-forming coralline algae (Hapalidiales, Rhodophyta), remarkable marine benthic microhabitats. Scientific Reports 7: 45850

Martin S, Clavier J, Chauvaud L, Thouzeau G (2007) Community metabolism in temperate maërl beds. I. Carbon and carbonate fluxes. Marine Ecology Programme Series 335: 19-29

Martin S, Gattuso J (2009) Response of Mediterranean coralline algae to ocean acidification and elevated temperature. Global Change Biology 15: 2089-2100

Martin S, Hall-Spencer JM (2017) Effects of ocean warming and acidification on rhodolith/maërl beds. In: Riosmena-Rodríguez R, Nelson W, Aguirre J (eds) Rhodolith/Maërl beds: A global perspective. Coastal Research Library, vol 15. Springer: Cham, Switzerland [doi: https://doi.org/10.1007/978-3-319-29315-8_3]

Milliman JD (1993) Production and accumulation of calcium carbonate in the ocean: budget of a nonsteady state. Global Biogeochemical Cycles 7: 927-957

Milliman JD, Droxler AW (1996) Neritic and pelagic carbonate sedimentation in the marine environment: ignorance is no bliss. Geologische Rundschau 85: 495-504

Moura RL, Abieri ML, Castro GM, Carlos-Júnior LA, Chiroque-Solano PM, Fernandes NC, Teixeira CD, Ribeiro FV, Salomon PS, Freitas MO, Gonçalves JT, Neves LM, Hackradt CW, Felix-Hackradt F, Rolim FA, Motta FS, Gadig OBF, Pereira-Filho GH, Bastos AC (2021) Tropical rhodolith beds are a major and belittled reef fish habitat. Scientific Reports 11: 794

Ordines F, Bauzá M, Sbert M, Roca P, Gianotti M, Massutí E (2015) Red algal beds increase the condition of nekto-benthic fish. Journal of Sea Resources 95: 115-123

Pena V, Barbara I, Grall J, Maggs C, Hall-Spencer J (2014) The diversity of seaweeds on maerl in the NE Atlantic. Marine Biodiversity 44: 533-551

Riosmena-Rodríguez R, Medina-Lopez M (2010) The role rhodolith beds in the recruitment of invertebrate

species from the Southwestern Gulf of California, México. In: Seckbach J, Einav R, Israel A (eds) Seaweeds and their role in globally changing environments. Springer, Netherlands. pp 127-138

Riosmena-Rodríguez R, Nelson W, Aguirre J (eds) (2017) Rhodolith/Maërl beds: A global perspective. Coastal Research Library 15. Springer: Cham, Switzerland. 362 pp

Schubert N, Salazar VW, Rich WA, Vivanco-Bercovich M, Almeida-Saa AC, Fadigas SD, Silva J, Horta PA (2019) Rhodolith primary and carbonate production in a changing ocean: The interplay of warming and nutrients. Science of the Total Environment 676: 455-468

Schubert N, Schoenrock KM, Aguirre J, Kamenos NA, Silva J, Horta PA, Hofmann LC (2020) Editorial: Coralline algae: Globally distributed ecosystem engineers. Frontiers in Marine Science 7: 1-3

Spalding MD, Grenfell AM (1997) New estimates of global and regional coral reef areas. Coral Reefs 16: 225-230

Steller DL, Riosmena-Rodriguez R, Foster MS, Roberts CA (2003) Rhodolith bed diversity in the Gulf of California: The importance of rhodolith structure and consequences of disturbance. Aquatic Conservation 13: S5-S20

Vecsei A (2000) Database on isolated low-latitude carbonate banks. Facies 43: 205-221

Vecsei A (2004a) A new estimate of global reefal carbonate production including the forereefs. Global Planet Change 43: 1-18

Vecsei A (2004b) Carbonate production on isolated banks since 20 k.a.BP: climatic implications. Palaeogeographical Palaeoclimatology and Palaeoecology 214: 3-10

Villas-Boas AB, Riosmena-Rodriguez R, de Oliveira Figueiredo MA (2014) Community structure of rhodolith-forming beds on the central Brazilian continental shelf. Helgol Marine Resources 68: 27-35

Vortsepneva E (2008) Review: Saya de Malha Bank - an invisible island in the Indian Ocean. Geomorphology, Oceanology, Biology. Lighthouse Foundation. 44 pp

First field observation of a *Thalassodendron ciliatum* bed on the Nazareth Bank, Mascarene Plateau

Sundy Ramah[1,2]*, Ranjeet Bhagooli[2]

[1] Albion Fisheries Research Centre, Ministry of Blue Economy, Marine Resources, Fisheries and Shipping, Albion, Petite Rivière 91001, Republic of Mauritius

[2] Department of Biosciences and Ocean Studies, Faculty of Science & Pole of Research Excellence in Sustainable Marine Biodiversity, University of Mauritius, Réduit 80837, Republic of Mauritius

* Corresponding author: sundy.ramah@gmail.com

Seagrass meadows are one of the most productive marine ecosystems in the world (Duarte and Cebrian, 1996). They play key ecological roles in providing important services such as nursery and feeding grounds for juvenile fish and other marine organisms, thus maintaining populations of commercially exploited fishery resources (Jackson *et al*., 2001). Seagrass has strong linkages with coral reefs and mangroves, forming one of the most productive coastal habitats, and can play a critical role in buffering the effects of ocean acidification on adjacent coral reefs (Anthony *et al*., 2011). They often form extensive meadows which can be of mono- or multi- specific species. They are commonly situated in shallow areas of lagoons up to 20 meters depth, or deeper if the environmental conditions permit photosynthesis. There are about 60 species of seagrasses worldwide and 13 species are known to occur in the Western Indian Ocean (Gullstrom *et al*., 2002), making up an important habitat in coastal waters (Gullstrom *et al*., 2002; Duarte *et al*., 2012). While it has been reported that 5 seagrass species prevail in Mauritian waters (Jagtap, 1993), very few studies have been carried out on seagrasses and their associated organisms (Paupiah *et al*., 2000; Daby, 2003; Nakamura *et al*., 2006; Ramah *et al*., 2014), and even less on their occurrence on distant fishing banks, creating a significant knowledge gap on this important ecosystem in the waters of the Republic of Mauritius.

During the EAF-Nansen Indian Ocean Research Expedition 2018, two shallow locations over the Nazareth Bank were explored; location SS45 (14° 10.852'S; 60° 56.465'E) and SS46 (14° 24.848'S; 61° 02.659'E) on the northeast of the bank with a depth range of 35-36 m and 34-38 m, respectively. The Nazareth Bank is found within the Exclusive Economic Zone of the Republic of Mauritius and is characterised by a surrounding slope of about 150 m with a shallow central part of about 50 - 60 m deep (Mees, 1996). With the aid of the Argus Remotely Operated Underwater Vehicle (ROV) attached to the Video-Assisted Multi-Sampler (VAMS), SS45 and SS46 were explored for 11 minutes along a transect of 37 m and 30 minutes along a transect of 110 m, respectively. Both areas were covered with the seagrass *Thalassodendron ciliatum* or mixed with organisms such as *Halimeda* spp. and sponges, among others (Fig. 1). Both locations indicated the occurrence of one dominant species of seagrass of approximately 90 – 100 % coverage within the studied area, similar to the Saya de Malha Bank. This observation provides new information on seagrass beds occurring on the Mascarene plateau, notably on the Nazareth Bank.

One of the very important services that seagrass beds provide, besides being important as nursery grounds for fish and other juvenile benthic organisms, is its blue carbon storage capacity. While seagrasses have been recognised for their carbon sequestration capacity since the 1980s (Smith, 1981), this topic has received very little attention until recently where they have been recognised as a blue carbon ecosystem that could potentially contribution in addressing climate change impacts (Duarte *et al*., 2005, 2013; Mcleod *et al*., 2011; Fourqurean *et al*., 2012; Gullstrom *et al*., 2018; Bedulli *et al*., 2020). Indeed, seagrass can absorb carbon dioxide from the atmosphere and the ocean for the process

http://dx.doi.org/10.4314/wiojms.si2021.2.13

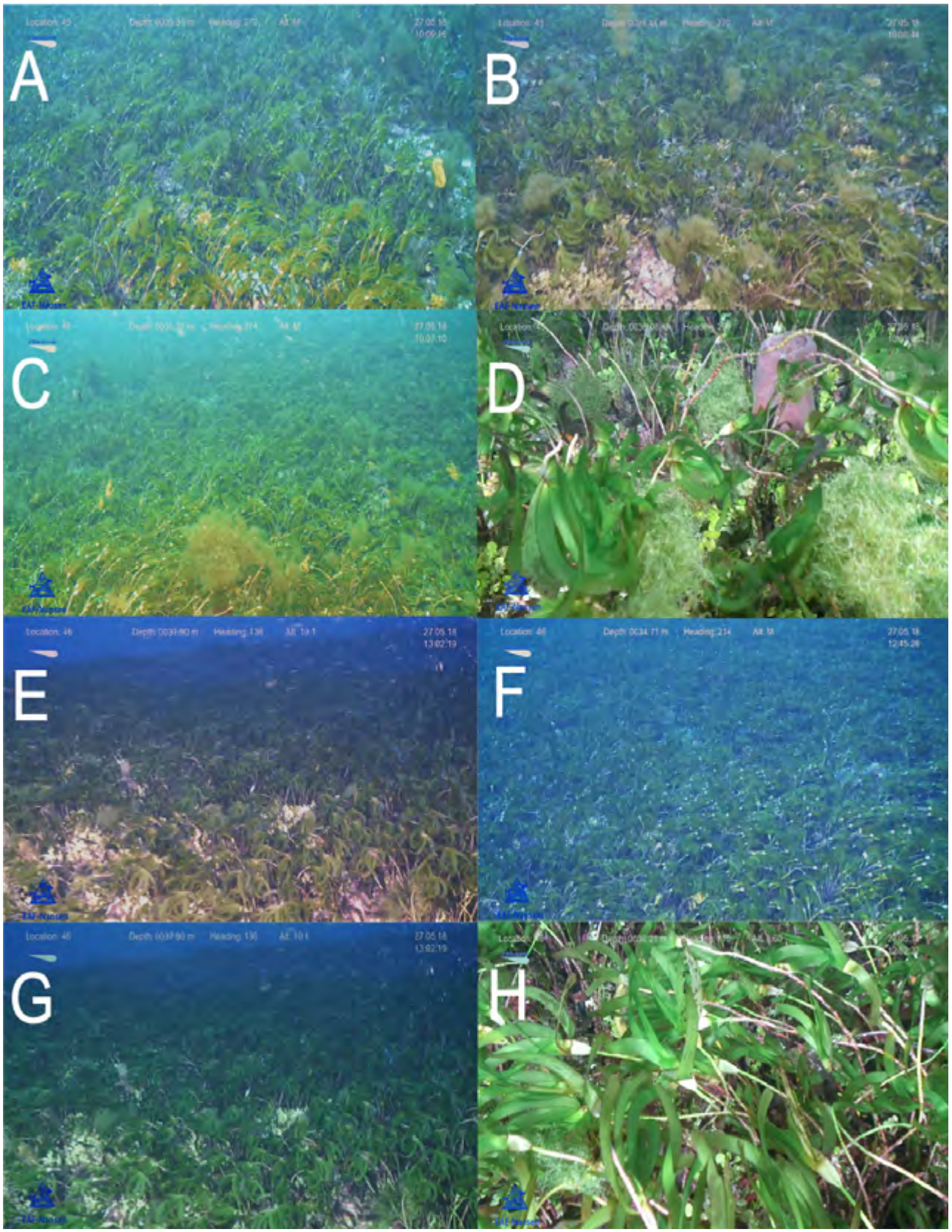

Figure 1. Presence of large seagrass beds (*T. ciliatum*) on the Nazareth Bank. A-D: Location 45 at a depth range of 35-36 m. E-H: Location 46 at a depth range of 34-38 m. D and H represents a closer view of the seagrass species at Location 45 and 46, respectively. Photographs were taken using the Argus Remotely Operated Underwater Vehicle (ROV).

of photosynthesis and store the organic carbon for a long time in the underlying sediments (McKenzie and Unsworth, 2009). Globally, they have been estimated to sequester between 27-44 Tg (approximately 10-18 %) of organic carbon per year in the ocean. This is comparable to terrestrial and mangrove forests (Duarte *et al*., 2005; Fourqurean *et al*., 2012). A study in 2012 by Gullstrom *et al*. (2018), conducted on the Eastern African coast of Tanzania and Mozambique, demonstrated that of the four species of seagrass meadows targeted, *Enhalus acoroides*, *Thalassia hemprichii*, *Cymodocea* spp., and *T. ciliatum*, meadows of both *E. acoroides* and *T. ciliatum* had a significantly higher organic carbon stock (approximately 7305 gm^{-2}) as compared to the other two species.

Research carried out on the Nazareth Bank is extremely limited and has been concentrated mainly on its fisheries resources (Caussy *et al*., 2019), primary productivity (Ramchandur *et al*., 2017) or oil and gas prospects (Meyerhoff and Kamen-Kaye, 1989), while no research has been carried out on its benthic habitats, especially on the presence of seagrass beds with potential for blue carbon sequestration. This first field observation on the presence of large *T. ciliatum* meadows at two shallow water areas within the Nazareth Bank brings forth new knowledge on the distribution of this species in the waters of the Republic of Mauritius. More work is however warranted to thoroughly explore the distribution of such meadows within the Bank as well as their potential for carbon capture.

Acknowledgements

The underlying work was made possible with the support of the EAF-Nansen Programme "Supporting the Application of the Ecosystem Approach to Fisheries Management considering Climate Change and Pollution Impacts" executed by Food and Agriculture Organization of the United Nations (FAO) and funded by the Norwegian Agency for Development Cooperation (Norad). The authors are thankful to FAO for funding and supporting the Indian Ocean research expedition 2018 on the Saya de Malha Bank and Nazareth Bank with the R/V *Dr Fridtjof Nansen*, the Department of Continental Shelf, Maritime Zones Administration & Exploration of Mauritius for co-leading and coordinating the scientific expedition, the Mauritius-Seychelles Joint Commission of the Extended Continental Shelf for their support and assistance and granting the necessary authorisations, the Ministry of Blue Economy, Marine Resources, Fisheries & Shipping for hosting and spearheading the Habitat Mapping Workshop in Mauritius and for granting necessary authorization to carry out research in the Nazareth Bank; the Institute of Marine Research, Norway for leading the expedition and providing the technical and logistic support. The authors also thank the participating scientists, the crew members and the VAMS / Argus ROV technicians for their work and contribution during the expedition and to the anonymous reviewers for their insightful comments which have significantly improved the manuscript.

References

Anthony KRN, Maynard JA, Diaz-Pulido G, Mumby PJ, Cao L, Marshall PA, Hoegh- Guldberg O (2011) Ocean acidification and warming will lower coral reef resilience. Global Change Biology 17: 1798–1808

Bedulli C, Lavery PS, Harvey M, Duarte CM, Serrano O (2020) Contribution of seagrass blue carbon toward carbon neutral policies in a touristic and environmentally-friendly Island. Frontiers in Marine Sciences 7: 1-12

Caussy L, Appadoo C, Sauer WHH, Potts WM (2019) Preliminary observations of the reproductive biology of the Frenchman seabream *Polysteganus baissaci* (Sparidae) from Mauritius. African Journal of Marine Science 41: 455-461

Daby D (2003) Some quantitative aspects of seagrass ecology in a coastal lagoon of Mauritius. Marine Biology 142: 193-203

Duarte CM, Cebrian J (1996) The fate of marine autotrophic production. Limnology and Oceanography 41: 1758-1766

Duarte CM, Middelburg JJ, Caraco N (2005) Major role of marine vegetation on the oceanic carbon cycle. Biogeosciences Discussions 1: 659-679

Duarte MC, Bandeira S, Romeiras MM (2012) Systematics and ecology of a new species of seagrass (*Thalassodendron, Cymodoceaceae*) from southeast African coasts. Novon a Journal of Botanical Nomenclature 22: 16-24

Duarte CM, Losada IJ, Hendriks IE, Mazarrasa I, Marbà N (2013) The role of coastal plant communities for climate change mitigation and adaptation. Nature Climate Change 3: 961-968

Fourqurean JW, Duarte CM, Kennedy H, Marbà N, Holmer M, Mateo MA, Apostolaki ET, Kendrick GA, Krause-Jensen D, McGlathery KJ, Serrano O (2012) Seagrass ecosystems as a globally significant carbon stock. Nature Geosciences 5: 505-509

Gullstrom M, de la Torre Castro M, Bandeira SO, Bjork M, Dahlberg M, Kautsky N, Ronnback P, Ohman MC (2002) Seagrass ecosystems in the western Indian Ocean. Ambio 31: 588-596

Gullstrom M, Lyimo LD, Dahl M, Samuelsson GS, Eggertsen M, Anderberg E, Rasmusson LM, Linderholm HW, Knudby A, Bandeira S, Nordlund LM, Bjork M (2018) Blue carbon storage in tropical seagrass meadows relates to carbonate stock dynamics, plant–sediment processes, and landscape context: insights from the Western Indian Ocean. Ecosystems 21: 551-566

Jackson EL, Rowden AA, Attrill M, Bossey SJ, Jones MB (2001) The importance of seagrass beds as a habitat for fishery species. Oceanography and Marine Biology 39: 269-304

Jagtap TG (1993) Studies on littoral and sublittoral macrophytes around the Mauritian coast. Atoll Research Bulletin 352: 1-23

McKenzie LJ, Unsworth RKF (2009) Great Barrier Reef water quality protection plan (Reef Rescue) – marine monitoring program: intertidal seagrass. Final report for the sampling period 1 September 2008 - 31 May 2009. Fisheries Queensland, Cairns. 143 pp

Mcleod E, Chmura GL, Bouillon S, Salm R, Björk M, Duarte CM, Lovelock CE, Schlesinger WH, Silliman BR (2011) Review: A blueprint for blue carbon: toward an improved understanding of the role of vegetated coastal habitats in sequestering CO_2. The Ecological Society of America, Frontiers in Ecology: 552-560

Mees CC (1996) The Mauritian banks fishery – A review and spatial analysis. MRAG, London. 62 pp

Meyerhoff AA, Kamen-Kaye M (1981) Petroleum prospects of Saya de Malha and Nazareth Banks, Indian Ocean. American Association of Petroleum Geologists Bulletin 65: 1344-1347

Nakamura Y, Terashima H, Samyan C, Sato N, Ida H (2006) Preliminary survey and diet analysis of seagrass bed fishes at Mauritius, Western Indian Ocean. Galaxea, Japanese Coral Reef Society 8: 61-69

Paupiah CN, Mosaheb JI, Mangar V, Leckraz S, Kulputtea D, Samyan C, Bookun V, Mungry K, Terashima H, Yamamoto M (2000) Present status of seagrass at Albion and Pointe aux Cannoniers, Mauritius, Indian Ocean – A preliminary study. Report on Marine Ecology Resources Institute 99301: 1-12

Ramah S, Etwarysing L, Auckloo N, Gopeechund A, Bhagooli R, Bahorun T (2014) Prophylactic antioxidants and phenolics of seagrass and seaweed species: A seasonal variation study in a Southern Indian Ocean Island, Mauritius. Internet Journal of Medical Update 9: 27-37

Ramchandur V, Rughooputh S, Boojawon R, Motah BA (2017) Assessment of chlorophyll-a and sea surface temperature variability around the Mascarene Plateau, Nazareth Bank (Mauritius) using satellite data. Indian Journal of Fisheries 64: 1-3

Smith SV (1981) Marine macrophytes as a global carbon sink. Science 211: 838-840

First field observations of *Halimeda* beds at depths of 37-62 m at Saya de Malha and Nazareth banks, Mascarene Plateau

Ranjeet Bhagooli[1,2,3]*, Sundy Ramah[1,4], Deepeeka Kaullysing[1,2], Arvind Gopeechund[1,2], Odd A. Bergstad[5]

[1] Department of Biosciences and Ocean Studies, Faculty of Science & Pole of Research Excellence in Sustainable Marine Biodiversity, University of Mauritius, Réduit 80837, Republic of Mauritius

[2] The Biodiversity and Environment Institute, Reduit, Republic of Mauritius

[3] The Society of Biology, Reduit, Republic of Mauritius

[4] Albion Fisheries Research Centre, Ministry of Blue Economy, Marine Resources, Fisheries and Shipping, Albion, Petite Rivière, 91001, Republic of Mauritius

[5] Institute of Marine Research (IMR), PO Box 1870 Nordnes, N-5817 Bergen, Norway

* Corresponding author: r.bhagooli@uom.ac.mu

Halimeda spp. are cosmopolitan benthic marine green calcifying macroalgae occurring in shallow and deep waters. Their leaf-like segments are produced in a branched and segmented manner. Reproduction occurs by the edges of the segments turning into whitish reproductive cells that release the protoplasmic contents of spores, a process known as holocarpy, followed by the death and disintegration of the *Halimeda* segments (Drew and Abel, 1988). The segments grow continuously with a maximum of one segment per branch per day (Vroom *et al*., 2003). This rapid segmental growth may have a full turnover of about 30 days or less (van Tussenbroek and van Dijk, 2007). Walters *et al*. (2002) documented the vegetative reproduction of fragments of *Halimeda* on Conch Reef, Key Largo, Florida, which generated 4.7 – 9.4 fragments m^{-2} day^{-1}. *Halimeda* beds, or bioherms, are important in fixing and storing atmospheric carbon in the long-term in the tropics (Kinsey and Hopley, 1991) and result in the production of extensive sediment deposits due to the large biomass resulting from the thick mats. Therefore, sediments from *Halimeda* may be considered as carbon sinks and carbonate buffers (Rees *et al*., 2007). In the tropics *Halimeda*'s calcareous segments provide a major carbonate sediment (Freile *et al*., 1995), contributing to a reef development framework and a build-up of carbonate platforms (Pomar and Kendall, 2007). This allows *Halimeda* spp. to significantly contribute to the carbon budget estimated to be similar to or exceeding that of corals within the reef (Rees *et al*., 2007).

The occurrence and increase of *Halimeda opuntia* cover from 1997 to 2002 in the shallow areas (<20 m) of the Ritchie Bank in the north of Saya de Malha has been reported by Hilbertz and Goreau (2002). They suggested these changes may be attributed to the coral bleaching/mortality of 1998, when some 77% on the windward and 87% on the leeward coasts bleached or died around St. Pierre, Republic of Seychelles (Spencer *et al*., 2000). A review by Vortsepneva (2008) indicated that Karpitenko and Bidenko (1980) reported that *Halimeda* algae were more frequently found on the low terrace, with study stations not clearly defined by depths, but related to the landscape of the submerged circular reef areas between the upper terrace and the slopes and foot of the reef. However, these studies in the 1980s, late 1990s and early 2000s did not thoroughly document the green coralline algae, *Halimeda*, in the dynamic southern bank of Saya de Malha, a region which is well known to be data deficient.

The May 2018 EAF-Nansen Programme research cruise provided a unique opportunity to visually document the green coralline algae-dominated beds at the studied locations (Fig. 1A) 36, 37, 39 and 40 at

http://dx.doi.org/10.4314/wiojms.si2021.2.14

Saya de Malha (Fig. 1B), and 44, 47 and 52 at Nazareth (Fig. 1C) Banks using the Video-Assisted Multi-Sampler (VAMS) for standard inspection of the seabed by video. The Van Veen grabs attached to the VAMS also collected some samples at the study locations. In this paper, the presence of quite large *Halimeda* beds is reported at depths ranging from about 37 to 43 m at locations 36 (Fig. 2 A, B, D, F), 37 (Fig. 2C), 39 (Fig. 2E) and 40 (Fig. 2G) at Saya de Malha, and locations 44 (Fig. 2H), 47 (Fig. 2I) and 52 (Fig. 2J, K) at Nazareth Bank, where such environments are considered as oligotrophic and receiving low irradiance. Ramah *et al*. (*in prep for submission in this Special Issue*) indicated that at locations 36, 37, 39, and 40, the general macroalgal cover was estimated at 23-72%, 52-71%, 21-71% and 48%, respectively. Based on the morpho-anatomy description in Oliveira *et al*. (2005), three species of *Halimeda* were observed, namely *H. opuntia*, *H. discoidea* and *H. tuna*, the latter being most dominant. *Halimeda* has been reported to live down to 130 m in clear tropical waters (Littler *et al*., 1985). In Mediterranean waters, *H. tuna* stands have been documented at 35 m at Tossa de Mar (Ballesteros, 1991), while in Maltese waters the species grew at a depth of 75 m (Drew, 1969).

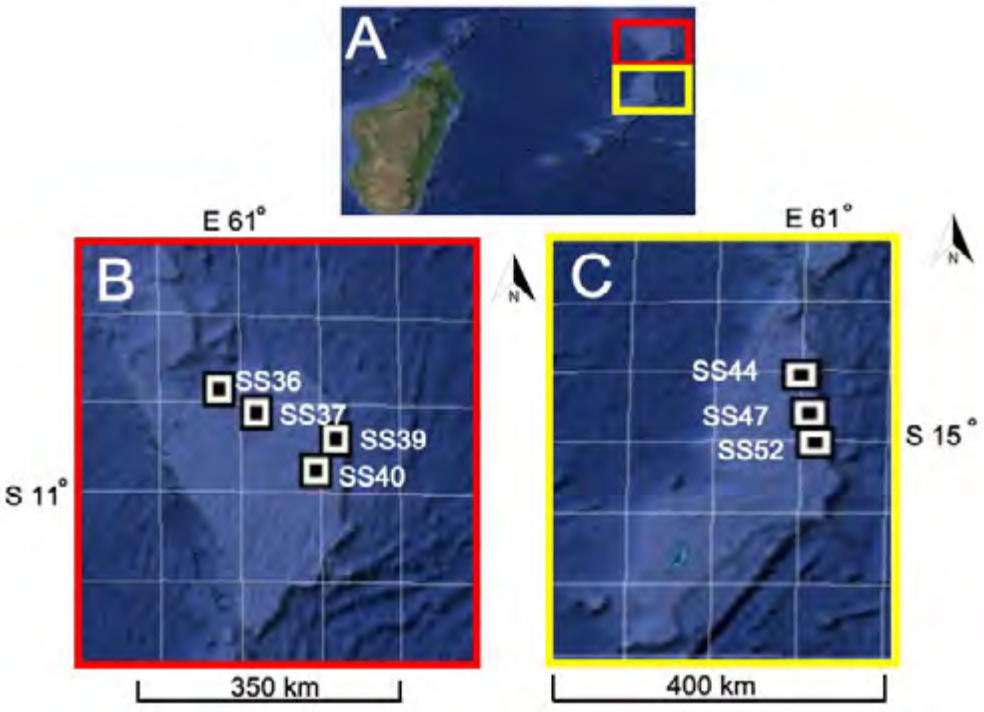

Figure 1 A. Map indicating the Saya de Malha and Nazareth banks studied during the EAF-Nansen 2018 research cruise on the Mascarene Plateau. B. Study locations 36, 37, 39 and 40 on the Southern Saya de Malha. C. Study locations 44, 47 and 52 on the Nazareth Bank.

Halimeda beds not only provide an important substrate but also a diverse habitat for marine organisms (Multer and Clavijo, 2004). For instance, the ophistobranchian *Bosellia mimetica* feeds on the chloroplast and camouflages itself in a green colour similar to *H. tuna* (J Ellis and Solander) JV Lamouroux 1816, segments. The *Halimeda* beds of the southern Saya de Malha bank harboured fishes like the regionally endemic *Amphiprion* sp. (Fig. 2B), commercially important red emperor, *Lutjanus sebae* (Fig. 2D) and the emperor, *Lethrinus* sp. (Fig. 2F). The *Halimeda* fields of the Nazareth bank were inhabited by *Helipora coerulea* and *Porites* sp. (Fig. 2G), *Seriatopora* sp. (Fig. 2H), and the elephant trunk sea cucumber, *Holothuria fuscopuntata* (Fig. 2K); the first record of this species at a depth as great as 61.64 m. McGrouther (2018) mentioned the accidental discovery of a *Halimeda* bed or meadow at 30-40 m depth near Lizard Island on the Great Barrier Reef in 1982. Out of the 14 fish species they recorded, a new goby species, *Minysicya caudimaculata*, was described by Larson in 2002 (McGrouther, 2018). In 2001, Leis and colleagues collected fish samples at depths of 23-27 m at the same *Halimeda* bed and found 378 fishes (35 species in 18 families), at least 4 gobies of the genus *Hetereleotris*, and 1 cardinal fish of the genus *Fowleria*

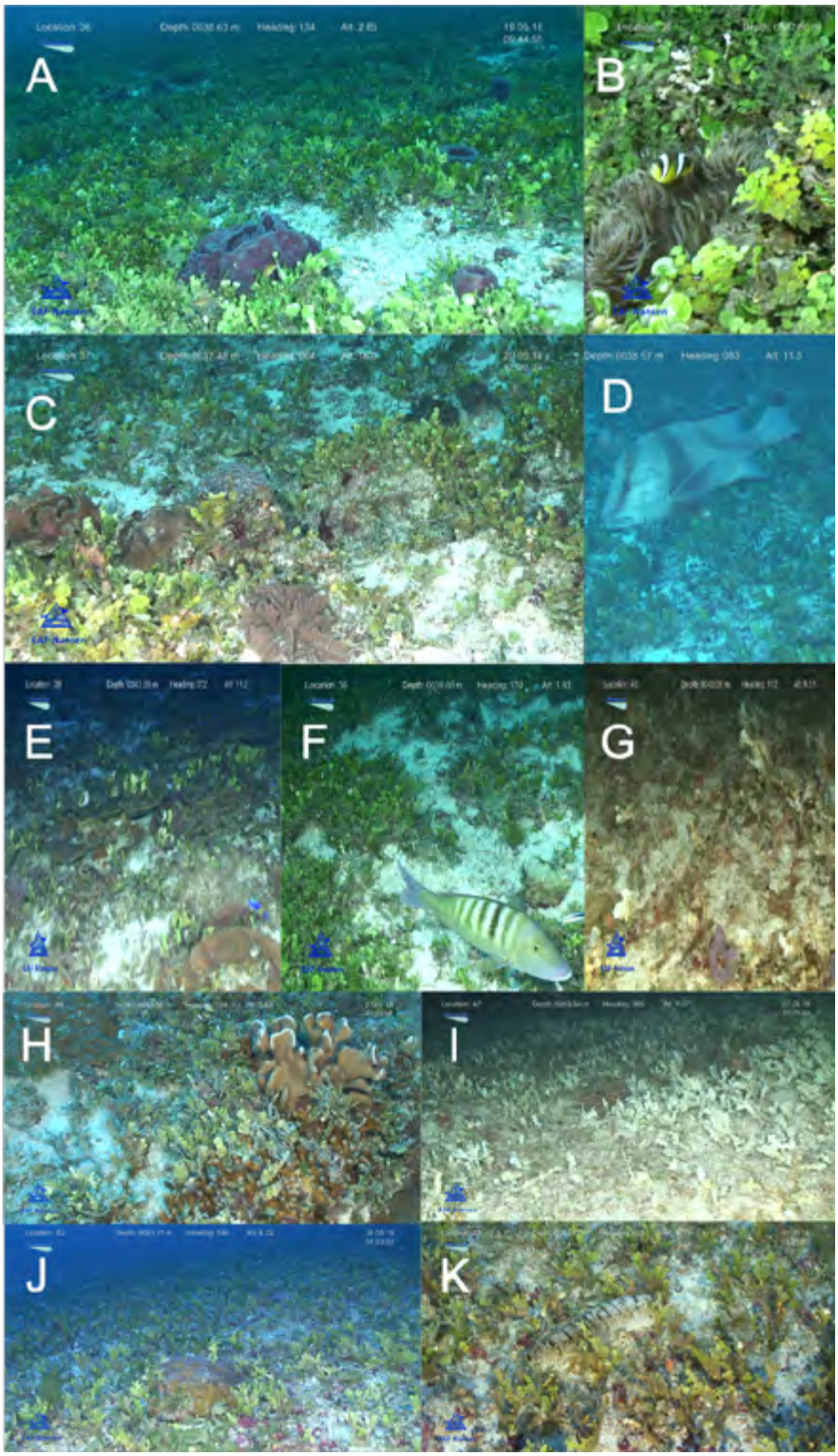

Figure 2. Fields of *Halimeda* at Saya de Malha Bank: A. Location 36 at a depth of 38.63 m – Sponges in the *Halimeda* bed; B. Location 36 at a depth of 37.86 m – Regionally endemic clownfish *Amphirion* sp.; C. Location 37 at a depth of 37.48 m – Corals in the *Halimeda* bed; D. Location 37 at a depth of 38.57 m – The emperor red snapper, *Lutjanus sebae*, native to the Indian Ocean and the Western Pacific region; E. Location 39 at a depth of 43.29 m – Plate corals in the *Halimeda* bed; F. Location 36 at a depth of 38.01 m – Commercially fished *Lethrinus* sp.; G. Location 40 at a depth of 43.05 m – *Halimeda* whitening. Fields of *Halimeda* at Nazareth Bank: H. Location 44 at depth 40.98 m - *Helipora coerulea* and *Porites* sp.; I. Location 47 at depth 59.64 m - *Seriatopora* sp.; J. Location 52 at depth 61.57 m - *Porites* sp.; K. Location 52 at depth 61.64 m - *Holothuria fuscopuntata* (elephant trunk sea cucumber, maximum depth previously reported is 30 m). Photos taken using the Argus Remote Operated Video (ROV). RV Dr Fridtjof Nansen, 2018.

(McGrouther, 2018). With only 3 collections, 8 fish species were recognised as new to Australia along with at least 5 undescribed ones, indicating that *Halimeda* beds are potential hotspots of biodiversity.

From a biotechnological perspective, in addition to antioxidant (De Oliveira e Silva *et al*., 2012), antimicrobial properties (*Escherichia coli, Klebsiella oxytoca, K. pneumonia, Lactobacillus vulgaris, Proteus mirabillis, Pseudomonas* sp., *Salmonella paratyphi, S. typhimurium, Staphylococcus aureus and Vibrio cholerae*), and antifungal (*Aspergillus flavus, A. niger, Alternaria alternaria, Candida albicans, Epidermophyton floccossum, Penicillium* sp., *Rhizopus* sp., *Trichophyton mentagrophytes* and *T. rubrum*) (Indira *et al*., 2013) properties, activity against the marine coronavirus A59 by Halitunal, an uncommon diterpene aldehyde isolated from *H. tuna*, has been documented (Koehn *et al*., 1991).

This first observation of quite large *Halimeda* beds at 37-62 m depths at the Saya de Malha and Nazareth Banks suggests the possibility of such a habitat acting as an important carbon sink, requiring conservation and preservation of the regionally endemic and commercially important biodiversity, and warranting further exploration and sustainable use of the potential associated biotechnological resources of the Mascarene Plateau. Further in-depth ecological and biotechnological investigations are imperative to thoroughly understand the potential of such a biodiversity hotspot and its related marine resources, especially within the framework of Sustainable Development Goal 14, life under the sea.

Acknowledgements

The underlying work was made possible with the support of the EAF-Nansen Programme “Supporting the Application of the Ecosystem Approach to Fisheries Management considering Climate Change and Pollution Impacts” executed by Food and Agriculture Organization of the United Nations (FAO) and funded by the Norwegian Agency for Development Cooperation (Norad). The authors are thankful to FAO for funding and supporting the Indian Ocean research expedition 2018 on the Saya de Malha Bank and Nazareth Bank with the R/V Dr Fridtjof Nansen, the Department of Continental Shelf, Maritime Zones Administration & Exploration of Mauritius for co-leading and coordinating the scientific expedition, the Mauritius-Seychelles Joint Commission of the Extended Continental Shelf for their support and assistance and granting the necessary authorisations, the Ministry of Blue Economy, Marine Resources, Fisheries and Shipping for granting the permits for sampling, and the University of Mauritius for logistic support and laboratory facilities." The authors are indebted to the fellow participants on the expedition. The authors are thankful to the reviewer’s comments that improved the paper.

References

Ballesteros E (1991) Structure of a deep-water community of *Halimeda tuna* (Chlorophyceae, Caulerpales) from the North-Western Mediterranean. Collectiona Botanica 20: 5-21

De Oliveira e Silva AM, Vidal-Novoa A, Batista-González AE, Pinto JR, Portari Mancini DA, Reina-Urquijo W, Mancini-Filho J (2012) *In vivo* and *in vitro* antioxidant activity and hepatoprotective properties of polyphenols from *Halimeda opuntia* (Linnaeus) Lamouroux. Redox Report 17 (2): 47-53

Drew EA (1969) Photosynthesis and growth of attached marine algae down to 130 meters in the Mediterranean. Proceedings of the VI International Seaweed Symposium 6: 151-159

Drew EA, Abel KM (1988) Studies on *Halimeda* II. Reproduction, particularly the seasonality of gametangia formation, in a number of species from the Great Barrier Reef Province. Coral Reefs 6: 207-218

Freile D, Milliman J, Hillis L (1995) Leeward bank margin *Halimeda* meadows and draperies and their sedimentary importance on the western Great Bahama Bank slope. Coral Reefs 14: 27-33

Hilbertz W, Goreau T (2002) Saya de Malha Expedition, March, 2002. 101 pp

Indira K, Balakrishnan S, Srinivasan M, Bragadeeswaran S, Balasubramanian T (2013) Evaluation of *in vitro* antimicrobial property of seaweed (*Halimeda tuna*) from Tuticorin coast, Tamil Nadu, Southeast coast of India. African Journal of Biotechnology 12 (3): 284-289

Karpitenko EA, Bidenko VG (1980) Trade investigations in the Indian Ocean. In: Fish economic investigations in north-east part of Indian Ocean, M. VNIRO. pp 53-65 (in Russian)

Kinsey D, Hopley D (1991) The significance of coral reefs as global carbon sinks–response to greenhouse. Palaeogsography, Palaeoclimatology, Palaeoecology (Global and Planetary Change Section) 89: 363-377

Koehn RE, Gunasekera SF, Niel DN, Cross SS (1991) Halitunal, an unusual diterpene aldehyde from the marine alga *Halmeda tuna*. Temhadron Letters 32 (2) 169-172

Littler MM, Littler DS, Blair SM, Norris JN (1985) Deepest known plant life discovered on an unchartered seamount. Science 227: 57-59

McGrouther M (2018) Halimeda, hot beds of biodiversity! [https://australian.museum/learn/animals/fishes/halimeda-hot-beds-of-biodiversity/]

Multer HG, Clavijo I (2004) *Halimeda* investigations: progress and problems. NOAA/RSMAS. pp 117-127

Oliveira EC, Osterlund K, Mtolera MS (2005) Marine plants of Tanzania – A field guide to the seaweeds and seagrasses. Botany Department, Stockholm University, Sweden. 267 pp

Pomar L, Kendall CGSC (2007) Architecture of carbonate platforms: a response to hydrodynamics and evolving ecology. In: Lukasik J, Simo JA (eds) Controls on carbonate platform and reef development. SEPM 89: 187-216

Rees SA, Opdyke BN, Wilson PA, Henstock TJ (2007) Significance of *Halimeda* bioherms to the global carbonate budget based on a geological sediment budget for the Northern Great Barrier Reef, Australia. Coral Reefs 26: 177-188

Spencer T, Teleki KA, Bradshaw C, Spalding MD (2000) Coral bleaching in the southern Seychelles during the 1997–1998 Indian Ocean warm event. Marine Pollution Bulletin 40 (7): 569-586

Van Tussenbroek BI, van Dijk JK (2007) Spatial and temporal variability in biomass and production of psammophytic *Halimeda incrassata* (Bryopsidales, Chlorophyta) in a Caribbean reef lagoon. Journal of Phycology 43: 69-77

Vortsepneva E (2008) Saya de Malha Bank – an invisible island in the Indian Ocean. Geomorfology, Oceanology, Biology. 44 pp

Vroom PS, Smith CM, Coyer JA, Walters LJ, Hunter CL, Beach KS, Smith JE (2003) Field biology of *Halimeda tuna* (Bryopsidales, Chlorophyta) across a depth gradient: comparative growth, survivorship, recruitment, and reproduction. Hydrobiologia 501: 149-166

Walters LJ, Smith CM, Coyer JA, Hunter, CL, Beach KS, Vroom PS (2002) Asexual propagation in the coral reef macroalga *Halimeda* (Chlorophyta, Bryopsidales): production, dispersal and attachment of small fragments. Journal of Experimental Marine Biology and Ecology 278: 47-65

First report of White Syndrome Disease on branching *Acropora* at Saya de Malha, Mascarene Plateau

Ranjeet Bhagooli[1,2,3]*, Shakeel Jogee[1], Deepeeka Kaullysing[1,2], Sundy Ramah[1,4]

[1] Department of Biosciences and Ocean Studies, Faculty of Science & Pole of Research Excellence in Sustainable Marine Biodiversity, University of Mauritius, Réduit 80837, Republic of Mauritius

[2] The Biodiversity and Environment Institute, Reduit, Republic of Mauritius

[3] The Society of Biology, Reduit, Republic of Mauritius

[4] Albion Fisheries Research Centre, Ministry of Blue Economy, Marine Resources, Fisheries and Shipping, Albion, Petite Rivière, 91001, Republic of Mauritius

* Corresponding author: r.bhagooli@uom.ac.mu

With the potential to cause rapid and large-scale reef decline, coral diseases represent a prominent global stressor to coral reef ecosystems (Aronson *et al.,* 2003; Harvell *et al.,* 2007). The Western Indian Ocean (WIO) is not spared from coral diseases. Observation of coral diseases in the WIO dates back to 1991 when the Skeletal Eroding Band (SEB) coral disease caused by the pathogenic protozoan, *Halofolliculina corallasia*, was reported around Mauritius Island (Antonius (1991) in Antonius and Lipscomb, 2000). A study by Goreau in 1998 (cited in Hilbertz and Goreau, 2002) observed Porites Line Disease in massive *Porites* sp. in 1997 in Seychelles. In Zanzibar, *Vibrio coralyticus* was isolated from diseased *Pocillopora damicornis* (Ben-Haim and Rosenberg, 2002). White Syndrome Disease (WSD) was reported, at prevalence levels below 1.5%, in the south-west reef systems of Madagascar (Sheridan *et al.,* 2014). Studies conducted around Reunion Island, Mayotte, and South Africa revealed the occurrence of six coral diseases: Growth Anomalies, Black Band Disease, Skeletal Eroding Band, WSD, Pink Line Syndrome and *Porites* White Patch Syndrome (Séré *et al.,* 2015). In the same study, spatial heterogeneity in disease prevalence among the sites was also observed, where Reunion Island had the highest disease prevalence rate (7.5 ± 2.2%) compared to South Africa (3.9 ± 0.8%) and Mayotte (2.7 ± 0.3%) (Séré *et al.,* 2015). It was further reported that WSD and Black Band Disease were more common, and *Porites* and *Acropora* were the most disease-vulnerable genera. WSD, amongst other coral diseases such as Brown Band, SEB, Black Band and Ulcerative White Spot, was also reported as one of the most prevalent coral diseases among seven islands of the Maldivian Archipelago where the overall estimated disease prevalence was around 1.51% (Montano *et al.,* 2015). More recently, Bhagooli *et al.* (2017) observed Brown Band, SEB, White Band, White Plague, Growth Anomalies, and Pink Pigmentation Response in corals in the lagoonal area of Mauritius.

The only coral disease observations from the poorly studied Saya de Malha region revealed two types of coral diseases: one isolated Black Band case and the highly abundant Porites Line Disease (PLD) (Hilbertz and Goreau, 2002) at the northern region on Ritchie bank and at depths of less than 20 m. The same PLD-affected corals that survived the 1998 bleaching event were found dead in 2002, most probably as a result of the disease (Hilbertz and Goreau, 2002). Although being remote and distant from terrestrial influences, the submerged Saya de Malha bank located in the WIO holds evidence of coral diseases and requires further studies.

The second leg of the EAF-Nansen research survey cruise in May 2018 at the Saya de Malha bank provided an opportunity to use the Video-Assisted Multi Sampler (VAMS) to collect coral samples. At location 39 (10° 22.6501'S; 62° 12.362035'E) on the Saya de Malha bank, WSD was observed on *Acropora* sp. which was collected (Fig. 1) from a depth of 30 m. Such environments are characterised by low coral

http://dx.doi.org/10.4314/wiojms.si2021.2.15

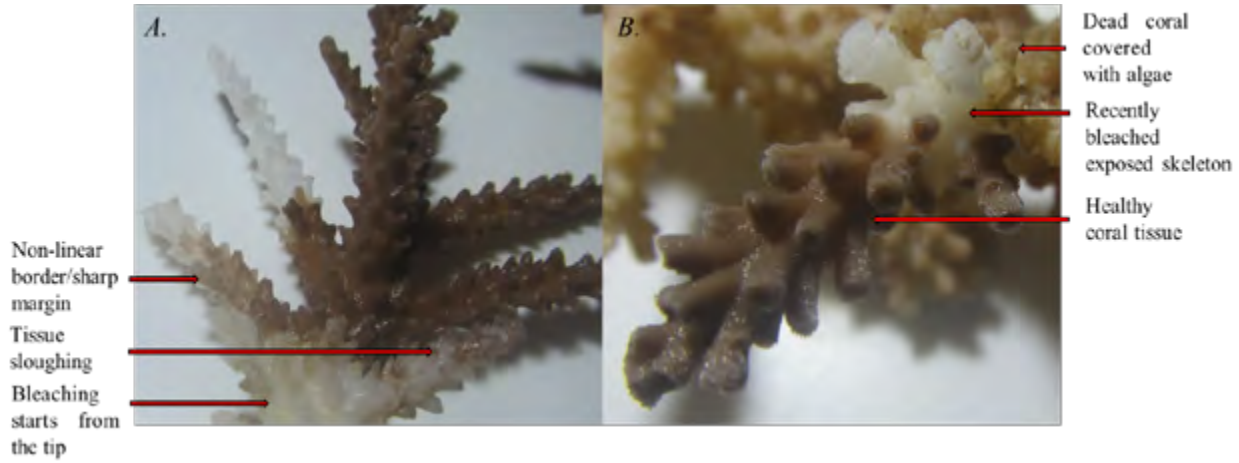

Figure 1. White Syndrome Disease (WSD) on *Acropora* sp. (A and B) collected from 30 m at Saya de Malha bank.

cover and possibly reduced frequency of warm temperature anomalies. Ramah *et al*. (2021) indicated that at location 39, the general live hard coral cover was estimated at 9-33%. The corals observed at location 39 included *Acropora*, *Porites*, *Lobophyllia*, *Goniastrea* and *Favites* species. WSD in *Acropora* sp. was observed only among the collected coral samples. It is noteworthy that high coral cover (>50%) and warm temperatures are two important prerequisites for outbreaks of WSD. Depth is also an important factor in the distribution of WSD, with a reduction of 89% and 43% in live coral cover at 5 m and 20 m, respectively, associated with WSD (Hobbs *et al.,* 2015). WSD on *Acropora* corals have been commonly reported from depth ranges of 5 m (Hobbs *et al.,* 2015; Hobbs and Frisch, 2010), 4-6 m (Roff *et al.,* 2011), and 20 m (Hobbs *et al.,* 2015).

It is also worth highlighting that corallivorous gastropods generally feed on Acroporids in large masses (high density aggregations) (Bruckner *et al.*, 2017; Kaullysing *et al.,* 2017; Kaullysing *et al.*, 2020). For instance, the corallivorous gastropods *Drupella* are attracted to other *Drupella* individuals forming an aggregation to feed over corals (Cumming, 2009a; 2009b). However, during this survey, not a single corallivorous individual was collected and/or observed in the vicinity of the coral. Moreover, it has been reported that corallivorous gastropods occur in lower densities in deeper waters (6-9 m) (Scott *et al.*, 2017). Thus, the possibility of the white patches being those of predation scars was ruled out.

WSD appears to be quite common in the WIO (Sheridan *et al.,* 2014; Séré *et al.,* 2015; Montano *et al.,* 2015). WSDs are a group of coral diseases characterised by diffuse patterns of tissue loss that expose the underlying bare white coral skeleton (Raymundo *et al.,* 2008; Roff *et al.,* 2011). The lesion boundaries of WSD can be linear, annular or irregular, and the coral tissue bordering the lesion can sometimes become pigmented (Roff *et al.,* 2011; Beeden *et al.,* 2008). In *Acropora* corals, the disease can be observed originating at the base of coral branches that are found in the middle of the colony (Roff *et al.,* 2011). The rate of tissue loss caused by this disease has been recorded to range from 0 to 1,146 cm^2 per week (Roff *et al.,* 2011). The bacterium *Vibrio owensii* has been isolated as the main pathogenic agent of WSD in *Monitpora capitata* (Ushijima *et al.,* 2012). WSDs have been observed to progress at a rate not exceeding 20 mm per day. The most common host of this disease is *Acropora* corals (Raymundo *et al.,* 2008; Roff *et al.,* 2011), but it has also been observed in *Turbinaria* (Dalton *et al.,* 2009). WSDs have been recorded in the reefs of the Indo-Pacific (Roff *et al.,* 2011; Dalton *et al.,* 2010), Caribbean (Weil and Hooten, 2008), Pacific Ocean (Aeby *et al.,* 2010). The prevalence of WSD is moderately high, usually not exceeding 10% (Roff *et al.,* 2011). The prevalence of WSD is usually higher in winter months (Roff *et al.,* 2011). However, Aeby *et al.* (2010) reported no influence of season on the prevalence of WSD. Bruno *et al*. (2004) also reported an increase in the prevalence of WSDs in densely populated coral communities with increasing temperatures.

This first observation of WSD on the branching *Acropora* coral at a depth of 30 m at the southern Saya de Malha bank is indicative of the possibility of more infectious biotic stressors to the deep and 'pristine' coral reef ecosystem at that bank. Further in-depth characterisation and distribution studies of prevalent diseases and inter-species susceptibility to diseases are warranted to thoroughly understand the impacts of coral diseases at the Saya de Malha bank, for enhanced and adaptive

coral reef management and conservation strategies and efforts, especially in an era of global climate change.

Acknowledgements

The underlying work was made possible with the support of the EAF-Nansen Programme "Supporting the Application of the Ecosystem Approach to Fisheries Management considering Climate Change and Pollution Impacts" executed by Food and Agriculture Organization of the United Nations (FAO) and funded by the Norwegian Agency for Development Cooperation (Norad). The authors are thankful to FAO for funding and supporting the Indian Ocean research expedition 2018 on the Saya de Malha Bank and Nazareth Bank with the R/V *Dr Fridtjof Nansen*, the Department of Continental Shelf, Maritime Zones Administration & Exploration of Mauritius for co-leading and coordinating the scientific expedition, the Mauritius-Seychelles Joint Commission of the Extended Continental Shelf for their support and assistance and granting the necessary authorisations, the Ministry of Blue Economy, Marine Resources, Fisheries & Shipping for hosting and spearheading the Habitat Mapping Workshop in Mauritius and for granting necessary authorization to carry out research in the Nazareth Bank; the Institute of Marine Research, Norway for leading the expedition and providing the technical and logistic support. The authors also thank the participating scientists, the crew members and the VAMS / Argus ROV technicians for their work and contribution during the expedition and to the anonymous reviewers for their insightful comments which have significantly improved the manuscript.

Reference

Aeby GS, Ross M, Williams GJ, Lewis TD, Work TM (2010) Disease dynamics of *Montipora* White Syndrome within Kaneohe Bay, Oahu, Hawaii: Distribution, seasonality, virulence, and transmissibility. Diseases of Aquatic Organisms 91: 1-8

Antonius AA, Lipscomb D (2000) First protozoan coral-killer identified in the Indo-Pacific. Atoll Research Bulletin 481: 1-21

Aronson RB, Bruno JF, Precht WF, Glynn PW, Harvell CD, Kaufman l, Rogers CS, Shinn EA, Valentine JF (2003) Causes of coral reef degradation. Science 302 (5650): 1502-1504

Beeden R, Willis BL, Raymundo LJ, Page CA, Weil E (2008) Underwater cards for assessing coral health on Indo-Pacific reefs. Coral Reef Targeted Research and Capacity Building for Management Program. Currie Communications, Melbourne. 26 pp

Ben-Haim Y, Rosenberg E (2002) A novel *Vibrio* sp. pathogen of the coral *Pocillopora damicornis*. Marine Biology 141 (1): 47-55

Bhagooli R, Mattan-Moorgawa S, Kaullysing D, Taleb-Hossenkhan N (2017) A first field report of coral diseases around Mauritius Island, Western Indian Ocean. Western Indian Ocean Journal of Marine Science, Special Issue 2017: 71-72

Bruckner AW, Coward G, Bimson K, Rattanawongwan T (2017) Predation by feeding aggregations of *Drupella* spp. inhibits the recovery of reefs damaged by a mass bleaching event. Coral Reefs 36: 1181-1187

Bruno JF, Selig ER, Casey KS, Page CA, Willis BL, Harvell CD, Sweatman H, Melendy AM (2007) Thermal stress and coral cover as drivers of coral disease outbreaks. PLoS Biology 5 (6): p.e124

Cumming RL (2009a) Case study: impact of *Drupella* spp. on reef-building corals of the Great Barrier Reef, Report to the Great Barrier Reef Marine Park Authority, Townsville, Australia. Research Publication Series (97). 124 pp

Cumming RL (2009b) Population outbreaks and large aggregations of the coral-feeding *Drupella* spp.: the importance of spatial scale, Report to the Great Barrier Reef Marine Park Authority, Townsville, Australia. Research Publication Series (96). 32 pp

Dalton SJ, Godwin S, Smith SDA, Pereg L (2010) Australian subtropical white syndrome: a transmissible, temperature-dependent coral disease. Marine and Freshwater Research 61 (3): 342-350

Harvell D, Jordán-Dahlgren E, Merkel S, Rosenberg E, Raymundo L, Smith G, Weil E, Willis B (2007) Coral disease, environmental drivers, and the balance between coral and microbial associates. Oceanography 20: 172-195

Hilbertz W, Goreau T (2002) Saya de Malha Expedition, March 2002. 101 pp

Hobbs JPA, Frisch AJ (2010) Coral disease in the Indian Ocean: taxonomic susceptibility, spatial distribution and the role of host density on the prevalence of white syndrome. Diseases of Aquatic Organisms 89 (1): 1-8

Hobbs JPA, Frisch AJ, Newman SJ, Wakefield CB (2015) Selective impact of disease on coral communities: outbreak of white syndrome causes significant total mortality of *Acropora* plate corals. PloS ONE 10 (7): p.e0132528

Kaullysing D, Taleb-Hossenkhan N, Kulkarni BG, Bhagooli R (2017) A first field report of various coral-eating gastropods and associated infestations around Mauritius Island, Western Indian Ocean. Western Indian Ocean Journal of Marine Science (Special Issue) 1: 73-75

Kaullysing D, Mehrotra R, Arnold S, Ramah S, Allchurch A, Haskin E, Taleb-Hossenkhan N, Bhagooli R (2020) Multiple substrates chosen in mass in-situ egg deposition by *Drupella* in Mauritius, a first record for the Western Indian Ocean waters. Journal of Molluscan Studies 86 (4): 427-430

Montano S, Strona G, Seveso D, Maggioni D, Galli P (2016) Widespread occurrence of coral diseases in the central Maldives. Marine and Freshwater Research 67 (8): 1253-1262

Ramah S, Gendron G, Bhagooli R, Soondur M, Souffre M, Melanie R, Coopen P, Caussy L, Bissessur D, Bergstad OA (2021) Distribution and diversity of the shallow water (23-50 m) macro-benthic habitats in the Saya de Malha bank, Mascarene plateau. Western Indian Ocean Journal of Marine Science, Special Issue 2/2021, 69-80.

Raymundo LJ, Couch CS, Harvell CD, Raymundo J, Bruckner AW, Work TM, Weil E, Woodley CM, Jordan-dahlgren E, Willis BL, Sato Y (2008) Coral disease handbook guidelines for assessment, monitoring & management. Coral Reef Targeted Research and Capacity Building for Management Program, 2008. 124 pp

Roff G, Kvennefors ECE, Fine M, Ortiz J, Davy JE, Hoegh-Guldberg O (2011) The ecology of 'Acroporid white syndrome', a coral disease from the southern Great Barrier Reef. PLoS ONE 6 (12): p.e26829

Scott CM, Mehrotra R, Hein MY, Moerland MS, Hoeksema BW (2017) Population dynamics of corallivores (*Drupella* and *Acanthaster*) on coral reefs of Koh Tao, a diving destination in the Gulf of Thailand. Raffles Bulletin of Zoology 65: 68-79

Séré MG, Chabanet P, Turquet J, Quod JP, Schleyer MH (2015) Identification and prevalence of coral diseases on three Western Indian Ocean coral reefs. Diseases of Aquatic Organisms 114 (3): 249-261

Sheridan C, Baele JM, Kushmaro A, Frejaville Y, Eeckhaut I (2014) Terrestrial runoff influences white syndrome prevalence in SW Madagascar. Marine Environmental Research 101: 44-51

Ushijima B, Smith A, Aeby GS, Callahan SM (2012) *Vibrio owensii* induces the tissue loss disease Montipora white syndrome in the Hawaiian reef coral *Montipora capitata*. PloS One 7 (10): p.e46717

Weil E, Hooten AJ (2008) Underwater cards for assessing coral health on Caribbean reefs. Coral reefs targeted research and capacity building for management. 24 pp

First in-situ observation of the endemic giant clam *Tridacna rosewateri* from the Nazareth Bank, Mascarene Plateau

Sundy Ramah[1,2]*, Deepeeka Kaullysing[2], Ranjeet Bhagooli[2]

[1] Albion Fisheries Research Centre, Ministry of Blue Economy, Marine Resources, Fisheries and Shipping, Albion, Petite Rivière 91001, Republic of Mauritius

[2] Department of Biosciences and Ocean Studies, Faculty of Science & Pole of Research Excellence in Sustainable Marine Biodiversity, University of Mauritius, Réduit 80837, Republic of Mauritius

* Corresponding author: sundy.ramah@gmail.com

Giant clams play an important ecological role in the structure and ecology of coral reef communities (Neo *et al*., 2015) and conducting research on these species is as important as the overwhelming attention being given to coral reefs worldwide. Giant clams (family: Cardiidae; sub family: Tridacninae) are the largest living bivalves; some species can live for a hundred years and reach a length over 1.5 m (Yonge, 1975; Nuryanto *et al*., 2007). Giant clams have a feeding behaviour similar to that of corals, exploiting nutrients in both heterotrophic and autotrophic conditions, thanks to their obligate symbiotic association with photosynthetic dinoflagellates (Jantzen *et al.,* 2008), and are able to concentrate most of their energy into growth (Griffiths and Klumpp, 1994). They usually grow in the warm waters of the Pacific and Indian Oceans (Purchon, 1977) and use substrates such as coral, rock, rubble or sand to attach themselves (Ramah *et al*., 2017). Most species are found within shallow lagoons and on reef flats, usually not deeper than 30 m (Neo *et al*., 2017) due to their relationship with symbionts requiring light. Presently, there are 12 recognized extant species of giant clams worldwide, comprising two species of the *Hippopus* genus and ten species of the *Tridacna* genus (Fauvelot *et al*., 2020; Tan *et al*., 2021).

Limited research on these invertebrates is available from the Western Indian Ocean (WIO) region, notably from the Comoros Islands (Mohamed *et al*., 2016) and from several other WIO countries (Fauvelot *et al*., 2020). Among the 12 species, only two are known to be widely distributed in the WIO (Othman *et al*., 2010); namely *Tridacna squamosa* (Lamarck, 1819) and *T. maxima* (Röding, 1798). Two other species, endemic to the WIO, *T. elongatissima* (Bianconi, 1856) and *T. rosewateri* (Sirenko and Scarlato, 1991), have narrow distribution ranges (Fauvelot *et al*., 2020). The two widespread species within the waters of the Republic of Mauritius, *T. maxima* and *T. squamosa,* have been the subject of ecological studies in Mauritius and Rodrigues Islands (Ramah *et al*., 2019). In addition, Mauritian waters are known to host the endemic species *T. rosewateri*, only known from the shallow bank of Saya de Malha (Sirenko and Scarlato, 1991) and Cargados Carajos archipelago (St Brandon) (Fauvelot *et al*., 2020). The only living specimens of *T. rosewateri* were sampled from Cargados Carajos archipelago and were described as "*Tridacna lorenzi*" (Monsecour, 2016), and recently synonymized with *T. rosewateri* (Fauvelot *et al*., 2020). The EAF-Nansen research survey expedition of 2018 provided an excellent opportunity to carry out some exploratory work within the waters of the Saya de Malha and Nazareth Banks in order to refine the geographic distribution of *T. rosewateri*.

With the aid of the Argus Remotely Operated Vehicle (ROV), it was possible to take stock of the different benthic communities of the Saya de Malha and Nazareth Banks. In this note, the *in-situ* observation of two individuals of the WIO endemic giant clam *T. rosewateri* in their natural habitat at depths of 38.60 m and 39.66 m (Fig. 1 B-H) within the Nazareth Bank are reported. Morphological identification of giant clams *in situ* can be challenging, especially when organisms are young, have different mantle colour, shells that are covered by epibionts, and when relevant morphological traits have not yet been fully developed (Ramah *et al*., 2017; 2019). Well-developed identification guides (Knop, 1996) are nevertheless available to easily identify species using morphological traits such as by observing

http://dx.doi.org/10.4314/wiojms.si2021.2.16

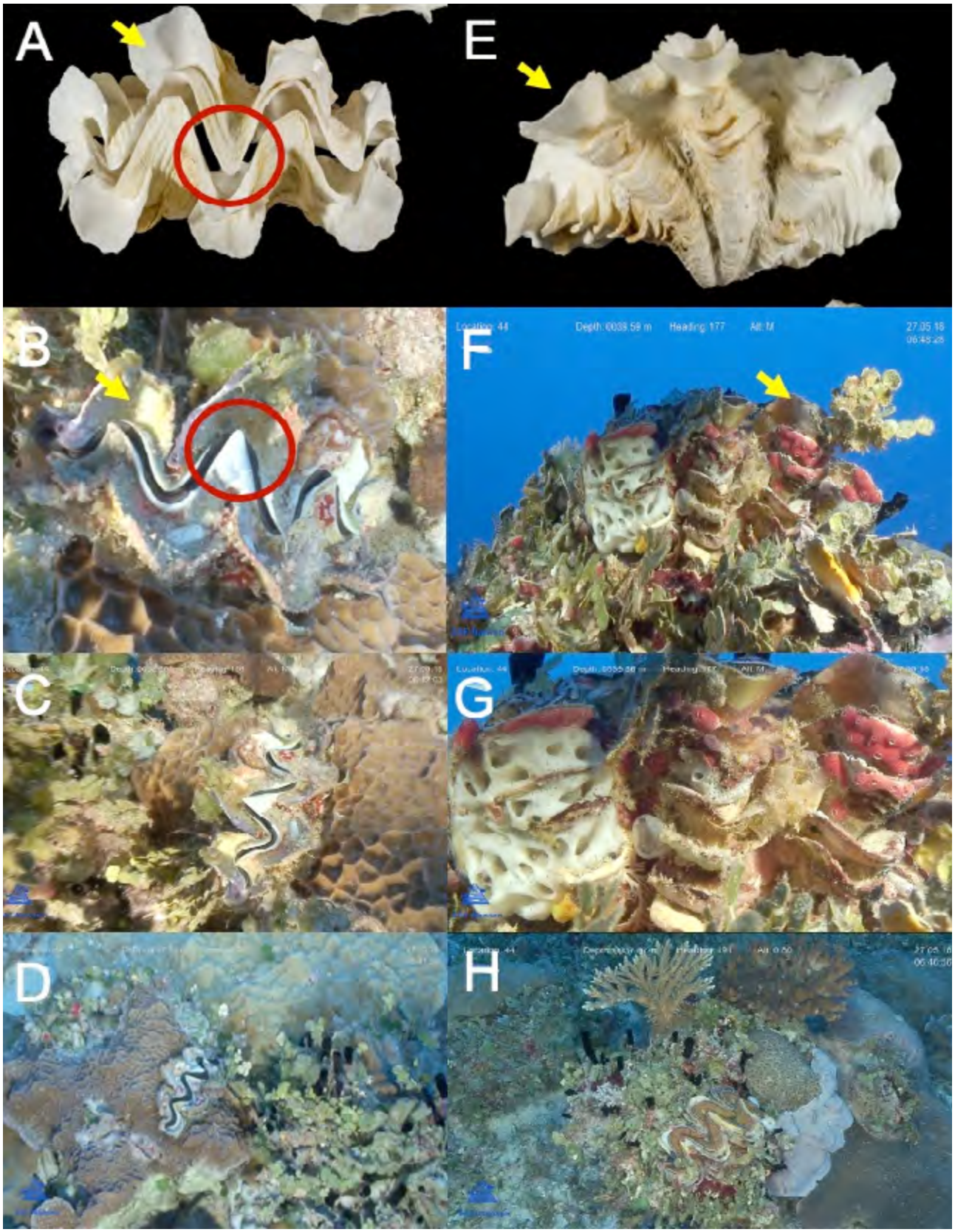

Figure 1. *T. rosewateri* from Musée national d'Histoire naturelle (MNHN) and *in situ* from the Nazareth Bank. A and E: Specimen photos from MNHN (photos adapted to show salient features only). B-D: Individual 1 recorded from Nazareth Bank at 38.60 m encrusted in coral. F-H: Individual 2 recorded from Nazareth Bank at depth at 39.66 m encrusted in coral and green coralline algae. Red circles indicate the shape of the valve margins, and the yellow arrows show the scutes projection on the primary folds.

the lateral, back and upper view of the organism's shell, the rib interstices and the byssal orifice (Norton and Jones, 1992). Photographs available from the Musée national d'Histoire naturelle (MNHN) of one *T. rosewateri* paratype (MNHN-IM-2013-49129, Fig 1A, E) were used for morphological comparison with the two individuals observed *in situ* (Fig. 1 B-D and F-H). Based on the Sirenko and Scarlato (1991) morphological description, a high number of similarities in morphological traits were easily observed between the two individuals recorded from the Nazareth Bank and that from the Saya de Malha Bank kept at the MNHN. Both specimens from the Nazareth Bank have an elongated shape, and the valve margins are large and sharp in a triangular shape (red circle in Fig. 1. A and C). The scutes at the primary folds are large and widely spaced (yellow arrow in Fig. 1 A, B, E and F) very similar to that of *T. squamosa*. However, as compared to the latter, *T. rosewateri* was found to be semi-encrusted in coral (Fig. 1 D and H) which is not a trait of *T. squamosa* in Mauritian waters (Ramah *et al*., 2017). *T. rosewateri* have 4 to 9 dense convex rib-like folds which become more concentrated on the ventral slope. This can be seen from the lateral view of the specimen observed in Fig. 1 F and G. The shells of giant clams are often used as a substrate and shelter by other organisms such as sponges, corals, molluscs, and coralline algae, among others (Neo *et al*., 2015). As recorded previously by Sirenko and Scarlato (1991), these were also observed for the two individuals recorded from the Nazareth Bank (Fig. 1 B, C, F and G).

This observation backed up by morphological evidence presents new data on the occurrence of *T. rosewateri* in the waters of the Republic of Mauritius, especially on its fishing banks. *T. rosewateri* that was previously thought to occur only at the Saya de Malha Bank and more recently in St Brandon is more regionally spread. It is noteworthy that no individuals of giant clams were observed in the surveyed water of the Saya de Malha Bank during this expedition, while two individuals of *T. rosewateri* were observed on the Nazareth Bank at a depth of about 40 m, which is quite unusual as giant clams prefer shallow waters for their symbiotic zooxanthellae to photosynthesize. The occurrence of *T. rosewateri* in the waters of Nazareth Bank is not improbable. Saya de Malha and Nazareth Banks and St Brandon are dominated by the South Equatorial Current (SEC) (New *et al*., 2013) which may play a role in the connectivity of the marine flora and fauna of the Banks and St Brandon. With this new observation, it can be confirmed that the distribution of this endemic species of giant clam likely covers the entire Mascarene Plateau and not only the Saya de Malha Bank.

Acknowledgements

The underlying work was made possible with the support of the EAF-Nansen Programme "Supporting the Application of the Ecosystem Approach to Fisheries Management considering Climate Change and Pollution Impacts" executed by Food and Agriculture Organization of the United Nations (FAO) and funded by the Norwegian Agency for Development Cooperation (Norad). The authors are thankful to FAO for funding and supporting the Indian Ocean research expedition 2018 on the Saya de Malha Bank and Nazareth Bank with the R/V *Dr Fridtjof Nansen*, the Department of Continental Shelf, Maritime Zones Administration & Exploration of Mauritius for co-leading and coordinating the scientific expedition, the Mauritius-Seychelles Joint Commission of the Extended Continental Shelf for their support and assistance and granting the necessary authorisations, the Ministry of Blue Economy, Marine Resources, Fisheries & Shipping for hosting and spearheading the Habitat Mapping Workshop in Mauritius and for granting necessary authorization to carry out research in the Nazareth Bank; the Institute of Marine Research, Norway for leading the expedition and providing the technical and logistic support. The authors also thank the participating scientists, the crew members and the VAMS / Argus ROV technicians for their work and contribution during the expedition and to the anonymous reviewers for their insightful comments which have significantly improved the manuscript.

References

Fauvelot C, Zuccon D, Borsa P, Grulois D, Magalon H, Riquet F, Andrefouet S, Berumen ML, Sinclair-Taylort TH, Gelin P, Behivoke P, Johan Ter Poorten J, Strong EE, Bouchet P (2020) Phylogeographical patterns and a cryptic species provide new insights into Western Indian Ocean giant clams phylogenetic relationships and colonization history. Journal of Biogeography: 1-20

Griffiths C, Klumpp D (1994) Contributions of phototrophic and heterotrophic nutrition to the metabolic and growth requirements of four species of giant clam (*Tridacnidae*). Marine Ecology Progress Series 115: 103-115

Jantzen C, Wild C, El-Zibdah M, Roa-Quiaoit HA, Haacke C, Richter C (2008) Photosynthetic performance of giant clams, *Tridacna maxima* and *T. squamosa*, Red Sea. Marine Biology 155: 211-221

Knop D (1996) Giant clams: A comprehensive guide to the identification and care of tridacnid clams. Ettlingen, Dähne Verlag GmbH. 255 pp

Lamarck JBM (1819) Histoire naturelle des animaux sans vertèbres. Tome sixième, 1re partie, Paris. 343 pp

Mohamed NA, Yu Q, Chanfi MI, Li Y, Wang S, Huang X, Bao Z (2016) Genetic diversity and population differentiation of small giant clam *Tridacna maxima* in Comoros islands assessed by micro- satellite markers. SpringerPlus 5: 1852

Monsecour K (2016) A new species of giant clam (Bivalvia: Cardiidae) from the Western lndian Ocean. Conchylia 46: 1-4

Neo ML, Eckman W, Vicentuan K, Teo SLM, Todd PA (2015) The ecological significance of giant clams in coral reef ecosystems. Biological Conservation 181: 111-123

Neo ML, Wabnitz CCC, Braley RD, Heslinga GA, Fauvelot C, Van Wynsberge S, Andréfouët S, Waters C, Tan AS-H, Gomez ED, Costello MJ, Todd PA (2017) Giant clams (Bivalvia: Cardiidae: Tridacninae): A comprehensive update of species and their distribution, current threats and conservation status. Oceanography and Marine Biology – An Annual Review 55: 87-388

New AL, Magalhaes JM, da Silva JCB (2013) Internal solitary waves on the Saya de Malha bank of the Mascarene Plateau: SAR observations and interpretation. Deep Sea Research Part I: Oceanographic Research Papers 79: 50-61

Norton JH, Jones GW (1992) The giant clams: An anatomical and histological atlas. Australian Centre for International Agricultural Research Monographs. 142 pp

Nuryanto A, Duryadi D, Soedharma D, Blohm D (2007) Molecular phylogeny of giant clams based on mitochondrial DNA cytochrome C oxidase I gene. HAYATI Journal of Biosciences 14: 1662-1665

Othman ASB, Goh GHS, Todd PA (2010) The distribution and status of giant clams (family: Tridacnidae) – a short review. The Raffles Bulletin of Zoology 58: 103-111

Purchon RD (ed)(1977) The biology of the mollusca, 2nd edition. Chapter 7 – Distribution of molluscs. Pergamon Press. pp 333-398

Ramah S, Taleb-Hossenkhan N, Bhagooli R (2017) Differential substrate affinity between two giant clam species, *Tridacna maxima* and *Tridacna squamosa,* around Mauritius. Western Indian Ocean Journal of Marine Science (Special Issue) 1: 13-20

Ramah S, Taleb-Hossenkhan N, Todd PA, Neo ML, Bhagooli R (2019) Drastic decline in giant clams (Bivalvia: Tridacninae) around Mauritius Island, Western Indian Ocean: implications for conservation and management. Marine Biodiversity 49: 815-823

Röding PF (1798) Museum Boltenianum sive Catalogus cimeliorum e tribus regnis naturae quae olim collegerat Joa. Fried. Bolten M. D. p. d. Pars secunda continens *Conchylia sive Testacea univalvia, bivalvia et multivalvia*. 171 pp

Sirenko BI, Scarlato OA (1991) *Tridacna rosewateri* sp. A new species of giant clam from Indian Ocean. La Conchiglia 22: 4-9

Tan EYW, Quek ZBR, Neo ML, Fauvelot C, Huang D (2021) Genome skimming resolves the giant clam (Bivalvia: Cardiidae: Tridacninae) tree of life. Coral Reefs [https://doi.org/10.1007/s00338-020-02039-w]

Yonge CM (1975) Giant clams. Scientific American 232. pp 96-105

Sightings of sea stars (Echinodermata, Asteroidea) and a first record of crown-of-thorns starfish *Acanthaster* at Saya de Malha Bank, Mascarene Plateau

Sundy Ramah[1,2]*, Deepeeka Kaullysing[2], Ranjeet Bhagooli[2]

[1] Albion Fisheries Research Centre, Ministry of Blue Economy, Marine Resources, Fisheries and Shipping, Albion, Petite Rivière 91001, Republic of Mauritius

[2] Department of Biosciences and Ocean Studies, Faculty of Science & Pole of Research Excellence in Sustainable Marine Biodiversity, University of Mauritius, Réduit 80837, Republic of Mauritius

* Corresponding author: sundy.ramah@gmail.com

Sea stars or starfish, belonging to the phylum Echinodermata and class Asteroidea, are ecologically important and diverse members of marine ecosystems. They are found at various depths ranging from the intertidal to abyssal zones (Gale, 1985). The estimated number of species in this class is 1900, belonging to seven extant orders (Mah and Blake, 2012). The rich fossil history of sea stars dates back to the early Paleozoic (Gale, 1985). Sea stars predate mostly on benthic invertebrates (Wells *et al*., 1961; Mauzey *et al*., 1968; Sloan and Robinson, 1983; Magnesen and Redmond, 2012), and are known to regenerate damaged parts or lost arms (Mladenov *et al*., 1989).

The ecologically important corallivorous crown-of-thorns starfishes (COTS) *Acanthaster* spp. have gained particular attention among the sea stars due to their significant contribution to the loss of hard coral cover globally (Conand, 2001; Emeras *et al*., 2004; Conand *et al*., 2016; Pratchett *et al*., 2017; Conand *et al*., 2018; Caragnano *et al*., 2021). The displacement of COTS principally occurs at night, ranging between less than 1 m to 19 m day^{-1}. This wide difference in the daily movement is dependent on the availability of the preferred coral prey, *Acropora* spp. (Ling *et al*., 2020). Despite the uncertainty about the main causes leading to COTS outbreaks, Babcock *et al*. (2016) proposed that elevated nutrients leading to phytoplankton blooms, acting as abundant food sources for *Acanthaster* larvae, and removal of key predators can cause or exacerbate an outbreak, eventually resulting in a decrease in coral cover. They also suggested that multiple factors act together to initiate an outbreak.

Numerous reports on the devastating effect of COTS have emanated from various regions globally, particularly from the Indo-Pacific region. The Great Barrier Reef (GBR) has witnessed four outbreaks since the 1960s (in 1962, 1979, 1993 and 2009) (Babcock *et al*., 2016; Pratchett *et al*., 2017), resulting in the average hard coral cover across the GBR halving during the period from 1985–2012, largely attributed to *Acanthaster* cf. *solaris* (Babcock *et al*., 2020; Westcott *et al*., 2020). Saponari *et al*. (2015) reported an average density of 120±51 COTS per 900 m^2 at Mama Ghiri, Ari Atoll in the Republic of Maldives. This led to approximately 70 % coral mortality comprised almost entirely of tabular *Acropora* mainly belonging to the species *A. cytherea, A. clathrata,* and *A. hyacinthus*. Moreover, Plass-Johnson *et al*. (2015) noted high densities of COTS reaching up to 37 individuals per 250 m^2 in a region close to two river mouths, which resulted in the loss of half the live coral at 2 out of the 12 islands studied in Indonesia.

In the Western Indian Ocean (WIO) region, there have been some reports of high densities of COTS; for instance in Seychelles in 1997 and 2014 (Obura *et al*., 2017). In 1994, a COTS outbreak was reported on the reefs of northern KwaZulu-Natal, South Africa, with the hard coral genera *Acropora*, *Montipora* and *Fungia* being initially favoured, followed by the frequently avoided colonies of *Pocillopora* (Schleyer, 1998). This was in contradiction with other observations where *Pocillopora* was found to be one of the preferred coral genera of COTS (Pratchett, 2001, 2007; De'ath and Moran, 1988). There appears to be a gap in

http://dx.doi.org/10.4314/wiojms.si2021.2.17

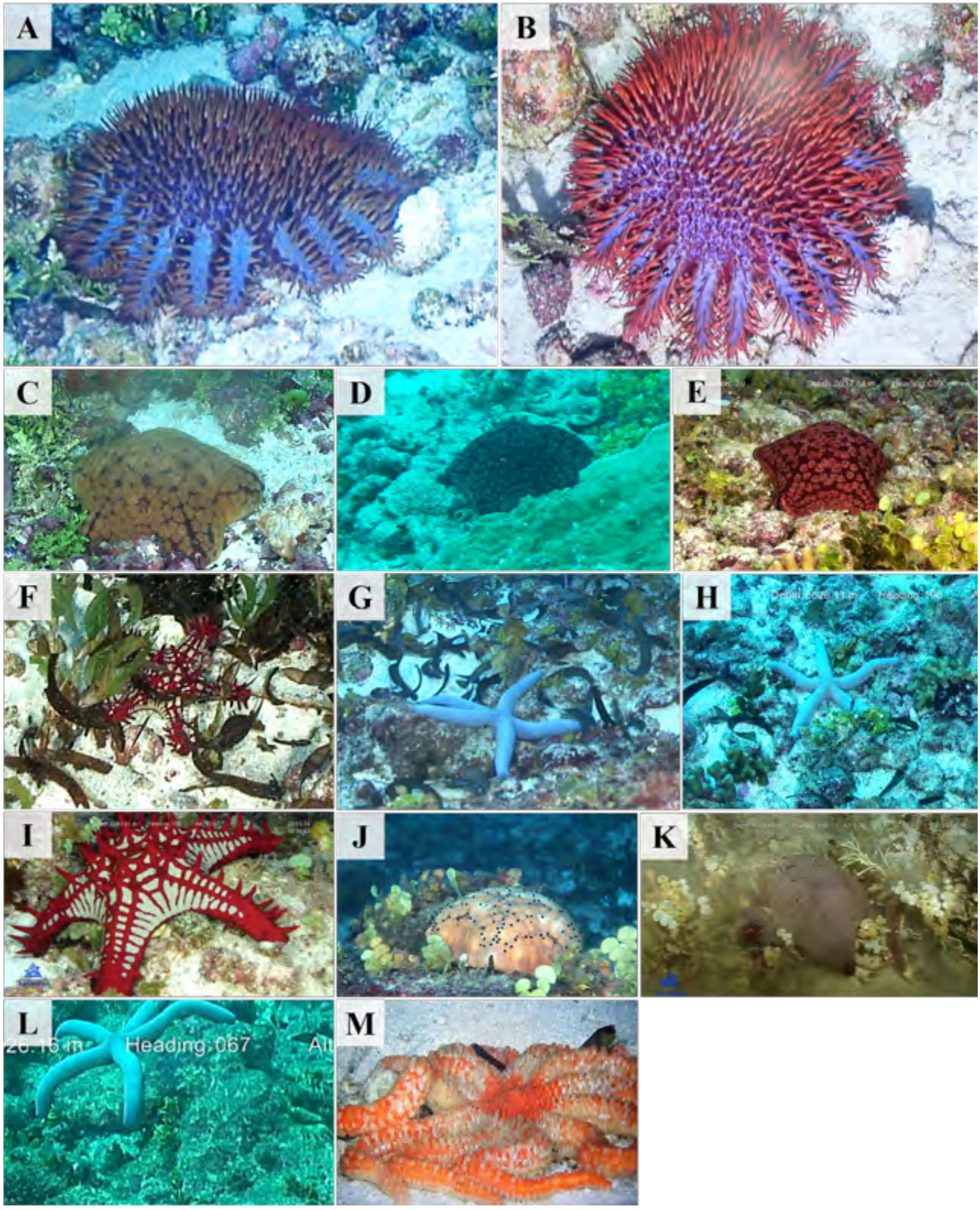

Figure 1. A, B. Crown-of-thorns starfish *Acanthaster* sp. spotted on a rhodolith bed at 38.11 m at Saya de Malha Bank; C–N. Sea stars spotted at Saya de Malha Bank. C. *Culcita* sp. 1 - Location 36 at a depth of 38.71 m and 25.07 m, respectively; D, E. *Culcita* sp. 2 - Location 39 at a depth of 37.84 m; F. *Protoreaster lincki* - Location 13 at a depth of 31.5 m; G. *Linckia* sp. - Location 39 at a depth of 33.09 m; H. *Linckia* sp. - Location 36 at a depth of 26.11 m; I. *Protoreaster lincki* - Location 39 at a depth of 41.81 m; J. *Culcita schmideliana* - Location 39 at a depth of 32.74 m; K. *Culcita* sp. 3 - Location 40 at a depth of 43.42 m; L. *Linckia* sp. - Location 36 at a depth of 26.16 m; M. *Rathbunaster* sp. - Location 38 at a depth of 175.23 m.

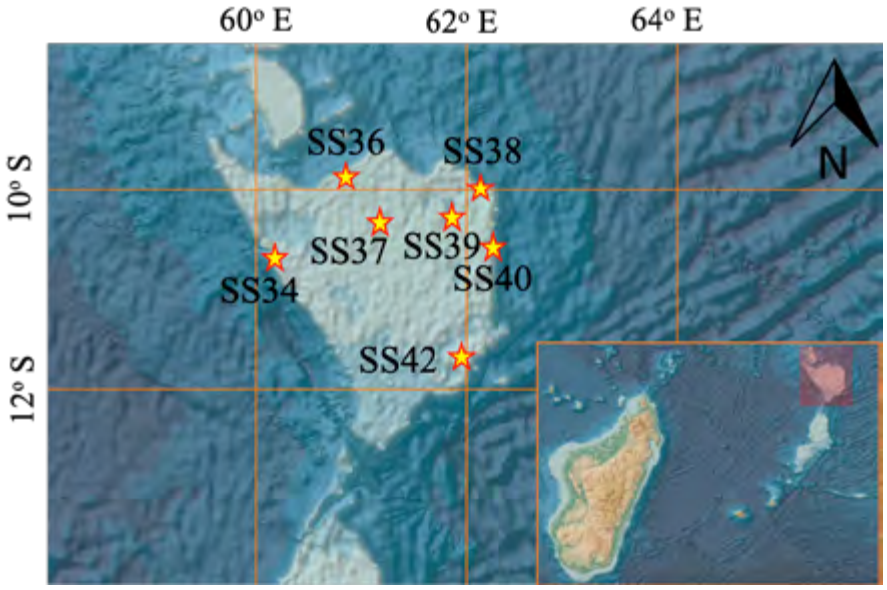

Figure 2. Map showing the seven locations (SS where the sea stars were observed indicated in yellow and red border stars. Map prepared using the GEBCO Bathymetry Grid layer data 2020.

the scientific information available in the WIO region on COTS species. Although research has shown the occurrence of *Acanthaster mauritiensis* in this region (Haszprunar *et al*., 2017), additional information is required to provide a broader understanding on the phylogeography and evolution of these species.

In May 2018, the Indian Ocean Research Expedition conducted under the EAF-Nansen Programme at the Saya de Malha Bank of the Mascarene Plateau enabled the sighting of one *Acanthaster* sp. individual (Fig. 1A, B) using the Argus Remotely Operated Vehicle (ROV). A total of 12 transects at 7 locations for an average of 30 min to 1 hour were covered. The *Acanthaster* sp. was observed at locations 38 (SS38) on a rhodolith bed at a depth of 38.11 m. The presence of the coralline green macroalga *Halimeda* on the bed was also noted while the corals in the vicinity were widely spaced and included *Porites* sp., branching *Acropora* sp., *Pocillopora* sp., *Heliopora coerulea* and other massive hard corals. Further visual inspection revealed the presence of at least 17 other individuals of non-corallivorous sea stars (with *Protoreaster* sp., *Linckia* sp. and *Culcita* spp. being more dominant) during the cruise at depths ranging between 23 m to 50 m (Fig. 1 C-M) at locations at locations SS34, SS36, SS37, SS38, SS39, SS40 and SS42 (Fig. 2). The substrata on which the sea stars were spotted were sand, rhodolith beds, corals, macroalgae and seagrass beds.

Koonjul *et al*. (2003) reported 28 COTS around Mauritius Island, spread over a reef area of 0.6 km^2 (about 4.67 x 10^{-5} per m^2, or 0.01 per 250 m^2, or 0.04 per 900 m^2) with a substrate mix comprising corals, algae, sand, and coral rubble. The first observation of only one individual of *Acanthaster* sp. at one location (out of 7) after 30 min of video time at Saya de Malha Bank does not signify any warning of significant damage to corals in that region. However, this information is noteworthy as it brings forth new knowledge on Asteroids from the Saya de Malha Bank, an unexplored region of the WIO which appears to harbour a high diversity of sea stars.

There are considerable challenges to addressing the knowledge gaps relating to the biology, ecology and genetics of *Acanthaster* spp. Differences in morphology, in particular colour patterns, among COTS species reported from the Pacific and the Indian Oceans suggest divergent biology and ecology (Haszprunar, 2017). Further research on and exploration of the seabed is required to build a more robust and in-depth understanding of the sea star distribution at the Bank, especially the corallivorous COTS. Thorough morphological, morphometric, and genetic analyses are necessary to characterize the COTS from this region to assist any future development of key actions required for management.

Acknowledgements

The underlying work was made possible with the support of the EAF-Nansen Programme "Supporting the Application of the Ecosystem Approach to Fisheries Management considering Climate Change and Pollution Impacts" executed by Food and Agriculture

Organization of the United Nations (FAO) and funded by the Norwegian Agency for Development Cooperation (Norad). The authors are thankful to FAO for funding and supporting the Indian Ocean research expedition 2018 on the Saya de Malha Bank and Nazareth Bank with the R/V *Dr Fridtjof Nansen*, the Department of Continental Shelf, Maritime Zones Administration & Exploration of Mauritius for co-leading and coordinating the scientific expedition, the Mauritius-Seychelles Joint Commission of the Extended Continental Shelf for their support and assistance and granting the necessary authorisations, the Ministry of Blue Economy, Marine Resources, Fisheries & Shipping for hosting and spearheading the Habitat Mapping Workshop in Mauritius and for granting necessary authorization to carry out research in the Nazareth Bank; the Institute of Marine Research, Norway for leading the expedition and providing the technical and logistic support. The authors also thank the participating scientists, the crew members and the VAMS / Argus ROV technicians for their work and contribution during the expedition and to the anonymous reviewers for their insightful comments which have significantly improved the manuscript.

References

Babcock RC, Dambacher JM, Morello EB, Plagányi ÉE, Hayes KR, Sweatman HPA, Pratchett MS (2016) Assessing different causes of crown-of-thorns starfish outbreaks and appropriate responses for management on the Great Barrier Reef. PLoSONE 11: e0169048 [doi:10.1371/journal.pone.0169048]

Babcock RC, Plagányi É, Condie SA, Westcott DA, Fletcher CS, Bonin MC, Cameron D (2020) Suppressing the next crown-of-thorns outbreak on the Great Barrier Reef. Coral Reefs 39: 1233-1244

Caragnano A, Basso D, Spezzaferri S, Hallock P (2021) A snapshot of reef conditions in North Ari Atoll (Maldives) following the 2016 bleaching event and *Acanthaster planci* outbreak. Marine and Freshwater Research 72: 987-996

Conand C (2001) *Acanthaster planci*. Bulletin des sciences naturelles et de géologie. Mayotte 5: 26-29

Conand C, Ribes-Beaudemoulin S, Trentin F, Mulochau T, Boissin E (2016) Oursins, étoiles de mer & autres echinodermes. Biodiversité de La Réunion. Les éditions du cyclone. 168 pp

Conand C, Ribes-Beaudemoulin S, Trentin F, Mulochau T, Boissin E (2018) Marine biodiversity of La Reunion Island: Echinoderms. Western Indian Ocean Journal of Marine Science 17: 111-124

De'ath G, Moran PJ (1988) Factors affecting the behaviour of crown-of-thorns starfish (*Acanthaster planci* L.) on the Great Barrier Reef, 1: Patterns of activity. Journal of Experimental Marine Biology and Ecology 220: 83-106

Emeras J, Falquet M-P, Conand C (2004) *Acanthaster planci* on La Reunion reefs (Western Indian Ocean). Reef Encounter 32: 26-27

Gale AS (1987) Phylogeny and classification of the Asteroidea (Echinodermata). Zoological Journal of the Linnean Society 89: 107-132

Haszprunar G, Vogler C, Wörheide G (2017) Persistent gaps of knowledge for naming and distinguishing multiple species of crown-of-thorns seastar in the *Acanthaster planci* species complex. Diversity 9: 22 [doi:10.3390/d9020022]

Koonjul MS, Mangar V, Luchmun JP (2003) Eradication of crown of thorns starfish (*Acanthaster planci*) infestation in a patch reef in the lagoon off Ile aux Cerfs, Mauritius. AMAS. Food and Agricultural Research Council, Réduit, Mauritius. pp 333-338

Ling SD, Cowan Z-L, Boada J, Flukes EB, Pratchett MS (2020) Homing behaviour by destructive crown-of-thorns starfish is triggered by local availability of coral prey. Proceedings of the Royal Society B 287: 20201341 [http://dx.doi.org/10.1098/rspb.2020.1341]

Magnesen T, Redmond KJ (2011) Potential predation rates by the sea stars *Asterias rubens* and *Marthasterias glacialis*, on juvenile scallops, *Pecten maximus*, ready for sea ranching. Aquaculture International 20: 189-199

Mah CL, Blake DB (2012) Global diversity and phylogeny of the Asteroidea (Echinodermata). PLoS ONE 7: e35644 [doi:10.1371/journal.pone.0035644]

Mauzey KP, Birkeland C, Dayton PK (1968) Feeding behavior of asteroids and escape responses of their prey in the Puget Sound region. Ecology 49: 603-619

Mladenov PV, Bisgrove B, Asotra S, Burke RD (1989) Mechanisms of arm-tip regeneration in the sea star, *Leptasterias hexactis*. Roux's Archives of Developmental Biology 198: 19-28

Obura D, Gudka M, Rabi FA, Bacha Gian S, Bijoux J, Freed S, Maharavo J, Mwaura J, Porter S, Sola E, Wickel J, Yahya S, Ahamada S (2017) Coral reef status report for the Western Indian Ocean. Global Coral Reef Monitoring Network (GCRMN)/International Coral Reef Initiative (ICRI). 144 pp

Plass-Johnson JG, Schwieder H, Heiden J, Weiand L, Wild C, Jompa J, Ferse SCA, Teichberg M (2015) A recent outbreak of crown-of-thorns starfish (*Acanthaster*

planci) in the Spermonde Archipelago, Indonesia. Regional Environmental Change 15: 1157-1162

Pratchett MS (2001) Influence of coral symbionts on feeding preferences of crown-of-thorns starfish *Acanthaster planci* in the western Pacific. Marine Ecology Progress Series 214: 111-119

Pratchett MS (2007) Feeding preferences of *Acanthaster planci* (Echinodermata: Asteroidea) under controlled conditions of food availability. Pacific Science 61: 113-120

Pratchett MS, Caballes CF, Wilmes JC, Matthews S, Mellin C, Sweatman HPA, Nadler LE, Brodie J, Thompson CA, Hoey J, Bos AR, Byrne M, Messmer V, Fortunato SAV, Chen CCM, Buck ACE, Babcock RC, Uthicke S (2017) Thirty years of research on crown-of-thorns starfish (1986–2016): Scientific advances and emerging opportunities. Diversity 9: 41 [https://doi.org/10.3390/d9040041]

Saponari L, Montano S, Seveso D, Paolo G (2015) The occurrence of an *Acanthaster planci* outbreak in Ari Atoll, Maldives. Marine Biodiversity 45: 599-600

Schleyer MH (1998) Observations on the incidence of crown-of-thorns starfish in the Western Indian Ocean. Reef Encounter 23: 25-27

Sloan NA, Robinson SMC (1983) Winter feeding by asteroids on a subtidal sandbed in British Columbia. Ophelia 22: 125-140

Wells HW, Wells MJ, Gray IE (1961) Food of the sea-star *Astropecten articulatus*. The Biological Bulletin 120: 265-271

Westcott DA, Fletcher CS, Kroon FJ, Babcock RC, Plagányi EE, Pratchett MS, Bonin MC (2020) Relative efficacy of three approaches to mitigate crown-of-thorns starfish outbreaks on Australia's Great Barrier Reef. Scientific Reports 10: 12594 [doi:10.1038/s41598-020-69466-1]

Instructions for Authors

Thank you for choosing to submit your paper to the Western Indian Ocean Journal of Marine Science. These instructions ensure we have everything required so your paper can move through peer review, production, and publication smoothly.
Any queries should be sent by e-mail to the Editorial Secretariat: wiojms@fc.ul.pt.

Editorial Policy

The Western Indian Ocean Journal of Marine Science (WIOJMS) is the research publication of the Western Indian Ocean Marine Science Association (WIOMSA). It publishes original research papers or other relevant information in all aspects of marine science and coastal management as original articles, review articles, and short communications (notes). While submissions on tropical and subtropical waters of the western Indian Ocean and the Red Sea will be given primary consideration, articles from other regions of direct interest to the western Indian Ocean will also be considered for publication.

All manuscripts submitted to the Western Indian Ocean Journal of Marine Science are accepted for consideration on the understanding that their content has not been published elsewhere and is not under consideration by any other journal. Manuscripts and all illustrations should be prepared according to the instructions provided below. Submissions will be subject to a pre-review by the Editor-in-Chief or a member of the Editorial Board and those that fall within the remit of the journal, make a substantial contribution to the field of research, and are in the correct style and format, will be sent for review. Manuscripts that do not meet these criteria will be rejected. Every manuscript will be double-blind reviewed by at least two referees competent in the field of interest.

The research studies must comply with international and national ethical guidelines, including the use of animals in research as well as sampling of endangered species and sensitive habitats.

Submission

Authors should submit an electronic version of the manuscript online by registering as an author on the AJOL website1 and following the submission prompts. This can be accessed directly or via the link provided at the journal's page on the WIOMSA website2. Authors are asked to suggest the names of at least two referees with respective email contacts in the submission message to the editor, avoiding suggested reviewers from the author(s) institution.

The submission must be accompanied by the following documents:

- Complete manuscript single file in word format with the following content sequence:
  - cover page with title, authors and affiliations;
  - manuscript (title, abstract, keywords, introduction, main body text, acknowledgements, and references);
  - tables in editable Word format;
  - figures (maps, graphs and others) in best possible resolution.
- Original files of graphs and diagrams (such as Excel, Power-point, e-Primer, R script, etc.).
- Files of maps (pdf, tiff or jpeg) in high resolution.

In each published WIOJMS issue, the cover has a different colour photograph relevant for the themes of the respective articles. Should the author(s) have high-quality images for which they hold the copyright, they may propose its inclusion as cover for the issue.

[1] https://www.ajol.info/index.php/wiojms/login

[2] https://www.wiomsa.org/publications-2/wio-journal-of-marine-science/

The Manuscript

1. The manuscript is your own original work, and does not duplicate any other previously published work, including your own previously published work.

2. The manuscript has been submitted only to the Western Indian Ocean Journal of Marine Science; it is not under consideration or peer review or accepted for publication or in press or published elsewhere.

3. By submitting your manuscript to the Western Indian Ocean Journal of Marine Science, you are agreeing to any necessary originality checks your manuscript may undergo during the peer-review and production process.

4. Contributions must be written in English. Any consistent spelling and publication styles may be used. Please use single quotation marks, except where 'a quote is "within" a quotation'. Long quotations of 40 words or more should be indented without quotation marks. If English is not your first language we suggest that an English-speaker edits the text, before submission.

5. The journal recommends that authors have their manuscripts checked for language by an English native speaker before submission.

6. All persons who have a reasonable claim to authorship should be named in the manuscript as co-authors and should have been involved in the fundamental aspects of the manuscript; the corresponding author acts on their behalf in all matters pertaining to publication of the manuscript. The order of names should be agreed by all authors.

7. The manuscript must be typed in a normal type font (e.g. Times New Roman font size 12, or Arial font size 11) and 1.5 line spacing. Sequential line numbers should be inserted on the manuscript. The total number of pages should not exceed 20 manuscript pages (excluding figures and tables), both for Original Articles and Review Articles. Short Communications must not exceed 8 manuscript pages.

8. Species names must be in italics; the genus is written in full at the first mention in the Abstract, again in the main text, figure and table legends, and abbreviated thereafter.

9. Tables and Figures (maps, graphs and others): originals of all figures should follow the **Guidelines for illustrations** referred below. The lettering should be of a size readable after reduction for the final layout. Authors are requested to indicate the recommended position of figures and tables in the left-hand margin of the text. A separate sheet at the end of the document should be used for each table and figure, with the corresponding legend.

10. The international system of units (SI Units) must be used throughout; abbreviations and acronyms should be identified where they first appear; mathematical symbols and formulae should be used only when absolutely necessary and should be clearly defined in the text.

11.A complete **Original Article** manuscript must include the following: title page, abstract, keywords, introduction, materials and methods, results, discussion, acknowledgements, references, tables and figures (with figure legends) in that order.

a. Title Page: this should contain a concise title and the names of authors followed by affiliations and their complete postal addresses, phone numbers, and email addresses. The corresponding author and email address must be indicated.

b. Abstract: the abstract should not exceed 200 words and should be a single paragraph. It should briefly describe the main points of the manuscript.

c. Keywords: four to six key words are required for indexing purposes. Keywords must be written in lower case letters unless when referring names, separated by comas. Avoid using the same words as in the title.

d. Introduction: a brief survey of relevant literature and objectives of the work should be given in this section. Thus, the introduction should largely be limited to the scope, purpose and rationale of the study.

e. Materials and Methods: the methodology used should be clearly explained, including relevant references, such that another person can repeat the procedures. It should provide the framework to gain answers to the questions or problems identified. Sampling methods must be elaborated as well as analytical frameworks and model specifications.

f. Results: the text should be as objective and descriptive as possible. Only material pertinent to the subject should be included. Avoid presenting the same information in both graphical and tabular form.

g. Discussion: this section could be combined with the above to present "Results and Discussion". It should interpret the results in view of the problems identified in the introduction, as well as in relation to other published work. The final paragraph of this section could include concluding remarks and recommendations for future work.

h. Citations: authors should be cited using their surnames, followed by the year of publication. Two authors should be separated by 'and'. If there are more than two authors, only the first author, followed by "*et al.*", should be given. This and other Latin or foreign terms should be italicized.

i. Acknowledgement/s: this section should be brief. Authors are advised to limit acknowledgements to substantial contributions to the scientific and technical aspects of the paper, financial support or improvements in the quality of the manuscript.

j. References: the reference section must contain an alphabetical list of all references mentioned in the text of the manuscript, and the journal rules should be followed strictly. Limit punctuation and special fonts as indicated and give all journal names in full. Cross checking of references in the text to the cited literature and vice-versa is the responsibility of the author(s). Examples for citations from periodicals, books and composite works are given below:

- **Periodicals.** Here the following should be sequentially listed: author's name/s, initials, year of publication, full title of paper, periodical (in full), volume, first and last page numbers.

  Example: Richardson K, Beardall J, Raven J (1983) Adaptation of unicellular algae to irradiance: An analysis of strategies. The New Phytologist 93: 157-191

- **Books.** The following should be listed: author's or editor's name, initials, year of publication, full title, publisher, place of publication, total pages.

  Example: Kirk TJO (1983) Light and photosynthesis in aquatic ecosystems. Cambridge University Press, Cambridge. 401 pp

- **Composite works or serials.** The sequence should be as above, but also should include full title of paper followed by In: editor(s) if any, full title of publication, publisher, etc., and the first and last page numbers.

  Example: Sathyendranath S, Platt T (1993a) Remote sensing of water-column primary production. In: Li WKW, Maestrini SY (eds) Measurement of primary production from the molecular to the global Scale. ICES Marine Science Symposia, Vol. 97, Copenhagen. pp 236-243

- **Articles with a Digital Object Identifier (DOI).**

  Example: Gooseff MN, McKnight DM, Lyons HJ, Blum RJ (2002) Weathering reactions and hyporheic exchange controls on stream water chemistry in a glacial meltwater stream in the McMurdo Dry Valleys. Water Resources Bulletin 38 [doi: 10.1029/2001WR000834]

k. Tables and Figures: each table and figure should be numbered consecutively, accompanied by a complete caption, and must be cited in the text. Please follow the **Guidelines for illustrations** for details.

l. Supplementary material: in case it is found relevant, authors may submit appendices with relevant information of major interest for the interpretation of the manuscript results. This is not applicable for the raw data of normal research. The editors will decide its eventual inclusion as appendices.

12. A complete **Review Article** manuscript must include the following: title page, abstract, keywords, introduction, main body text (the central sections vary with specific divisions according to the theme), acknowledgements, references, tables and figures (with figure legends) in that order.

13. A complete **Short Communication** manuscript must include the same structure as an Original Article in a shorter format.

Failure to follow any point of these guideline may delay or compromise the editorial process. Unless there are communication problems, all communications and exchange of documents shall be made strictly via the AJOL editorial interface. Authors must comply with timing for processing manuscripts, either requested revisions or proof check, or otherwise inform the editors of any delays.

Please refer to the Ajol website for full instructions including graphical guidelines.

The Western Indian Ocean Journal of Marine Sciences is the research publication of the Western Indian Ocean Marine Science Association (WIOMSA). It publishes original research papers or other relevant information in all aspects of marine science and coastal management as articles, reviews, and short communications (notes).